Cyclometallation at Pd, Mn and Co: functionalisation of C-H and C≡C bonds involving cyclisation, rearrangement and isomerisation processes

Nasiru Pindiga Yahaya

Doctor of Philosophy

University of York

Chemistry

December 2015

Abstract

This thesis describes cyclometallation at Pd, Mn and Co: functionalisation of C-H and C≡C bonds involving cyclisation, rearrangement and isomerisation processes. The use of $NaNO_2/NaNO_3$ as an oxidant in oxidative Pd-catalyzed processes has recently been reported as a complementary co-catalyst to other common oxidants (*e.g.* Cu^{II}/Ag^{I} salts). In view of this (Chapter two) the synthesis of a series of palladacyclic complexes containing a C^N ligand backbone, and the geometry and linkage isomerism at NO_2-Pd, has been studied. The geometry about the $Pd^{(II)}$ centre shows the crucial role played by bulky ligands in creating hindrance and affecting phosphine dissociation.

Mn-catalysed C-H bond activation is a powerful strategy for the functionalisation of organic compounds containing metal-directing groups. Chapter three of this thesis reports the characterisation of a highly reactive 7-membered Mn^{I} species which acts as anvil point between protonation and reductive elimination to deliver alkenylated and/or pyridinium products respectively. Both processes are exemplified through the reactions of a substrate containing a 2-pyridyl directing group and electron-deficient 2-pyrone motif at Mn^{I}, where C-H bond activation occurs regioselectively at C3 within the 2-pyrone. An unprecedented regioselective Diels-Alder reaction also occurs on both the pyridine and 2-pyrone ring systems. These findings provide a unique insight into Mn^{I}-mediated C-H bond activation processes, especially how relatively minor changes in substrate structure influence the product distribution. The study shows that Mn^{I}-based metallocycles warrant further study more generally in organic and organometallic chemistry

The intermolecular Pauson-Khand (PK) reactions of sterically comparable (2-pyridylethynyl)-heteroaromatic compounds with norbornene, mediated by $Co_2(CO)_8$ to give cyclopentenone products, were examined in Chapter four of this thesis. The π-deficient heteroaromatic substrate, 2-pyrone, favoured the α-position while the π-rich heteroaromatics such as 2-thiophene favour the β-position. The position of the nitrogen in pyridyl-containing alkyne substrates also affects the regiochemical outcome of the PK reaction. A 2-pyridyl alkyne, possessing a proximal nitrogen atom, influences the regioselectivity relative to a 4-pyridyl variant, quite dramatically, favouring the β-position in the newly formed cyclopentenone ring. Overall, the type of heteroaromatic group greatly influences PK regioselectivity. The PK cycloadducts undergo a 6π-electrocyclisation–oxidative aromatisation reaction in the presence of light, which is promoted by a LED UV-light controlled system, affording benzo[*h*]indeno[1,2-*f*]isochromene type products.

List of Contents

List of Figures

List of Schemes

List of Tables

Acknowledgements

First I would like to thank my supervisors, Professors Ian Fairlamb and Simon Duckett, for giving me the opportunity to work under their intensive care in their respective laboratory (both academically and otherwise). I am specifically very indebted to Professor Ian Fairlamb for absolute support especially during the difficult times and also for giving me the freedom in my research project and flexibility on working hours, I have learn a lot from you (Ian Fairlamb).

I would also like to thank all the good people in both the Fairlamb and Duckett groups, especially the Fairlamb group, who I have been working with in the Laboratory and made my time so easy in York. I would especially like to thank past and present Fairlamb group whom have shared their experience with me in group meetings and lab work over the past 4 years, particularly Tom Williams (for showing me the way in and around the department),

Special thanks to Lyndsay, Tom, Kate, Josh and Ben for giving their time to proofread this thesis. I am grateful for the technical support from Dr. Karl Heaton (Mass Spectrometry), Dr. Adrian Whitwood (X-Ray Crystallography), Dr. Pedro Aguiar and Heather Fish (NMR), Chris Rhodes (Electrical LED system), Chris Mortimer (Mechanical LED system), Graeme McAllister (Elemental Analysis) and Dr. Charlotte Elkington (IJSF Lab. motivator).

Finally I am deeply thankful to my family, especially my parents, my wife and son (Abdulrahaman) and uncle; it would not have been possible without their support and encouragement, and I am very grateful to them for everything they have done for me, and of course the rest of them.

Author's Declaration

The work presented in this thesis is my own except where referenced or clearly indicated in the body of the text. This work has not previously been presented for an award at this, or any other, University. The work was carried out at the University of York between November 2011 and November 2015.

Chapter 1: General Introduction

3.1 Transition metal mediated C–C, C–O and C–N bond formation

Transition metal complexes are employed extensively as catalysts in modern organic chemistry, natural product synthesis, therapeutics, advanced materials and chemical biology. They allow the production of high value chemicals for use in manufacturing drugs and specialised chemicals,[1-5] through cross-coupling reactions which are powerful methods for the construction of C–C, C–O and C–N bonds.[6-8] Researchers have used a variety of ligand types to promote catalytic activity at Pd and high turnover numbers (TONs) are obtained with many phosphine ligands.[9, 10] The development of metal-catalysed methods for converting sp^3-C–H bonds (*e.g.* **1)** into C–O bonds (*e.g.* **2**), using dioxygen as a terminal oxidant, remains a grand challenge in organometallic chemistry[11] (Scheme 1).

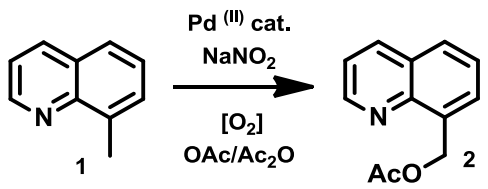

Scheme 1 Typical oxidative acetoxylation reaction mediated by Pd.

Furthermore, the use of acyl anion equivalents in the formation of C–C and or C–O bonds is a powerful strategy used widely in chemical synthesis.[12] Interesting effects of nitrate/nitrite anions at Pd has been reported recently.[11, 13, 14]

3.1.1 Palladium in C-X/C-H cross-coupling bond functionalisation

Metal-catalysed cross-coupling, particularly using Pd, continues to grow, as evidenced by the total number of publications/patents[15] recoded by a SciFinder

search (Figure 1).[15] Pd-catalysed cross-coupling reactions comprise of one of the most important classes of transformations in synthetic chemistry, providing chemists with an exceptionally powerful tool for the construction of C-C and C-X bonds (X = heteroatom).[16] These, and many related transformations, are indispensable reactions used widely in modern industry and academia.

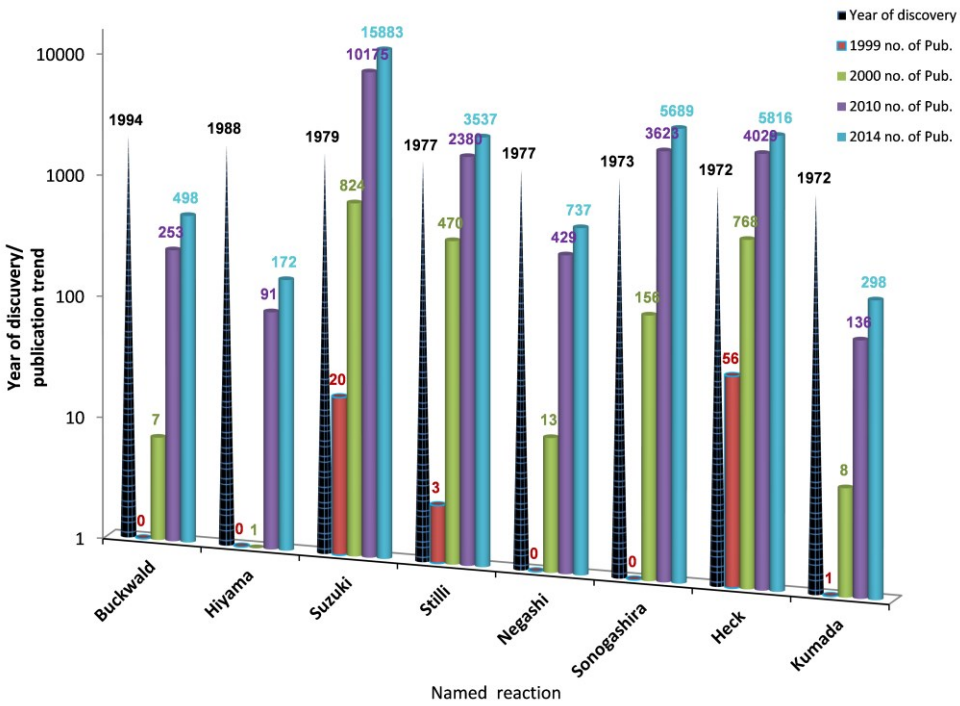

Figure 1 Trend in discovery and number of publications 1999, 2000, 2010 and 2014 of Pd-catalysed cross-coupling reactions (Based on SciFinder searches, May 2014).

A direct C–H bond functionalisation reaction (Scheme 2) is widely attractive to the organic community, although it is considered to be limited by two fundamental issues:

(i) the inert nature of most carbon-hydrogen bonds, and;

(ii) the requirement to control site selectivity in molecules that contain diverse C–H groups.

Many studies have addressed the first challenge by demonstrating that transition metals can react with C–H bonds to produce C–M bonds in a process known as C–H bond activation, which occurs by distinct mechanisms (exemplified in Scheme 2).[17] The resulting C–M bonds are far more reactive than their C–H counterparts, and in many cases they can be converted to new useful functional groups under mild reaction conditions. The latter are typically reactions conducted at or below 40 ºC, although it does depend on the system.

3.1.2 Recent developments in metal C–C bond formation via C–H bond activation – examples from natural product synthesis

Suzuki–Miyaura cross-coupling remains the most widely used Pd-mediated reaction[18] (Figure 1) Heck shared the 2010 Nobel Prize for Pd-catalysed cross-coupling with both Suzuki and Negishi. Mizoroki and Heck, first reported functionalisation of a terminal alkene,[19, 20] using Pd catalysts to enable reactions with aryl, benzyl or vinyl halides (Scheme 2). The Stille (coupling organopseudohalides with organotin reagents),[21-23] Suzuki-Miyaura (coupling organopseudohalides with organoboronic acids),[24] Sonogashira (coupling organopseudohalides with terminal alkynes),[25, 26] Kumada-Corriu (coupling organopseudohalides with Grignard reagents) and Hiyama (coupling organopseudohalides with organosilanes) reactions are also well developed, taking advantage of the unique reactivity of Pd, usually shuttling between Pd^0 and Pd^{II}.[18]

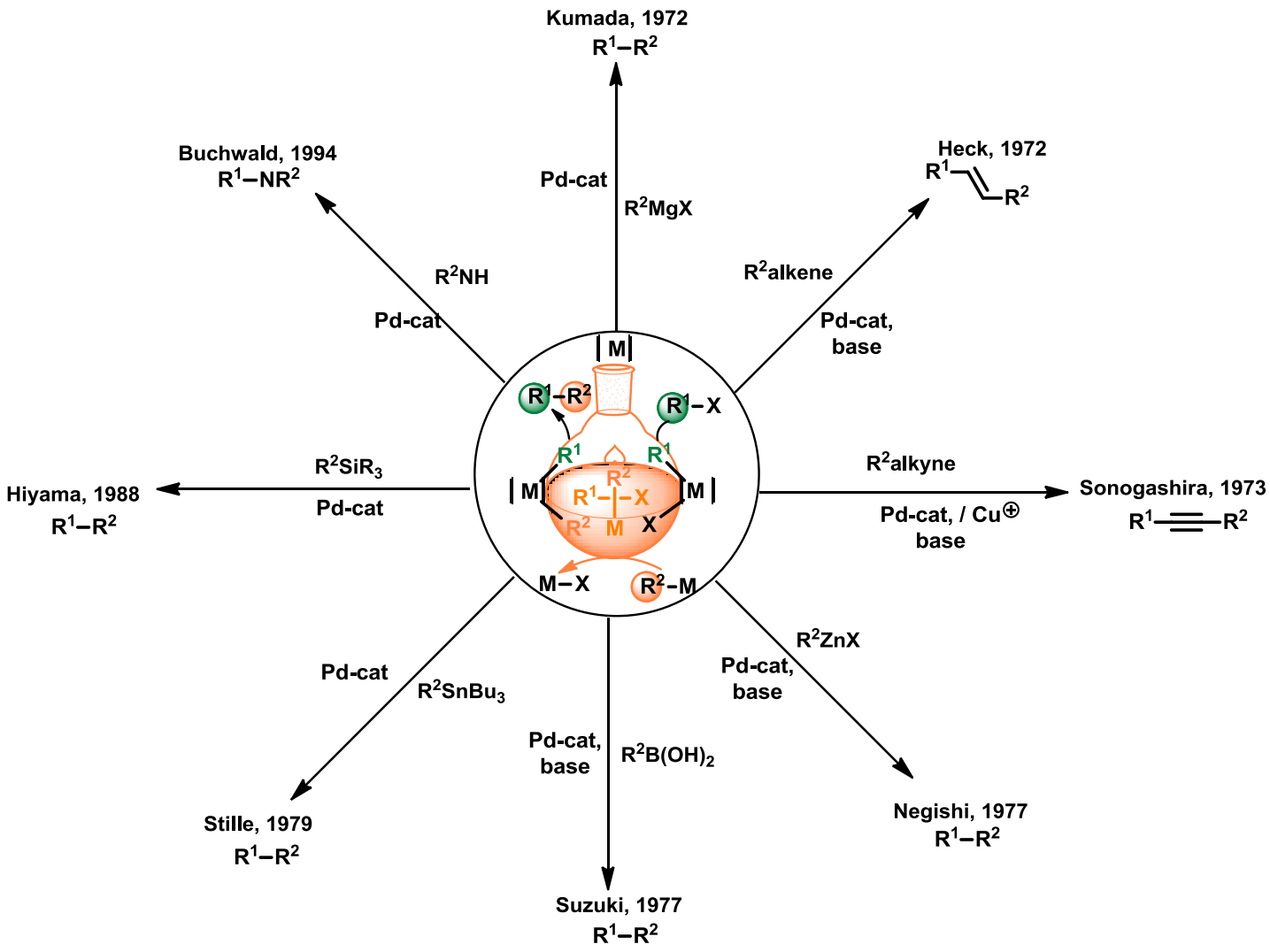

Scheme 2 A timeline of cross-coupling processes

Sasaki and Tsukano[27-30] examined how the Suzuki-Miyaura reaction can be used in the total synthesis of gymnocin A,[31-33] using a highly complex synthetic strategy as highlighted in Scheme 3. The exocyclic enol ether (**3A)** was transformed with 9–borabicyclo[3.3.1]nonane (9-BBN); the resultant alkyl borane adduct was treated with cyclic ketene acetal phosphate (**3B),** under Johnson's conditions, to afford a trisubstituted enol ether product (**3C)** in good yield (72 %). Illustration of the coupling product (**3C**), via a cyclic ketene acetal triflate (**3D)** resulted in the second key *β*-alkyl Suzuki–Miyaura fragment coupling reaction of an alkyl borane species, derived from hydroboration of the ABCD-ring exocyclic enol ether unit (**3E)**, to give compound (**3F)** in 81 % yield. Intermediate (**3F)** was then used to complete of the total synthesis of gymnocin A **3G**.[34]

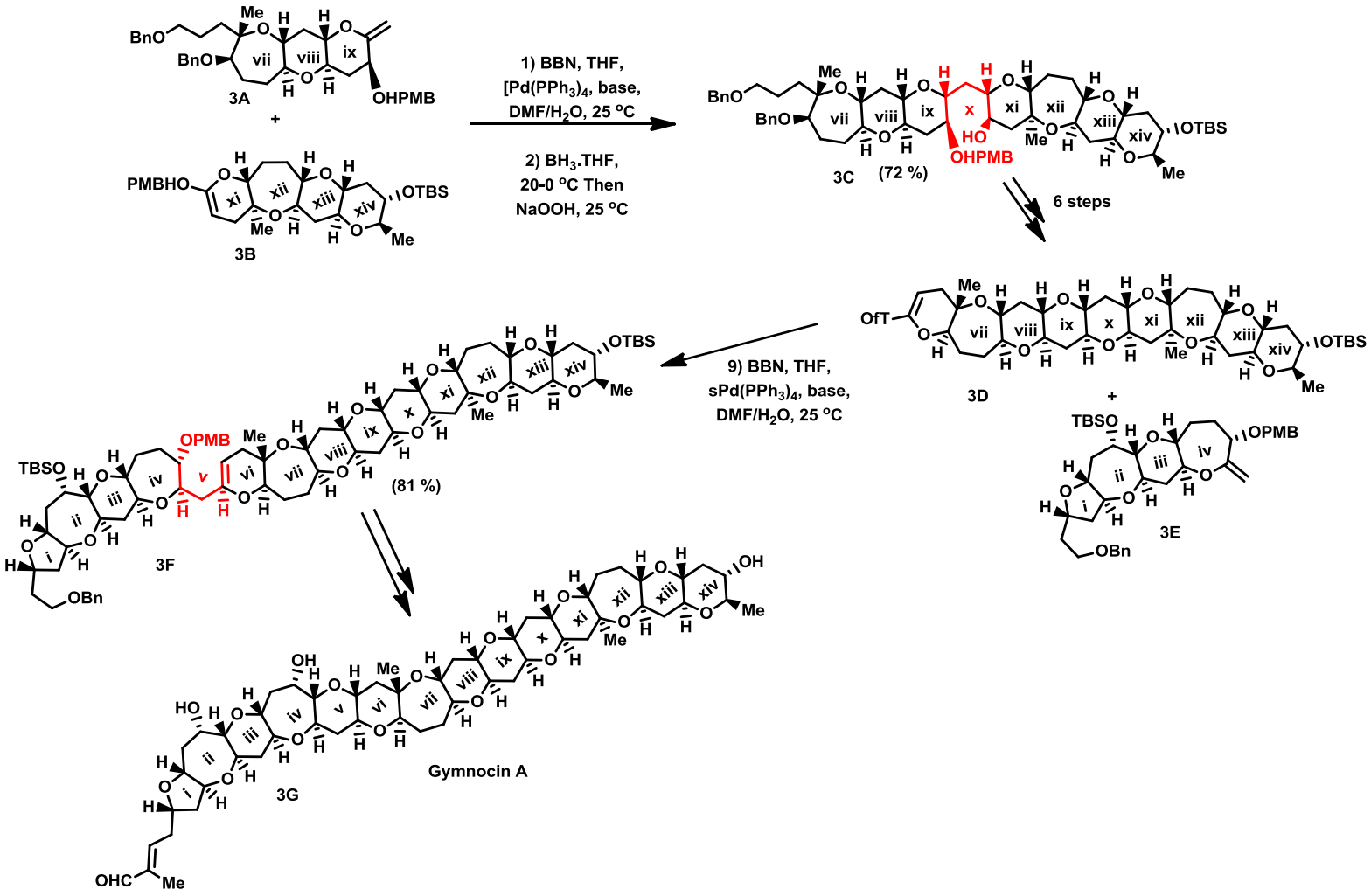

Scheme 3 Intermolecular Suzuki–Miyaura coupling exemplified in the total synthesis of gymnocin A

Schreiber *et al.* used inter- and intramolecular Sonogashira reactions to prepare the core structure of dynemicin A (Scheme 4).[35, 36, 37, 38] The potential viability of two different strategies to prepare the putative macrocyclic transannular Diels–Alder precursor **4B** was investigated. In the first of these, it was proposed that the macrocyclic ring could be generated via a terminal alkyne and the bromide-bearing vinyl carbon atom in ester **3A** through a Sonogashira coupling reaction (Scheme 4). Surprisingly, when ester **4A** was treated under Sonogashira conditions in toluene, it was found that the Diels–Alder cycloadduct **4C** was formed as a single stereoisomer in 25 % yield, via a transient intermediate of macrocycle **4B**. The second approach made use of an intermolecular Sonogashira coupling between enediyne **4D** and bromoacrylate **4E**, followed by basic ester hydrolysis, to generate the corresponding polyunsaturated carboxylic acid with retention of the alkene geometry. When the acid was subjected[39] to a Yamaguchi macrocyclisation protocol, cyclisation gave a lactone **4B** which spontaneously participated in a transannular Diels–Alder reaction at room temperature to give **4C**. Such cascade processes serve to highlight the utility and potential of the Sonogashira reaction in generating molecular complexity.

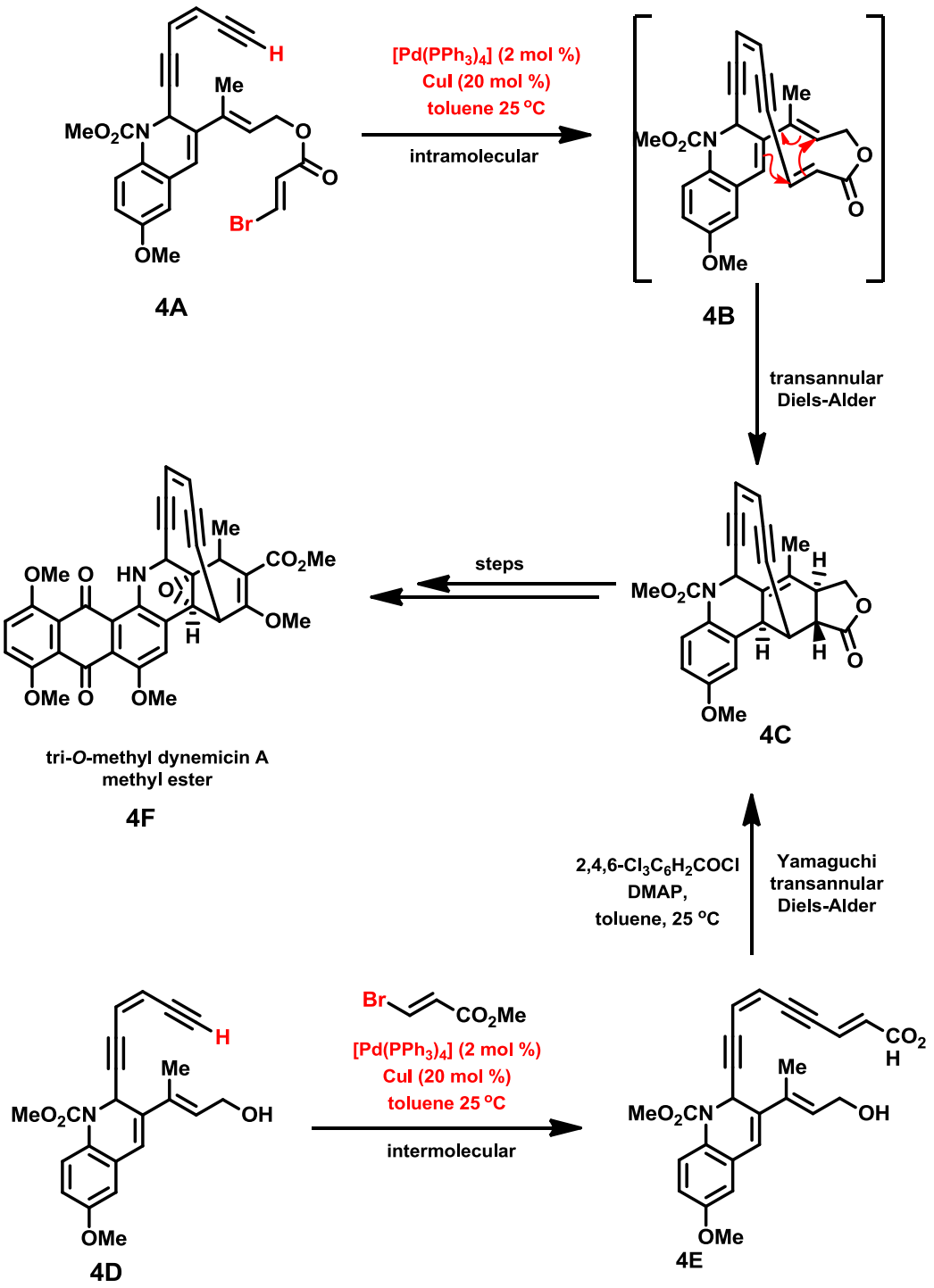

Scheme 4 Different uses of the Sonogashira coupling in cascade reactions *en route* to dynemicin A

3.1.3 C-H bond activation methodologies

Pd-catalysed C–H activation/C–C bond forming reactions excel as promising new catalytic transformations; however, development in this field is still at an early stage compared to the state-of-the-art in classical cross-coupling reactions using aryl and alkyl halides (note: involving two substrates which are both preactivated by functional groups). Direct arylation reactions *via* C–H bond functionalisation has become economically attractive (Figure 2), although one should bear in mind the formation of stoichiometric side-products, which are not necessarily green.[40]

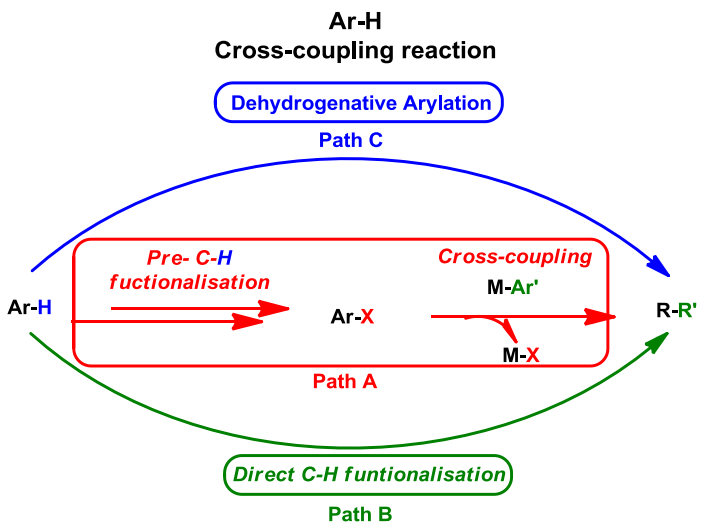

Figure 2 Classical vs modern pathways for metal-catalysed C-H bond functionalisation

There are typically four modes of activation for forming C–C or C–O bonds from C–H bonds at Pd. They use various redox couples, *e.g.* $Pd^{(II)/(0)}$, $Pd^{(II)/(IV)}$, $Pd^{(0)/(II)/(IV)}$ and $Pd^{(II)/(III)}$.[11, 13] Each catalytic manifold offers something quite different – Pd^{IV} is hard, whereas Pd^{0} is soft. Pd^{II} can be hard or soft, although is usually consider harder than soft. Pd^{III} is usually seen in bimetallic species and is likely hard too.

Chapter two of this thesis focuses on the synthesis of Pd^{II}-nitrito complexes, which are of potential significance in C-H bond functionalisation. Indeed, nitrite linkage isomerisation and associated ligand effects, *e.g.* Pd–NO_2 → Pd–ONO, are interesting to study.[41] This has enhanced significance, as the anionic nitrate or nitrite ligands offer potential as co-catalysts/oxidants in oxidative processes mediated by Pd^{II} salts,[11, 41] particularly when the NO_x species are redox-active under the reaction conditions (Figure 3).[42]

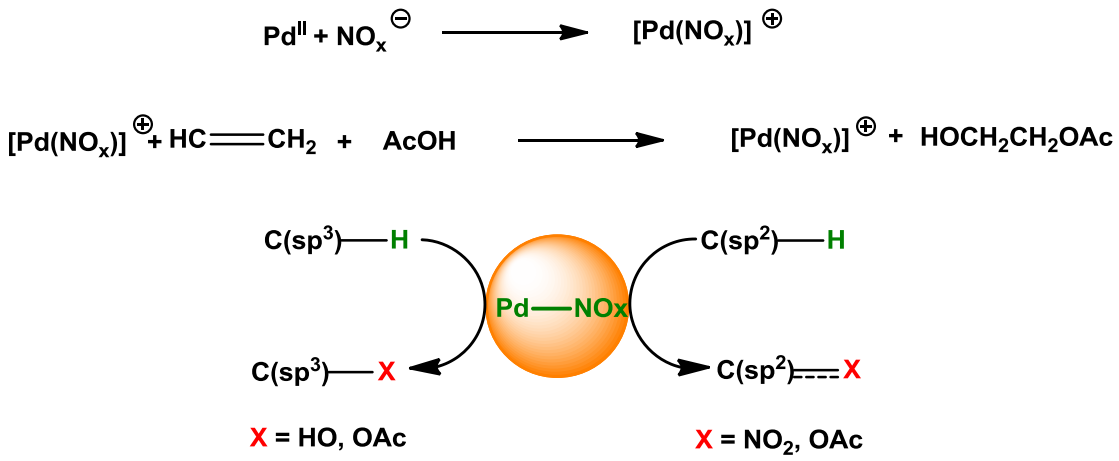

Figure 3 Synthesis methodology using NO_x with Pd

A variety of substrates containing both oxime ether- and pyridine-directing groups undergo aerobic $Pd(OAc)_2/NaNO_3$-catalysed sp^3-C–H bond acetoxylation[42] at sites adjacent to the directing group. Sanford *et al.* hypothesised that these transformations proceed via decomposition of nitrate to $NO_2(g)$, [11] which can lead to a NO_x redox cycle. They reported that NO_2 and 2 equiv. of AcOH react with a cyclopalladated intermediate to form Pd^{II} along with NO and H_2O.[43] This is followed by carbon–oxygen bond-formation *via* reductive elimination, with the NO being oxidized by O_2 to regenerate NO_2.[44, 45] Sanford proposed that generation of NO is a key intermediate in this reaction (Scheme 5).

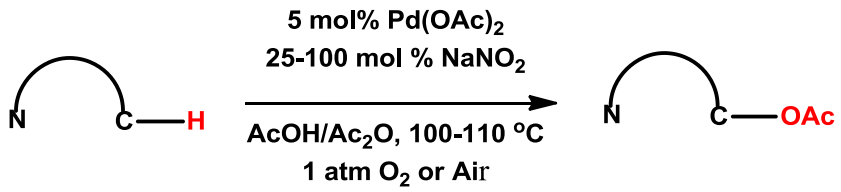

Scheme 5 C–H bond acetoxylation reaction reported by Sanford *et al.*

Pd–NO_2 coordination and "Pd–NO_2"→"Pd–ONO" linkage isomerisation has been investigated within the Fairlamb group in York (Scheme 6),[41] although other examples are known.[11]

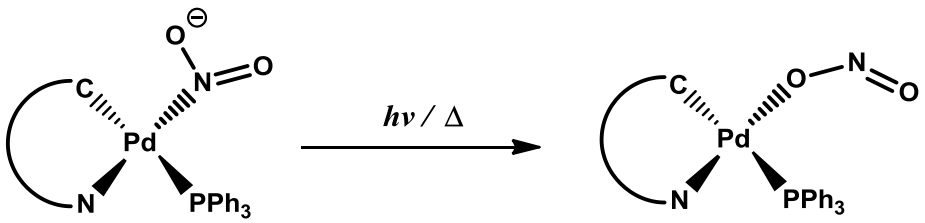

Scheme 6 Linkage isomerisation in a palladacycle containing a Pd^{II} centre.

Previously a complex, $Pd(OAc)_2(pip)_2$ (where pip = piperidine), was synthesised within the group.[41] The synthesis of this complex was accompanied by the surprising formation of $Pd(OAc)(NO_2)(pip)_2$, which also proved to be catalytically competent.[41] The source of the NO_2 then was a mystery in this chemistry, but further investigation revealed that NO_2 ligand came from a nitrite impurity found in commercial batches of $Pd(OAc)_2$, which was able to replace one of the acetate ligands in $Pd_3(OAc)_6$ giving $Pd_3(OAc)_5NO_2$ (Scheme 7).[46] The impurity arises from the synthesis: Pd + $4HNO_3 \rightarrow Pd(NO_3)_2 + 2NO_2 + 2H_2O$ and $Pd(NO_3)_2 + 2CH_3COOH \rightarrow Pd(OAc)_2 + 2HNO_3$.[41, 42]

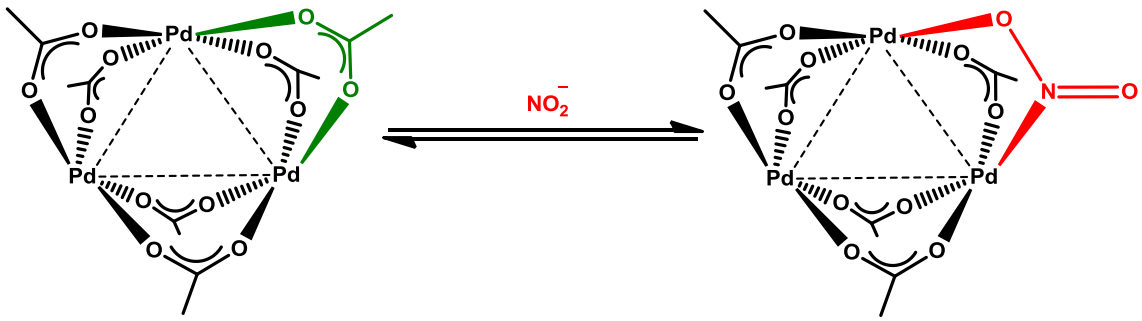

Scheme 7 Nitrite adduct of $[Pd_3(OAc)_5NO_2]$.

The nitrite anion replaced one acetate anion bridging ligand between two Pd atoms; a similar process was reported by Murillo *et al.*,[46] in which one acetate bridging ligand was replaced by H_2O from the wet $CDCl_3$ solvent used (Scheme 8).[46]

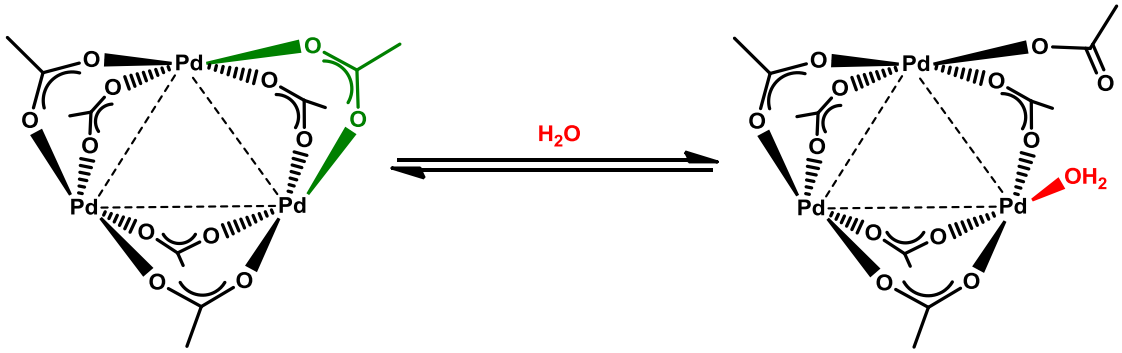

Scheme 8 Water adduct of $[Pd_3(OAc)_6 \cdot H_2O]$

It is not obvious that the hydrolysis is consistent with the well-established reactivity of $Pd_3(OAc)_6$ toward ligands such phosphines and arsines,[47] but recent work has shown that alcoholic solvents have a profound effect in a similar way to water.[48]

3.2 Mn-catalysed cross-coupling processes

3.2.1 Mn catalysed cross-coupling with organolithium and Grignard reagents

Manganese was first used as a catalyst for cross-coupling reactions by Cahiez, Normant in 1976.[49] They found that the homo-coupling of alkenyl lithium reagents

(generated *in situ* from alkenyl iodides and *n*-BuLi), gave conjugated 1,3-dienes with excellent *E*-selectivity and high yield (Scheme 9)

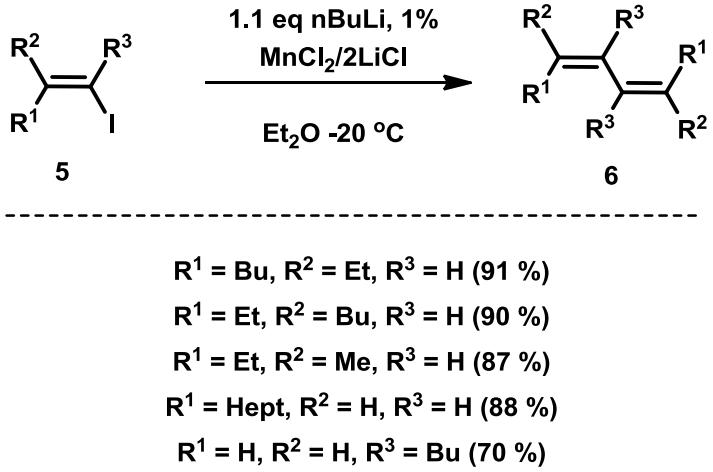

Scheme 9 $MnCl_2$/2LiCl-catalyzed homocoupling of alkenyllithium derivatives

The reaction is catalysed by simple $MnCl_2$ or $MnBr_2$, but for preparative purposes, they utilised $MnCl_2$/2LiCl was initialised. Their choice of ether as a solvent was crucial since more polar solvents like THF favour an undesirable alkylation of alkenyl iodides with *n*-BuLi, even in the absence of the manganese catalyst.[50] Daugulis reported the application of a similar[51] synthetic protocol in the dimerisation of aryl and heteroaryl Grignard reagents generated[52] *in situ* upon aromatic deprotonation with the super-base[51] TMPMgCl/LiCl. The coupling of activated alkyl Grignard reagents can also be achieved with higher catalyst loadings;[51-55] but the reaction suffers poor chemoselectivity[52] (Scheme 10).

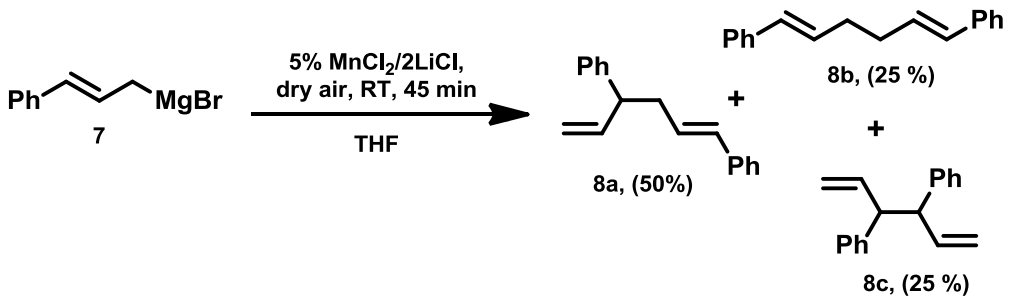

Scheme 10 $MnCl_2$-catalysed homocoupling of Grignard reagents with low chemoselectivity

3.2.2 Cross-coupling processes leading to carbon-heteroatom bond formation

Mn-based catalysis can be effective for the amination of aryl and heteroaryl halides **9** with a broad variety[56-59] of nucleophiles, *e.g.* benzamide **10** (Scheme 11). The reactions work well in water, while in other polar (DMF, DMSO, THF, MeCN) or apolar (toluene) solvents, the yields were considerably lower.

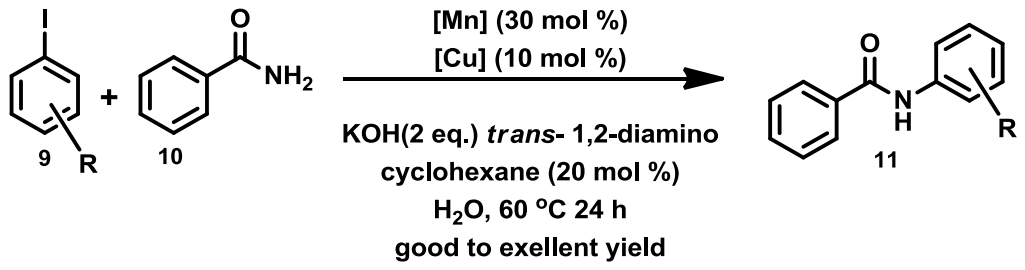

Scheme 11 Mn/Cu catalytic systems for the N-arylation of benzamide in H_2O

The presence of a chelating diamine ligand is crucial for the success of the reaction using MnF_2 (20 mol%) or a mixed MnF_2 (20 mol%)/ CuI (10 mol%) catalyst system. For nucleophilic heterocyclic amines such as pyrazoles, indazole and 7- azaindole, the reaction can be performed using $MnCl_2$,[58] whereas for less nucleophilic amines and amides the catalytic system based on MnF_2 provides the best results.[56, 57,56, 60] Aryl bromides such as PhBr, *m*-ArBr, and *p*-ArBr can be coupled as well, giving similar product yields as their iodide counterparts.

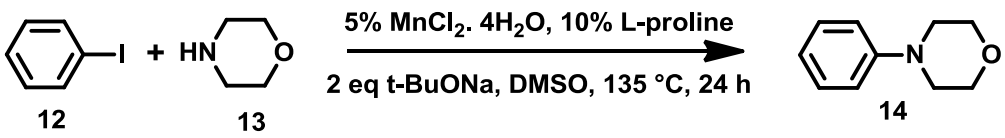

Scheme 12 Mn-catalysed amination of aryl iodides with aliphatic amines

3.2.3 Mn-catalysed carbonylation reactions

Calderazzo reported a Mn-catalysed reaction of amines[61] to give ureas and hydrogen, at high temperature and high CO pressure (Scheme 13). Both $Mn_2(CO)_{10}$ and $MnMe(CO)_5$, are equally effective catalysts in heptane, showing TONs of 94 and 102 respectively.[61]

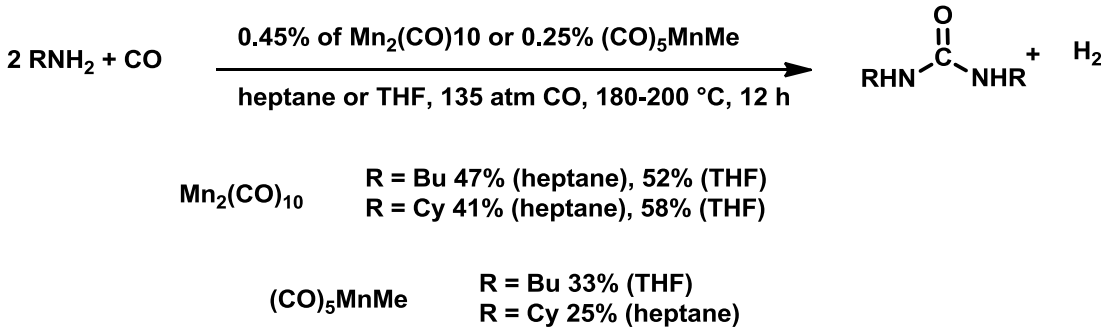

Scheme 13 Mn-catalyzed dehydrogenative carbonylation of primary alkylamines

The most important example involves the methylene moiety of a *β*-ketoester. The reaction of these substrates types affords 2-pyranones (2-pyrones)[62-64] in good yields, instead of the expected tetra-substituted arenes (Scheme 14). The reaction was found to work well for aryl- and alkenyl-substituted terminal alkynes.[65]

The proposed catalytic cycle begins with complex **A** bearing both the coordinated alkyne and enol form of the *β*-ketoester (Scheme 14). It then rearranges intramolecularly to metallacyclopentene **B**, which undergoes a reductive elimination

liberating cyclobutenol **C** and regenerating **A**. The cyclobutenol **C** undergoes a ring-opening rearrangement to give δ-ketoester **E**, followed by a sequence of base-catalysed double bond migrations, deprotonation of **F** and intramolecular cyclisation of enolate **G** to give 2-pyranone **H**.

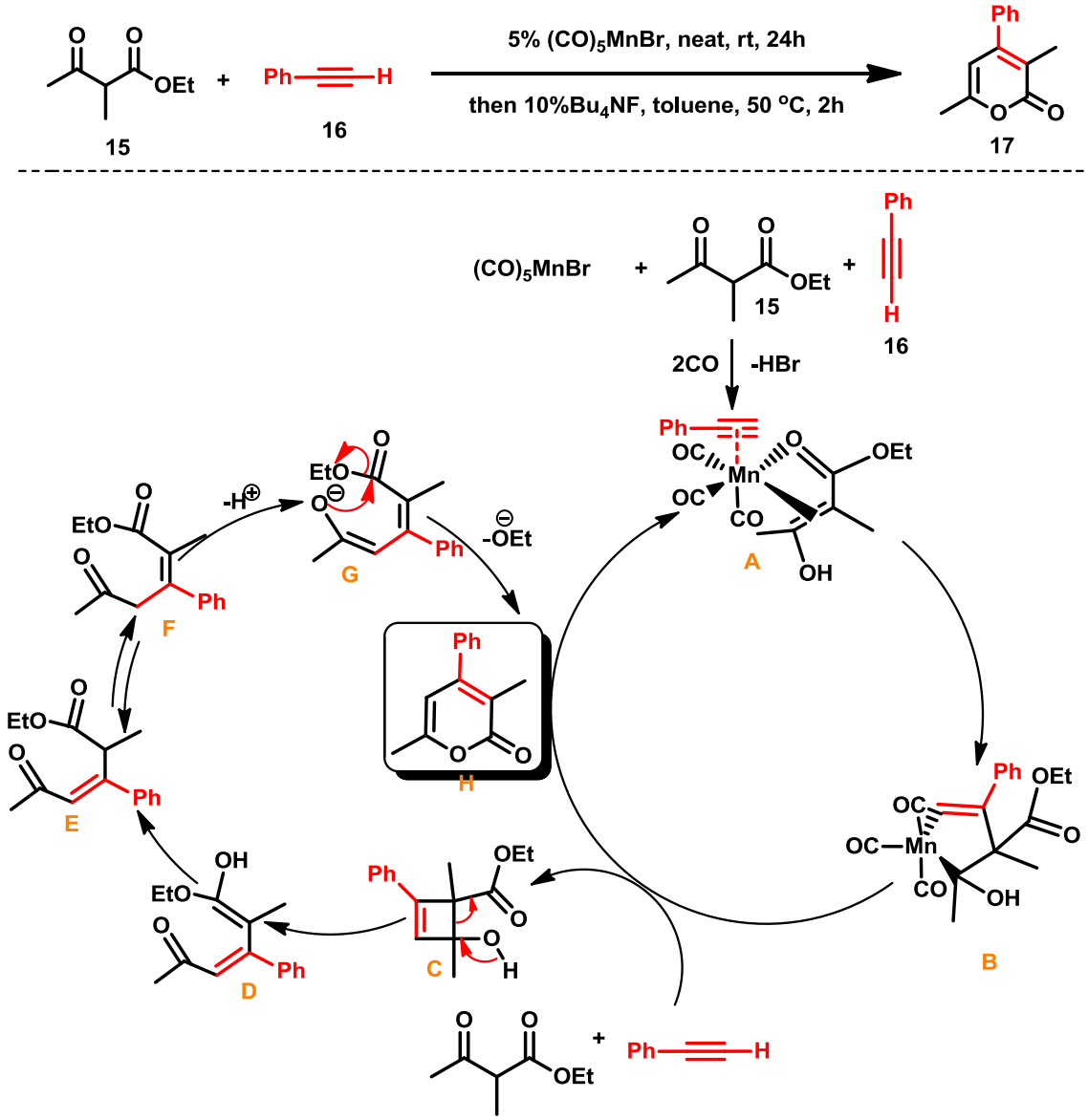

Scheme 14 Proposed mechanism for Mn-catalysed formation of 2-pyrones

3.2.4 Mn-catalysed C–H bond activation processes

Hartwig *et al.*[66] reported the catalytic C–H bond activation reaction based on an organometallic manganese complex. The study consisted of a borylation of pentane and benzene with PinB–BPin, promoted by $Cp'Mn(CO)_3$ (10%) at RT under UV irradiation and in the presence of CO (2 atm) to give PentBPin, and PhBPin in 36%, and 76% yields respectively. Later, Kuninobu,[67, 68] reported the catalytic C–H activation of phenyl and alkenyl moieties bearing a directing nitrogen donor group, in the presence of an aldehyde and tertiary silane. The imidazole and imidazoline moieties were good directing groups, giving excellent yields of the silyl ethers products. Interestingly, $Mn_2(CO)_{10}$ and $MnMe(CO)_5$ exhibited the same efficiency as $MnBr(CO)_5$. More recently it was shown by Chen and Wang[69] that $MnBr(CO)_5$ induces the selective insertion of terminal alkynes into the C–H bond of *ortho*-phenylpyridines, in the presence of co-catalytic Cy_2NH (Scheme 15). Terminal alkynes are considered as tricky reaction partners in C–H alkenylation reactions, due to their tendency to undergo competitive cyclotrimerisation to give arenes. Here, the reaction shows good scope and provides alkenylated products in moderate to good yield, with excellent chemo- and stereoselectivity. When two *ortho* C–H bonds are available, typically the less hindered site is activated selectively.

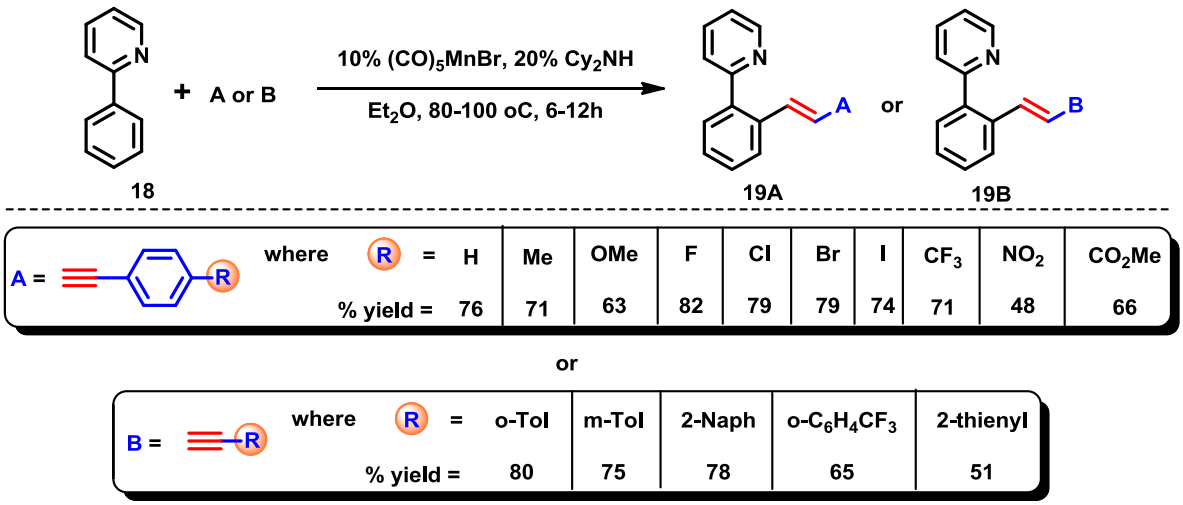

Scheme 15 Mn-catalysed aromatic C–H bond alkenylation using terminal alkynes

The work by Chen and Wang led our research group to investigate the use of the electron-deficient 2-pyrone ring, containing a pyridyl directing group at the 4-positions. In this context, chapter three will give details about this work, involving C-H alkenylation reactions of a 2-pyrone derivative containing a 2-pyridyl directing-group at Mn^{I}, including a plethora of other types of chemistry.

3.3 Introduction to Pauson-Khand reaction

Ihsan Ullah Khand (1935-1980), working as a postdoctoral associate with Peter L. Pauson,[70] first reported the Pauson-Khand Reaction (PKR) in 1973.[71] The reaction consists of a transition metal-catalysed [2+2+1] cycloaddition of an alkene, alkyne and carbon monoxide to give cyclopentenone (Scheme 16).[70-73]

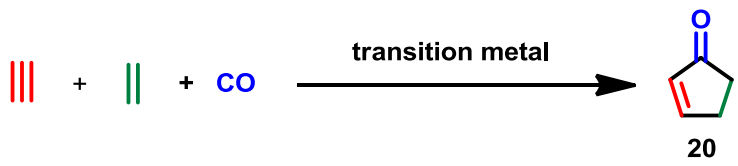

Scheme 16 Transition-mediated Pauson-Khand reaction

The cyclopentenone ring is an important structural unit found in natural products and pharmaceuticals.[74, 75] This one-pot reaction, which can be both intermolecular and intramolecular, can display regiochemical preferences, depending on the substituents on the alkene and alkyne substrates. Despite the successes of the intramolecular PKR,[71] the intermolecular PKR suffers from less predictable regioselectivity, especially in new substrates (Scheme 17). Here, unsymmetrical alkynes and alkenes give rise to various regioisomeric products. The link to the work described within this thesis examines intermolecular PKRs and the regiochemical outcome specifically.

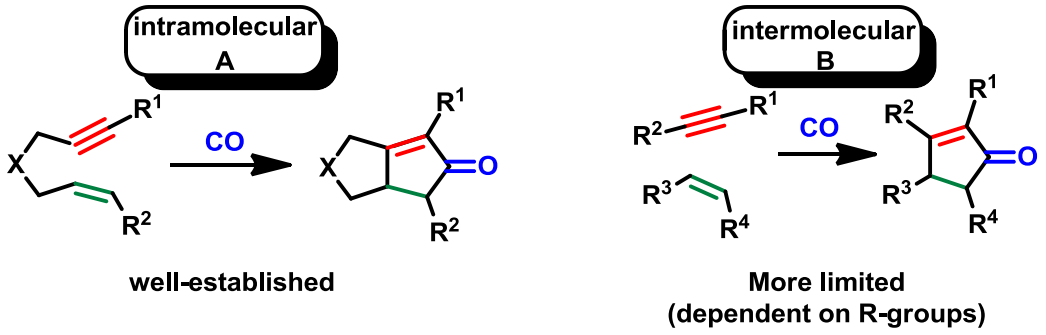

Scheme 17 Cobalt-mediated Pauson-Khand reactions

The PKR reaction was first mediated by cobalt and this is still the most common transition metal used; however, PKRs can also be mediated with rhodium[76], iridium[77], iron[78, 79], chromium[80], molybdenum[81, 82], tungsten[83, 84] and palladium[85, 86]. This thesis focuses on intermolecular Co^0-mediated reactions, as there are interesting regiochemical observations that require more detailed understanding.

3.3.1 Mechanism of Pauson-Khand reaction

The general PKR mechanism starts with the formation of a stable alkyne-cobalt complex **I**. A pentacarbonyl complex forms via a vacant coordination site, loses one

CO ligand in a reversible step which gives **II**. The free site reversibly occupied by coordination of an alkene (Scheme 18), followed by the regiochemical determining step through the cobaltacycle where alkene insertion occurs between cobalt and the original alkyne carbon, forming a five-membered ring **IV**. Then, carbonyl insertion into the bond between the former alkene and the cobalt gives **V**. The next step is reductive elimination, in which a bond is formed between the carbonyl carbon and the other end of the alkyne, so that five-membered carbocycle is formed **VI**. The final step is decomplexation of the weakly-bonded cyclopentenone-cobalt complex, after which the PKR is complete. Several key intermediates were characterised within the literature by IR, UV and NMR, *e.g.* **II**[87-90], **III**[91-93] and **IV**[94].

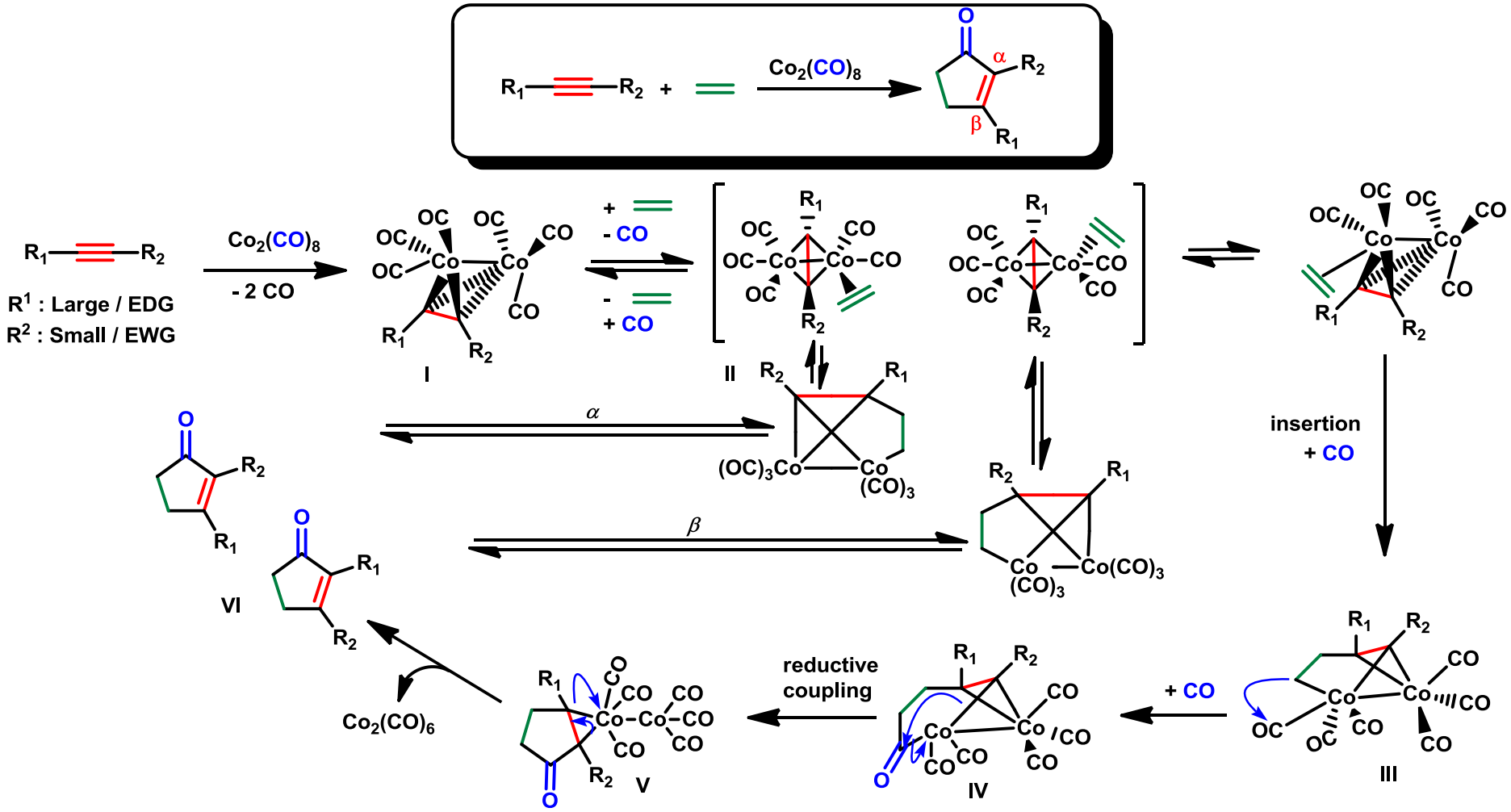

Scheme 18 Magnus's Mechanism for the intermolecular PKR

The mechanism originally proposed by Magnus was based on general organometallic knowledge,[95, 96] and supported by theoretical studies by Nakamura (Figure 4),[97] although the purpose of Magnus's hypothesis was to explain the observed stereoselectivity of certain intramolecular reactions. Nevertheless, it fits well with other experimental findings.

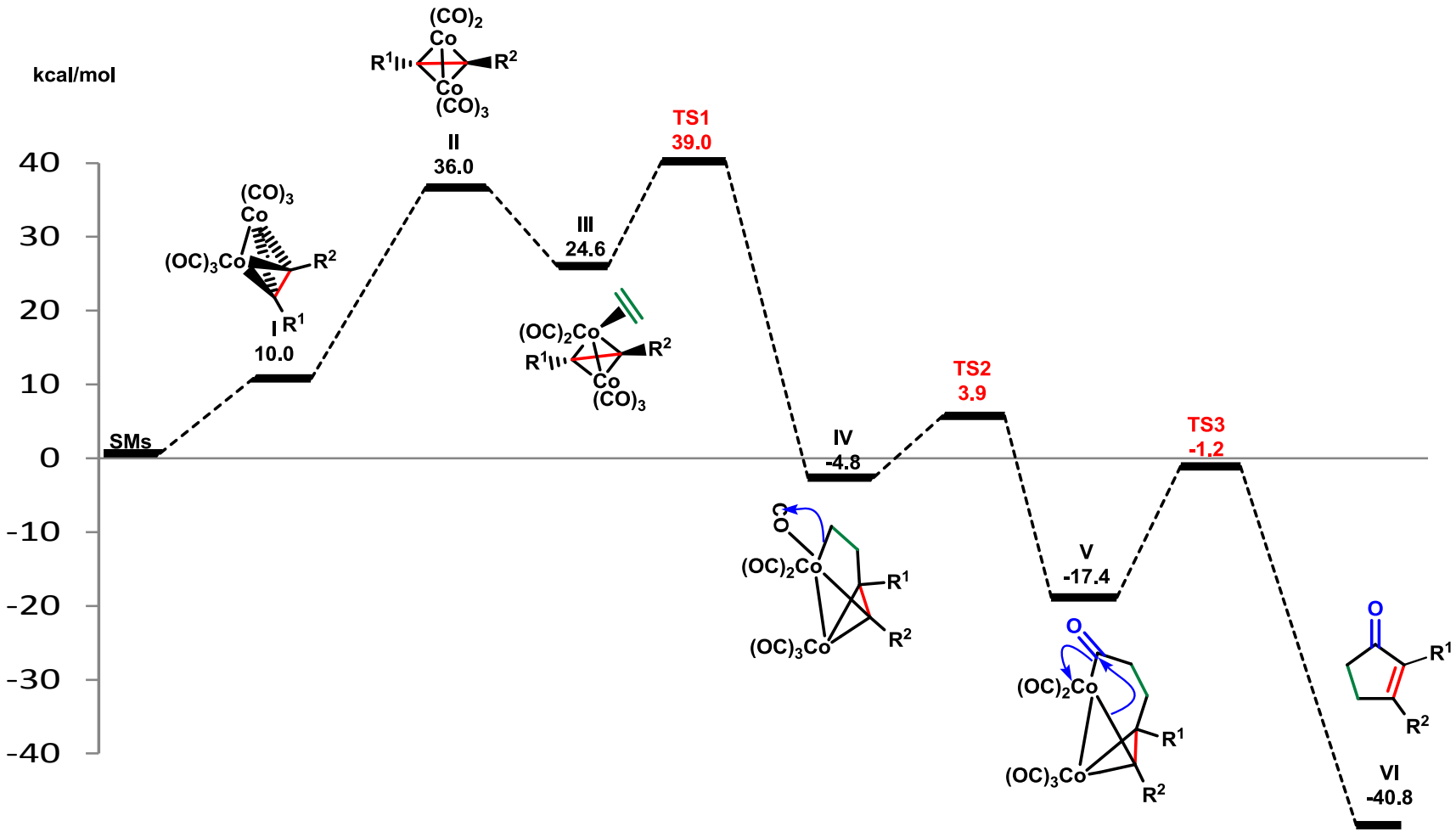

Figure 4. Nakamura's calculated of Energies in PKR using DFT methods. These values were for acetylene as an alkyne and ethene as an alkene

3.3.2 Regioselectivity in the Pauson-Khand reaction

A total of four different isomeric products are possible in the PKR – two are related to the alkyne regioselectivity (R^1 and R^2) in Scheme 19, and two to the alkene regioselectivity, giving four regioisomers (racemic) in total (Figure 5). The number of possible stereoisomers is limited to two in this reaction mechanism, the alkene stereochemistry is significant, one alkene stereo-centre was used for clarity of the mechanism to show how alkene insertion plays a vital role in controlling selectivity.

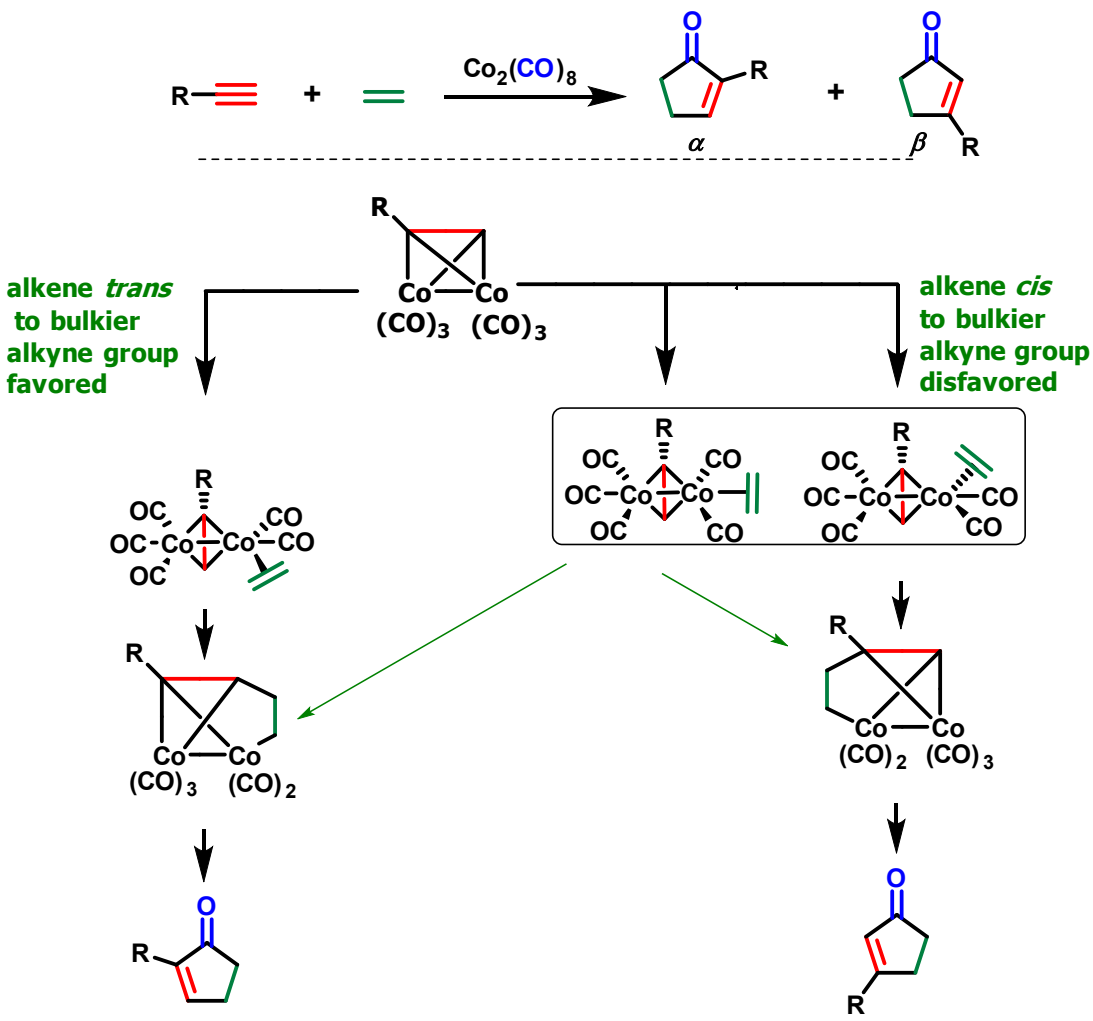

Figure 5 PKR regioselectivity regarding alkene insertion vs. steric effect

The alkene substituents R^3 and R^4 (Scheme 19) are on the same side of the ring. Choosing a symmetrical alkene starting material limits the possible isomeric products. However, regioselectivity is often a problem for synthetic applications of PKR and a great effort has gone into predicting and controlling the selectivity (Scheme 19). The regio and stereochemical outcome of the intermolecular PKR are substrate-controlled. The intermolecular reaction has been less exploited, mainly because of the small range of reactive alkene partners (Scheme 19).[98]

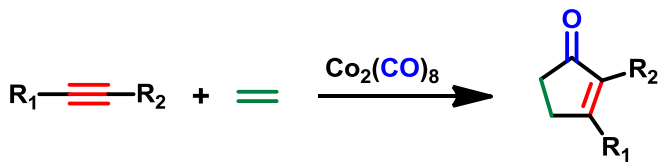

Scheme 19 Intermolecular Pauson-Khand reaction

3.3.3 Significance of alkene regioselectivity in intermolecular PKRs

Gimbert and co-workers' study, examining the reactivity of alkenes in the intermolecular PKR,[98, 99] showed good reactivity for cyclohexene, cyclopentene and norbornene towards the intermediate hexacarbonyldicobalt(0) complex of 1-propyne. The reactivity of the alkenes is related to the extent of π-back donation of electrons from the d orbitals of the cobalt atom to the π*-orbital of the alkene (Figure 6).

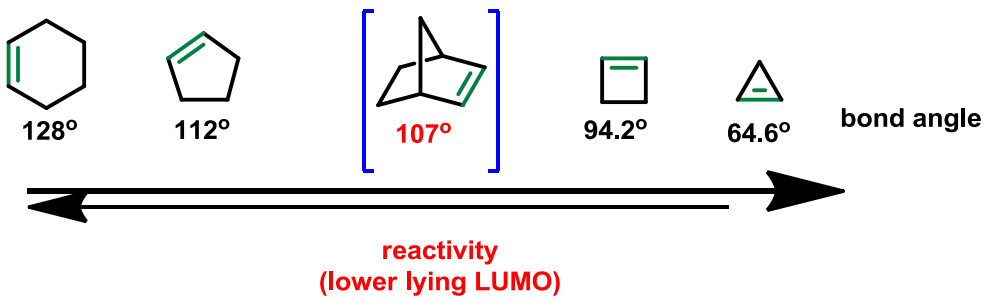

Figure 6 Alkene reactivity in the intermolecular PKR

The favourable back-donation from Co^0 to the alkene is due to the highest energy occupied molecular orbital and lowest energy unoccupied molecular orbital interaction (HOMO-LUMO interaction) respectively. The greater the back-donation, the higher the reactivity – a low energy LUMO gives rise to a lower energy barrier for PKRs.[98, 99] The frontier-leading molecular orbitals are shown for the simplest alkene in Figure 7.

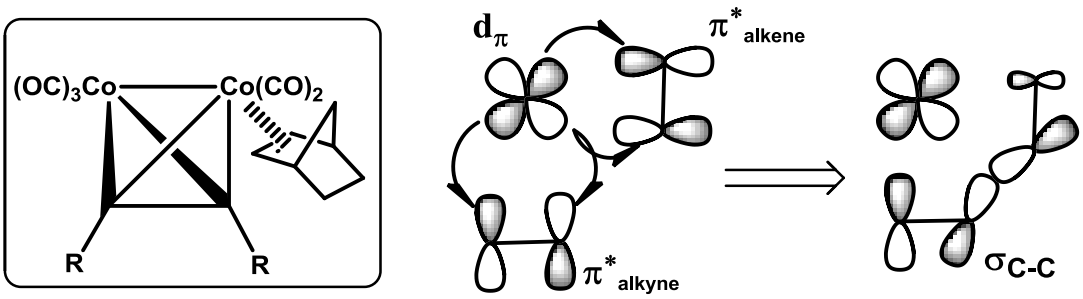

Figure 7 HOMO-LUMO orbital interaction of a transition metal d-orbital with ethene [99]

An important property of the ethene molecule, and alkenes in general, is the existence of a high barrier to rotation about the C=C bond.

3.3.4 Competition between steric and electronic factors

The reported regiochemistry in a number of different systems is a complex issue, especially for intermolecular PKR. The dividing line between complete selectivity and non-selective reaction can be quite thin, depending on four variables: alkene reactivity, alkyne chemical structure (steric *vs.* electronic), CO insertion and the metal used (relating to π-back donation). Several research groups have been aiming to address these issues.[100-107] As can be seen from Scheme 20 and Scheme 21, the electron-withdrawing ester group typically occupies the β-position in products employing internal disubstituted alkynes.[107]

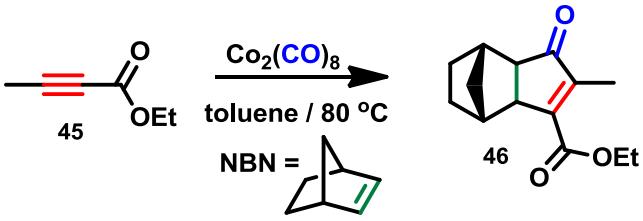

Scheme 20 Norbornene effect on the regioselectivity which is completely selective, despite the sterically hindered group (example 1)

If the methyl group is changed to a strongly electron-withdrawing and sterically similar trifluoromethyl group (Scheme 21), the reaction outcome still remains the same.[108] For electronic reasons the trifluoromethyl might prefer the β-position. However, the electron-withdrawing ester group (by mesomeric effects) again prefers to go into the β-position, placing the electron-withdrawing CF_3 group (by inductive effects) into the α-position (Scheme 21).

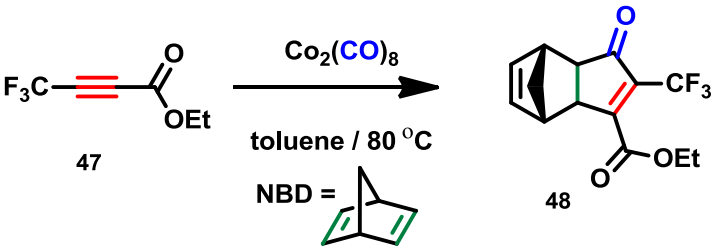

Scheme 21 Norbornene effect on the regioselectivity which is completely selective, despite the sterically hindered group (example 2)

Riera *et al.*[107] have run a series of experiments (Scheme 22), varying the alkyne substituents. In reactions with NBD, the reaction was completely regioselective giving the product with a trifluoromethyl group in the α-position. On the other hand, Konno *et al.*[106] reported another set of experiments, where regioisomeric mixtures of cyclopentenones α- and β-products formed. The reaction conditions for both experiments were close to each other, the main differences being the alkenes and solvents used (NBD vs. NBN and toluene vs. DCE, respectively) and the

temperature (70 °C vs. 84 °C). The reason for this unexpected difference in results is not obvious, but it might indicate that the more reactive NBD is, for some reason, affecting the regioselectivity outcome than NBN. This may be due to mono- versus bi-dentate coordination of NBN and NBD to Co^0 respectively.

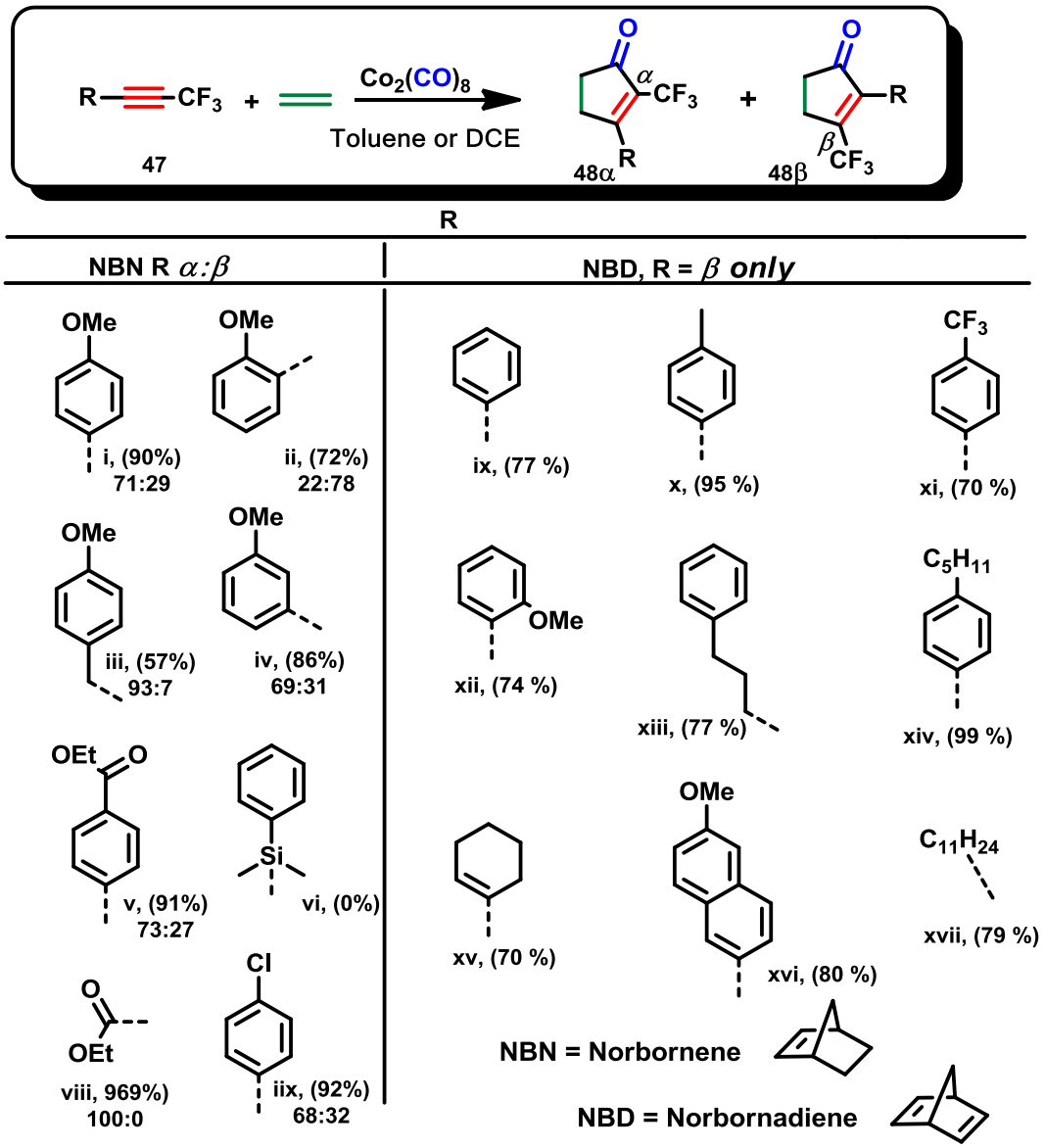

Scheme 22 Summary of two reported studies probing the effect of alkene substituents in reactions of trifluoromethyl-substituted internal alkynes with norbornene and norbornadien.

3.3.5 Regiochemistry determination with sterically near-equivalent alkynes

The examples above showcase the competition between steric and electronic factors and how they influence regiochemistry – clearly it is difficult to predict. In order to gain more information about the electronics guidance, the steric effect has to be minimised. A few studies with sterically equivalent or near-equivalent diarylalkynes have been reported. For example, Fairlamb *et al.*[104, 105, 109] reported PKRs of heteroaromatic diarylalkynes, with interesting results. To be critical, these results could not be fully explained by the electronic properties of the alkynes alone. The alkynes were classified by the types of heteroaromatics tested, *e.g.* as π-deficient (**iv-ix**, Scheme 23) or π-excessive (**i-iii** and **x-xii**, Scheme 23). All π-deficient heteroaromatics preferred the β-position, but results varied with alkynes having π-excessive substituents. It was suggested that, aside from steric and electronic effects, that dynamic ligand effects and stabilisation provided by the aromatic or heteroaromatic group might subtly influence the regiochemical outcome of intermolecular PKR. This will be elaborated upon within Chapter 4.

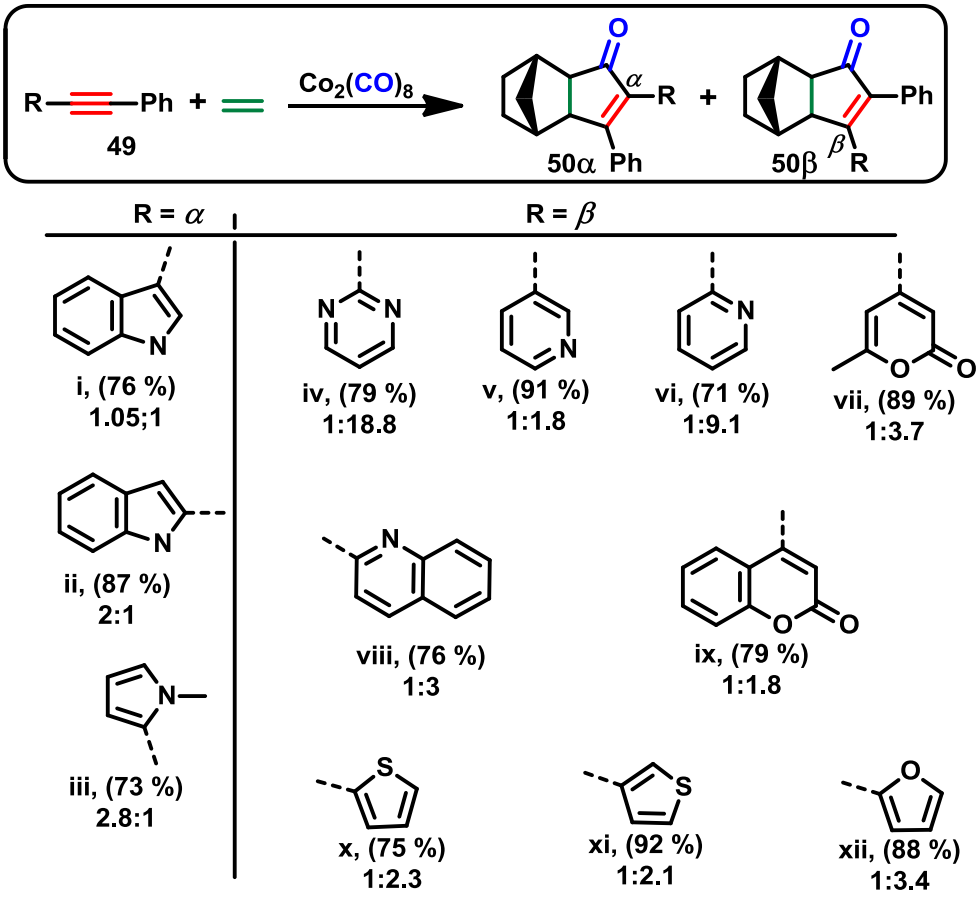

Scheme 23 PKRs of heteroaromatic diarylalkynes reported by Fairlamb *et al.*[105]

Gimbert[103] led a computational DFT study on the alkyne-dicobalt hexacarbonyl complexes[103] to probe whether electronic differences in the acetylenic substituents could affect the regiochemistry of the PKR (Scheme 24). This provides an alternative to the "steric effect" for mechanistic interpretation of this important aspect of the PKR. For example, the ethyl benzoate group was found exclusively in the β-position of the newly-formed cyclopentenone.[58] The dichotomy between steric *vs*. electronic effects is still a subject of debate, which makes regiochemical predictions still difficult.

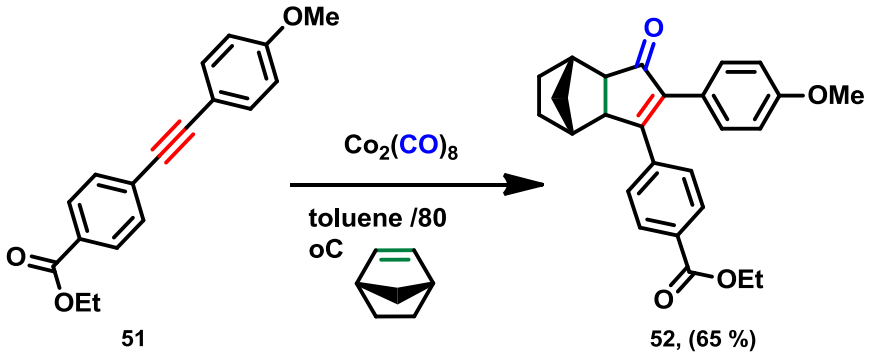

Scheme 24 Formation of one regioisomeric product.

3.4 PKR/6π-electrocyclisation/aromatisation reactions

Electrocyclisation, a subclass of pericyclic reactions, enable the formation of a ring system from an open-chain conjugated system, [110] with a σ-bond forming across the ends of a conjugated system on both sides.[111] Intramolecular 6π-electrocyclisation of the PKR product of various heteroaromatic systems provided the stimulus for this part of the project (Scheme 25).[104]

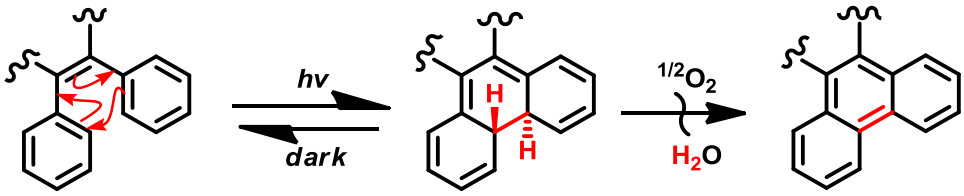

Scheme 25 6π-electrocyclisation/oxidative aromatisation reaction

Electrocyclisation reactions[109] can occur thermally or photochemically, *via* two possible modes known as *conrotatory* and *disrotatory*. The simplest examples of photochemical electrocyclisation are illustrated in Scheme 25.

3.4.1 Examples of orbital symmetry and torquoselectivity in 6π–electrocyclisations

The Woodward–Hoffman rules were put forth over a series of publications in 1965, the first of which concerned itself with the stereochemistry of electrocyclic reactions, and the landmark synthesis of vitamin B_{12}.[110] Orbital symmetry rules state that the ground state of the HOMO controls the key bond forming steps of the reaction, thus the terminal substituents during a thermal 6π-electrocyclic reaction move in a disrotatory manner (Scheme 26).[112]

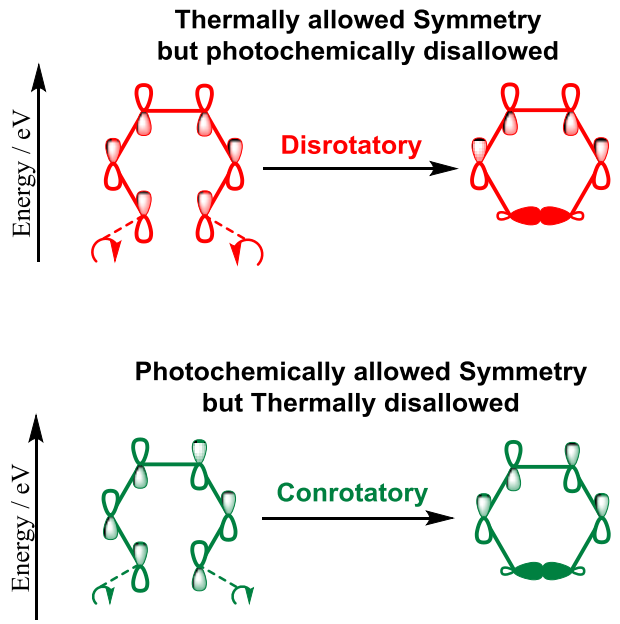

Scheme 26 Thermal vs photochemical induced cyclisation

Orbital symmetry rules predict that the thermal 6π-electrocyclisation is disrotatory, while the photochemical process is conrotatory (Scheme 26); thus two modes of disrotation exist for all thermal 6π-electrocyclisations.[111]

3.5 Project Aims and Objectives

3.5.1 Aims

The focus of the thesis is split principally into three parts. The first aim is to synthesise Pd^{II}-nitrito compounds, which are of potential relevance to catalytic C–H bond functionalisation reactions. The second aim is to examine Mn-mediated C–H bond alkenylation of substrates containing a 2-pyrone moiety with a pyridyl directing group. The third aim of the project is to further examine the regioselectivity in selected intermolecular Co-mediated PKRs (PKR). A follow-on aim is to examine the light-induced 6π-electrocyclisation/oxidative aromatisation reactions of the PKR cycloadducts. A common thread throughout the whole thesis is the use of 2-pyrone ring systems and pyridyl directing groups, and their reactions and coordination to Mn, Co and Pd.

3.5.2 Objectives

The following objectives underpin the content of this thesis:

I. To examine the reactivity of directed C–H bond activation by reaction of $Pd(OAc)_2$ with 2-benzyl- and 2-phenyl-pyridines (Chapter 2).

II. Prepare and characterise palladacyclic complexes containing NO_2 ligands and establish nitrite linkage isomerisation at Pd^{II} (Chapter 2).

III. To study the reactivity of a 2-pyrone-containing pyridyl group as a substrate for Mn-mediated C–H bond functionalisation (Chapter 3).

IV. To examine secondary reactions from Mn-mediated C–H bond functionalisation processes, *e.g.* pyridyl fragmentation and Diels-Alder reactions of the 2-pyrone derivatives (Chapter 3).

V. To examine the regioselectivity in Co-mediated intermolecular PKRs, specifically the role of a pyridyl moiety and related heteroaromatic ring systems (Chapter 4).

VI. Investigate the 6π-electrocyclisation/aromatisation of PKR cycloadducts mediated by light (400 nm) and air (Chapter 4).

Chapter 2: Synthesis and Characterisation of Cyclopalladated C^N Complexes

4.1 Introduction

Most Pd-catalysed mediated cross-coupling reactions require pre-functionalised carbon atoms in the organic substrate.[13] These functional groups are usually halogens or oxygen-containing (Scheme 27),[14] the challenge for direct C–H functionalisation is site-selectivity as there are usually many different C–H bonds in a single organic molecule. For this purpose, Pd^{II} complexes with μ^2–acetate-bridged ligands, were prepared from 2-phenylpyridine, 2-benzylpyridine and 4-(2'-pyridyl)-6-methyl-2-pyrone, in all cases acting as the C^N ligand backbone of the cyclopalladated derivatives, *e.g.* **60**.

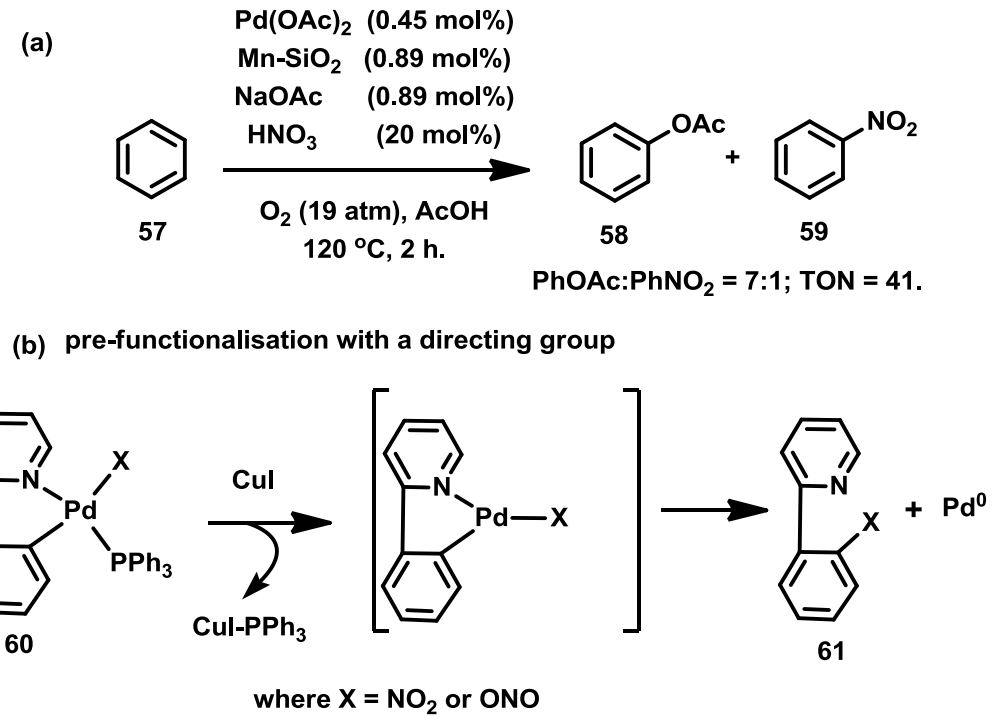

Scheme 27 Potential products from the reaction of (a) benzene with $Pd/O_2/NO_x$ and (b) $[Pd]-NO_2$ for acetoxylation/nitration[14]

The pyridyl moiety serves as a directing group for Pd to harness the challenge of directing functionality at the *ortho*-C-H bond. Two of the key aims of this chapter are to understand the effect of phosphine substituents on the regio- and linkage isomerisation of Pd–NO_2/Pd–ONO complexes – a fundamental study will pave the way for studying whether Pd–NO_2 species are present and active in oxidative C–H bond functionalisation processes.[41] If the geometry of the 'Pd(C^N)X' complexes with nitrite ligands does influence the reactivity, then their independent synthesis and characterisation could be important in defining a more specific role for the redox active ligands in catalysis. With this in mind, novel Pd^{II} complexes were prepared as part of this chapter. Also, within this chapter the effect of bulky phosphine substituents within the Pd^{II}-nitrite dimer complexes containing 2-phenylpyridine have been examined.

4.1.1 μ^2-Acetate-bridged palladacyclic complexes of 2-phenylpyridine

Pd^{II} complexes with acetate bridging ligands were prepared using 2-phenylpyridine as the C^N ligand. Cyclopalladated complexes were isolated in good yields *via* the reaction pathway shown in Scheme 28. Katsuma and co-workers[113] demonstrated that similar syntheses of cyclopalladated derivatives proceed in good to excellent yields. The μ^2-acetato-bridged dimer **62** was prepared by the reaction of 2-phenylpyridine with $Pd(OAc)_2$ in acetic acid. An NMR study suggests that both *syn*- and *anti*-geometrical isomers are formed (Figure 8).

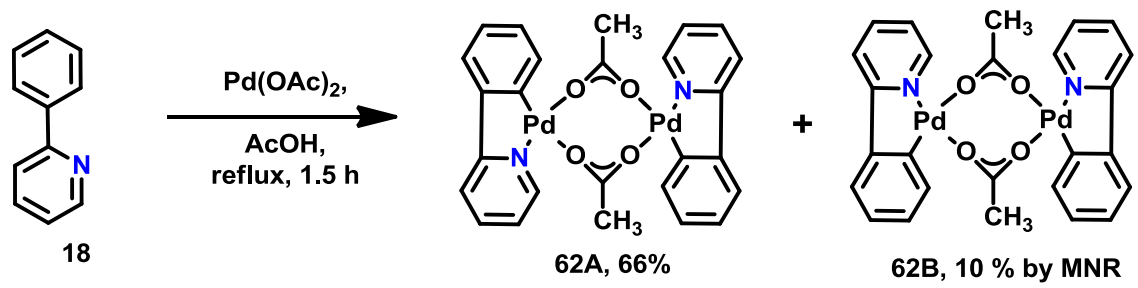

Scheme 28 Synthesis of palladacyclic complexes of 2-phenylpyridine

The *syn* and *anti*-isomers are inseparable by conventional chromatographic methods, even though isomer **62B** is only present in a small quantity; both isomers **62A** and **62B** could be catalytically competent species. This was not elaborated upon in the work reported by Sanford and co-workers, who proposed a mechanism for the acetoxylation reaction (Scheme 29).[13]

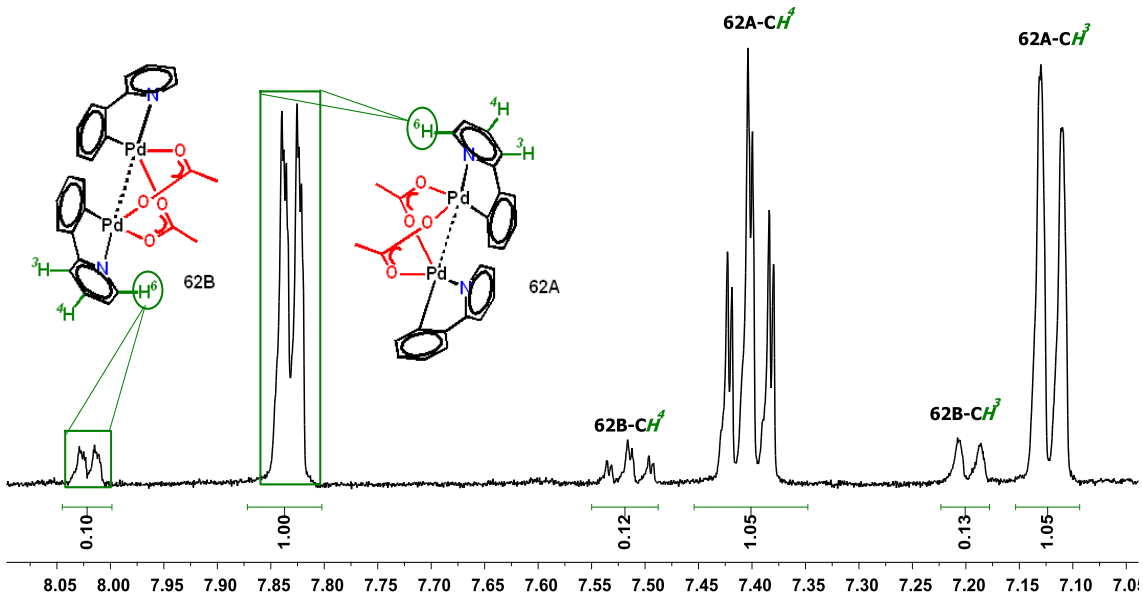

Figure 8 Aromatic region of some ^{1}H NMR spectra containing a mixture **62A** and **62B**

The ^{1}H NMR spectra shows that the pyridine ring within **62** is a useful diagnostic tool when distinguishing between **62A** and **62B** (Table 1). The proton α- to the

nitrogen atom in **62B** is deshielded by 0.15 ppm with respect to its equivalent proton in **62A**. In fact, with the exception of the phenyl moiety and methyl of the acetate bridge, all the protons of the pyridyl moiety in compound **62B** are more deshielded compared to **62A** (the proton attributes were confirmed by ^{1}H COSY). The aromatic protons within the two isomers **62A** and **62B** appear in a similar chemical shift range (6.80 - 6.95 ppm) as shown in Table 1 and Figure 8; changing from *trans* **62B** to *cis* **62A** causes an upfield shift of ca. 0.13 ppm.

Although the geometrical isomerism has no effect when **62A**/**62B** is transformed from a dimeric palladacycle in to a monomeric palladacycle, it is well established that a palladium-nitrogen (c.a Å = 1.985) bond is longer than a palladium-carbon bond (c.a Å = 1.855) in this type of C^N palladacycle system,[114] which explains why the proton chemical shifts of the pyridyl system are so diagnostic (Figure 8).

Table 1 Comparison of selected ^{1}H NMR shifts for compounds **62A** and **62B**

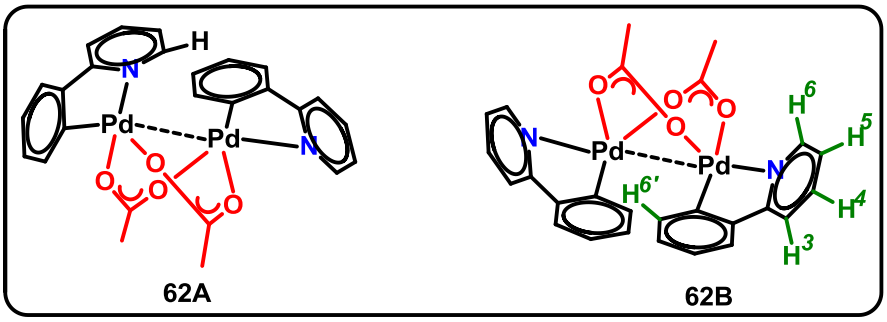

Position	Compound (**62A**) δ δ/ppm	Compound (**62B**) δ/ppm	Δ / ppm
6	7.87	8.02	0.15
4	7.37	7.51	0.14
3	7.08	7.2	0.12
6'	6.67	6.71	0.04

Note: multiplets are given by a centre point average; NMR standard is residual CD_2Cl_2.

Efficient synthetic methods have been developed for ligand-directed C–H oxygenation in identical palladacyclic complexes (Scheme 29). The transformations generally involve reaction with oxidants such as IOAc,[11] $PhI(OAc)_2$,[115] or Oxone®.[116] However, formation of stoichiometric quantities of by-products means that there is a requirement for expensive or non-commercial reagents – poor atom economy has suppressed the use of these methods in large scale production. The ideal method is the use of O_2 as the oxidant, especially from an atom economy perspective. The mechanism of Pd-catalysed C–H oxygenation, with acetate-bridging Pd species, has been explored in detail by Sanford and co-workers.[1, 6]

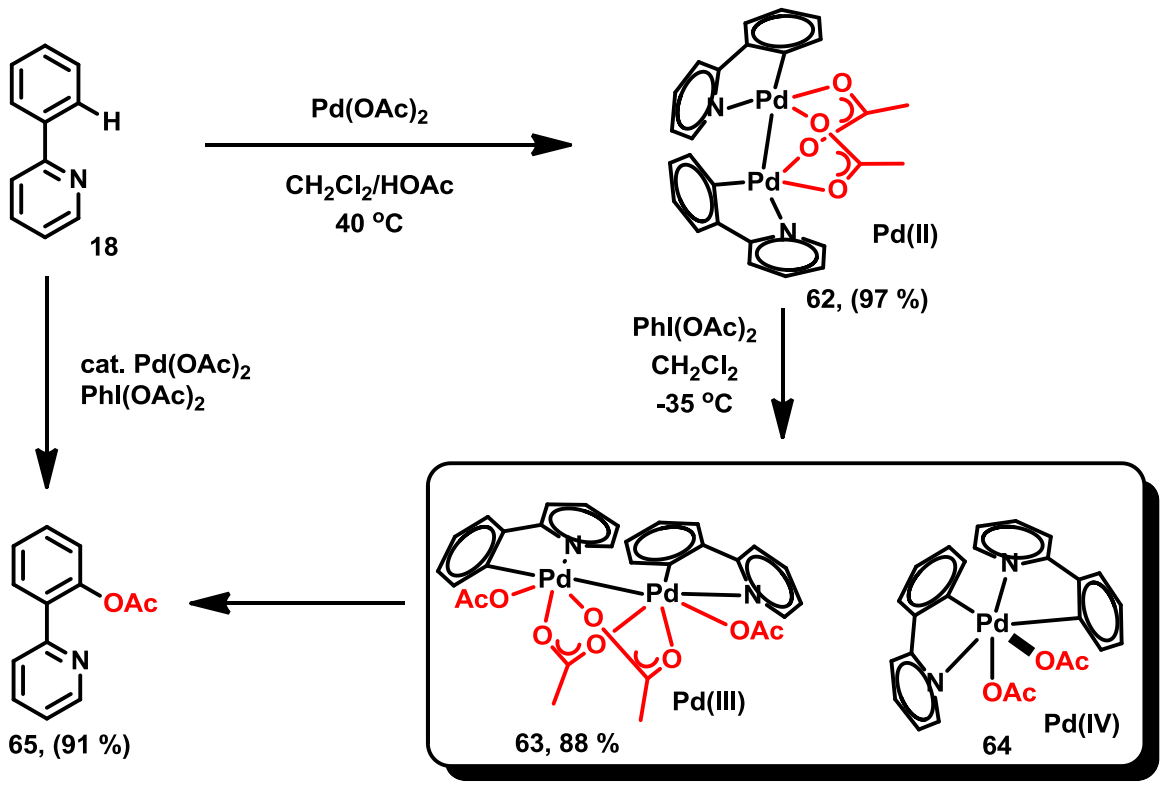

Scheme 29 Pd^{III}/Pd^{IV} species implicated in acetoxylation reactions starting at Pd^{II}

4.2 Nitrido palladacyclic complexes of 2-phenylpyridine

The main aim of this chapter was to synthesise novel nitrito–cyclopalladated complexes with sterically bulky phosphine ligands, enabling steric effects relating to nitrite linkage isomerisation to be studied. In view of this, a series of novel Pd-nitrite complexes were synthesised, following the literature procedures.[11,114,115] The chloro-dimer was synthesised according to the method described by Hiraki *et al.*,[113] which involved treatment of **62** with an excess of lithium chloride to afford the insoluble chloride-bridged Pd dimer **66**.[113] This was then converted to the phosphine monomer **67** *via* addition of triphenylphosphine, and followed by reaction with silver nitrite to form compound **60** in excellent yield (Scheme 30).

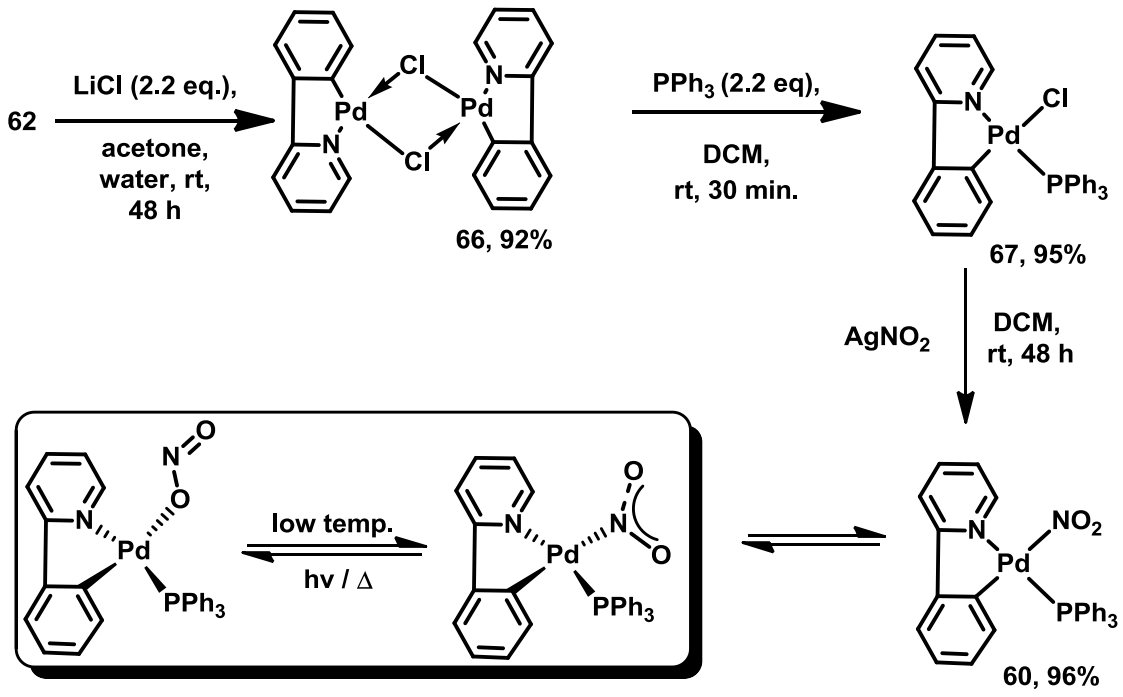

Scheme 30 Synthesis of novel Pd^{II} nitrito complexes of 2-phenylpyridine and different nitrite geometries

All the complexes prepared have been studied by electrospray ionization (ESI-MS) or liquid injection field desorption ionization (LIFDI-MS), infra-red (IR) and nuclear magnetic resonance (NMR) spectroscopic analysis (Table 2). An NMR study suggested the phosphine ligand has a profound effect on coupling with the proton of the C^N backbone ligand in the palladacycle owing to dramatic change on *J*-coupling splitting pattern. The J_{HP}-coupling splitting patterns were diagnostic for the proton α to nitrogen within the pyridyl moiety (Figure 9).

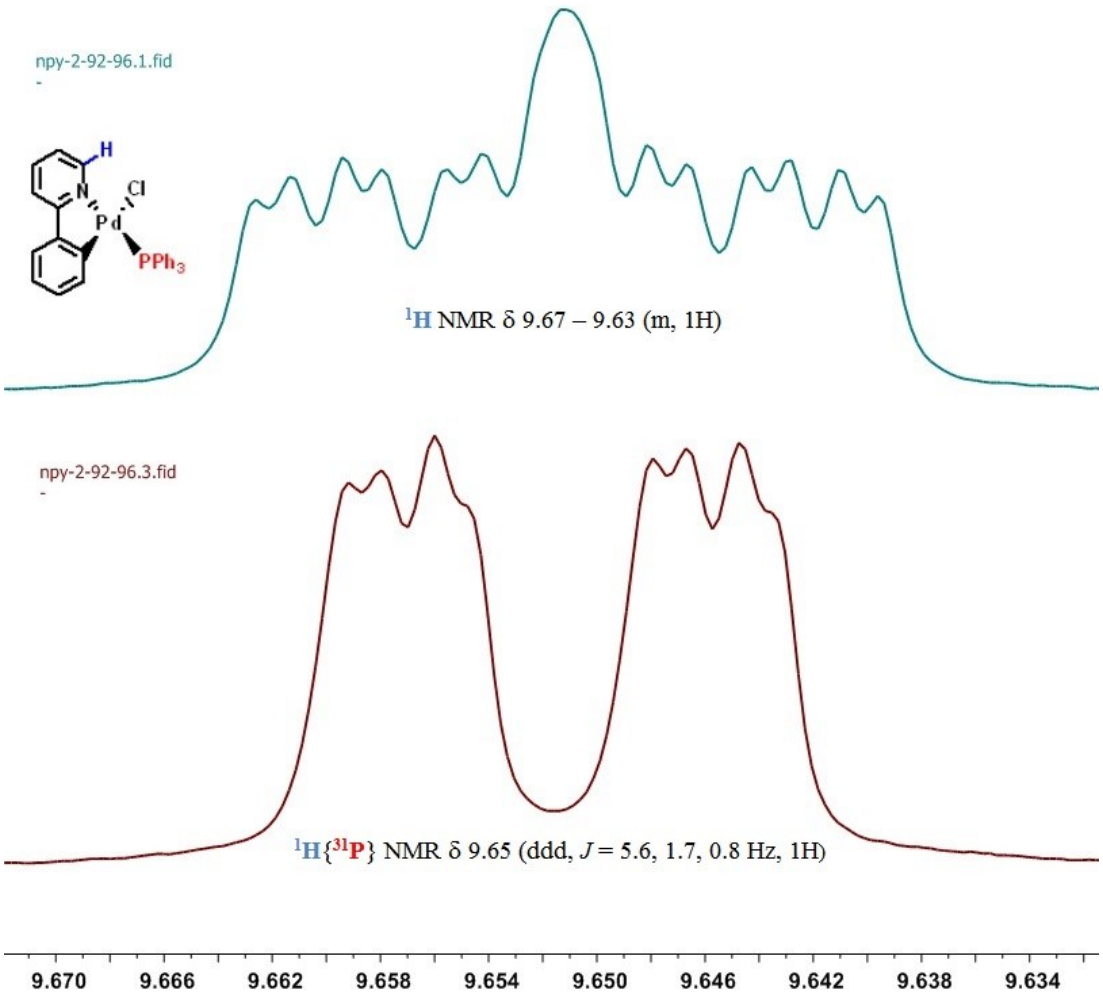

Figure 9 Phosphorus coupling/de-coupling ^{1}H NMR effect on monomeric palladacycle containing phosphine ligand

Resolution enhancement by free induction delay (FID) modification allows the multiplicity of the peaks to be seen – here, a sine-bell apodisation function was employed. An example of the effect of their peaks is shown in Figure 10. The two stacked ^{1}H NMR spectra, showing the ^{31}P coupled and decoupled result gave a clear indication of the effect of phosphorus.

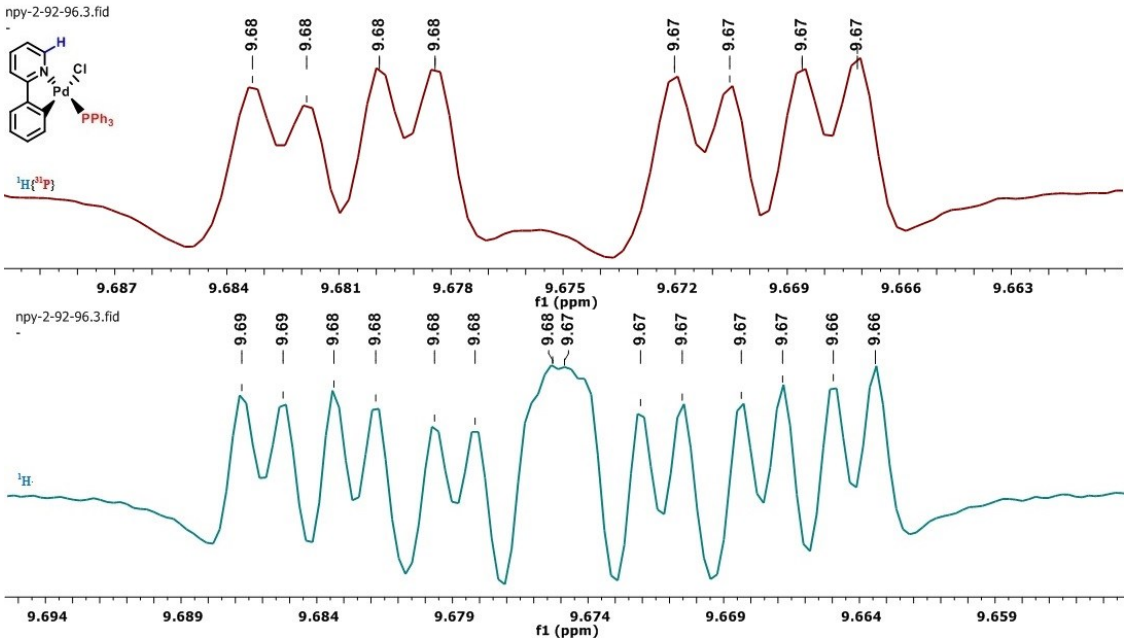

Figure 10 Sine-bell enhancement of ^{1}H and $^{1}H\{^{31}P\}$ NMR spectra effect on complex illustrating the α-N resonance of **67** (red $^{1}H\{^{31}P\}$ – green ^{1}H)

4.2.1 Geometry and linkage isomerism in Pd–NO_2 and Pd–ONO species

Following a successful synthesis of the novel nitrito cyclopalladated complex **60** a crystal suitable for X-ray diffraction was grown from a solution of dichloromethane with petroleum ether as the anti-solvent. The single crystal structure obtained is displayed in Figure 11. The crystal structure confirmed that the nitrite ligands occupy a coordination site *trans* to the Pd–C bond. A mixture of Pd–NO_2 and Pd–ONO isomers were evident. The bond lengths (Å) and bond angles (º) are all in agreement with those typical for complexes of this type.

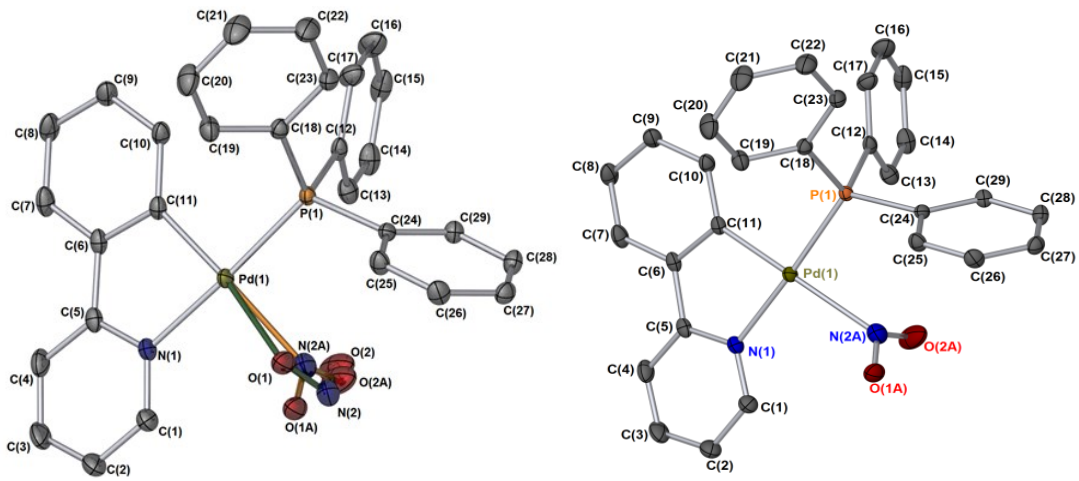

Figure 11 Single crystal X-ray diffraction structure of complex **60**

Hydrogen atoms omitted for clarity. Thermal ellipsoids shown with probability of 50%. (left; a mixture of N- and O-bonded NO_2 forms.) and (right; N-bond structure only shown for clarity). Selected bond lengths (Å); Pd(1) – C(11) 2.0083(18), Pd(1) – N(1) 2.0666(15), Pd(1) – P(1), Pd(1) – O(1) 2.1227(17), Pd(1) – N(2A) 2.2200(2)

Previously the Fairlamb group worked on a similar complex with a different C^N backbone,[41] showing that when the complex is exposed to light (400 nm) 150 K, a 1:3 mixture of Pd–η^1-NO_2 and Pd–η^1-ONO linkage isomers of Pd(η^1-ONO)(C^N)PPh_3 (C^N = papaverine) converted fully into the Pd–η^1-ONO species.[3] Irradiation of **60** revealed that only isomer remained, which supported the idea that linkage isomerisation in this type of complex is temperature and light dependent. This was further studied by Raithby *et al.,*[117] who examined the nitro/nitrito photomediated linkage isomerisation of [Ni(dppe)(η^1-ONO)Cl].[117-119]

4.2.2 Geometry and linkage isomerism in Pd–NO_2 and Pd–ONO species – a theoretical perspective

An independent study was carried out within the Fairlamb group[41] in order to ascertain the stability of the Pd–NO_2 or Pd–ONO forms of the nitrite ligand and the geometry of the nitrito palladacycle complexes by DFT. For these complexes to

function as precatalytic species, their *cis*/*trans* geometry and the preferred linkage isomerism of the nitrite ligand could be of great importance. In a catalytic system, it is anticipated that the nitrite ligand could undergo reductive elimination, along with an organic substrate, to form a C–NO_2 or C–ONO contains products, the ratio of these products could be determined by the relative geometry of the Pd–C and Pd–NO_2/ONO bonds; typically the two anionic ligands would need to be *cis*- to each other to form a product via a concerted reductive elimination process. The stability of Pd–NO_2 or Pd–ONO species could determine whether the ligand is likely to be involved in reductive elimination or act as a spectator ligand. The density functional theory (DFT) were computed by Dr. Jason Lynam in York, the purpose being to determine single point energies at 298 K for the *O*-bound and *N*-bound isomers of [Pd(C^N)(NO_2)PR_3], where C^N = 2-phenylpyridine, 2-benzylpyridine and PR_3 = PPh_3. Calculations were also performed on *cis*- and *trans*-isomers. The Gibbs free energies of each substituent at the pbe0/TZVPP level of theory are shown in Figure 12.

***Trans;* geometry**

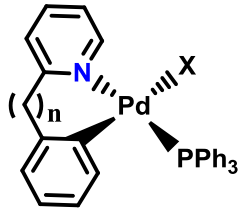

Relative free energies (ΔE) at TZVPP /kJ mol^{-1}		
n =	**0**	**1**
***N*-bound isomer**	0	0
***O*-bound isomer**	-1	+13

***cis;* geometry**

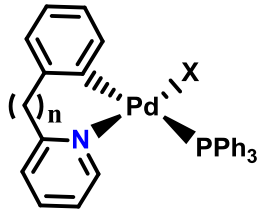

X = NO_2 or ONO

Relative free energies (ΔE) at TZVPP /kJ mol^{-1}		
n =	**0**	**1**
***N*-bound isomer**	+15	+17
***O*-bound isomer**	+44	+48

Figure 12 Single point energies of complexes of the type [Pd(Ligand)(NO_2)PPh_3]

These values suggest that in any species that is set-up for reductive elimination, the nitrite ligand would be likely to be bound through the nitrogen atom. For this geometry, the DFT results showed that the difference in free energy between *O*- and *N*- bound forms of the complex is negligible. For the *trans*-isomer, as the length of the alkyl linker, and therefore the steric bulk of the C^N ligand, increases, the *O*-bound isomer was found to increase in energy.

This suggests that the *N*-bound form of the nitrite ligand has less steric clash with the neighbouring ligands, and therefore is preferred over the *O*-bound when a bulky C^N ligand is present (Figure 12). However, the lower energy forms of complex **60** contain a nitrite ligand which is *trans*- to the Pd–C bond. Therefore the likely-hood for complex **60** to participate in catalytic C-H bond activation is hindered by the

geometry it possesses (Figure 11). A series of related Pd(η^1-ONO/NO_2)(C^N)PR_3 were synthesised to ascertain the effect of the ligand substituent.

$Pd(OAc)_2$ was added to the C^N ligand in the presence of LiCl. Subsequently the phosphine and nitrite were added according to Scheme 31.

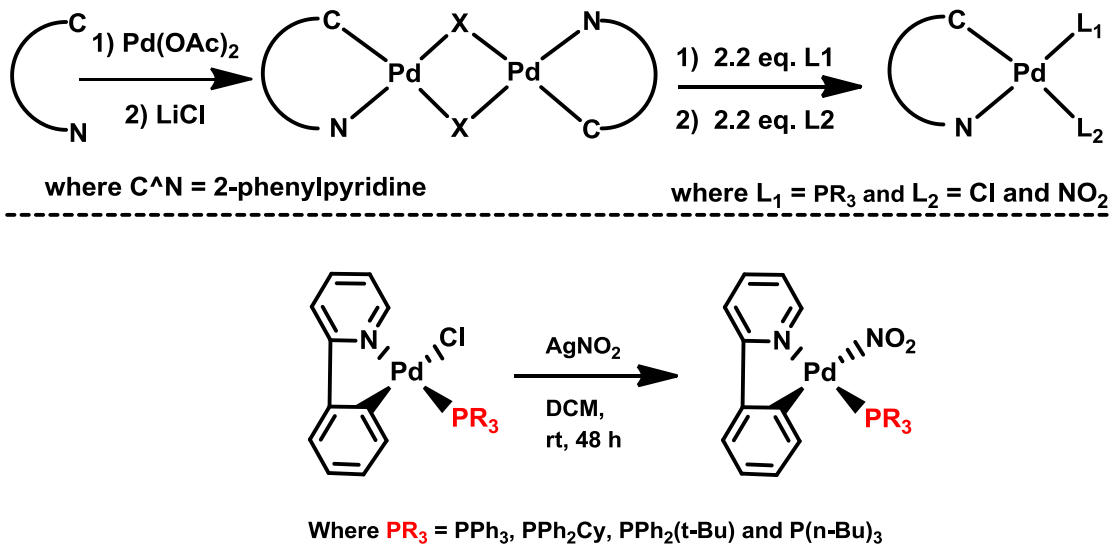

Scheme 31 General synthetic pathway to novel Pd^{II} nitrito complexes of 2-phenylpyridine

Although nitrite chemistry is under investigation for its role in catalysis[11, 41, 42, 117-120] as well as anthropogenic toxicity,[121, 122] their coordination with N^C bound Pd has received less attention, which has caught the attention of the Fairlamb group in York.[41, 42]

Table 2 summarises the novel palladacycles synthesised in this study. Changing phosphine from a less sterically hindered to more bulky / sterically hindered phosphine proved to not change the nitrite linkage isomerisation, studying these complexes by single crystal diffraction reveals unusual structural changes in complexes **74a** and **74b** (Figure 13 and Figure **14**), which result from the elimination of the bulky phosphine (PPh_2Cy and PPh_2(*t*-Bu)) and transformation into dimeric

complexes containing μ^2-NO_2 bridging ligand. The effect of phosphine substituents on the nitrite palladacycle is therefore significant as revealed in Scheme 33.

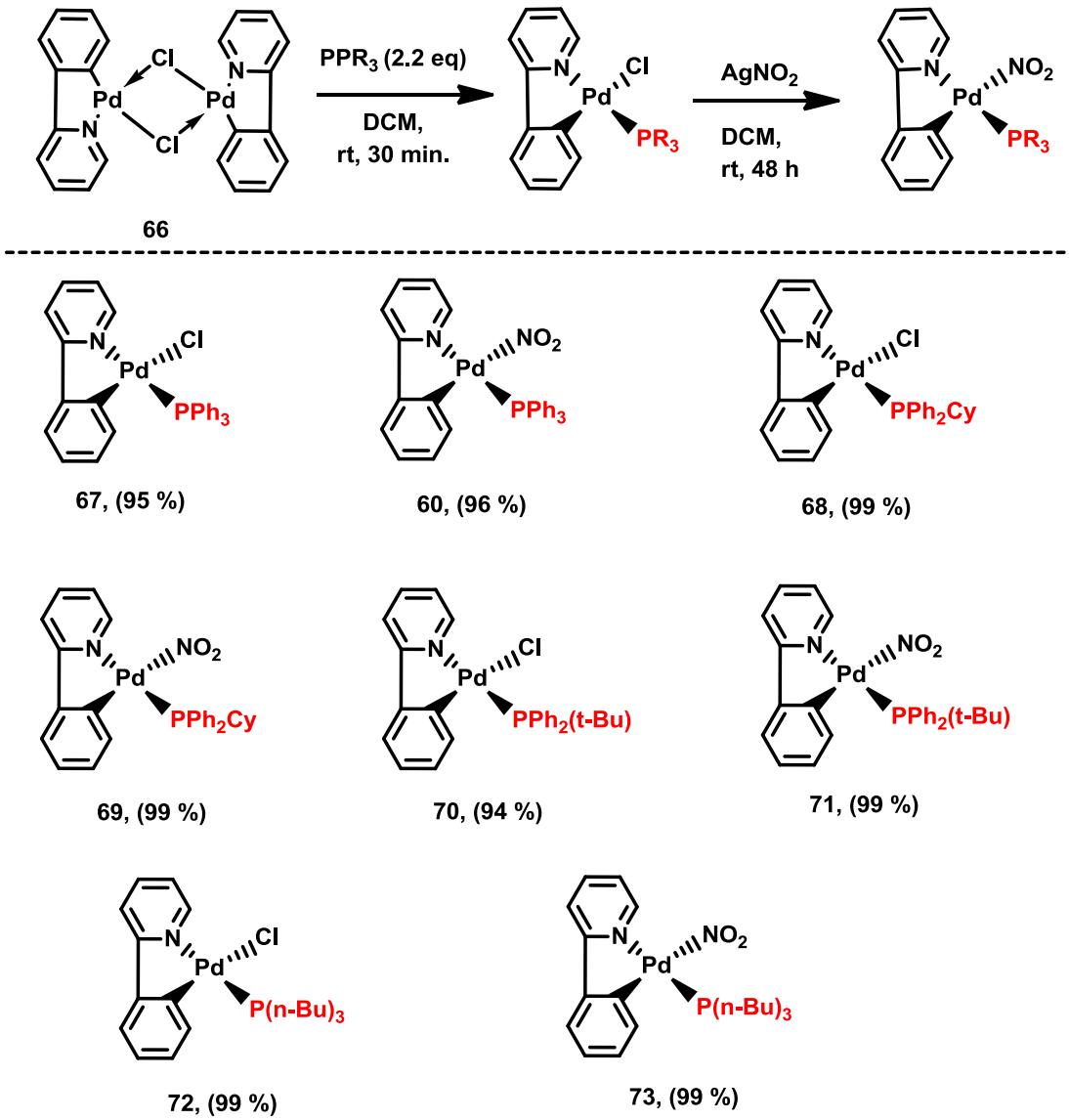

Scheme 32 Synthesis of novel nitrite palladacycles containing 2-phenylpyridine

Table 2 Physical properties of complexes **60** and **67-73** 2-phenylpyrine palladacycles (dimers to monomers)

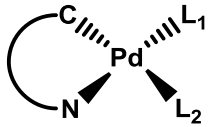

where C^N = 2-phenylpyridine
L_1 = PPh_3, PPh_2Cy, PPh_2(t-Bu), P(n-Bu)$_3$
L_2 = Cl and NO_2

Compound	L_1	L_2	M.P / ^oC	C:H:N (cal. / observed)	MS *m/z*	Yield (%)
67	PPh_3	Cl	220–223	62.38:4.15:2.51 / 63.03:4.71:2.62	558.99	95
60	PPh_3	NO_2	215–216	61.23:4.07:4.92 / 65.63:4.32:2.69	588.90	96
68	PPh_2Cy	Cl	172 – 173	61.71:5.18:2.48 / 62.23:5.33:2.50	564.10	99
69	PPh_2Cy	NO_2	195–196	60.58:5.08:4.87 / 65.81:5.50:2.69	574.08	99
70	PPh_2(t-Bu)	Cl	160 – 161	60.24:5.06:2.60 / 61.13:5.44:3.01	538.11	94
71	PPh_2(t-Bu)	NO_2	163–167	--	548.07	99
72	P(n-Bu)$_3$	Cl	--	--	497.12	>99
73	P(n-Bu)$_3$	NO_2	--	--	508.17	>99

Some of the experimental CHN values were found to be outside of the error limits of the calculated values, which may be due to the presence of CH_2Cl_2 in the samples.

4.2.3 Metastable Pd(η^1-ONO)(C^N)PR_3 and an unusual Pd dimer structure (C^N = ligand)

Raithby and co-workers[117, 119] studied similar low temperature, single crystal photocrystallography, suggesting that similar square planar complexes can be formed *e.g.* $[Ni(PEt_3)(NO_2)_2]$, $[Pd(PPh_3)_2(NO_2)_2]$ and $[Pd(AsPh_3)_2(NO_2)_2]$. In their Pd complexes, the two nitro groups adopt a *trans*-configuration at the metal centre. Upon irradiation with UV light, at 100 K, photoisomerisation of η^1-NO_2 nitro to the η^1-ONO nitrito form occurs. Under the same experimental conditions, $[Pt(PPh_3)_2(NO_2)_2]$ showed no isomerisation. Based on these experimental details, our study suggests that complexes **69** and **71** dimerised via phosphine loss at low temperature (Scheme 33).

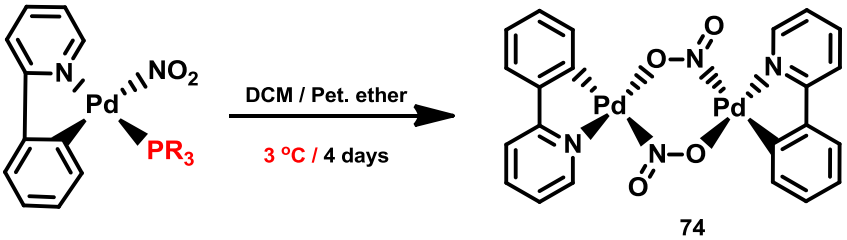

Where PR_3 = PPh_2Cy complex 69 and PPh_2(*t*-Bu) complex 71

Scheme 33 Metastable Pd(η^1-ONO)(C^N)PR_3 and an unusual $Pd^{(II)}$ dimer structure

In order to transform from the η^1-NO_2 to the η^1-ONO nitrito complex, a lone pair of electrons on the nitrogen atom replaces the bulky phosphine according to Scheme 34. Such transformation occurred only in complexes containing PPh_2Cy (Figure 13) and PPh_2(t-Bu) (Figure 14). The complex, containing the PPh_3 ligand, gave the expected monomeric palladacycle linkage nitrite isomer (Figure 11).

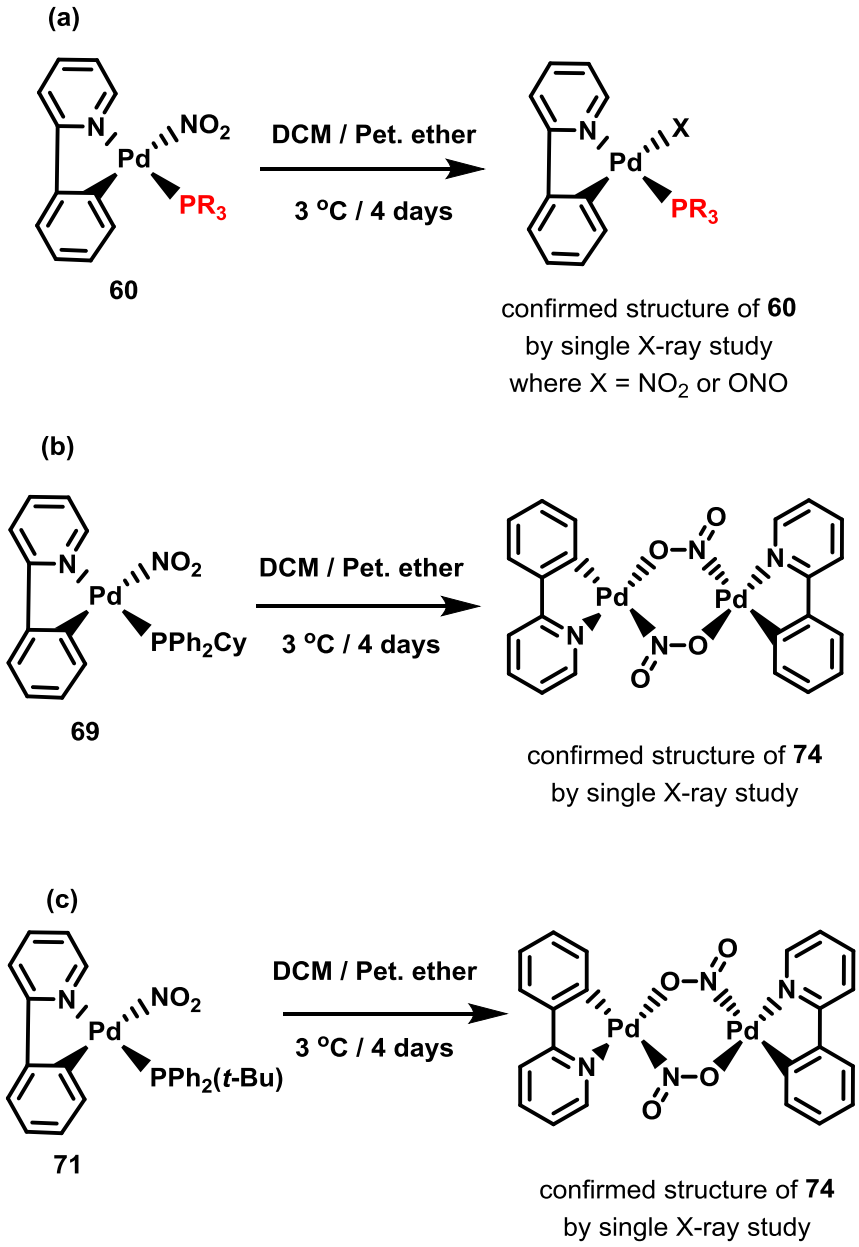

Scheme 34 Effect of bulky phosphine on nitrito cyclopalladated complexes containing phenylpyridine open crystallisation

The crystal structures of the monomeric and dimeric palladacycles **60** and **68-71** (Scheme 32) have been unequivocally proven by X-ray diffraction studies example Figure 13 and Figure 14. The monomeric N^C palladacycles having monophosphine, chloro and or nitrite ligands **60** and **67-73** (Table 2) were initially studied by NMR spectroscopic analysis, which confirmed their expected structure in each case (Scheme 32, Table 2). NMR also confirmed the formation of **74** (Scheme 34, Figure

13 and Figure **14**). It is important to note that these complexes only formed during the process of growing crystals at low temperature (Scheme 34, Figure 13 and Figure **14**). For X-ray crystallographic analysis, complex **74** is described as **74a** and **74b** (different crystals from the separate reactions detailed above), as there is marginal increase in all bond lengths (Å), along with a decrease in bond angles (˚), although these can be considered within error.

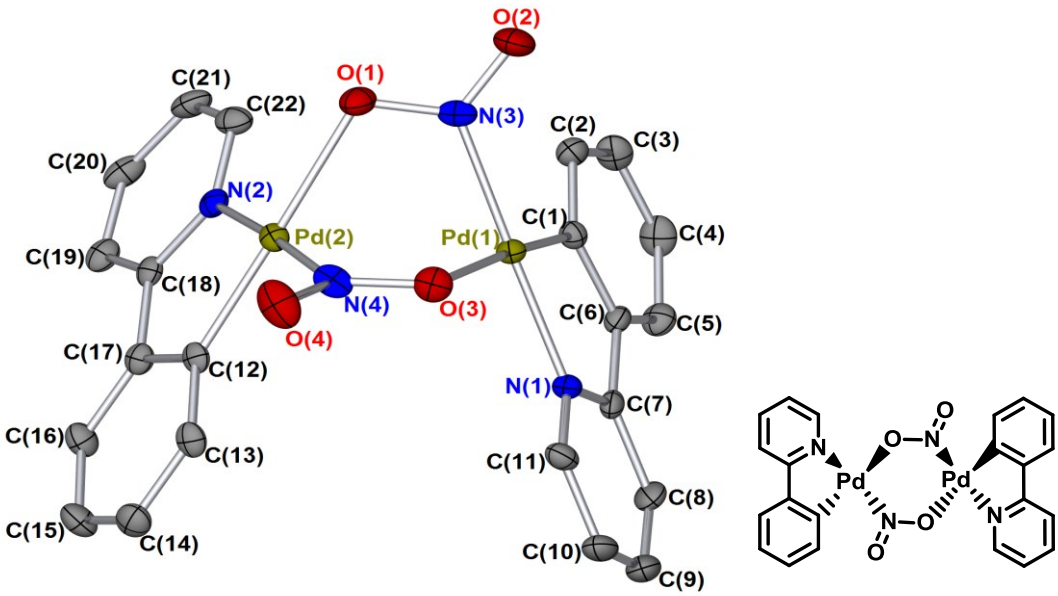

Figure 13 Single crystal X-ray diffraction structure of complex **74a**; Hydrogen atoms removed for clarity. Thermal ellipsoids shown with probability of 50%. Selected bond lengths (Å); Pd(1)–C(1) 1.972(4), Pd(1)–O(3) 2.173(3), Pd(1)–N(1) 2.017(3), Pd(1)–N(3) 2.034(3), Pd(1)–Pd(2) 2.9802(5), Pd(2)–C(12) 1.964(4), Pd(2)–N(4) 2.027(3), Pd(2)–O(1) 2.172(3), Pd(2)–N(2) 2.024(3)

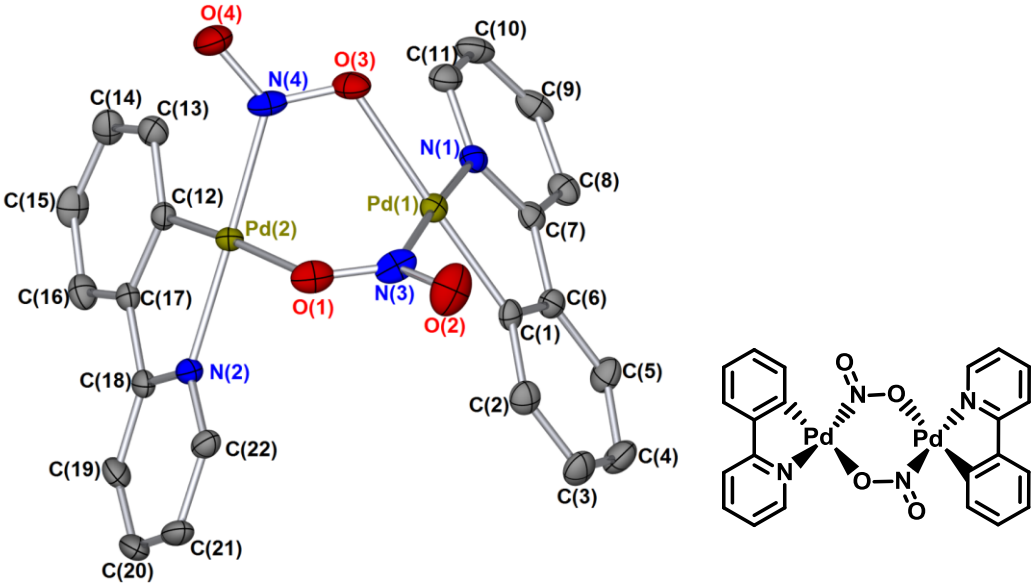

Figure 14 Single crystal X-ray diffraction structure of complex **74b**; Hydrogen atoms removed for clarity. Thermal ellipsoids shown with probability of 50%. Selected bond lengths (Å); Pd(1)–C(1) 1.964(3), Pd(1)-N(1) 2.016(2), Pd(1)–N(3) 2.033(3), Pd(1)–O(3) 2.172(2), Pd(1)–Pd(2) 2.9707(4), Pd(2)–C(12) 1.962(3), Pd(2)–N(2) 2.012(2), Pd(2)–N(4) 2.037(2), Pd(2)–O(1) 2.184(2).

Upon re-dissolving the crystal submitted for X-ray diffraction study, an unusual structure was ascertained in deuterated solvents and also in solid state NMR, in both cases the phosphine ligand was found to be in the complexes. These presumably dissolve the entire sample in phosphine and equilibrate the sample and phosphine in solution. However the crystal structure of chloro-monomers of this type of product did not deviate from that expected (Figure 15).

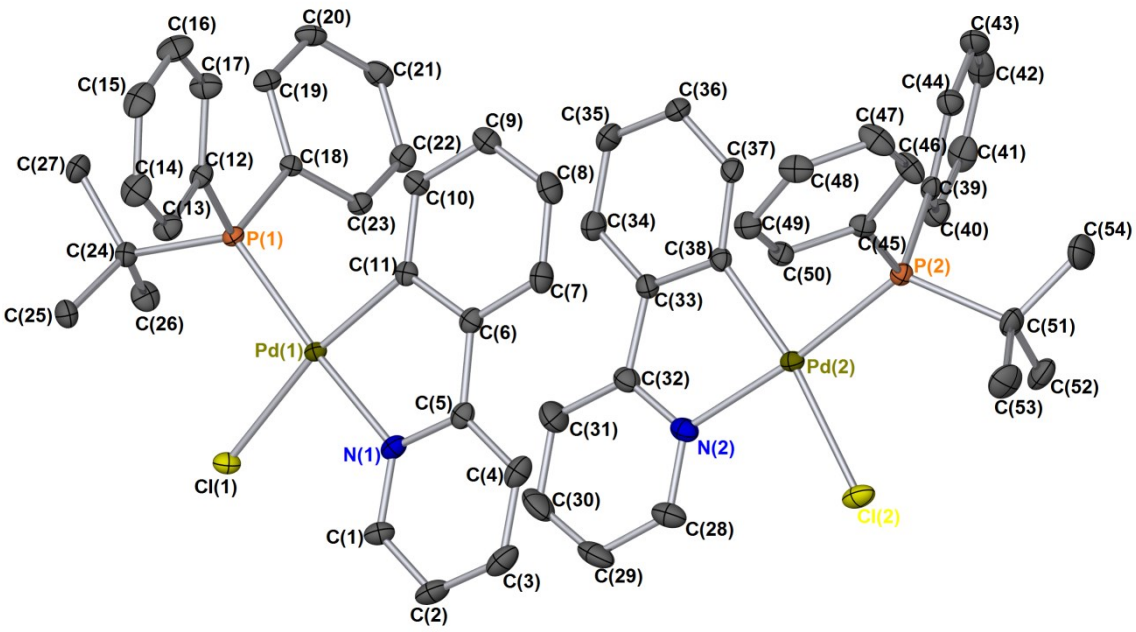

Figure 15 Single crystal X-ray diffraction structure of complex **70** showing two molecules (left – single molecule and right – showing the two independent molecules in the unit cell). Hydrogen atoms omitted for clarity. Thermal ellipsoids shown with probability of 50%. For selected bond lengths and bond angles see Table 3 page 78.

Table 3 summarises the X-ray crystallographic data of these palladacyclic complexes. They adopt square planar geometries around palladium with the phosphorus atom *trans* to the donor N atom. The angle P–Pd–N bond angle in the nitrite isomer of **60** is 176.36(5)º, while that for the corresponding complex **70** is 171.57(4)º. This suggested that the nitrite containing complex distorts the square plane less than the chloride counterpart. However the Pd–N bond length **70** 2.0982(15) Å is longer compared to 2.0666(15) Å of complex **60**. As expected, complexes **74a** and **74b** (nitrite dimer) show a dramatic increase in the N–Pd–X bond angles and a decrease in the O–Pd–X bond angles, when compared to **60**.

Table 3 Selected bond lengths (Å) and bond angles (º) for complexes **60**, **70**, **74a** and **74b**

Lengths/Angles	**60 (ijsf1213)**	**70 (ijsf1219)**	**74a (ijsf1225)**	**74b (ijsf1226)**
Pd-C Å	2.0083(18)	2.0183(18)	1.972(4)	1.964(3)
Pd-P Å	2.2447(5)	2.2846(5)	2.173(3)*	2.172(2)*
Pd-N Å	2.0666(15)	2.0982(15)	2.017(3)	2.016(2)
Pd-X Å	2.22(2)	2.3891(5)	2.034(3)	2.012(2)
Pd-Pd Å	--	--	2.9802(5)	2.9707(4)
C-Pd-N º	81.49(7)	81.13(7)	81.62(15)	81.85(10)
C-Pd-P º	95.03(5)	92.57(5)	173.32(14)*	176.86(9)*
C-Pd-X º	162.2(5)	170.15(5)	95.81(15)	94.45(11)
P-Pd-N º	176.36(5)	171.57(4)	94.11(13)	95.02(9)
P-Pd-X º	91.0(5)	96.842(16)	88.45(13)*	88.69(9)*
N-Pd-X º	92.0(5)	89.77(5)	177.43(14)	176.04(10)
C-Pd-Pd º	--	--	112.17(11)	117.20(8)

X = Cl for **70**; X = N for **60**, **74a** and **74b**; * = (ligand change from Pd-P → Pd-O in **74a** and **74b**)

4.3 Palladacyclic complexes of 2-benzlpyridine

An acetate-bridged cyclopalladated complex of benzylpyridine, **76** $[(Pd(OAc)(N^C)]_2$, was obtained by reaction of benzylpyridine **75** with $Pd(OAc)_2$.[113] A chloro-bridged analogue **77**, $[PdCl(N^C)]_2$, formed by metathetical reaction of the μ^2-acetato-bridged complex with LiCl, undergoes a bridge-exchange reaction to form **77**. Whereas treatment of **75** directly with $PdCl_2$ in methanol yielded only mononuclear complex **78** (Scheme 35).

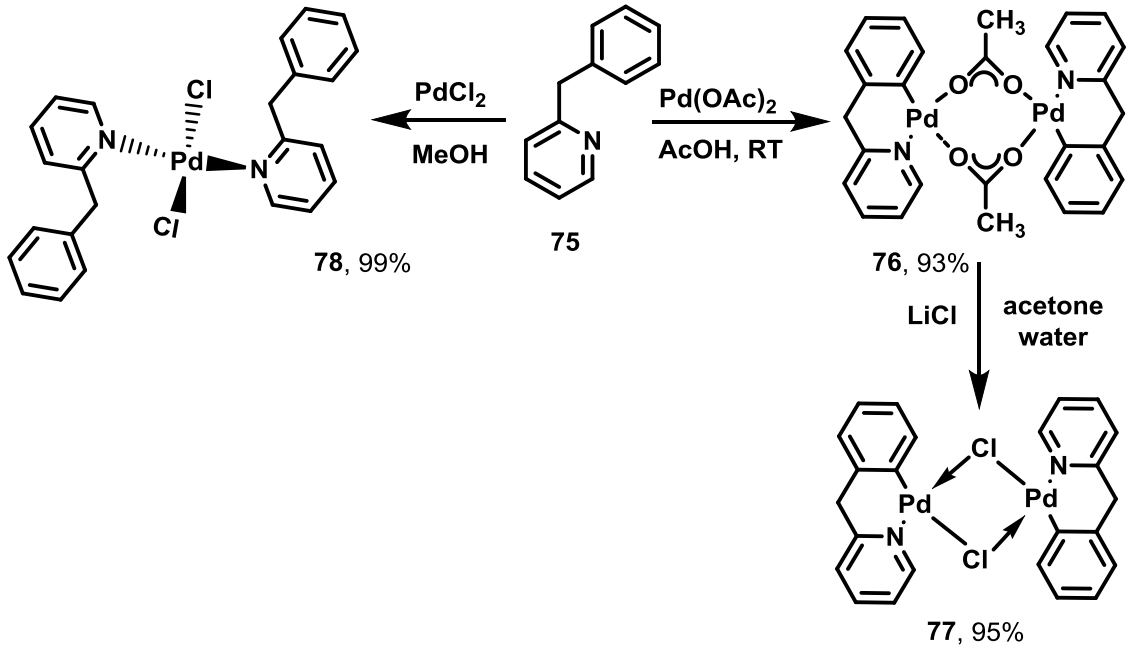

Scheme 35 Synthesis of cyclopalladated 2-benzylpyridine complexes

These Pd complexes were characterised by means of elemental analysis, IR and NMR spectroscopy. NMR study reveals that the acetato-cyclopalladated-bridged complex **76** prefers a higher energy boat conformation rather than a chair conformation, an observation reported by Hiraki and co-workers, who studied the geometry of these types of complexes[113] with different substituents (Figure 16).

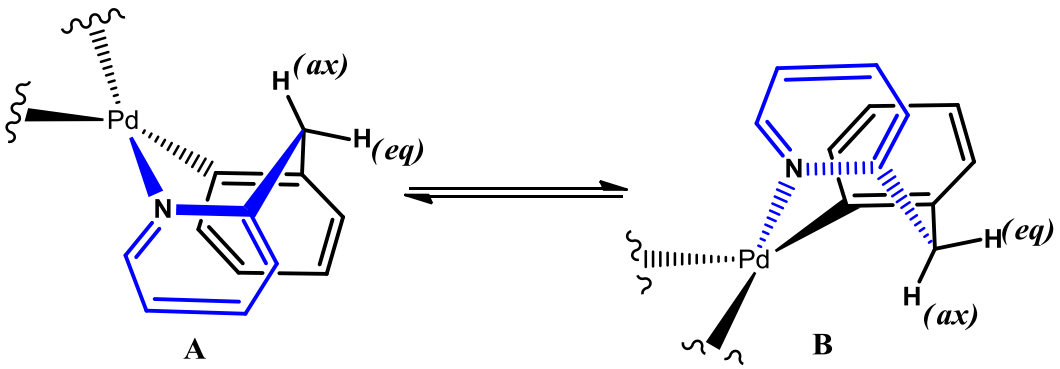

Figure 16 Geometry of cyclopalladation of 2-benzylpyridine

4.3.1 Geometrical aspects of the Pd complexes

NMR spectroscopic analysis suggested two isomers were present for complexes **76**, **A** and **B**, with **A** being the major isomer. In consideration of the two coordination planes in an acetato-bridged cyclopalladated dimers which possess two mutually *cis* acetato ligands, **76** was expected to adopt two configurations **A** and **B** (Figure 16). The mixture of **76** was simplified by addition of deuterated pyridine (C_5D_5N) in CD_2Cl_2, giving the mononuclear cyclopalladated complex [Pd(OAc)(N^C)(C_5D_5N)] **80** only (Scheme 36). This simplifies the NMR spectra as only one isomer is seen where the pyridine nitrogen of the cyclopalladated ligand and pyridyl donor ligand assume to be are mutually *trans*. One isomer was only observed for **80**, as evidenced by the simplified proton signals within the ^{1}H NMR spectra (Figure 17, page 82).

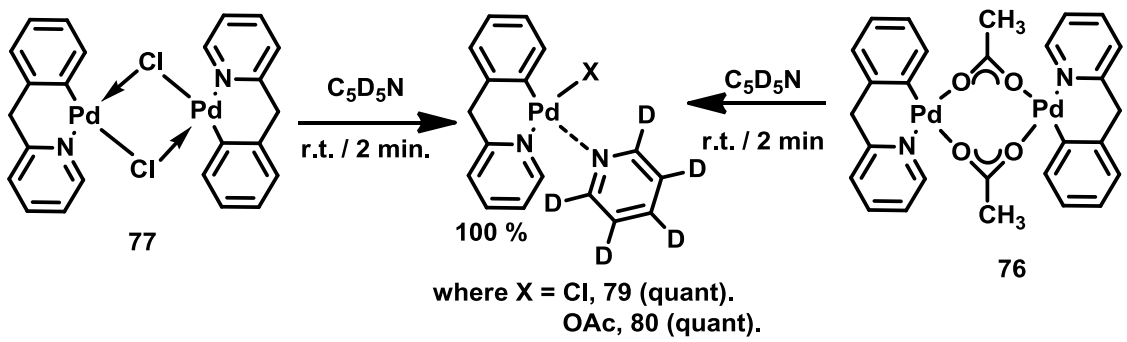

Scheme 36 Synthesis of palladacycles of 2-benzylpyridine containing a pyridine ligand

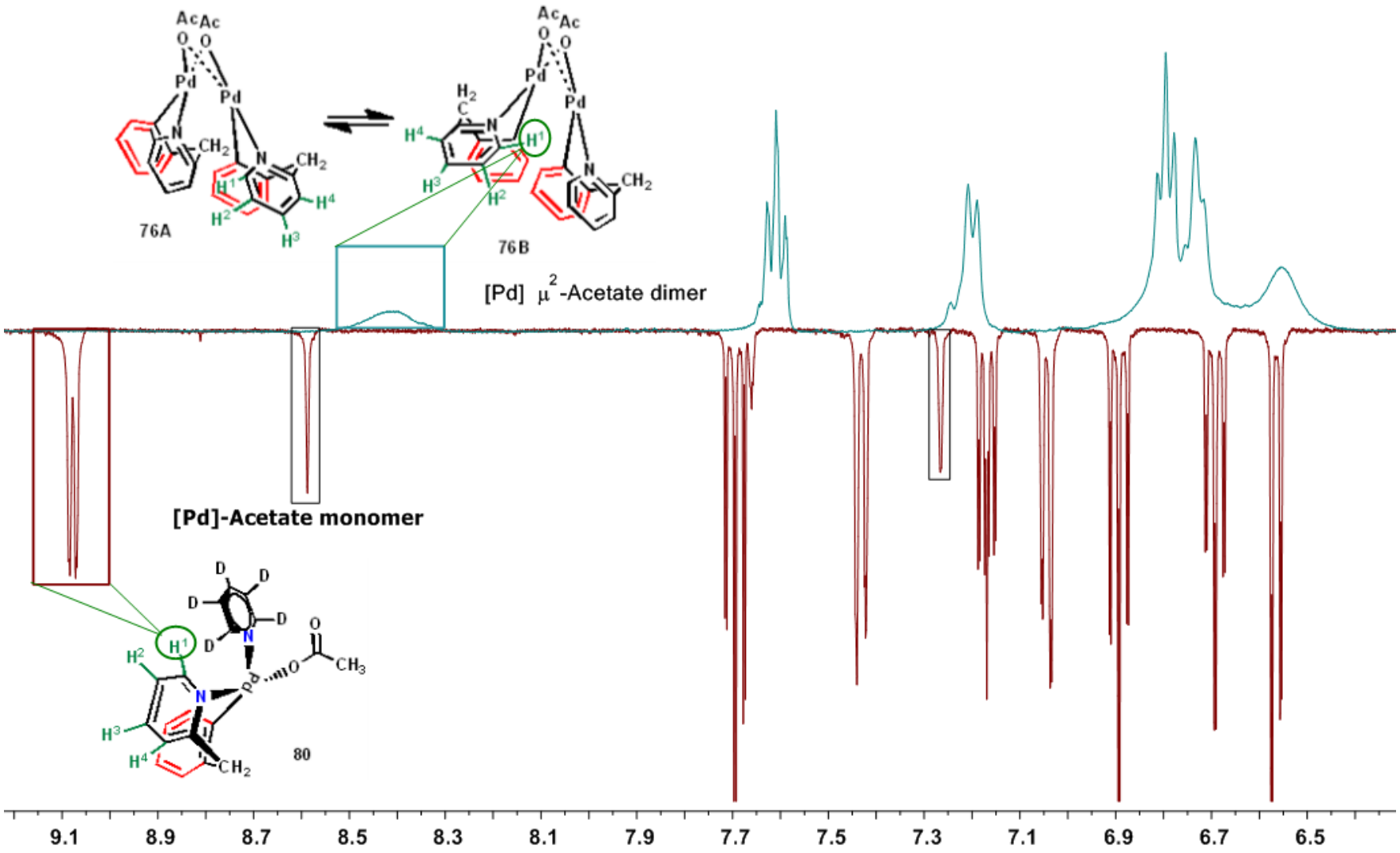

Figure 17 Comparison of ^{1}H NMR spectra of **76A/B** (positive spectra) and **80** (negative spectra) at (400 MHz, CD_2Cl_2). I- the negative spectra the protons of the pyridiyl group are highlighted

A similar acetate bridged complex was synthesised using 4-(2'-pyridyl)-6-methyl-2-pyrone as the N^C backbone. Reaction of $PdCl_2$ with a two-fold excess of 2-benzylpyridine, in refluxing methanol, yielded **68** (Scheme 35, page 79), and the ^1H NMR spectra of this complex suggested two isomers, present in an equimolar mixture. Hiraki and co-workers postulated that this is associated with the quenching of the rotation about the two bulky N^C ligands, about the Pd-N bond.

4.4 Palladacyclic complexes of 4-(2-pyridyl)-6-methyl-2-pyrone

4-(2'-Pyridyl)-6-methyl-2-pyrone **81** was prepared by Negishi cross-coupling in an excellent yield (Scheme 37). This provides a more bulky (N^C) ligand with respect to 2-phenylpyridine **18**. Treatment of **81** with $PdCl_2$ in methanol does not give a monomer complex **86**, but rather gives chloro-bridged dimer complex **83**. Refluxing ligand **81** with $Pd(OAc)_2$ yielded acetate-bridged dimer complex **82**, present as four possible isomers. Treatment of **83** with triphenylphosphine allowed the formation of monomeric palladacycle **84**. Dissolving **83** in deuterated pyridine at room temperature for ca. 5 min., gave complex **85**.

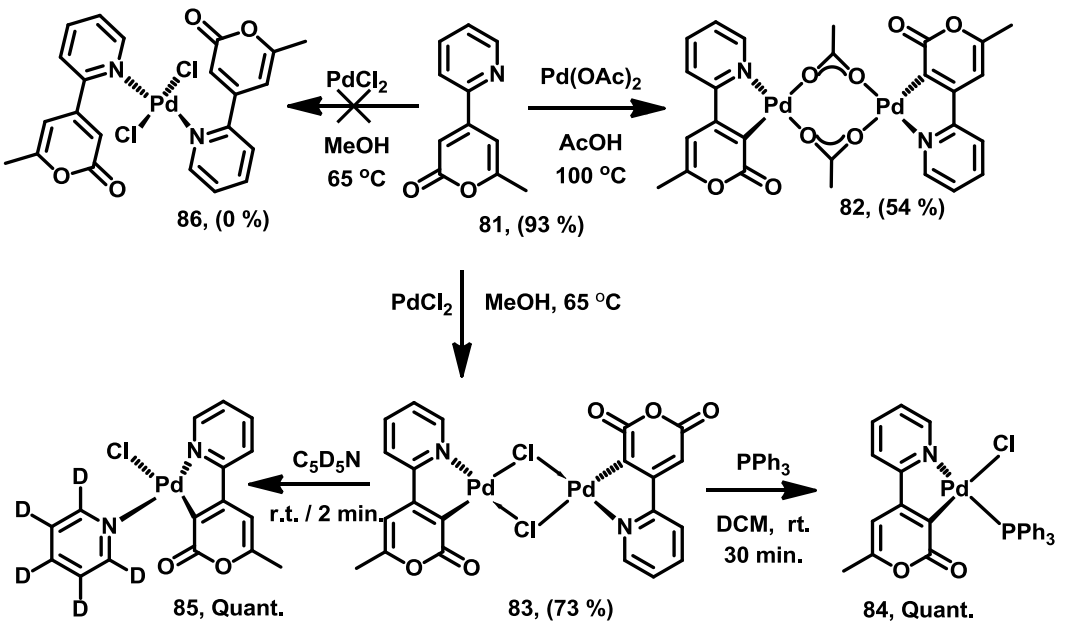

Scheme 37 Synthesis of cyclopalladated 4-(2'-pyridyl)-6-methyl-2-pyrone complexes

These complexes were characterised by MS (LIFDI and ESI) and NMR. The NMR spectra of complex **82** proved to be four different geometrical isomers (Scheme 38). The remaining proton of the 2-pyrone moiety in complex **82** is indicative when following the transformations between **82A**, **82B**, **82C** and **82D** by NMR (Scheme 38). It appears that both C3 and C5 protons have been activated by Pd^{II} in these reactions.

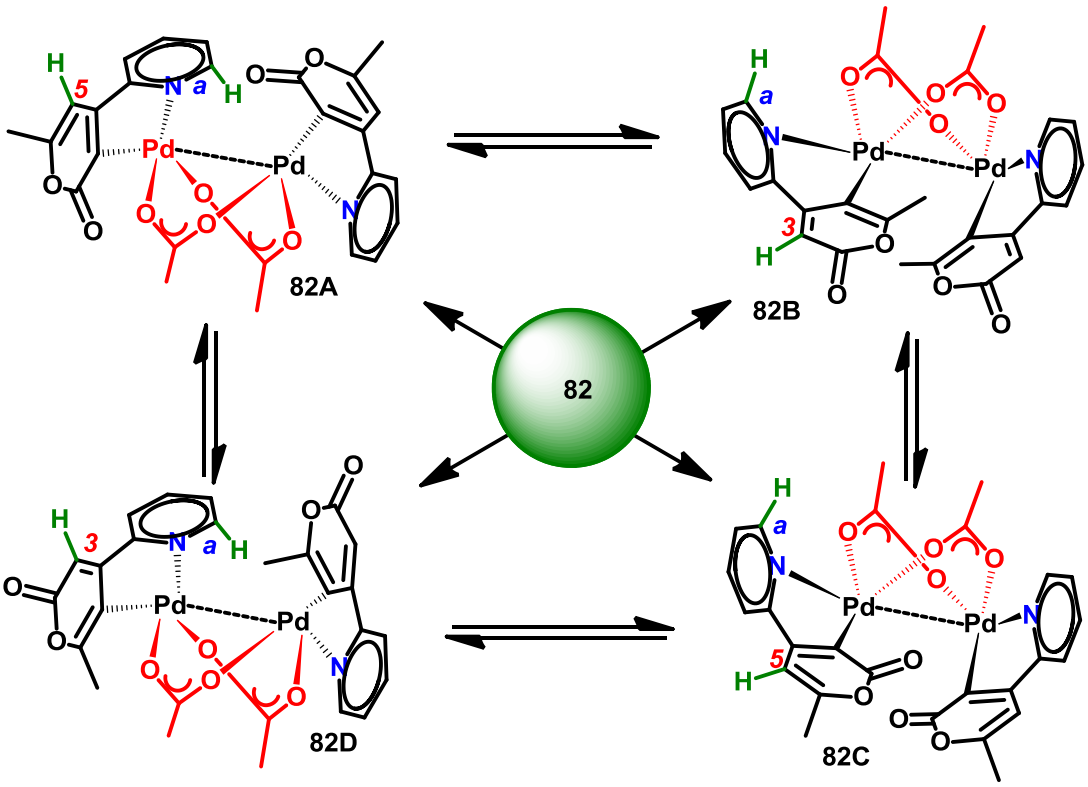

Scheme 38 Possible *syn / anti* vs C3 / C5 isomers of **82**

This is illustrated by ^{1}H NMR spectra in Figure 18 to support the structures proposed in Scheme 38, where the proton chemical shift at δ 5.95 (s, 1H) and 5.65 (s, 1H), correspond to C3 of **82B** and **82D,** whereas proton chemical shift at δ 5.79 (s, 1H) and 5.56 (s, 1H) correspond to C5 of **82A** and **82C**.respectively. This was further supported by COSY spectroscopy which confirmed the presence of four sets of protons *α*- to nitrogen in the pyridyl moiety. These correspond to the protons on each aromatic ring of the pyridyl moiety. These appear at proton chemical shift δ 8.54, 8.52, 8.29 and 8.22 (Figure 18).

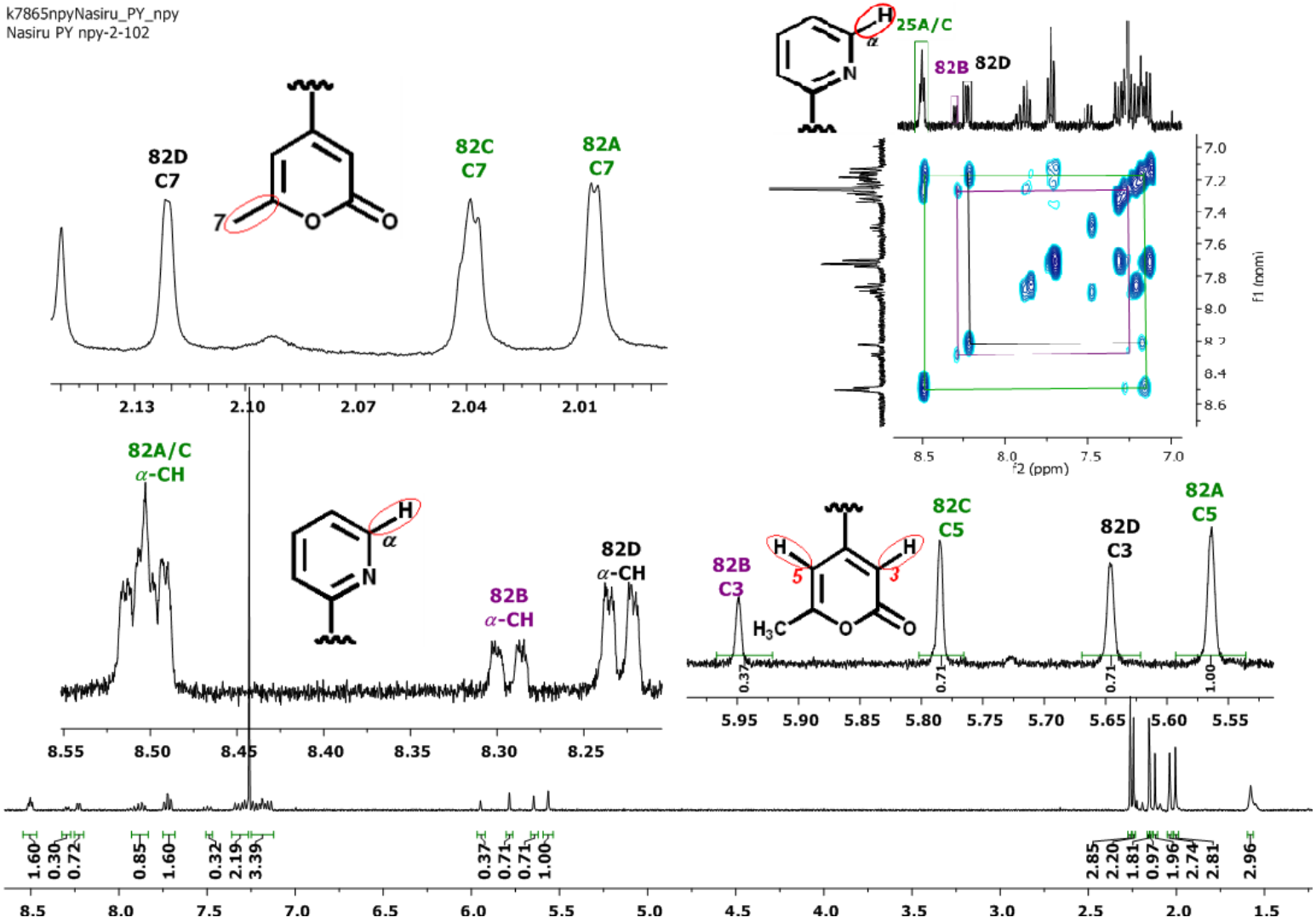

Figure 18 NMR spectroscopic analysis of complex **82** (400 MHz, $CDCl_3$) – inset (top right) is the ^{1}H COSY spectra

For compound **85**, crystals suitable for X-ray diffraction were grown by layering a solution of **83** in deuterated pyridine d_6; the single crystal structure is displayed in Figure 19. This confirmed that chloride occupies the coordination site *trans*- to the Pd–C bond.

The bond distance for a similar complex **70** was directly compared with **85 (**Figure 19). The Pd(1)–C(1) bond in **85** was 1.9931(18) Å, which is shorter than the same bond within **70**, 2.0183(18) Å. Similarly, the Pd(1)–N(1) bond in **85** was 2.0353(16) Å, slightly shorter than **70**, with 2.0982(15) Å. While, Pd(1)–Cl(1) was 2.3967(5) Å in **85** and 2.3891(5) Å in **70**.

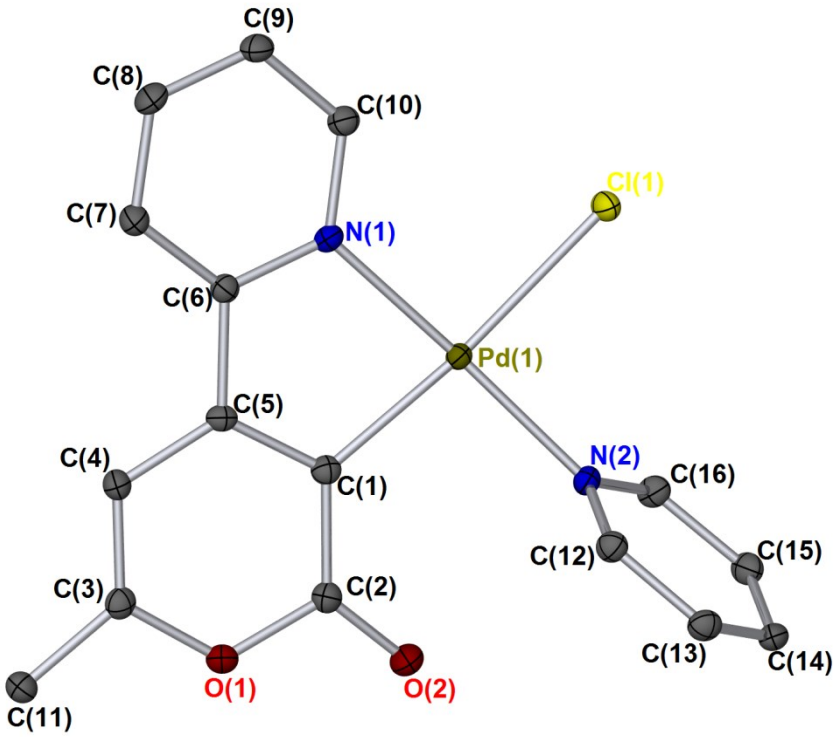

Figure 19 Single crystal X-ray diffraction structure of complex **85**. Hydrogen atoms removed for clarity. Thermal ellipsoids shown with probability of 50%. Selected bond lengths (Å); Pd(1)–C(1) 1.9931(18), Pd(1)–Cl(1) 2.3967(5), Pd(1)–N(1) 2.0353(16), Pd(1)–N(2) 2.0287(15).

4.5 Nitrito-palladacyclic complexes of 2-benzylpyridine

The nitrito containing palladacycle with N^C backbone as 2-benzylpyridine was synthesised according to the method described by Hiraki *et al.* – treatment of **76** with an excess of LiCl gave give chloride-bridged dimer **77**,[1] which was then converted to the phosphine monomer **87** *via* addition of PPh_3, followed by reaction with $AgNO_2$ to form **88** in excellent yield (Scheme 39)

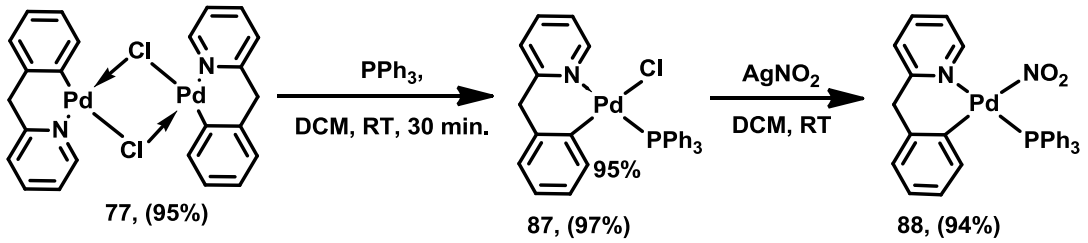

Scheme 39 Synthesis of Pd^{II} nitrito-cyclopalladated complex of 2-benzylpyridine

The reaction mechanisms of cyclopalladation reactions of this type have been recently given due consideration with 2-phenylpyridines[2], *N*-benzylideneamines[3] and N-benzyltriamines[4] as N-donor ligands. Although it is commonly assumed that the first step in the cyclopalladation reaction is coordinative bonding of the N^C nitrogen to the palladium atom,[5, 6] this assumption being quite logical, direct experimental proof has been lacking. What remains clear is that N^C bounded nitrogen is a directing group in C-H bond activation/functionalisation, as shown in Scheme 40. The geometry of all the monomeric palladacycles under this study depend on the steric and electronic nature of the incoming ligands, for example complexes **76-87** gives preference to the N^C nitrogen of the pyridine moiety which direct the overall geometry. Earlier in the chapter the geometry of the Pd complexes containing 2-phenylpyridine as N^C ligand were found to be less sterically hindered, here was introduced a more sterically bulky N^C as 2-benzylpyridine to ascertain the

enhancement or suppressing outcome of the nitrite anion **88**, with its various coordination modes that it can adopt at Pd^{II}. A series of nitrito cyclopalladated complexes were synthesised with varying phosphines, all in excellent yields (Scheme 41, and Table 4).

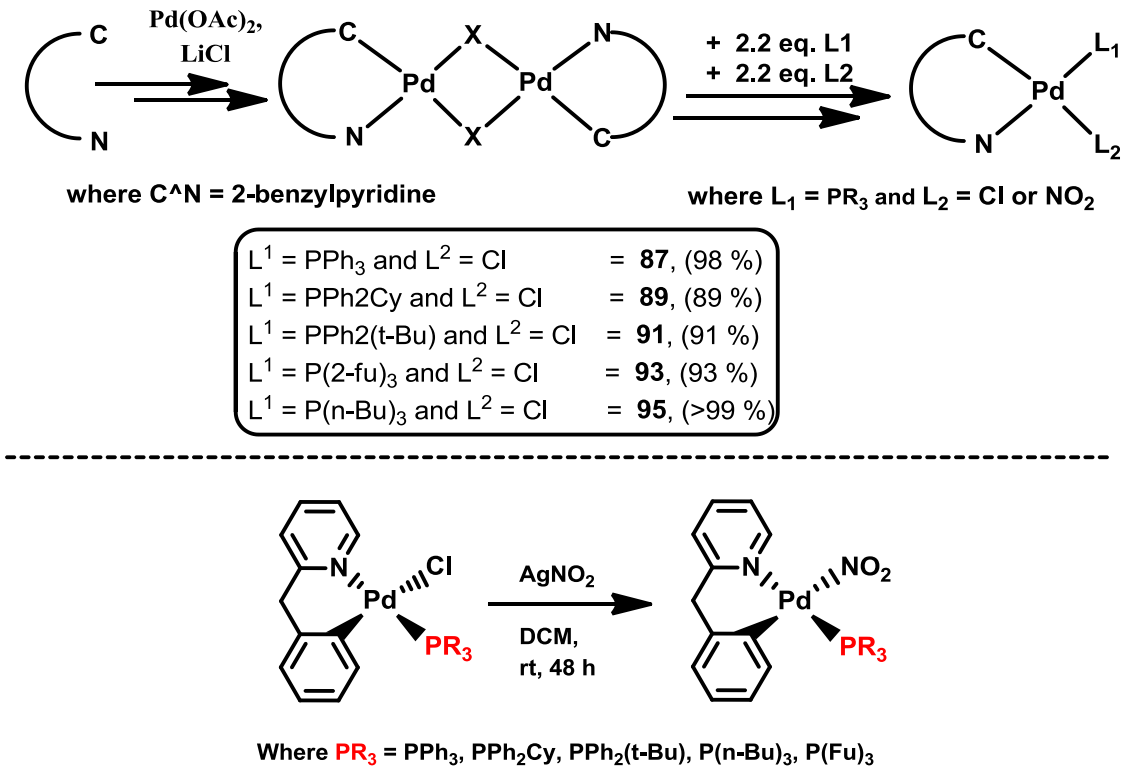

Scheme 40 General synthetic pathway to novel Pd^{II} nitrito complexes of 2-benzylpyridine **75**

The ^{1}H-NMR spectra of **79** and **87-96**, recorded in CD_2Cl_2, are given in Table 4. The signal assignments are based on the chemical shifts and spin/spin couplings, 2D NMR experiments and by comparison of the ^{1}H chemical shifts of related compounds (Scheme 41and Table 4).

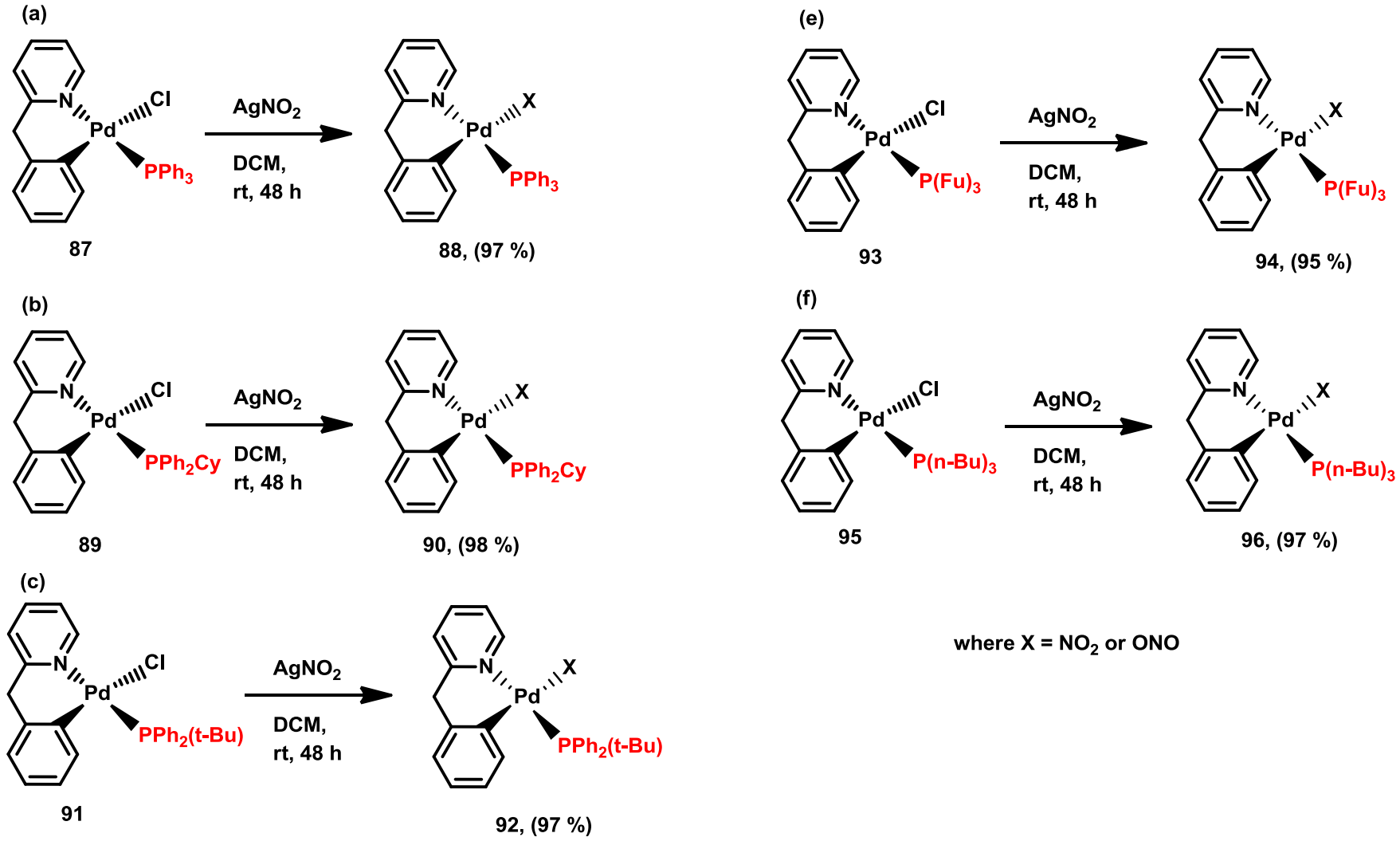

Scheme 41 Synthesis of novel nitrite-containing palladacycles of 2-benzylpyridine

4.5.1 NMR study of nitrito-palladacyclic complexes of 2-benzylpyridine

Coordination of the metal atom with a phosphine in complexes **87-96** (Scheme 41, and Table 4) results in a CH_2 protons splitting from a singlet within the ligand to a doublet (diastereotopic protons) with a large downfield shift seen for the equatorial proton at HCH_{eq} (δ 4.71-5.01 ppm) and large upfield shift for the axial proton H_{ax}CH (δ 3.97 – 4.08 ppm) with respect to complex **79**. Here, both protons of CH_2 are observed as a broad signal at upfield (δ 4.30 ppm).

However the dichotomy between complexes with 2-phenylpyridine with respect to 2-benzylpyridine is that, the ^{1}H coupling phosphorus has no profound effect on 2-benzylpyridine ligand compared to the 2-phenylpyridine, this may be due to the bulky nature of 2-benzylpyridine, see Table 4, where the proton *α* to nitrogen Py-H^1 shows the expected attribute of doublet (d) with the exception of complex **88** broad singlet (br.s) and **81** doublet of doublet (two doublet, dd), which is not observed in 2-phenylpyridine.

In the complexes **79** and **87-96** the protons on pyridyl moiety (py-H^1, py-H^2, py-H^3 and py-H^4) and phenyl moiety (ph-H^1, ph-H^2, ph-H^3 and ph-H^4) are matching the expected attribute with the exception of complex **90** where multiplets dominates the attributes. The proton *α* to nitrogen Py-H^1 of chloromonomer complexes are de-shielded with respect to their corresponding nitrito monomers (ca 0.60 ppm).

The δ of phosphorus in chloro bound complexes observed at lowfield with respect to nitrite complexes displays a profound difference between complexes containing chloro and ntrito with similar phosphine was observed in the complexes **87** and **88** (δ 35.26 ppm and 32.45 ppm, Δ 2.81 ppm), **89** and **90** (δ 36.83 ppm and 34.60 ppm, Δ 2.23 ppm), **91** and **92** (δ 54.75 ppm and 52.94 ppm, Δ 1.81 ppm), **93** and **94** (δ -

19.24 ppm and -22.17 ppm, Δ 2.93 ppm) and **95** and **96** (δ 21.14 ppm and 19.01 ppm, Δ 2.13 ppm) respectively.

Table 4 ^{1}H and ^{13}P NMR chemical shift (δ) data from the spectra of complexes **79** and **89-96**

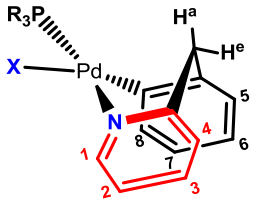

Comolexes	piph-CH_2	py-H^1	py-H^2	py-H^3	py-H^4	ph-H^5	ph-H^6	ph-H^7	ph-H^8	^{13}P
79	4.30 s	9.29 *dd*	7.14	7.68 *t*	7.41 *d*	7.07 *dd*	6.91 *td*	6.70 *td*	6.56 *dd*	--
87	4.90 *d*, 4.01 *d*	9.17 *d*	7.24 *ddd*	7.74 *ddd*	7.46 *d*	6.95 *dd*	6.66 *td*	6.62 *dr. s*	6.25 *td*	35.26
88	5.01 *d*, 4.08 *d*	8.55 *br. s*	7.15 *t*	7.74 *td*	7.50 *d*	7.02 *d*	6.74 *t*	6.33 *t*	6.48 *d*	32.45
89	4.91 *d*, 4.07 *d*	9.04 *d*	7.18 *dd*	7.71 *td*	7.45 *d*	7.06 *dd*	7.00 *ddd*	6.82 *td*	6.61 *t*	36.83
90	4.93 *d*, 4.07 *d*	8.40 *d*	7.15 *m*	7.73 *m*	7.73 *m*	7.03 *m*	6.88 *dd*	6.66 *t*	6.83 *d*	34.60
91	4.84 *d*, 3.95 *d*	9.25 *dd*	7.25 *dd*	7.72 *td*	7.41 *d*	6.77 *d*	6.4s8 *dd*	6.04 *t*	6.44 *ddd*	54.75
92	4.93 *d*, 3.99 *d*	8.52 *d*	7.73 *td*	7.13 *dd*	7.47 *d*	6.79 *d*	6.52 *td*	6.13 *t*	6.45 *ddd*	52.94
93	4.90 *d*, 4.00 *d*	9.24 *d*	7.22 *ddd*	7.70 *td*	7.42 *d*	6.99 *d*	6.78 *td*	6.48 *td*	6.84 *d*	-19.24
94	4.98 *d*, 4.05 *d*	8.75 *d*	7.23 *d*	7.75 *dd*	7.49 *d*	7.06 *d*	6.82 *m*	6.56 *dd*	6.87 *d*	-22.17
95	4.71 *d*, 3.97 *d*	9.00 *d*	7.18 *t*	7.69 *t*	7.40 *d*	7.04 *d*	7.28 *dd*	6.85 *m*	6.90 *d*	21.14
96	4.80 *d*, 401 *d*	8.53 *d*	7.13 *m*	7.71 *td*	7.44 *d*	7.04 *dd*	7.23 *ddd*	6.71 *m*	6.92 *dd*	19.01

Note: multiplets, are given as a centre point average; NMR standard (5.32 ppm) is residual CH_2Cl_2.

The ^{13}P NMR chemical shift is indicative of the phosphine ligand within the complexes (Figure 20) – complexes containing $P(Fu)_3$ **93** and **94** appeared at higher field (upfield) δ = -19.24 and -22.17 ppm with difference of chloro- to nitrito- Δδ = -2.93, complexes **95** and **96** containing [$P(n\text{-}Bu)_3$] appeared at 21.14 and 19.01 ppm and Δδ of Cl- to NO_2- = 2.13, while complexes **91** and **92** containing [PPh_2(t-Bu)] appeared at low field (downfield) δ = 54.75 and 52.94 with Δδ = 1.81. However, complexes containing PPh_3 and PPh_2Cy show similar properties, which both coordinated to phosphine with a cyclic six membered ligand through a quaternary carbon – complexes **89** and **90** δ = 36.83 and 34.60 with Δδ = 2.23, complexes **87** and **88** δ 35.26 and 32.45 with Δδ = 2.81. These values differentiate between the complexes containing Cl- and NO_2- (Figure 20).

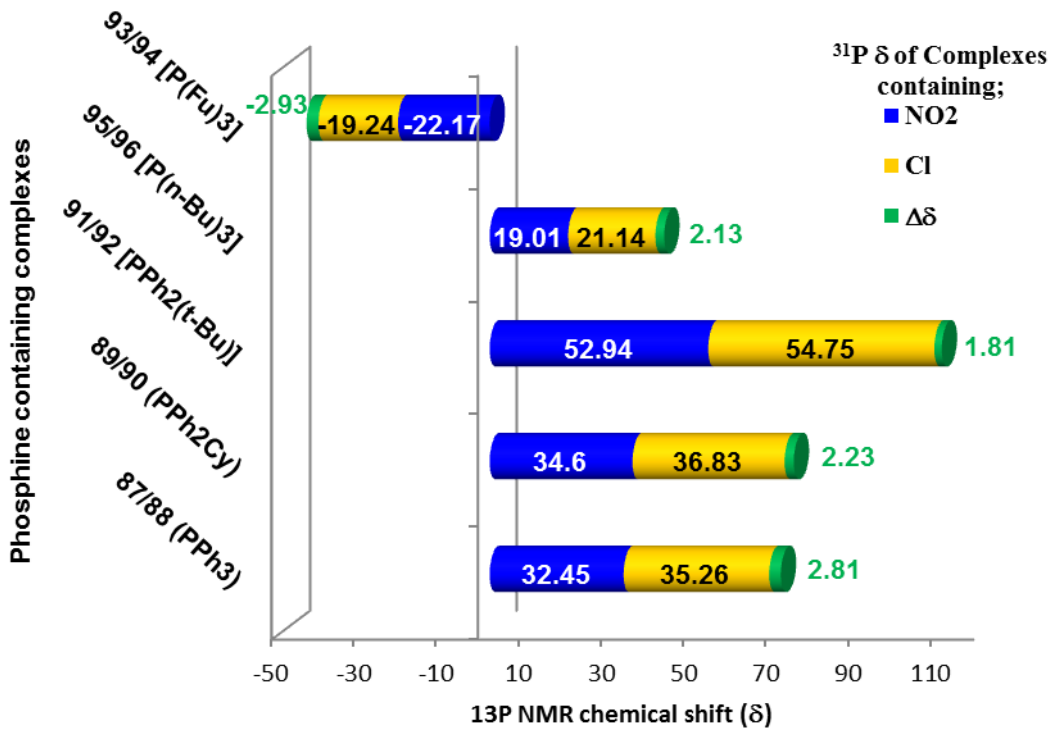

Figure 20 ^{13}P NMR chemical shift (δ) data from the spectra of complexes **87-96**

4.5.2 Single crystal study of nitrito-palladacyclic complexes of 2-benzylpyridine

From the X-ray crystallographic data it can be noticed that the palladacyclic complexes are square planar geometries at the palladium centre and the phosphorus atom is in *trans* position to the donor N atom. The angle P–Pd–N varies from 166.79 to 174.73˚ and Pd–N bond length varies from 2.093-2.1119 Å, complex **91** bond length of Pd centred are longer with respect to its nitrito counterpart **92** (Table 5). When the phosphine ligand is similar, *e.g.* complexes **91** and **92**, there is an increase in the P–Pd–N bond angles 171.57˚ and 173.25˚ and a decrease in the N–Pd–X bond angles (89.77˚ and 87.72˚). For complex **93**, having a $P(Fu)_3$ ligand, the C-Pd-X 175.13˚ and P-Pd-N 174.73˚ increase by a margin of *ca.* 3˚ and 2 ˚ respectively and a decrease in N-Pd-X (92.98˚) bond angles by ca. 5˚, with respect to complexes **88-92**. See the crystallographic data for the complexes **88-94**, are also summarised in Figure 21.

Table 5 Selected bond lengths (Å) and bond angles (º) for complexes **88-93**

Lengths/Angles	**88** (ijsf1209)	**89** (ijsf1215)	**90**(ijsf1217)	**91** (ijsf1216)	**92** (ijsf1218)	**93** (ijsf1314)
Pd-C Å	2.017(2)	2.0183(18)	2.0004(18)	2.0077(12)	2.0070(18)	2.006(2)
Pd-P Å	2.2568(6)	2.2846(5)	2.2667(5)	2.2791(3)	2.2743(5)	2.2413(7)
Pd-N Å	2.1166(17)	2.0982(15)	2.1067(16)	2.1119(11)	2.081(12)	2.093(2)
Pd-X Å	2.219(3)	2.3891(5)	2.1332(19)	2.4046(4)	2.1061(15)	2.3978(6)
C-Pd-N °	86.60(8)	81.13(7)	86.18(7)	84.55(5)	84.51(7)	85.61(9)
C-Pd-P °	92.02(6)	92.57(5)	90.69(6)	87.06(4)	87.20(5)	91.88(7)
C-Pd-X °	171.69(9)	170.15(5)	173.88(8)	171.32(4)	169.1(4)	175.13(7)
P-Pd-N °	175.79(5)	171.57(4)	173.25(5)	166.79(3)	166.93(5)	174.73(6)
P-Pd-X °	93.08(7)	96.842(16)	95.42(5)	100.978(12)	100.9(4)	92.98(2)
N-Pd-X °	88.75(8)	89.77(5)	87.72(7)	88.09(3)	88.7(4)	89.51(6)

X = Cl for **89**, **91** and **93**; X = N for **88**, **90** and **92**

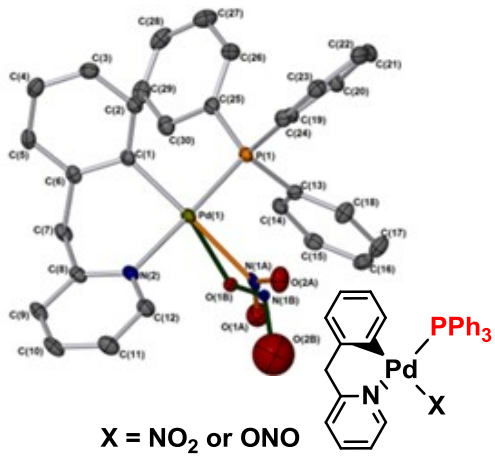

A Single crystal X-ray diffraction structure of **88** with a mixture of N- and O-bonded NO_2 forms

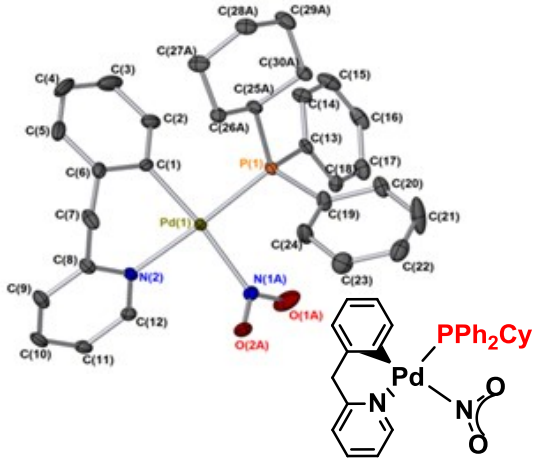

A Single crystal X-ray diffraction structure of **90** with only N- bonded NO_2 forms

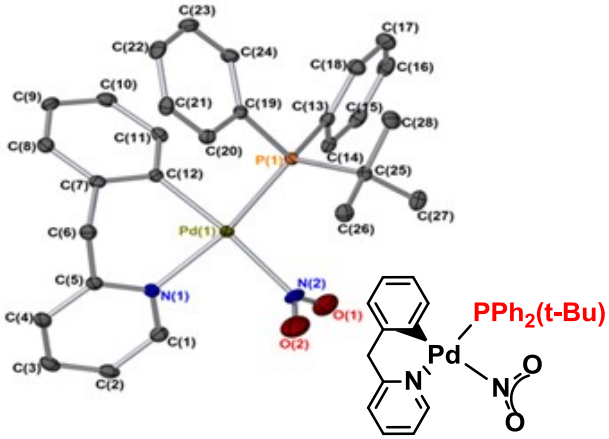

A Single crystal X-ray diffraction structure of **92** with only N- bonded NO_2 forms

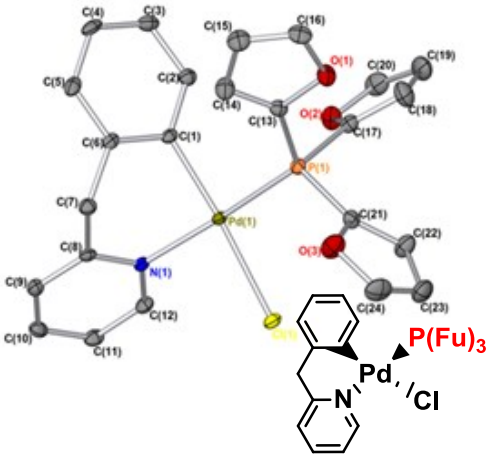

A Single crystal X-ray diffraction structure of **93**

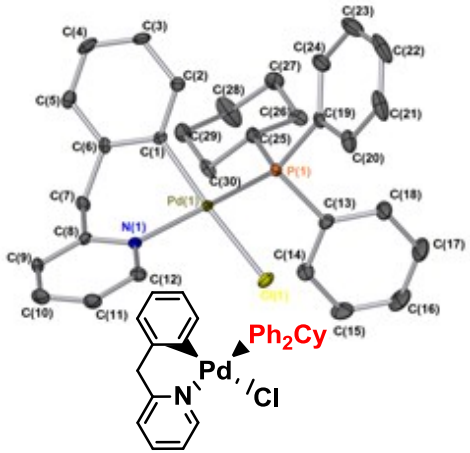

A Single crystal X-ray diffraction structure of **89**

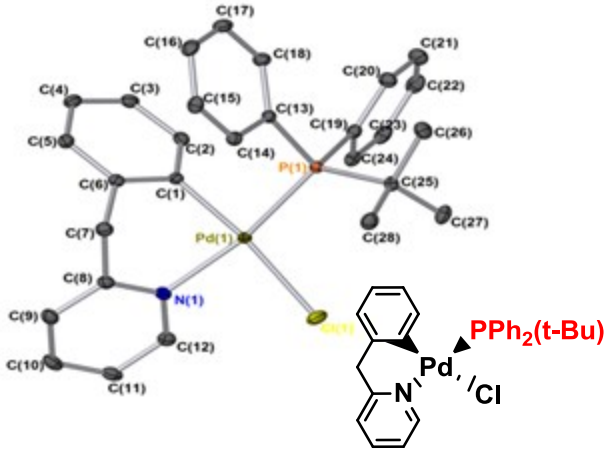

Single crystal X-ray diffraction structure of **91**

Figure 21 Single crystal X-ray diffraction structures of complexes **88-93**.

4.5.3 Pd-catalysed C–H bond functionalisation processes

Nitroaromatic compounds are of great importance to both the pharmaceutical industry and academia.[123] The C-H bond activation/functionalisation of ligands involved in this study is the key test to catalytic activity of the Pd complexes synthesised in this thesis. The potential C-H bond acetoxylation reaction process with the complexes prepared in this thesis is under investigation within the Fairlamb group in York, and believed to proceed *via* a $Pd^{(II/III)}$ or $Pd^{(II/IV)}$ C-H bond functionalisation pathway as shown in Scheme 44. However, the potential application of these complexes is the formation of C–N bonds (sp^2 C-H bonds to form nitroaromatic compounds) *via* reductive elimination of Pd–NO_2 complexes was noted. It was anticipated that reductive elimination is the key to forming carbon–carbon and carbon–heteroatom in the majority of metal-catalysed transformations, and reductive elimination processes from both $Pd^{(II)}$ and $Pd^{(IV)}$ (Scheme 42)

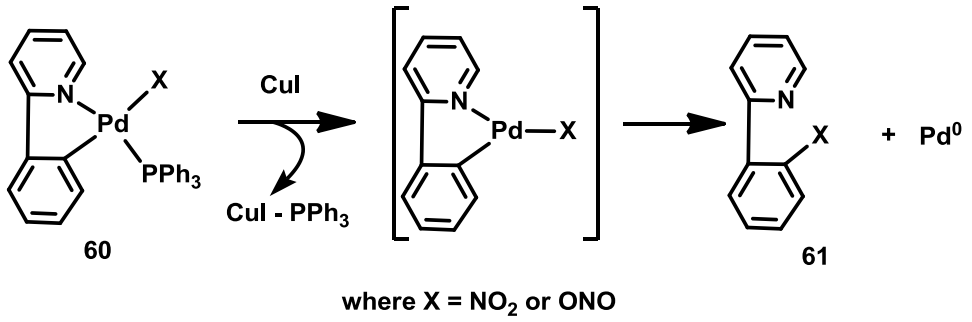

Scheme 42 Anticipated reductive elimination via complex **60** with CuI

4.5.4 Pd Cat. C-H bond activation the dichotomy between nitration vs acetoxylation

Liu and co-workers,[124] reported palladium-catalyzed nitration of 8-methylquinolines **1** with t-BuONO to give 8-nitromethylquinolines **2** in a good yields, involving sp^3 C−H bond activation, their report examined the nitrite source and atmospheric

conditions; $NaNO_2$, $AgNO_2$ and KNO_2 supressed the formation of product with respect to t-BuONO under an atmosphere of dioxygen at 1 atm. (Scheme 43).

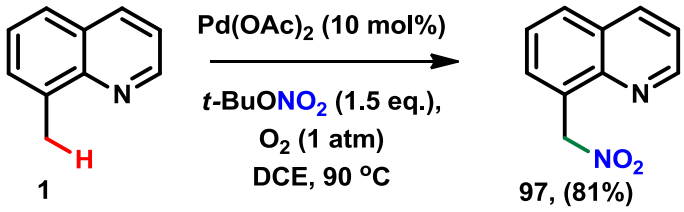

Scheme 43 Example demonstrating the catalytic nitration reaction by Liu and co-workers,[124]

The above observation Liu and co-workers,[124] proves that the nitrite source has profound effect in enhancing the nitration reaction. The Fairlamb group (Dr. Margot Wenzel and Philippa Owens) set $Pd(OAc)_2$ (**c**) as the benchmark catalyst to evaluate the aerobic oxidation of **1** to give **2** in Scheme 44. Although the catalyst has excellent activity, using 1 eq. of $NaNO_3$ (Figure 22), complexes (**a**) to (**d**) are less catalytically competent with respect to $NaNO_3$. The dinuclear $Pd^{(II)}$ complexes (**d**) and (**c**) showing a relatively similar reactivity profile. The PPh_3-containing complex (**a**) is also a viable catalyst, with (**b**) being more active under the conditions using 0.1 eq. of $NaNO_3$ with respect to (**a**) (Figure 22).

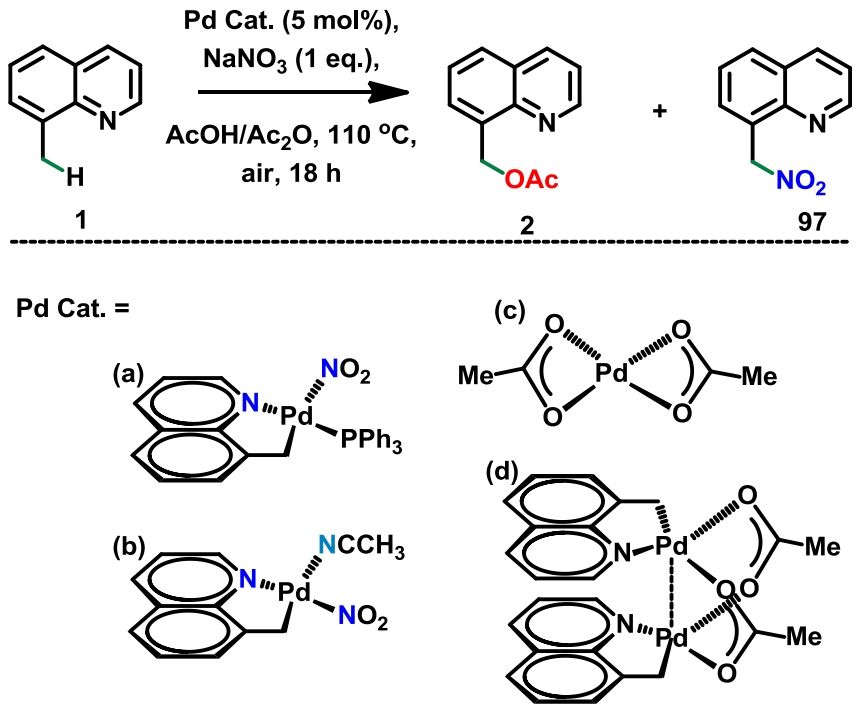

Scheme 44 Acetoxylation of **1** to **2** and a possible nitration side product **97**

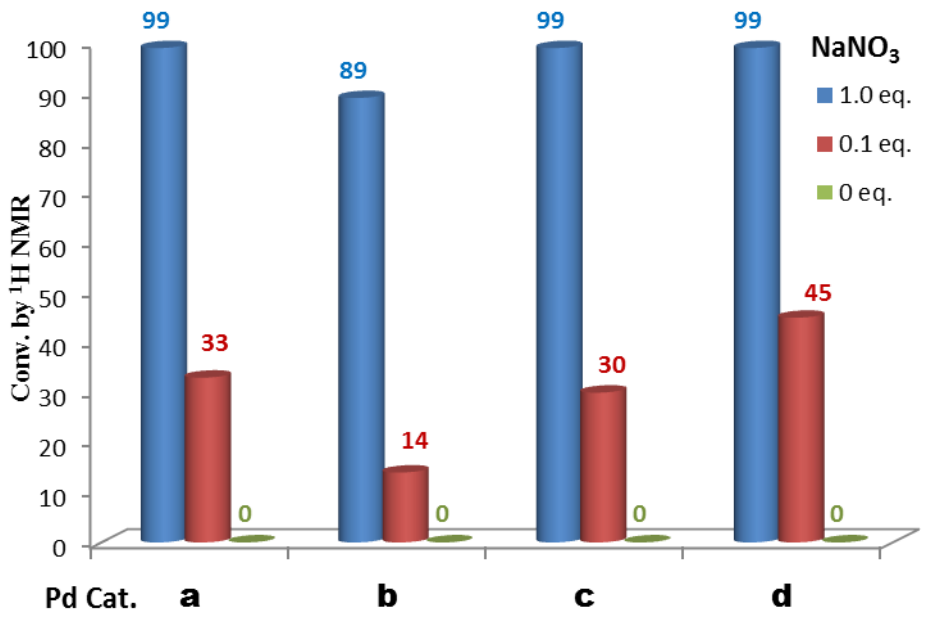

Figure 22 Catalytic activity of Pd complexes. (**a**) and (**b**) with respect to (**c**) and (**d**) (5 mol%) with varying equivalents of $NaNO_3$, in the aerobic oxidation of compounds **1- 2**.

4.6 Conclusion

A series of novel palladacyclic complexes have been prepared, with differing C^N ligands **60**, **68 - 73**, **82-85** and **88-96**. The work allowed a greater understanding of the cyclopalladation behaviour of several C^N ligands to be gained. Furthermore, the successful synthesis and characterisation of a series of C^N palladacyclic complexes containing nitrite and nitrite ligands has paved the way into understanding how NO_2 interacts with $Pd^{(II)}$. When assessing the role that such ligands can play in catalysis, and in particular the potential for reductive elimination of useful "C–NO_2" type products, the geometry and linkage isomerism of the complexes is of paramount importance. However, for more bulky phosphine ligands, monomeric $Pd^{(II)}$ complexes could be characterised by NMR spectroscopy, however crystallisation of N^C (2-phenylpyridine) with bulky phosphines (PPh_2Cy and PPh_2(t-Bu)) **69** and **71** upon crystallisation yielded novel $Pd^{(II)}$ dimer complex **74**, where the bulky ligand had been ejected and the μ^2-nitrito ligand is found bridging two $Pd^{(II)}$ centres. This was only seen where C^N = 2-phenylpyridine and not for 2-benzylpyridine (Figure 13 and Figure **14**)

Calculated free energy values suggest that the energy difference between *cis* and *trans* geometric isomers with respect to the pyridyl moiety in the complexes studied increases with increasing steric bulk of the C^N ligand and reductive elimination experiments, where elimination of C–NO_2 type products, which would normally require the two ligands being eliminated to be mutually *cis*, was not observed. The crystal structure of all the nitrite complexes prepared in this thesis showed a mixture of N- and O- bound linkage isomers.

Chapter 3 Manganese catalysed C-H alkenylation / Diels-Alder Reactions

5.1 Introduction

The nucleophilic addition of species generated by C-H activation,[125] has been widely investigated at palladium,[126] rhodium,[127] rhenium,[128] and nickel.[69] It has however been difficult to mediate such reactions with first-row transition metals. In a recent report, Chen and co-workers[69] showed that environmentally-friendly Mn^{I} mediates a catalytic C-H alkenylation of 2-phenylpyridine derivatives, by a highly chemo-, regio- and stereoselective reaction with terminal alkynes in diethyl ether at 100 °C (Scheme 45).

Indeed, intermediate structures proposed by Chen and co-workers (Scheme 45) in Mn^{I}-mediated C-H bond activation reactions (intermediate) are often speculative and unsubstantiated by experimental evidence.

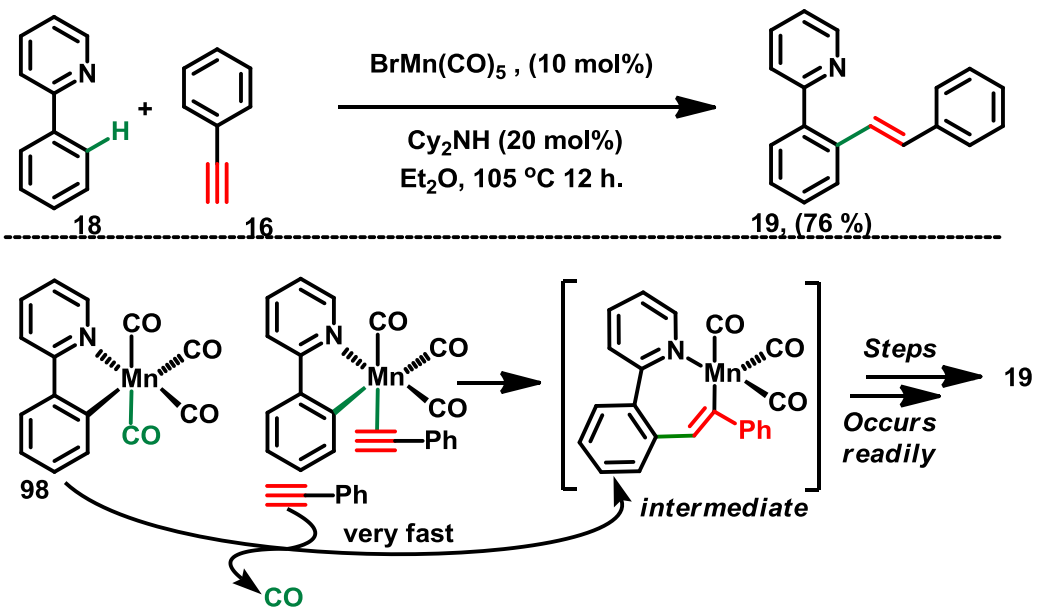

Scheme 45 Chen and co-workers alkenylation process[69]

A number of related manganese-mediated C-H functionalisation processes have been reported,[69] which have been proposed to proceed *via* the intermediacy of manganacycles related to **98**. Complex **98** has been of interest to the Fairlamb group because it acts as a source of therapeutic CO,[129] in addition to synthetic applications,[130] specifically the regioselective alkenylation of biologically-relevant 2-pyrones, which is currently limited to Pd.[131] Structural details on reaction intermediates relating to protonation and reductive elimination, from **18** to **19**, has been missing. The pyridyl-directing group exerts a profound effect in determining alkenylation regioselectivity. 2-Phenylpyrazine **99** is altered by a second nitrogen atom *para* to the nitrogen-directing group.

Compound **99** was synthesised via a Suzuki cross-coupling reaction. The five-membered manganacycle **100** was formed in a 62 % yield by cyclometallation of **99** with $BnMn(CO)_5$ – the reaction confirmed that the nitrogen in the *ortho*-nitrogen acted as the directing atom (Scheme 46).

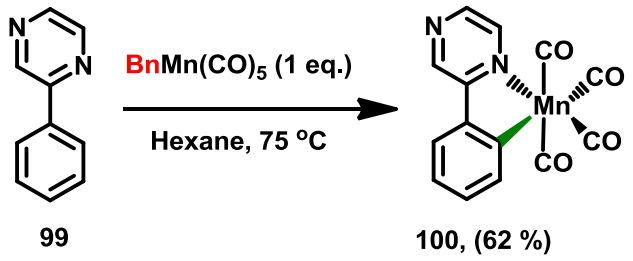

Scheme 46 Novel five-membered manganacycle 100

The *E/Z* isomerisation is possible in manganese-catalysed alkenylation, as it often occurs in the transition metal catalysed hydroarylation of alkynes.[131, 132] A proposed mechanistic scheme is shown in Scheme 47, involving several intermediates (**I-III/III'**). Isomerisation is possible within the key seven-membered manganacycle

III. This could equilibrate with a manganese carbene complex **II**, via path A. This can afford a *E*-isomer by protonation with alkyne.[133] Another possibility is the homolytic cleavage of the *C*vinyl-Mn bond in **I**, followed by isomerisation giving **III'**. Reformation of the *C*vinyl-Mn bond **I** (path B) can also deliver the *E*-isomer.

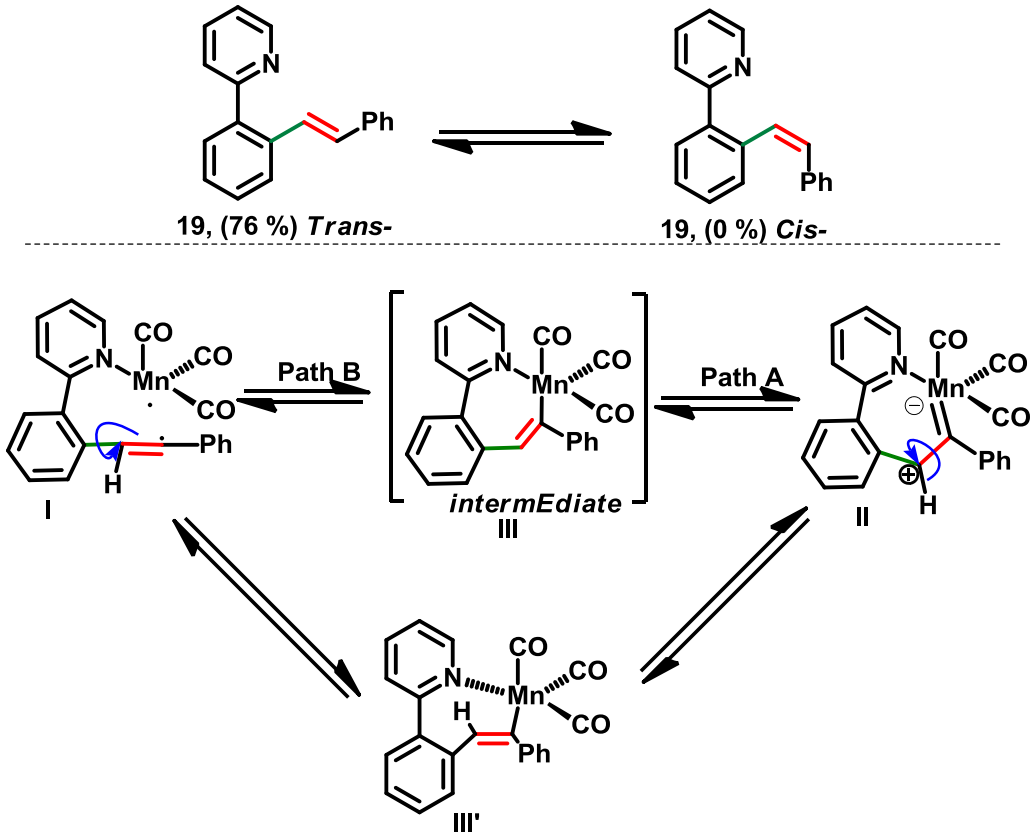

Scheme 47 Possible pathways for *E*/*Z* isomerization

Chen and co-workers also reported, based on DFT calculations,[69] that the step of insertion of phenyl acetylene into the Mn-*C*aryl bond, leading to **III,** favoured the *anti*-Markovnikov addition product **Iva**, which is more stable than the Markovnikov addition product **IVb** by 5.1 kcal/mol (Figure 23).[69] Alkyne insertion mediated by $Cy_2NH_2^+$ **IVd**, to generate the final alkenylation product, is disfavoured due to a higher energy barrier (2.3 kcal/mol) with respect to direct insertion with phenyl acetylene **IVc** (Figure 23b).[69]

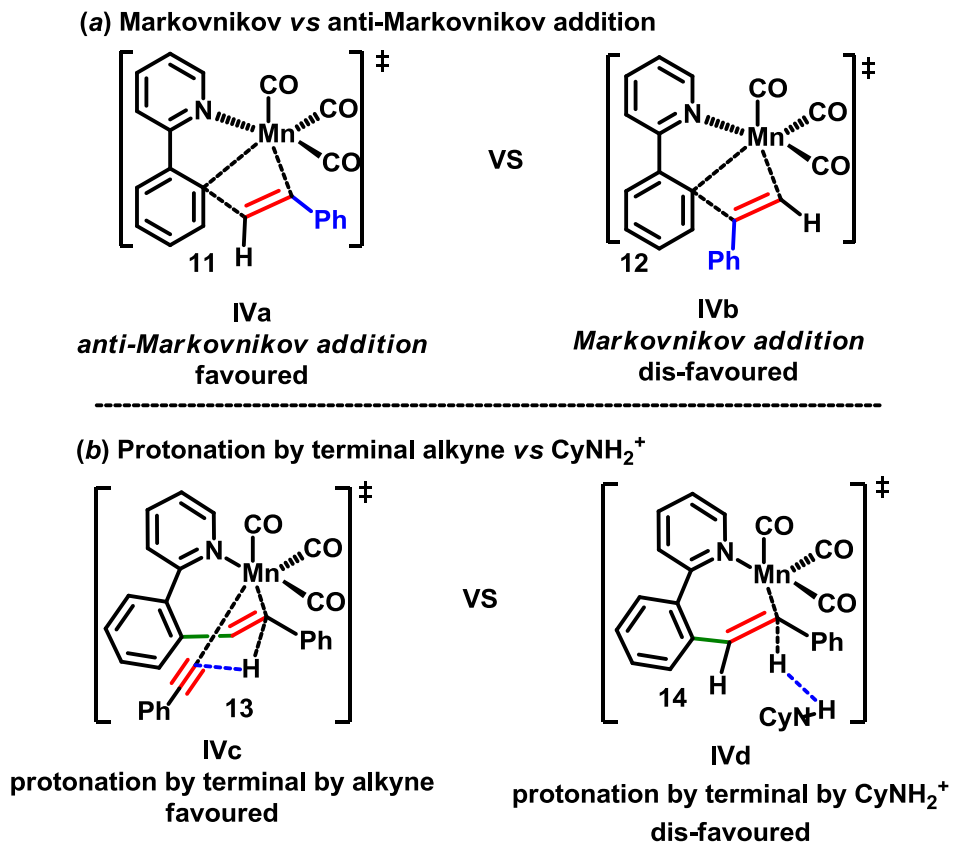

Figure 23 Markovnikov and anti-markovnikov addition vs protonation by terminal alkyne and $CyNH_2^+$ possibilities

5.2 Synthesis of 4-(2'-pyridyl)-6-methyl-2-pyrone derivatives 81 and 104

Based on the experimental evidence above, the investigation focused on the use of the 4-(2'-pyridyl)-6-methyl-2-pyrone **81** moiety as the nitrogen-directing group. This novel compound is available *via* Negishi cross-coupling of 4-bromo-6-methyl-2-pyrone[134] **103** with PhZnCl **102**, formed by lithiation of **101**, mediated by $Pd(PPh_3)_4$ (Scheme 48).

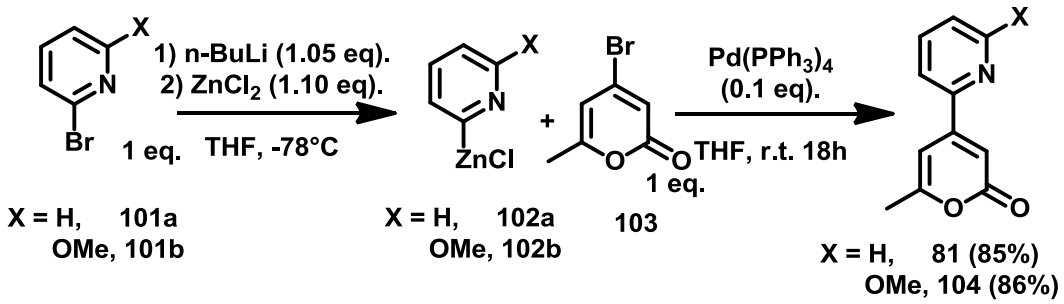

Scheme 48 Negishi cross-coupling reactions of 4-bromo-6-methyl-2-pyrone **103** with pyridyl zinc reagents **102a** and **102b**

5.3 Synthesis of five membered manganacycles

Given the intermediates proposed in Scheme 45 (page 102) the related complexes **81** and **104** were synthesised. Compounds **81**, **104a** and **104b** were used in a mangana-cyclometallation reaction with $BnMn(CO)_5$, in a stoichiometric reaction to give a five membered manganacycle **105a** and **105b** (Scheme 49). The direct reaction of **81** with $BnMn(CO)_5$ in hexane at 75 °C gave **105a** in 96% and **105b** 98% yield. The complexes were characterised by spectroscopic methods, and a single crystal was subjected to X-ray diffraction (Figure 24), which showed that regioselective C3 C-H bond activation had taken place.

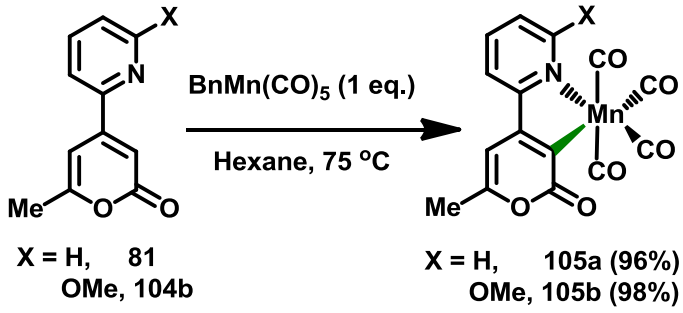

Scheme 49 Stoichiometric reaction of $MnBn(CO)_5$ with 2-pyrone **104** affording five-membered manganacycle **105a** and **105b**

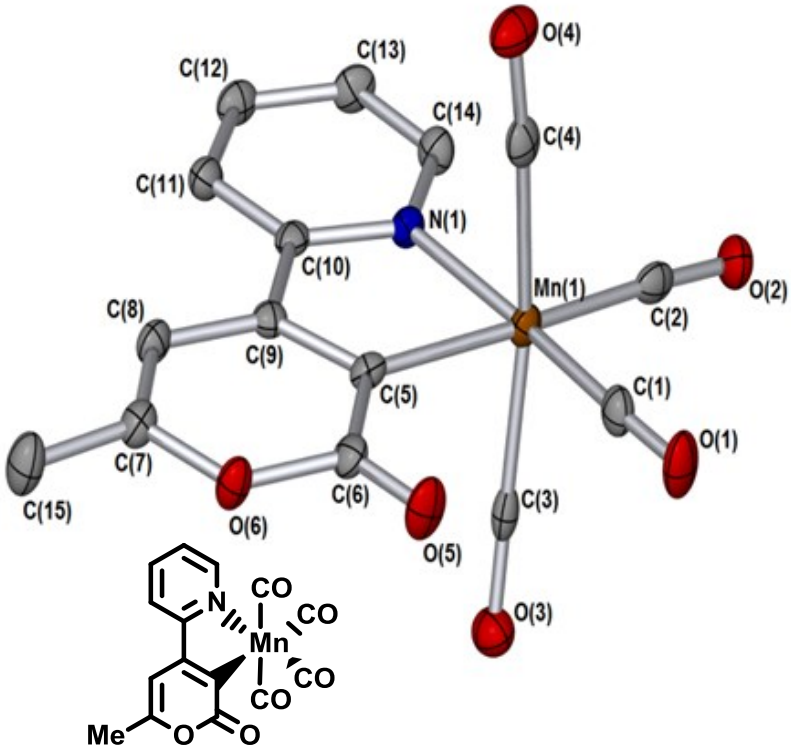

Selected bond lengths (Å) of **105a**: C1-Mn1 = 1.817(3), C2-Mn1 = 1.827(3), C3-Mn = 11.842(3), C9-C10 = 1.467(3), C4-Mn1 = 1.866(3), C10-N1 = 1.353(3), C5-Mn1 = 2.042(2), Mn1-N1 = 2.0651(19)

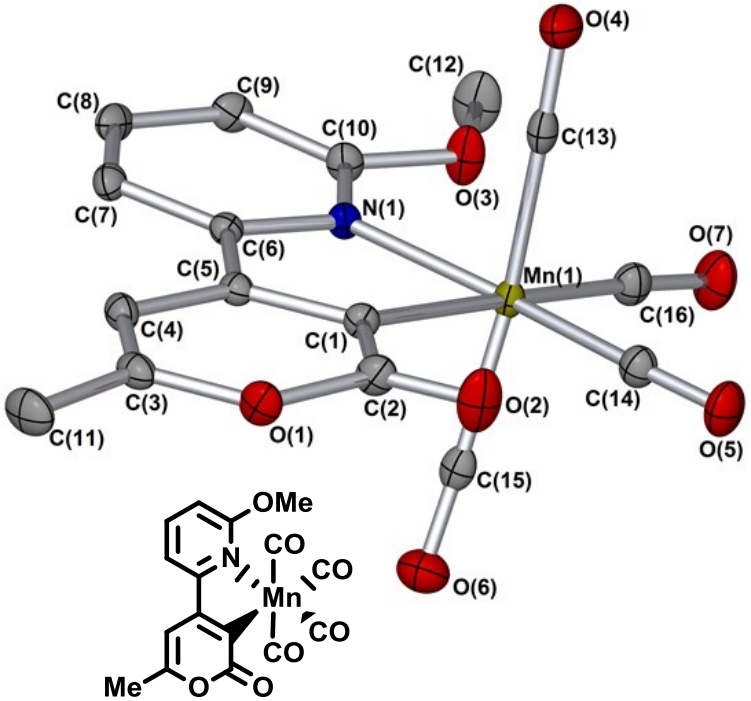

Selected bond lengths (Å) of **105b**: Selected bond lengths (Å) of 104b: C1 - Mn1 = 2.0357(15), C13-Mn1 = 1.8487(17), C14-Mn1 = 1.8097(16), C15--Mn1 = 1.8617(17), C5-C6 = 1.464(2), C16-Mn1 = 1.8396(17), C6-N1 = 1.3645(18), Mn1-N1 = 2.1032(13), C1-C5 = 1.363(2)

Figure 24 X-ray crystal structures of **105a** and **105b** (note: arbitrary atom numbering used and thermal ellipsoids set to 50%; H-atoms omitted for clarity).

5.3.1 C-H bond alkenylation

Chen *et al.*[69] described their conditions for the 2-phenylpyridine alkenylation by heating 2-phenylpyridine **18** and phenylacetylene **16**, catalysed by $BrMn(CO)_5$, with or without amine in Et_2O.[69] Using the pyrone moiety surprisingly, these conditions did not produce the expected product **106**. In work initially conducted by an Erasmus exchange student, Conrad Wagner, the product obtained was a stable six membered manganacycle **107** (Scheme 50). The ^{1}H NMR spectra of **107** (acetone-d_6, 400 MHz) exhibited a new resonance at δ 5.79 as a singlet. An equivalent reaction, run with PhC≡^{13}CH, confirmed that this proton was directly connected to the ^{13}C label ($^1J_{CH}$ = 181 Hz). The most characteristic information was obtained from the ^{13}C NMR spectra of the unlabelled product which showed four unusual but characteristic carbon environments (at δ 62.0, 77.2(*), 85.8 and 92.0) (* denotes enriched in ^{13}C-label). The observation indicates that the Mn atom is bound to four contiguous carbon centres in an η^4-coordination mode **107**.

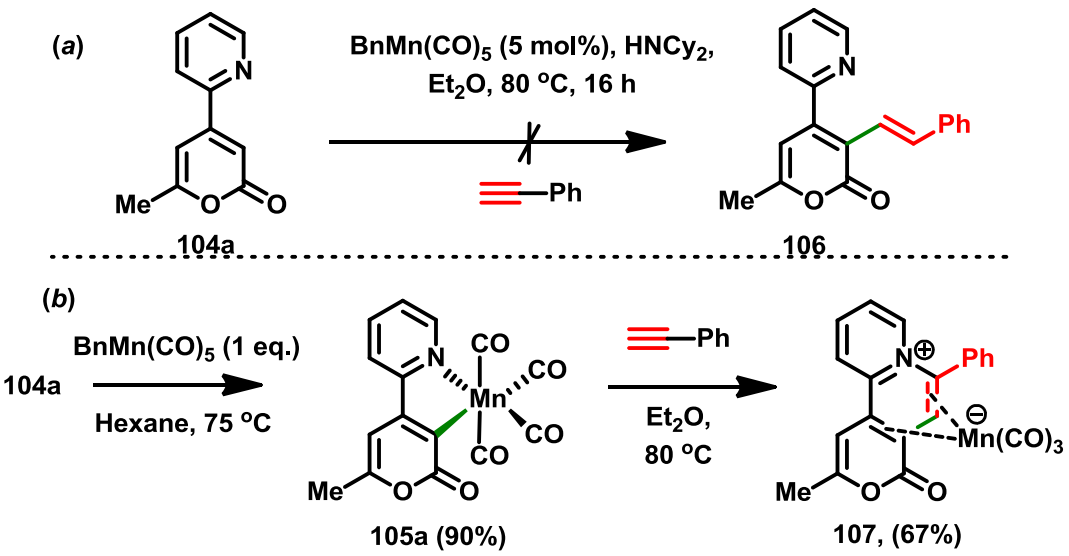

Scheme 50 Unexpected alkyne insertion giving cyclomanganesiated complex **107**

Crystallisation of **107** from acetone-d_6 gave single crystals suitable for X-ray diffraction, which confirmed its structure (work conducted by a summer project student, Magdalene Teh, Figure 25).

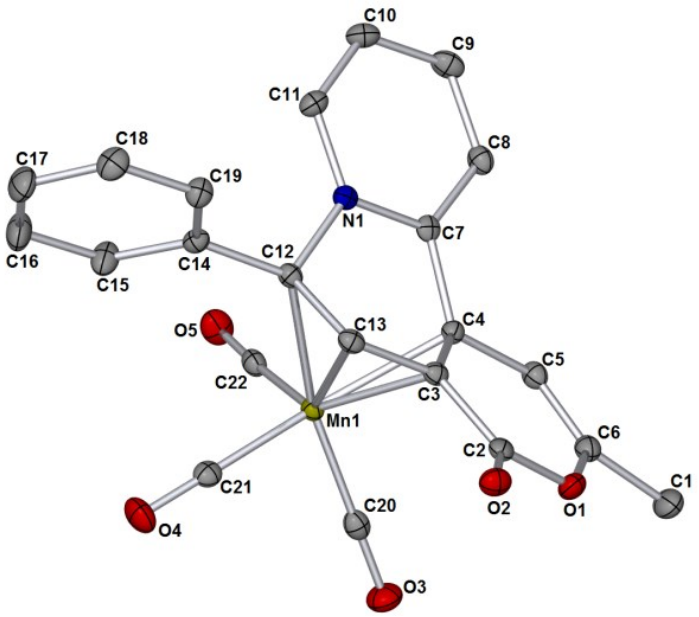

Figure 25 X-ray crystal structure of 2-methyl-4-oxo-6-phenyl-4*H*-3,7λ^5-pyrano[4,3-a]quinolizin-7-ylium-η^4-3,3a,5,6-tricarbonylmanganesuide **107** (note: arbitrary atom numbering used). Selected torsion angles (°), bond angles (°) and bond lengths (Å): C4-C3-C13-C12 = 4.2(2), C3-C4-C7-N1 = -38.4(2), N1-C12-C13-C3 = 44.4(2); C13-C12-N1 = 114.38(14), C3-C4-C7 = 116.31(15); C3-Mn1 = 2.0769(17), C4-Mn1 = 2.1843(17), C12-Mn1 = 2.1060(18), C13-Mn1 = 2.0908(18) (Figure prepared by Ian Fairlamb).

5.3.2 Density functional theory (DFT) evaluation for 107

The mechanistic steps leading to the formation of **107** were evaluated using density functional theory by Dr. Jason Lynam in York. Starting from **I** (Figure 24), formed via loss of a CO ligand from **19a**, insertion of the coordinated alkyne into the Mn-C(pyrone) bond proceeds through a low energy transition state **II** to give **III**. Carbon-nitrogen reductive elimination from **II**, *via* transition state **IV**, results in the formation of the 2-methyl-4-oxo-6-phenyl-4H-3,7λ^5-pyrano[4,3-a]quinolizin-7-ylium ring system. An analysis of **IV** revealed that the imaginary eigenvector led to

107' (coordination isomer of **107**); a π-slip (not modelled) would lead to **107**(Figure 26).

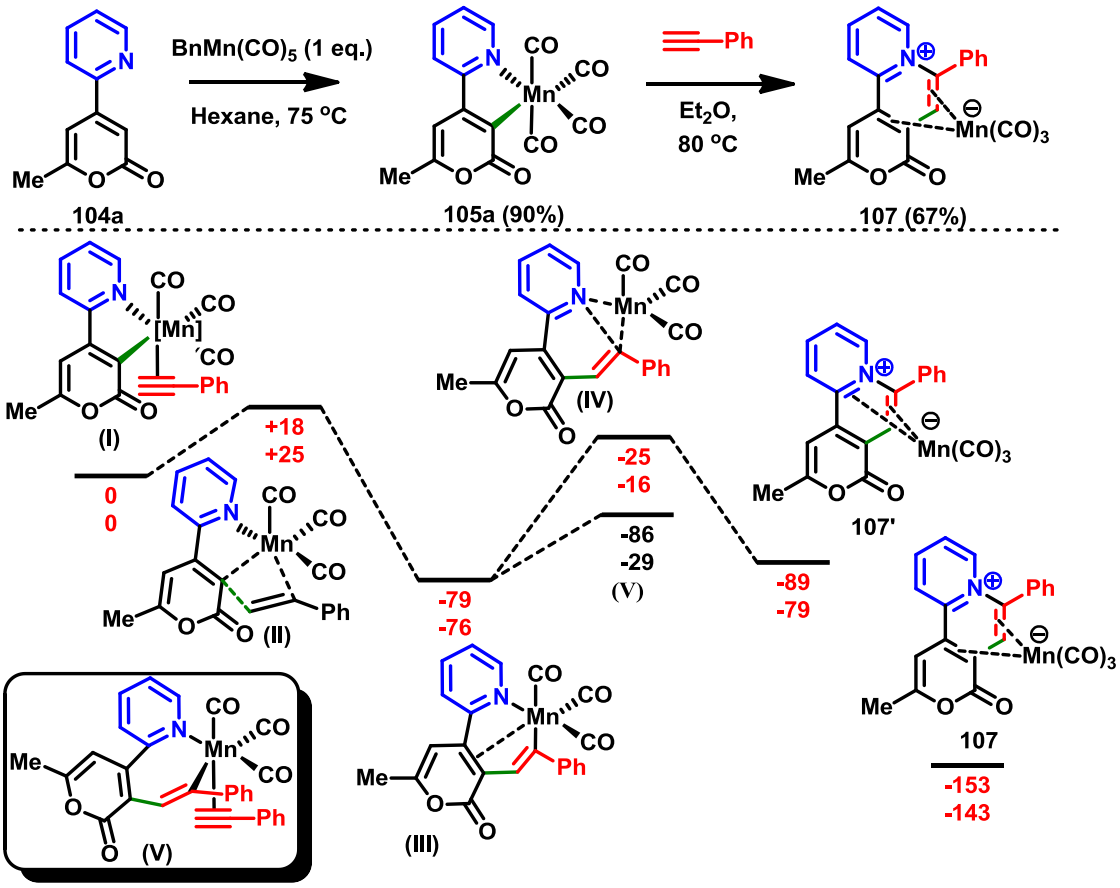

Figure 26 Density functional theory (DFT) showing potential energy surface for the formation of **107**; Energies are zero point-corrected electronic energies (top) and Gibbs free energies at 298.15 K (bottom) in kJ mol^{-1} at the PBE0-D3/def2-TZVPP//BP86/SV(P) level with solvation corrections applied in Et_2O (COSMO, ε = 4.33 for Et_2O at 25 °C).

A series of experiments were conducted to gain evidence for reaction intermediates. Taking 10 mg of **105a** with 1.1 equivalents of phenylacetylene, dissolved in d_8-THF (0.5 mL), the reaction mixture was cooled to 243 K. UV light was used to irradiate the sample at 243 K for 15 mins. NMR simulation of the reaction mixture reveals signals corresponding to **107**. However further irradiation reveals new signals. These may be due to the formation of the intermediate (**III**). The intermediate (**III**)

detection was conducted in collaboration with Kate Appleby, who did the NMR analysis and photochemical measurements (Figure 27).

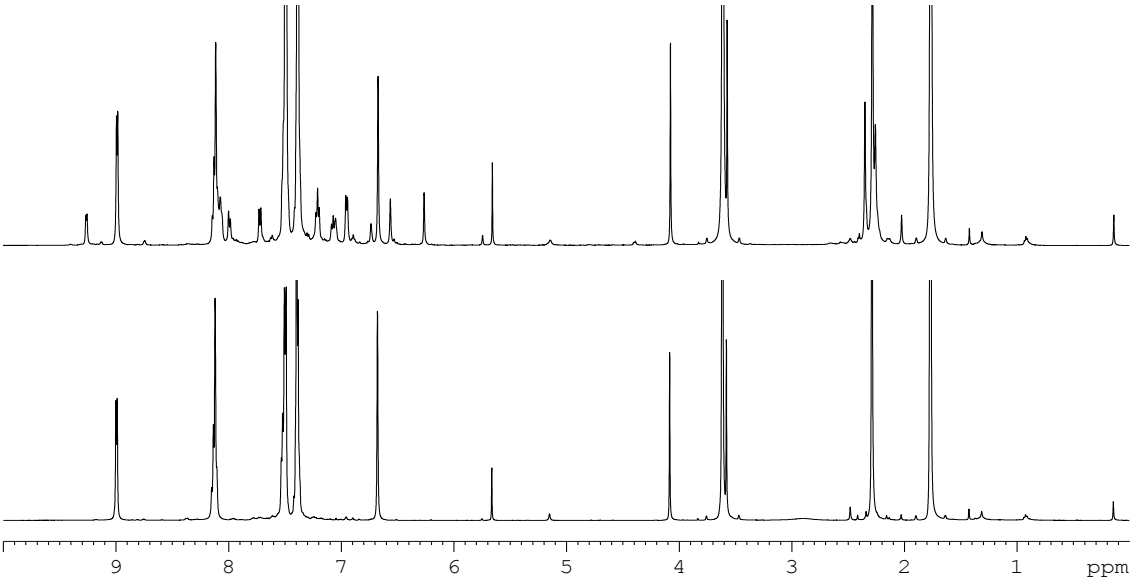

Figure 27; ^{1}H NMR spectra of the manganese starting material **105a**. and the solution after 15 min irradiation with UV light (above). New signals belong to the intermediate (**III**).

2D NMR paves the way in confirming the proposed intermediate (Figure 28). LIFDI-MS analysis confirmed a radical cation at *m/z* 427 $[M]^{+}$. ESI-MS also showed a pseudomolecular ion $[MH]^{+}$ at *m/z* 428, with MS-MS analysis revealing loss of CO *m/z* 400 $[MH\text{-}CO]^{+}$. Warming of the solution of (**III**) to room temperature led to formation of **107**, confirming (**III**) as a viable intermediate (Figure 28).

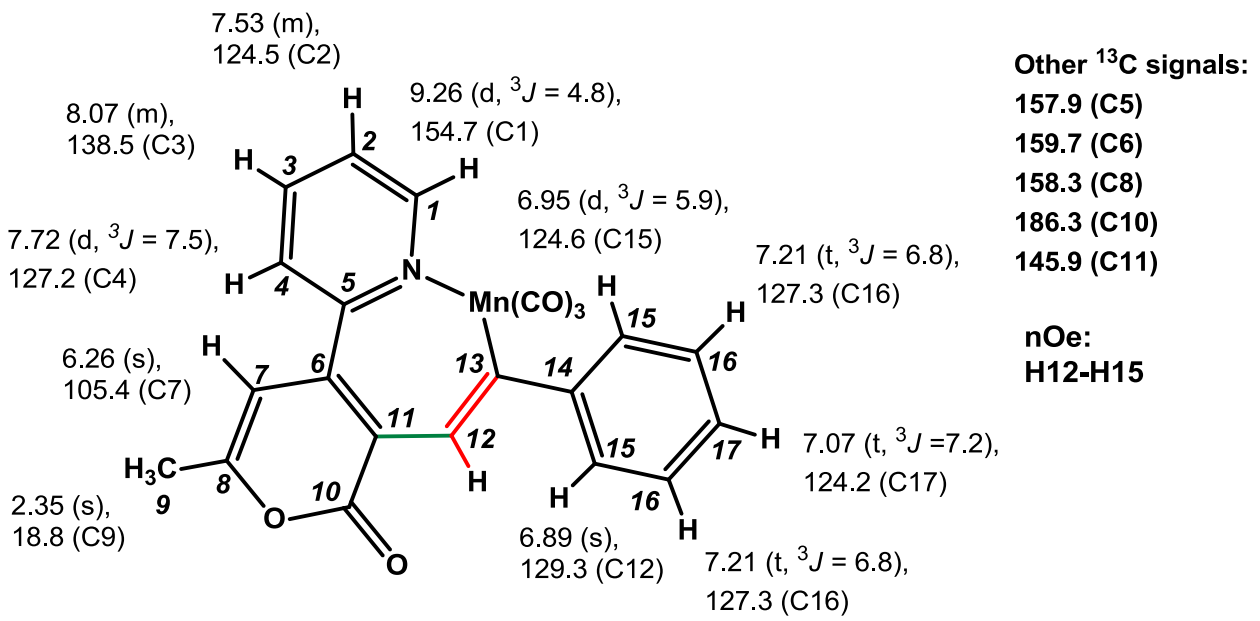

Figure 28 Correlation methods (HMQC and HMBC) and selective nOe experiments confirmed intermediate (**III**) (Figure prepared by Kate Appleby and Ian Fairlamb).

DFT calculation of corresponding potential energy surface for the phenyl-substituted system (Figure 29) revealed similar pathway was viable. In this case insertion of alkyne remains a barrier between the two as 2-pyrone moiety is slightly greater in Gibbs energies relative to the respective compound **I** = +25 kJ mol^{-1} versus (**Ia** = +34 kJ mol^{-1}) and that **III** was higher in energy than **111a** (-76 kJ mol^{-1} versus -95 kJ mol^{-1}). Therefore, the energetic spans for reductive elimination are 60 kJ mol^{-1} (2-pyrone) and 129 kJ mol^{-1} (phenyl). When compared with the formation of **Va** and **V**, *i.e.* the next steps in forming of **19** and **106** respectively, it is evident that the reductive elimination to form **107** is competitive, but in the case of intermediate **V** in Figure 29, the much larger energetic span to reductive elimination allows for productive catalysis via **Va**.

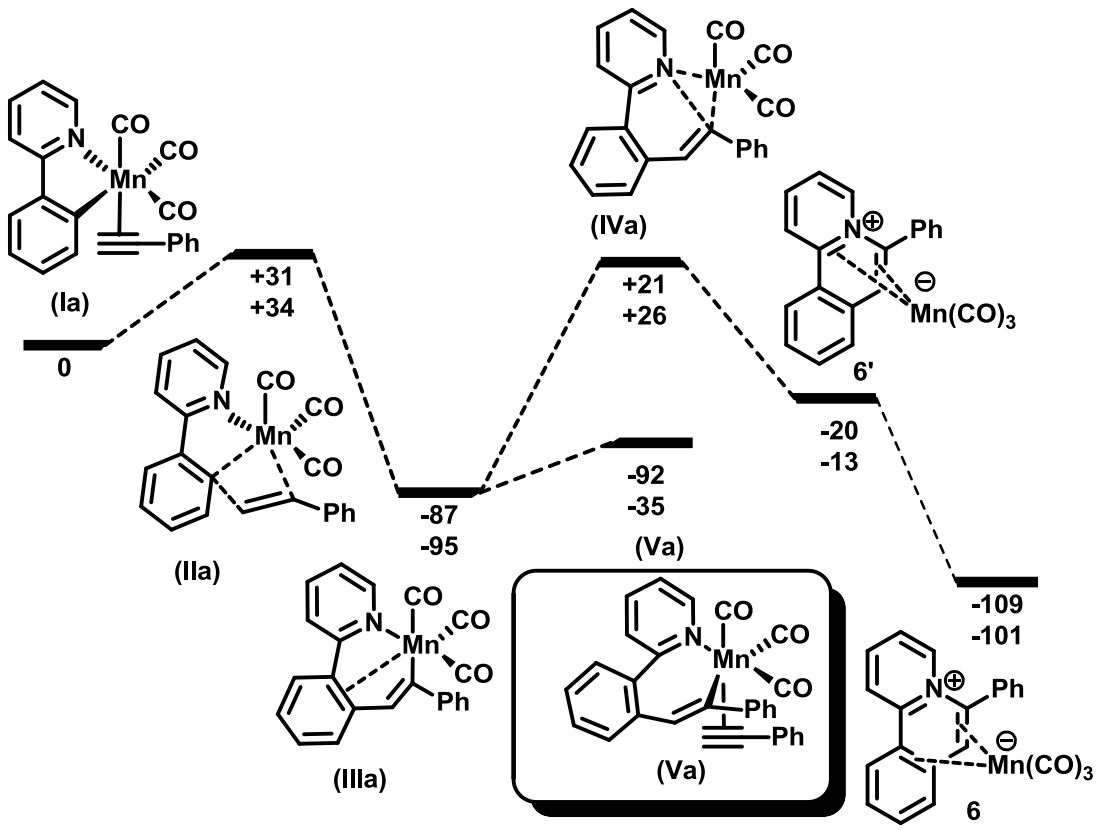

Figure 29 Density functional theory (DFT) showing Potential energy surface for the formation of **IIIa**; Energies are zero point-corrected electronic energies (top) and Gibbs free energies at 298.15 K (bottom) in kJ mol^{-1}at the PBE0-D3/def2-TZVPP//BP86/SV(P) level with solvation corrections applied in Et_2O (COSMO, ε = 4.33 for Et_2O at 25 °C)

5.3.3 Alkenylation reaction/Diels-Alder product

The DFT results led us to believe that the reaction of **105** with higher concentrations of phenyl acetylene **16** could give product **106** by alkyne protonation (cf. similar to that proposed in Chen's studies).[69] Heating **105a** in neat **16** at 100 °C for 5 h, gave four compounds (Scheme 51).

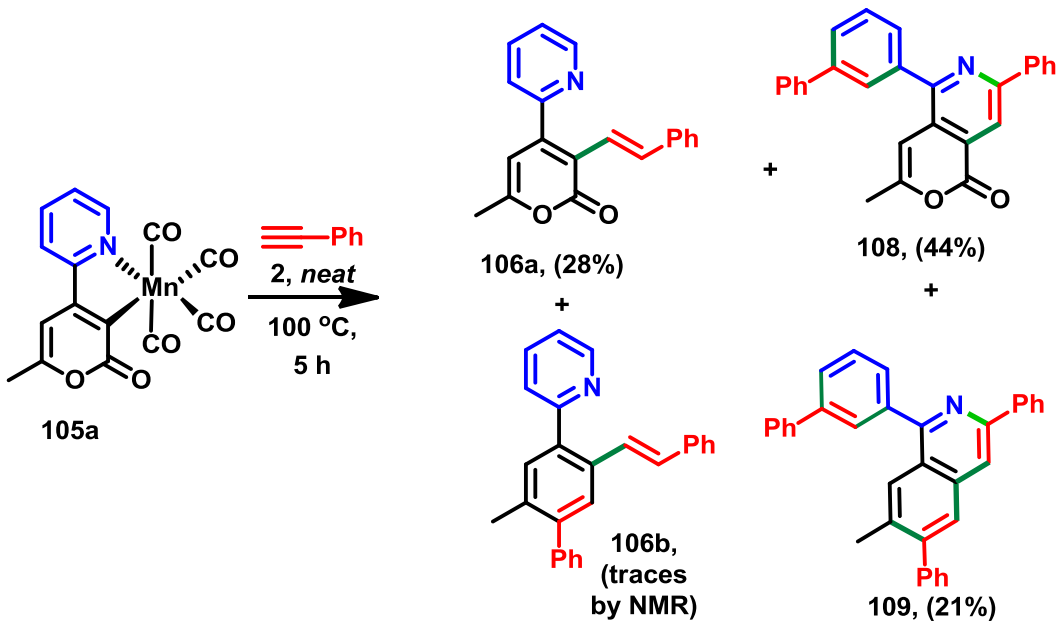

Scheme 51 Reaction of **105a** with neat phenyl acetylene 16 at 100 °C afforded alkenylated product **106a** and Diels-Alder products **106b**, **108** and **109**

The first compound was determined to be novel compound **106a**, which was isolated in a yield of 28%. Rather remarkably, the second and major product from the reaction was found to be an entirely novel compound **108**, isolated in a yield of 44%. Here, four new bonds have been formed, including C-C and C-N bonds, in addition to the cleavage of the pyridyl ring and elimination of the $Mn(CO)_n$ moiety. The final product from the reaction was found to be novel compound **109**, isolated in a 21% yield, with a remarkable six new bond from three alkyne insertions in a systematic fashion by manipulating both the pyridyl and pyronyl moiety of the ligand and fourth compound **106b** which was detected by (ESI-MS).

Compound **106** was synthesised via a protonation reaction (Scheme 51). However compounds **106b**, **108** and **109** are formed by a fragmentation and Diels-Alder reaction, involving the 2-pyridine group to give **108**. A second Diels-Alder reaction at **108** *via* the 2-pyrone also occurs, regioselectively, giving compound **109**, also was detected a Diels-Alder reaction at **106a** *via* the 2-pyrone to form **106b**. These

compounds were characterised by NMR and other spectroscopic technique, however compound **106** exhibited a precedented character at protons J_{HH} coupling in the alkene region δ 7.88 (1H, d, J_{HH} = 16.1) and 6.95 (1H, d, J_{HH} = 16.1) which confirm the *trans* alkene formation as drawn in Scheme 51, typically the *trans* alkene gave J_{HH} coupling constant 16 Hz while *cis* alkene 12 Hz. However surprisingly the proton geminal to phenyl in the alkene region **106a** resonated at relatively low-field δ 7.88 with respect to corresponding geminal proton at the alkene region compound **19** δ 7.05, (Scheme 45) with a δ difference of (Δδ = 0.83)

The full NMR spectroscopic analysis of **108** and **109** was possible, using correlation methods (HMQC and HMBC) and selective nOe experiments, which confirmed that the proposed structure **108** had been formed regioselectively (Figure 30). It can be seen that the J_{HH} coupling matched the typical structure, example (Figure 30a) proton (11') δ 7.94 (1 H, td, J_{HH} = 1.8, 0.6), (13'/15') δ 7.78 (2 H, dt, J_{HH} = 7.1, 1.8) and (14') δ 7.67 (1 H, t, J_{HH} 1.8) both in the same ring system and are coupled with a J_{HH} value = 1.8 more detail coupling see Figure 30a. The selective nOe experiments further confirmed the proposed structure having observed the nOe of the protons that lie close in space especially nOe ^{1}H-^{1}H of (C***H-8*** and C***H-11***) and (C***H-5*** and C***H-11'***) (Figure 30b). ESI-MS analysis confirmed a radical cation at *m/z* $[M+H]^+$ 390.1484, $[M+Na]^+$ 412.1304 (Figure 34).

(**a**) ^{1}H NMR spectroscopic data of **108**

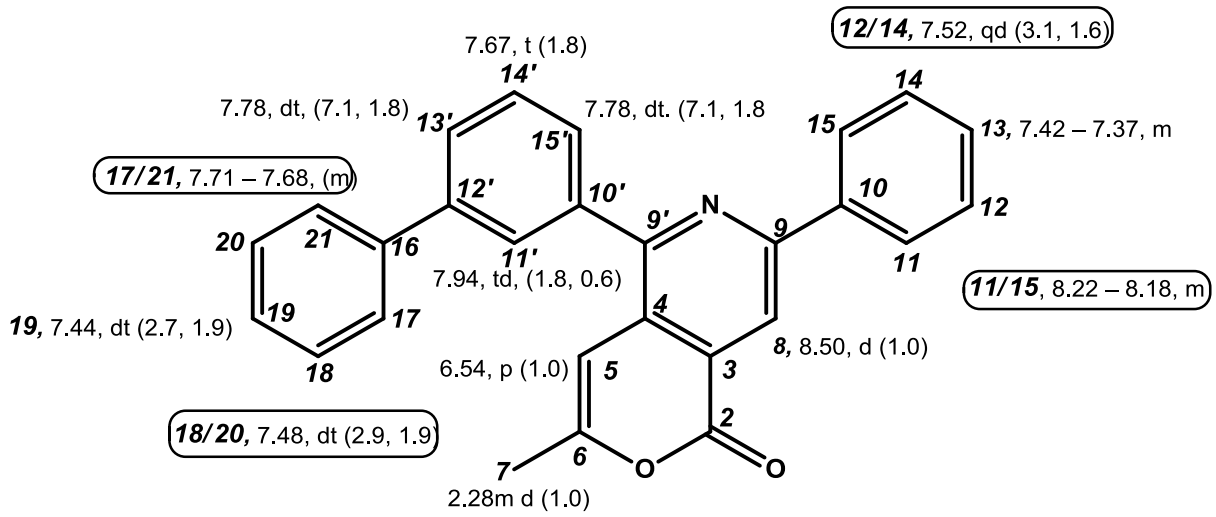

(**b**) Key nOe interactions of **108**

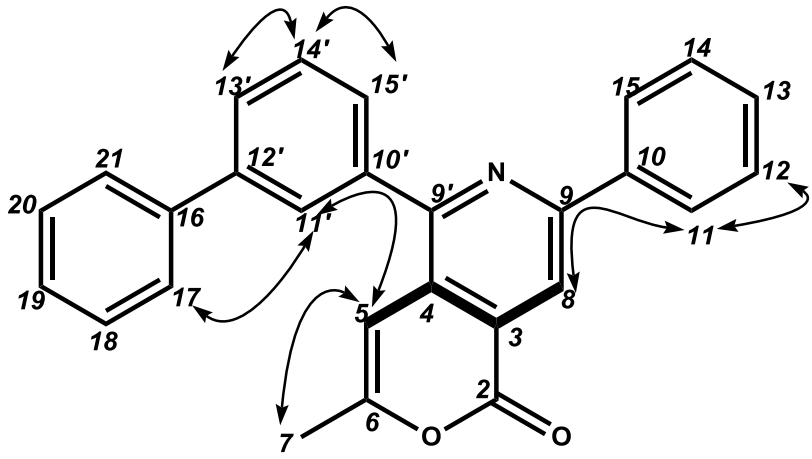

Figure 30 ^{1}H NMR spectroscopic data (700 MHz, CD_2Cl_2) for compound **108**; (a) chemical shifts (in ppm) are followed by the multiplicity of the signal and the coupling constant in Hz. (b) Key nOe interactions for compound 108, confirming the stereochemistry around the 2-pyrone moiety.

Further evidence for a 2-pyrone was the characteristic UV absorption band at 262 nm, and infrared bands at 1681, 1633, and 1596 cm^{-1}, in addition to ^{13}C NMR resonances at 162.26, 156.95 and 156.06 ppm, all of which were in agreement with an authentic reference compound, 4-(2'-pyridyl)-2-pyrone **81**.

Crystallisation of the product from dichloromethane and hexane gave single crystals suitable for X-ray diffraction, which confirmed the structure as **108** (Figure 31).

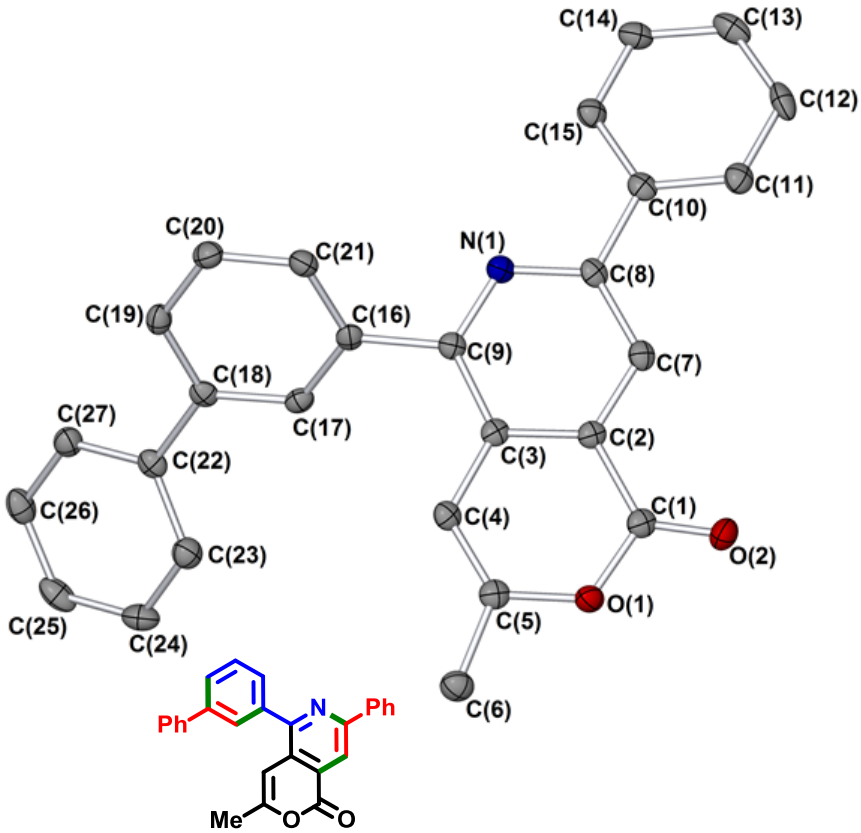

Figure 31 X-ray crystal structure of **108** (note: arbitrary atom numbering used; thermal ellipsoids set to 50%; H-atoms omitted).

It is important to note that the rearrangement occurred only in the presence of tricarbonylmanganesuide, in η^4-coodination mode from **107**, which was ascertained by treatment of **108** with excess **16** at 110 ^{o}C for several hours (ca. 24 h.); however reaction monitoring by TLC suggested that no reaction occurred (Scheme 52).

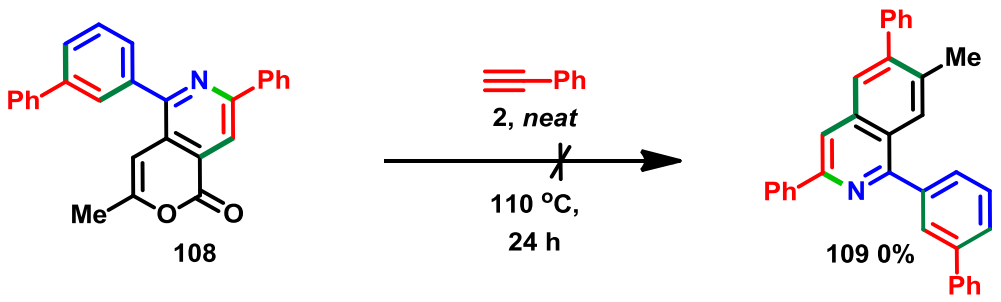

Scheme 52 Control Diels-Alder reaction in the absence of Mn

A plausible mechanism for the formation of **108** and **109** (Scheme 53) is shown where **108** and **109** are formed by a fragmentation and Diels-Alder reaction involving the 2-pyridyl group. The Diels-Alder reaction may be caused by ionisation of nitrogen on the pyridyl moiety by coordination of tricarbonylmanganese. This may manipulate the bonds on the pyridyl moiety, especially the nitrogen, subsequently paving the way for phenylacetylene **16** cycloaddition via **I**, as shown in the proposed mechanism. This is a fragmentation process, proceeding via **II** to give **III**. Aromatisation gives **108**. A second known Diels-Alder addition at the 2-pyrone also occurs, regioselectively, giving compound **109**.

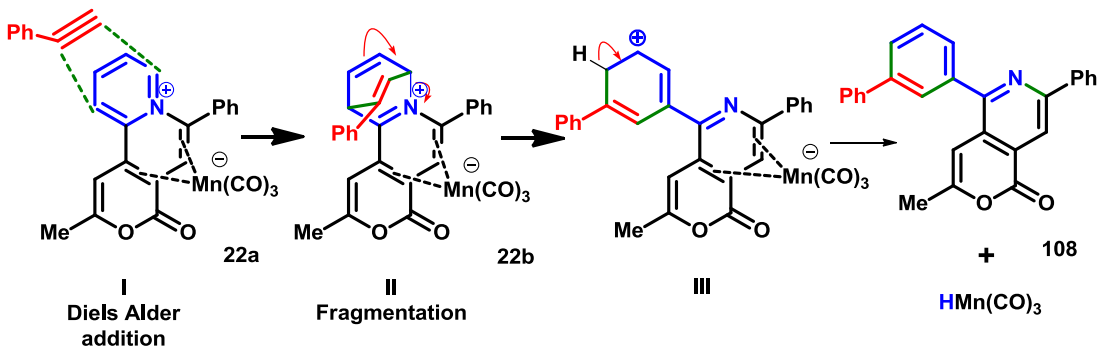

Scheme 53 Proposed mechanism for the formation of Diels-Alder product **108.**

Compound **109** was ascertained by NMR, IR, UV-vis and single crystal X-ray diffraction. The correlation methods (HMQC and HMBC) and selective nOe experiments, and UV absorption at 262 nm confirmed the proposed structure of **109**.

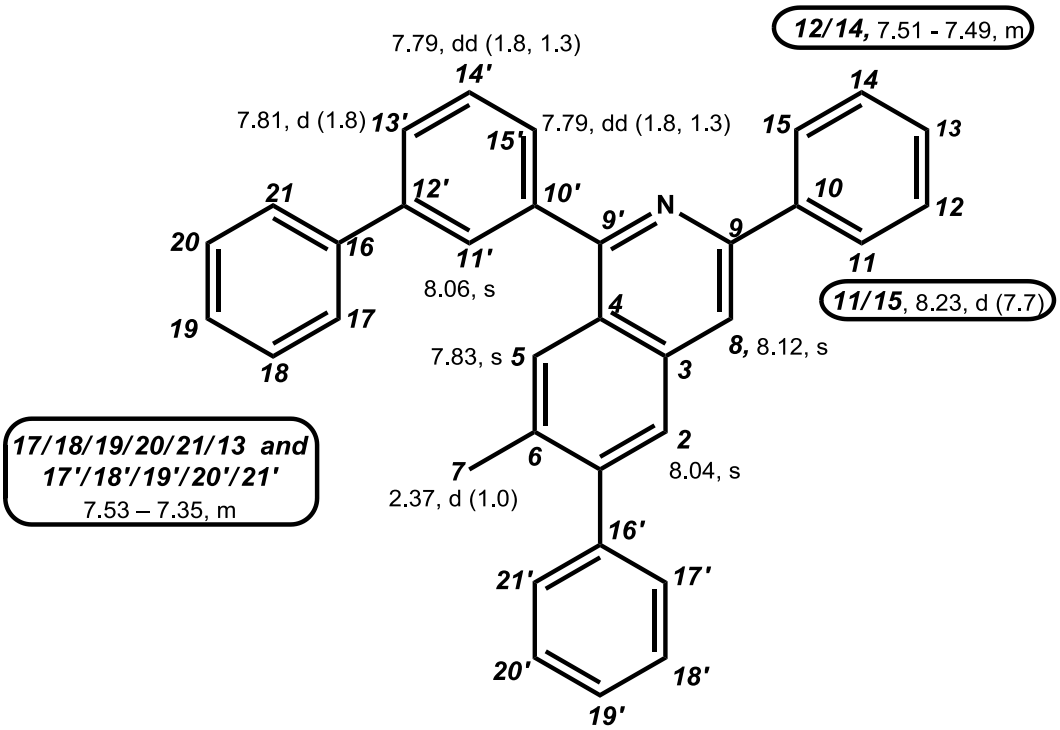

Figure 32 ^{1}H NMR spectroscopic data (700 MHz, CD_2Cl_2) for compound **109**; chemical shifts (in ppm) are followed by the multiplicity of the signal and the coupling constant in Hz.

A single crystal suitable for X-ray diffraction analysis was obtained from DCM and hexane, which confirmed the structure as **109** (Figure 33)

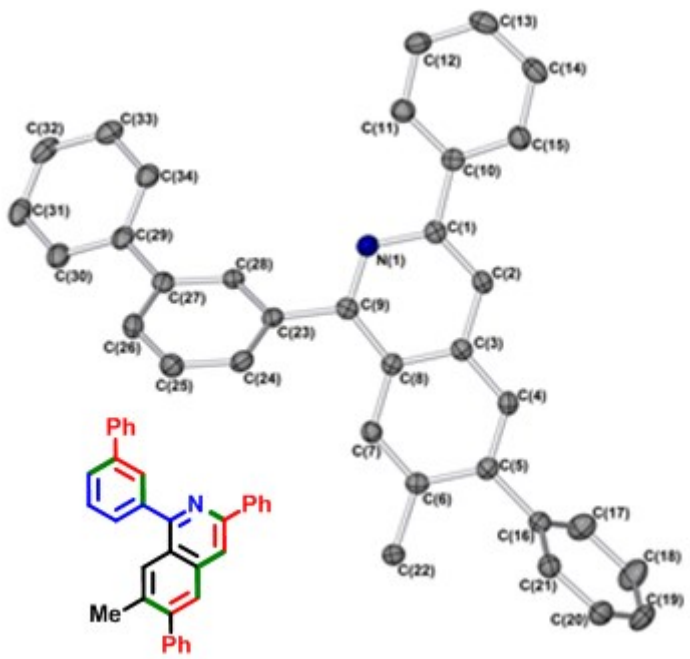

Figure 33 X-ray crystal structure of **109** (note: arbitrary atom numbering used; thermal ellipsoids set to 50%; H-atoms omitted).

The hypothesis above is implicated by observing both the intermediate and product using mass spectrometry (ESI-MS) at *m/z* 530.0778 and the product **109** at *m/z* 448.2035. The Diels-Alder reaction was also seen for **106** via addition to the 2-pyrone moiety. Similarly, alkyne insertion was observed in **106b**, where **I** was also observed by ESI-MS (Figure 34).

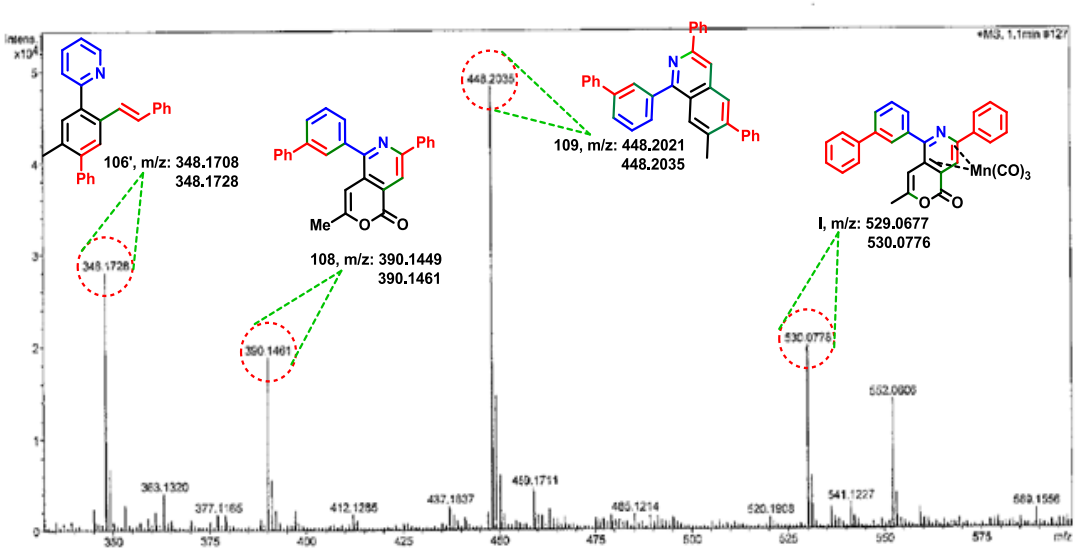

Figure 34 ESI-MS of the reaction of alkenylation and Diels-Alder product

The ^{1}H NMR spectroscopic data for compound **108**, which contains a pyrone moiety, can be compared to that for **109**, which does not have a pyrone but a sterically bulky phenyl (Table 1). Some selected ^{1}H NMR (*e.g.* the H-7, H-11&15, H-12&14, H-13 and H-15 portion) match closely ($\Delta\delta < 0.1$ ppm), however other parts do not. The largest chemical shift difference in this category arises for the proton at H-5, and is $\Delta\delta = 1.29$ ppm, followed by H-8 where $\Delta\delta = 1.29$ ppm. This confirms that the two double bonds in the enol ether are more electron deficient in the pyrone-containing system, owing to the ^{1}H NMR signals for compound **108** observed at $-\Delta\delta$ ppm reported values with respect to compound **109**, which is more electron-rich (Table 6)

Table 6 Comparison of selected ^{1}H NMR shift data for the compounds **108** and **109**

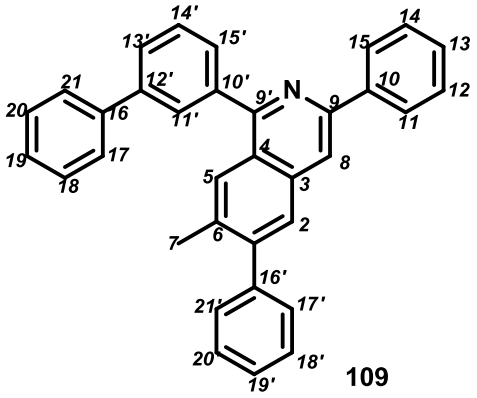

109

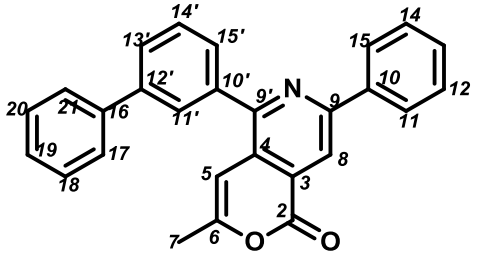

108

Position	Compound (**109**) δ/ppm	Compound (**108**) δ/ppm	Δδ / ppm
5	7.83	6.54	1.29
7	2.37	2.28	0.09
8	8.12	8.5	0.7
11 & 15	8.23	8.2	0.03
12 & 14	750	7.52	-0.02
11'	8.06	7.94	0.12
13'	7.79	7.78	0.01
14'	7.81	7.67	0.14
15'	7.68	7.64	0.04

Note: multiplets are given as a centre point average; NMR standard (δ 5.32) was residual CH_2Cl_2.

The proposed route to the final product (

Scheme **54**) begins with $MnBn(CO)_5$ which reacts with 2-phenylpyridine **104a** by reductively eliminating toluene and CO, affording a five-membered manganacycle **105a**. Next is the reaction of five-membered manganacycle **105a** with phenyl

acetylene **16** to form manganacycle **(II)**, via a fast regioselective alkyne insertion **I**. Interestingly, the seven-membered manganacycle intermediate **III**, was formed via selective alkyne migration into **II**. Transition state **IV** sets up reductive elimination from **III**. The dichotomy here is that alkenylated product **106** formed via protonation and the μ^2-alkyne complex **V** to form **106**; complex **107** forms *via* reductive elimination. Complex **107** then rearranges intramolecularly to manganacyclohexyl intermediate **VII** by a Diels-Alder addition of phenyl acetylene **16**. Intermediate **VII** undergoes pyridyl ring-opening and rearrangement to give **VIII**. H-loss and aromatisation affords **108** and regenerates $HMn(CO)_3$, which feasibly can participate in further reaction.

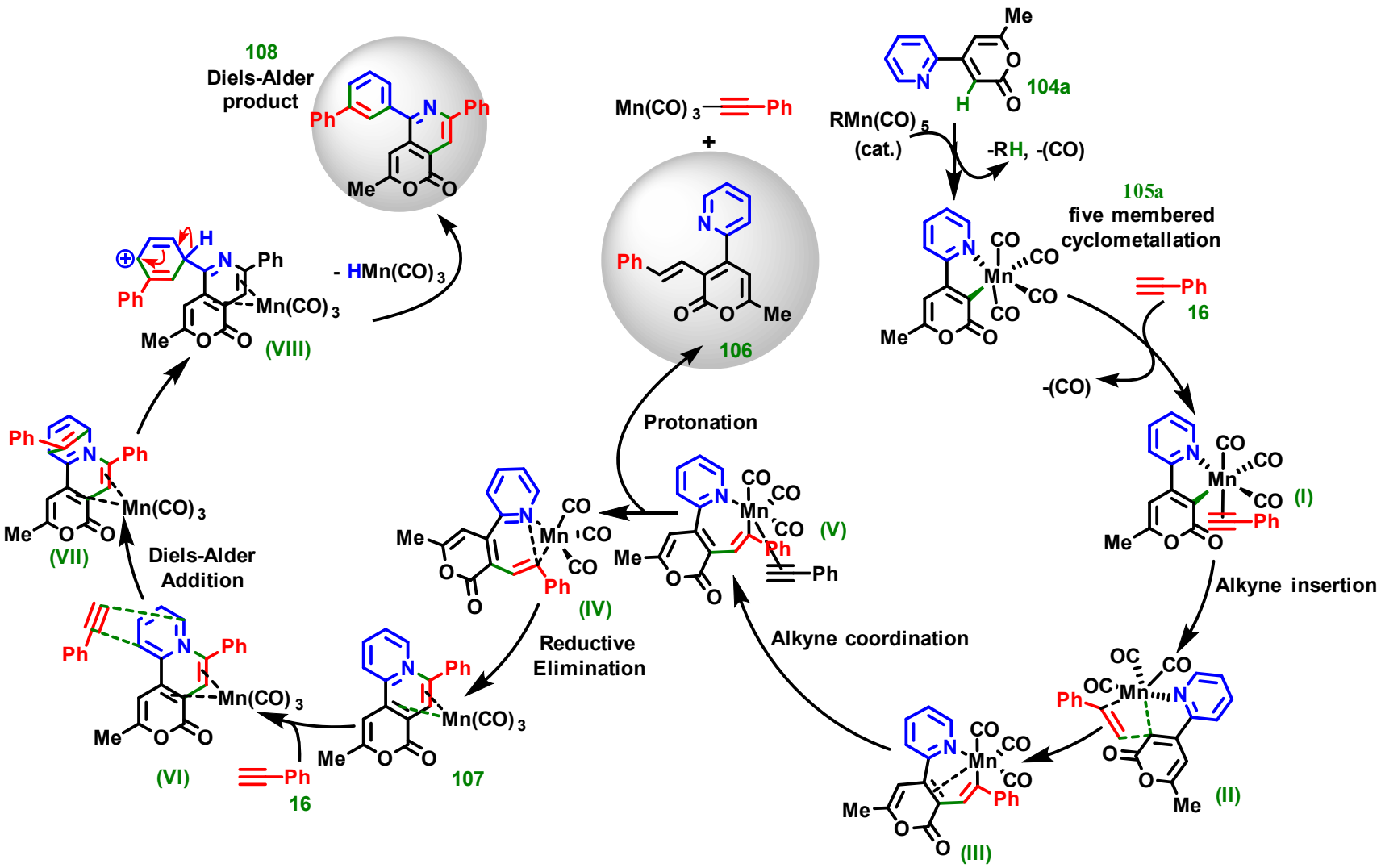

Scheme 54 proposed route for alkenylation/Diel-Alder Product.

5.4 Effect of substituted 2-pyridine moiety with 6-methoxy-2-pyridyl moiety on 2-pyrone

Noticed was a profound effect when a substituted 2-pyridine **105b** was used with a similar reaction conditions with respect to Scheme 50 (page 108) and Scheme 51 (page 114) (Scheme 55). Although the alkenylated product **111** was only observed in trace amounds by ESI-MS, complex **110** was isolated in a good yield (76%). The structure of the double alkyne insertion product **110** was ascertained by NMR, IR and UV-vis.

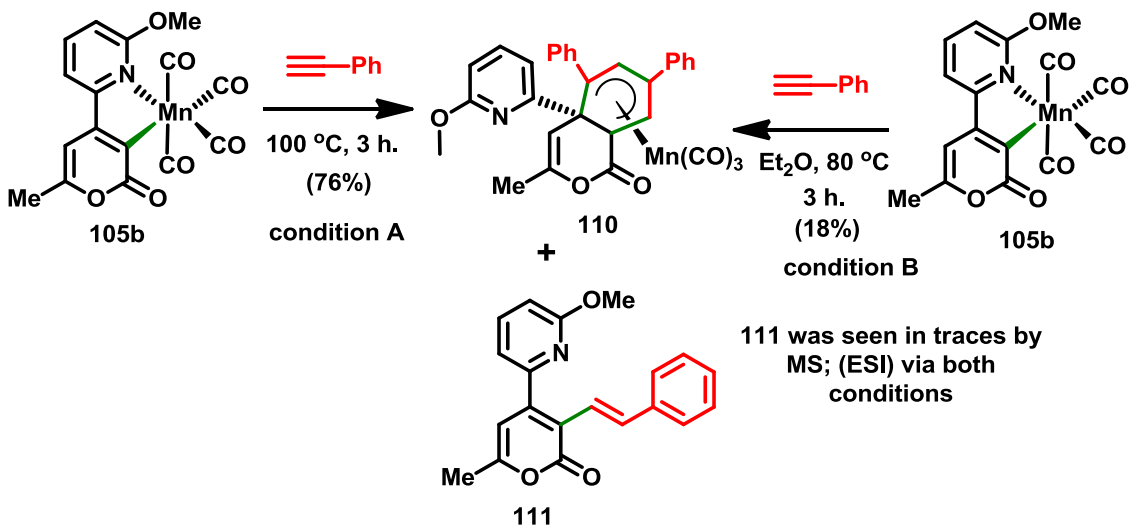

Scheme 55 Double alkyne insertion into cyclomanganesiated complex **110** and alkenylated product **111**

A single crystal suitable for X-ray diffraction analysis was obtained from DCM and hexane, which gave the structure as can be seen in Figure 35.

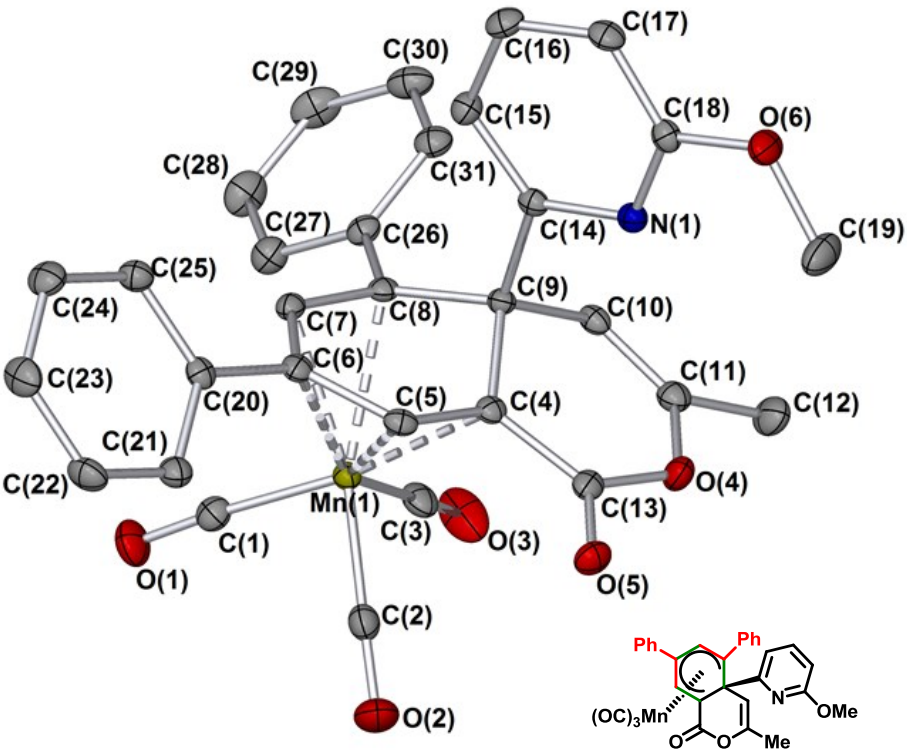

Figure 35 X-ray crystal structure of **110** (note: arbitrary atom numbering used) dotted lines have been used to show the Mn-coordination in complex for clarity (thermal ellipsoids set to 50%; H-atoms omitted). Selected torsion angles (°), bond angles (°) and bond lengths (Å): C4-C3-C13-C12 = 4.2(2), C3-C4-C7-N1 = -38.4(2), N1-C12-C13-C3 = 44.4(2); C13-C12-N1 = 114.38(14), C3-C4-C7 = 116.31(15); C3-Mn1 = 2.0769(17), C4-Mn1 = 2.1843(17), C12-Mn1 = 2.1060(18), C13-Mn1 = 2.0908(18)

5.5 Conclusion

This study has shown that a 2-pyridyl directing group can become directly involved in Mn^{I}-mediated alkenylation reactions. Replacement of a phenyl group with a 2-pyrone (more electron-accepting) group had a profound effect on the preferred reaction path, affording a stable and isolable manganese adduct **107**. Critically, for the first time, evidence of a commonly proposed manganacyclic 16-electron 5-coordinate intermediate **III** has been gathered, which is found to be the key intermediate controlling whether direct reductive elimination or protonation and metal de-coordination occurs, affording **106** or **107**, as proposed in the catalytic chemistry.

The stoichiometric reactions conducted in neat phenyl acetylene showed that other products such as **106b**, **108**, **109** and **I**, can be readily formed. Remarkably, this is an unprecedented C-H bond activation and Diels-Alder reaction, involving 2-pyridyl ring-cleavage and a recombination process to give **108**, was observed. Related double Diels-Alder compound **109** was also isolated.

An unprecedented complex **110** was isolated, using the 6-methoxy-2-pyridyl electron-donating group, which was found to have a profound effect on the preferred alkyne insertion reaction pathway, affording a stable and isolable manganese adduct **110.**

The combined experimental and computational approach used in this study has allowed delineation of some of the reaction paths available in Mn^{I}-mediated C-H bond activation. These findings could provide insight for the future design of Mn^{I}-mediated C-H bond activation processes, especially how relatively minor changes in substrate structure influence product selection – Mn^{I}-based metallocycles offer

interesting chemistry and reactivity which could be exploited in advanced chemical synthesis.

Chapter 4 Pauson-Khand / 6π-electrocyclisation reactions of internal alkynes possessing cobalt-directing groups

6.1 Introduction

Fairlamb and co-workers[105, 109] reported a push-pull effect in the PKR with several sterically equivalent, heteroaromatic-substituted **112** alkynes containing π-electron deficient pyrones **113** (Scheme 56).[105]

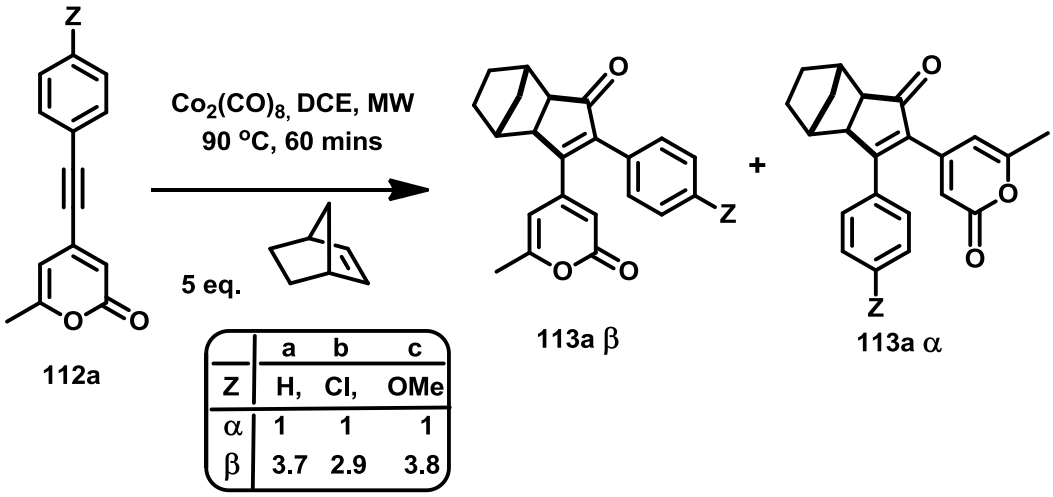

Scheme 56 Sterically, near-equivalent, heteroaromatic-substituted alkynes in PKR

The π-deficient 2-pyrone moiety is found to preferentially occupy the β-position with respect to the enone of cyclopentenone product.[105] The electronic factor is not enough to predict that the 2-pyrone electron donating group (EDG) favoured the β-position, as for other more π-electron rich examples, *e.g.* furan and thiophene,[105] the β-regioisomer predominated, which violates the notion, rule if you will, for internal alkynes that predicts placement of electron-donating groups (EDG) at the α-regioisomer.[135] It was thus necessary to study further PKR reactions of internal alkynes containing heteroaromatic rings to assess the regioselectivity outcome. It is proposed that the ratio of different PKR cycloadducts will be sensitive to the

heteroaromatic rings used (**a**) to (**e**) (Figure 36). Also, it was anticipated that the position of the nitrogen atom within pyridyl-containing alkynes might control the regiochemical outcome of the PKR reaction.

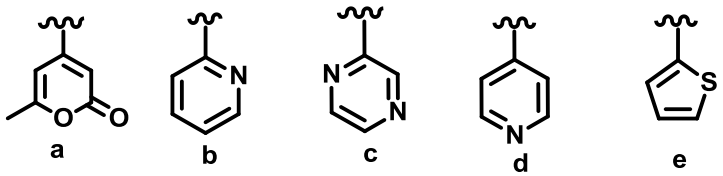

Figure 36 Heteroaromatic ring systems used in this study

The internal alkynes required for the PKR study were prepared by a Sonogashira cross-coupling protocol. The precatalyst, $PdCl_2(PPh_3)_2$ (1 mol %), was employed and the catalytic cycle involved Pd^0 (**I**), oxidative addition of organic substrate (**II**), follow by Cu^I to activate the alkyne by π-coordination (**IIIa**), then cupration to form (**IIIb**). On transmetallation (**IV**) is formed along with the regeneration of (**IIIc**). Isomerisation at $Pd^{(II)\ (II)}$ (**V**), followed by reductive elimination, affords the internal alkyne product and also regenerates the Pd^0 catalyst (Scheme 57).[25]

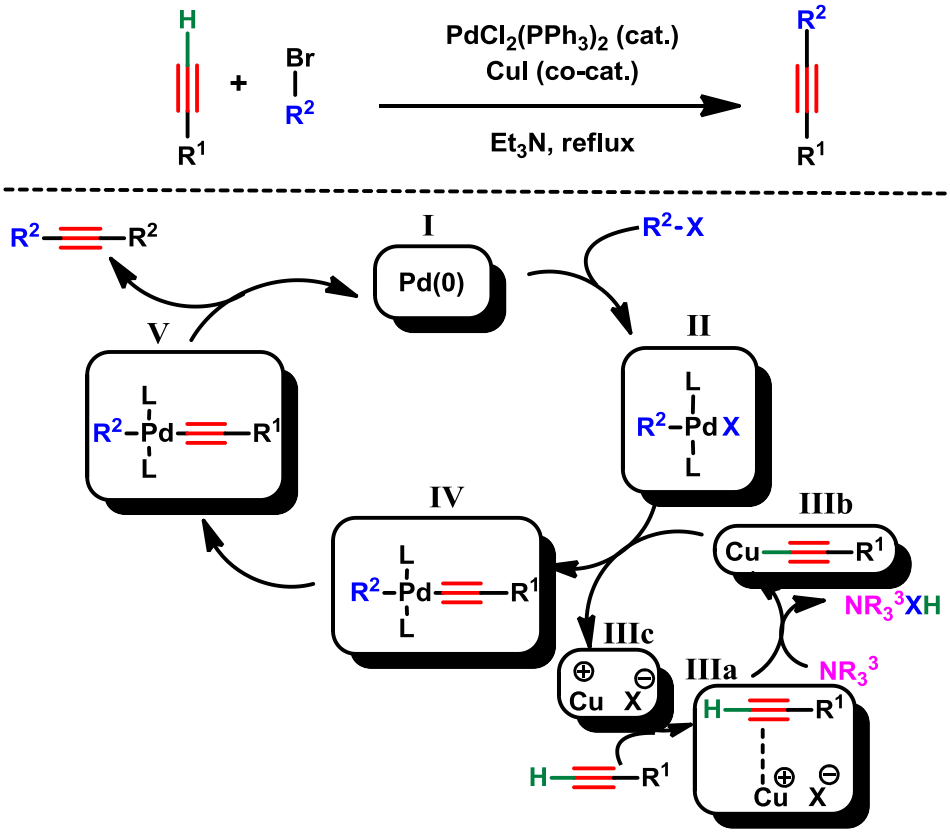

Scheme 57 Postulated mechanism for the Sonogashira cross-coupling reaction

The pyridyl derivatives of ethynyltrimethylsilane, *i.e.* 2-[2'-(trimethylsilyl)ethynyl] pyridine **114a**, 4-[4'-(trimethylsilyl)ethynyl]pyridine **115a** and 2-[2'-(trimethylsilyl)ethynyl]pyrazine **116a** were prepared in excellent yields, with the exception of 2-[2'-(trimethylsilyl)ethynyl]thiophene **117a**, which is satisfactory (Scheme 58).

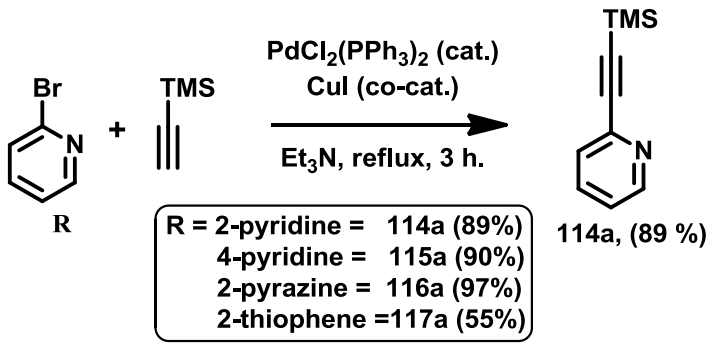

Scheme 58 Synthesis of initial alkyne **114a** using the Sonogashira cross-coupling reaction

The terminal alkynes were accessed *via* deprotection of **114a-117a** using NaOH in methanol / dichloromethane (1:1 v/v) under a N_2 atmosphere for 2 h. The compounds 2-ethynylpyridine **114b**, 4-ethynylpyridine **115b**, 2-ethynylpyrazine **116b** and 2-ethynylthiophene **117b** in good yield, with the exception of 2-ethynylthiophene **117b** which was isolated in 48% yield.

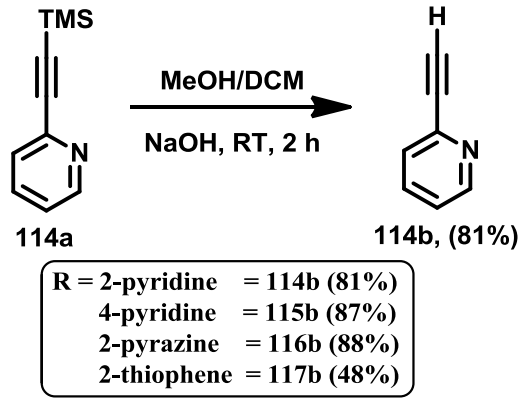

Scheme 59 Deprotection of silyl-protected alkynes to deliver terminal alkynes for Sonogashira cross-coupling

Table 7 Synthesis of heteroaromatic ethynyl substrates, all substrates were synthesised using a standard Sonogashira protocol

Lebel	ArX	Akynes / Yield (%)	Product / Yield (%)
1	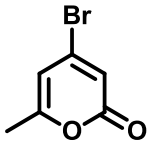	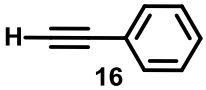 16	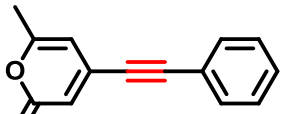 112a, (91%)
3	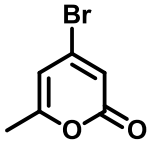	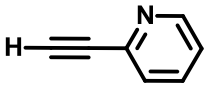 114b, (89%)	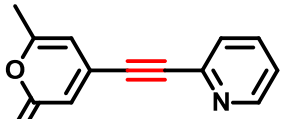 114c, (88%)
4	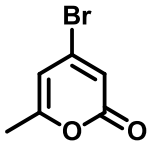	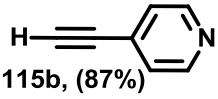 115b, (87%)	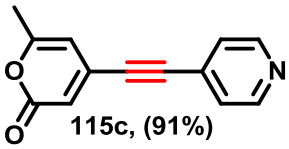 115c, (91%)
5	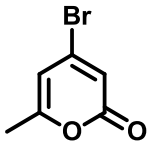	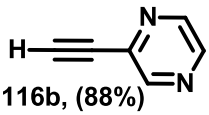 116b, (88%)	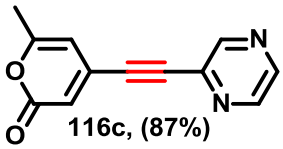 116c, (87%)
6	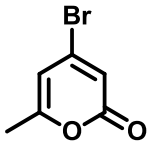	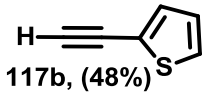 117b, (48%)	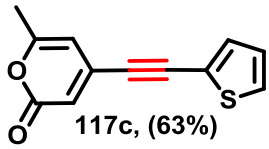 117c, (63%)
7	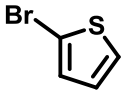	115b	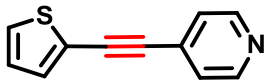 118, (58%)
8	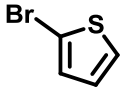	114b	 119, (71%)
9	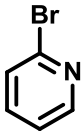	115b	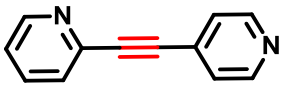 120, (85%)

6.1.1 Synthesis of sterically and electronically near-equivalent alkynes

The terminal alkyne was synthesised via a Sonogashira cross-coupling reaction of ethynyl pyridine with 4-bromo-6-methyl-2-pyrone, 2-bromopyridine and 2-bromothiophene. These allowed access to the alkyne compounds, 6-methyl-4-(2'-

pyridylethynyl)-2-pyrone **114c**, 6-methyl-4-(4'-pyridylethynyl)-2-pyrone **115c**, 6-methyl-4-(2'-pyrazylethynyl)-2-pyrone **116c**, 6-methyl-4-(2'-thienylethynyl)-2-pyrone **117c**, 4-(2'-thienylethynyl)pyridine, 118 2-(2'-thienylethynyl)pyridine and 2-(4'-pyridylethynyl)pyridine **119**. Compounds **114c–116c** allow the relative position of the nitrogen atom to be probed with respect to 2-pyrones, whereas 2-thiophene derivatives **117c–119** offer a sterically distinct but electronically similar alternative to the pyridyl ring system.

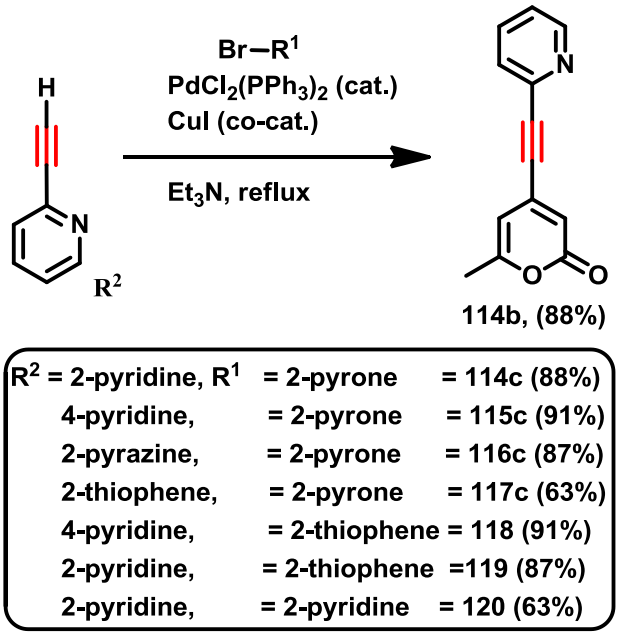

Scheme 60 Synthesis of sterically and electronically near-equivalent terminal alkyne using Sonogashira cross-coupling reaction

A series of π–electron-deficient 2-pyrone derivatives **114c-116c** and 2-thiophene derivatives π-electron rich **116c–119** were prepared for comparison with reported alkynes from the Fairlamb group.[104, 105, 109] These particular derivatives were synthesised to evaluate regiochemistry pertaining to the structure of the internal alkynes, containing a heteroaromatic ring moiety (pyridine) with respect to 2-pyrone in PKR , *i.e.* **114c–117c** (Scheme 60).

Crystallisation of products **114c** and **115c** from dichloromethane and hexane gave single crystals suitable for X-ray diffraction study, which confirmed their postulated chemical structures (Figure 37).

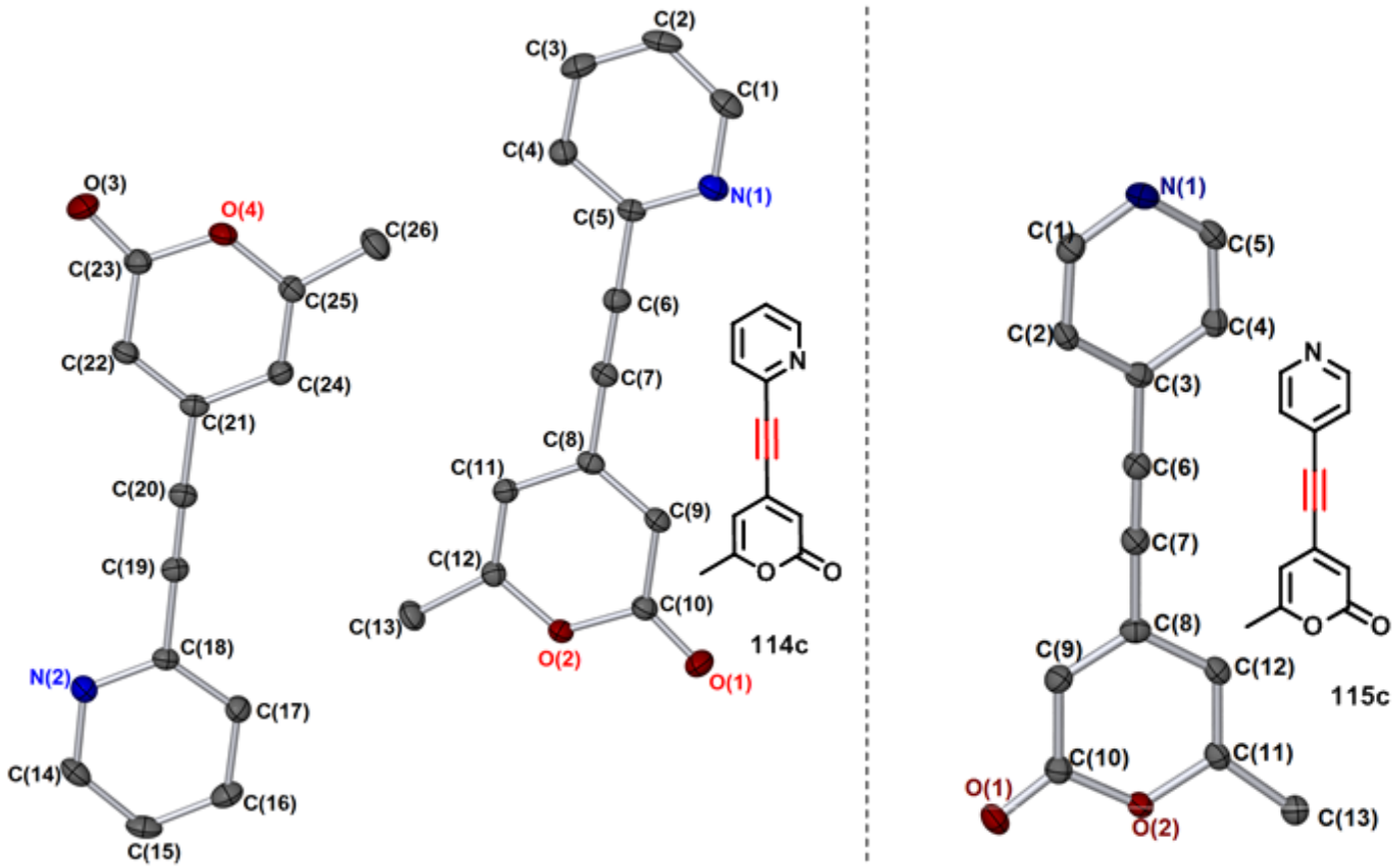

Figure 37 X-ray diffraction structures of compound **114c** and **115c**. Compound **114c** left hand side, showing the packing between the atoms in the molecules. Hydrogen atoms removed for clarity. Thermal ellipsoids shown with probability of 50%.

6.2 Synthesis of sterically and electronically near-equivalent heteroaromatic PKR protocol

The first step in the synthesis of the cyclopentanones was carried out by the reaction between the cobalt carbonyl complex, $Co_2(CO)_8$, internal alkyne at room temperature, *ca.* 23 ^oC for 30 min. follow by alkene alkene insertion via microwaving for about 60 min that lead to PKR. However, reacting an equimolar quantity of $Co_2(CO)_8$ and alkyne in THF at room temperature under nitrogen atmosphere for 16 hours afforded the first intermediate complexes, which were isolable, *e.g.* complexes **121(I)-123(I)** and **125(I)**, and formed in good yield (Scheme 61). However on comparing the proton chemical shift of the internal alkyne **114c-116c** and alkynyl-$Co_2(CO)_6$ **121(I)-123(I)** suggested no significant difference in the heteroaromatic region containing pyridine, while a difference was observed at C5/H5 in all of the pyrone containing moieties, *e.g.* δ 6.28 for **114c** and δ 6.10 for **121(I)**, Δδ 0.18. The second step involved PKR reaction with norbornene under typical thermal conditions (microwave assisted synthesis at 90 ^oC for one hour). The reaction proceeded smoothly and gave the PK cycloadduct **121** in 68% yield as only one *β* isomer (Scheme 61 and Table 8).

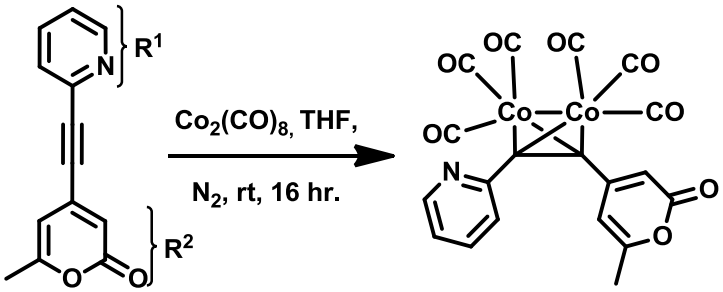

121(I), (86%)

R^1 = 2-pyridine,	R^2 = 2-pyrone	=	121(I), (86%)
4-pyridine,	= 2-pyrone	=	122(I), (84%)
2-pyrazine,	= 2-pyrone	=	123(I), (76%)
4-pyridine,	= 2-thiophene	=	125(I), (68%)

Scheme 61 PKR via the intermediate μ^2-alkynyl-pyrone-phenyl-$Co_2(CO)_6$ complex

6.2.1 Evaluation of heteroaromatic containing nitrogen atom or 2-pyrone in PKR

Here the alkene was kept constant (norbornene), as other alkenes may alter the regiochemical outcome[98] (Table 8). Previously Fairlamb and co-workers[105] reported that the presence of a proximal nitrogen on the alkyne heteroaromatic group in pyridyl-containing alkyne substrates has a profound effect on the regiochemical outcome of the PK reaction.[105] Compound containing 2-pyrone, **113** and **121-124** (Scheme 61) were studied for their selectivity, however nitrogen containing atom at α position to the substituent compound **121** and **124** favour the β-position exclusively. The compound containing a nitrogen atom at the *meta*-position to the cyclopentenone substituent **122** shows no selectivity at all. Selectivity towards the β-position was observed for the pyrone containing 2-thiophene **124**. However nitrogen containing in both ring system **127** favoured the 2-pyridine at the β-position exclusively, suggesting that there may be an interaction of 2-pyridine with the cobalt complex. Further evidence is provided by 2-thiophene **125**, where the 2-pyridine controls the regiochemical outcome, even though the α-isomer was observed **125**.

The 2-thiophene was observed controlling the regioselectivity over 4-pyridine **126**. This suggested that the position of the nitrogen atom in pyridyl-containing system (with respect to the 2-pyrone) dramatically affects the regiochemical outcome of the PKR. Remarkably, 2-pyridine shows unique behaviour by having a significant effect on the selectivity of both the π-electron deficient 2-pyrone **121**-**124** and π-electron rich 2-thiophene **125**.

Table 8 PKR of nitrogen and pyrone containing (heteroaromatic alkynes) compounds.

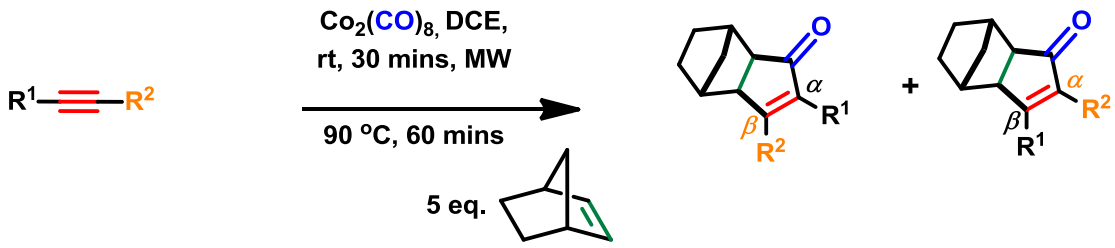

Entry	Substrate	β %	α %	Entry	Substrate	β %	α %
1	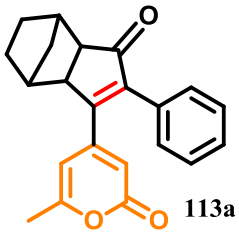 113a	71	11	5	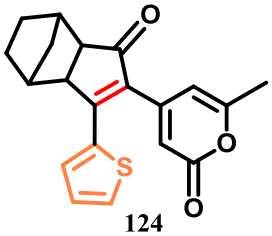 124	55	12
2	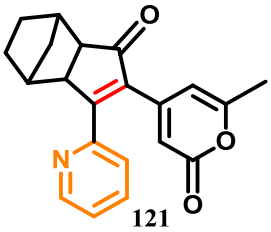 121	68	--	6	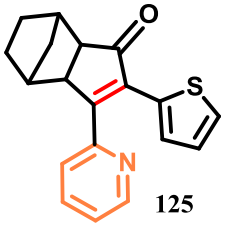 125	58	29
3	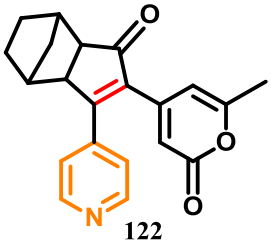 122	42	42	7	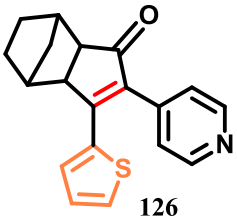 126	67	10
4	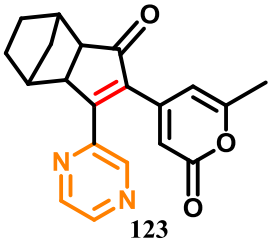 123	77	--	8	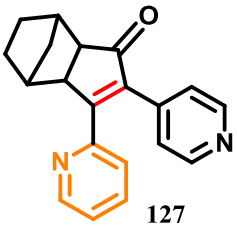 127	76	--

All PKR cycloadducts were characterised by NMR, IR, UV-Vis, and elemental analysis. The NMR spectroscopic study shows that the regioisomeric structures can be discerned by chemical shift, with the aid of ^{1}H COSY, nOe interactions and ^{13}C information, provided by HMQC and HMBC. The ^{1}H NMR spectra (400 MHz, $CDCl_3$) of the two protons α to the nitrogen atom in **122β** (note: β is in respect of the pyridyl ring position within the cyclopentenone ring system) resonated at downfield δ 8.70, while the proton α to nitrogen in **122α** regioisomeric resonated slightly upfield with respect to **122β** at δ 8.63. The proton β to nitrogen in **122β** appears at δ 7.22 (d, J_{HH} = 5.9 Hz, 2H) and at 7.17 (d, J_{HH} = 5.9 Hz, 2H) for **122α**. The C3 and C5 protons within the 2-pyrone moiety appeared at δ 6.18 (s, J_{HH} = 3.1 Hz, 1H), 6.03 (s, J_{HH} = 3.1 Hz, 1H) for **122β** and δ 5.71 (s, J_{HH} = 3.1 Hz, 1H) and 5.59 (s, J_{HH} = 3.1 Hz, 1H) for **122α** (Figure 38).

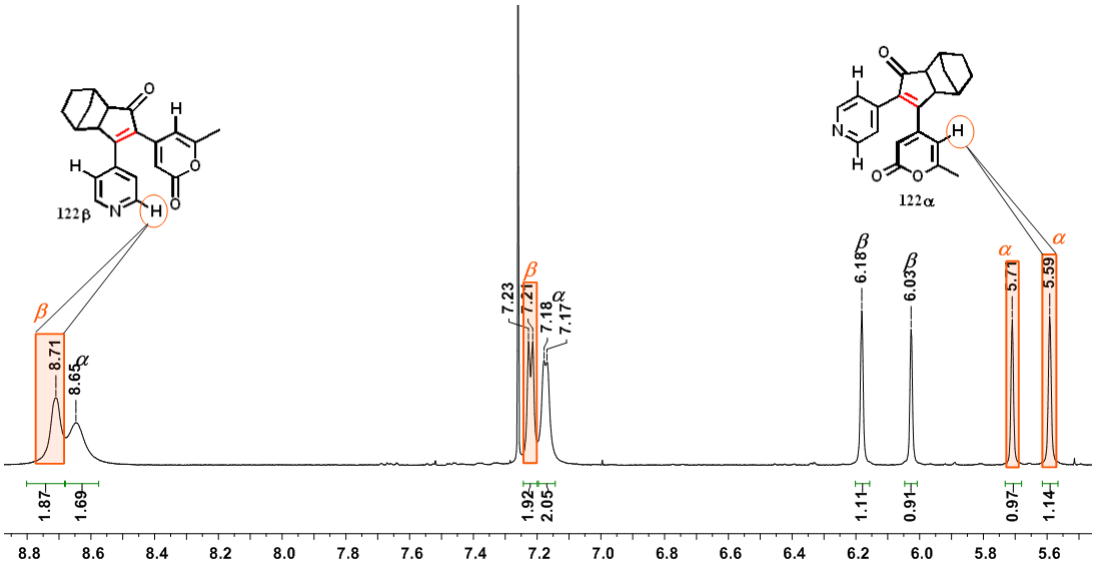

Figure 38 ^{1}H NMR spectra (400 MHz, $CDCl_3$) of PKR compound **122** reaction mixture of 1:1, **122α** and **122β** which possess the same R_f value by TLC.

The ^{1}H NMR spectra of **124**, containing 2-thiophene and 2-pyrone, with a relative α and β regioselectivity reveals significant chemical shift differences, especially the protons on the thiophene moiety α, β and γ to sulphur **124β** resonated at lower field δ

7.61 (dd, J_{HH} = 5.1, 1.1 Hz, 1H), 7.49 (dd, J_{HH} = 3.8, 1.1 Hz, 1H), 7.14 (dd, J_{HH} = 5.1, 3.8 Hz, 1H) respectively with respect to **124α** δ 7.41 (dd, J_{HH} = 5.1, 1.2 Hz, 1H), 7.34 (dd, J_{HH} = 3.8, 1.2 Hz, 1H), 7.03 (dd, J_{HH} = 5.1, 3.8 Hz, 1H). The ^{1}H-^{1}H *J* coupling of thiophene moiety with respect to **124β** ^{1}H J_{HH} α to β = 1.1, α to γ = 5.1 and β to γ =3.8 and **124α** ^{1}H J_{HH} α to β = 1.2, α to γ = 5.1 and β to γ =3.8 is in agreement with the expected coupling constant in both regioisomers (Figure 39). The chemical shift of the of pyrone moiety *C3*H and *C5*H of **124α** absorbed at low field δ 6.18 (s, *J* = 2.6 Hz, 1H), 5.86 (t, *J* = 1.2 Hz, 1H) with respect to **124β** 6.08 (dd, *J* = 1.4, 0.7 Hz, 1H) and 5.84 – 5.82 (m, 2H) contrary to **122** (Figure 39 and Table 9).

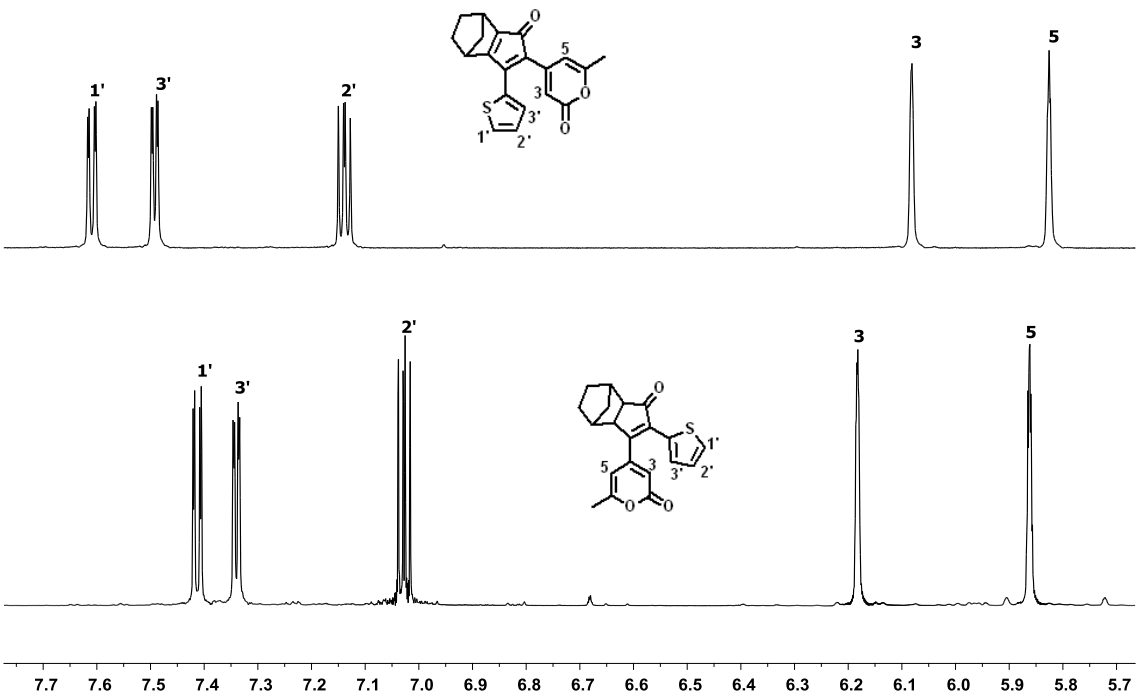

Figure 39 ^{1}H NMR spectra (400 MHz, $CDCl_3$) of PKR compound **124** showing simulation at different δ of **124β** above and **124α** see Table 9.

Table 9 summarises the NMR spectroscopic data of PKR compounds containing the 2-pyrone moiety, *i.e.* **121**, **122α**, **122β**, **123**, **124α** and **124β**. 2D NMR analysis allowed the regiochemistry to be determined. The protons of the β-regioisomer

resonated at lower field in compound **122β**, especially protons in the pyridyl and pyrone moiety.

The protons of the α-regioisomer resonated downfield in **125α**, especially the proton in the thienyl and pyrone moiety (Table 9). It is generally observed that in 2-pyrone moiety the *C3*H (proton) resonates downfield with respect to *C5*H (in most cases containing the 2-pyrone). The ^{1}H-^{1}H nOe of the PK cycloadducts are also diagnostic. The ^{1}H (δ) *ortho* to nitrogen in the pyridyl moiety shows a ^{1}H-^{1}H nOe contact with the *C*H4a of the cyclopentenone in **121β**, while in compound **122β** the ^{1}H-*β* to nitrogen show ^{1}H-^{1}H 2D nOe with C4a of cyclopentenone, likewise **122β** ^{1}H-*β* to nitrogen show ^{1}H-^{1}H nOe with *C*3 of pyrone moiety is nOe the ^{1}H C-H4a of cyclopentenone is said to be *α*– region-selective isomer **122α**, (Table 9). The compound containing a pyrazine moiety **124β** showed exclusively *β*-selectivity. In the case of **125β** the proton that is γ to sulphur within the thienyl moiety shows an nOe contact between H1-H4a.

Table 9 The ^{1}H δ shift of PKR product involving 2-pyrones with regiochemical outcome supported by COSY, nOe ^{1}H-^{1}H and HMQC ^{1}H-^{13}C coupling experiments.

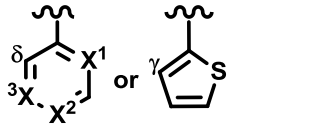			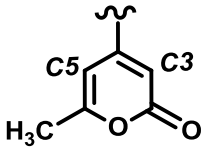			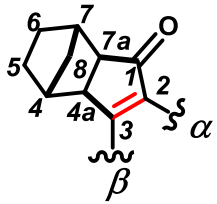				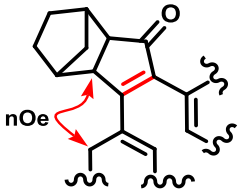
Entry	α-N	β-N	^{1}H δ C5	^{1}H δ C3	^{1}H δ CH_3	^{1}H δ C7a	^{1}H δ C7	^{1}H δ C4a	^{1}H δ C4	^{1}H-^{1}H nOe
121β	8.72	7.39	5.77	6.01	2.17	3.41	2.50	2.58	2.20	(C-Hδ–N)-C-H4a
122β	8.71	7.22	6.03	6.18	2.17	3.15	2.52	2.60	2.23	(C-Hβ–N)-C-H4a
122α	8.65	7.17	5.59	5.71	2.15	3.01	2.52	2.60	2.23	C-H5-C-H4a
123β	8.57	8.64	5.72	5.99	2.18	3.41	2.52	255	2.18	(C-Hδ–N)-C-H4a
124β	7.61*	7.14*	5.83	6.08	2.22	3.16	2.48	2.48	2.48	(C-Hγ–S)-C-H4a
124α	7.39*	7.02*	5.84	6.22	2.24	2.88	2.47	2.59	2.23	C-H5-C-H4a

^{1}H NMR (400 MHz, $CDCl_3$) Note: multiplets are given as a centre point average. **(121)** X^1 = N, X^2 = C, X^3 = C. **(122),** X^1 = C, X^2 = N, X^3 = C**. (123),** X^1 = N, X^2 = C, X^3 = N

Crystallisation of the major regioisomeric product of PKR adducts from dichloromethane and hexane gave single crystals suitable for study by X-ray diffraction, which confirmed the structure, consistent with NMR spectroscopic analysis (Figure 40).

The crystal structures of **121** and **127** exclusively β, and **126β** as a major isomer which predict that the position of the nitrogen atom has a greater influence to the substituent presumably due to the interaction of nitrogen α to the substituent with the cobalt intermediate. Substituting the 2-pyridyl ring with 2-pyrazine, in a system containing 2-pyrone, **123**, led to exclusive formation of the β-regioisomer. This supports the prediction that the position of the nitrogen atom in the pyridine ring system exerts greater influence in controlling the regiochemical outcome of the PKR.

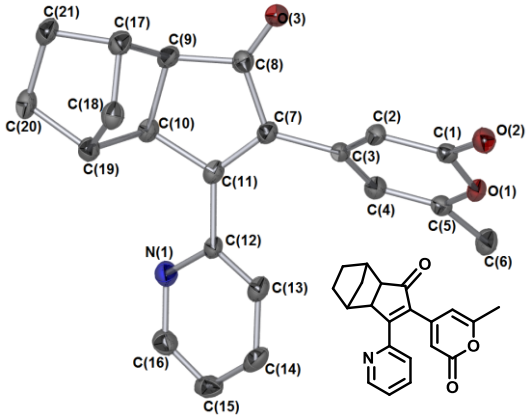

Figure 40(I) Single Crystal X-ray structure of **121** showing exclusive β selectivity

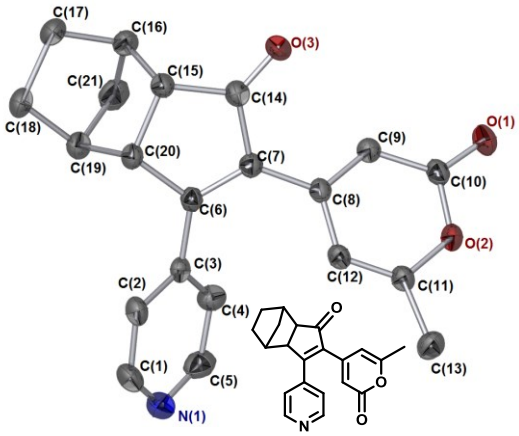

Figure 40(II) Single Crystal X-ray structure of **122β** showing β selectivity

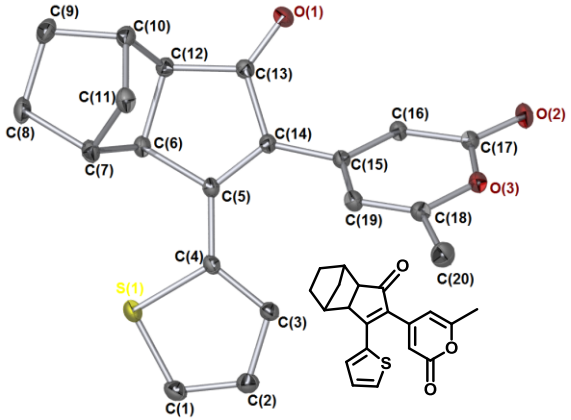

Figure 40(III) Single Crystal X-ray structure of **124β** showing β selectivity as a major isomer

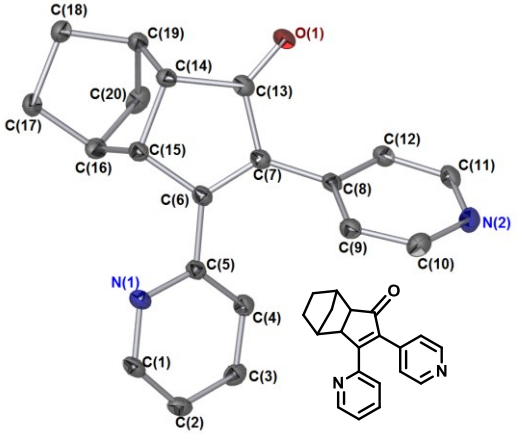

Figure 40(IV) Single Crystal X-ray structure of **127β** showing exclusive β selectivity

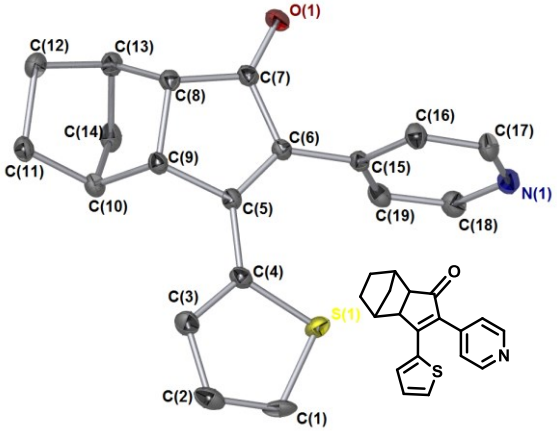

Figure 40(VI) Single Crystal X-ray structure of **125α** disordered thiophene deleted for clarity

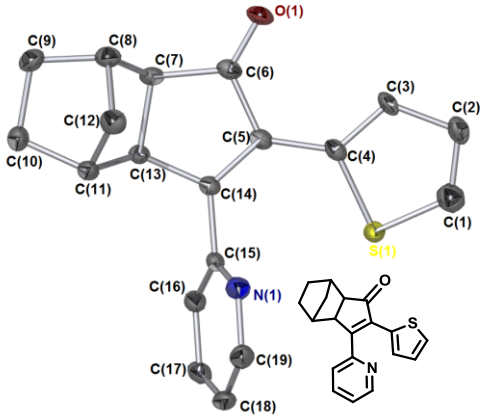

Figure 40(VIII) Single Crystal X-ray structure of **126β,** one thiophene deleted for clarity

Figure 40 Single Crystal X-ray structure of PKR for 121β, 122β, 124β, 125α, 126β and 127β

6.2.2 Significance of the alkene in determining PKR regioselectivity

Kanno *et al.*[102, 106, 108] and Riera *et al.* [107] explained that it is difficult to ignore the fact that the alkyne and solvent influence the regiochemical outcome of PKRs, while also acknowledging that the alkene can play a role. The findings in this project provide supporting evidence that varying alkene structure can have a profound influence on the PKR regio-selectivity, by using alkynes such as **114c** (Scheme 62). Norbornadiene influenced the selectivity outcome quite dramatically, affording cycloadducts **128β** in 57% and **128α** in 35% yield. While **128β** was still the major regioisomer; previously the reaction with norbornene gave this particular regioisomer, exclusively, *i.e.* **121β** – the results are summarised in Scheme 62.

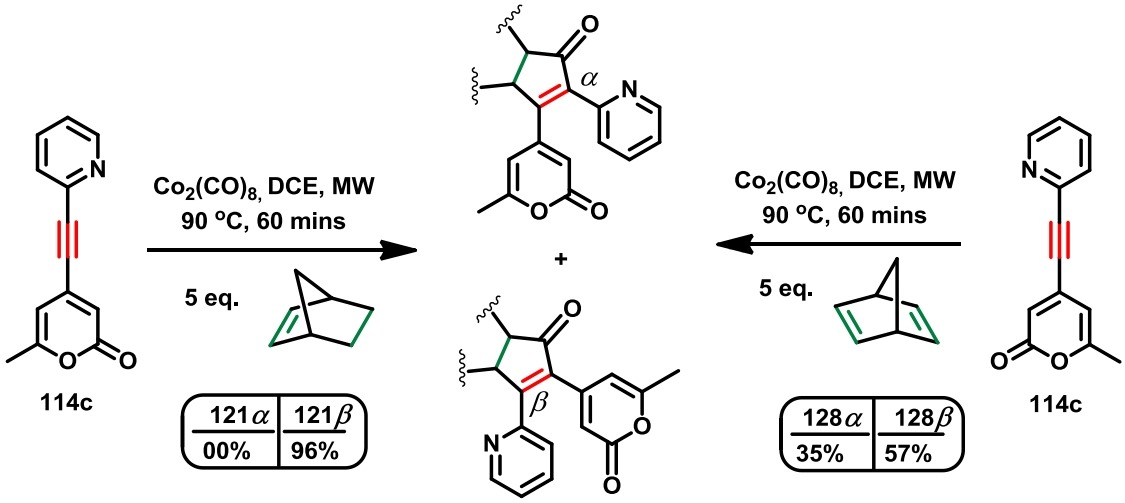

Scheme 62 PKR with norbornene and norbornadiene showing the significance of alkene structure in the affecting the regiochemical outcome of **121** and **128**.

The regiochemical outcome of the PK reaction of 2-pyridylalkynyl-2-pyrone **114c** with $Co_2(CO)_8$ and norbornadiene did not mirror the equivalent reaction with norbornene, presumably due to the former substrate being able to act as a bidentate ligand at Co.

The selectivity seen for **121** could also be explained based on bulky nature of the alkyne group toward alkene insertion. The alkene insertion toward bulky group favoured *trans*- **II** while *cis*- insertion is disfavoured **III** for compound **121**, exclusively (Scheme 63). The regiochemical outcome of the PKR with $Co_2(CO)_8$ and norbornadiene behaved as expected, giving **128β** as the major product not to ignore that the **128α** is also significant. The alkene insertion to both *cis*- and *trans*- is possible for PKR **128** *via* **IV** to give both **128β** and **128α** through **V** and **VI**, it was precedented that **128β** is the major product given that steric effect pay a vital role in controlling the selectivity outcome in PKR. Here is a speculative possibility for **128** to dimerise to form a compound similar to **VII** even though it was not detected. This chapter classifies the effect of the different heteroaromatic moieties and alkene insertion. The results suggest that a subtle combination of steric, electronic and alkene insertion factors control the regioselectivity.

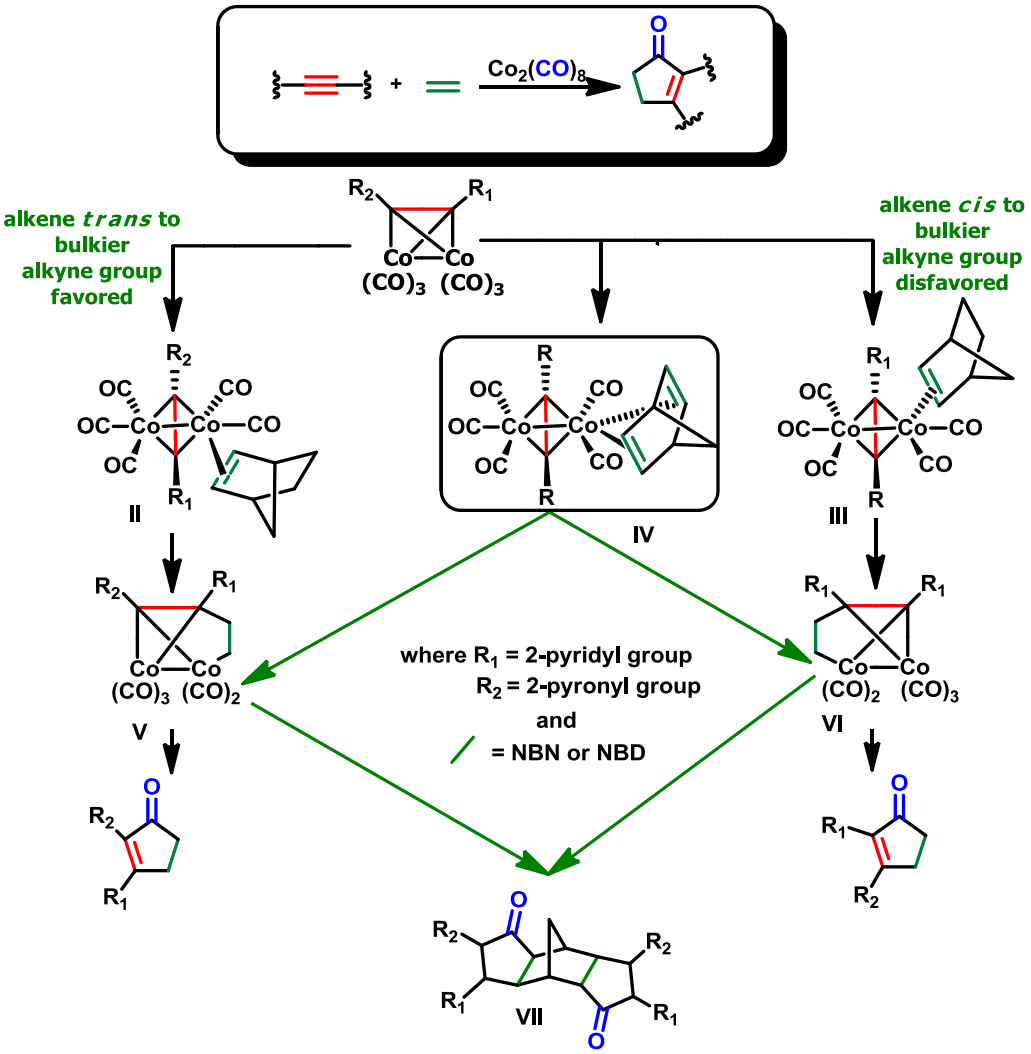

Scheme 63 Possible mechanism showing effect of alkene insertion on the regioselectivity outcome

6.2.3 Microwave-assisted PKR – a tool for forming other cyclic products

Besides the PKR cycloadducts, the microwave-assisted PKR protocol used in this study generated a by-product, *e.g.* Coogan lactone **129** via intermediate **129(I)** in good yield (42%) – the limiting regent in this case was norbornene (Scheme 64). Coogan and co-workers first reported that "treatment of norbornene with either dicobaltoctacarbonyl or with preformed alkyne-dicobalthexacarbonyl complexes affording the enol-lactone dimer" **129**.[136] The Fairlamb group previously reported observing trace amounts of **129**, under microwave-assisted PKR.[105]

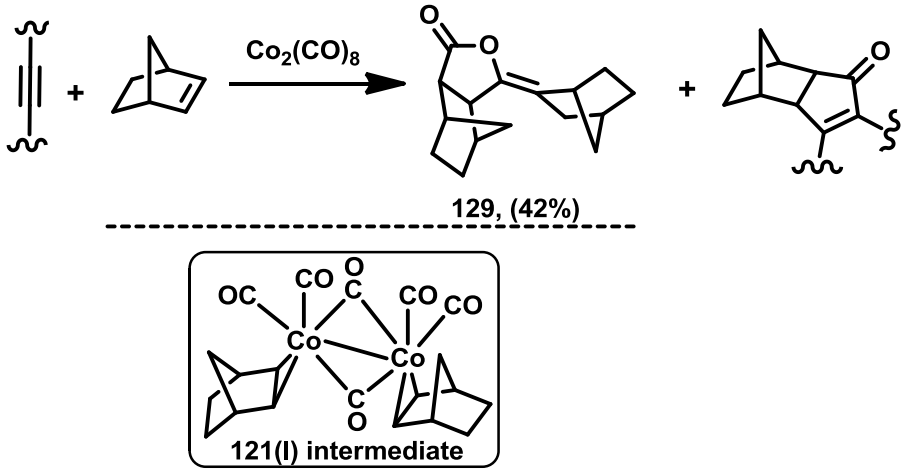

Scheme 64 Coogan lactone **129** as a side product in the PKR

An investigation was initiated to understand how and why these side products were forming, besides the desired PKR product. Three products were observed; Coogan lactone **129** and the formation of two hydrogenated alkynes **130** and **131** (Scheme 65). Formation of **130** and **131** from high pressures of carbon monoxide and cobalt catalysts in an air free environment is precedented. However, this is believed to be the first observation of hydrogenated alkynes from a PKR. The initial thought was that wet conditions might assist the hydrogenation process (Scheme 65).

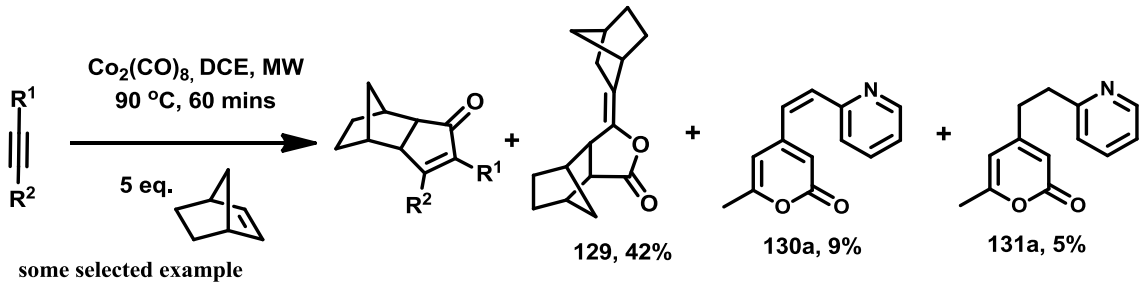

R^2 = 2-pyridine, R^1	= 2-pyrone	= 129(42%),	130a (9%),	130a (5%)
4-pyridine,	= 2-pyrone	= 129 (40%),	130b (11%),	130b traces
2-thiophene,	= 2-pyrone	= 129 (41%),	130c (10%),	130c traces

Scheme 65 Novel alkyne hydrogenation observed during microwave-assisted PK reaction

These compounds were characterised by spectroscopic methods. An example is shown in Figure 41, showing the NMR spectra of starting material **114c**, proton of C3 and C5 resonated at 6.07 and 5.30 ppm with Δδ = 0.77,while **130a** and **131a** resonated at δ C3 δ = 5.92, C5 δ = 5.87 and C3 δ = 6.08, C5 δ = 5.77 and their Δδ 0.31 and 0.05 respectively.

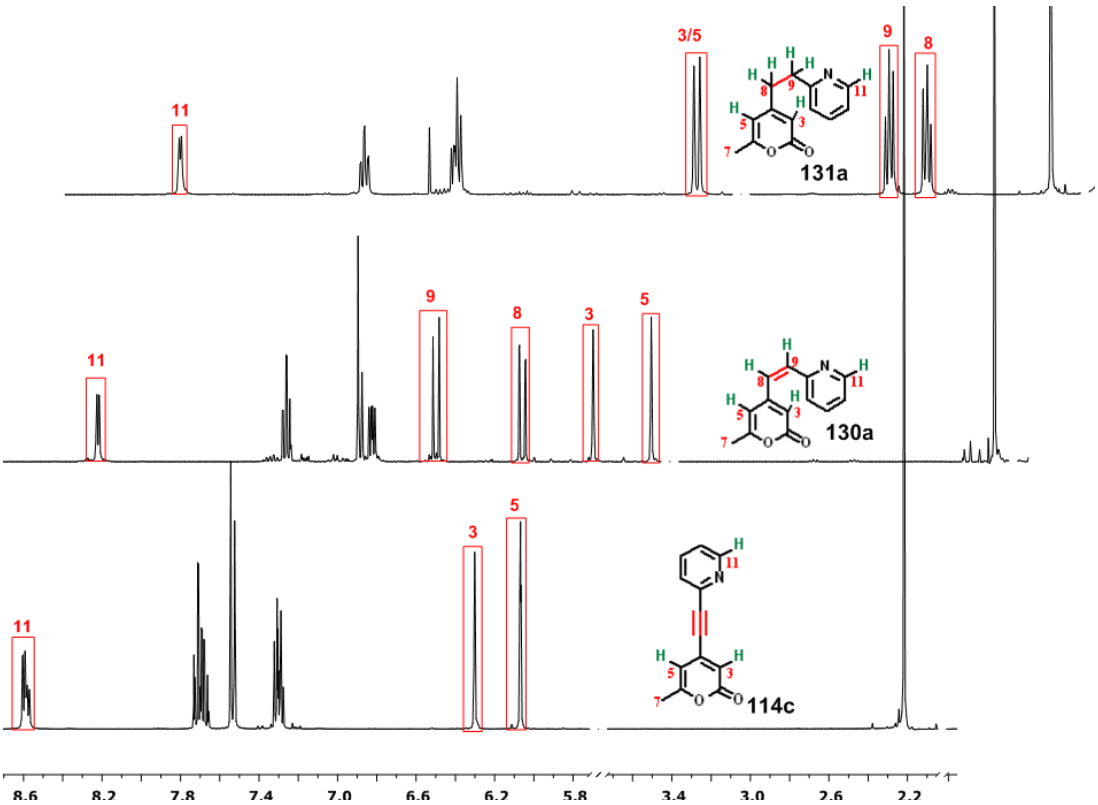

Figure 41 Stack plot of ^{1}H NMR spectra (400 MHz, $CDCl_3$) of **114c**, **130a** and **131a** (reaction conducted under various conditions along with reference spectra).

The reaction conditions affected the formation of lactone **129**, hydrogenated alkyne **130a** and double hydrogenated alkyne **131a**. Entry 1 in Table 10 employed dried solvent, where there was no hydrogenated alkyne **130a** or **131a** product observed, with **129** formed in 40 % yield. When using normal DCE, as purchased without further drying (entry 2), both lactone **129** and hydrogenated product **130a** and **131a** were observed in 42, 9, and 5 % yields respectively. Entry 3 revealed the addition of water (DCE/H_2O: 19/1 v/v) increased **129** (65%) and **131a** (17%) but decreased **121**

and **130a** (Table 10). Entry 4 revealed an increase in yield in both hydrogenated products. Addition of benzoquinone which acts as a scavenger to take up hydrogen in hydrogenation process and is known for hydrogenating agent increases the yields of **129**, **130a** and **131a** to 48, 15, and 18 % yields respectively.

Table 10 Study on the formation of side-products in PKR

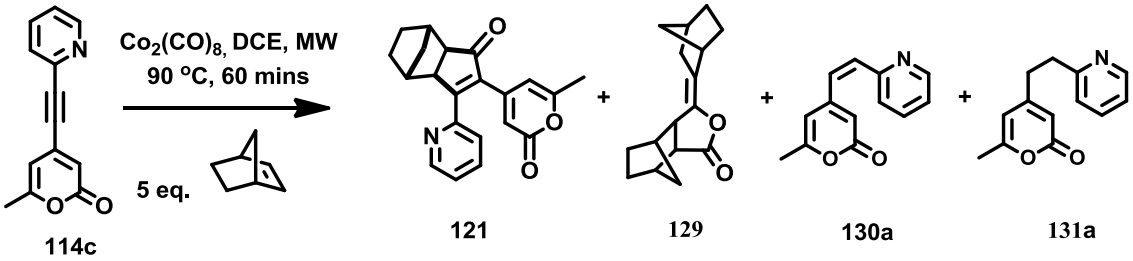

	Compounds	121	129	130a	131a
Entry	**Solvent condition**	**(% yield)**	**(% yield)[a]**	**(% yield)[b]**	**(% yield)[b]**
1	Dried DCE	76	40	00	00
2	Normal DCE (AR)	73	42	9	5
3	Wet DCE	46	65	trace	17
4	Wet DCE/Benzoquinone	60	48	15	18

[a] Yield based on excess norbornene used in reaction (5 eq). [b] Yield based on alkyne starting material.

In relation to alkene reactivity, Gimbert and co-workers,[98, 99] reported the reactivity of alkenes in the PKR, which showed the reactivity of cyclohexene, cyclopentene, and norbornene towards the hexacarbonyldicobalt(0) complex, the reactivity of which is related to the back donation of electrons from the d orbitals of the cobalt atom to the π*-orbital of the alkene.

Interaction of lower-lying LUMO alkenes give different lactones; an example is given in Scheme 66a, where norbornene reacts with dicobaltoctacarbonyl complex

by using (5 eq.) norbornene, $Co_2(CO)_8$ (1 eq.), in reagent grade DCE, this form compound **129** in a good yield (73%), higher than reported in literature.[136] It is well established in the literature that the better the back-donation the greater the reactivity and the lower the angle of the alkene the lower the LUMO, so the lower the LUMO the lower the energy barrier[98, 99] so using a larger angle (º) than norbornene, for example Scheme 66b cyclopentene (5 eq.), $Co_2(CO)_8$ (1 eq.), reagent grade DCE, gave lactone **132** although it was only characterised by ESI-MS. Reaction of norbornene and cyclopentene (Scheme 66c, in (1 eq.) norbornene, (4 eq.) cyclopentene and $Co_2(CO)_8$ (1 eq.), in DCE, gave cross-lactone **133**, although again this was only characterised by ESI-MS.

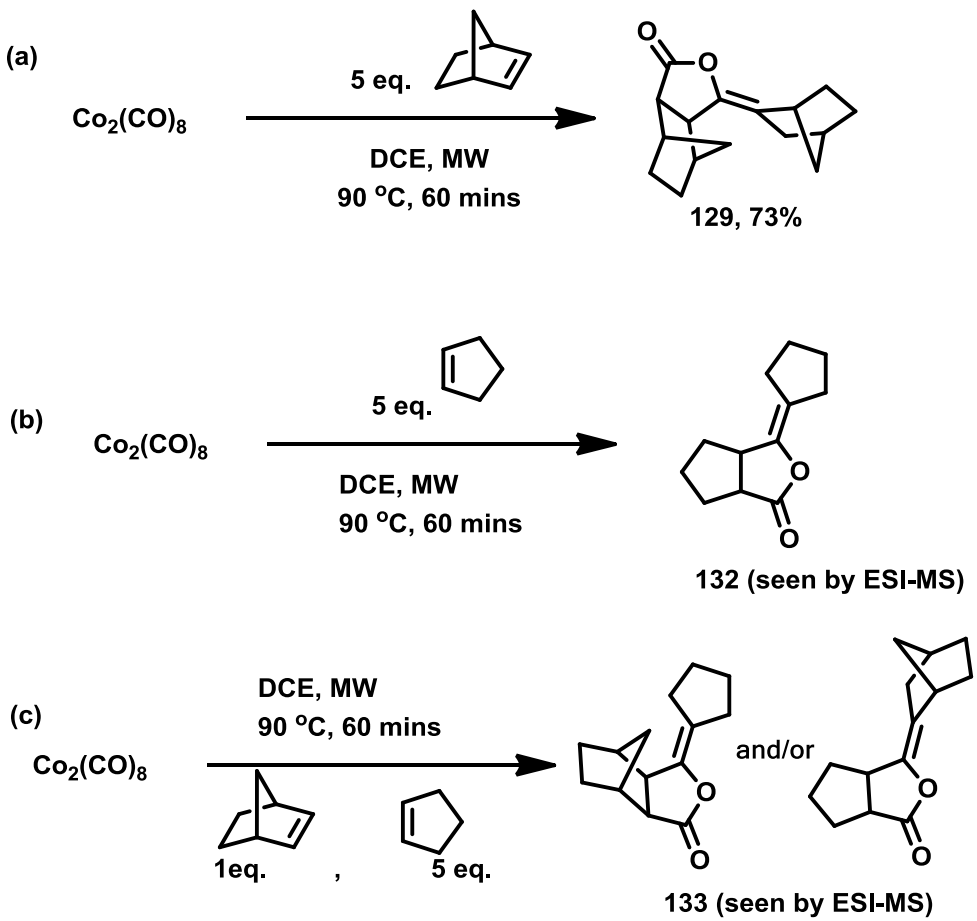

Scheme 66 Synthesis of Coogan-type lactones using two different alkenes.

6.3 Photochemical 6π-electrocyclisation reaction

Cyclopentene-2-one derived from the PKR readily undergo photochemically-induced 6π-electrocyclisation reactions, especially with compounds containing 2-pyrones, which on oxidation reveal benzo[h]indeno[1,2-f]isochromene type products.[109] The reaction occurs readily in natural light, and this thesis is interested in why, and how structural changes affect the efficacy of the electrocyclisation reactions with a control UV-light especially with compound involving 2-pyrones and related ring systems (**A**) to (**B**) via the intermediate showing in Scheme 67.

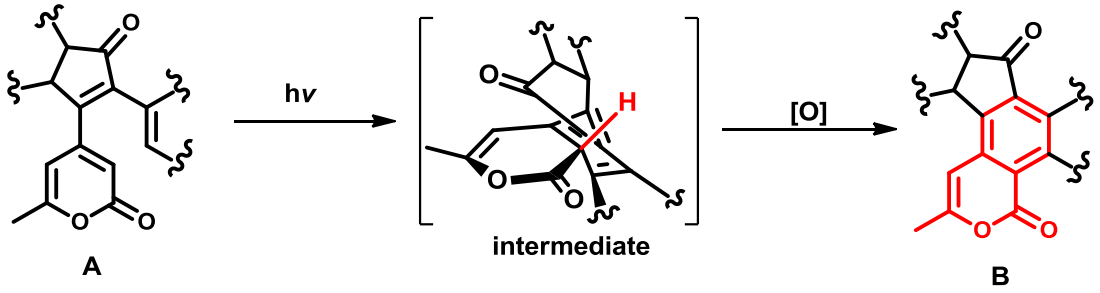

Scheme 67 General synthesis route for cyclisation and aromatisation of PK cycloadduct.

McKendry and Barboiu[137, 138] studied the light-induced electrocyclisation reactions of the 2-pyrone moiety giving encapsulated cyclobutadiene structures (**V**) *via* a suitable Dewar lactone (calixarene) (**II**) or to form extremely unstable aldehydeketene (**III**) (Scheme 68).[137] Sequence of photofragmentation of (**II**) occurs via cyclobutenecarboxylate zwitterion intermediates by eliminating CO_2, producing butadiene cyclo-compound (CBD) (**V**). The unstable (**V**) dimerizes to form (**VI**) that rearranges to cyclooctatetraene (**VII**).[137,138] (Scheme 68). This type of photochemistry particularly, with PKR cycloadducts, stimulated further interest in the photochemistry of these compounds.

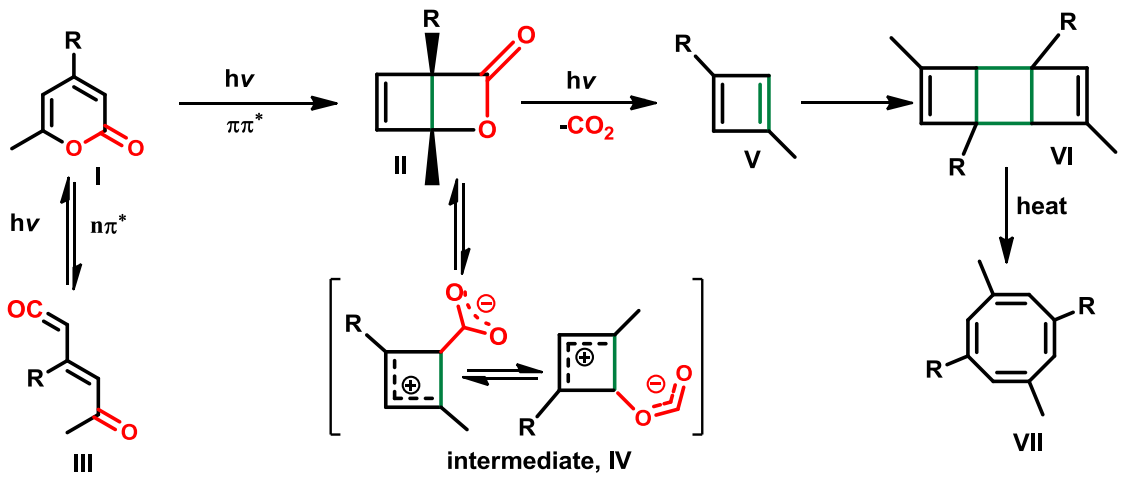

Scheme 68 α-Pyrone photolysis: electrocyclic opening of α-pyrone and formation of cyclobutadiene **V** and cyclooctatetraene **VII**.

6.3.1 Orbital symmetry and thermal versus photochemical selective activation in 6π electrocyclisations of PKR compound containing 2-pyrone system

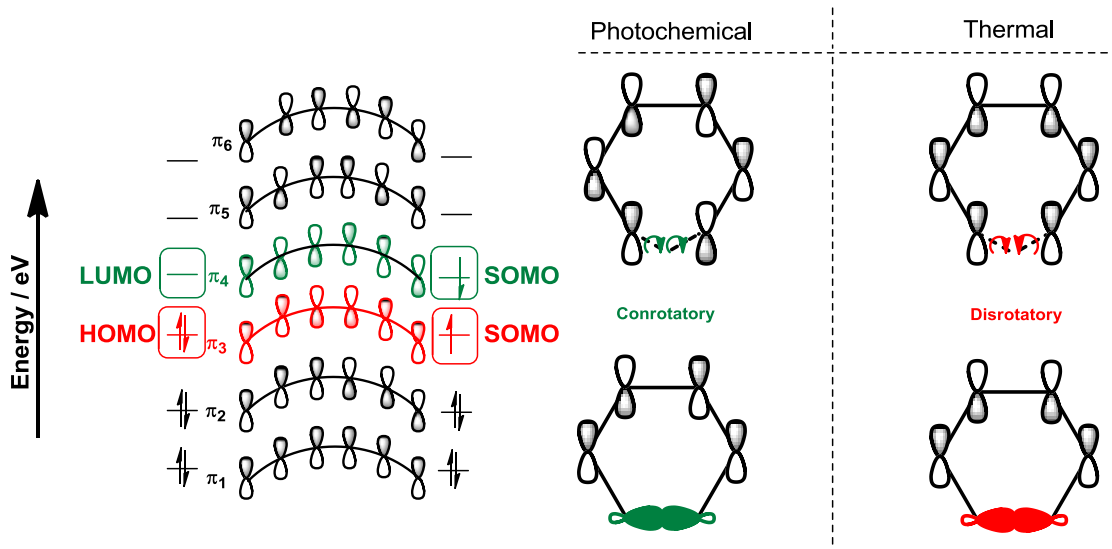

Figure 42 Thermal vs photochemical Symmetry allowed induced cyclization

A generally photochemical way of dihydrophenanthrene irreversibly converts to phenanthrene in the presence of air and oxygen, by hydrogen-elimination (loss of H_2O).[139, 140] It is proposed that the oxidant rapidly reacts with the dihydrophenanthrene intermediate to give **121B**, even in sun light.

In order to accelerate the reaction, a solution of compound **121A** in CD_2Cl_2 was irradiated using a purpose-built Amber LED UV lamp with a filter at 400 nm, in a reaction vessel with an air inlet. In ca. 40 min, the reaction was essentially complete with quantitative conversion >90%. The ^{1}H NMR spectra confirmed the formation of **121B** (Scheme 69).

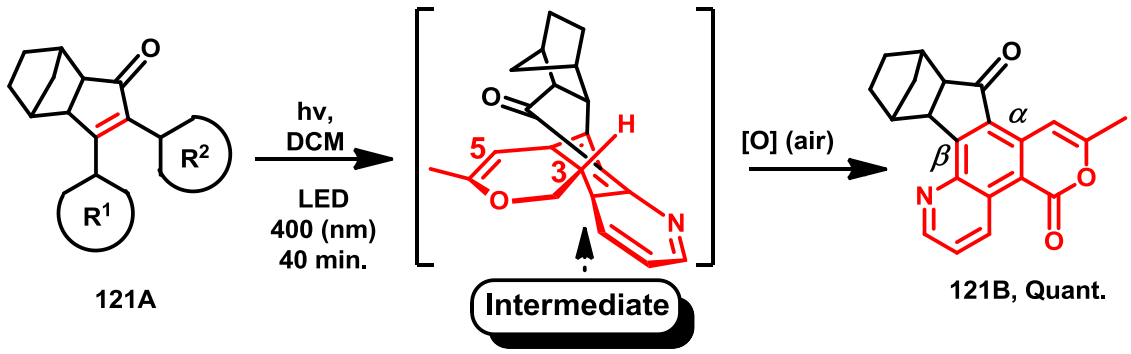

			A → Bβ	Bα
R^1 = Phenyl,	R^2 = 2-pyrone	= 113,	--	(>90%)
2-pyridine,	= 2-pyrone	= 121,	(>90%)	--
4-pyridine,	= 2-pyrone	= 122,	(>90%)	(>90%)
2-pyrazine,	= 2-pyrone	= 123,	--	–
2-thiophene,	= 2-pyrone	= 124,	(>90%)	(25%)
4-pyridine,	= 2-thiophene	= 125,	(50%)	(>90%)
2-pyridine,	= 2-thiophene	= 126,	(>90%)	(55%)
2-pyridine,	= 2-pyridine	= 127,	–	–

Scheme 69 Photochemical reactions of PKR the cycloadducts

The Fairlamb group in York conducted B3LYP density functional theory calculations (DFT) on a related system **113**.[104,109] It is proposed that a similar series of intermediates arise with **121A(I)**, given two local minima, relating to conformers **121A(I)** and **121A(II)** (Figure 43). The rotation of the 2-pyrone group about the cyclopentanone single bond of both **121A(I)** and **121A(II)** possesses similar stabilities. Conformer **121A(I)** is less stable by only 1.2 kcal/mol than **121A(II)**. Isolation of **I** was not successful. The only two possible routes are **I→III** and

I→II→III (Figure 43). It was of interest to study the effect of 2-pyridyl group, and other heteroaromatic moieties, to evaluate whether they possess similar characteristics (Figure 43).

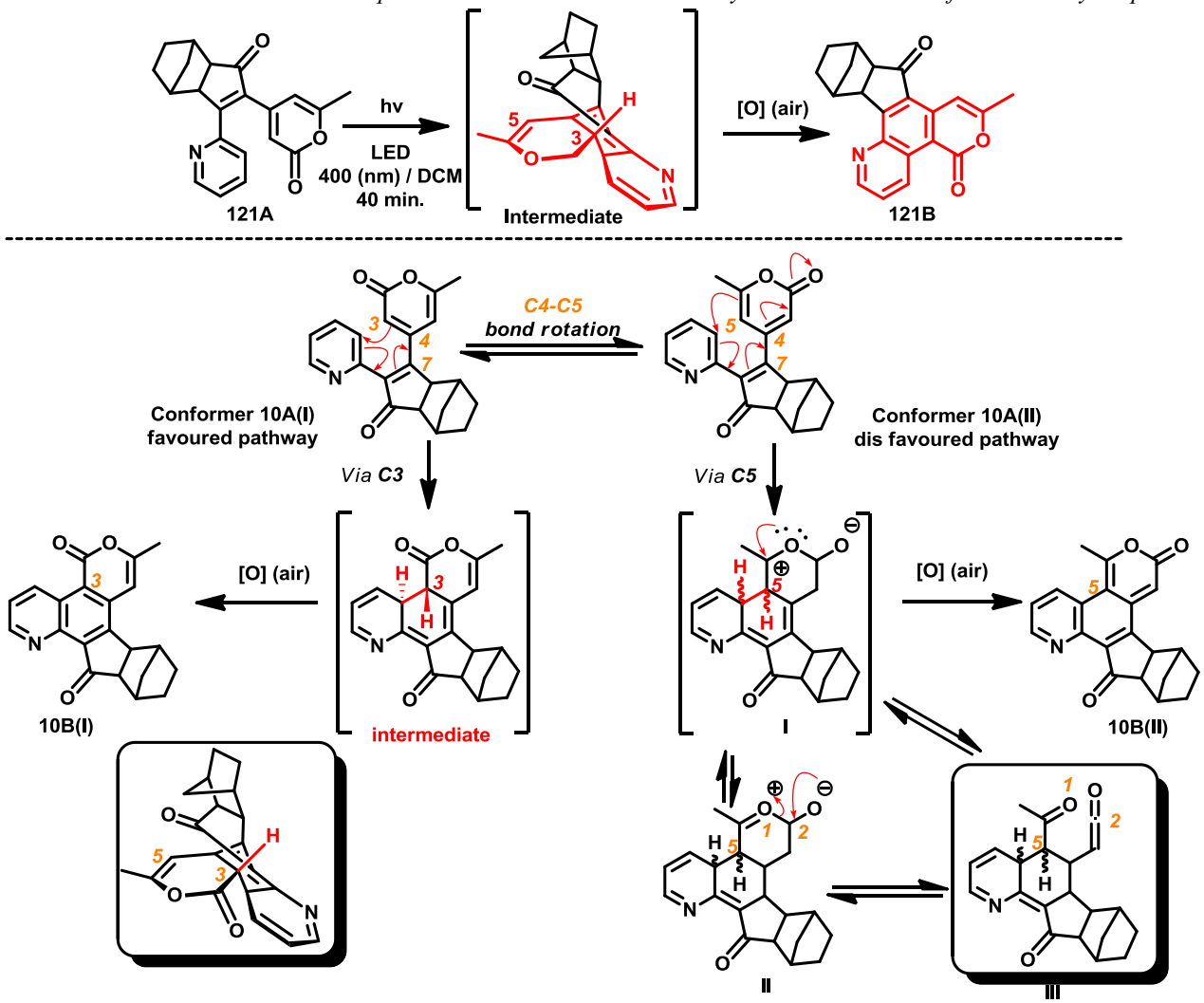

Figure 43 Mechanism and possible regioselective C3 and C5 paths for the formation of **121B** from **121A**

6.3.2 Spectroscopic analysis

Exposure of **121A** to ambient light leads to cyclisation and subsequent aromatisation to give **121B**. This strategy was applied to PKR compounds **121-128** of both α and β respectively (Table 8). Although the aromatisation occurs very fast, it was hoped that the dihydrophenanthrene could be detected during the conversion of **121A** to the aromatised **121B** using the Signal amplification by reversible exchange (SABRE) technique. First there is a need to understand the timeframe for complete cyclisation and aromatisation, using controlled UV-vis light at a given intensity which would undergo 6π-electrocyclisation (Scheme 69). Irradiation of **121** gave complete cyclisation and aromatisation (Figure 44). Experiments were performed with an Amber LED (0.2 amp) (400 nm), to irradiate a 5 x 10^{-6} mol/dm^3 solution in a quartz cuvette for 30 sec. followed by a hold period of 2 mins and 33 sec. The UV-Vis spectrometer was set to scan every 4620 sec.; the first scan was run before irradiation under air, in DCM. The photoconversion of **121A** to **121B** was monitored at a low concentration of **121A** in DCM by UV-vis spectroscopy. The spectral changes upon irradiation of a solution of **121A**, at 30 second intervals at 400 nm from 0 to 240 sec. suggested complete cyclisation; further irradiation shown no significant change (Figure 44). Furthermore, further data for **113β**, **124β**, **124α**, **125β** and **126α** can be seen in Appendix 2.

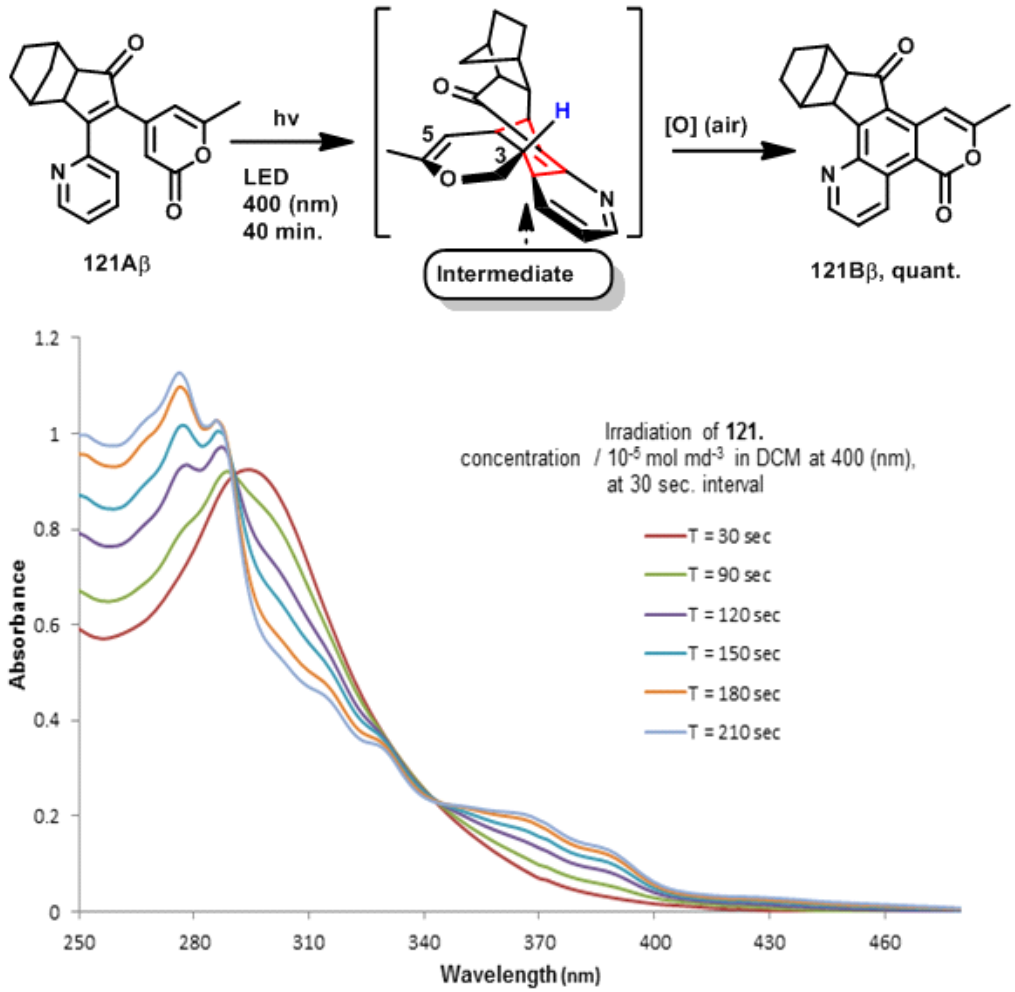

Figure 44 UV analysis; monitoring the 6π-photo-electrocyclization and aromatization of **121*β*** with respect to time

The resulting irradiated solution of **121B** was characterised by ESI-MS and NMR. The ^{1}H NMR suggested complete cyclisation and aromatisation, determined by the disappearance of C3H of the pyronyl moiety for **121A** and ^{1}H α– to the substituent in the pyridyl moiety of **121A**. However, the C5 proton chemical shift of 2-pyrone moiety resonated at δ 5.69 ppm for **121A** and the cyclised product **121B** resonated at δ 7.90 ppm with a difference Δδ = 2.21 ppm, ^{1}H α to the substituent in the pyridyl moiety of **121A** δ 8.70 ppm and the cyclised product δ 10.01 ppm with Δδ = 1.31 also the ^{1}H's of cyclopentanone showed significant δ changes example ^{1}H β to enone

of cyclopentanone for pre-cyclised compound 10A δ 3.42 ppm and cyclised product δ 3.78 ppm with Δδ = 0.36 confirmed the formation of product **121B** (Figure 45).

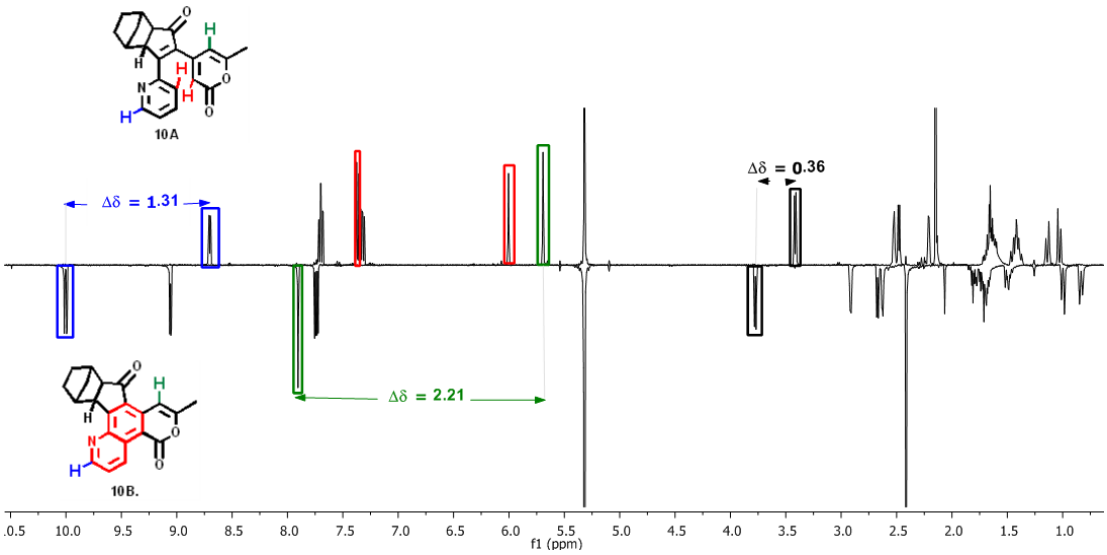

Figure 45 Stacked spectra plot showing the pre-cyclised **121A** over complete cyclised product **121B** and Δδ of some new signals

A sample of **121A** (10 mg) was dissolved in 0.6 mL CD_2Cl_2 in an NMR tube and the solution was then monitored by ^{1}H NMR (Figure 46). After <30 minutes of irradiation (interval of 1 min.) at ambient temperature, a set of new peaks (Figure 46) can clearly be observed to be appearing next to the starting material example protons of pyridine group (especially proton α– to nitrogen) at time zero (0) relative integration 100% pre-cyclised **121A** δ 8.70 ppm while 0 % cyclised product **121B** δ 10.01. However, after irradiation for 26 minutes at ambient temperature (ca. 23 ^{o}C) the relative integration changed completely to 0% pre-cyclised **121A** δ 8.70 ppm while 100% cyclised product **121B** δ 10.01. The time difference between UV and NMR analysis (3 min and 26 min for complete cyclisation) respectively, could best be explained based on concentration (Figure 46).

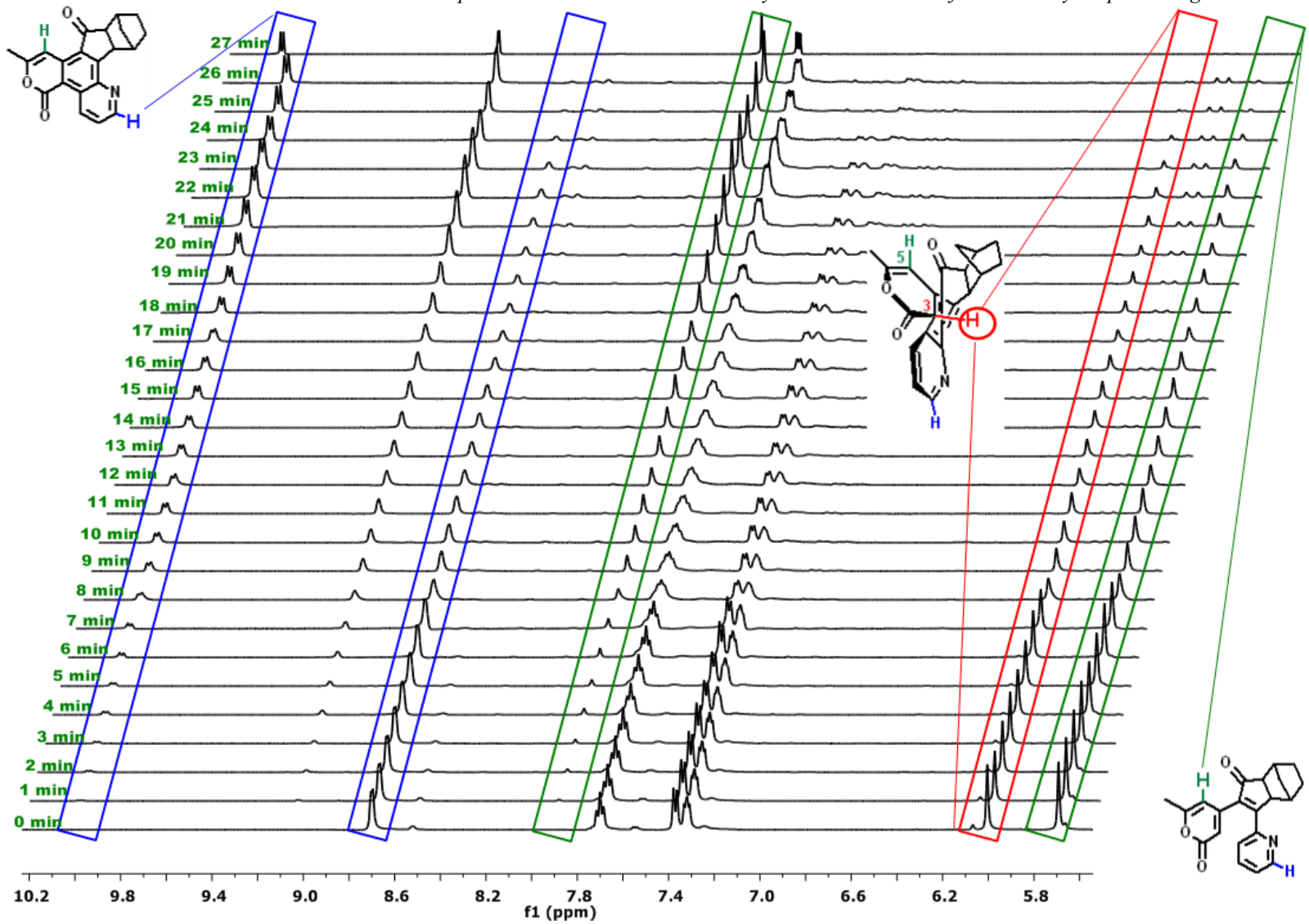

Figure 46 Stack spectral plot of irradiation cycles showing conversion of the pre-cyclised **121Aβ** to cyclised product **121Bβ** over a period of 28 min. at 1 min. intervals (λ = 400nm)

However, after heating the starting material **121A** at 35 °C for 30 minutes there was no difference with respect to unheated **121A**. Also, heating in a water bath to 35 °C, upon irradiating the sample, shows no relative integration decrease or increase in respect to unheated **121A** to **121B** at 4 min. intervals (Figure 47).

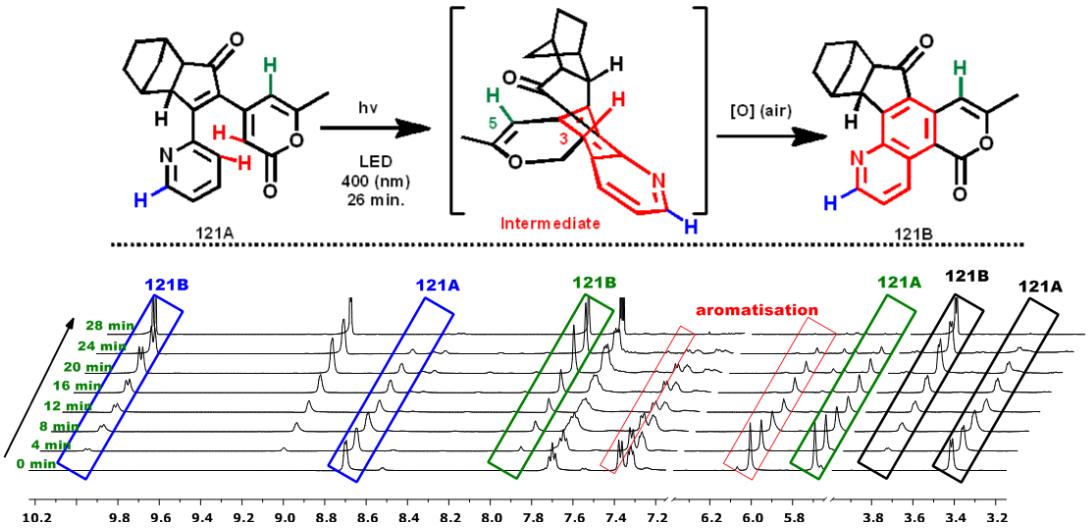

Figure 47 Stack spectral plot of irradiation cycles showing the heated (35 °C) pre-cyclised **121A*β*** to cyclised product **121B*β*** over a period of 28 min. at 4 min. intervals (λ = 400nm)

Table 11 summarise the electrocyclisation and relative rate of the electrocyclisation – aromatisation reactions for **121** to **127** α- and β-, in CD_2Cl_2 solutions. Each compound was irradiated for between 1 min. to 1 h at 400 nm and monitored by UV-Vis. The ^{1}H NMR after which time the relative ratios of the starting compounds to products **121-127** α– and β–, were determined by a relative integral ratio of ^{1}H NMR spectroscopy with respect to starting material (Figure 44 and Figure 46,). It was noted that the rate of cyclisation of compound containing thienyl moiety at α– to enone of cyclopentanone is significantly affected with respect to the β– moiety, the β-thienyl moiety gave complete cyclisation within ca. 30 min. while the α-thienyl moiety gave ca. 25%, 55% and 50%, see entries 5, 8 and 9 respectively (Table 11). Also no cyclisation was observed in entries 3 and 10.

Table 11 Synthesis of PKR cyclic adduct and respective α and β regio-isomers (note the regioisomer is w.r.t cyclopentanone)

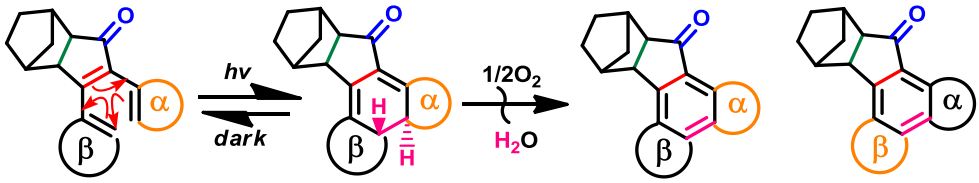

Entry	Substrate	α	β	Entry	Substrate	α	β
1	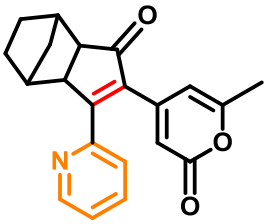	121B --	121B quant.	6	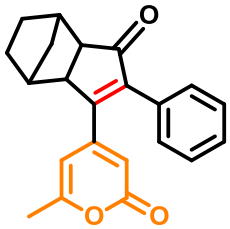	113B --	113B quant.
2	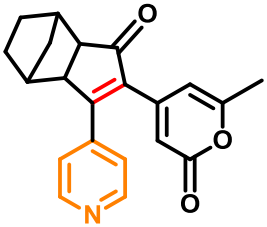	122B quant .	122B quant.	8	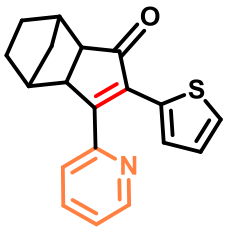	125B quant.	15B ca. 55
3	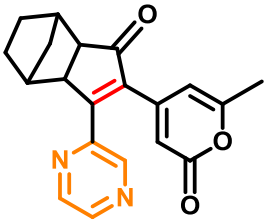	123B --	123B --	9	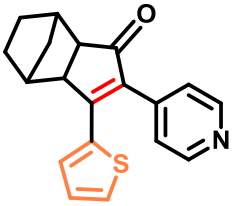	126B ca. 50	126B quant.
5	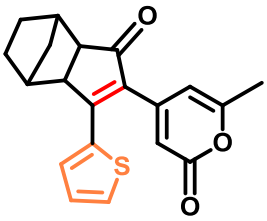	124B ca. 25	124B quant.	10	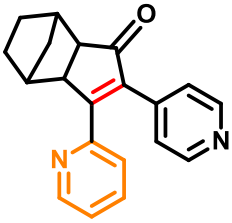	127B --	127B --

Concentration of reagents entry 1-10 (60 mM in CD_2Cl_2) irradiation for 30 min. and percentage yield given as starting material: to product as determined by ^{1}H NMR spectroscopy (400 MHz). (-- = no cyclisation observed).

6.4 Conclusion

This chapter has examined the regioselectivity of the PK reaction by substituting the heteroaromatic group, especially with the 2-pyrone group, using a series of unsymmetrical internal alkynes. The position of nitrogen α– (ortho-) to the substituent prove to be useful in controlling the regioselectivity outcome, as seen with compounds **121**, **123**, **125** and **127** (Table 8, page 140). Furthermore compounds **122**, **126** and **128**, where the nitrogen is γ– (meta-) to the substituent depended on steric influence of the next nearest atom. This proved a useful dichotomy with respect to the position of nitrogen in the pyridyl (heteroaromatic) moiety, especially compound **127**, where 2-pyridyl overrode the 4-pyridyl group. This chapter has also demonstrated that varying the alkene substrate affects the regiochemical outcome of **128** with respect to **121** which may be due to the "push–pull" effect of internal alkynes and $Co_2(CO)_8$ (Scheme 62 and Scheme **63**).

For the first time an alkyne hydrogenation processes is reported as a side-product in the microwave-assisted synthesis of the PKR (Scheme 65 and Table 10). Mechanistic studies are required to fully understand the regiochemical observations made in this and in other studies. Further breakthroughs could be achieved if mechanistic studies reveal how the positions of nitrogen in the heteroaromatic group affects the Co-Co bond order in intermediate complexes such as **121(I)** to **127(I)** (Scheme 61) and subsequent intermediate species to the final product.

The major and minor PKR regioisomeric products **121-128** readily undergo a photochemically-induced 6π-electrocyclisation–oxidative aromatisation reaction with the exception of **123** and **127** to reveal aromatised and functionalised type products **121B**, **122B** and **124B-126B** α and β respectively.

Chapter 5 Over-arching conclusions

7.1 General conclusions

Chapter two: Palladacyclic complexes have been prepared with differing C^N backbones, and OAc, Cl, PPh_3, PPh_2Cy, PPh_2(*t*-Bu), P(*n*-Bu)$_3$, P(Fu)$_3$ and NO_2 ligands. This has allowed a greater understanding of the cyclopalladation behaviour of several organic substrates (ligands) to be gained. Furthermore, the successful synthesis and characterisation of a series of C^N palladacyclic complexes containing nitrite ligands has paved the way into understanding how NO_2 bonds to Pd with each showing a *trans*-geometry.

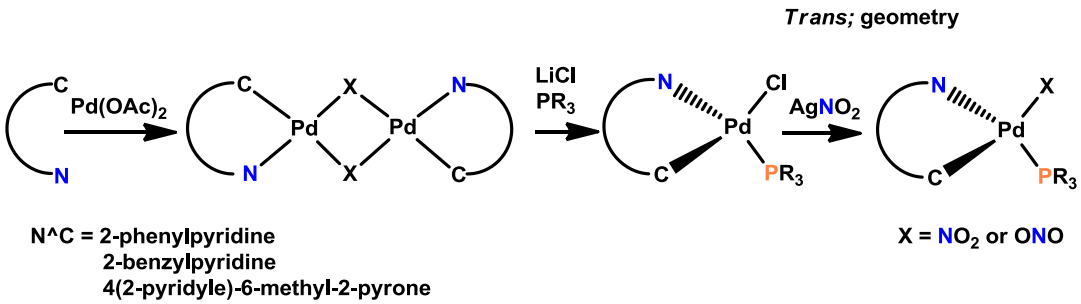

Scheme 70 Synthesis of novel Pd$^{(II)}$-nitrito-cyclopalladated complexes by a general synthetic route

When assessing the role that such ligands can play in catalysis, and in particular the potential for reductive elimination of useful "C–NO_2" type products, the geometry and linkage isomerism of the complexes is of paramount importance. However for more bulky phosphine (PPh_2Cy and PPh_2(*t*-Bu)) ligands with N^C = (2-phenylpyridine), monomeric Pd$^{(II)}$ complexes could be characterised by NMR spectroscopy, although crystallisation yielded a novel Pd^{II} dimer complex where the bulky phosphine ligand had been ejected and the nitrito ligand is now found bridging two Pd^{II} centres (Figure 48).

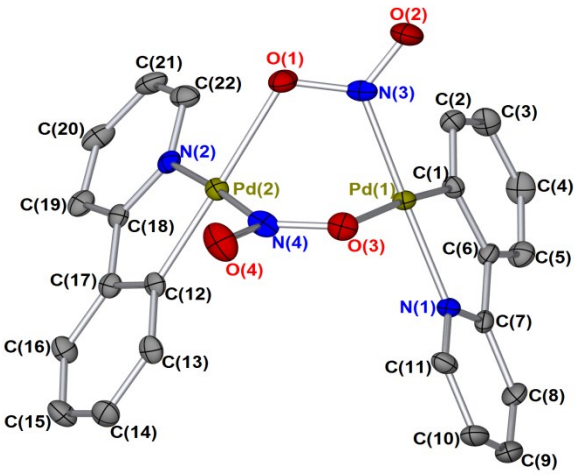

Figure 48 Single crystal X-ray diffraction structure of complex **74a**

Calculated free energy values (DFT) suggest that the energy difference between *cis* and *trans* geometric isomers with respect to pyridyl moiety in all the Pd complexes increases with increasing steric bulk of the C^N ligand and reductive elimination experiments, where elimination of C–NO_2 type products, which would normally require the two ligands being eliminated to be mutually *cis*, was not observed. The crystal structure of all the nitrite complexes prepared in this thesis showed a mixture of *N*- and *O*- bound linkage isomers. The DFT calculations, suggest for this complexes to be catalytically active the nitrite ligand should be *cis* to pyridyl moiety in all the nitrite complexes, which suggested they are catalytically less active.

Chapter three: A 2-pyridyl directing group can become directly involved in Mn(I)-mediated alkenylation reactions.[69] Replacement of a phenyl group with a 2-pyrone (more electron-accepting) group had shown a profound effect on the preferred reaction path, affording stable and isolable intermediate manganese adduct. Critically, for the first time evidence for a commonly-proposed manganacycle 16-electron 5-coordinate intermediate has been gathered (Scheme 71, in work conducted in collaboration Kate Appleby from the Fairlamb/Duckett group), which is found to

be the pivotal intermediate controlling whether direct reductive elimination or protonation and metal de-coordination occurs affording the intermediate, alkenylated or Diels-Alder products (Scheme 71).

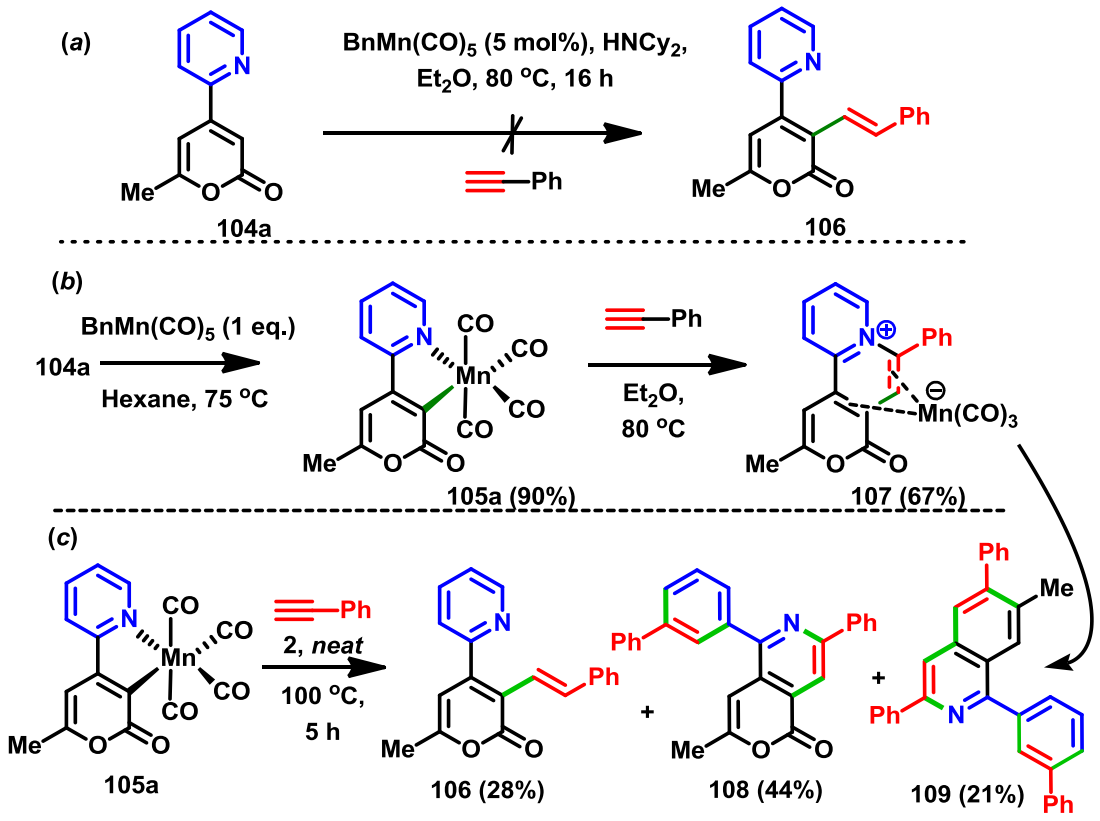

Scheme 71 Unprecedented alkyne insertion into cyclomanganesiated complex and alkenylation / Diels-Alder rearrangement

The stoichiometric reactions conducted in neat phenyl acetylene showed that other products in addition to **106** can be readily formed. Remarkably, unprecedented C-H bond activation and Diels-Alder adduct process involving 2-pyridyl ring-cleavage and a recombination process to give **108** and a plausible regioselective second Diels-Alder addition in to pyrone pave the way for six, C-H bond functionalisation in a single molecule **109**. When the 2-pyridyl group replaced with a 6-methoxy-2-pyridyl unprecedented complexed **110** was isolated, the anticipation was due to a more electron-donating group in the pyridine moiety and had shown a profound

effect on the preferred alkyne insertion reaction path, affording stable and isolable manganese adduct **110**.

The combined experimental and computational approach used in this study has allowed the delineation of a mechanistic dichotomy in Mn(I)-mediated C-H bond activation. These believe to be the findings in this study provide an insight into future design of Mn(I)-mediated C-H bond activation processes involving electron deficient compound like 2-pyrone.

Chapter four: Here, the regioselectivity of the PKRs of alkynes containing heteroaromatic moieties, substituting with 2-pyrone especially, was examined with two alkenes (norbornene and norbornadiene). The position of nitrogen $\alpha-$ (ortho-) to the substituent prove to be useful in affecting the regioselectivity outcome, *e.g.* compounds **121**, **123**, **125 and 127** (Table 8, page 140). Furthermore, compounds **122**, **126** and **128**, where the nitrogen is at $\gamma-$ (meta-) to the substituent, depend on the steric influence of the next nearest substituent. This revealed a useful dichotomy with respect to the position of nitrogen in the pyridyl (heteroaromatic) moiety especially compound **127**, where the 2-nitro overrides the 4-nitro group exclusively. This thesis also demonstrated that varying the alkene substrate affect the regiochemical outcome **128** with respect to **121** which may be due to push pull effect of internal alkynes and $Co_2(CO)_8$ (Scheme 62 and Scheme **63**). For the first time an alkyne hydrogenation processes is reported as a side product in a microwave-assisted synthesise of PKR product (Scheme 65 and Table 10). Further mechanistic studies are required to fully understand the regiochemical observations, made in this and in other studies. Furthermore breakthrough could be achieved if, for example, a mechanistic study revealed how the positions of the nitrogen atom in the heteroaromatic group affect the Co-Co bond order in intermediate complexes such as

121(I)-127(I) (Scheme 61 page 138) and subsequent intermediate species to the final product.

The major and minor PKR regioisomeric products **121-128** readily undergo a photochemically-induced 6π-electrocyclisation–oxidative aromatisation reaction, with the exception of **123** and **127**, to reveal aromatised and functionalised type products, *e.g.* **121B**, **122B** and **124B-126B** α and β respectively. The precise arrangement of atoms in **124B-126B** suggested that the α-thienyl regioisomer supresses the photochemically-induced electrocyclisation process with respect to the β-regioisomer.

Chapter 6: Experimental section

8.1 General experimental techniques

Solvents and reagents

All commercially sourced reagents were purchased and used as received unless otherwise noted from Alfa Aesar, Acros Organics, Sigma-Aldrich, or Fluorochem. Dry solvents used were obtained from a Pure Solv MD-7 solvent machine and stored under nitrogen. Trimethylamine was dried by the condensation method, under nitrogen or argon conditions, and THF was also deoxygenated by bubbling nitrogen gas though the solvent with sonication.

All reactions requiring anhydrous or air-free conditions were carried out in dry solvents under an argon or nitrogen atmosphere

Nuclear magnetic resonance spectroscopy

Proton (^{1}H), Carbon-13 (^{13}C decoupled ^{1}H) and Phosphorus-31 (^{31}P decoupled ^{1}H) spectra were recorded on a Jeol ECX400 or Jeol ECS400 spectrometer at 400 and 100 MHz respectively, or on a Bruker AV500 operating at 500 and 125 MHz respectively. Chemical shifts are reported in parts per million (ppm) of tetramethylsilane using residual solvent as an internal standard CD_2Cl_2 δ H = 5.32 ppm; CD_2Cl_2 δ C = 54.84 ppm or $CDCl_3$ δ H = 7.26 ppm; $CDCl_3$ δ C = 77.16 ppm). Multiplicities are described as singlet (s), doublet (d), triplet (t), quartet (q), pentet (p), multiplet (m), apparent (app.) and broad (br). Coupling constants (*J*) are quoted to the nearest 0.1 Hz. Spectra were processed using MestreNova; apodization (Sine-Bell 0°) was used to enhance the (*J*) couplings, where necessary. Spectra were

exported as JPEG (or similar format) images into the appropriate document. Copies of ^{1}H and ^{13}C NMR spectra for all compounds are given in a CD Appendix.

Phosphorus-31 (^{31}P) spectra are referenced externally to H_3PO_4 and reported in parts per million (ppm).

Chromatography

Thin layer chromatography (TLC) was carried out using Merck aluminium backed 5554 plates. Spots were visualised by the quenching of ultraviolet light (λ_{max} = 254 nm) and then stained and heated with one of anisaldehyde, potassium permanganate or phosphomolybdic acid as appropriate. Flash column chromatography was ordinarily performed using Merck 60 silica gel. Preparatory TLC was carried out using Analtech UNIPLATE glass-backed silica plates.

Melting points

Melting points were determined using a Stuart SMP3 melting point apparatus using a temperature ramp of 3 °C min^{-1}.

UV–Visible spectroscopy

UV–visible spectroscopy was performed on a Jasco V-560 spectrometer, with a background taken in the appropriate solvent prior to recording spectra, using a cell with a path length of 1 cm. The wavelength of maximum absorption (λ_{max}) is reported in nm along with the extinction coefficient (ε) in mol dm^{-3} cm^{-1}. Copies of the appropriate absorption spectra and Beer–Lambert plots are given in Appendix 6.

Elemental analysis

Elemental analysis was carried out using an Exeter Analytical CE-440 Elemental Analyser, with the percentages reported as an average of two runs.

X-Ray crystallography

Diffraction data were collected at 110 K on an Agilent SuperNova diffractometer with MoKα radiation (λ = 0.7107 Å). Data collection, unit cell determination and frame integration were carried out with CrysalisPro. Absorption corrections were applied using face indexing and the ABSPACK absorption correction software within CrysalisPro. Structures were solved and refined using Olex2252 implementing SHELX algorithms and the Superflip253-255 structure solution program. Structures were solved by charge flipping, Patterson or direct methods and refined with the ShelXL256 package using full-matrix least squares minimisation. All non-hydrogen atoms were refined anisotropically and structures presented were processed using X-seed soft wire.

8.1.1 General procedures

General procedures A: Synthesis of palladacycle dimers[113]

(A1) *Procedures for [Pd(OAc)(N^C)]$_2$*: An acetic acid (30 mL) suspension containing palladium(II) acetate (1 eq.) and ligand (1 eq.) was refluxed for 1.5 h and then filtered. Water (150 mL) was added to the yellow filtrate, and the mixture was left standing overnight. Precipitated solid was filtered and then recrystallised from dichloromethane and hexane to afford the desired complex.

(A2) *Procedures for [PdCl(N^C)]$_2$*: Lithium chloride (2.2 eq.) in water (10 mL) was added to an acetone (20 mL) suspension of [Pd(OAc)(N^C)]$_2$ (1.0 eq.) and the resulting mixture was stirred for 48 h at room temperature. After filtration, the filtered residue was washed well with a methanol/water (1/1, *v*/*v*) mixed solvent, to afford the desired complex.

(A3) *Procedures for Pd[Cl(N^C)]$_2$*: A methanol suspension (10 mL) containing palladium(II) chloride (1 eq.) and ligand (2 eq.) was refluxed for 2 h. The resulting yellow solid was filtered off and then recrystallised from dichloromethane and hexane to afford the desired complex.

General procedures B: Synthesis of palladacycle monomers[114]

(B1) *Procedures for [PdCl(N^C)(PPh$_3$)]:* A solution of μ^2-chlorido-bridged complex, [PdCl(N^C)]$_2$ (1 eq.) and triphenylphosphine (1.2 eq.) in dichloromethane (10 mL) was stirred at room temperature for 30 min, under nitrogen atmosphere. The reaction mixture was filtered through Celite and hexane was added to induce precipitation. The product was collected by filtration and recrystallised from dichloromethane/hexane to afford the desired complex.

(B2) *Procedures for [Pd(NO$_2$)(N^C)(PPh$_3$)]*: A solution of [PdCl(N^C)(PPh$_3$)] (1 eq.) and silver nitrite (2.2 eq.) in dichloromethane (18 mL) was stirred at room temperature for 48 h. The reaction mixture was filtered and the filtrate concentrated *in vacuo* to afford the desired complex.

General procedure C: Negishi cross-coupling reaction

(**C**) *Procedure for 4-(2'-pyridyl)-6-methyl-2-pyrone* **81** *and its derivatives*: To a flame-dried Schlenk tube under N_2, equipped with a magnetic stirrer bar, was added 2-bromopyridine (2.78 mmol, 440 mg, 1.05 eq.) in dry THF (30 mL). The solution was cooled to -110 ^{o}C and then *n*-BuLi (2.78 mmol, 1.2 mL, 1.05 eq.) was added dropwise over 10 min with stirring, which was left to continue stirring for a further 30 min. To a separate, flame-dried Schlenk tube under N_2, equipped with a magnetic stirrer bar, was added high vacuum line-dried $ZnCl_2$ (2.91 mmol, 400 mg, 1.1 eq.; dried to constant weight, *ca.* 12 h). The lithiated 2-pyridine was transferred *via* cannula at -110 ^{o}C to the $ZnCl_2$, over 5 mins. The mixture was allowed to warm to -40 ^{o}C, with constant stirring for 30 min.

To a separate flame-dried Schlenk tube under N_2, equipped with a magnetic stirrer bar, was added 4-bromo-6-methyl-2-pyrone (2.65 mmol, 500 mg, 1 eq.), $Pd(PPh_3)_4$ (0.13 mmol, 150 mg, 5 mol%) sequentially and dry THF (20 mL). The zincated 2-pyridine was rapidly transferred *via* cannula and the reaction mixture allowed to stir at 22 ^{o}C for 12 h. The reaction was monitored by TLC analysis. Upon completion, it was quenched with saturated NH_4Cl (ca. 30 mL), and the mixture was filtered through Celite^{TM}. The mixture was extracted with EtOAc (2x25 mL). The crude product was purified by silica gel column chromatography (petroleum ether:EtOAc, 60:40, *v/v*) to afford the product as a creamy solid (485 mg, 85 %).

General procedure D: Synthesis of manganacycle.[69]

(D1) *Synthesis of five membered manganacycle:*[69] To a flame-dried Schlenk tube was equipped with a magnetic stir bar. $MnBr(CO)_5$ (0.05 mmol, 10 mol %, 13.75

mg), hexane (1.2 ml), 4-(2'-pyridyl)-6-methyl-2-pyrone **81** (1.0 mmol, 155 mg), phenyl acetylene **16** (0.5 mmol, 51 mg) and dicyclohexylamine (0.1 mmol, 18.1 mg) were added sequentially under nitrogen. The closed tube was put into a pre-heated oil bath at 80 ^{o}C and stirred for 6 h. After completion of the reaction, the resulting mixture was cooled down to room temperature, diluted with dichloromethane (10 mL), filtered through a short pad of silica gel and washed with EtOAc (30 mL). The filtrate was pre-absorbed on silica gel and concentrated by rotary evaporation. The crude product was purified by silica gel column chromatography (petroleum ether:EtOAc = 40:1, *v*/*v*) to afford the product.

(D2) *Synthesis of six membered manganacycle via Alkyne insertion:* a flame-dried Schlenck tube was equipped with a magnetic stir bar. [Mn(CO)$_4$(C^N)] (0.57 mmol, 200 mg), *n*-Bu$_2$O (8.0 ml), phenyl acetylene **16** (0.68 mmol, 70 mg) was added sequentially under nitrogen. The closed tube was put into a pre-heated oil bath at 80 ^{o}C and stirred for 8 h. After completion of the reaction, the resulting mixture was cooled down to room temperature, filtered through Celite and washed with EtOAc (30 mL). The filtrate was pre-absorbed on silica gel and concentrated by rotary evaporation. The crude product was purified by silica gel column chromatography (petroleum ether:EtOAc = 60:40, *v*/*v*) that afforded the product as yellow solid of 0.210 mg (87 %).

General procedures E: Synthesis of Mn-catalyzed alkenylation/Diels-Alder-product

(**E**) To a flame-dried Schlenk tube equipped with a magnetic stir bar, [Mn(CO)$_4$(C^N)] (1 eq.), in neat phenylacetylene **16** (100 eq., excess) were added

sequentially under nitrogen. The sealed tube was put into a pre-heated oil bath at 110 ^{o}C and stirred for 4 h. After completion of the reaction (monitored by TLC analysis), the resulting mixture was cooled to room temperature, filtered through Celite and washed with dichloromethane (30 mL). The filtrate was pre-absorbed on to silica gel and concentrated by rotary evaporation (with care). The crude product was purified by silica gel column chromatography, for which several fractions were identified. The column was eluted with petroleum ether / EtOAc:dichloromethane:MeOH = 90:10:0:0 – 0:0:95:5, *v/v*.

General procedures F: Synthesis of alkyne derivatives.[105]

(**F1**) *Sonogashira cross-coupling reaction;* To an oven-dried Schlenk tube charged with a magnetic stirrer bar was added a solution of the bromopyridine derivative (1.0 eq), CuI (0.03 eq.) and $Pd(PPh_3)_2Cl_2$ (0.01 eq.) in dried acetonitrile (90 eq.) and dried trimethylamine (10 eq.). A solution of terminal alkyne (1.2 eq.) was then added dropwise via syringe under nitrogen. The resulting solution was refluxed for 3-4 h. The reaction mixture was allowed to cool to room temperature, filtered through Celite and the solvent was removed by rotary evaporation. The residue was treated with water and extracted with ethyl ether. The combined organic layer was washed with brine and dried over magnesium sulfate, the filtered. After the removal of solvent, the crude product was purified with silica gel column chromatography (ethyl acetate/petroleum ether, 20/80, *v/v*) affording the products.

(**F2**) *Synthesis of pyridylacetylene derivatives via desilylation reactions;* To a solution of trimethyl(pyridylethynyl)silane derivatives (1 eq.) in methanol (75 eq.) and dichloromethane (25 eq.) was added potassium carbonate (5 eq.) and stirred at

r.t. for 6 h. The resulting mixture was treated with water and extracted with ethyl ether. The combined organic layer was washed with brine and dried over magnesium sulfate, then filtered. The solvent was removed *in vacuo* and the residue was distilled carefully under reduced pressure or purified by silica gel column chromatography to afford the pure products.

(**F3**) *Synthesis of η4-alkynyl-derivatives-$Co_2(CO)_6$ complex;* An equimolar mixture of dicobaltoctacarbonyl and the alkyne were added to a pre-dry Schleck tube charged with magnetic stirrer bar. Dry THF (6 mL per mmol) was added and the reaction mixture was stirred for 16 h., at room temperature. The resulting mixture was filtered through Celite^{TM} and washed with dichloromethane (12 mL). The filtrate was pre-absorbed on to silica gel and concentrated by rotary evaporation. The crude product was purified by silica gel column chromatography; the column was eluted with EtOAc / petroleum ether: 80/20, *v*/*v* to afford the complex.

General procedures G: Synthesis of cyclopentenones derivatives (Pauson-Khand reaction):[105]

(**G1**) To a microwave tube charged with a magnetic stirrer bar and filled with argon was added alkyne derivatives (1.0 eq.), $Co_2(CO)_8$ (1.2 eq.) and a deoxygenated dichloroethane DCE (80 eq.). The mixture was stirred at room temperature for 30 min., norbornene (5.0 eq.) was added in one portion and the reaction heated in the microwave (90 °C, 100 W) for 1 h. The resulting mixture was filtered through Celite, the filtrate was tested by TLC using ethyl acetate: petroleum ether (2/8, *v*/*v*), (in some reactions four distinct TLC sport was observed), this was pre-absorbed on to silica gel and concentrated by rotary evaporation (with care) and dry-loaded onto a

silica plug and eluted using ethyl acetate: petroleum ether (2/8, *v*/*v*). The eluted fractions were concentrated *in vacuo*, to afford the PKR products.

For a typical reaction, where four distinct products were observed by TLC: Fraction F1 (test tube number 3 to 5 = Coogan enol-lactone), F2 (test tube number 7 to 11 = hydrogenated alkyne), F3 (test tube number 12 to 19 = α PKR product, with respect to cyclopentenone) and F4 (test tube number 20 to 27 = β PKR product, with respect to cyclopentenone).

General procedure H: UV light controlled irradiation (cyclization / aromatization):

An in house (York) new irradiation system has been developed to provide controlled irradiation in which the wavelength and intensity of the light can be adjusted when required. The system (device) uses a small 5W LED's that attach directly on to the top of a cuvette. The LED's circuit is mechanically in-built in a special cuvette cap to a flexible wire, to allow the cuvette to be placed in the UV spectrometer for UV irradiation (Figure 49). A heat absorbing system (device) was developed for irradiating the NMR sample in the NMR tube for NMR simulation. The current LEDs in the system irradiate at 400 nm.

Figure 49 An irradiation system using the 400 nm 5W LED drawing a current of 20 mA.

(**H1**) *UV vis. irradiation;* The Amber LED (400 nm) 0.2A was set to irradiate $5*10^{-6}$ mol/dm^3 solution of an analyte in DCM, in a quartz cuvette for 30 sec. followed by a wait period of 2 min and 33 sec. the UV Vis was set to scan every 9240 seconds). First scan was run before the irradiation. The analyte was irradiated for 4 to 5 minute to afford the required product.

(**H2**) *NMR sample irradiation;* To a PKR cycloadduct (15 mg) was added DCM 0.6 (mL) in to an NMR tube the resulting solution was irradiated for 40 minute in an air ventilated NMR tube. The resulting product was NMR and MS (ESI) simulated directly to confirm the required product (Figure 49).

8.2 Synthetic procedures and compound data

[Pd(NO_2)(2-Phpy)(PPh_3)] (60)

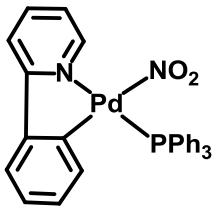

Following the general procedure B2; **67** (50 mg, 0.100 mmol) and silver nitrite (30 mg, 0.197 mmol) to afford the desired product as a pale orange solid crystals (51 mg, 96 % yield). MP 215–216 °C.

^{1}H NMR (400 MHz, CD_2Cl_2) δ 8.27 - 8.24 (br. s, 1H, H-1), 7.89 (dd, J_{HH} = 7.4, 1H, H-3), 7.82 (dd, J_{HH} = 7.4, 1.1, 1H, H-4), 7.79 – 7.73 (m, 4H, H-PPh_3), 7.56 (d, J_{HH} = 1.1, 1H, H-7), 7.49 – 7.44 (m, 7H, H- PPh_3), 7.42 – 7.36 (m, 4H, H- PPh_3), 7.22 (ddd, J_{HH} = 7.4, 2.3, 1.1, 1H, H-2), 6.98 (ddd, J_{HH} = 7.4, 5.7, 2.0, 1H, H-8), 6.55 – 6.53 (m, 1H, H-10), 6.53 – 6.50 (m, 1H, H-7). ^{13}C NMR (101 MHz, CD_2Cl_2) δ 152.45 (C-5), 149.54 (C-1), 147.85 (C-6), 147.73 (C-11), 140.20 (C-10), 140.02 (C-2), [135.55 (C-PPh_3), 135.42 (C- PPh_3), 134.33 (C- PPh_3), 134.17 (C- PPh_3), 132.35 (C- PPh_3), 131.66 (C- PPh_3), 131.45 (C- PPh_3), 130.78 (C- PPh_3), 130.28 (C- PPh_3), 129.71 (C- PPh_3), 129.60 (C- PPh_3), 129.14 (C- PPh_3), 128.93 (C- PPh_3), 128.75 (C-PPh_3), 128.64 (C- PPh_3)], 125.12 (C-8), 124.36 (C-7), 123.30 (C-2), 119.22 (C-4). ^{31}P NMR (162 MHz, CD_2Cl_2) δ 41.02. MS; LRMS (LIFDI-MS) m/z: calcd for $C_{29}H_{23}N_2O_2PPd$ 588.90; Found 590.02, Elemental Analysis: calcd C 61.23, H 4.07, N 4.92; Found C 65.63, H 4.32, N 2.69. The low carbon content is likely due to the presence of DCM in the final product.

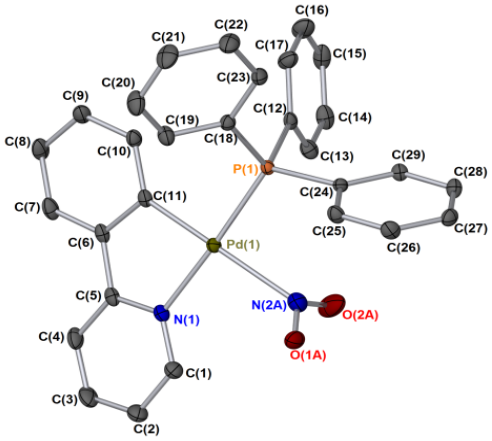

Lab book reference number: *NPY-2-128*

[Pd(OAc)(2-PhPy)]$_2$[113] *cis*- (62A)

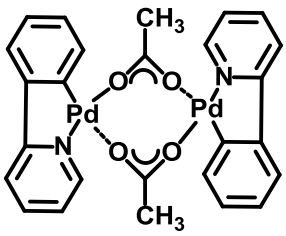

Following the general procedure A1; palladium(II) acetate (290 mg, 1.29 mmol) and **18** (200 mg, 1.29 mmol) to afford the product as a pale greenish yellow solid crystal (721 mg, 88% overall yield).

^{1}H NMR (400 MHz, $CDCl_3$) δ 7.87 (dd, J_{HH} = 5.7, 1.3, 2H, H-1), 7.37 (, td, J_{HH} = 7.3, 1.3, 2H, H-3), 7.08 (d, J_{HH} = 7.3, 2H, H-4), 6.91 (dd, J_{HH} = 7.4, 1.3, 2H, H-7), 6.88 – 6.78 (m , 6H, H-8/9/10), 6.45 (ddd, J_{HH} = 7.3, 5.7, 1.3, 2H, H-2), 2.27 (s, 6H, H-12). ^{13}C NMR (101 MHz, $CDCl_3$) δ 181.82 (C-13), 164.25 (C-5), 151.94 (C-11), 150.18 (C-1), 144.50 (C-6), 137.59 (C-3), 131.88 (C-10), 128.55 (C-9), 124.00 (C-7), 122.43 (C-8), 121.12 (C-2), 117.20 (C-4), 24.96 (C-12). IR (solid-state ATR, cm-^{1}) 3042, 2361, 2337, 1605, 1559, 1567, 1484, 1415, 1407, 1023, 726, 682, 408. MS;

LRMS (LIFDI-MS) m/z: calculated (calcd) for $C_{26}H_{23}N_2O_2Pd_2$ 639.96; Found 639.98, Elemental Analysis: calcd C 48.85, H 3.47, N 4.38; Found C 48.55, H 3.38, N 4.09.

Lab book reference number: *NPY-1-51*

[Pd(OAc)(2-PhPy)]$_2$ *trans*- (62B)

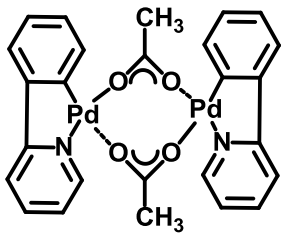

Following the general procedure A1; palladium(II) acetate (290 mg, 1.29 mmol) and **18** (200 mg, 1.29 mmol) to afford product as a pale greenish yellow solid crystals (10 % yield by ^{1}H MNR with respect to *cis*- isomer).

^{1}H NMR (400 MHz, CD_2Cl_2) 8.02 (d, J_{HH} = 5.7, H-1), 7.51 (td, J_{HH} = 7.9, 1.7, H-3), 7.20 (d, J_{HH} = 8.7, H-4), 6.88 (dd, J_{HH} = 2.6, 1.5, 1H, H-7), 6.79 – 6.63 (m, 4H, H-2/8/9/10), 2.22 (s, 6H, H-12).MS; LRMS (LIFDI-MS) m/z: calcd for $C_{26}H_{23}N_2O_2Pd_2$ 639.96; Found 639.98, Elemental Analysis: calcd C 48.85, H 3.47, N 4.38; Found C 48.55, H 3.38, N 4.09.

Lab book reference number: *NPY-1-51*

[PdCl(2-PhPy)]$_2$ (66)[113]

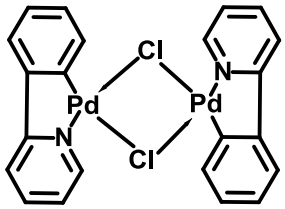

Following the general procedure A2; Lithium chloride (29 mg, 0.688 mmol), and **62** (200 mg, 0.313mmol), to afford the desired product as a pale yellowish solid (170 mg, 92% yield). MP >320 °C. NMR; Pyridine-d_5 was added to an NMR tube containing a sample of complex [PdClPhPy)]$_2$ in CD_2Cl_2 in order to increase its solubility in NMR solvents 3 Drops of pyridine-*d*5 a clear light yellow solution was formed and NMR spectra was taken immediately, keeping it longer resulted in a clear orange-yellow solution presumably due to the formation of the monomeric complex [PdCl($_2$-Phpy)(py-d_5)]. Residual pyridine signals have been omitted from the reported ^{13}C NMR data for clarity.

^{1}H NMR (400 MHz, CD_2Cl_2) δ 9.47-9.43 (br. s, 2H, H-1), 7.80 (ddd, J_{HH} = 8.0, 7.6, 1.7, 2H, H-3), 7.67 (d, J_{HH} = 7.7, 2H, H-4), 7.49 (dd, J_{HH} = 7.7, 1.4, 2H, H-7), 7.16 – 7.13 (m, 2H, H-2), 7.13 – 7.07 (m, 2H, H-8), 6.94 (td, J_{HH} = 7.6, 1.4, 2H, H-9), 6.25 (d, J_{HH} = 5.9 Hz, 2H, H-10). ^{13}C NMR (101 MHz, CD_2Cl_2) δ 165.99 (C-5), 155.16 (C-11), 152.23 (C-1), 146.13 (C-6), 139.24 (C-3), 132.98 (C-10), 129.81 (C-9), 125.05 (C-8), 123.71 (C-7), 122.47 (C-2), 118.80 (C-4). IR (solid-state ATR, cm-^{1}) 3045, 1605, 1579, 1487, 1421, 1277, 1160, 1028, 737, 719. MS; LRMS (LIFDI-MS) m/z: calcd for $C_{22}H_{16}N_2Cl_2Pd_2$ 591.87; Found 591.88, Elemental Analysis: calcd C 44.63, H 2.72, N 4.73, observed C 44.47, H 2.61, N 4.72.

Lab book reference number: *NPY-1-52*

[PdCl(2-Phpy)(PPh3)] (67)[114]

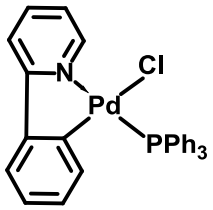

Following the general procedure B1; **62** (100 mg, 0.169 mmol) and triphenylphosphine (97 mg, 0.372 mmol), to afford the desired product as light orange solid crystals (180 mg, 95 % yield). MP 220–223 °C

^{1}H NMR (400 MHz, CD_2Cl_2) δ 9.58 (dd, J_{HH} = 5.6, 1.3, 1H, H-1), 7.90 (dd, J_{HH} = 7.5, 1.4, 1H, H-3), 7.80 (d, J_{HH} = 7.5, 1H, H-4), 7.74 (dd, J_{HH} = 10.6, 8.0, 6H, H-PPh_3), 7.56 (dd, J_{HH} = 7.6, 1.2, 1H, H-7), 7.49 – 7.43 (m, 3H, 1H, H- PPh_3), 7.41 – 7.35 (m, 6H, 1H, H- PPh_3), 7.29 (ddd, J_{HH} = 7.5, 5.6, 1.3, 1H, H-2), 6.97 (dd, J_{HH} = 7.6, 5.7, 1H, H-8), 6.56 – 6.49 (m, 2H, H-9/10). ^{13}C NMR (101 MHz, CD_2Cl_2) δ 165.30 (C-8), 155.67 (C-8), 150.76 (C-8), 147.87 (C-8), 139.61 (C-8), 139.44 (C-8), 135.66 (C-8), 135.53 (C-8), 130.91 (C-8), 130.89 (C-8), 129.11 (C-8), 128.53 (C-8), 128.43 (C-8), 124.74 (C-8), 124.22 (C-8), 122.68 (C-8), 118.80 (C-8). IR (solid-state ATR, cm-1) 3056, 1601, 1578, 1479, 1434, 1097, 743, 689, 531, 460. MS; LRMS (LIFDI-MS) m/z: calcd for $C_{29}H_{23}ClNPPd$ 557.03; Found 558.99, Elemental Analysis: calcd C 62.38, H 4.15, N 2.51; Found C 63.03, H 4.71, N 2.62.

Lab book reference number: *NPY-2-127*

[PdCl(2-Phpy)(PPh$_2$Cy)] (68)

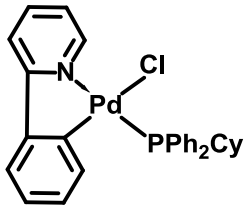

Following the general procedure B1; **66** (200 mg, 0.338 mmol) and Cyclohexyldiphenylphosphine (199 mg, 0.743 mmol) to afford the desired product as a white solid crystals (390 mg, 99 % yield). MP 172 – 173 ^{o}C.

^{1}H NMR (400 MHz, CD_2Cl_2) δ 9.58 (d, J_{HH} = 5.7, 1H, H-1), 7.72 – 7.78 (br. s, 1H, H-3), 7.88 – 7.81 (m, 4H, H- PPh$_2$), 7.73 (d, J_{HH} = 7.3, 1H, H-4), 7.50 (dd, J_{HH} = 5.5, 1.5, 1H, H-7), 7.49 – 7.39 (m, 6H, H- PPh$_2$), 7.27 (ddd, J_{HH} = 7.3, 5.7, 1.3, 1H, H-2), 6.95 (ddd, J_{HH} = 7.5, 5.5, 1.5, 1H, H-8), 6.69 (d, J_{HH} = 7.5, 1H, H-10), 6.61 (dd, J_{HH} = 7.5, 5.5, 1H, H-9), 2.10 – 1.92 (br. s, 2H, H-PCy), 1.72 – 1.55 (m, 3H, H-PCy), 1.42 – 1.31 (m, 2H, H- PCy), 1.05 – 0.81 (m, 3H, H- PCy). ^{13}C NMR (101 MHz, CD_2Cl_2) δ 164.99 (C-5), 155.99 (C-6), 150.39 (C-1), 147.66 (C-11), 139.43 (C-3), 138.68 (C-10), 134.48 (C-PPh$_2$), 134.37 (C- PPh$_2$), 130.75 (C- PPh$_2$), 129.22 (C-9), 128.71 (C- PPh$_2$), 128.61 (C- PPh$_2$), 124.62 (C-8), 124.07 (C-7), 122.50 (C-2), 118.68 (C-4), 29.18 (C-PCy), 27.34 (C- PCy), 27.21 (C- PCy), 26.58 (C- PCy), 15.50 (C- PCy). ^{31}P NMR (162 MHz, CD_2Cl_2) δ 42.36. MS; LRMS (LIFDI-MS) m/z: calcd for $C_{29}H_{29}ClNPPd$ 563.08; Found 564.10, Elemental Analysis: calcd C 61.71, H 5.18, N 2.48; Found C 62.23, H 5.33, N 2.50.

Lab book reference number: *NPY-3-144*

[Pd(NO_2)(2-Phpy)(PPh_2Cy)] (69)

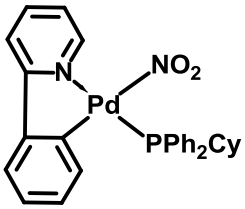

Following the general procedure B2; **68** (100 mg, 0.177 mmol) and silver nitrite (60 mg, 0.390 mmol) to afford the desired product as pale orange solid crystals (101 mg, 99 % yield). MP 195–196 ^{o}C .

^{1}H NMR (400 MHz, CD_2Cl_2) δ 8.49 – 8.45 (m, 1H, H-1), 8.02 – 7.95 (m, 4H, H-PPh_2), 7.91 (td, J_{HH} = 7.6, 1.5 Hz, 1H, H-3), 7.78 (d, J_{HH} = 7.6 Hz, 1H, H-4), 7.76 – 7.71 (m, 1H, H-PPh_2), 7.55 – 7.43 (m, 6H, H-PPh_2/8), 7.34 – 7.28 (m, 1H, H-2), 7.00 – 6.94 (m, 1H, H-7), 6.68 – 6.58 (m, 2H, H-9/10), 2.66 – 2.49 (m, 1H, H-PCy), 1.93 – 1.84 (m, 1H, H-PCy), 1.67 (dd, J_{HP} = 14.2, 10.3 Hz, 3H, H-PCy), 1.37 – 1.23 (m, 3H, H-PCy), 1.05 – 0.96 (m, 2H, H-PCy). IR (solid-state ATR, cm-^{1}) 3050, 2924, 2849, 1601, 1484, 1434, 1352, 1313, 1267, 1097, 1174, 999,745, 693, 518. MS; LRMS (LIFDI-MS) m/z: calcd for $C_{29}H_{29}N_2O_2PPd$ 574.10; Found 574.08, Elemental Analysis: calcd C 60.58, H 5.08, N 4.87; Found C 65.81, H 5.50, N 2.69.

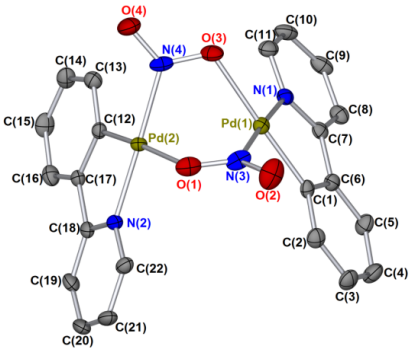

Lab book reference number: *NPY-2-105*

[PdCl(2-Phpy)(PPh$_2$(t-Bu)] (70)

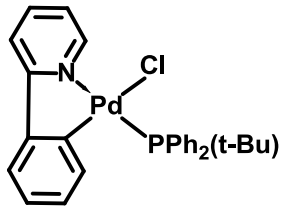

Following the general procedure B1; **66** (200 mg, 0.338 mmol) and tert-butyl diphenylphosphine (180 mg, 0.743 mmol) to afford the product as white solid crystals (360 mg, 94 % yield). MP 160–161 ^{o}C.

^{1}H NMR (400 MHz, CD_2Cl_2) δ 9.74 (d, J_{HH} = 5.7, 1H, H-1), 8.39 – 8.28 (br. s, 3H, H-PPh$_2$), 7.88 (ddd, J_{HH} = 7.3, 5.7, 1.5, 1H, H-3), 7.74 (d, J_{HH} = 8.0, 1H, H-4), 7.50 – 7.39 (m, 7H, H-PPh$_2$), 7.39 (d, J_{HH} = 4.5, 1H, H-7), 7.33 (ddd, J_{HH} = 7.3, 5.7, 1.5, 1H, H-2), 6.78 (ddd, J_{HH} = 7.7, 5.3, 1.3, 1H, H-8), 6.31 (d, J_{HH} = 1.3, 1H, H-10), 6.36 – 6.25 (m, 1H, H-9), 1.35 (d, J_{HP} = 15.0, 9H, H-P(t-Bu)). ^{13}C NMR (101 MHz, CD_2Cl_2) δ 165.43 (C-5), 156.44 (C-6), 149.87 (C-1), 146.95 (C-11), 139.41 (C-3), 138.82 (C-10), 136.34 (C-PPh$_2$), 136.21 (C-PPh$_2$), 131.03 (C-PPh$_2$), 128.74 (C-9), 128.35 (C- PPh$_2$), 128.25 (C- PPh$_2$), 124.12 (C-7), 123.62 (C- PPh$_2$), 122.34 (C-2), 118.73 (C-4), 28.66 (C-P(t-Bu), 28.62 (C-P(t-Bu). ^{31}P NMR (162 MHz, CD_2Cl_2) δ 61.10. MS; LRMS (LIFDI-MS) m/z: calcd for $C_{27}H_{27}ClNPPd$ 537.06; Found 538.11, Elemental Analysis: calcd C 60.24, H 5.06, N 2.60; Found C 61.13, H 5.44, N 3.01.

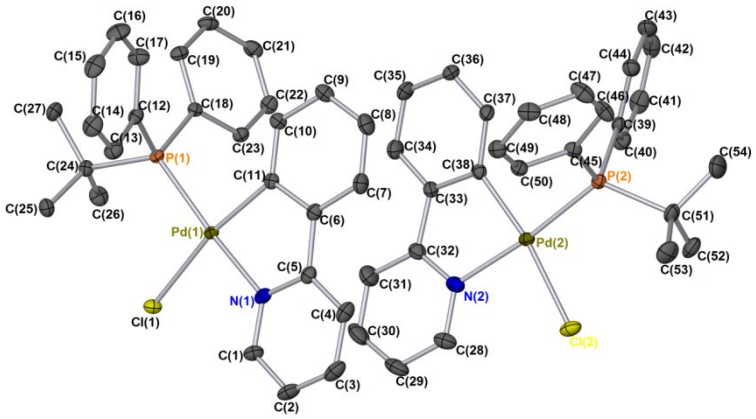

Lab book reference number: *NPY-3-143*

[Pd(NO$_2$)(2-Phpy)(PPh$_2$(t-Bu)] (71)

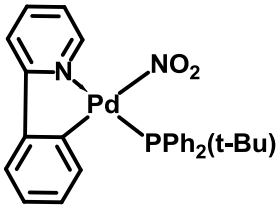

Following the general procedure B2; **70** (100 mg, 0.186 mmol) and silver nitrite (63 mg, 0.409 mmol) to afford the desired product as off-white crystals (101 mg, 99 % yield). MP 163–167 ^{o}C.

^{1}H NMR (400 MHz, $CDCl_3$) δ 8.46 – 8.38 (m, 1H, H-1), 8.43 – 8.38 (m, 3H, H-PPh$_2$), 7.85 (dd, J_{HH} = 7.4, 1.5, 1H, H-3), 7.73 (d, J_{HH} = 7.4, 1H, H-4), 7.51 – 7.41 (m, 7H, H-PPh$_2$), 7.36 (dd, J_{HH} = 7.7, 1.4, 1H, H-7), 7.21 (dd, J_{HH} = 7.4, 5.7, 1H, H-2), 6.89 – 6.80 (m, 1H, H-10), 6.34 (dd, *JHH* = 7.7, 5.6, 1H, H-8), 6.25 – 6.19 (m, 1H, H-9), 1.22 (d, J_{HH} = 15.1, 9H, H- P(t-Bu)). ^{31}P NMR (162 MHz, $CDCl_3$) δ 59.28. MS; LRMS (LIFDI-MS) m/z: calcd for $C_{27}H_{27}N_2O_2PPd$ 548.09; Found 548.07.

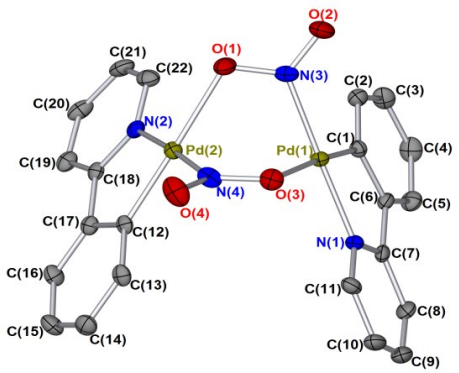

Lab book reference number: *NPY-2-92* / *NPY-145B*

[PdCl(2-Phpy)P(n-Bu)$_3$] (72)

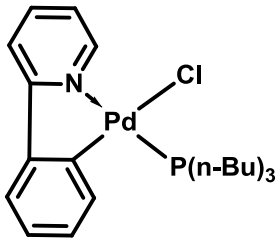

Following the general procedure B1; **66** (60 mg, 0.100 mmol) and triphenylphosphine (45 mg, 0.223 mmol) to afford the product as a colourless liquid (50.1 mg, >99 % yield).

^{1}H NMR (400 MHz, CD_2Cl_2) δ 8.83 – 8.80 (br. s, 1H, H-1), 8.20 (d, J_{HH} = 7.7, 1H, H-4), 7.71 (td, J_{HH} = 7.7, 1.6, 1H, H-3), 7.63 – 7.58 (m, 1H, H-8), 7.48 (dd, J_{HH} = 5.6, 1.6, 1H, H-7), 7.19 (dd, J_{HH} = 7.7, 5.4, 1H, H-2), 7.02 (d, J_{HH} = 1.6, 1H, H-10), 7.01 (dd, J_{HH} = 5.6, 1.6, 1H, H-9), 1.46 (d, J_{HH} = 8.9, 14H, H-P(n-Bu)$_3$), 1.34 – 1.19 (m, 22H, H-P(n-Bu)$_3$), 0.93 (dd, J_{HH} = 8.8, 5.4, 2H, H-P(n-Bu)$_3$), 0.83 (t, J_{HH} = 7.0, 16H, H-P(n-Bu)$_3$). ^{13}C NMR (101 MHz, CD_2Cl_2) δ 162.74 (C-5), 154.83 (C-6), 149.39 (C-1), 145.54 (C-1), 137.74 (C-11), 136.59 (C-7), 127.99 (C-3), 127.70 (C-9), 123.24 (C-10), 121.81 (C-2), 121.44 (C-4), 26.53 (C-1), 24.90 (C-P(n-Bu)$_3$),

23.40 (C-P(n-Bu)$_3$), 13.89 (C-P(n-Bu)$_3$).^{31}P NMR (162 MHz, CD_2Cl_2) δ 57.19, 47.89, 34.33, 3.90. IR (solid-state ATR, cm-^{1}) 3049, 2956, 2929, 2859, 1581, 1464, 1413, 1377, 1302, 1247, 120, 1153, 1092, 1051, 1017, 905, 799, 740, 619. MS; LRMS (LIFDI-MS) m/z: calcd for $C_{23}H_{35}ClNPPd$ 497.12; Found 497.12.

Lab book reference number: *NPY-2-77*

[Pd(NO$_2$)(2-Phpy)P(n-Bu)$_3$] (73)

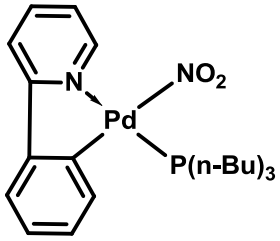

Following the general procedure B2; **72** (50 mg, 0.100 mmol) and silver nitrite (34 mg, 0.221 mmol) to afford the desired product as pale orange solid crystals (52 mg, >99 % yield).

^{1}H NMR (400 MHz, CD_2Cl_2) δ 8.17 – 8.14 (br. s, 1H, H-1), 7.88 – 7.83 (m, 1H, H-3), 7.79 (d, J_{HH} = 8.0, 1H, H-4), 7.60 (dd, J_{HH} = 7.4, 1.9, 1H, H-7), 7.19 (dd, J_{HH} = 4.0, 1.9, 1H, H-2), 7.17 (d, J_{HH} = 1.9, 1H, H-10), 7.16 (t, J_{HH} = 2.2, 1H, H-8), 7.12 (dd, J_{HH} = 9.5, 1.9, 1H, H-9), 1.86 (dd, J_{HH} = 16.7, 9.3, 2H, H-P(n-Bu)$_3$), 1.68 (dd, J_{HH} = 16.2, 8.5, 4H, H-P(n-Bu)$_3$), 1.59 (ddd, J_{HH} = 14.1, 6.7, 3.4, 2H, H-P(n-Bu)$_3$), 1.52 – 1.37 (m 10H, H-P(n-Bu)$_3$), 0.97 – 0.86 (m, 9H, H-P(n-Bu)$_3$). ^{31}P NMR (162 MHz, CD_2Cl_2) δ 21.64, 10.14. MS; LRMS (LIFDI-MS) m/z: calcd for $C_{23}H_{35}N_2O_2PPd$ 508.15; Found 508.17.

Lab book reference number: *NPY-2-79*

[Pd(OAc)(piph)]$_2$ (76) [113]

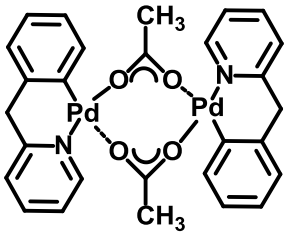

Following the general procedure A1; palladium(II) acetate (2.6 mmol) and **75** (2.6 mmol) to afford product as pale greenish yellow crystals (1.65 g 93 %).

^{1}H NMR (400 MHz, CD_2Cl_2) δ 8.45 – 8.41 (br. s, 2H, H-1), 7.61 (dd, J_{HH} = 7.5, 5.7, 2H, H-3), 7.20 (d, J_{HH} = 7.5, 2H, H-4), 6.95 – 6.35 (m, 10H, H-2/8/9/10/11), 3.90 (d, J_{HH} = 13.6, 4H, H-6), 2.01 (d, J_{HH} = 2.6, 6H, H-13). ^{13}C NMR (101 MHz, CD_2Cl_2) δ 180.87 (C-14), 159.88 (C-5), 141.59 (C-1), 138.35 (C-3), 136.71 (C-7), 134.24 (C-12), [125.68, 124.76, 124.22, 124.19 (C-8/9/10/11)], 121.99 (C-2), 48.83 (C-6), 24.73 (C-13). IR (solid-state ATR, cm-^{1}) 30441, 3019, 1603, 1577, 1484, 1421, 1276, 1155, 1019, 741, 425. MS; LRMS (LIFDI-MS) m/z: calcd for $C_{28}H_{28}N_2O_4Pd_2$ 668.01; Found 668.00, Elemental Analysis: calcd C; 50.24, H; 4.22, N; 4.19; Found C; 50.74, H; 4.22, N; 4.20.

Lab book reference number: *NPY-1-53*

[PdCl(PiPh)]$_2$ (77) [113]

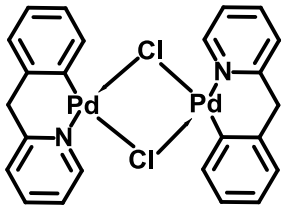

Following the general procedure A2; Lithium chloride (110 mg, 2.60 mmol) and **76** (200 mg, 1.182 mmol), to afford product as a pale yellow solid, (780 mg, 99% yield). For NMR measurement, Pyridine-d_5 was added to an NMR tube containing the sample of complex [PdClPhPy)]$_2$ in CD_2Cl_2, this was to increase its solubility for NMR measurement, a clear light yellow solution was formed and NMR spectra was taken immediately, keeping it longer resulted in a clear orange-yellow solution, presumably due to the formation of the monomeric complex [PdCl($_2$-Phpy)(py-d_5)]. Residual pyridine signals have been omitted from the report.

^{1}H NMR (400 MHz, CD_2Cl_2) δ 9.30 (dd, J_{HH} = 5.7, 1.2, 1H, H-1), 7.68 (td, J_{HH} = 7.6, 1.2, 1H, H-3), 7.41 (d, J_{HH} = 7.6, 1H, H-4), 7.14 (t, J_{HH} = 5.7, 1H, H-2), 7.07 (dd, J_{HH} = 7.3, 1.2, 1H, H-8), 6.91 (td, J_{HH} = 7.3, 1.2, 1H, H-9), 6.70 (td, J_{HH} = 7.3, 1.2, 1H, H-10), 6.56 (dd, J_{HH} = 7.3, 1.2, 1H, H-11), 3.06 (s, 1H, H-6). ^{13}C NMR (101 MHz, CD_2Cl_2) δ 160.00 (C-5), 159.55 (C-1), 154.74 (C-3), 138.78 (C-4), 137.50 (C-12), 135.27 (C-7), 126.19 (C-8), 125.46 (C-10), 124.53 (C-9), 124.08 (C-11), 122.01 (C-2), 49.68 (C-6). IR (solid-state ATR, cm-^{1}) 3109, 3080, 3053, 3038, 2870, 2962, 2822, 1708, 2168, 1606, 1559, 1484, 1443, 1338, 1156, 1028, 759, 619, 448.

Lab book reference number: *NPY-1-54*

[$PdCl_2$(Hpiph)$_2$] (78)[113]

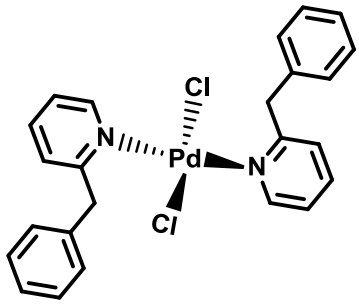

Following the general procedure A3; palladium(II) chloride (147 mg, 0.827 mmol) and **75** (280 mg, 1.655 mmol) to afford product as lemon yellow crystals (85 mg >99 %).

^{1}H NMR (400 MHz,) δ 9.06 (d, J_{HH} = 5.4 Hz, 1H, H-1), 8.89 (d, J_{HH} = 5.4 Hz, 1H, H-1'), 7.65 (t, J_{HH} = 7.7 Hz, 2H, H-3/3'), 7.50 – 7.30 (m, 10H, H-8/8'/9/9'/10/10'11/11'/12/12'), 7.30 – 7.20 (m, 2H, H-2/2'), 7.02 (d, J_{HH} = 7.9 Hz, 1H, H-4'), 6.96 (d, J_{HH} = 7.9 Hz, 1H, H-4), 5.41 (s, 2H, H-6'), 5.29 (s, 2H, H-6). ^{13}C NMR (101 MHz, CD_2Cl_2) δ 163.94 (C-5), 163.68 (C-5'), 152.78 (C-1), 152.41 (C-1'), 138.75 (C-3), 137.85 (C-7), 137.58 (C-7'), [130.54, 130.35, 129.30, 129., 127.54, 127.43 (C-8/8'/9/9'/10/10'11/11'/12/12')], 126.45 (C-4), 126.40 (C-4), 123.04 (C-2), 122.94 (C-2), 46.56 (C-6), 45.83 (C-6). IR (solid-state ATR, cm-^{1}) 3086, 3060, 3027, 2905, 1601, 1568, 1478, 1433, 1411, 1328, 1218, 1154, 1066, 1102, 1244, 1029, 969, 816, 768, 743, 721, 694, 620, 452. MS; LRMS (LIFDI-MS) m/z: calcd for $C_{24}H_{22}Cl_2N_2Pd$ 514.02; Found 514.01, Elemental Analysis: calcd C; 55.89, H; 4.30, N; 5.43; Found C; 56.12, H; 4.33, N; 5.45.

Lab book reference number: *NPY-1-20*

[Pd(OAc)(PiPh)(Py-d$_5$)] (80)[113]

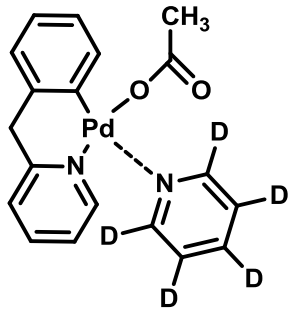

To a vial containing palladium complex **76** c.a. (10 mg) was added deuterated dichloromethane c.a. (0.6 mL) the solution was yellowish, upon addition of pyridine-d_5 (0.3 mL), the solution changed to light yellow immediately (100 % conversion by NMR).

^{1}H (400 MHz, C_5D_5) δ 9.08 (d, J_{HH} = 5.5, 1H, H-1), 7.69 (td, J_{HH} = 7.6, 1.2, 1H, H-3), 7.43 (d, J_{HH} = 7.6, 1H, H-4), 7.19 – 7.14 (m, 1H, H-2), 7.04 (dd, J_{HH} = 7.3, 1.2, 1H, H-8), 6.89 (td, J_{HH} = 7.3, 1.2, 1H, H-9), 6.69 (td, J_{HH} = 7.3, 1.2, 1H, H-10), 6.57 (dd, J_{HH} = 7.3, 1.2, 1H, H-11), 4.46 (s, 2H, H-6), 1.88 (s, 3H, H-13). ^{13}C NMR (101 MHz, CD_2Cl_2) δ 160.06 (C-1), 153.69 (C-9), 138.72 (C-9), 138.22 (C-9), 135.99 (C-9), 125.98 (C-9), 125.36 (C-9), 124.29 (C-9), 124.12 (C-9), 122.50 (C-9), 49.62 (C-9), 24.95 (C-9).

Lab book reference number: *NPY-1-53*

4-(2-Pyridyl)-2-Pyrone (81)

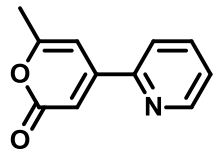

Following the general procedure C1; 4-bromo-6-methyl-2-pyrone **103** (500 mg, 2.65 mmol) was used to afford the product as a creamy solid (485 mg, 85 % yield). MP 89-90 °C.

^{1}H NMR (400 MHz, CD_2Cl_2) δ 8.74 – 8.65 (m, 1H, H-12), 7.83 (td, J_{HH} = 7.7, 1.5 Hz, 1H, H-10), 7.76 (d, J = 7.7 Hz, 1H, H-9), 7.38 (ddd, J_{HH} = 7.7, 4.8, 1.5 Hz, 1H, H-11), 6.81 (s, 1H, H-3), 6.68 (s, 1H, H-5), 2.32 (s, 3H, H-7). ^{13}C NMR (101 MHz, CD_2Cl_2) δ 163.64 (C-2), 162.74 (C-4), 153.75 (C-6), 152.65 (C-8), 150.34 (C-12), 137.46 (C-10), 125.27 (C-11), 121.76 (C-9), 109.16 (C-5), 102.31 (C-3), 20.41 (C-7). IR (solid-state ATR, cm-1) 3073, 2952, 1702, 1632, 1551, 1432, 785, 842, 874. MS; HRMS (ESI$^+$) m/z: $[M + H]^+$ calcd for $C_{11}H_9NO_2$ 188.0633; Found 188.0685. Elemental Analysis: calcd C 70.58, H 4.85, N 7.48; Found C 71.12, H 4.79, N 2.46.

Lab book reference number: *NPY-3-149*

[Pd(OAc)((4-Py)-2-Pyr)]$_2$ (82)

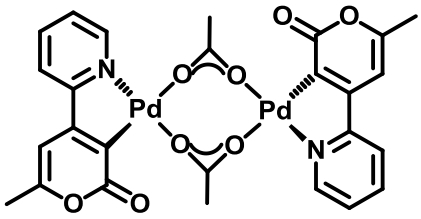

Following the general procedure A1; palladium(II) acetate (314 mg, 1.40 mmol) and **81** (100 mg, 0.64 mmol) were reacted to afford the product as a pale greenish yellow solid (490 mg, 54 % yield).

^{1}H NMR (400 MHz, CD_2Cl_2) δ 8.26 (d, J_{HH} = 5.7 Hz, 2H, H-12), 7.90 – 7.87 (m, 2H, H-10), 7.51 (d, J_{HH} = 8.2, 2H, H-9), 7.29 – 7.26 (m, 2H, H-11), 5.94 (s, 2H, H-5), 2.11 (d, J_{HH} = 0.9, 6H, H-7), 2.02 (s, 6H, H-13). IR (solid-state ATR, cm-^{1}) 3080, 2910, 7970, 2870, 1230, 1180, 1490, 1370, 1300, 1290, 1270, 1250, 1130, 1115, 1050, 910, 820, 750, 710, 610, 580. MS; LRMS (LIFDI-MS) m/z: calcd for $C_{26}H_{24}N_2O_8Pd_2$ calcd 707.96; Found 707.96.

Lab book reference number: *NPY-4-266F3*

[PdCl((4-Py)-2-Pyr)]$_2$ (83)

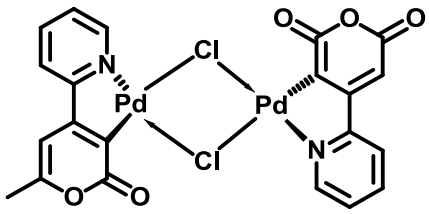

Following the general procedure A3; palladium(II) chloride (113 mg, 0.640 mmol) and **81** (100 mg, 0.534 mmol) to afford product as lemon yellow crystals (515 mg 73 %).

^{1}H NMR (400 MHz, C_5H_5N) δ 9.32 (br. s, 2H, H-12), 8.04 (td, J_{HH} = 7.8, 1.6 Hz, 2H, H-10), 7.66 (d, J_{HH} = 7.8 Hz, 2H, H-9), 7.41 (ddd, J_{HH} = 7.8, 5.7, 1.6 Hz, 2H, H-11), 6.25 (d, J_{HH} = 0.8 Hz, 2H, H-5), 2.15 (s, 6H, H-7). IR (solid-state ATR, cm-^{1}) 3067, 3182, 172, 1641, 1551, 1476, 1435, 1321, 1387, 1284, 1208, 1162, 1137, 1071, 1024, 899, 842, 780, 682, 550, 456. MS; LRMS (LIFDI-MS) m/z: calcd for $C_{21}H_{13}C_{l2}N_2O_5Pd_2$ calcd 656.83; Found [M – (NO_2)] 653.82.

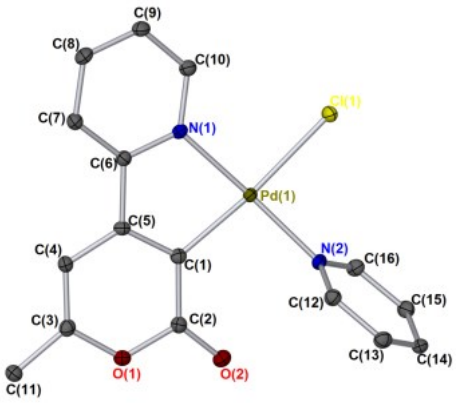

Lab book reference number: *NPY-4-270*

[PdCl((4-Py)-2-Pyr)(PPh$_3$)] (84)

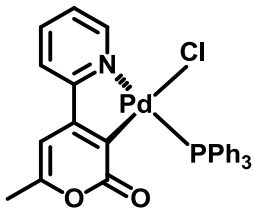

Following the general procedure B1; **83** (200 mg, 0.304 mmol) and triphenylphosphine (176 mg, 0.638 mmol) to afford the desired product as white solid crystals (151 mg, 84 % yield). MP 167–170 ^{o}C.

^{1}H NMR (400 MHz, CD_2Cl_2) δ 9.46 (d, J_{HH} = 4.8 Hz, 1H, H-12), 7.93 (td, J_{HH} = 7.8, 1.7 Hz, 1H, H-10), 7.74 – 7.67 (m, 6H, H-PPh$_3$), 7.66 – 7.61 (m, 2H, H-9/PPh$_3$), 7.45 – 7.42 (m, 1H, H-2), 7.39 (t, J_{HH} = 1.2 Hz, 2H, H-PPh$_3$), 7.34 (t, J_{HH} = 7.3 Hz, 6H, H-1), 6.08 (s, 1H, H-5), 2.06 (d, J_{HH} = 1.0 Hz, 3H, H-7). ^{13}C NMR (101 MHz, CD_2Cl_2) δ 164.22 (C-2), 159.54 (C-6/8), 151.20 (C-12), 143.50 (C-4), 139.53 (C-10), [134.61, 134.49, 132.35, 132.25, 130.23 (C-PPh$_3$)], 128.94 (C-11), [128.82, 128.11, 128.02, 124.70 (C-PPh$_3$)], 121.16 (C-9), 99.82 (C-5), 19.66 (C-7). IR (solid-state ATR, cm-^{1}) 3067, 3053, 2914, 1731, 1697, 1673, 1633, 1599, 1552, 1478, 1433, 1387, 1320, 1286, 1256, 1208, 1186, 1160, 1096, 1071, 1025, 998, 920, 900, 843, 781, 742, 691, 508, 455. MS; LRMS (LIFDI-MS) m/z: calcd for $C_{29}H_{23}ClNO_2PPd$ calcd 591.0194; Found $[M – (Cl)]^+$ 556.0505.

Lab book reference number: *NPY-4-272*

[PdCl(PiPh)(PPh$_3$)] (87)[113]

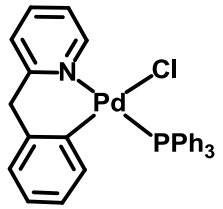

Following the general procedure B1; **77** (200 mg, 0.322 mmol) and triphenyl phosphine (186 mg, 0.709 mmol) to afford the product as white crystals (353 mg, 98 % yield). MP 210–211 ^{o}C.

^{1}H NMR (400 MHz, $CDCl_3$) δ 9.26 (d, J_{HH} 5.7, 1H, H-1), 7.71 – 7.67 (m, 1H, H-3), 7.67 – 7.60 (m, 6H, H- PPh$_3$), 7.43 – 7.41 (m, 1H, H-4), 7.41 – 7.37 (m, 3 H, H-PPh$_3$), 7.35 – 7.29 (m, 6H, H- PPh$_3$), 7.21 (dd, J_{HH} 7.3, 5.7, 1H, H-2), 6.94 (dd, J_{HH} 7.6, 1.3, 1H, H-8), 6.68 (td, J_{HH} 7.6, 1.3, 1 H, H-9), 6.63 (ddd, J_{HH} 7.6, 5.7, 1.3, 1 H, H-10), 6.27 (d, J_{HH} 7.6, 1H, H-11), 4.91 (d, J_{HH} 13.7, 1H, H-6), 3.97 (d, J_{HH} 13.7, 1H, H-6). ^{13}C NMR (101 MHz, $CDCl_3$) δ 159.22 (C-5), 153.31 (C-1), 153.23 (C-3), 138.49 (C-7), 138.18 (C-4), [135.08, 134.97, 131.63, 131.13, 130.35, 130.32, 128.17, 128.06, 125.86, 125.29, 125.25, 123.52, 123.49, 123.38 (C-PPh$_3$/8/9/10/11/12/)], 122.01 (C-2), 50.34 (C-6). ^{31}P NMR (162 MHz, $CDCl_3$) δ 35.47. IR (solid-state ATR, cm-1) 3420, 3047, 1607, 1573, 1480, 1435, 1096, 1183, 1025, 747, 691, 532, 499. MS; LRMS (LIFDI-MS) m/z: calcd for $C_{30}H_{25}ClNPPd$ 571.05; Found 571.06, Elemental Analysis: calcd C 62.95, H 4.40, N 2.45; Found C 63.13, H 4.77, N 2.33.

Lab book reference number: *NPY-1-56*

[Pd(NO_2)(PiPh)(PPh_3)] (88)

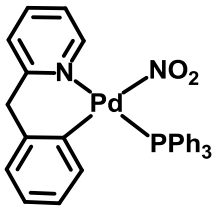

Following the general procedure B2; **87** (100 mg, 0.175 mmol) and silver nitrite (59 mg, 0.384 mmol) to afford the desired product as pale orange crystals (101 mg, 97 % yield). MP 201–204 °C.

^{1}H MNR (500 MHz, CD_2Cl_2) δ 8.54 – 8.56 (br. s, 1H, H-1), 7.74 (td, J_{HH} = 7.7, 1.6, 1H, H-3), 7.61 – 7.53 (m, 7H, H-PPh_3), 7.50 (d, $_{JHH}$ = 7.7, 1H, H-4), 7.44 (t, J_{HH} = 6.7, 3H, H-PPh_3), 7.36 (d, J_{HH} = 6.7, 8H, H-PPh_3), 7.15 (t, J_{HH} = 6.7, 1H, H-2), 7.02 (d, J_{HH} = 7.1, 1H, H-8), 6.74 (t, J_{HH} = 7.1, 1H, H-9), 6.49 – 6.47 (d, J_{HH} = 5.3, 1H, H-11), 6.33 (t, J_{HH} = 7.1, 1H, H-10), 5.01 (d, J_{HH} = 12.7, 1H, H-6), 4.08 (d, J_{HH} = 12.7, 1H, H-6). ^{13}C NMR (126 MHz, CD_2Cl_2) δ 159.78 (C-5), 151.59 (C-1), 147.42 (C-7), 139.53 (C-3), 137.82 (C-12), 137.75 (C-11), [135.04, 134.95, 132.39, 132.31, 131., 130.87, 130.47, 128.95, 128.86, 128.69, 128.61 (C-PPh_3)], 126.99 (C-8), 125.34 (C-10), 124.59 (C-9), 124.48 (C-4), 122.55 (C-2), 50.52 (C-6). IR (solid-state ATR, cm-1) 3056, 2960, 2922, 2850, 1604, 1573, 1479, 1435, 1359, 1309, 1260, 1093, 1021, 745, 693, 515. MS; LRMS (LIFDI-MS) m/z: calcd for $C_{30}H_{25}N_2O_2PPd$ 582.07; Found 582.07, Elemental Analysis: calcd C 61.81, H 4.32, N 4.81; Found C 66.63, H 4.71, N 2.69. The low carbon content is likely due to the presence of DCM in the final product.

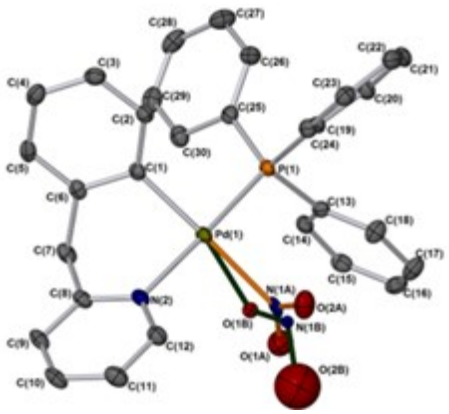

Lab book reference number: *NPY-1-42*

[PdClPiPh)(PPh$_2$Cy)] (89)

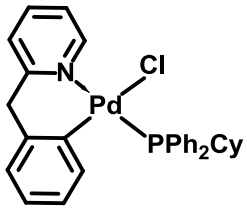

Following the general procedure B1; **77** (60 mg, 0.097 mmol) and cyclohexyldiphenylphosphine (57 mg, 0.213 mmol) to afford the desired product as white crystals (111 mg, >99 % yield). MP 172–173 °C.

^{1}H NMR (500 MHz, CD_2Cl_2) δ 9.04 (d, J_{HH} = 5.6, 1H, H-1), 7.88 – 7.82 (m, 2H, H-PPh$_2$), 7.71 (td, J_{HH} = 7.6, 1.6, 1H, H-3), 7.56 – 7.46 (m, 5H, H-PPh$_2$), 7.45 (d, J_{HH} = 7.6, 1H, H-4), 7.43 – 7.39 (m, 1H, H-PPh$_2$), 7.33 (td, J_{HH} = 7.6, 1.7, 2H, H-PPh$_2$), 7.18 (dd, J_{HH} = 7.6, 5.6, 1H, H-2), 7.06 (dd, J_{HH} = 7.3, 1.2, 1H, H-8), 7.00 (ddd, J_{HH} = 7.3, 5.1, 1.2, 1H, H-9), 6.82 (td, J_{HH} = 7.3, 1.2, 1H, H-10), 6.61 (t, J_{HH} = 7.3, 1H, H-11), 4.91 (d, J_{HH} = 13.8, 1H, H-6), 4.07 (d, J_{HH} = 13.8, 1H, H-6), 2.89 – 2.79 (m, 1H, H- P(Cy)), 2.35 (s, 1H, H- P(Cy)), 1.72 – 1.61 (m, 2H, H- P(Cy)), 1.51 (s, 2H,

H- P(Cy)), 1.32 (dtd, J_{HH} = 13.0, 9.8, 3.4, 1H, H- P(Cy)), 1.04 – 0.93 (m, 1H, H-P(Cy)), 0.90 – 0.62 (m, 2H, H- P(Cy)). ^{13}C NMR (126 MHz, CD_2Cl_2) δ 159.63 (C-5), 153.17 (C-1), 152.02 (C-7/12), 138.96 (C-3), 136.28 (C-9), [134.85, 134.78, 134.47, 134.55, 130.49, 130.39, 130.04, 128.28, 128.20, 128.11, 128.03, 127.78 (C-PPh_2)], 126.95 (C-8), 125.52 (C-11), 124.18 (C-10), 123.96 (C-4), 122.16 (C-2), 50.70 (C-6), [36.31 (C-1), 36.07, 29.50, 27.34, 26.47 (C-P(Cy))]. ^{31}P NMR (162 MHz, CD_2Cl_2) δ 36.83. IR (solid-state ATR, cm^{-1}) 3051, 2929, 2849, 1605, 1573, 1475, 1432, 1291, 1187, 1151, 1094, 1025, 997, 769, 738, 695, 519, 474. MS; LRMS (LIFDI-MS) m/z: calcd for $C_{29}H_{29}ClNPPd$ 563.08; Found 564.10, Elemental Analysis: calcd C 61.71, H 5.18, N 2.48; Found C 62.23, H 5.33, N 2.50.

Lab book reference number: *NPY-2-66*

[Pd(NO_2)(PiPh)(PPh_2Cy)] (90)

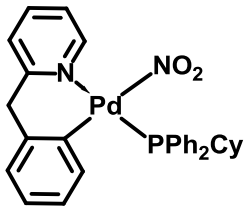

Following the general procedure B2; **89** (50 mg, 0.175 mmol) and silver nitrite (59 mg, 0.384 mmol) to afford the desired product as pale orange solid crystals (50 mg, 98 % yield). MP 176–178 °C.

^{1}H NMR (400 MHz, CD_2Cl_2) δ 8.47 – 8.34 (m, 1H, H-1), 7.77 – 7.71 (m, 2H, H-3/4), 7.70 – 7.61 (m, 3H, H-PPh_2), 7.53 – 7.40 (m, 7H, H-PPh_2), 7.13 – 7.08 (m, 1H, H-2), 7.05 – 7.01 (m, 1H, H-8), 6.88 (dd, $_{JHH}$ = 7.7, 5.5, 1H, H-9), 6.83 (d, J_{HH} = 7.7, 1H, H-10), 6.64 (t, J_{HH} = 7.7, 1H, H-11), 4.93 d, J_{HH} = 13.9, 1H, H-6), 4.07 (d, J_{HH}

= 13.9, 1H, H-6), 2.14 (d, J_{HP} = 37.0, 2H, H-PCy), 1.68 (dd, J_{HP} = 58.9, 23.4, 2H, H- PCy), 1.50 (d, J_{HH} = 10.6, 1H, H- PCy), 1.36 – 1.19 (m, 2H, H- PCy), 0.85 (d, J_{HH} = 8.1, 3H, H- PCy), 0.56 (d, J_{HH} = 12.6, 1H, H- PCy). ^{31}P NMR (162 MHz, CD_2Cl_2) δ 34.60. IR (solid-state ATR, cm-^{1}) 3056, 2934, 2849, 1601, 1578, 1483, 1433, 1360, 1314, 1268, 210, 1160, 1119, 1097, 1065, 1001, 915, 891, 851, 750, 704, 533, 473, 501, 414.5456. MS; LRMS (LIFDI-MS) m/z: calcd for $C_{30}H_{31}N_2O_2PPd$ 588.12; Found [M – (NO_2)] 542.02; Elemental Analysis: calcd C 61.18, H 5.31, N 4.76; Found C 66.33, H 5.67, N 2.50.

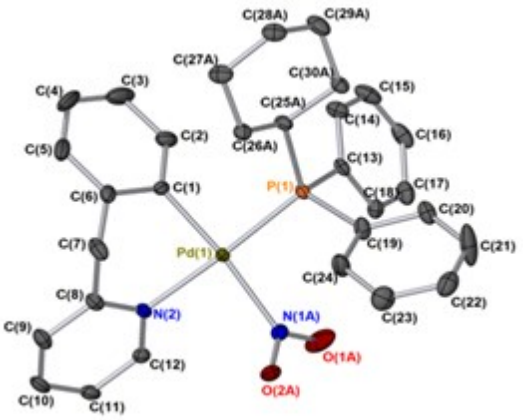

Lab book reference number: *NPY-2-67*

[PdCl(PiPh)(PPh$_2$(t-Bu))] (91)

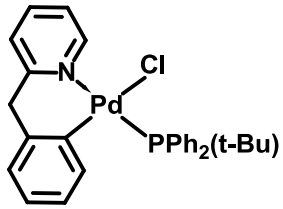

Following the general procedure B1; **77** (100 mg, 0.161 mmol) and tert-butyldiphenylphosphine (86 mg, 0.355 mmol) to afford the desired product as white solid crystals (60 mg, 98 % yield). MP 162–165 °C.

^{1}H NMR (400 MHz, CD_2Cl_2) δ 9.25 (dd, J_{HH} = 5.2, 1.7, 1H, H-1), 8.51 (dd, J_{HH} = 14.1, 6.3, 2H, H-PPh$_2$), 7.72 (td, J_{HH} = 7.6, 1.7, 1H, H-3), 7.67 – 7.62 (m, 3H, H-PPh$_2$), 7.41 (d, J_{HH} = 7.6, 1H, H-4), 7.25 (dd, J_{HH} = 7.6, 5.2, 1H, H-2), 7.21 (dd, J_{HH} = 10.1, 1.5, 2H, H-PPh$_2$), 7.11 (td, J_HH = 7.2, 1.7, 1H, H-PPh$_2$), 7.01 (td, J_{HH} = 7.6, 1.9, 2H, H-PPh$_2$), 6.77 (d, J_{HH} = 7.3, 1H, H-8), 6.48 (dd, J_{HH} = 7.3, 1.2, 1H, H-9), 6.44 (ddd, J_{HH} = 7.3, 5.4, 1.2, 1H, H-10), 6.04 (t, J_{HH} = 7.4, 1H, H-11), 4.84 (d, J_{HH} = 13.7, 1H, H-6), 3.95 (d, J_{HH} = 13.7, 1H, H-6), 1.38 (d, J_{HH} = 15.2, 9H, H-P(t-Bu)). NMR (101 MHz, CD_2Cl_2) δ 159.94 (C-5), 154.54 (C-7), 153.12 (C-1), 138.89 (C-3), 138.17 (C-9), 138.06 (C-12), [137.89, 137.74, 137.61, 133.13, 133.09, 133.00, 132.70, 131.71, 129.04, 128.74, 127.61, 127.51 (C-PPh$_2$)], 126.01 (C-9), 124.97 (C-11), 123.66 (C-4), 123.27 (C-10), 122.12 (C-2), 50.55 (C-6), 36.09 (C-P(t-Bu)), 35.84 (C-P(t-Bu)), 30.16 (C-P(t-Bu)), 30.11 (C-P(t-Bu)). ^{31}P NMR (162 MHz, CD_2Cl_2) δ 54.75. IR (solid-state ATR, cm-^{1}) 3064, 2987, 2954, 2901, 2863, 1602, 1562, 1474, 143, 1363, 1292, 1328, 1261, 1183, 1159, 1097, 1014, 761, 744, 695, 617, 587, 523. MS; LRMS (LIFDI-MS) m/z: calcd for $C_{28}H_{29}ClNPPd$ 553.08; Found 553.08.

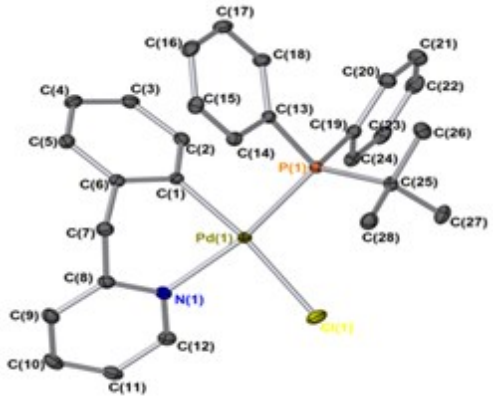

Lab book reference number: *NPY-2-136*

[Pd(NO$_2$)(PiPh)(PPh$_2$(t-Bu))] (92)

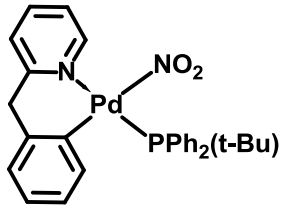

Following the general procedure B2; **91** (60 mg, 0.112 mmol) and silver nitrite (38 mg, 0.245 mmol) to afford the desired product as pale orange solid crystals (60 mg, 97 % yield). MP 182–187 °C.

^{1}H NMR (400 CD_2Cl_2) δ 8.52 (d, J_{HH} = 5.4, 1H, H-1), 8.49 – 8.42 (m, 2H, H-PPh$_2$), 7.73 (td, J_{HH} = 7.7, 1.2, 1H, H-3), 7.64 (dd, J_{HH} = 4.4, 2.5, 3H, H-PPh$_2$), 7.51 (dd, J_{HH} = 7.9, 7.8, 2H, H-PPh$_2$), 7.47 (d, J_{HH} = 7.6, 1H, H-4), 7.28 – 7.14 (m, 3H, H-PPh$_2$), 7.13 (dd, J_{HH} = 5.4, 1.2, 1H, H-2), 6.79 (d, J_{HH} = 7.3, 1H, H-8), 6.52 (td, J_{HH} = 7.5, 1.2, 1H, H-9), 6.45 (ddd, J_{HH} = 7.3, 5.4, 1.2, 1H, H-11), 6.13 (t, J_{HH} = 7.3, 1H, H-10), 4.93 (d, J_{HH} = 13.6, 1H, H-6), 3.99 (d, J_{HH} = 13.6, 1H, H-6), 1.16 (d, J_{HH} = 15.2, 9H, H- P(t-Bu)). ^{13}C NMR (101 MHz, CD_2Cl_2) δ 160.06 (C-5), 151.25 (C-1), 139.37 (C-3), 138.55 (C-7), 138.11 (C-11), 138.01 (C-12), 137.15 (C-1), [137.02,

133.59, 133.49, 131.84, 129.66), 128.92, 128.82, 127.97, 127.87 (C-PPh_2)], 126.26 (C-8), 124.87 (C-10), 124.43 (C-4), 123.82 (C-9), 122.52 (C-2), 50.51 (C-6), [35.08, 34.83, 28.92, 28.87 (C-P(t-Bu))]. ^{31}P NMR (162 MHz, CD_2Cl_2) δ 52.94. MS; LRMS (LIFDI-MS) m/z: calcd for $C_{28}H_{29}N_2O_2PPd$ 562.10; Found [M – (NO_2)] 516.06.

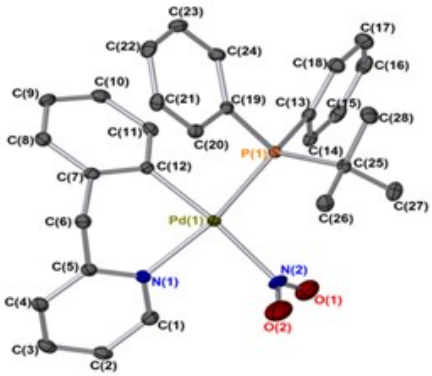

Lab book reference number: *NPY-2-135*

[PdCl(PiPh)(P(2-Furyl)$_3$)] (93)

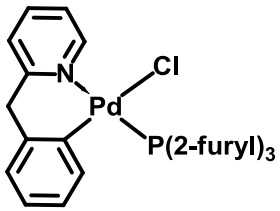

Following the general procedure B1; **77** (30 mg, 0.048 mmol) and tri-2-furyl phosphine (25 mg, 0.106 mmol) to afford the desired product as a light orange liquid (50 mg, 95 % yield). MP 145–147 °C.

^{1}HNMR (400 MHz, $CDCl_3$) δ 9.24 (d, J_{HH} = 5.6, 1H, H-1), 7.70 (td, J_{HH} = 7.6, 1.7, 1H, H-3), 7.60 (br s, 4H, H-P(Fu)$_3$), 7.42 (d, J_{HH} = 7.6, 1H, H-4), 7.22 (ddd, J_{HH} = 7.6, 5.6, 1.4, 1H, H-2), 7.18 – 7.06 (m, 3H, H-P(Fu)$_3$)), 6.99 (d, J_{HH} = 5.9, 1H, H-8),

6.84 (d, J_{HH} = 7.6, 1H, H-11), 6.78 (td, J_{HH} = 7.5, 1.6, 1H, H-9), 6.48 (td, J_{HH} = 7.5, 1.6, 1H, H-10), 6.44 (dt, J_{HH} = 3.3, 1.6, 4H, H-P(Fu)$_3$), 4.90 (s, 1H, H-6), 4.00 (s, 1H, H-6). ^{13}C NMR (101 MHz, $CDCl_3$) δ 159.05 (C-5), 153.14 (C-1), 150.13 (C-7), 148.44 (C-P(Fu)$_3$), 138.85 (C-3), 137.81 (C-12), 136.79 (C-11), 126.32 (C8), 125.19 (C-10), 123.95 (C-9), 123.72 (C-3), 122.19 (C-2), 111.29 (C-P(Fu)$_3$), 50.16 (C-6). ^{31}P NMR (162 MHz, $CDCl_3$) δ -19.24. MS; LRMS (LIFDI-MS) m/z: calcd for $C_{24}H_{19}ClNO_3PPd$ 542.98; Found 542.99, Elemental Analysis: calcd C 53.16, H 3.53, N 2.58; Found C 51.77, H 3.52, N 2.59.

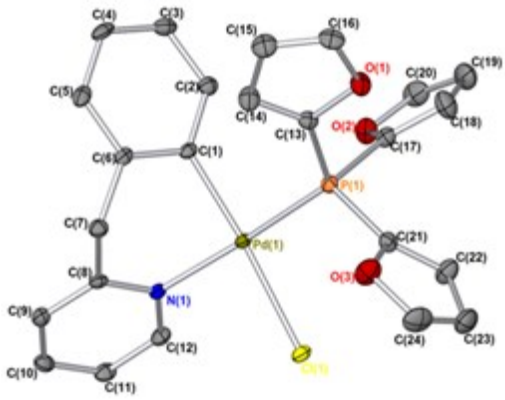

Lab book reference number: *NPY-2-109*

[Pd(NO$_2$)(PiPh)(P(Fu)$_3$)] (94)

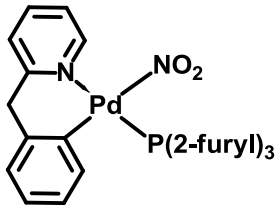

Following the general procedure B2; **93** (20 mg, 0.037 mmol) and silver nitrite (13 mg, 0.081 mmol) to afford the desired product as a colourless liquid (49 mg, 95 % yield).

^{1}H NMR (400 MHz, $CDCl_3$) δ 8.75 (d, J_{HH} = 2.5, 1H, H-1), 7.77 – 7.74 (m, 1H, H-3), 7.68 (br s, 4H, H-P(Fu)$_3$), 7.49 (d, J_{HH} = 7.7, 1H, H-4), 7.23 (d, J_{HH} = 6.0, 1H, H-2), 7.06 (d, J_{HH} = 7.2, 1H, H-8), 6.97 (t, J_{HH} = 7.8, 4H, H-P(Fu)$_3$), 6.87 (d, J_{HH} = 7.1, 1H, H-11), 6.85 – 6.80 (m, 1H, H-9), 6.56 (dd, J_{HH} = 8.3, 6.7, 1H, H-10), 6.50 – 6.40 (m, 4H, H-P(Fu)$_3$), 4.98 (d, J_{HH} = 13.5, 1H, H-6), 4.05 (d, J_{HH} = 13.5, 1H, H-6). ^{31}P NMR (162 MHz, $CDCl_3$) δ -22.17. MS; LRMS (LIFDI-MS) m/z: calcd for $C_{24}H_{19}N_2O_5PPd$ calcd 552.01; Found [M – (NO_2)] 506.02.

Lab book reference number: *NPY-2-110*

[PdCl(PiPh)(P(n-Bu)$_3$)] (95)

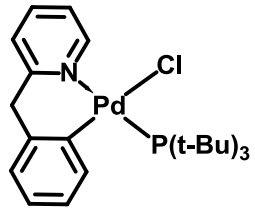

Following the general procedure B1; **77** (50 mg, 0.081 mmol) and tri-n-butylphosphine (36 mg, 0.177 mmol) to afford the desired product as a colourless liquid (83 mg, >99 % yield).

^{1}H NMR (400 MHz, CD_2Cl_2) δ 9.09 – 8.98 (m, 1H, H-1), 7.69 (t, J_{HH} = 7.5, 1H, H-3), 7.40 (d, J_{HH} = 7.5, 1H, H-4), 7.28 (dd, J_{HH} = 7.5, 2.4, 1H, H-9), 7.18 (t, J_{HH} = 7.5, 1H, H-2), 7.04 (d, J_{HH} = 6.7, 1H, H-8), 6.90 (d, J_{HH} = 6.7, 1H, H-10), 6.88 – 6.82 (m, 1H, H-11), 4.71 (d, J_{HH} = 13.7, 1H, H-6), 3.97 (d, J_{HH} = 13.7 1H, H-6), 1.81 (dd, J_{HH} = 16.6, 8.9, 5H, H-P(n-Bu)), 1.68 – 1.22 (m, 13H, H-P(n-Bu)), 0.98 – 0.76 (m, 9H, H-P(n-Bu)). ^{13}C NMR (101 MHz, CD_2Cl_2) δ 159.53 (C-5), 152.80 (C-1), 152.33 (C-12), 138.80 (C-3), 137.14 (C-8), 126.70 (C-7), 125.65 (C-10), 124.10

(C-11), 123.89 (C-4), 122.06 (C-2), 50.38 (C-6), [26.75, 24.77, 24.64, 24.48, 13.83 (C-P(n-Bu)$_3$)]. ^{31}P NMR (162 MHz, CD_2Cl_2) δ 21.14. IR (solid-state ATR, cm-^{1}) 3047, 345, 2955, 2927, 2869, 1605, 1573, 1442, 1378, 1291, 1209, 1156, 1091, 1058, 1027, 904, 742, 724, 620, 451. MS; LRMS (LIFDI-MS) m/z: calcd for $C_{28}H_{29}ClNPPd$ 511.13; Found 511.10.

Lab book reference number: *NPY-2-76*

[Pd(NO$_2$)(PiPh)(P(n-Bu)$_3$)] (96)

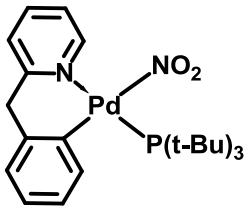

Following the general procedure B2; **95** (50 mg, 0.098 mmol) and silver nitrite (33 mg, 0.215 mmol) to afford the desired product as a colourless liquid (48 mg, 97 % yield).

^{1}H NMR (400 MHz, CD_2Cl_2) δ 8.53 (d, J_{HH} = 5.1, 1H, H-1), 7.71 (td, J_{HH} = 7.7, 1.6, 1H, H-3), 7.44 (d, J_{HH} = 7.7, 1H, H-4), 7.23 (ddd, J_{HH} = 7.2, 3.4, 1.5, 1H, H-9), 7.16 – 7.10 (m, 1H, H-2), 7.04 (dd, J_{HH} = 7.2, 1.5, 1H, H-8), 6.92 (dd, J_{HH} = 7.2, 1.5, 1H, H-11), 6.90 – 6.84 (m, 1H, H-10), 4.80 (d, J_{HH} = 13.8, 1H, H-6), 4.01 (d, J_{HH} = 13.8, 1H, H-6), 1.87 – 1.22 (m, 18H, H-P(n-Bu)$_3$), 0.99 – 0.79 (m, 9H, H-P(n-Bu)$_3$). ^{13}C NMR (101 MHz, CD_2Cl_2) δ 159.72 (C-5), 151.00 (C-1), 149.21 (C-7), 140.49 (C-12), 139.33 (C-3), 137.00 (C-9), 126.90 (C-8), 125.68 (C-10), 124.60 (C-11), 124.54 (C-4), 122.46 (C-2), 50.31 (C-6), [28.26, 26.47, 24.66, 23.39, 13.77 (C-P(n-Bu)$_3$)]. ^{31}P NMR (162 MHz, CD_2Cl_2) δ 19.01. IR (solid-state ATR, cm-^{1}) 3049, 2956, 2956,

2928, 2870, 1606, 1571, 1442, 1345, 1282, 1212, 1155, 1092, 1026, 1050, 968, 905, 745, 620, 447, 3436. MS; LRMS (LIFDI-MS) m/z: calcd for $C_{24}H_{37}N_2O_2PPd$ calcd 522.16; Found [M – (NO_2)] 476.17.

Lab book reference number: *NPY-2-78*

2-Phenylpyrazine (99)[141]

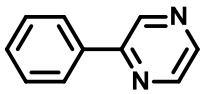

A mixture of 2-chloropyrazine (29 mg, 0.25 mmol), arylboronic acid (46 mg, 0.375 mmol), K_2CO_3 (70 mg, 0.5 mmol), $Pd(OAc)_2$ (1 mg, 0.00375 mmol), distilled water (1 mL) and ethanol (3 mL) was stirred at 80 °C in air for 20 min. The reaction mixture was added to brine (15 mL) and extracted with ethyl acetate (4 × 15 mL). The reaction mixture was filtered through Celite and washed with EtOAc (30 mL). The filtrate was pre-absorbed on silica gel and concentrated by rotary evaporation. The crude product was purified by silica gel column chromatography (petroleum ether:EtOAc = 40:60, *v*/*v*) and the filtrate concentrated *in vacuo* to afford the desired product as a shiny reddish brown solid (34 mg, 86% yield). MP 60–61 °C.

^{1}H NMR (400 MHz, $CDCl_3$) δ 9.03 (d, *J* = 1.5 Hz, 1H), 8.64 (dd, *J* = 2.5, 1.5 Hz, 1H), 8.51 (d, *J* = 2.5 Hz, 1H), 8.02 (dd, *J* = 8.0, 1.5 Hz, 2H), 7.62 – 7.40 (m, 3H). ^{13}C NMR (101 MHz, $CDCl_3$) δ 152.96, 144.30, 143.04, 142.36, 136.46, 130.05, 129.18, 128.86, 127.27, 127.06.

Lab book reference number: *NPY-3-201*

[Mn(CO)$_4$(2-Phenylpyrazine)] (100)

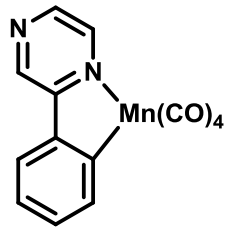

Following the general procedure D1; MnBn(CO)$_5$ (183 mg, 0.64 mmol), hexane (8 ml), 2-phenylpyrazine (100 mg, 0.64 mmol), to afford the desired product as a sticky solid yellow (142 mg, 68% yield). MP 97–100 $^{\circ}$C.

^{1}H NMR (400 MHz, $CDCl_3$) δ 9.17 (br. s, 1H, H-3), 9.17 (br. s, 1H, H-1), 8.68 (br. s, 1H, H-2), 8.34 (br. s, 1H, H-7), 8.00 (d, J_{HH} = 7.4 Hz, 1H, H-6), 7.93 (d, J_{HH} = 7.9 Hz, 1H, H-8), 7.33 (d, J_{HH} = 7.9 Hz, 1H, H-9). MS; HRMS (ESI$^+$) m/z: $[M + H]^+$ calcd for $C_{14}H_8MnN_2O_4$ 322.9820; Found 322.9787.

Lab book reference number: *NPY-4-210F6-9*

4-(3-Methoxy-2-pyridyl)-2-Pyrone (104)

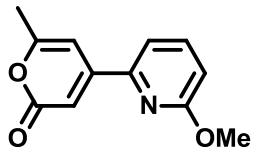

Following the general procedure C1; 4-bromo-6-methyl-2-pyrone **103** (500 mg, 2.65 mmol) with 2-Bromo-6-methoxypyridine **101b** (547 mg, 2.91 mmol) to afford the compound as a Creamy solid (496 mg, 86 % yield). MP 80-82 °C.

^{1}H NMR (400 MHz, CD_2Cl_2) δ 7.69 (dd, J_{HH} = 8.3, 7.3, 1H, H-10), 7.36 (d, J_{HH} = 7.3, 1H, H-9), (d, J_{HH} = 8.3, 1H, H-11), 6.78 (s, 1H, H-3), 6.71 (s, 1H, H-5), 3.99 (s, 3H, H-13), 2.32 (s, 3H, H-7). ^{13}C NMR (101 MHz, CD_2Cl_2) δ 193.21 (C-2), 164.28 (C-4), 162.54 (C-6), 153.33 (C-12), 149.83 (C-8), 139.77 (C-10), 114.85 (C-9), 113.35 (C-11), 108.87 (C-3), 102.08 (C-5), 53.79 (C-13), 20.44 (C-7). IR (solid-state ATR cm-1) 3110, 2080, 2075, 1750, 1700, 1680, 1550, 1480, 1330, 1291, 1030, 988, 830, 805, 514. MS; HRMS (ESI^{+}) m/z: $[M + H]^{+}$ calcd for $C_{12}H_{12}NO_3$ 218.0739; Found 218.0772. Elemental Analysis: calcd C 66.35, H 5.10, N 6.45; Found C 67.15, H 5.22, N 6.46.

Lab book reference number: *NPY-5-Mn-OMe C-HF5*

[Mn(CO)$_4$(4-(2-pyridyl)-2-Pyrone)] (105a)

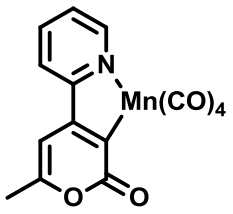

Following the general procedure D1; MnBn(CO)$_5$ (764 mg, 2.67 mmol,), hexane (20 ml), **81** (500 mg, 2.67 mmol), to afford the desired product as a yellow powdered (943 mg, 96% yield). MP 155–156 °C.

^{1}H NMR (400 MHz, $CDCl_3$) δ 8.86 (d, J_{HH} = 5.0 Hz, 1H, H-12), 7.91 (td, J_{HH} = 7.8, 1.6 Hz, 1H, H-10), 7.71 (d, J_{HH} = 7.9 Hz, 1H, H-9), 7.33 – 7.27 (m, 1H, H-11), 6.27 (s, 1H, H-5), 2.30 (s, 3H, H-7). ^{13}C NMR (101 MHz, $CDCl_3$) δ 167.62 (C-2), 162.66 (C-6), 159.16 (C-4), 158.31 (C-8), 157.50 (C-3), 155.51(C-12), 139.46 (C-10), 125.80 (C-11), 122.80 (C-9), 99.94 (C-5), 19.22 (C-7). IR (solid-state ATR cm-1)

2081, 1966, 1927, 1681, 1633, 1596, 1259, 1015, 783, 629, 545, 449. MS; HRMS (ESI^+) m/z: $[M + H]^+$ calcd for $C_{15}H_9MnNO_6$ 353.9766; Found 353.9769.

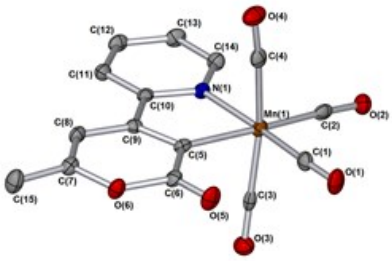

Lab book reference number: *NPY-5-313*

[Mn(CO)$_4$(4-(3-methoxy-2-pyridyl)-2-Pyrone)] (105b)

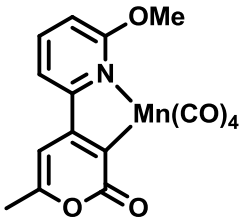

Following the general procedure D1; $MnBn(CO)_5$ (395 mg, 1.38 mmol,), THF (15 ml), **104** (300 mg, 1.38 mmol) to afford the desired product as a sticky yellow solid (52 mg, 98% yield). MP 159–160 °C.

^{1}H NMR (400 MHz, CD2Cl2) δ 7.92 – 7.86 (m, 1H, H-10), 7.37 (d, J_{HH} = 7.5, 1H, H-9), 6.79 (d, J_{HH} = 8.0Hz, 1H, H-11), 6.27 (s, 1H, H-5), 4.07 (s, 3H, H-13), 2.27 (s, 3H, H-7). ^{13}C NMR (176 MHz, CD_2Cl_2) δ 212.84 (C-2), 168.96 (C-4), 167.15 (C-5), 164.01 (C-6), 163.45 (C-12), 158.10 (C-8), 141.46 (C-9), 114.90 (C-10), 105.66 (C-11), 100.00 (C-5), 56.56 (C-13), 19.94 (C-7). IR (solid-state ATR cm^{-1}) 3084, 3020, 2957, 2923, 2853, 2073, 1993, 1946, 1685, 1633, 1473, 1597, 1569, 1509, 1425,

1368, 1318, 1286, 1260, 1093, 1049, 1016, 929, 883, 799, 745, 659, 631. MS; HRMS (ESI$^+$) m/z: $[M + H]^+$ calcd for $C_{16}H_{11}MnNO_7$ 382.9838; Found 382.9872.

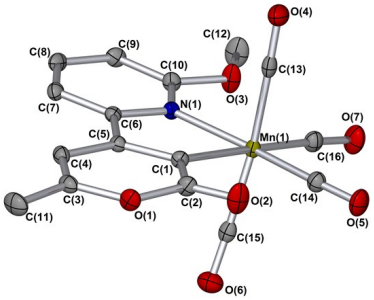

Lab book reference number: *NPY-5-[Mn]-OMe*

4-[(2-Pyridyl)-3-(ethenylphenyl)-2-pyrone (106)

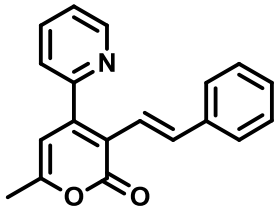

Following the general procedure E1; **105a** (0.28 mmol, 100 mg), in neat phenylacetylene **16** (1.5 mL., excess) to afforde the third (fraction) product as a pale orange viscous liquid (23.3 mg, 28 %)

^{1}H NMR (400 MHz, CD_2Cl_2) δ 8.76 (ddd, J_{HH} = 4.8, 1.8, 1.0 Hz, 1H, H-12), 7.87 (d, J_{HH} = 16.1 Hz, 1H, H-14), 7.81 (td, J_{HH} = 7.7, 1.8 Hz, 1H, H-10), 7.50 – 7.47 (m, 1H, H-9), 7.38 (ddd, J_{HH} = 7.7, 4.8 Hz, 1.0, 1H, H-11), 7.35 – 7.31 (m, 2H, H-16/20), 7.31 – 7.25 (m, 2H, H-17/19), 7.24 – 7.19 (m, 1H, H-18), 6.95 (d, J_{HH} = 16.1 Hz, 1H, H-13), 6.31 (s, 1H, H-5), 2.30 – 12.34 (s, 3H, H-7). 13C NMR (101 MHz,

CD_2Cl_2) δ 161.91 (C-2), 159.33 (C-6), 155.39 (C-4), 150.48 (C-8), 150.13 (C-12), 137.92 (C-3), 136.41 (C-10), 134.32 (C-14), 128.61 (C-17/19), 127.87 (C-18), 126.70 (C-16/20), 124.94 (C-9), 123.66 (C-11), 121.08 (C-13), 117.65 (C-15), 106.43 (C-5), 19.73 (C-7). IR (solid-state ATR, cm-^{1}) 340, 288, 269, 2970, 3015, 1739, 1367, 1263, 1216, 836, 795, 687, 738, 613, 567, 539, 463.2464. UV Vis. λ max. = 262 and 364. MS; HRMS (ESI^+) m/z: [M + H]+ calcd for $C_{19}H_{16}NO_2$ 290.1176; Found 290.1177, $[M + Na]^+$ 312.0990.

Lab book reference number: *NPY-5-315/316 F4F2*

6-Methylpyrano-4,3-quinolizin(14-phenyl)-8-ylium-η^4-tricarbonylmanganesuide (107)

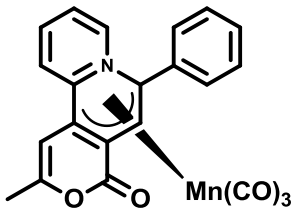

Following the general procedure C2; **105a** (200 mg, 0.57 mmol), phenyl acetylene **16** (70 mg, 0.68 mmol) to afford the product as yellow powder (210 mg, 87 %). MP 89 - 90 °C.

^{1}H NMR (400 MHz, CD_2Cl_2) δ 7.62 (d, J_{HH} = 7.6 Hz, 1H, H-12), 7.55 – 7.41 (m, 4H, H-16/17/19/20), 7.36 (t, J_{HH} = 7.5 Hz, 1H, H-18), 7.26-7.31 (m, 1H, H-10), 6.98 (d, J_{HH} = 8.2 Hz, 1H, H-9), 6.72 (s, 1H, H-13), 6.69 – 6.60 (m, 1H, H-11) 5.46 (s, 1H, H-5), 2.03 (s, 3H, H-7). ^{13}C NMR (101 MHz, CD_2Cl_2) 170.85 (C-2), 157.98 (C-8), 146.67 (C-6), 139.45 (C-10), 137.39 (C-12), 135.91 (C-15), 129.55 (C-16/20), 128.82 (C-17/19), 128.36 (C-18), 119.54 (C-11), 119.33 (C-9), 101.44 (C-5), 85.19 (C-4), 76.47 (C-13), 75.13 (C-14), 60.67 (C-3), 18.79 (C-7). IR (solid-state ATR,

cm^{-1}) 3073, 2952, 2080, 1965, 1702, 1632, 1551, 1432, 1015, 785, 842, 874, 783, 630, 544. MS; HRMS (ESI^{+}) m/z: [M + H]$^{+}$ calcd for $C_{22}H_{15}MnNO_5$ 427.0252; Found 430.0320.

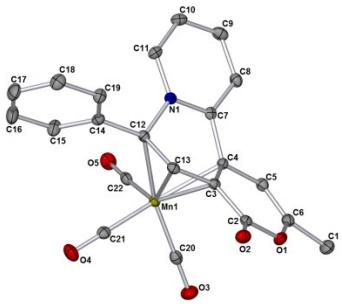

Lab book reference number: *NPY-5-314*

8-Biphenyl-6-methyl-9-phenyl-4,3-isoquinolizin-2-pyrone (108)

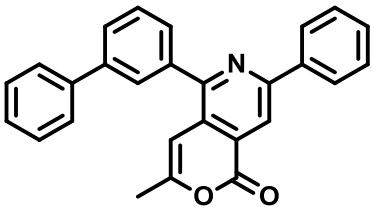

Following the general procedure E1; **105a** (0.28 mmol, 100 mg), in neat phenylacetylene **16** (1.5 mL., excess) to afforde the second (fraction) product as dirty white solid (47.10 mg, 44 %). MP 115–116 °C.

^{1}H NMR (400 MHz, CD_2Cl_2) δ 8.50 (d, J_{HH} = 1.0 Hz, 1H, H-10), 8.22 – 8.18 (m, 2H, H-12/16), 7.94 (td, J_{HH} = 1.8, 0.6 Hz, 1H, H-18), 7.78 (dt, J_{HH} = 7.1, 1.8 Hz, 1H, H-22), 7.71 – 7.68 (m, 2H, H-25/27), 7.67–7.62 (m, 2H, H-20/21), 7.52 (qd, J_{HH} = 2.9, 1.8 Hz, 2H, H-24/28), 7.39–7.48 (m, 4H, H-13/14/15/26), 6.54 (6.59 – 6.45 (m, 1H, H-5), 2.28 (d, J = 1.0 Hz, 3H, H-7). ^{13}C NMR (176 MHz, CD_2Cl_2) δ 162.26 (C-

2), 156.95 (C-8/19), 156.06 (C-6), 155.02 (C-9), 141.94 (C-23), 140.99 (C-17), 139.38 (C-13/15), 138.46 (C-3), 129.84 (C-25/27), 129.35 (C-26), 129.29 (C-11), 129.23 (C-24/28), 128.90 (C-20), 128.68 (C-18), 128.31 (C-4), 128.08 (C-22), 127.99 (C-21), 127.61 (C-14), 127.19 (C-12/16), 116.53 (C-10), 100.84 (C-5), 20.37 (C-7). IR (solid-state ATR, cm-^{1}) 2081, 1966, 1927, 1681, 1633, 1596, 1259, 1015, 783, 629. UV Vis. λ max. = 252, 304 and 372. MS; HRMS (ESI^{+}) m/z: $[M + H]^{+}$ calcd for $C_{27}H_{20}NO_2$ 389.1416; Found 390.1484, $[M + Na]^{+}$ 412.1304, Elemental Analysis: calcd C; 83.27, H; 4.92, N; 3.60; Found C; 82.27, H; 4.60, N; 3.23.

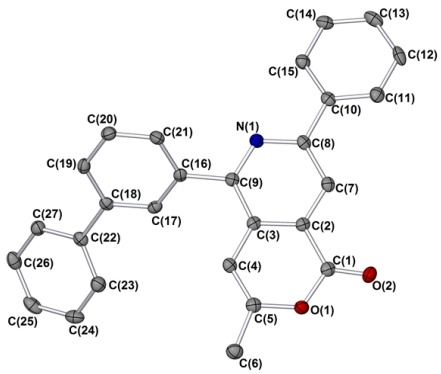

Lab book reference number: *NPY-5-315/316 F2F2*

7-methyl-2,6-diphenyl-10-(benzo-3-phenyl)isoquinoline (109)

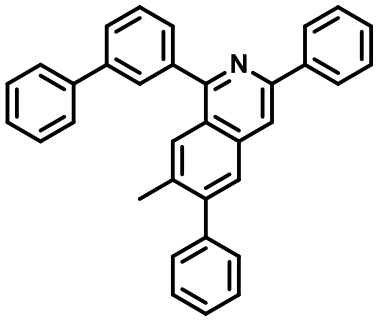

Following the general procedure E1; **105a** (0.28 mmol, 100 mg), in neat phenylacetylene **16** (1.5 mL., excess) to afforde the First (fraction) product as a light orange solid (39.15 mg, 32 %). MP 150.5–152.0 °C.

^{1}H NMR (700 MHz, CD_2Cl_2) δ 8.23 (d, J_{HH} = 7.7 Hz, 2H, H-17/21), 8.12 (s, 1H, H-14), 8.06 (s, 1H, H-24), 8.04 (s, 1H, H-3), 7.83 (s, 1H, H-6), 7.82–7.74 (m, 2H, H-26/28), 7.73 (d, J_{HH} = 7.7 Hz, 2H, H-9/13), 7.68 (ddd, J_{HH} = 8.0, 7.4, 0.5 Hz, (small J_{HH} = 0.5 confirmed by ^{1}HCosy), 1H, H-27), 7.52 – 7.51 (m, 1H, H-19), 7.51 – 7.38 (br m, 10H, H-10/11/12/18/20/30/31/32/33/34), 2.37 (d, J_{HH} = 0.7 Hz, 3H, H-1). ^{13}C NMR (176 MHz, CD_2Cl_2) δ 159.74 (C-22), 149.85 (C-16), 145.74 (C-2), 141.32 (C-8), 141.31 (C-23), 136.81 (C-4), 136.19 (C-7), 129.48 (C-26), 129.45 (C-25), 129.39 (C-9/13), 129.34 (C-10/12), 129.27 (C-30), 129.16 (C-24), 129.04 (C-18/20), 129.01 (C-27), 128.83 (C-11), 128.77 (C-34), 128.66 (C-32), 128.26 (C-15), 128.25 (C-6), 127.94 (C-19), 127.92 (C-3), 127.64 (C-28), 127.60 (C-31/33), 127.58 (C-29), 127.19 (C-17/21), 125.57, (C-5), 115.75 (C-14), 21.64 (C-1). IR (solid-state ATR, cm-^{1}) 3054, 3029, 2958, 2921, 2853, 2008, 1931, 1553, 1477, 1446, 1378, 1313, 1259, 1073, 1024, 898, 803, 757, 693. UV Vis. λ max. = 262. MS; HRMS (ESI^{+}) m/z: $[M + H]^{+}$ calcd for $C_{34}H_{26}N$ 448.2065; Found448.2065.

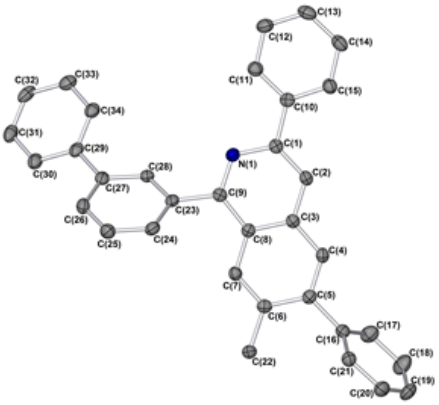

Lab book reference number: *NPY-5-315/316 F3F3*

η^4-Tricarbonylmanganese complex (110)

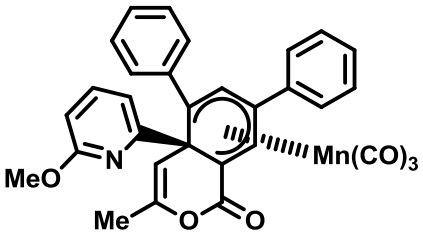

Following the general procedure E1; **105b**, (0.25 mmol, 100 mg), in neat phenylacetylene **16** (1.5 mL., excess), column chromatography with petroleum ether:EtOAc (90:10, *v*/*v*), to afford the product as a pale orange solid (107 mg, 76 %). MP 110.5–111.0 °C.

^{1}H NMR (400 MHz, CD_2Cl_2) δ 7.71 (dd, J_{HH} = 7.9, 1.7 Hz, 2H, H-14/16), 7.46 (s, 1H, H-9), 7.43 – 7.29 (m, 9H, H-13/15/17/19/20/21/22/23/26), 6.61 (d, J_{HH} = 7.5 Hz, 1H, H-27), 6.52 (d, J_{HH} = 7.5 Hz, 1H, H-25), 6.49 (s, 1H, H-11), 5.93 (d, J_{HH} = 1.1, 1H, H-9), 5.47 (s, 1H, H-5), 3.71 (s, 3H, H-29), 2.03 (s, 3H, H-7). ^{13}C NMR (176 MHz, CD_2Cl_2) δ 168.59 (C-2), 163.79 (C-2), 162.64 (C-6), 149.52 (C-24), 139.52 (C-9), [137.38, 136.06, 129.70, 129.40, 129.30, 128.69, 128.63

(C-12/13/15/18/19/20/21/22/23/26/28)], 126.89 (C-17/13), 111.81 (C-27), 109.64 (C-25), 104.07 (C-5), 99.95 (C-3), 94.94 (C-11), 86.76 (C-8), 53.61 (C-10) 48.50 (C-4), 44.12 (C-29), 19.50 (C-7). IR (solid-state ATR, cm-^{1}) 3087, 3027, 2923, 2853, 2073, 1993, 1946, 1634, 1599, 1261, 1260, 1093, 1049, 782, 629, 559, 455. MS; HRMS (ESI^{+}) m/z: $[M + H]^{+}$ calcd for $C_{31}H_{24}MnNO_6$ 560.0906; Found 560.0859.

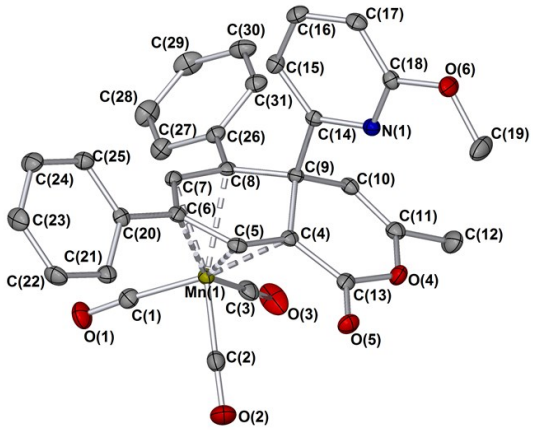

Lab book reference number: *NPY-5-OMe C-H F2F3*

6-Methyl-4-(phenylethynyl)-2-pyrone (112a)[109]

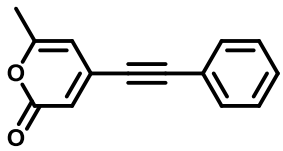

Following the general procedure F1; with 4-bromopyrone (250 mg, 1.32 mmol) and phenylacetylene (162 mg, 1.58 mmol), to afford the compound as a Cream solid (320 mg, 91%). MP 107–110 °C.

^{1}H NMR (400 MHz, $CDCl_3$) δ 7.52 (dd, J_{HH} = 8.0, 1.6 Hz, 2H, H-11/15), 7.45 – 7.34 (m, 3H, H-12/13/14), 6.29 (d, J_{HH} = 0.6 Hz, 1H, H-3), 6.04 (d, J_{HH} = 0.6 Hz, 1H, H-5), 2.24 (s, 1H, H-7). ^{13}C NMR (101 MHz, $CDCl_3$) δ 162.35 (C-2), 162.06 (C-6), 139.06 (C-4), 132.2435 (C-11/15), [130.07, 128.71 (C-12/13/14)], 121.34 (C-10), 114.51 (C-3), 105.50 (C-5), 98.71 (C-9), 85.51 (C-8), 20.0235 (C-7). IR (solid-state ATR, cm-^{1}) 2203, 1721, 1703, 1643, 1534, 1439, 1309, 1206, 1135, 955, 838, 760, 692, 530, 1392, 1485. MS; HRMS (ESI^{+}) m/z: [M + H]$^{+}$ calcd for $C_{14}H_{11}O_2$ 211.0681; Found 211.0753. Elemental Analysis: calcd C 79.98, H 4.79,; Found C 79.48, H 4.79.

Lab book reference number: *NPY-4-287*

(*β*)-(*3aSR,4RS,7SR,7aRS*)-6-Methyl-4-(1-oxo-3-phenyl-3a,4,5,6,7,7a-hexahydro-1H-4,7-methanoinden-2-yl)- 2*H*-pyran-2-one (*β*–113a)[109]

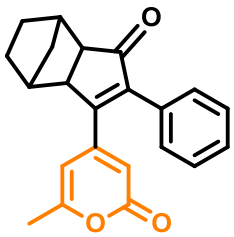

Synthesised following the general procedure G; with **112a** (55 mg, 0.26 mmol), to afford to afford the desired product as a creamy solid (85 mg, 98 % yield). MP 115–116. °C.

^{1}H NMR (400 MHz, $CDCl_3$) δ 7.37 – 7.31 (m, 3H, H-12/13/14), 7.20 (dd, J_{HH} = 6.7, 3.0 Hz, 2H, H-11/15), 6.22 (d, J_{HH} = 0.6 Hz, 1H, H-3), 5.60 (s, 1H, H-5), 2.99 (d, J_{HH} = 5.5 Hz, 1H, H-18), 2.61 (d, J_{HH} = 3.3 Hz, 1H, H-17), 2.49 (d, J_{HH} = 5.5 Hz,

1H, H-19), 2.22 (d, J_{HH} = 3.3 Hz, 1H, H-22), 2.10 (s, 3H, H-7), 1.80 – 1.58 (m, 2H, H-21), 1.39 (d, J_{HH} = 8.8 Hz, 2H, H-20/23), 1.10 (d, J_{HH} = 8.8 Hz, 2H, H-20/23). ^{13}C NMR (101 MHz, $CDCl_3$) δ 207.81 (C-16), 163.55 (C-2), 162.72 (C-6), 162.25 (C-4), 151.44 (C-8), 146.22 (C-9), [129.19, 128.66, 128.40 (C-12/13/14)], 111.59 (C-3), 103.54 (C-5), 54.08 (C-20), 50.13 (C-19), 39.78 (C-18), 38.21 (C-22), 31.77 (C-17), 29.02 (C-21), 28.67 (C-23), 20.17 (C-7). IR (solid-state ATR, cm^{-1}) 1634, 1573, 2954, 2871, 1695, 1717, 1444, 1306, 1196, 980, 854, 695, 750. MS; HRMS (ESI$^+$) m/z: [M + H]$^+$ calcd for $C_{22}H_{21}O_3$ 333.1446; Found 333.1396.

Lab book reference number: *NPY-4-288F2*

(*α*)-(*3aSR,4RS,7SR,7aRS*)-6-Methyl-4-(1-oxo-3-phenyl-3a,4,5,6,7,7a-hexahydro-1*H*-4,7-methanoinden-2-yl)- 2*H*-pyran-2-one (*α*–113a)[109]

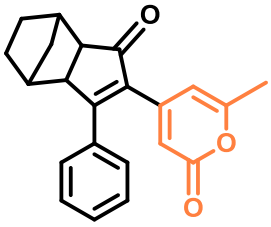

Synthesised following the general procedure G; with **112a** (55 mg, 0.26 mmol), to afford to afford the desired product as a creamy solid (46 % yield by ^{1}H MNR with respect to *α*- isomer). MP 116–118 °C.

^{1}H NMR (400 MHz, $CDCl_3$) δ 7.44 – 7.37 (m, 3H, H-12/13/14), 7.36 (d, *J* = 2.3 Hz, 2H, H-11/15), 6.08 (s, 1H, H-3), 5.74 (s, 1H, H-5), 3.20 (d, *J* = 5.5 Hz, 1H, H-18), 2.58 (d, *J* = 3.2 Hz, 1H, H-17), 2.49 (d, *J* = 5.4 Hz, 3H, H-19), 2.15 (s, 3H, H-7),

2.09 – 2.07 (m, 1H, H-22), 1.77 – 1.58 (m, 2H, H-21), 1.39 (d, J = 8.5 Hz, 2H, H-20/23), 1.03 (d, J = 8.5 Hz, 2H, H-20/23). ^{13}C NMR (101 MHz, $CDCl_3$) δ 206.52 (C-16), 174.37 (C-2), 162.98 (C-6), 162.72 (C-4), 161.98 (C-8), 148.51 (C-9), [130.87, 130.37, 129.11, 129.07 (C-11/12/13/14/15)], 112.66 (C-3), 104.79 (C-5), 54.43 (C-20), 51.49 (C-19), 39.78 (C-18), 38.57 (C-22), 31.77 (C-17), 29.07 (C-21), 28.76 (C-23), 20.14 (C-7). IR (solid-state ATR, cm^{-1}) 1634, 1573, 2954, 2871, 1695, 1717, 1444, 1306, 1196, 980, 854, 695, 750. MS; HRMS (ESI$^+$) m/z: [M + H]$^+$ calcd for $C_{22}H_{21}O_3$ 333.1446; Found 333.1396.

Lab book reference number: *NPY-4-288F2*

(*9aRS,10SR,13RS,13aSR*)-2-Methyl-4,9,9a,10,11,12,13,13aoctahydro-10,13-methanobenzo[*h*]indeno[1,2-*f*]isochromene-4,9-dione (113*B*)

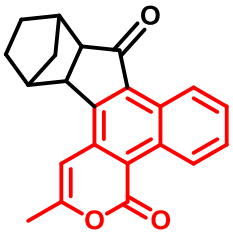

Synthesised following the general procedure H2; with irradiation of **113a** (ca.15 mg), in CD_2Cl_2 (0.6 mL) to afford to afford the desired product as a creamy solid. (100 % conversion by NMR). MP 201–203 °C.

^{1}H NMR (400 MHz, CD_2Cl_2) δ 9.67 (dd, J_{HH} = 7.9, 1.5 Hz, 1H, H-11), 9.28 (dd, J_{HH} = 8.2, 1.4 Hz, 1H, H-14), 7.76 (ddd, J_{HH} = 8.7, 6.9, 1.8 Hz, 1H, H-12), 7.74 – 7.69 (m, 1H, H-13), 6.70 (s, 1H, H-5), 3.32 (d, J_{HH} = 5.8 Hz, 1H, H-18), 2.69 (d, J_{HH} = 5.8 Hz, 1H, H-19), 2.66 (d, J_{HH} = 4.0 Hz, 1H, H-17), 2.56 (d, J_{HH} = 4.2 Hz, 1H, H-22), 2.45 (d, J_{HH} = 0.9 Hz, 3H, H-7), 1.85 – 1.65 (m, 4H, H-20/21), 1.00 (ddt, J_{HH} =

10.8, 2.8, 1.5 Hz, 1H, H-23), 0.85 (ddt, J_{HH} = 10.5, 3.4, 1.8 Hz, 1H, H-23). ^{13}C NMR (101 MHz, CD_2Cl_2) δ 211.60 (C-16), 160.39 (C-2), 156.44 (C-6), 140.22 (C-4), 139.99 (C-8), 133.62 (C-9), 131.49 (C-12), 131.17 (C-15), 130.85 (C-13), 130.69 (C-10), 128.71 (C-11), 126.45 (C-3), 102.96 (C-5), 58.94 (C-19), 48.57 (C-18), 42.86 (C-17), 42.29 (C-22), [34.29, 31.69 (C-20/21)], 30.70 (C-23), 22.15 (C-7). MS; HRMS (ESI$^+$) m/z: [M + H]$^+$ calcd for $C_{21}H_{18}O_3$ 331.1289; Found 331.1257. Elemental Analysis: calcd C, 79.98; H, 5.49; Found C, 79.73; H, 5.47.

Lab book reference number: *NPY-3-161*

2-(2'-Tetramethylsilyl-ethynyl)pyridine (114a)[142]

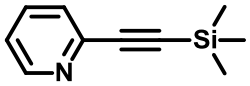

Following the general procedure F1; with 2-bromopyridine (1000 mg, 6.32 mmol) and TMS-acetylene (1367 mg, 13.94 mmol), to afford the compound as a colourless liquid (990 mg, 89%).

^{1}H NMR (400 MHz, $CDCl_3$) δ 8.51 (ddd, J_{HH} = 4.9, 1.8, 1.0 Hz, 1H, H-1), 7.56 (td, J_{HH} = 7.7, 1.8 Hz, 1H, H-3), 7.38 (dt, J_{HH} = 7.8, 1.0 Hz, 1H, H-2), 7.15 (ddd, J_{HH} = 7.7, 4.9, 1.8 Hz, 1H, H-4), 0.22 – 0.21 (m, 9H, H-8/9/10). IR (solid-state ATR, cm-1) 3126, 3298, 2962, 1584, 1259, 1094, 1013. MS; HRMS (ESI$^+$) m/z: [M + H]$^+$ calcd for $C_{10}H_{14}NSi$ 176.0851; Found 176.0821.

Lab book reference number: *NPY-3-168*

2-Ethynylpyridine (114b)[142]

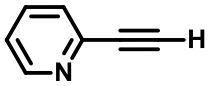

Following the general procedure F1; with **114b** (500 mg, 2.85 mmol), to afford the compound as a colourless liquid (230 mg, 81 %).

^{1}H NMR (400 MHz, $CDCl_3$) δ 8.55 (ddd, J_{HH} = 4.8, 1.8, 1.0 Hz, 1H, H-1), 7.62 (td, J_{HH} = 7.8, 1.8 Hz, 1H, H-3), 7.44 (ddt, J_{HH} = 7.8, 1.8, 1.0 Hz, 1H, H-2), 7.23 (ddd, J_{HH} = 7.7, 4.9, 1.0 Hz, 1H, H-4), 3.13 (s, 1H, H-7). ^{13}C NMR (101 MHz, $CDCl_3$) δ 150.11 (C-1), 142.40 (C-5), 136.27 (C-3), 127.53 (C-2), 123.50 (C-4), 82.79 (C-6), 77.21 (C-7). IR (solid-state ATR, cm^{-1}) 3299, 3046, 2962, 2900, 2166, 2066, 1582, 1562, 1461, 1427, 1250, 873.

MS; HRMS (ESI$^+$) m/z: $[M + H]^+$ calcd for C_7H_6N 104.0456; Found 104.0425.

Lab book reference number: *NPY-3-169*

6-Methyl-4-(2-pyridilethynyl)-2-pyrone (114c)

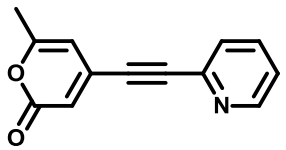

Following the general procedure F1; with 4-bromopyrone **103** (500 mg, 2.65 mmol) and 2-pyridilacetylene (327 mg, 3.17 mmol), to afford the compound as a Cream solid (490 mg, 88 % yield). MP 102–104 °C.

^{1}H NMR (400 MHz, CD_2Cl_2) δ 8.63 (ddd, J = 4.8, 1.7, 0.9 Hz, 1H, H-14), 7.74 (td, J = 7.8, 1.7 Hz, 1H, H-12), 7.56 (dt, J_{HH} = 7.8, 1.7 Hz, 1H, H-11), 7.33 (ddd, J_{HH} = 7.8, 4.8, 1.7 Hz, 1H, H-13), 6.33 (d, J_{HH} = 0.6 Hz, 1H, H-3), 6.10 (s, 1H, H-5), 2.25 (d, J_{HH} = 0.6 Hz, 3H, H-7). ^{13}C NMR (101 MHz, CD_2Cl_2) δ 162.89 (C-2), 161.92 (C-6), 150.83 (C-14), 142.07 (C-10), 138.25 (C-4), 136.71 (C-12), 128.36 (C-11), 124.49 (C-13), 115.80 (C-3), 105.24 (C-5), 96.81 (C-9), 84.25 (C-8), 20.17 (C-7). IR (solid-state ATR, cm-^{1}) 3068, 2214, 1704, 1632, 1579, 1537, 1461, 1430, 1312, 1214, 1138, 1028, 961, 854, 812, 776, 739, 533. MS; HRMS (ESI^{+}) m/z: $[M + H]^{+}$ calcd for $C_{13}H_{10}NO_2$ 212.0633; Found 212.0706, Elemental Analysis: calcd C 73.92, H 4.29, N 6.63; Found C 72.62, H 4.17, N 6.69.

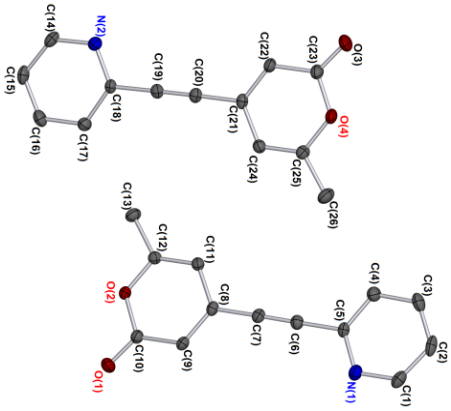

Lab book reference number: *NPY-3-119*

4-(2'-Tetramethylsilyl-ethynyl)pyridine (115a)[142]

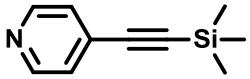

Following the general procedure F1; with 4-bromopyridine (500 mg, 3.16 mmol) and TMS-acetylene (341 mg, 3.48 mmol), to afford the compound as a colourless liquid (500 mg, 90 %).

^{1}H NMR (400 MHz, $CDCl_3$) δ 7.37 (d, J_{HH} = 4.2 Hz, 2H, H-1/5), 7.30 (d, J_{HH} = 4.2 Hz, 2H, H-2/4), 0.25 (s, 9H, H-8/9/10). MS; HRMS (ESI$^+$) m/z: $[M + H]^+$ calcd for $C_{10}H_{14}NSi$ 176.0890; Found 176.0896. *Lab book reference number*: *NPY-5-325*

4-Ethynylpyridine (115b)[142]

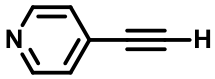

Following the general procedure F1; with **115a** (500 mg, 2.85 mmol), to afford the compound as a dirty white solid (255 mg, 87 %).

^{1}H NMR (400 MHz, $CDCl_3$) δ 8.59 (dd, J_{HH} = 4.4, 1.6 Hz, 2H, H-1/5), 7.34 (dd, J_{HH} = 4.4, 1.6 Hz, 2H, H-2/4), 3.29 (s, 1H, H-7). ^{13}C NMR (101 MHz, $CDCl_3$) δ 149.96 (C-1/5), 130.42 (C-3), 126.20 (C-2/4), 81.99 (C-6), 81.07 (C-7). IR (solid-state ATR, cm-1) 3044, 2097, 1590, 1539, 1402, 1217, 991, 813, 772, 745, 723, 543, 513, 469. MS; HRMS (ESI$^+$) m/z: $[M + H]^+$ calcd for C_7H_6N 104.0456; Found 104.0446.

Lab book reference number: *NPY-4-257*

6-Methyl-4-(4'-pyridylethynyl)-2-pyrone (115c)

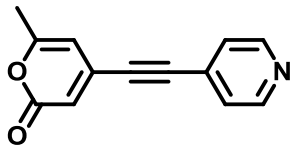

Following the general procedure F1; with 4-bromopyridine **103** (500 mg, 2.65 mmol) and 4-pyridilacetylene (327 mg, 3.17 mmol), to afford the compound as a Cream solid (510 mg, 91 % yield). MP 98–99 °C.

^{1}H NMR (400 MHz, $CDCl_3$) δ 8.66 (d, J_{HH} = 5.2 Hz, 2H, H-13/14), 7.38 (dd, J_{HH} = 5.2, 1.5 Hz, 2H, H-11/14), 6.35 (d, J_{HH} = 0.6 Hz, 1H, H-3), 6.05 (d, J_{HH} = 0.6 Hz, 1H, H-5), 2.27 (s, 3H, H-7). ^{13}C NMR (101 MHz, $CDCl_3$) δ 162.65 (C-2), 161.96 (C-6), 149.99 (C-12/13), 125.85 (C-11/14), 115.87 (C-9), 105.20 (C-3), 94.71 (C-5), 88.94 (C-9), 77.16 (C-8), 20.12 (C-7).IR (solid-state ATR, cm-^{1}) 2213, 1707, 1632, 1587, 1536, 1486, 1440, 1400, 1312, 1136, 1032, 959, 824, 536, 502, 555, 210. MS; HRMS (ESI^{+}) m/z: $[M + H]^{+}$ calcd for $C_{13}H_{10}NO_2$ 212.0633; Found 212.0706, Elemental Analysis: calcd C 73.92, H 4.29, N 6.63; Found C 73.87, H 4.28, N 6.63.

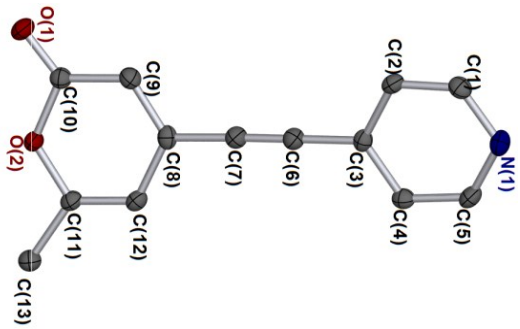

Lab book reference number: *NPY-3-182*

2-(Tetramethylsilyl-2'-ethynyl)pyrazine (116a)[142]

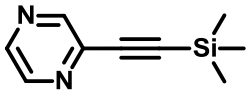

Following the general procedure F1; with 2-bromopyrazine (1000 mg, 6.30 mmol) and TMS-acetylene (1358 mg, 13.83 mmol), to afford the compound as a colourless liquid (1.07 g, 97 %).

^{1}H NMR (400 MHz, $CDCl_3$) δ 8.61 (d, J_{HH} = 1.3 Hz, 1H, H-1), 8.49 (d, J_{HH} = 2.5 Hz, 1H, H-3), 8.38 (dd, J_{HH} = 2.5, 1.4 Hz, 1H, H-2), 0.28 (s, 9H, H-7/8/9). IR (solid-state ATR, cm-^{1}) 3064, 2960, 2899, 1459, 1391, 1249, 1141, 1011, 839, 760 MS; HRMS (ESI$^+$) m/z: $[M + H]^+$ calcd for $C_9H_{13}N_2Si$ 177.0803; Found 177.0779.

Lab book reference number: *NPY-4-213*

2-Ethynylpyrazine (116b)[142]

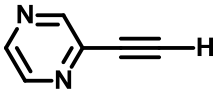

Following the general procedure F1; with **116a** (500 mg, 2.84 mmol), to afford the compound as a colourless liquid (260 mg, 88 %).

^{1}H NMR (400 MHz, $CDCl_3$) δ 8.71 (d, J_{HH} = 1.4 Hz, 1H, H-1), 8.56 (dd, J_{HH} = 2.5, 1.4 Hz, 1H, H-2), 8.52 (d, J_{HH} = 2.5 Hz, 1H, H-3), 3.35 (s, 1H, H-6). IR (solid-state ATR, cm-^{1}) 3242, 3217, 2109, 1459, 1380, 1143, 1049, 1013, 850, 735, 695, 672, 529.MS; HRMS (ESI$^+$) m/z: $[M + H]^+$ calcd for $C_6H_5N_2$ 105.0408; Found 105.0404.

6-Methyl-4-(2'-pyrazylethynyl)-2-pyrone (116c)

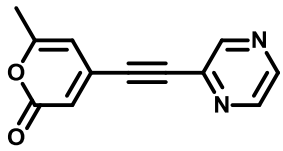

Following the general procedure F1; with 2-bromopyrone **103** (1.0 g, 5.29 mmol) and 2-pyrazylacetylene (66 mg, 6.35 mmol), to afford the compound as a creamy solid (0.98 g, 87 %). MP 97–99 °C.

^{1}H NMR (400 MHz, CD_2Cl_2) δ 8.77 (d, J_{HH} = 1.5 Hz, 1H, H-11), 8.62 (dd, J_{HH} = 2.4, 1.5 Hz, 1H, H-12), 8.58 (d, J_{HH} = 2.5 Hz, 1H, H-13), 6.40 (d, J_{HH} = 0.5 Hz, 1H, H-3), 6.09 (s, J_{HH} = 1.1 Hz, 1H, H-5), 2.26 (s, 3H, H-7). ^{13}C NMR (101 MHz, CD_2Cl_2) δ 162.77 (C-2), 161.72 (C-6), 148.25 (C-11), 144.95 (C-12), 144.37 (C-13), 138.71 (C-10), 137.22 (C-10), 116.29 (C-3), 104.85 (C-5), 93.32 (C-9), 87.89 (C-8), 20.14 (C-7). IR (solid-state ATR, cm-^{1}) 3088, 1709, 1628, 1533, 1464, 1381, 1315, 1315, 1139, 1012, 858, 536, 510, 409. MS; HRMS (ESI^{+}) m/z: $[M + H]^{+}$ calcd for $C_{12}H_9N_2O_2$ 213.0586; Found 213.0596.

Lab book reference number: *NPY-4-215*

2-(Tetramethylsilyl-2'-ethynyl)thiophene (117a)[142]

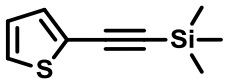

Following the general procedure F1; with 2-bromothiophene (1000 mg, 6.14 mmol) and TMS-acetylene (1.325 g, 13.49 mmol), to afford the compound as a colourless liquid (530 mg, 48 %).

^{1}H NMR (400 MHz, CD_2Cl_2) δ 7.25 (dd, J_{HH} = 5.2, 1.1 Hz, 1H, H-1), 7.21 (dd, J_{HH} = 3.6, 1.1 Hz, 1H, H-3), 6.95 (dd, J_{HH} = 5.2, 3.6 Hz, 1H, H-2), 0.22 (s, 9H, H-7/8/9). MS; HRMS (ESI$^+$) m/z: $[M + H]^+$ calcd for $C_9H_{13}SSi$ 181.0463; Found 181.0459.

Lab book reference number: *NPY-4-232*

6-Methyl-4-(2-thienylethynyl)-2-pyrone (117c)

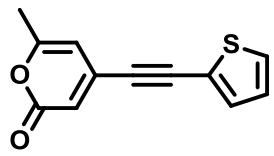

Following the general procedure F1; with 4-bromopyrone **103** (500 mg, 2.65 mmol) and 2-ethynylthiophene (343 mg, 3.17 mmol), to afford the compound as a cream solid (360 mg, 63 % yield). MP 61–62 °C.

^{1}H NMR (400 MHz, CD_2Cl_2) δ 7.43 (dd, J_{HH} = 5.2, 1.1 Hz, 1H, H-13), 7.38 (dd, J_{HH} = 3.7, 1.1 Hz, 1H, H-11), 7.06 (dd, J_{HH} = 5.1, 3.7 Hz, 1H, H-12), 6.26 (d, J_{HH} = 0.6 Hz, 1H, H-3), 6.03 (s, J_{HH} = 0.6 Hz, 1H, H-5), 2.25 (s, 3H, H-7). ^{13}C NMR (101 MHz, CD_2Cl_2) δ 162.29 (C-2), 162.13 (C-6), 138.68 (C-4), 134.59 (C-11), 130.17 (C-13), 127.72 (C-12), 121.22 (C-10), 113.92 (C-3), 105.08 (C-5), 92.26 (C-9), 89.53 (C-8), 20.07 (C-7). MS; HRMS (ESI$^+$) m/z: $[M + H]^+$ calcd for $C_{12}H_9O_2S$ 217.0245; Found 217.0343, Elemental Analysis: calcd C 66.65, H 3.73, N 6.63; Found C 66.45, H 3.73.

Lab book reference number: *NPY-4-240F1F2F1*

[4-(2'-Thienylethynyl)pyridine] (118)

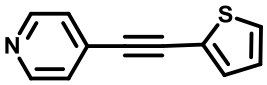

Following the general procedure F1; with 2-bromothiophene (500 mg, 3.07 mmol) and 4-pyridilacetylene (380 mg, 3.68 mmol), to afford the compound as a cream solid (330 mg, 58 % yield). MP 58–62 °C.

^{1}H NMR (400 MHz, CD_2Cl_2) δ 8.60 (dd, J_{HH} = 4.6, 1.4 Hz, 1H, H-1/5), 7.39 – 7.34 (m, 4H, H-2/4/9/11), 7.05 (dd, J_{HH} = 5.1, 3.7 Hz, 2H, H-10). ^{13}C NMR (101 MHz, CD_2Cl_2) δ 149.59 (C-1/5), 133.90 (C-11), 131.93 (C-5), 129.38 (C-2/4), 127.86 (C-10), 125.68 (C-9), 122.20 (C-8), 90.61 (C-7), 87.88 (C-6). IR (solid-state ATR, cm-^{1}) 3071, 2200, 1694, 1589, 1404, 1208, 1007, 818, 705, 540, 504. MS; HRMS (ESI^{+}) m/z: $[M + H]^{+}$ calcd for $C_{11}H_8NS$ 186.0299; Found 186.0381.

Lab book reference number: *NPY-4-224*

[2-(2'-Thienylethynyl)pyridine] (119)[143]

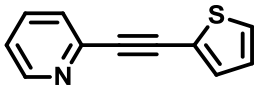

Following the general procedure F1; with 2-bromothiophene (700 mg, 4.30 mmol) and 2-ethenylpyridine (531 mg, 5.15 mmol), to afford the compound as a Cream solid (562 mg, 71 % yield). MP 56–59 °C.

^{1}H NMR (400 MHz, $CDCl_3$) δ 8.60 (ddt, J_{HH} = 4.9, 1.8, 0.8 Hz, 1H, H-1), 7.66 (tdd, J_{HH} = 7.8, 1.8, 0.8 Hz, 1H, H-3), 7.49 (dd, J_{HH} = 7.8, 0.8 Hz, 1H, H-4), 7.39 – 7.36

(m, 1H, H-11), 7.33 (dt, J_{HH} = 5.1, 1.0 Hz, 1H, H-9), 7.22 (dd, J_{HH} = 7.8, 4.9 Hz, 1H, H-2), 7.01 (ddd, J_{HH} = 5.1, 3.6, 1.0 Hz, 1H, H-10). ^{13}C NMR (101 MHz, $CDCl_3$) δ 150.24 (C-1), 143.34 (C-3), 136.29 (C-5), 133.43 (C-11), 128.49 (C-9), 127.33 (C-4), 127.02 (C-10), 122.90 (C-2), 122.33 (C-8), 92.41 (C-6), 82.79 (C-7). IR (solid-state ATR, cm^{-1}) 3077, 2202, 1666, 1642, 1631, 1577, 1558, 1458, 1414, 1275, 1211, 1151, 1043, 986, 835, 775, 706, 568, 502. MS; HRMS (ESI$^+$) m/z: [M + H]$^+$ calcd for $C_{11}H_8NS$ 186.0299; Found 186.0372.

Lab book reference number: *NPY-4-255*

[2-(4'-Pyridylethynyl)pyridine] (120)[144]

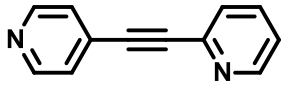

Following the general procedure F1; with 4-bromopyridine (200 mg, 1.27 mmol) and 2-ethenylpyridine (157 mg, 1.52 mmol), to afford the compound as a cream solid (194 mg, 85 % yield). MP 83–86 °C.

^{1}H NMR (400 MHz, $CDCl_3$) δ 8.35 (ddd, J_{HH} = 4.9, 2.0, 1.0 Hz, 2H, H-1/5), 7.53 (ddd, J_{HH} = 8.0, 7.2, 2.0 Hz, 2H, H-11/12), 7.46 (dt, J_{HH} = 8.0, 1.0 Hz, 2H, H-10/13), 7.24 (ddd, J_{HH} = 7.2, 4.9, 1.0 Hz, 2H, H-2/4). ^{13}C NMR (101 MHz, $CDCl_3$) δ 150.34 (C-1/5), 142.37 (C-6/9), 138.57 (C-11/12), 134.00 (C-8), 128.72 (C-7), 128.35 (C-10/13), 122.71 (C-2/4). IR (solid-state ATR, cm^{-1}) 3041, 1593, 1576, 1460, 1408, 987, 825, 776, 736, 545, 508. MS; HRMS (ESI$^+$) m/z: [M + H]$^+$ calcd for $C_{12}H_9N_2$ 181.0687; Found 181.0768.

Lab book reference number: *NPY-4-282*

(*β*)-(*3aSR*,4RS,7SR,7aRS)-6-Methyl-4-(1-oxo-3-(2-pyridyl-3a,4,5,6,7,7a-hexahydro-1*H*-4,7-methanoinden-2-yl)-2*H*-pyran-2-one (*β*–121)

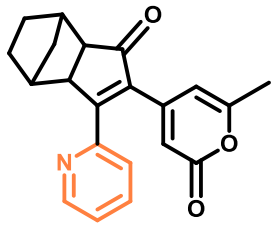

Synthesised following the general procedure G; with **114c** (55 mg, 0.26 mmol), to afford to afford the desired product as a creamy solid (84 mg, 95 % yield). MP 107–110 °C.

^{1}H NMR (400 MHz, $CDCl_3$) δ 8.71 (d, J_{HH} = 4.2 Hz, 1H, H-14), 7.69 (td, J_{HH} = 7.8, 1.8 Hz, 1H, H-13), 7.35 – 7.28 (m, 2H, H-12/14), 6.02 (s, 1H, H-3), 5.77 (s, 1H, H-5), 3.42 (d, J_{HH} = 5.4 Hz, 1H, H-17), 2.58 (d, J_{HH} = 2.1 Hz, 1H, H-16), 2.50 (d, $_{JHH}$ = 5.3 Hz, 1H, H-18), 2.20 (d, J_{HH} = 3.2 Hz, 1H, H-21), 2.17 (s, 3H, H-7), 1.73 – 1.58 (m, 2H, H-19), 1.49 – 1.34 (m, 2H, H-20), 1.14 (d, J_{HH} = 10.7 Hz, 1H, H-22), 1.04 (d, J_{HH} = 10.7 Hz, 1H, H-22). ^{13}C NMR (101 MHz, $CDCl_3$) δ 207.19 (C-15), 172.34 (C-2), 162.85 (C-6), 162.06 (C-4), 152.75 (C-8), 150.45 (C-14), 148.58 (C-9), 140.26, 136.56 (C-12), 124.64 (C-11/13), 112.50 (C-3), 104.84 (C-5), 54.42 (C-18), 50.71 (C-17), 40.00 (C-16), 38.64 (C-19), 31.79 (C-22), 29.18, 28.64 (C-20), 20.16 (C-7). MS; HRMS (ESI$^+$) m/z: [M + H]$^+$ calcd for $C_{21}H_{20}NO_3$ 334.1365; Found 334.1443, Elemental Analysis: calcd C 75.66, H 5.74, N 4.20; Found C 74.96, H 5.72, N 4.13.

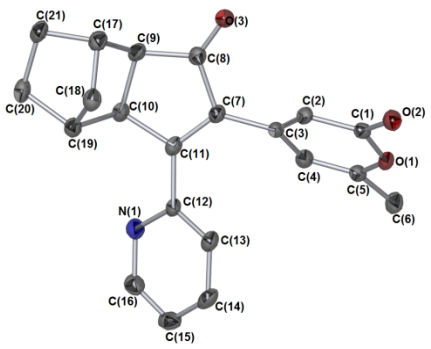

Lab book reference number: *NPY-3-160*

(*9aRS,10SR,13RS,13aSR*)-7-Pyridyl-2-methyl-4,9,9a,10,11,12,13,13a-octahydro-10,13- methanobenzo[*h*]indeno[1,2-*f*]isochromene-4,9-dione (*β*–121B)

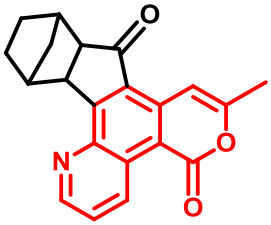

Synthesised following the general procedure H2; with irradiation of ***β*–121A** (ca.15 mg), in CD_2Cl_2 (0.6 mL) at 400 nm, 20 mA for 40 min. to afford the product as a creamy solid (100 % conversion by NMR). MP 197–199 °C.

^{1}H NMR (700 MHz, CD_2Cl_2) δ 10.00 (dd, J_{HH} = 8.7, 1.6 Hz, 1H, H-14), 9.05 (dd, J_{HH} = 4.1, 1.6 Hz, 1H, H-12), 7.90 (d, J_{HH} = 0.9 Hz, 1H, H-5), 7.74 (dd, J_{HH} = 8.7, 4.1 Hz, 1H, H-13), 3.77 (d, J_{HH} = 5.8 Hz, 1H, H-17), 2.90 (d, J_{HH} = 3.3 Hz, 1H, H-16), 2.67 (d, J_{HH} = 5.7 Hz, 1H, H-18), 2.62 (d, J_{HH} = 3.3 Hz, 1H, H-21), 2.41 (d, J_{HH} = 0.6 Hz, 3H, H-7), 1.83 – 1.77 (m, 1H, H-19), 1.73 – 1.67 (m, 2H, H-19/20), 1.51 – 1.46 (m, 1H, H-20), 0.99 (d, J_{HH} = 10.7 Hz, 1H, H-22), 0.83 (d, J_{HH} = 10.7 Hz, 1H, H-22). ^{13}C NMR (101 MHz, CD_2Cl_2) δ 211.60 (C-16), 160.39 (C-2), 156.44 (C-6),

140.22 (C-4), 139.99 (C-8), 133.62 (C-9), 131.49 (C-12), 131.17 (C-15), 130.85 (C-13), 130.69 (C-10), 128.71 (C-11), 126.45 (C-3), 102.96 (C-5), 58.94 (C-19), 48.57 (C-18), 42.86 (C-17), 42.29 (C-22), [34.29, 31.69 (C-20/21)], 30.70 (C-23), 22.15 (C-7). IR (solid-state ATR, cm-^{1}) 2951, 2870, 1693, 1644, 1556, 1499, 1346, 1294, 1186, 1134, 1049, 994, 855, 795, 759, 565, 730. MS; HRMS (ESI^{+}) m/z: $[M + H]^{+}$ calcd for $C_{21}H_{18}NO_3$ 332.1242; Found 332.1209. Elemental Analysis: calcd C, 76.12; H, 5.17; N; 4.23,; Found C, 76.01; H, 5.23; N; 4.26.

Lab book reference number: *NPY-3-160*

[μ_2-6-Methyl-4-(2-(2-pyridylethynyl))-2H-pyran-2-one]-hexacarbonyl dicobalt (121*I*)

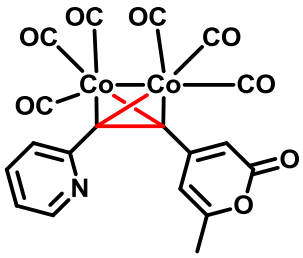

Following the general procedure F3; dicobaltoctacarbonyl (324 mg, 0.95 mmol) and the alkyne (200 mg, 0.95 mmol) to afford the complex as brownish crystals (410 mg, 86 % yield) MP 86–88 ^{o}C.

^{1}H NMR (400 MHz, $CDCl_3$) δ 8.63 (ddd, J = 4.8, 1.8, 0.9 Hz, 1H, H-14), 7.71 (td, J_{HH} = 7.7, 1.8 Hz, 1H, H-12), 7.52 (dt, J_{HH} = 7.8, 1.0 Hz, 1H, H-11), 7.25 – 7.22 (m, 1H, H-2), 6.62 (d, J_{HH} = 0.9 Hz, 1H, H-3), 6.28 (s, J_{HH} = 0.9 Hz, 1H, H-5), 2.29 (s, 3H, H-7). MS; LRMS (LIFDI) m/z: $[M + H]^{+}$ calcd for $C_{19}H_{16}Co_2NO_8$ 503.94; Found 503.93.

Lab book reference number: *NPY-5-293*

(*β*)-(*3aSR,4RS,7SR,7aRS*)-6-Methyl-4-(1-oxo-3-(4-pyridyl-3a,4,5,6,7,7a-hexahydro-1*H*-4,7-methanoinden-2-yl)-2*H*-pyran-2-one (*β*–122)

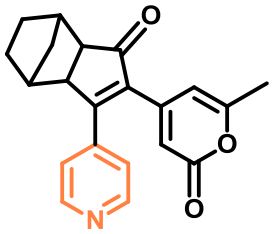

Synthesised following the general procedure G; with **115c** (200 mg, 0.95 mmol), to afford to afford the desired product as a creamy solid (313 mg, 99 % overall yield) (mixture of 50/50 regioisomers by ^{1}H NMR). MP 114–120 °C.

^{1}H NMR (400 $CDCl_3$) δ 8.77 – 8.67 (br. s, 2H, H-12/13), 7.21 (d, J_{HH} = 5.9 Hz, 2H, H-11/14), 6.17 (s, 1H, H-3), 6.01 (s, 1H, H-5), 3.14 (d, J_{HH} = 5.4 Hz, 1H, H-17), 2.64 – 2.57 (m, 1H, H-18), 2.22 (d, J_{HH} = 3.5 Hz, 1H, H-16), 2.14 (s, 3H, H-7), 2.07 (d, J_{HH} = 3.5 Hz, 1H, H-21), 1.78 – 1.59 (m, 2H, H-20), 1.39 (d, J_{HH} = 8.4 Hz, 1H, H-19/22), 1.09 (d, J_{HH} = 9.0 Hz, 1H, H-19/22). ^{13}C NMR (101 MHz, CD_2Cl_2) δ 206.68 (C-15), 166.99 (C-2), 163.42 (C-6), 162.68 (C-4), 150.88 (C-12/13), 150.26 (C-8), 143.27 (C-9), 138.63 (C-10), 123.94 (C-11/14), 104.39 (C-3), 103.18 (C-5), 54.38 (C-18), 51.00 (C-17), 40.21 (C-18), 38.35 (C-21), 31.88 (C-19), 29.15 (C-20), 28.78 (C-22), 20.29 (C-7). IR (solid-state ATR, cm-^{1}) 2953, 2872, 1698, 1636, 1590, 1542, 1406, 1307, 1196, 982, 836, 855, 539, 656. MS; HRMS (ESI^{+}) m/z: $[M + H]^{+}$ calcd for $C_{21}H_{20}NO_3$ 334.1365; Found 334.1434, Elemental Analysis: calcd C 75.59, H 5.73, N 4.21; Found C 75.96, H 5.72, N 4.13.

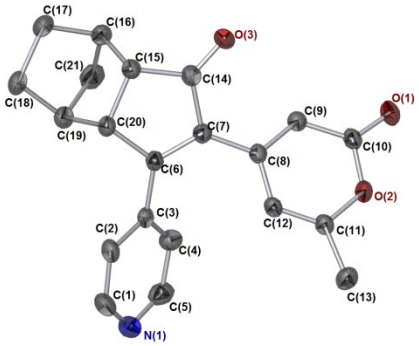

Lab book reference number: *NPY-4-241*

(*α*)-(*3aSR,4RS,7SR,7aRS*)-6-Methyl-4-(1-oxo-2-(4-pyridyl-3a,4,5,6,7,7a-hexahydro-1*H*-4,7-methanoinden-3-yl)-2*H*-pyran-2-one (*α*–122)

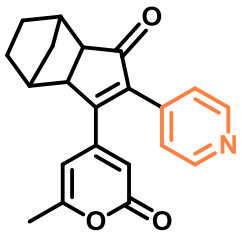

Synthesised following the general procedure G; with **115c** (200 mg, 0.95 mmol), to afford to afford the desired product as a creamy solid (313 mg, 99 % overall yield) (mixture of 50/50 regioisomers by ^{1}H NMR).

^{1}H NMR (400 MHz, $CDCl_3$) δ 8.66 – 8.75 (br. s, 2H, H-12/13), 7.16 (d, J_{HH} = 5.1 Hz, 1H, H-11/14), 5.70 (s, 1H, H-3), 5.58 (s, 1H, H-5), 3.00 (d, J_{HH} = 5.4 Hz, 1H, H-17), 2.64 – 2.58 (m, 1H, H-16), 2.54 – 2.48 (m, 1H, H-18), 2.16 (s, 3H, H-7), 2.07 (d, J_{HH} = 3.7 Hz, 1H, H-21), 1.77 – 1.60 (m, 2H, H-20), 1.39 (d, J_{HH} = 8.5 Hz, 2H, H-19/22), 1.09 (d, J_{HH} = 8.5 Hz, 2H, H-19/22). ^{13}C NMR (101 MHz, CD_2Cl_2) δ 206.05 (C-15), 170.81 (C-2), 162.45 (C-4), 151.04 (C-12/13), 147.57 (C-8), 141.99 (C-9), 22.47 (C-11/14), 112.87 (C-3), 111.72 (C-5), 54.38 (C-18), 51.47 (C-17),

40.21 (C-21), 38.57 (C-16), 31.88 (C-19), 29.15 (C-20), 28.78 (C-22), 20.20 (C-7). IR (solid-state ATR, cm^{-1}) 2953, 2872, 1698, 1636, 1590, 1542, 1406, 1307, 1196, 982, 836, 855, 539, 656. MS; HRMS (ESI^+) m/z: $[M + H]^+$ calcd for $C_{21}H_{20}NO_3$ 333.1365; Found 334.1434, Elemental Analysis: calcd C 75.59, H 5.73, N 4.21; Found C 75.96, H 5.72, N 4.13.

Lab book reference number: *NPY-4-241*

(9aRS,10SR,13RS,13aSR)-5-Pyridyl-2-methyl-4,9,9a,10,11,12,13,13a-octahydro-10,13-methanobenzo[h]indeno[1,2-f]isochromene-4,9-dione (*α*-122*B*)

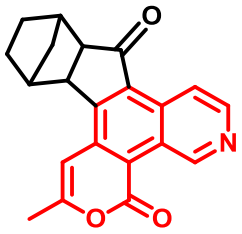

Synthesised following the general procedure H2; with irradiation of ***α*-124A** (15 mg), in CD_2Cl_2 (0.6 mL) at 400 nm, 20 mA for 40 min. to afford the product as a creamy solid (100 % conversion by NMR). MP 211–213 °C.

^{1}H NMR (700 MHz, CD_2Cl_2) δ 10.00 (dd, J_{HH} = 8.8, 1.6 Hz, 1H, H-14), 9.05 (dd, J_{HH} = 4.1, 1.6 Hz, 1H, H-12), 7.90 (d, J_{HH} = 0.9 Hz, 1H, H-5), 7.74 (dd, J_{HH} = 8.8, 4.1 Hz, 1H, H-13), 3.77 (d, J_{HH} = 5.8 Hz, 1H, H-16), 2.90 (d, J_{HH} = 3.8 Hz, 1H, H-15), 2.67 (d, J_{HH} = 5.8 Hz, 1H, H-17), 2.62 (d, J_{HH} = 3.8 Hz, 1H, H-20), 2.41 (d, J_{HH} = 0.6 Hz, 3H, H-7), 1.86 – 1.76 (m, 2H, H-19), 1.73 – 1.63 (m, 1H, H-20), 1.53 – 1.44 (m, 1H, H-20), 0.99 (d, J_{HH} = 10.7 Hz, 1H, H-22), 0.83 (d, J_{HH} = 10.7 Hz, 1H, H-22). ^{13}C NMR (101 MHz, CD_2Cl_2) δ 208.88 (C-15), 167.76 (C-9), 161.70 (C-2),

160.30 (C-6), 150.48 (C-12), 145.22 (C-8), 137.47 (C-10), 135.28 (C-14), 133.07 (C-4), 131.39 (C-11), 125.93 (C-13), 113.21 (C-3), 100.16 (C-5), 56.78 (C-18), 47.26 (C-17), 41.16 (C-21), 40.91 (C-16), 32.61 (C-22), 29.87 (C-19), 28.92 (C-20), 20.25 (C-7). IR (solid-state ATR, cm-^{1}) 2956, 2871, 1705, 1646, 1601, 1538, 1498, 1414, 1349, 1296, 1184, 948, 853, 565, 508. MS; HRMS (ESI^{+}) m/z: $[M + H]^{+}$ calcd for $C_{21}H_{18}NO_3$ 333.1320; Found 333.1297.

Lab book reference number: *NPY-4-241cyc.*

(9aRS,10SR,13RS,13aSR)-5-pyridyl-2-methyl-4,9,9a,10,11,12,13,13a-octahydro-10,13- methanobenzo[h]indeno[1,2-f]isochromene-4,9-dione (*β*-122*B*)

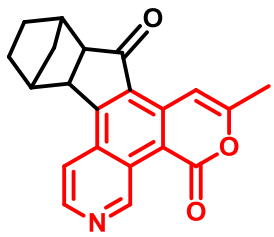

Synthesised following the general procedure H2; with irradiation of ***β*-124A** (ca.15 mg), in CD_2Cl_2 (0.6 mL) at 400 nm, 20 mA for 40 min. to afford the product as a creamy solid (100 % conversion by NMR). MP 211–213 °C.

^{1}H NMR (400 MHz, CD_2Cl_2) δ 10.93 (s, 1H, H-12), 8.84 (d, J_{HH} = 5.5 Hz, 1H, H-13), 8.03 (d, J_{HH} = 5.5 Hz, 1H, H-14), 7.89 (s, 1H, H-5), 3.57 (d, J_{HH} = 5.8 Hz, 1H, H-17), 2.72 (d, J_{HH} = 5.8 Hz, 3H, H-18), 2.65 (d, J_{HH} = 3.6 Hz, 1H, H-16), 2.58 (d, J_{HH} = 3.6 Hz, 1H, H-21), 2.42 (s, 3H, H-7), 1.89 – 1.71 (m, 2H, H-19), 1.68 – 1.45 (m, 2H, H-20), 1.03 (d, J_{HH} = 10.8 Hz, 1H, H-22), 0.83 (d, J_{HH} = 10.8 Hz, 1H, H-22). ^{13}C NMR (101 MHz, CD_2Cl_2) δ 208.46 (C-15), 168.68 (C-8), 167.14 (C-9),

160.68 (C-2), 159.65 (C-6), 158.66 (C-11), 150.57 (C-12), 146.61 (C-14), 139.69 (C-4), 138.85 (C-10), 131.20 (C-3), 116.75 (C-13), 100.82 (C-5), 56.925 (C-18), 47.15 (C-17), 40.88 (C-21), 40.29 (C-16), 32.40 (C-19), 29.72 (C-20), 28.63 (C-22), 20.25 (C-7). IR (solid-state ATR, cm^{-1}) 2956, 2871, 1705, 1646, 1601, 1538, 1498, 1414, 1349, 1296, 1184, 948, 853, 565, 508. MS; HRMS (ESI^+) m/z: $[M + H]^+$ calcd for $C_{21}H_{18}NO_3$ 333.1320; Found 333.1297.

Lab book reference number: *NPY-4-241cyc.*

[μ_2-6-methyl-4-(2-(4-pyridylethynyl))-2H-pyran-2-one]-hexacarbonyl dicobalt (122*I*)

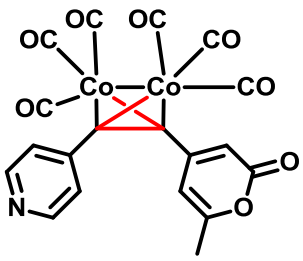

Following the general procedure F1; dicobaltoctacarbonyl (324 mg, 0.95 mmol) and the alkyne (200 mg, 0.95 mmol) to afford the complex as brownish crystals (350 mg, 70 % yield). M.P 87–88 ^oC.

^1H NMR (400 MHz, $CDCl_3$) δ 8.63 (s, 2H, H-12/13), 7.32 (s, 2H, H-11/14), 6.33 (s, 1H, H-3), 5.89 (s, 1H, H-5), 2.28 (s, 3H, H-7). MS; LRMS (LIFDI) m/z: $[M + H]^+$ calcd for $C_{19}H_{16}Co_2NO_8$ 503.95; Found 503.95.

Lab book reference number: *NPY-5-290*

(*β*)-(*3aSR,4RS,7SR,7aRS*)-6-Methyl-4-(1-oxo-3-(2-pyrazyl-3a,4,5,6,7,7a-hexahydro-1*H*-4,7-methanoinden-2-yl)-2*H*-pyran-2-one (*β*–123)

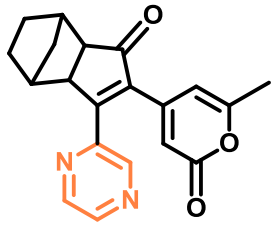

Synthesised following the general procedure G; with **116c** (200 mg, 0.94 mmol), to afford to afford the desired product as a creamy solid (250 mg, 79 % overall yield). MP 110–111 °C.

^{1}H NMR (400 MHz, CD_2Cl_2) δ 8.69 (dd, J_{HH} = 2.3, 1.6 Hz, 1H, H-12), 8.63 (d, J_{HH} = 1.6 Hz, 1H, H-11), 8.56 (d, J_{HH} = 2.3 Hz, 1H, H-13), 5.99 (d, J_{HH} = 0.6 Hz, 1H, H-3), 5.71 (s, 1H, H-5), 3.40 (d, J_{HH} = 5.5 Hz, 1H, H-16), 2.55 (d, J_{HH} = 3.6 Hz, 1H, H-15), 2.51 (d, J_{HH} = 5.5 Hz, 1H, H-17), 2.25 (d, J_{HH} = 3.6 Hz, 1H, H-20), 2.18 (s, 3H, H-7), 1.75 – 1.61 (m, 2H18), 1.49 – 1.37 (m, 2H, H-19), 1.14 (d, J_{HH} = 10.8 Hz, 1H, H-21), 1.06 (d, J_{HH} = 10.8 Hz, 1H, H-21). ^{13}C NMR (101 CD_2Cl_2) δ 206.64 (C-14), 194.12 (C-2), 168.15 (C-6), 162.86 (C-4), 162.49 (C-8), 148.42 (C-4), 145.58 (C-11/13), 145.22 (C-12), 141.85 (C-10), 112.63 (C-3), 104.62 (C-5), 54.66 (C-17), 50.42 (C-16), 40.36 (C-15), 39.14 (C-20), 31.95 (C-18), 29.39 (C-19), 28.78 (C-21), 20.28 (C-7). IR (solid-state ATR, cm-^{1}) 2954, 2873, 1698, 1716, 1639, 1612, 1540, 1446, 1394, 866, 1014, 1138, 1198, 1206, 1314, 1335. MS; HRMS (ESI^{+}) m/z: [M + H]$^{+}$ calcd for $C_{20}H_{19}N_2O_3$ 334.1317; Found 335.1374, Elemental Analysis: calcd C 71.84, H 5.43, N 8.38; Found C 70.11, H 5.12, N 8.39.

Lab book reference number: *NPY-4-219*

[μ_2-6-methyl-4-(2-(2-pyrazinethynyl))-2H-pyran-2-one]-hexacarbonyl dicobalt (123*I*)

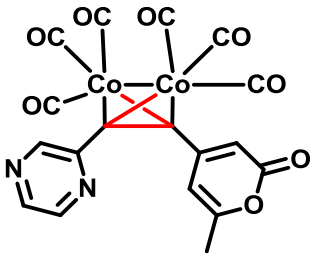

Following the general procedure F3; dicobaltoctacarbonyl (324 mg, 0.95 mmol) and the alkyne (200 mg, 0.95 mmol) to afford the complex as brownish crystals (430 mg, 91 % yield) M.P 86–88 ^{o}C.

^{1}H NMR (400 MHz, $CDCl_3$) δ 8.77 (d, J_{HH} = 1.3 Hz, 1H, H-12), 8.60 (dd, J_{HH} = 2.4, 1.5 Hz, 1H, H-11), 8.52 (d, J_{HH} = 2.4 Hz, 1H, H-10), 6.56 (s, 1H, H-3), 6.16 (s, 1H, H-5), 2.29 (s, 3H, H-7). MS; LRMS (LIFDI) m/z: $[M + H]^+$ calcd for $C_{18}H_{15}Co_2N_2O_8$ 504.94; Found 504.94.

Lab book reference number: *NPY-5-291*

(*β*)-(*3aSR*,4RS,7SR,7aRS)-6-Methyl-4-(1-oxo-3-(2-thienyl-3a,4,5,6,7,7a-hexahydro-1*H*-4,7-methanoinden-2-yl)-2*H*-pyran-2-one (*β*–124)

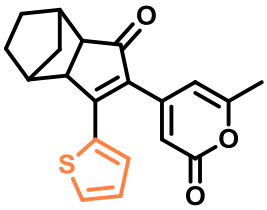

Synthesised following the general procedure G; with **117c** (100 mg, 0.46 mmol), to afford to afford the desired product as a creamy solid (85 mg, 54 % yield). MP 85 - 87 °C.

^{1}H NMR (400 MHz,) δ 7.41 (dd, J_{HH} = 5.1, 1.1 Hz, 1H, H-13), 7.34 (dd, J_{HH} = 3.7, 1.1 Hz, 1H, H-11), 7.03 (dd, J_{HH} = 5.1, 3.7 Hz, 1H, H-12), 6.18 (d, J_{HH} = 0.6 Hz, 1H, H-3), 5.86 (s, 1H, H-5), 2.91 (d, J_{HH} = 5.5 Hz, 1H, H-16), 2.53 (d, J_{HH} = 3.7 Hz, 1H, H-15), 2.45 (d, J_{HH} = 5.5 Hz, 1H, H-17), 2.23 (d, J_{HH} = 0.6 Hz, 3H, H-7), 1.73 – 1.58 (m, 3H, H-18/20), 1.41 – 1.30 (m, 2H, H-19), 1.09 (d, J_{HH} = 10.8 Hz, 1H, H-20), 1.05 (d, J_{HH} = 10.7 Hz, 2H, H-20). ^{13}C NMR (101 MHz,) δ 206.74 (C-14), 163.60 (C-2), 162.38 (C-6), 162.37 (C-4), 153.16 (C-8), 137.46 (C-9), 130.86 (C-10), 128.90 (C-13), 128.37 (C-12), 127.18 (C-11), 111.04 (C-3), 103.26 (C-5), 54.07 (C-16), 51.67 (C-15), 40.08 (C-14), 38.19 (C-19), 31.83 (C-17), 29.00 (C-18), 28.74 (C-20), 20.32 (C-7). IR (solid-state ATR, cm-^{1}) 3099, 2954, 2871, 1724, 1698, 1637, 1540, 1424, 1296, 1215, 980, 848, 706, 1137, 1046. MS; HRMS (ESI^{+}) m/z: [M + H]+ calcd for $C_{20}H_{18}O_3S$ 338.0977; Found 339.1062, Elemental Analysis: calcd C 70.98, H 5.36,; Found C 69.56, H 5.23.

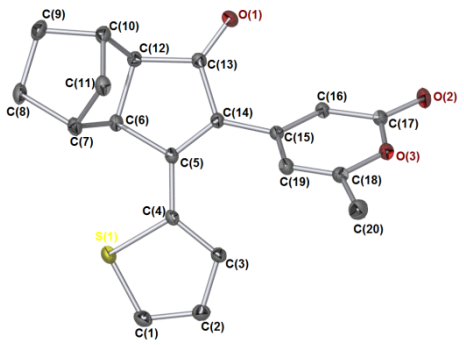

Lab book reference number: *NPY-5-300*

(*α*)-(*3aSR,4RS,7SR,7aRS*)-6-Methyl-4-(1-oxo-3-(2-thienyl-3a,4,5,6,7,7a-hexahydro-1*H*-4,7-methanoinden-2-yl)-2*H*-pyran-2-one (*α*–124)

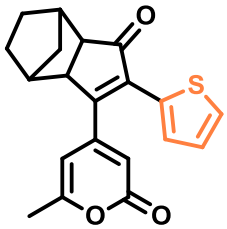

Synthesised following the general procedure G; with **117c** (100 mg, 0.46 mmol), to afford to afford the desired product as a creamy solid (19 mg, 12 % yield). MP 90–93 °C.

^{1}H NMR (400 MHz, CD_2Cl_2) δ 7.61 (dd, J_{HH} = 5.1, 1.1 Hz, 1H, H-13), 7.49 (dd, J_{HH} = 3.8, 1.1 Hz, 1H, H-11), 7.14 (dd, J_{HH} = 5.1, 3.8 Hz, 1H, H-12), 6.08 (d, J_{HH} = 0.6 Hz, 1H, H-5), 5.83 (s, J_{HH} = 1.1 Hz, 1H, H-3), 3.16 (d, J_{HH} = 5.6 Hz, 1H, H-15), 2.51 – 2.45 (m, 3H, H-14/16/19), 2.23 (s, 3H, H-7), 1.80 – 1.63 (m, 2H, H-17), 1.54 – 1.35 (m, 2H, H-18), 1.16 (d, J_{HH} = 7.1 Hz, 1H, H-20), 1.09 (d, J_{HH} = 10.7 Hz, 1H, H-20). ^{13}C NMR (101 MHz, CD_2Cl_2) δ 205.70 (C-14), 163.26 (C-2), 163.08 (C-6), 162.69 (C-4), 149.95 (C-8), 136.93 (C-9), 136.63 (C-10), 132.13 (C-13), 132.09 (C-11), 128.39 (C-12), 113.35 (C-3), 105.00 (C-5), 54.83 (C-17), 51.43 (C-16), 40.91 (C-15), 39.72 (C-19), 32.33 (C-17), 29.46 (C-18), 28.81 (C-20), 20.30 (C-20). IR (solid-state ATR, cm-^{1}) beta; 3083, 2962, 2870, 1735, 1690, 1538, 1419, 1295, 1197, 980, 861, 714. MS; HRMS (ESI^{+}) m/z: [M + H]$^{+}$ calcd for $C_{20}H_{19}O_3S$ 338.0977; Found 339.1070, Elemental Analysis: calcd C 70.98, H 5.36,; Found C 70.56, H 5.37.

Lab book reference number: *NPY-5-300*

(*9aRS*,*10SR*,*13RS*,*13aSR*)-6-thienyl-2-methyl-4,9,9a,10,11,12,13,13a-octahydro-10,13- methanobenzo[h]indeno[1,2-f]isochromene-4,9-dione (β-124*B*)

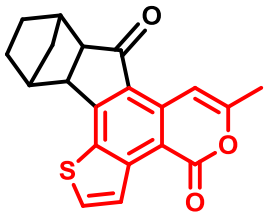

Synthesised following the general procedure H2; with irradiation of **β-124A** (15 mg), in CD_2Cl_2 (0.6 mL) at 400 nm, 20 mA for 40 min. to afford the product as a creamy solid (100 % conversion by NMR). MP 138–141 °C.

^{1}H NMR (400 MHz, CD_2Cl_2) δ 8.58 (d, J_{HH} = 5.5 Hz, 1H, H-13), 7.85 (d, J_{HH} = 5.5 Hz, 1H, H-12), 6.66 (s, 1H, H-5), 3.42 (d, J_{HH} = 5.8 Hz, 1H, H-16), 2.73 (d, J_{HH} = 5.8 Hz, 1H, H-15), 2.67 (d, J_{HH} = 3.7 Hz, 1H, H-17), 2.58 (d, J_{HH} = 3.9 Hz, 1H, H-20), 2.42 (d, J_{HH} = 1.0 Hz, 3H, H-7), 1.81 (ddd, J_{HH} = 15.4, 8.3, 4.1 Hz, 1H, H-18), 1.71 (ddd, J_{HH} = 11.7, 9.8, 3.9 Hz, 1H, H-18), 1.65 – 1.57 (m, 1H, H-19), 1.52 – 1.43 (m, 1H, H-19), 1.01 (d, J_{HH} = 10.8 Hz, 1H, H-21), 0.81 (d, J_{HH} = 10.8 Hz, 1H H-21). ^{13}C NMR (101 MHz, CD_2Cl_2) δ 207.40 (C-14), 156.57 (C-8), 150.25 (C-9), 139.60 (C-4), 139.44 (C-10), 137.76 (C-2), 136.70 (C-6), 134.93 (C-11), 131.60 (C-12), 124.57 (C-13), 117.85 (C-3), 100.59 (C-5), 56.86 (C-17), 47.88 (C-16), 40.71 (C-20), 40.46 (C-15), 32.60 (C-21), 29.42 (C-18), 28.78 (C-19), 20.13 (C-7). MS; HRMS (ESI$^+$) m/z: $[M + H]^+$ calcd for $C_{20}H_{17}O_3S$ 337.0854; Found 337.0823.

Lab book reference number: *NPY-5-300 Cyc.*

(*9aRS*,*10SR*,*13RS*,*13aSR*)-6-thienyl-2-methyl-4,9,9a,10,11,12,13,13a-octahydro-10,13- methanobenzo[h]indeno[1,2-f]isochromene-4,9-dione (*α*-124*B*)

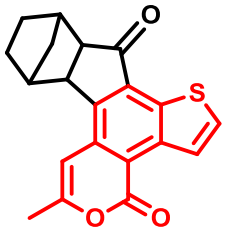

Synthesised following the general procedure H2; with irradiation of ***α*-124A** (15 mg), in CD_2Cl_2 (0.6 mL) at 400 nm, 20 mA for 40 min. to afford the product as a creamy solid (100 % conversion by NMR). MP 147–148 °C.

^{1}H NMR (400 MHz, $CDCl_3$) δ 8.64 (d, J_{HH} = 5.5 Hz, 1H, H-13), 7.84 (d, J_{HH} = 5.5 Hz, 1H, H-12), 6.63 (s, 1H, H-5), 3.41 (d, J_{HH} = 5.7 Hz, 1H, H-15), 2.78 – 2.72 (m, 2H, H-14/16), 2.59 (d, J_{HH} = 3.9 Hz, 1H, H-19), 2.44 (s, 3H, H-7), 1.83 (tt, J_{HH} = 11.3, 4.1 Hz, 1H, H-17), 1.77 – 1.67 (m, 1H, H-17), 1.65 – 1.59 (m, 1H, H-18), 1.53 – 1.44 (m, 1H, H-18), 1.03 (d, J_{HH} = 10.9 Hz, 1H, H-20), 0.85 (d, J_{HH} = 10.9 Hz, 1H, H-20). ^{13}C NMR (101 MHz,) δ 207.04 (C-14), 156.21 (C-8), 149.82 (C-9), 139.05 (C-2), 137.40 (C-6), 136.30 (C-10), 134.56 (C-4), 132.26 (C-11), 131.24 (C-12), 124.21 (C-13), 117.48 (C-3), 100.23 (C-5), 56.51 (C-17), 47.52 (C-16), 40.34 (C-15), 40.10 (C-20), 32.23 (C-21), 29.10 (C-18), 28.41 (C-19), 19.77 (C-7). HRMS (ESI^+) m/z: $[M + H]^+$ calcd for $C_{20}H_{17}O_3S$ 337.0854; Found 337.0842.

Lab book reference number: *NPY-5-300 Cyc.*

(*β*)-(*3aSR,4RS,7SR,7aRS*)-2-thienyl-3-(2-pyridyne-4-yl)-3a,4,5,6,7,7a-hexahydro-1*H*-4,7-methanoinden-one (*β*–125)

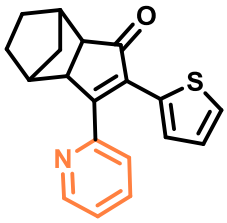

Synthesised following the general procedure G; with **119** (30 mg, 0.16 mmol), to afford to afford the desired product as a creamy solid (29 mg, 58 % yield). MP 115–117 °C.

^{1}H NMR (400 MHz, CD_2Cl_2) δ 8.75 (ddd, J_{HH} = 4.8, 1.6, 1.1 Hz, 1H, H-1), 7.67 (td, J_{HH} = 7.8, 2.3 Hz, 1H, H-3), 7.35 (dt, J_{HH} = 7.8, 1.1 Hz, 1H, H-2), 7.32 (td, J_{HH} = 2.3, 1.1 Hz, 1H, H-4), 7.30 (dd, J_{HH} = 5.1, 1.0 Hz, 1H, H-11), 7.14 (dd, J_{HH} = 3.7, 1.0 Hz, 1H, H-9), 6.96 (dd, J_{HH} = 5.1, 3.7 Hz, 1H, H-10), 3.28 (d, J_{HH} = 5.5 Hz, 1H, H-14), 2.54 (d, J_{HH} = 3.2 Hz, 1H, H-13), 2.47 (d, $J_{H}H$ = 5.5 Hz, 1H, H-15), 2.17 (d, J_{HH} = 3.2 Hz, 1H, H-18), 1.67 – 1.60 (m, 2H, H-16), 1.42 – 1.34 (m, 2H, H-17), 1.21 (d, J_{HH} = 10.6 Hz, 1H, H-19), 1.02 (d, J_{HH} = 10.6 Hz, 1H, H-19). ^{13}C NMR (101 MHz, CD_2Cl_2) δ 208.12 (C-12), 168.17 (C-6), 155.34 (C-7), 150.57 (C-1), 136.76 (C-5), 136.54 (C-3), 132.24 (C-8), 128.08 (C-9), 127.23 (C-4), 126.97 (C-10), 124.38 (C-2), 123.99 (C-11), 54.20 (C-15), 51.57 (C-14), 40.21 (C-13), 38.56 (C-18), 31.89 (C-16), 29.22 (C-17), 28.95 (C-19). IR (solid-state ATR, cm-^{1}) 3085, 2959, 2870, 1736, 1692, 1640, 1538, 1420, 1296, 1211, 980, 861, 713. MS; HRMS (ESI^{+}) m/z: $[M + H]^{+}$ calcd for $C_{19}H_{18}NOS$ 307.1031; Found 308.1103, Elemental Analysis: calcd C 74.23, H 5.57, N 4.56; Found C 74.33, H 5.58, N 4.55.

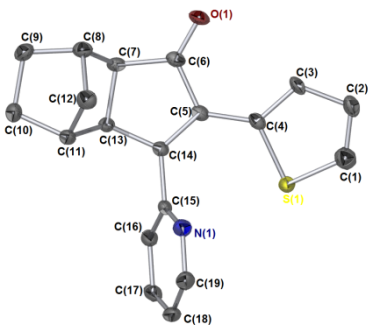

Lab book reference number: *NPY-5-301*

(*α*)-(*3aSR,4RS,7SR,7aRS*)-2-Thienyl-3-(2-pyridyne-4-yl)-3a,4,5,6,7,7a-hexahydro-1*H*-4,7-methanoinden-one(*α*–125)

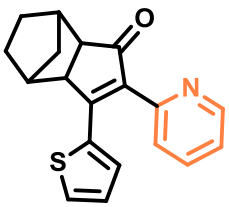

Synthesised following the general procedure G; with **119** (30 mg, 0.16 mmol), to afford to afford the desired product as a creamy solid (15 mg, 30 % yield). MP 123–126 °C.

^{1}H NMR (400 MHz, CD_2Cl_2) δ 8.69 (ddd, J_{HH} = 4.9, 1.8, 1.2 Hz, 1H, H-1), 7.79 (td, J_{HH} = 7.7, 1.8 Hz, 1H, H-3), 7.43 (ddd, J_{HH} = 4.9, 4.4, 1.1 Hz, 2H, H-9/11), 7.34 – 7.31 (m, 1H, H-2, H-2/4), 7.30 (dt, J_{HH} = 8.0, 0.9 Hz, 1H, H-10), 3.23 (d, J_{HH} = 5.5 Hz, 1H, H-14), 2.54 (d, J_{HH} = 3.2 Hz, 1H, H-13), 2.51 (d, J_{HH} = 5.5 Hz, 1H, H-15), 2.50 (d, J_{HH} = 3.2 Hz, 1H, H-18), 1.82 – 1.64 (m, 2H, H-16), 1.57 – 1.40 (m, 2H, H-17), 1.31 (d, J_{HH} = 10.7 Hz, 1H, H-19), 1.11 (d, J_{HH} = 10.7 Hz, 1H, H-19). ^{13}C NMR (101 MHz, CD_2Cl_2) δ 207.60 (C-12), 162.89 (C-6), 152.98 (C-7), 150.39 (C-1),

140.46 (C-5), 137.91 (C-8), 136.89 (C-3), 131.48 (C-9/11), 131.42 (C-10), 127.67 (C-11), 125.61 (C-2), 123.53 (C-4), 54.77 (C-15), 51.12 (C-14), 40.96 (C-13), 39.62 (C-18), 32.47 (C-16), 29.60 (C-17), 28.97 (C-19). MS; HRMS (ESI^+) m/z: $[M + H]^+$ calcd for $C_{19}H_{18}NOS$ 307.1031; Found 308.1107.

Lab book reference number: *NPY-5-301*

(*β*)-(*9aRS,10SR,13RS,13aSR*)-2-Thienyl-3-(2-pyridyne-4-yl)-4,9,9a,10,11,12,13,13aoctahydro-10,13--methanoinden-one (*β*-125*B*)

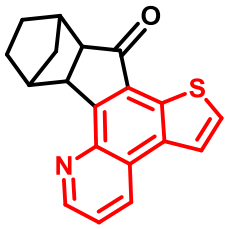

Synthesised following the general procedure H2; with irradiation of ***β*-125A** (15 mg), in CD_2Cl_2 (0.6 mL) at 400 nm, 20 mA for 40 min. to afford the product as a creamy solid (100 % conversion by NMR after 2 h irradiation). MP 122–123 °C.

^{1}H NMR (400 MHz, CD_2Cl_2) δ 9.03 (dd, J_{HH} = 4.3, 1.7 Hz, 1H, H-1), 8.66 (dd, J_{HH} = 8.4, 1.7 Hz, 1H, H-3), 7.96 (d, J_{HH} = 5.4 Hz, 1H, H-11), 7.76 (d, J_{HH} = 5.4 Hz, 1H, H-10), 7.64 (dd, J_{HH} = 8.4, 4.3 Hz, 1H, H-2), 3.76 (d, J_{HH} = 5.5 Hz, 1H, H-14), 2.89 (d, J_{HH} = 3.9 Hz, 1H, H-13), 2.67 (d, J_{HH} = 5.5 Hz, 1H, H-15), 2.62 (d, J_{HH} = 3.9 Hz, 1H, H-18), 1.84 – 1.67 (m, 2H, H-16), 1.67 – 1.61 (m, 1H, H-17), 1.51 – 1.45 (m, 1H, H-17), 0.95 (d, J_{HH} = 10.6 Hz, 1H, H-19), 0.81 (d, J_{HH} = 10.6 Hz, 1H, H-19). ^{13}C NMR (101 MHz, CD_2Cl_2) δ 207.79 (C-12), 156.46 (C-5), 149.73 (C-1), 144.93 (C-6), 137.23 (C-8), 135.13 (C-7), 132.69 (C-3), 130.07 (C-9), 129.01 (C-12), 128.53

(C-4), 123.87 (C-2), 121.27 (C-11), 56.43 (C-15), 48.34 (C-14), 40.51 (C-13), 40.36 (C-18), 32.50 (C-16), 29.65 (C-17), 29.08 (C-19). MS; HRMS (ESI^+) m/z: $[M + H]^+$ calcd for $C_{19}H_{16}NOS$ 306.0908; Found 306.0875. Elemental Analysis: calcd C, 74.72; H, 4.95; N, 4.59; Found C, 75.23; H, 5.37; N, 4.57.

Lab book reference number: *NPY-5-PKR3cyc.*

(*β*)-(*3aSR,4RS,7SR,7aRS*)-2-Thienyl-3-(4-pyridyne-4-yl)-3a,4,5,6,7,7a-hexahydro-1*H*-4,7-methanoinden-one (*β*–126)

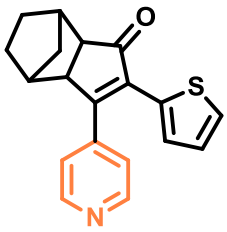

Synthesised following the general procedure G; with **118** (100 mg, 0.54 mmol), to afford to afford the desired product as a creamy solid (110 mg, 67 % yield). MP 131–135 °C.

^{1}H NMR (400 MHz, CD_2Cl_2) δ 8.66 (dd, J_{HH} = 4.4, 1.7 Hz, 2H, H-1/5), 7.31 (dd, J_{HH} = 5.1, 1.1 Hz, 1H, H-11), 7.26 (dd, J_{HH} = 4.4, 1.7 Hz, 2H, H-2/4), 7.15 (dd, J_{HH} = 3.7, 1.0 Hz, 1H, H-9), 6.93 (dd, J_{HH} = 5.1, 3.7 Hz, 1H, H-10), 3.00 (d, J_{HH} = 5.5 Hz, 1H, H-14), 2.55 (d, J_{HH} = 3.7 Hz, 1H, H-13), 2.48 (d, J_{HH} = 5.5 Hz, 1H, H-15), 2.09 (d, J_{HH} = 3.7 Hz, 1H, H-18), 1.70 – 1.59 (m, 2H, H-16), 1.45 – 1.29 (m, 2H, H-17), 1.20 (d, J_{HH} = 10.6 Hz, 1H, H-19), 1.05 (d, J_{HH} = 10.6 Hz, 1H, H-19). ^{13}C NMR (101 MHz,) δ 207.19 (C-12), 165.75 (C-6), 150.84 (C-1/5), 144.94 (C-7), 137.05 (C-8), 131.74 (C-5), 128.16 (C-11), 127.51 (C-9), 126.98 (C-10), 122.41 (C-2/4), 54.27 (C-

15), 52.49 (C-14), 40.14 (C-13), 38.15 (C-18), 31.84 (C-16), 29.09 (C-17), 28.88 (C-19). MS; HRMS (ESI$^+$) m/z: [M + H]$^+$ calcd for $C_{19}H_{18}NOS$ 307.1031; Found 308.1114,

Lab book reference number: *NPY-4-230*

(*α*)-(*3aSR,4RS,7SR,7aRS*)-2-Thienyl-3-(4-pyridyne-4-yl)-3a,4,5,6,7,7a-hexahydro-1*H*-4,7-methanoinden-one (*α*–126)

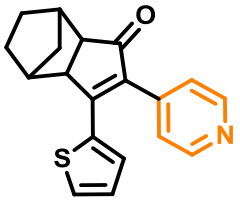

Synthesised following the general procedure G; with **118** (100 mg, 0.54 mmol), to afford to afford the desired product as a creamy solid (17 mg, 10 % yield). MP 115–117 °C.

^{1}H NMR (400 MHz, CD_2Cl_2) δ 8.66 (dd, J_{HH} = 4.4, 1.7 Hz, 2H, H-1/5), 7.31 (dd, J_{HH} = 5.1, 1.1 Hz, 1H, H-11), 7.26 (dd, J_{HH} = 4.4, 1.7 Hz, 2H, H-2/4), 7.15 (dd, J_{HH} = 3.7, 1.0 Hz, 1H, H-9), 6.93 (dd, J_{HH} = 5.1, 3.7 Hz, 1H, H-10), 3.00 (d, J_{HH} = 5.5 Hz, 1H, H-14), 2.55 (d, J_{HH} = 3.7 Hz, 1H, H-13), 2.48 (d, J_{HH} = 5.5 Hz, 1H, H-15), 2.09 (d, J_{HH} = 3.7 Hz, 1H, H-18), 1.70 – 1.59 (m, 2H, H-16), 1.45 – 1.29 (m, 2H, H-17), 1.20 (d, J_{HH} = 10.6 Hz, 1H, H-19), 1.05 (d, J_{HH} = 10.6 Hz, 1H, H-19). ^{13}C NMR (101 MHz,) δ 207.19 (C-12), 165.75 (C-6), 150.84 (C-1/5), 144.94 (C-7), 137.05 (C-8), 131.74 (C-5), 128.16 (C-11), 127.51 (C-9), 126.98 (C-10), 122.41 (C-2/4), 54.27 (C-15), 52.49 (C-14), 40.14 (C-13), 38.15 (C-18), 31.84 (C-16), 29.09 (C-17), 28.88 (C-

19). MS; HRMS (ESI$^+$) m/z: $[M + H]^+$ calcd for $C_{19}H_{18}NOS$ 308.1031; Found 308.1081.

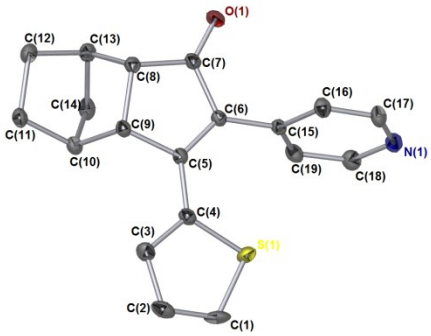

Lab book reference number: *NPY-4-230*

μ_2-1-(2'-thienyl)-2-(4'-Pyridyl)-ethynylhexacarbonyl dicobalt(0) (126*I*)

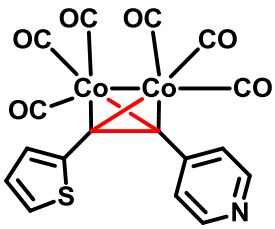

Following the general procedure F3; dicobaltoctacarbonyl (369 mg, 1. 08 mmol) and the alkyne (200 mg, 1.08 mmol) to afford the complex as brownish solid crystals (350 mg, 68 % yield). MP 67–70 ^oC.

^1H NMR (400 MHz, $CDCl_3$) δ 8.63 (s, 2H, H-1/5), 7.51 (s, 2H, H-2/4), 7.41 (d, J_{HH} = 5.1 Hz, 1H, H-11), 7.33 (s, 1H, H-10), 7.05 (s, 1H, H-9). MS; LRMS (LIFDI) m/z: $[M + H]^+$ calcd for $C_{17}H_{13}Co_2NO_6S$ 477.91; Found 477.92.

Lab book reference number: *NPY-5-292*

(*β*)-(*3aSR,4RS,7SR,7aRS*)-4-pyridyl-3-(2-pyridyne-4-yl)-3a,4,5,6,7,7a-hexahydro-1*H*-4,7-methanoinden-one (*β*–127)

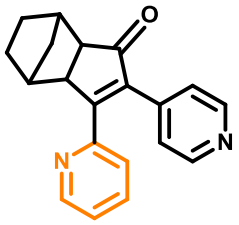

Synthesised following the general procedure G; with **120** (100 mg, 0.56 mmol), to afford to afford the desired product as a creamy solid (130 mg, 77 % yield). MP 210– 214 °C.

^{1}H NMR (400 MHz, CD_2Cl_2) δ 8.68 (ddd, J_{HH} = 4.8, 1.8, 1.0 Hz, 1H, H-1), 8.52 (dd, J_{HH} = 4.4, 1.6 Hz, 2H, H-10/11), 7.55 (td, J_{HH} = 7.8, 1.8 Hz, 1H, H-3), 7.26 (ddd, J_{HH} = 7.6, 4.8, 1.2 Hz, 1H, H-2), 7.13 – 7.07 (m, 3H, H-4/9/12), 3.47 (d, J_{HH} = 5.5 Hz, 1H, H-15), 2.55 (d, J_{HH} = 3.5 Hz, 1H, H-14), 2.50 (d, J_{HH} = 5.5 Hz, 1H, H-16), 2.22 (d, J_{HH} = 3.5 Hz, 1H, H-19), 1.74 – 1.59 (m, 2H, H-17), 1.50 – 1.37 (m, 2H, H-18), 1.23 (d, J_{HH} = 102 Hz, 1H, H-20), 1.05 (d, J_{HH} = 10.2 Hz, 1H, H-20). ^{13}C NMR (101 MHz, CD_2Cl_2) δ 208.19 (C-13), 171.35 (C-6), 153.75 (C-7), 150.48 (C-1), 150.17 (C-10/11), 141.98 (C-5), 140.68 (C-8), 136.42 (C-3), 125.07 (C-2), 124.41 (C-4/9/12), 54.54 (C-16), 50.82 (C-15), 40.30 (C-14), 38.93 (C-17), 31.90 (C-19), 29.42 (C-18), 28.97 (C-20). IR (solid-state ATR, cm-^{1}) 2956, 2866, 1696, 1626, 1588, 1455, 1351, 1168, 1195, 990, 737, 555, 524, 408. MS; HRMS (ESI^{+}) m/z: $[M + H]^{+}$ calcd for $C_{20}H_{19}N_2O$ 302.1419; Found 303.1492.

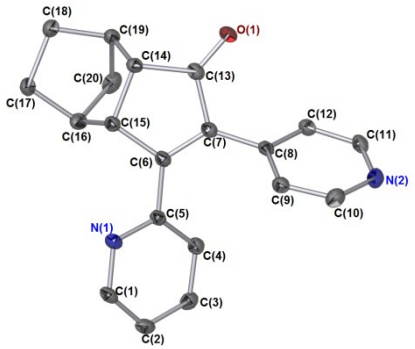

Lab book reference number: *NPY-5-299*

(*β*)-(*3aSR*,4RS,7SR,7aRS)-6-Methyl-4-(1-oxo-3-(2-pyridyl-3a,4,5,6,7,7a-tetrahydro-1*H*-4,7-methanoinden-2-yl)-2*H*-pyran-2-one (*β*–128)

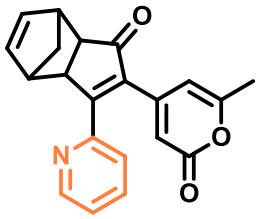

Synthesised following the general procedure G; with **114c** (55 mg, 0.26 mmol), norbornadiene (120 mg, 1.30 mmol) to afford to afford the desired product as a creamy solid (52 mg, 60 % yield). MP 85–88 °C.

^{1}H NMR (400 MHz, CD_2Cl_2) δ 8.72 (dd, J_{HH} = 5.8, 0.9 Hz, 1H, H-14), 7.71 (td, J_{HH}= 7.7, 1.9 Hz, 1H, H-12), 7.39 (d, J_{HH} = 7.7 Hz, 1H, H-11), 7.34 (dd, J_{HH} = 7.7, 5.8 Hz, 1H, H-123), 6.37 (dd, J_{HH} = 5.6, 3.0 Hz, 1H, H-19), 6.30 (dd, J_{HH} = 5.6, 3.0 Hz, 1H, H-20), 6.02 (s, 1H, H-3), 5.70 (s, 1H, H-5), 3.55 (d, J_{HH} = 5.4 Hz, 1H, H-17), 3.05 (d, J_{HH} = 0.9 Hz, 1H, H-16), 2.80 – 2.74 (m, 1H, H-21), 2.60 (dd, J_{HH} = 5.4, 1.5 Hz, 1H, H-18), 2.15 (s, 3H, H-7), 1.44 (dt, J_{HH} = 9.5, 1.5 Hz, 1H, H-22), 1.37 (d, J_{HH} = 9.5 Hz, 1H, H-22). ^{13}C NMR (101 MHz, CD_2Cl_2) δ 205.58, 171.98, 162.75,

162.28, 152.80, 150.58, 148.62, 141.15, 139.16, 137.82, 136.73, 125.15, 124.95, 112.50, 104.88, 53.53, 50.45, 44.94, 44.12, 42.00, 20.19. MS; HRMS (ESI^+) m/z: $[M + H]^+$ calcd for $C_{21}H_{18}NO_3$ 332.1208; Found 332.1287, Elemental Analysis: calcd C 76.12, H 5.17, N 4.23; Found C 74.98, H 5.18, N 4.23.

Lab book reference number: *NPY-5-370 Diene 1F3*

(*α*)-(*3aSR*,4RS,7SR,7aRS)-6-Methyl-4-(1-oxo-3-(2-pyridyl-3a,4,5,6,7,7a-hexahydro-1*H*-4,7-methanoinden-2-yl)-2*H*-pyran-2-one (*α*–128)

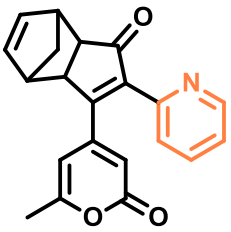

Synthesised following the general procedure G; with **114c** (55 mg, 0.26 mmol), norbornadiene (120 mg, 1.30 mmol) to afford to afford the desired product as a creamy solid (21 mg, 24 % yield). MP 87–88 °C.

.^{1}H NMR (400 MHz,) δ 8.59 (ddd, J_{HH} = 4.8, 1.8, 0.9 Hz, 1H, H-14), 7.77 (td, J_{HH} = 7.8, 1.8 Hz, 1H, H-12), 7.61 – 7.55 (m, 2H, H-11/13), 6.37 – 6.32 (m, 2H, H-19/20), 6.16 (s, 1H, H-3), 5.68 (s, 1H, H-5), 3.67 (d, J_{HH} = 5.5 Hz, 1H, H-18), 3.18 (d, J_{HH} = 6.3 Hz, 2H, H-21), 2.89 (s, 1H, H-17), 2.56 (s, 1H, H-16), 2.18 (s, 3H, H-7), 1.55 (d, J_{HH} = 9.5 Hz, 1H, H-22), 1.43 (d, J_{HH} = 9.5 Hz, 2H, H-22). MS; HRMS (ESI^+) m/z: $[M + H]^+$ calcd for $C_{21}H_{18}NO_3$ 332.1208; Found 332.1285.

Lab book reference number: *NPY-5-370 Diene 1F5*

(*Z*)-4-(2'-Pyridylethenyl)-6-methyl-2-pyrone (*Z*-130a)

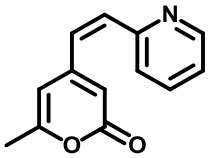

Synthesised following the general procedure G; with **114c** (55 mg, 0.26 mmol), to afford to afford the desired product as a creamy solid (6 mg, 11 % yield).

^{1}H NMR (400 MHz, $CDCl_3$) δ 8.58 (ddd, J_{HH} = 4.9, 1.8, 0.9 Hz, 1H, H-14), 7.62 (td, J_{HH} = 7.7, 1.8 Hz, 1H, H-12), 7.27 – 7.23 (m, 1H, H-13), 7.19 (ddd, J_{HH} = 7.6, 4.9, 0.9 Hz, 1H, H-11), 6.86 (d, J_{HH} = 12.5 Hz, 1H, H-19), 6.42 (dd, J_{HH} = 12.5, 1.1 Hz, 1H, H-8), 6.06 (s, 1H, H-3), 5.78 – 5.75 (m, 1H, H-5), 2.12 (s, 3H, H-7). ^{13}C NMR (101 MHz, $CDCl_3$) δ 163.41 (C-2), 161.11 (C-6), 154.40 (C-10), 152.55 (C-4), 149.77 (C-14), 136.41 (C-9), 135.80 (C-8), 128.75 (C-13), 124.59 (C-12), 123.02 (C-11), 111.64 (C-3), 104.77 (C-5), 20.02 (C-7). MS; HRMS (ESI$^+$) m/z: $[M + H]^+$ calcd for $C_{13}H_{12}NO_2$ 214.0823; Found 214.0860.

Lab book reference number: *NPY-4-243F3*

(*E*)-4-(4'-pyridylethenyl)-6-methyl-2-pyrone (*E*-130b)

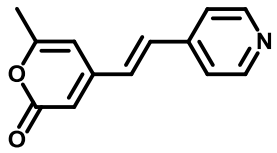

Synthesised following the general procedure G; with 6-methyl-4-(2'-pyridylethynyl)-2-pyrone) (55 mg, 0.26 mmol), to afford the desired product as a creamy solid (7 mg, 13 % yield). MP 82–85 °C.

^{1}H NMR (400 MHz, CD_2Cl_2) δ 8.54 (d, *J* = 5.1 Hz, 2H), 7.16 (dd, *J* = 4.8, 1.6 Hz, 2H), 6.77 (d, *J* = 12.4 Hz, 1H), 6.48 – 6.43 (m, 1H), 5.97 (s, 1H), 5.69 (s, 1H), 2.11 (s, 3H). MS; HRMS (ESI$^+$) m/z: [M + H]$^+$ calcd for $C_{12}H_{12}NO_2$ 214.0790; Found 214.0870. IR (solid-state ATR, cm-^{1}) 3042, 2919, 2956, 2995, 1698, 1620, 1540, 1456, 1328, 1140, 983, 983, 842, 776, 741, 651.

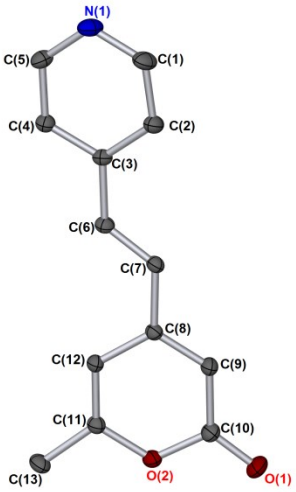

Lab book reference number: *NPY-4*

(*Z*)-4-(2'-Thienylethenyl)-6-methyl-2-pyrone (*E*-130c)

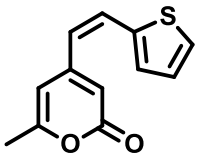

Synthesised following the general procedure G; with (6-methyl-4-(2-pyridilethynyl)-2-thiophene) (100 mg, 0.46 mmol), to afford to afford the desired product as a brownish solid (21 mg, 21 % yield). MP 57–59 °C.

^{1}H NMR (400 MHz, $CDCl_3$) δ 7.34 (d, J_{HH} = 5.1 Hz, 1H, H-13), 7.31 (d, J_{HH} = 16.0 Hz, 1H, H-9), 7.19 (d, J_{HH} = 3.5 Hz, 1H, H-14, H-11), 7.05 (dd, J_{HH} = 5.1, 3.6 Hz, 1H, H-12), 6.59 (d, J_{HH} = 16.0 Hz, 1H, H-8), 6.19 (s, 1H, H-3), 6.04 (s, 1H, H-2), 2.26 (s, 3H, H-7). ^{13}C NMR (101 MHz, $CDCl_3$) δ 163.98 (C-2), 161.78 (C-6), 151.84 (C-4), 141.24 (C-10), 129.87 (C-11), 129.78 (C-9), 128.54 (C-12), 128.00 (C-13), 123.99 (C-8), 109.33 (C-5), 100.84 (C-3), 20.53 (C-7). IR (solid-state ATR, cm-^{1}) 3083, 2960, 1699, 1612, 1546, 1406, 1330, 987, 945, 823, 854, 715, 659, 533. MS; HRMS (ESI^{+}) m/z: $[M + H]^{+}$ calcd for $C_{12}H_{11}O_2S$ 219.0402; Found 219.0473.

Lab book reference number: *NPY-4-240F1F2F2*

4-(2'-Pyridylethyl)-6-methyl-2-pyrone (131a)

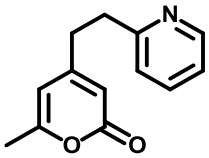

Synthesised following the general procedure G; with **114c** (55 mg, 0.26 mmol), to afford the product as a colourless liquid (9 mg, 16 % yield).

^{1}H NMR (400 MHz, $CDCl_3$) δ 8.53 (d, J_{HH} = 4.4 Hz, 1H, H-14), 7.59 (td, J_{HH} = 7.6, 1.8 Hz, 1H, H-12), 7.13 (dd, J_{HH} = 7.0, 4.7 Hz, 1H, H-13), 7.11 (d, J_{HH} = 7.5 Hz, 1H, H-11), 5.91 (s, 1H, H-3), 5.88 (s, 1H, H-5), 3.02 (dd, J_{HH} = 8.8, 6.7 Hz, 1H, H-9), 2.83 (dd, J_{HH} = 9.1, 6.4 Hz, 1H, H-8), 2.20 (s, 3H, H-7). ^{13}C NMR (101 MHz, $CDCl_3$) δ 163.40 (C-2), 161.63 (C-6), 159.54 (C-10), 159.41 (C-14), 149.61 (C-4), 136.71 (C-13), 123.12 (C-12), 121.78 (C-11), 110.04 (C-3), 105.63 (C-5), 36.54 (C-9), 34.81 (C-8), 20.00 (C-7). MS; HRMS (ESI$^+$) m/z: [M + H]+ calcd for $C_{13}H_{13}NO_2$ 216.0946; Found 216.1011. MS; HRMS (ESI$^+$) m/z: [M + H]$^+$ calcd for $C_{13}H_{14}NO_2$ 216.0980; Found 216.0947.

Lab book reference number: *NPY-4-243F4*

Appendices

9.1 Appendix 1: X -Ray Diffraction Data

Crystallographic data for complexes **70**, **74a** and **74b**.

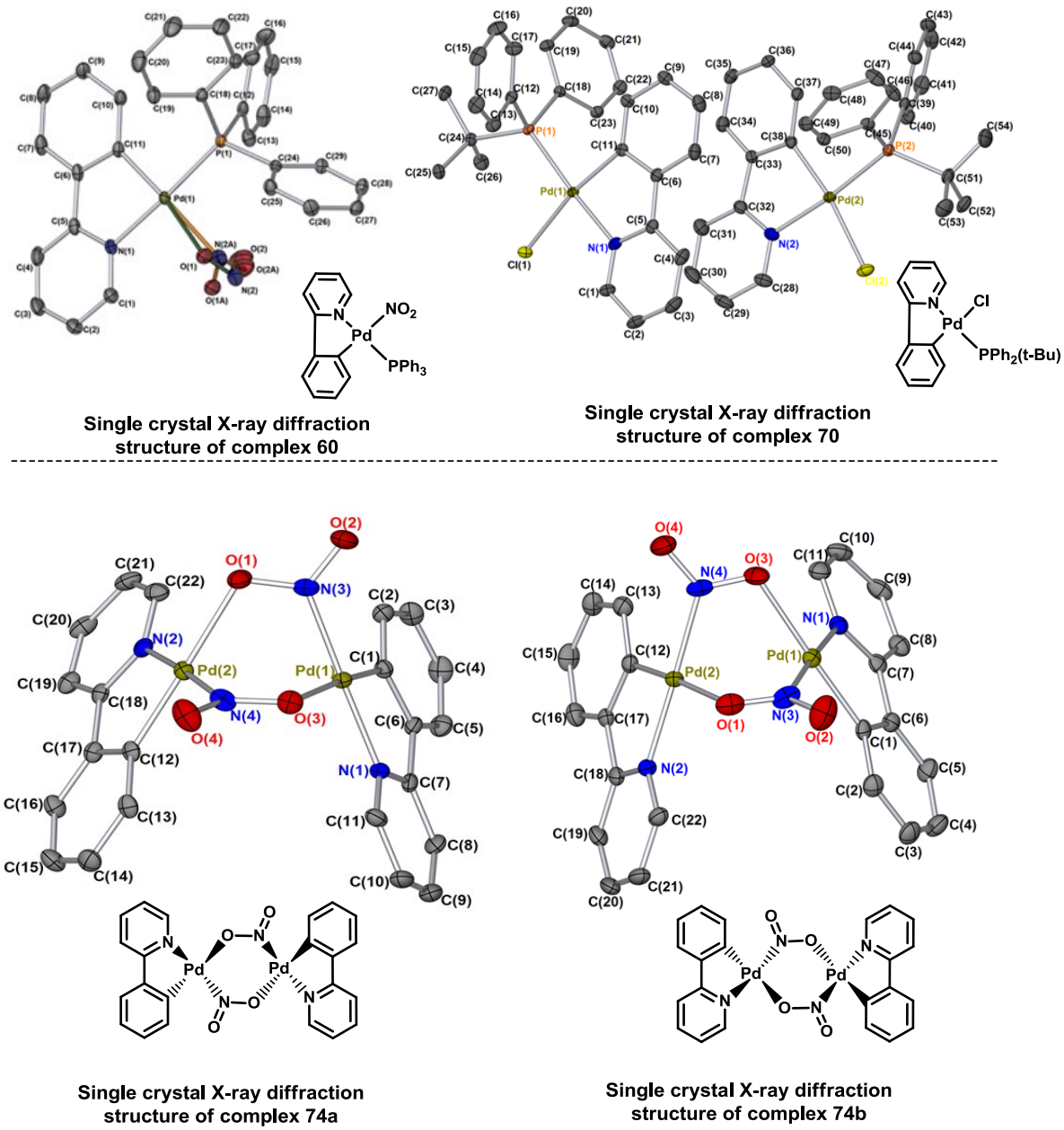

Single crystal X-ray diffraction structure of complex 60

Single crystal X-ray diffraction structure of complex 70

Single crystal X-ray diffraction structure of complex 74a

Single crystal X-ray diffraction structure of complex 74b

Figure 50 Single crystal X-ray diffraction structure of complexes **60**, **70**, **74a** and **74b**. Hydrogen atoms removed for clarity. Thermal ellipsoids shown with probability of 50%.

Table 12 Summary of X-ray data for complexes **60**, **70**, **74a** and **74b**

Identification code	**60** (ijsf1213)	**70** (ijsf1225)	**74a** (ijsf1219)	**74b** (ijsf1226)
Empirical formula	$C_{29.5}H_{24}ClN_2O_2PPd$	$C_{22}H_{16}N_4O_4Pd_2$	$C_{27}H_{27}ClNPPd$	$C_{22}H_{16}N_4O_4Pd_2$
Formula weight	611.33	613.19	538.32	613.19
Temperature/K	110	110.00(10)	110	110.00(10)
Crystal system	monoclinic	triclinic	triclinic	triclinic
Space group	$P2_{1/c}$	P-1	P-1	P-1
a/Å	16.9489(8)	8.9266(7)	10.5100(6)	8.9039(5)
b/Å	9.3636(3)	11.2223(8)	14.8251(5)	11.2328(8)
c/Å	17.3554(6)	12.2242(5)	16.6444(6)	12.2055(8)
α/°	90.00	68.542(5)	80.535(3)	68.568(6)
β/°	109.856(4)	69.674(5)	72.777(4)	69.609(6)
γ/°	90.00	67.921(7)	70.959(4)	67.907(6)
Volume/Å^3	2590.61(18)	1024.38(13)	2334.94(18)	1020.91(13)
Z	4	2	4	2
ρ_{calc}mg/mm^3	1.567	1.988	1.531	1.995
m/mm^{-1}	0.912	1.795	0.993	1.801
F(000)	1236.0	600.0	1096.0	600.0
Crystal size/mm^3	0.2526 × 0.2205 × 0.0868	0.1637 × 0.1002 × 0.0466	0.2162 × 0.1351 × 0.0728	0.1454 × 0.1019 × 0.0675
2Θ range for data collection	5.8 to 64.26°	6.2 to 60.06°	5.72 to 60.16°	6.2 to 60.06°
Index ranges	$-20 \leq h \leq 23$, $-11 \leq k \leq 13$, $-21 \leq l \leq 24$	$-12 \leq h \leq 11$, $-15 \leq k \leq 15$, $-17 \leq l \leq 17$	$-10 \leq h \leq 14$, $-19 \leq k \leq 20$, $-23 \leq l \leq 20$	$-7 \leq h \leq 12$, $-13 \leq k \leq 15$, $-17 \leq l \leq 17$
Reflections collected	15564	11052	20406	10464
Independent reflections	8183[R(int) = 0.0224]	5986[R(int) = 0.0261]	13090[R(int) = 0.0231]	5917[R(int) = 0.0233]
Data/restraints/parameters	8183/3/363	5986/0/289	13090/0/565	5917/0/289
Goodness-of-fit on F^2	1.026	1.162	1.039	1.047
Final R indexes [I>=2σ (I)]	R_1 = 0.0318, wR2 = 0.0731	R_1 = 0.0393, wR_2 = 0.0843	R_1 = 0.0263, wR_2 = 0.0637	R_1 = 0.0305, wR_2 = 0.0622
Final R indexes [all data]	R_1 = 0.0377, wR2 = 0.0772	R_1 = 0.0470, wR_2 = 0.0878	R_1 = 0.0313, wR_2 = 0.0672	R_1 = 0.0388, wR_2 = 0.0664
Largest diff. peak/hole / e Å^{-3}	1.06/-1.21	1.22/-0.99	0.51/-0.60	0.82/-0.54

Crystallographic data for complexes **85**, **89**, **91** and **93**.

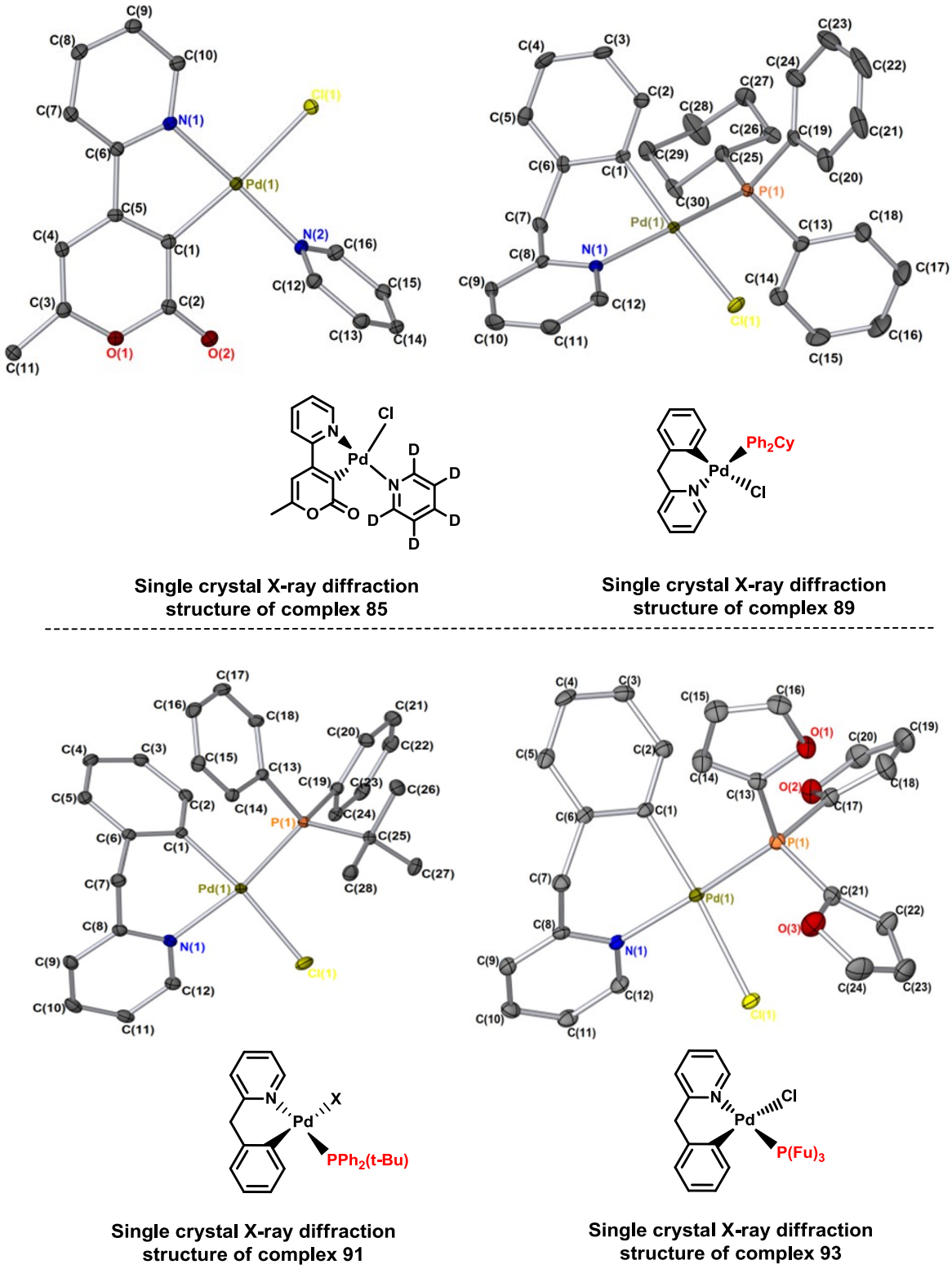

Figure 51 Single crystal X-ray diffraction structure of chloromonomer complexes **85**, **89**, **91** and **93**. Hydrogen atoms removed for clarity. Thermal ellipsoids shown with probability of 50%.

Table 13 Summary of X-ray data for complexes **85**, **89**, and **91**

Identification code	**91** (ijsf1216)	**93** (ijsf1314)	**85** (ijsf1313)
Empirical formula	$C_{28}H_{29}ClNPPd$	$C_{25}H_{20}Cl_4NO_3PPd$	$C_{16}H_{13}ClN_2O_2Pd$
Formula weight	552.34	661.59	407.13
Temperature/K	110.00(10)	110.05(10)	110.05(10)
Crystal system	monoclinic	monoclinic	orthorhombic
Space group	$P2_1/n$	$P2_1/c$	Pbca
a/Å	8.43431(6)	18.6500(7)	12.9846(3)
b/Å	18.79277(14)	8.38258(17)	10.9888(2)
c/Å	15.43388(11)	18.3610(6)	20.1211(6)
α/°	90.00	90.00	90.00
β/°	101.4672(7)	116.269(4)	90.00
γ/°	90.00	90.00	90.00
Volume/$Å^3$	2397.50(3)	2574.03(13)	2870.98(12)
Z	4	4	8
ρ_{calc}mg/mm^3	1.530	1.707	1.884
m/mm^{-1}	0.969	1.228	1.486
F(000)	1128.0	1320.0	1616.0
Crystal size/mm^3	0.2201 × 0.166 × 0.1273	0.2991 × 0.151 × 0.0679	0.2152 × 0.1579 × 0.0984
2Θ range for data collection	5.8 to 64.42°	6.4 to 59.9°	6.28 to 64.3°
Index ranges	$-12 \leq h \leq 12$, $-28 \leq k \leq 27$, $-22 \leq l \leq 23$	$-18 \leq h \leq 24$, $-11 \leq k \leq 10$, $-25 \leq l \leq 19$	$-16 \leq h \leq 19$, $-16 \leq k \leq 15$, $-29 \leq l \leq 28$
Reflections collected	41976	12973	18815
Independent reflections	7983[R(int) = 0.0289]	6602[R(int) = 0.0275]	4729[R(int) = 0.0265]
Data/restraints/parameters	7983/0/292	6602/12/329	4729/0/200
Goodness-of-fit on F^2	1.042	1.083	1.092
Final R indexes [I>=2σ (I)]	$R_1 = 0.0226$, $wR_2 = 0.0515$	$R_1 = 0.0345$, $wR_2 = 0.0672$	$R_1 = 0.0259$, $wR_2 = 0.0593$
Final R indexes [all data]	$R_1 = 0.0264$, $wR_2 = 0.0534$	$R_1 = 0.0491$, $wR_2 = 0.0733$	$R_1 = 0.0375$, $wR_2 = 0.0671$
Largest diff. peak/hole / e $Å^{-3}$	0.78/-0.67	0.70/-0.61	0.61/-1.11

Crystallographic data for complexes **88**, **90** and **92**.

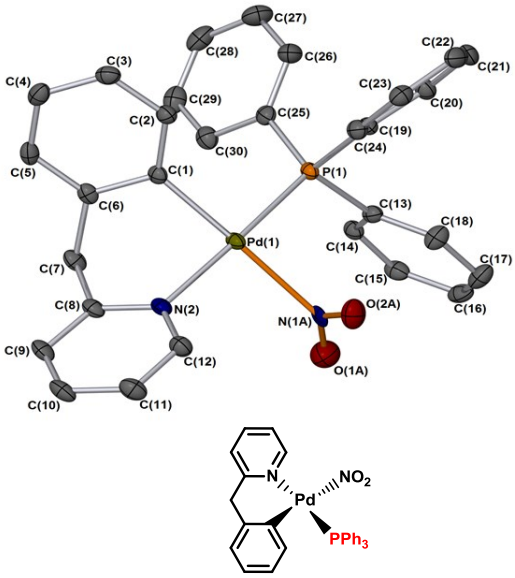

Single crystal X-ray diffraction structure of complex 88

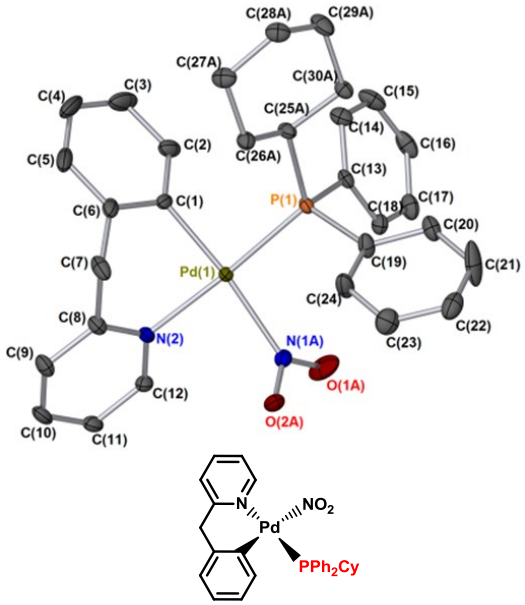

Single crystal X-ray diffraction structure of complex 90

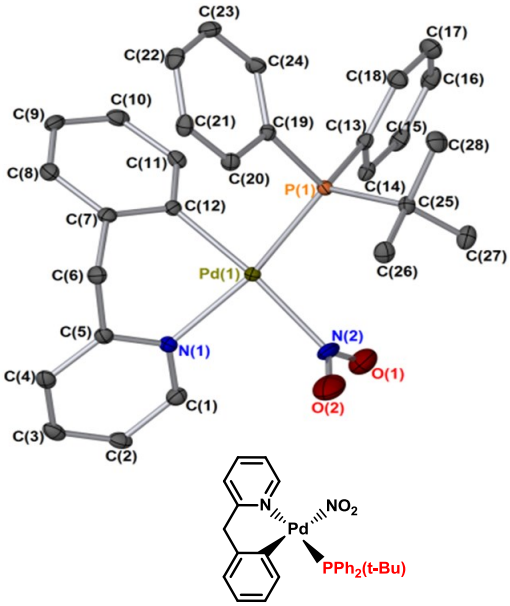

Single crystal X-ray diffraction structure of complex 92

Figure 52 Single crystal X-ray diffraction structure of complexes **88, 90** and **92**. Hydrogen atoms removed for clarity. Thermal ellipsoids shown with probability of 50%.

Table 14 Summary of X-ray data for complexes **88**, **90** and **92**

Identification code	**88**(ijsf1209)	**90**(ijsf1217)	**92**(ijsf1218)
Empirical formula	$C_{30}H_{25}N_2O_2PPd$	$C_{31}H_{33}Cl_2N_2O_2PPd$	$C_{28}H_{29}Cl_{0.76198}N_{1.23802}O_{0.47604}PPd$
Formula weight	582.89	673.86	554.86
Temperature/K	110.00(10)	110.00(10)	110.00(10)
Crystal system	monoclinic	monoclinic	monoclinic
Space group	$P2_1/n$	$P2_1/n$	$P2_1/n$
a/Å	8.5484(3)	8.40880(15)	8.42346(12)
b/Å	19.0146(8)	18.9504(3)	18.7653(3)
c/Å	15.6947(7)	18.6891(3)	15.4050(2)
α/°	90.00	90.00	90.00
β/°	99.449(5)	95.4843(17)	101.5786(15)
γ/°	90.00	90.00	90.00
Volume/$Å^3$	2516.45(18)	2964.48(9)	2385.49(6)
Z	4	4	4
ρ_{calc}mg/mm^3	1.539	1.510	1.545
m/mm^{-1}	0.832	0.892	0.950
F(000)	1184.0	1376.0	1133.2
Crystal size/mm^3	0.2146 × 0.119 × 0.0907	0.1595 × 0.1188 × 0.0468	0.1437 × 0.1234 × 0.0426
2Θ range for data collection	5.68 to 64.16°	5.92 to 64.34°	5.56 to 60.16°
Index ranges	$-11 \leq h \leq 12$, $-27 \leq k \leq 13$, $-14 \leq l \leq 23$	$-12 \leq h \leq 12$, $-27 \leq k \leq 28$, $-27 \leq l \leq 27$	$-11 \leq h \leq 9$, $-22 \leq k \leq 26$, $-21 \leq l \leq 21$
Reflections collected	14773	36957	13606
Independent reflections	7922[R(int) = 0.0233]	9644[R(int) = 0.0475]	6996[R(int) = 0.0294]
Data/restraints/parameters	7922/0/338	9644/15/381	6996/1/314
Goodness-of-fit on F^2	1.114	1.064	1.048
Final R indexes [I>=2σ (I)]	R_1 = 0.0378, wR_2 = 0.0797	R_1 = 0.0363, wR_2 = 0.0765	R_1 = 0.0294, wR_2 = 0.0605
Final R indexes [all data]	R_1 = 0.0432, wR_2 = 0.0824	R_1 = 0.0454, wR_2 = 0.0817	R_1 = 0.0372, wR_2 = 0.0645
Largest diff. peak/hole / e $Å^{-3}$	1.69/-1.34	0.82/-1.05	0.61/-0.66

Crystallographic data for complexes **105a**, **105b**, **107** and **110**.

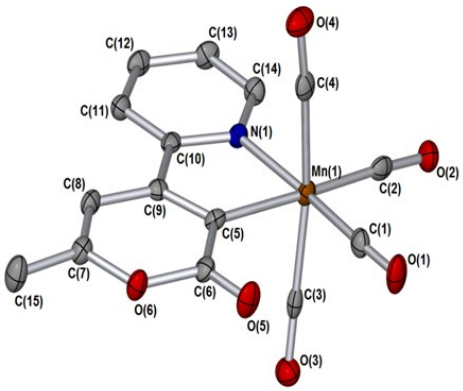

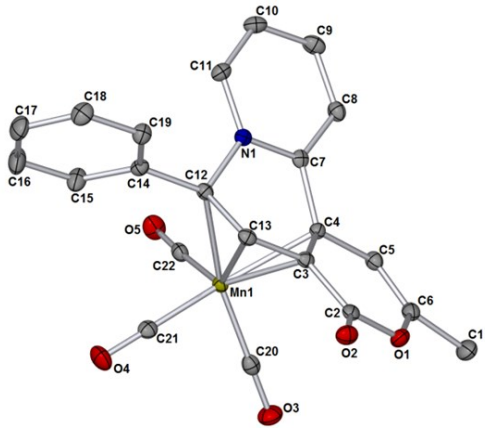

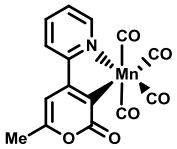

Single crystal X-ray diffraction structure of complex 105a

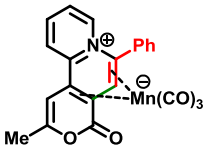

Single crystal X-ray diffraction structure of complex 107

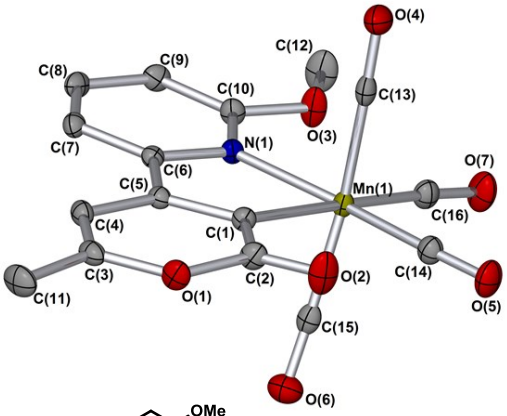

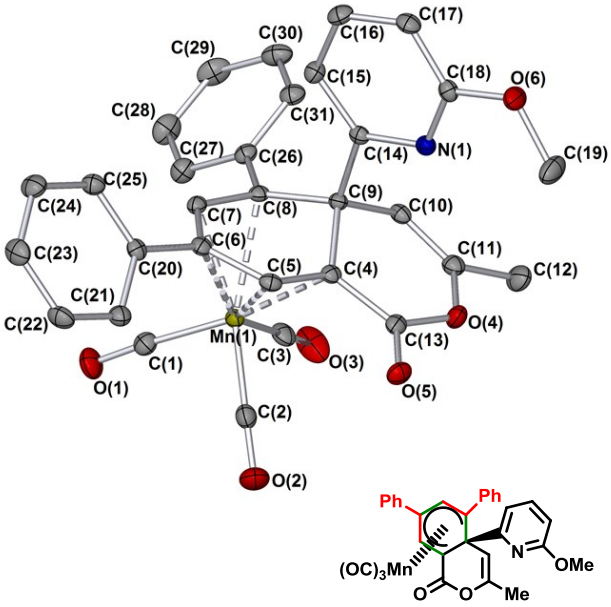

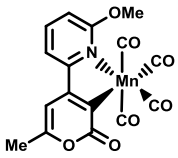

Single crystal X-ray diffraction structure of complex 105b

Single crystal X-ray diffraction structure of complex 110

Figure 53 Single crystal X-ray diffraction structure of complexes **105a**, **105b**, **107** and **110**. Hydrogen atoms removed for clarity. Thermal ellipsoids shown with probability of 50%.

Table 15 Summary of X-ray data for complexes **105b**, **107** and **110**

Identification code	**105b**(ijsf1510)	**107**(ijsf1416)	**110**(ijsf1512)
Empirical formula	$C_{16}H_{10}MnNO_7$	$C_{22}H_{14}MnNO_5$	$C_{31}H_{22}MnNO_6$
Formula weight	383.19	427.28	559.43
Temperature/K	110.05(10)	110.05(10)	110.05(10)
Crystal system	triclinic	monoclinic	monoclinic
Space group	P-1	$P2_1/c$	$P2_1/n$
a/Å	6.9469(5)	7.4809(3)	10.9613(2)
b/Å	10.1635(6)	19.0446(15)	19.3911(3)
c/Å	12.3849(9)	12.8808(4)	13.0063(3)
α/°	67.194(6)	90	90
β/°	83.812(6)	93.949(3)	110.468(3)
γ/°	71.460(7)	90	90
Volume/$Å^3$	764.12(10)	1830.78(17)	2589.97(10)
Z	2	4	4
ρ_{calc}g/cm^3	1.665	1.550	1.435
μ/mm^{-1}	0.905	0.757	4.540
F(000)	388.0	872.0	1152.0
Crystal size/mm^3	MoKα (λ = 0.7107)	MoKα (λ = 0.71073)	CuKα (λ = 1.54184)
Radiation	0.3277 × 0.0793 × 0.0616	0.2039 × 0.0557 × 0.0213	0.1513 × 0.0527 × 0.0334
2Θ range for data collection/°	6.764 to 64.15	5.856 to 60.688°	8.57 to 142.028
Index ranges	$-10 \leq h \leq 10$, $-15 \leq k \leq 14$, $-17 \leq l \leq 17$	$-7 \leq h \leq 10$, $-24 \leq k \leq 26$, $-14 \leq l \leq 18$	$-12 \leq h \leq 13$, $-23 \leq k \leq 17$, $-15 \leq l \leq 15$
Reflections collected	12875	8927	17168
Independent reflections	4850 [R_{int} = 0.0350, R_{sigma} = 0.0420]	4803 [R_{int} = 0.0258, R_{sigma} = 0.0453]	4964 [R_{int} = 0.0316, R_{sigma} = 0.0286]
Data/restraints/parameters	4850/0/228	4803/0/263	4964/0/354
Goodness-of-fit on F^2	1.056	1.048	1.047
Final R indexes [I>=2σ (I)]	R_1 = 0.0349, wR_2 = 0.0736	R_1 = 0.0374, wR_2 = 0.0808	R_1 = 0.0294, wR_2 = 0.0744
Final R indexes [all data]	R_1 = 0.0441, wR_2 = 0.0779	R_1 = 0.0507, wR_2 = 0.0876	R_1 = 0.0336, wR_2 = 0.0770
Largest diff. peak/hole / e $Å^{-3}$	0.47/-0.42	0.41/-0.42	0.30/-0.34

Crystallographic data for compound **108** and **109**

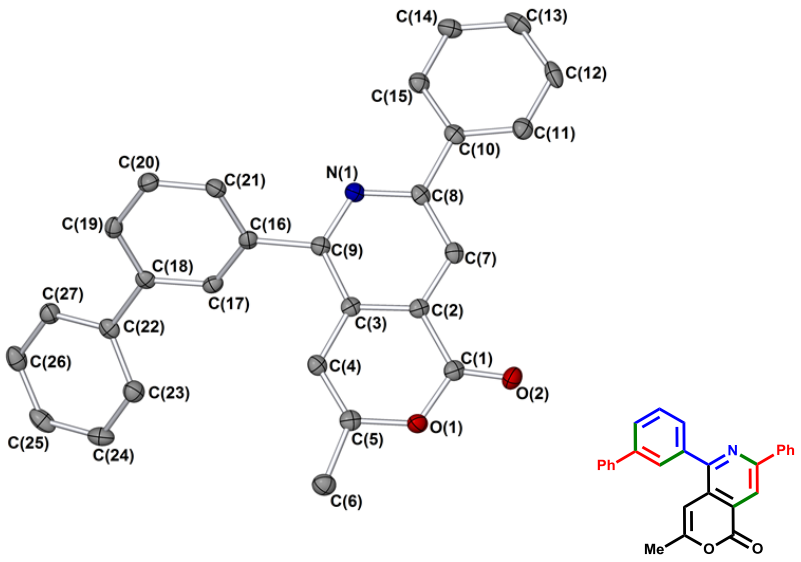

Single crystal X-ray diffraction structure of compound 108

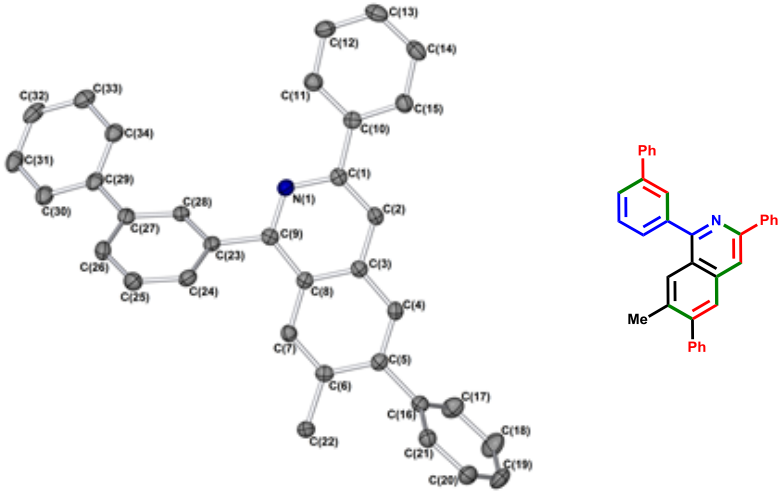

Single crystal X-ray diffraction structure of compoud 109

Figure 54 Single crystal X-ray diffraction structure of compound **108** and **109**. Hydrogen atoms removed for clarity. Thermal ellipsoids shown with probability of 50%.

Table 16 Summary of X-ray data for compound **108** and **109**

Identification code	**108**(ijsf1489)	**109**(ijsf1516a)
Empirical formula	$C_{27}H_{19}NO_2$	$C_{34}H_{25}N$
Formula weight	389.43	447.55
Temperature/K	110.05(10)	110.05(10)
Crystal system	monoclinic	tetragonal
Space group	$P2_1/c$	$P4_3$
a/Å	11.4500(3)	13.86719(18)
b/Å	13.3633(3)	13.86719(18)
c/Å	12.4539(3)	12.4237(3)
α/°	90	90.00
β/°	93.005(2)	90.00
γ/°	90	90.00
Volume/Å^3	1902.96(8)	2389.07(7)
Z	4	4
ρ_{calc}mg/mm^3	1.359	1.244
m/mm^{-1}	0.677	0.543
F(000)	816.0	944.0
Radiation	CuKα (λ = 1.54184)	CuKα (λ = 1.54184)
Crystal size/mm^3	0.233 × 0.1307 × 0.0883	0.1414 × 0.1144 × 0.0722
2Θ range for data collection	7.732 to 134.144	9.02 to 141.98
Index ranges	$-10 \leq h \leq 13$, $-14 \leq k \leq 15$, $-14 \leq l \leq 14$	$-16 \leq h \leq 16$, $-11 \leq k \leq 16$, $-9 \leq l \leq 14$
Reflections collected	6811	6885
Independent reflections	3383 [R_{int} = 0.0207, R_{sigma} = 0.0273]	3277 [R_{int} = 0.0217, R_{sigma} = 0.0313]
Data/restraints/parameters	3383/0/272	3277/1/317
Goodness-of-fit on F^2	1.038	1.016
Final R indexes [I>=2σ (I)]	R_1 = 0.0393, wR_2 = 0.0970	R_1 = 0.0307, wR_2 = 0.0783
Final R indexes [all data]	R_1 = 0.0447, wR_2 = 0.1024	R_1 = 0.0327, wR_2 = 0.0801
Largest diff. peak/hole / e Å^{-3}	0.47/-0.25	0.15/-0.12

Crystallographic data for compound **114c**, **115c** and **130a**

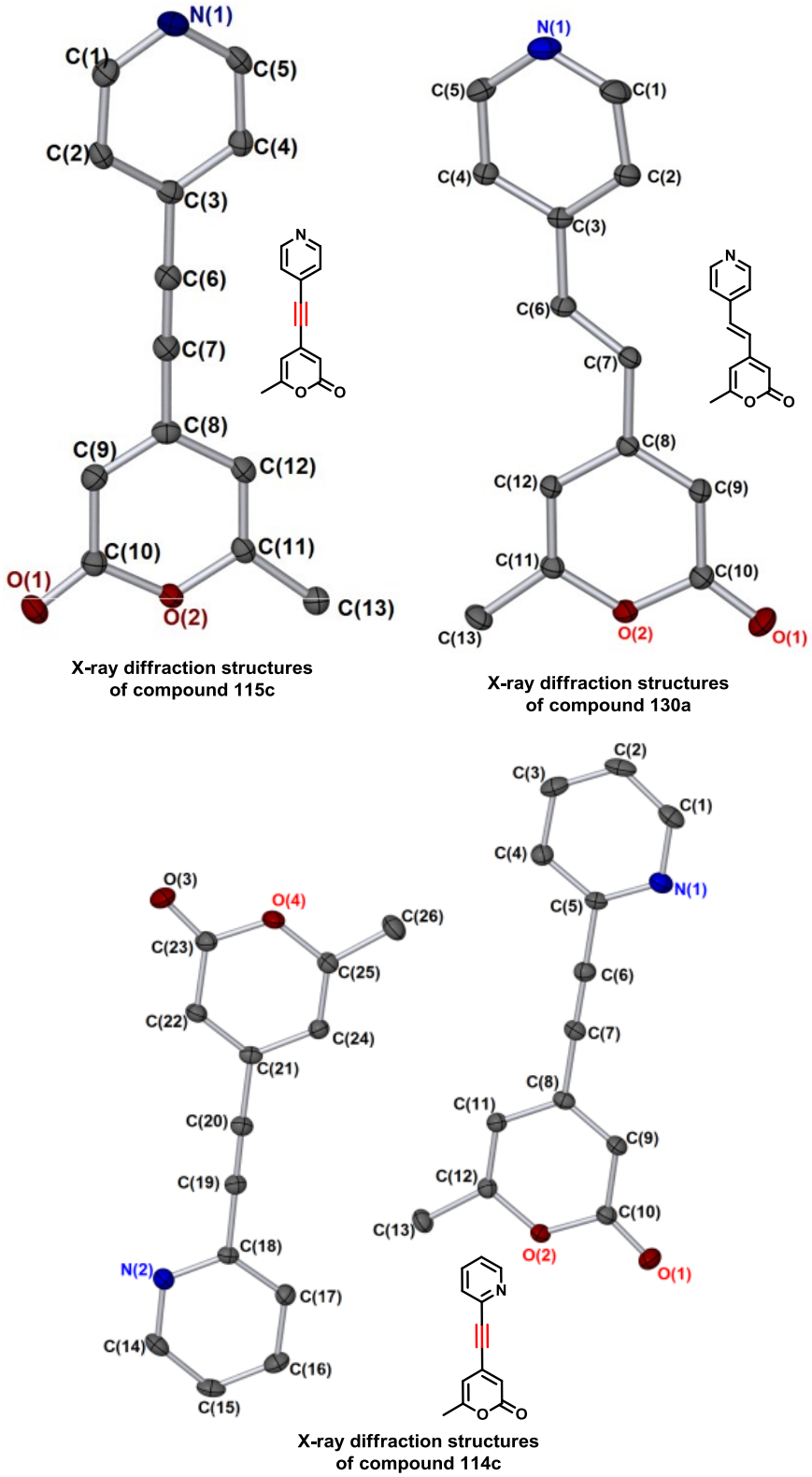

Figure 55 Single crystal X-ray diffraction structure of complexes **114c**, **115c** and **130a**. Compound **114c** bottom, showing the packing between the molecules. Hydrogen atoms removed for clarity. Thermal ellipsoids shown with probability of 50%.

Table 17 Summary of X-ray data for complexes **114c**, **115c** and **130b**

Identification code	**114c**(ijsf1410)	**115c**(ijsf1327)	**130b**(ijsf1329)
Empirical formula	$C_{13}H_9NO_2$	$C_{13}H_9NO_2$	$C_{13}H_{11}NO_2$
Formula weight	211.21	211.21	213.23
Temperature/K	110.05(10)	110.05(10)	110.05(10)
Crystal system	monoclinic	monoclinic	monoclinic
Space group	$P2_1/c$	$P2_1/n$	$P2_1/c$
a/Å	12.2868(3)	7.7732(2)	7.0432(3)
b/Å	23.6736(4)	9.9544(3)	12.8083(5)
c/Å	7.24297(15)	13.2388(4)	11.6581(4)
α/°	90	90.00	90.00
β/°	101.605(2)	97.545(3)	97.187(3)
γ/°	90	90.00	90.00
Volume/$Å^3$	2063.72(7)	1015.52(6)	1043.43(6)
Z	8	4	4
ρ_{calc}mg/mm^3	1.360	1.381	1.357
m/mm^{-1}	0.093	0.094	0.092
F(000)	880.0	440.0	448.0
Crystal size/mm^3	0.2968 × 0.1839 × 0.1127	0.2855 × 0.1649 × 0.0866	0.1849 × 0.1003 × 0.0826
Radiation	MoKα (λ = 0.7107)	Mo Kα (λ = 0.7107)	Mo Kα (λ = 0.7107)
2Θ range for data collection	5.988 to 60.482°	5.76 to 55.62°	5.82 to 64.44°
Index ranges	$-8 \leq h \leq 17$, $-33 \leq k \leq 26$, $-9 \leq l \leq 7$	$-7 \leq h \leq 9$, $-12 \leq k \leq 11$, $-13 \leq l \leq 16$	$-4 \leq h \leq 10$, $-18 \leq k \leq 16$, $-17 \leq l \leq 16$
Reflections collected	9966	3918	6204
Independent reflections	5432 [R_{int} = 0.0212, R_{sigma} = 0.0333]	2063[R(int) = 0.0194]	3352[R(int) = 0.0172]
Data/restraints/parameters	5432/0/291	2063/0/146	3352/0/146
Goodness-of-fit on F^2	1.063	1.089	1.070
Final R indexes [I>=2σ (I)]	R_1 = 0.0482, wR_2 = 0.1155	R_1 = 0.0434, wR_2 = 0.1048	R_1 = 0.0470, wR_2 = 0.1250
Final R indexes [all data]	R_1 = 0.0647, wR_2 = 0.1243	R_1 = 0.0567, wR_2 = 0.1122	R_1 = 0.0577, wR_2 = 0.1331

Crystallographic data for compound **121β**, **122β** and **124β**.

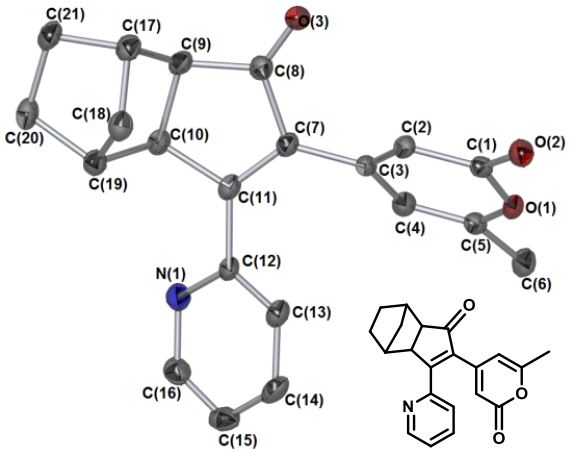

Single Crystal X-ray structure of 121 showing β selectivity

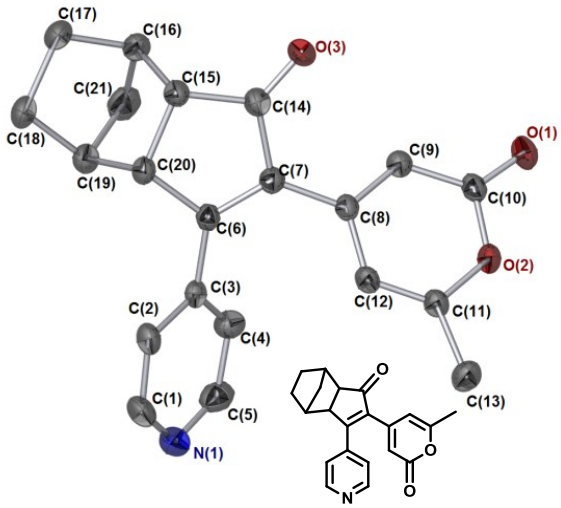

Single Crystal X-ray structure of 122 of β selectivity

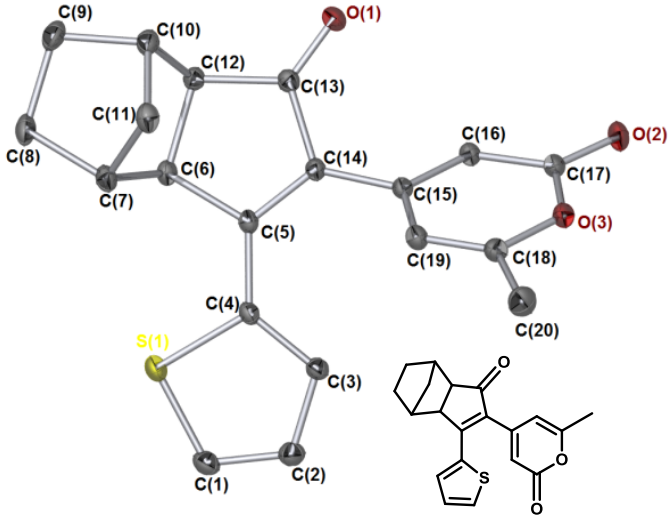

Single Crystal X-ray structure of 124 showing β selectivity

Figure 56 Single crystal X-ray diffraction structure of PKR compound containing 2-pyrone for **121*β***, **122*β*** and **124*β***. Hydrogen atoms removed for clarity. Thermal ellipsoids shown with probability of 50%.

Table 18 Summary of X-ray data for complexes **121*β***, **122*β*** and **124*β***

Identification code	**121*β*** (ijsf1325)	**122*β*** (ijsf1421)	**124*β*** (ijsf1440)
Empirical formula	$C_{21}H_{19}NO_3$	$C_{21}H_{19}NO_3$	$C_{20}H_{18}O_3S$
Formula weight	333.37	333.37	338.40
Temperature/K	110.05(10)	110.05(10)	110.00(10)
Crystal system	monoclinic	monoclinic	triclinic
Space group	$P2_1/n$	$P2_1/c$	P-1
a/Å	11.0079(3)	19.1782(5)	9.3885(5)
b/Å	10.2293(3)	8.3438(3)	9.7319(4)
c/Å	15.0673(4)	10.3712(3)	9.9642(5)
α/°	90.00	90	102.963(4)
β/°	100.220(3)	95.910(2)	93.132(4)
γ/°	90.00	90	114.627(5)
Volume/$Å^3$	1669.71(8)	1650.76(8)	795.15(7)
Z	4	4	2
ρ_{calc}mg/mm^3	1.326	1.341	1.413
m/mm^{-1}	0.089	0.090	0.219
F(000)	704.0	704.0	356.0
Crystal size/mm^3	0.1479 × 0.1252 × 0.0913	0.2384 × 0.1758 × 0.0449	0.2706 × 0.2322 × 0.1678
2Θ range for data collection	6.42 to 56.08°	6.274 to 56.194°	5.882 to 64.45
Index ranges	$-12 \leq h \leq 13$, $-8 \leq k \leq 12$, $-13 \leq l \leq 19$	$-23 \leq h \leq 24$, $-10 \leq k \leq 4$, $-11 \leq l \leq 12$	$-13 \leq h \leq 13$, $-14 \leq k \leq 14$, $-14 \leq l \leq 14$
Reflections collected	6179	5958	17495
Independent reflections	3346[R(int) = 0.0221]	3297 [R_{int} = 0.0236, R_{sigma} = 0.0388]	5216 [R_{int} = 0.0289, R_{sigma} = 0.0297]
Data/restraints/parameters	3346/0/227	3297/0/227	5216/0/218
Goodness-of-fit on F^2	1.056	1.042	1.073
Final R indexes [I>=2σ (I)]	R_1 = 0.0543, wR_2 = 0.1127	R_1 = 0.0544, wR_2 = 0.1273	R_1 = 0.0417, wR_2 = 0.1080
Final R indexes [all data]	R_1 = 0.0746, wR_2 = 0.1237	R_1 = 0.0708, wR_2 = 0.1388	R_1 = 0.0497, wR_2 = 0.1148
Largest diff. peak/hole / e $Å^{-3}$	0.34/-0.23	0.26/-0.22	0.50/-0.39

Crystallographic data for compound **125β**, **126α** and **127β**

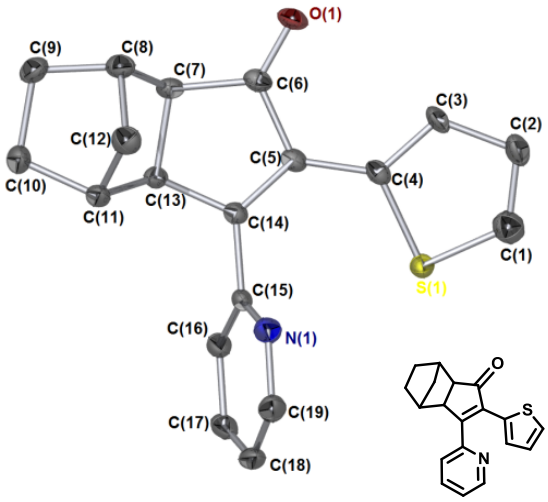

Single crystal X-ray diffraction structure of complex 125β

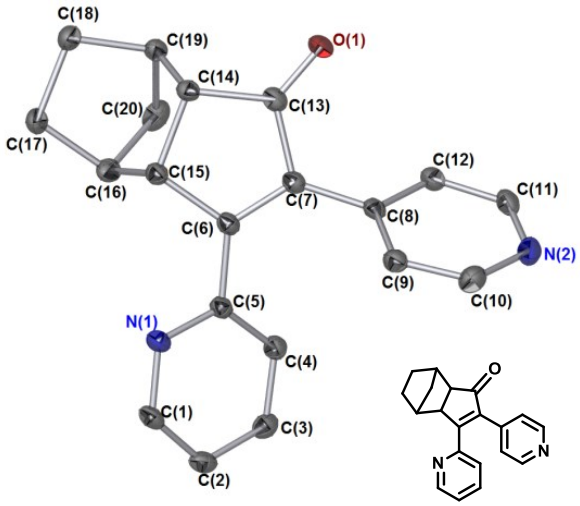

Single crystal X-ray diffraction structure of complex 127β

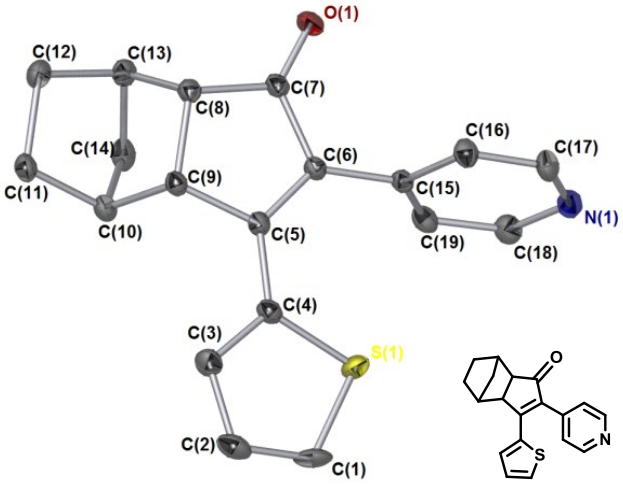

Single crystal X-ray diffraction structure of complex 126α

Figure 57 Single crystal X-ray diffraction structure of PKR compound of **125*β***, **126*α*** and **127*β***. Hydrogen atoms removed for clarity. Thermal ellipsoids shown with probability of 50%.

Table 19 Summary of X-ray data for complexes 125β, 126α and 127β

Identification code	**125β** (ijsf1460)	**126α** (ijsf1406)	**127β** (ijsf1463a)
Empirical formula	$C_{19}H_{17}NOS$	$C_{19}H_{17}NOS$	$C_{20}H_{18}N_2O$
Formula weight	307.39	307.39	302.36
Temperature/K	110.05(10)	110.05(10)	110.05(10)
Crystal system	monoclinic	monoclinic	orthorhombic
Space group	$P2_1/n$	$P2_1/c$	Pbca
a/Å	8.8893(3)	5.88552(11)	8.7098(5)
b/Å	19.7148(5)	18.4965(4)	10.0132(4)
c/Å	9.2543(3)	13.9295(3)	35.1795(16)
α/°	90	90	90
β/°	111.117(4)	97.2089(19)	90
γ/°	90	90	90
Volume/Å^3	1512.91(8)	1504.40(5)	3068.1(3)
Z	4	4	8
ρ_{calc}mg/mm^3	1.350	1.357	1.309
m/mm^{-1}	1.895	0.216	0.641
F(000)	648.0	648.0	1280.0
Crystal size/mm^3	0.2525 × 0.1996 × 0.0803	0.3773 × 0.1124 × 0.0594	0.2622 × 0.1912 × 0.0305
2Θ range for data collection	8.972 to 142.16	5.89 to 64.4°	10.058 to 142.332
Index ranges	$-10 \leq h \leq 10$, $-23 \leq k \leq 19$, $-11 \leq l \leq 10$	$-8 \leq h \leq 7$, $-19 \leq k \leq 26$, $-10 \leq l \leq 19$	$-5 \leq h \leq 10$, $-10 \leq k \leq 12$, $-40 \leq l \leq 42$
Reflections collected	5420	8811	6657
Independent reflections	2814 [R_{int} = 0.0183, R_{sigma} = 0.0248]	4764 [R_{int} = 0.0243, R_{sigma} = 0.0418]	2887 [R_{int} = 0.0273, R_{sigma} = 0.0360]
Data/restraints/parameters	2814/0/206	4764/5/212	2887/0/208
Goodness-of-fit on F^2	1.033	1.033	1.051
Final R indexes [I>=2σ (I)]	R_1 = 0.0362, wR_2 = 0.0905	R_1 = 0.0447, wR_2 = 0.1057	R_1 = 0.0490, wR_2 = 0.1173
Final R indexes [all data]	R_1 = 0.0425, wR_2 = 0.0957	R_1 = 0.0599, wR_2 = 0.1163	R_1 = 0.0604, wR_2 = 0.1259
Largest diff. peak/hole / e Å^{-3}	0.26/-0.20	0.40/-0.28	0.41/-0.23

9.2 Appendix 2: UV–Visible spectroscopic data for compound 108 and 109

UV–visible spectroscopic data for compound **108**

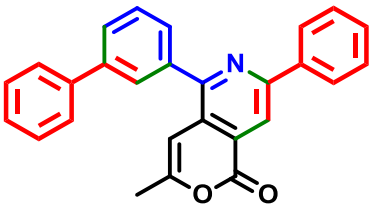

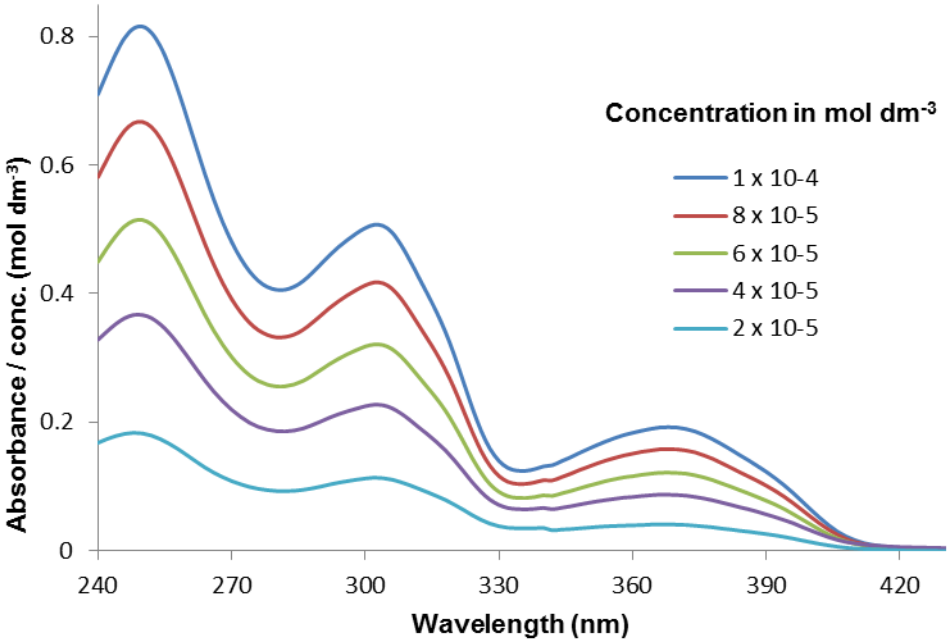

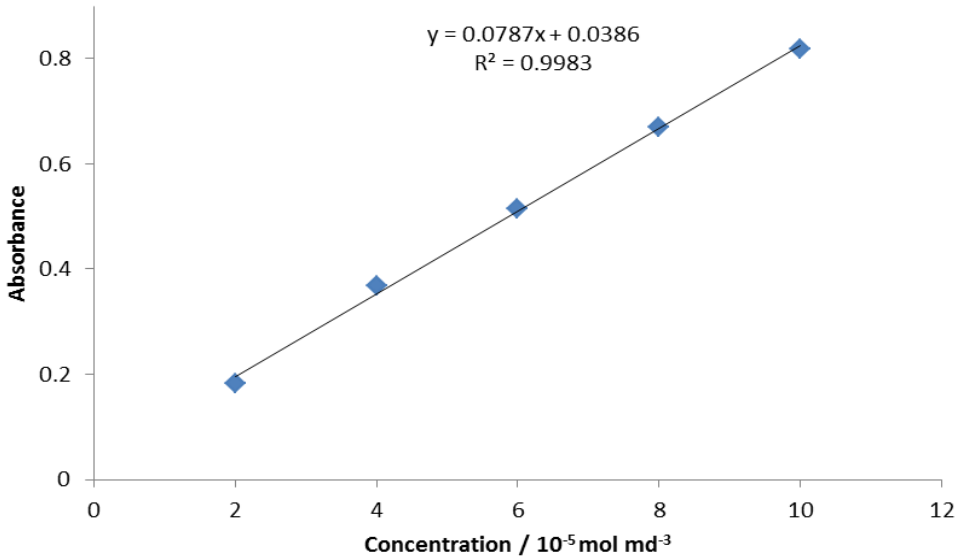

Figure 58 UV–visible spectroscopic data for compound **108**

UV–visible spectroscopic data for compound **109**

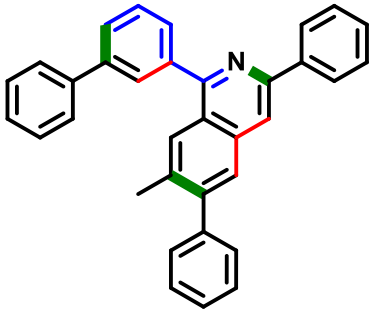

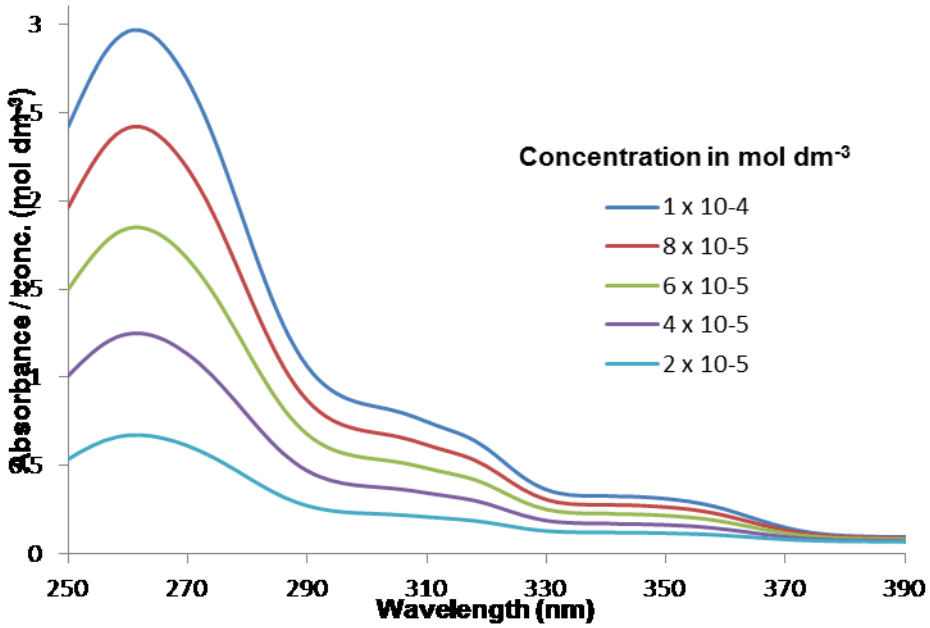

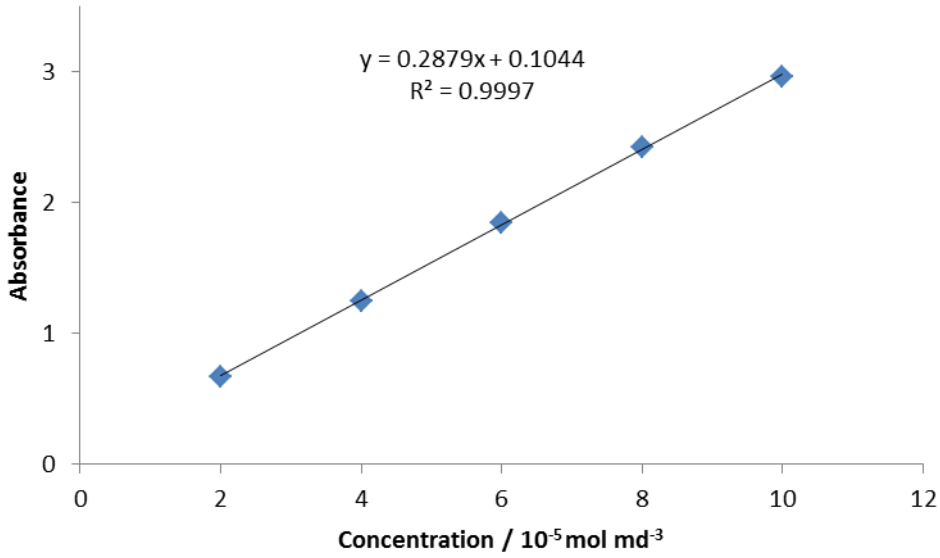

Figure 59 UV–visible spectroscopic data for compound **109**

9.3 Appendix 3: UV–Visible irradiation Spectroscopic Data

9.3.1 General procedure for the UV light-controlled irradiation for cyclisation / aromatisation

An in house new UV-vis. irradiation system developed in York to provide controlled irradiation in which the wavelength and intensity of the light can be adjusted when required were used for PK adduct irradiation. The system (device) uses a small 5W LED's that attach directly on to the top of a cuvette. The LED's circuit is mechanically in-built in a special cuvette cap to a flexible wire, to allow the cuvette to be placed in the UV spectrometer for UV. A heat absorbing system (device) was developed for irradiating the NMR sample in the NMR tube for NMR simulation. The current LEDs in the system irradiate at 400 nm (Figure 60)

Figure 60 An irradiation system using the 400 nm 5W LED drawing a current of 20 mA

UV–visible irradiation spectroscopic data for compound **113Aβ** to form **113Bβ**

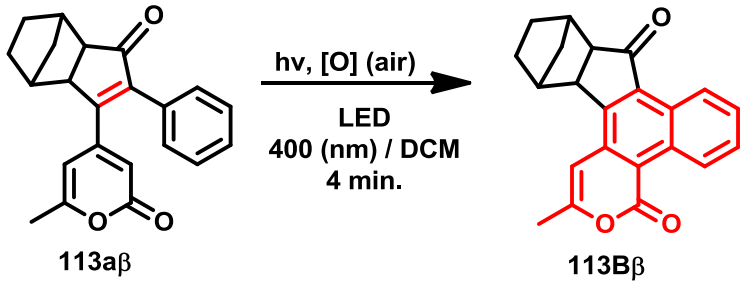

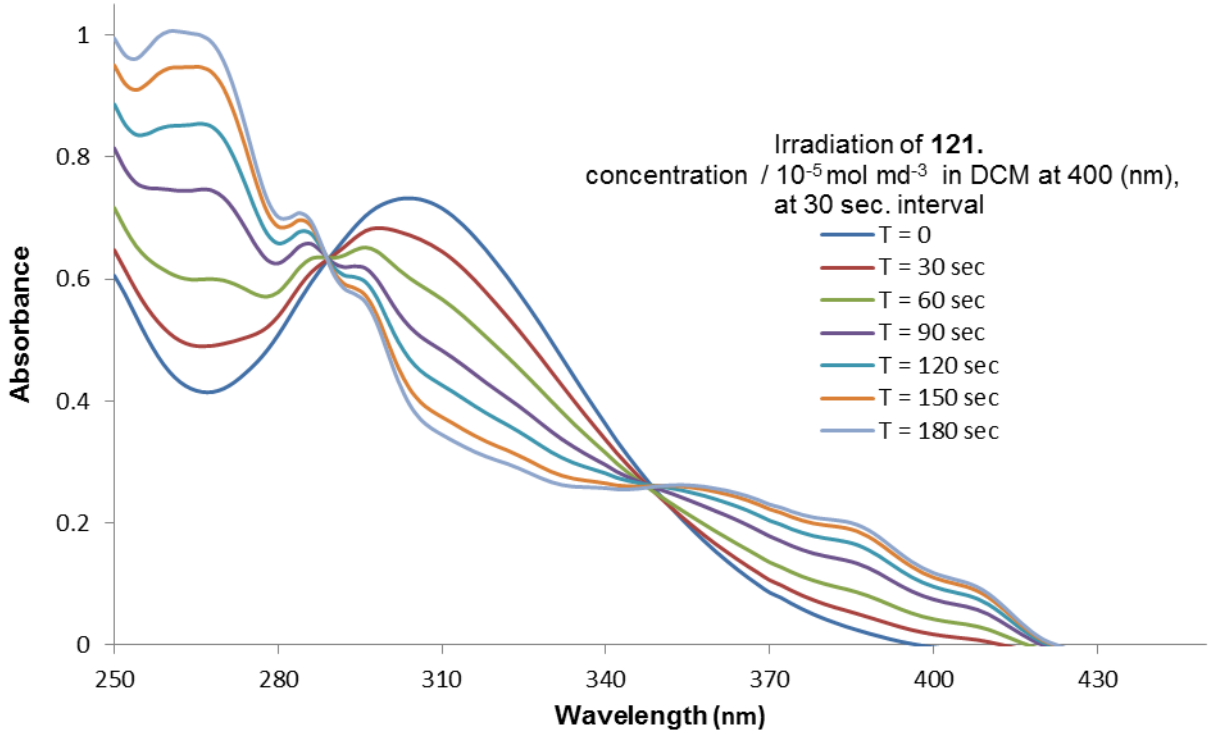

Figure 61 UV–visible irradiation spectroscopic data for compound **113Aβ** to form **113Bβ**

UV–visible irradiation spectroscopic data for compound **121A** to form **121B**

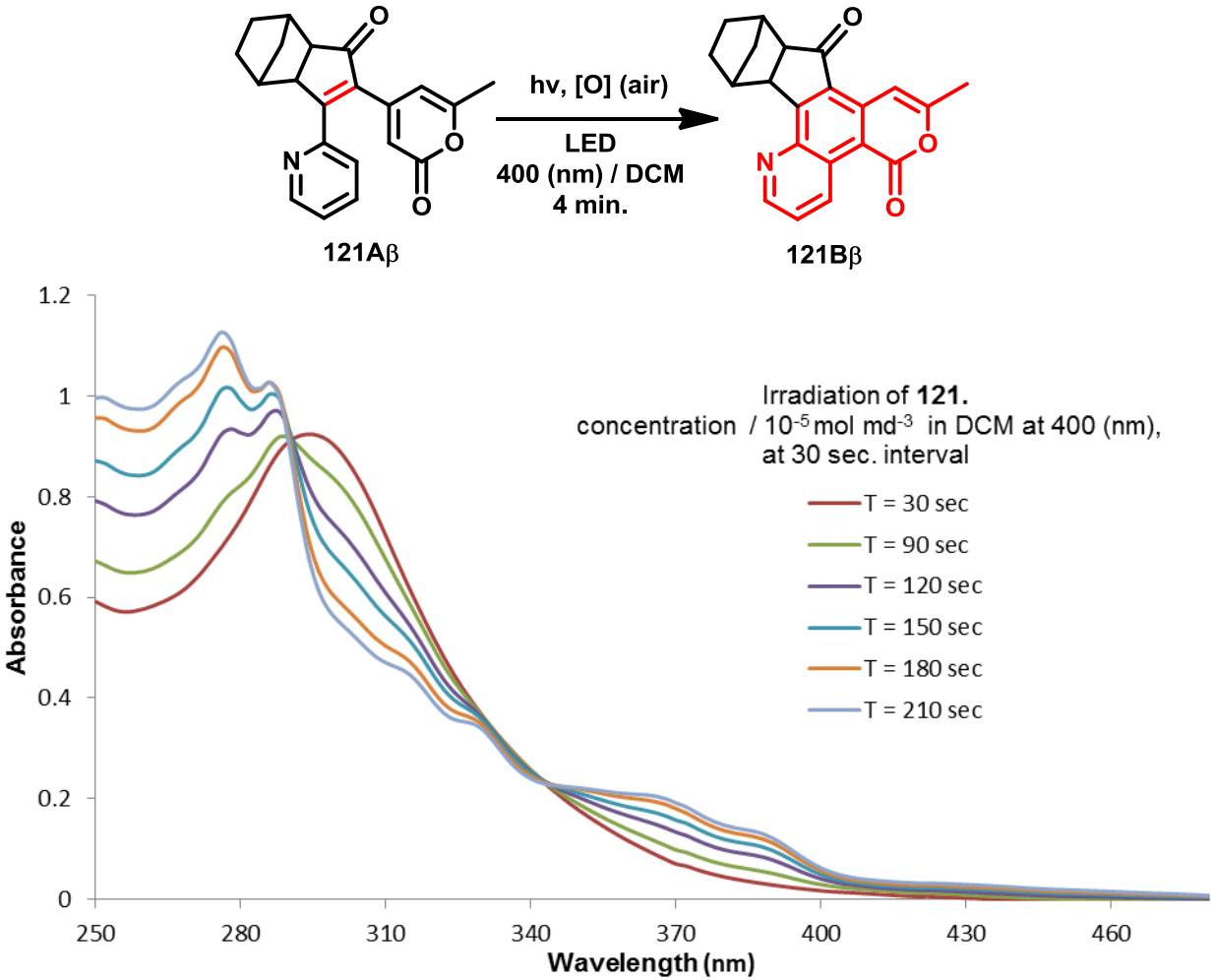

Figure 62 UV–visible irradiation spectroscopic data for compound **121A** to form **121B**

UV–visible irradiation spectroscopic data for compound **124Aβ** to form **124Bβ**

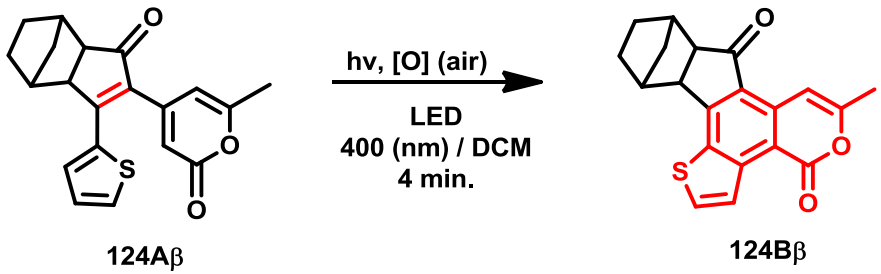

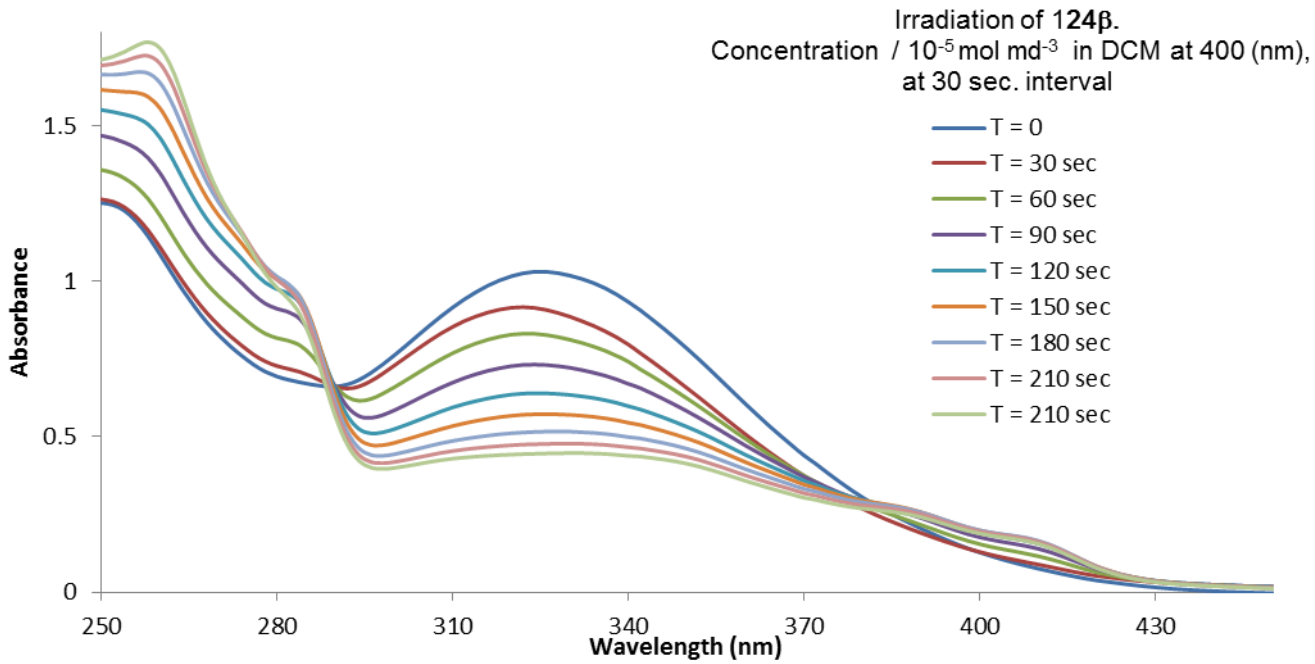

Figure 63 UV–visible irradiation spectroscopic data for compound **124Aβ** to form **124Bβ**

UV–visible irradiation spectroscopic data for compound **124Aα** to form **124Bα**

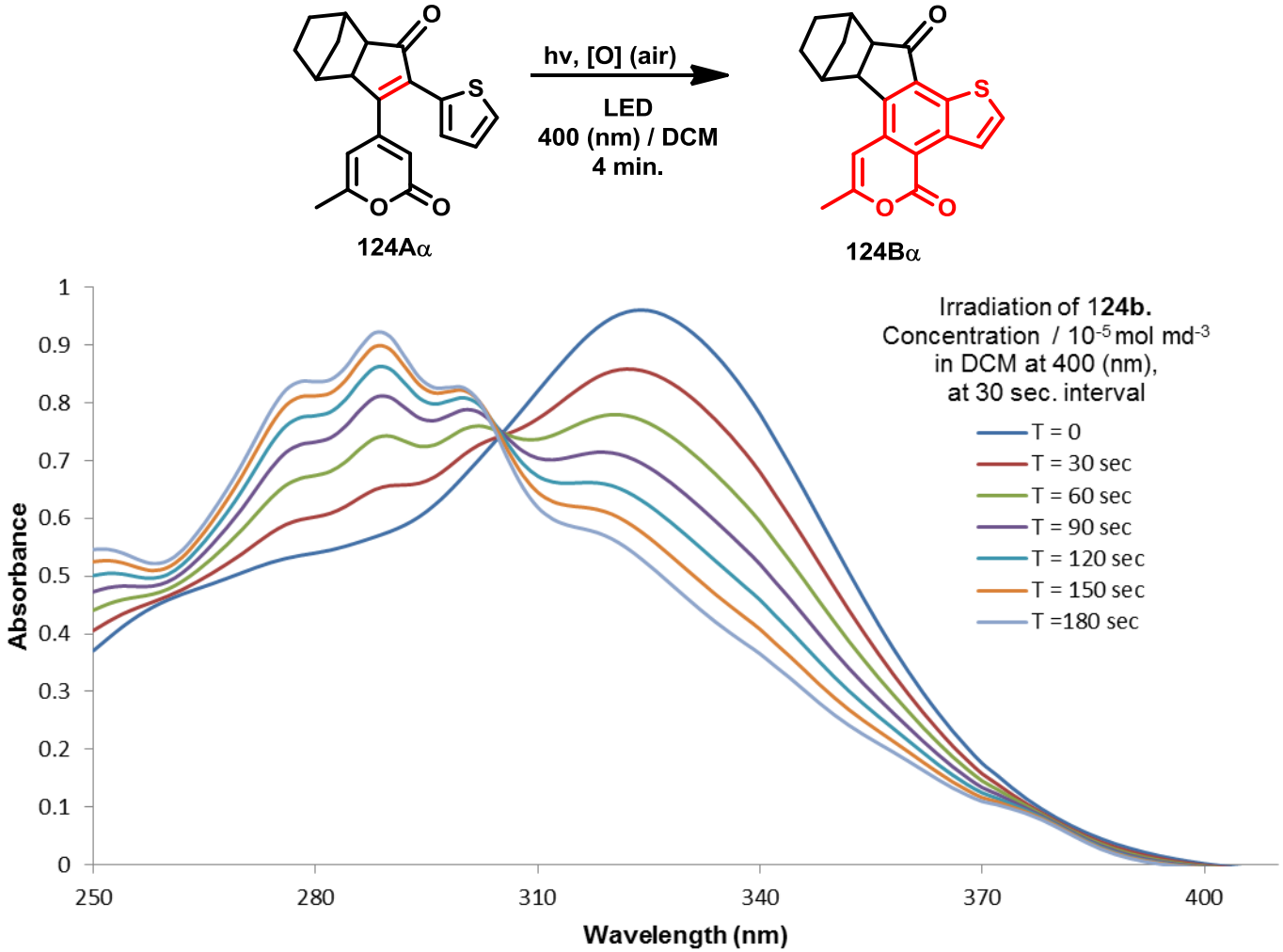

Figure 64 UV–visible irradiation spectroscopic data for compound **124Aα** to form **124Bα**

UV–visible irradiation spectroscopic data for compound **125Aβ** to form **125Bβ**

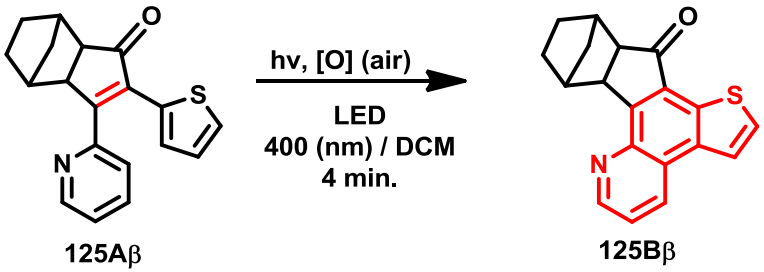

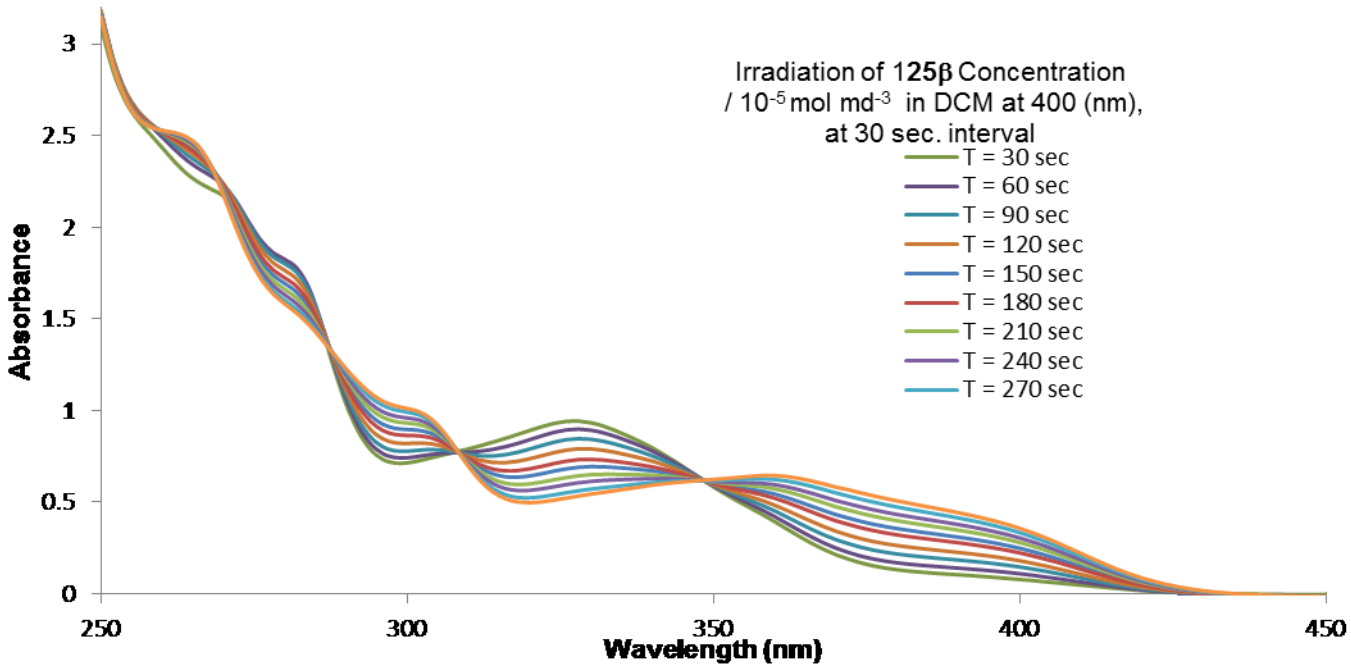

Figure 65 UV–visible irradiation spectroscopic data for compound **125Aβ** to form **125Bβ**

UV–visible irradiation spectroscopic data for compound **126Aα** to form **126Bα**

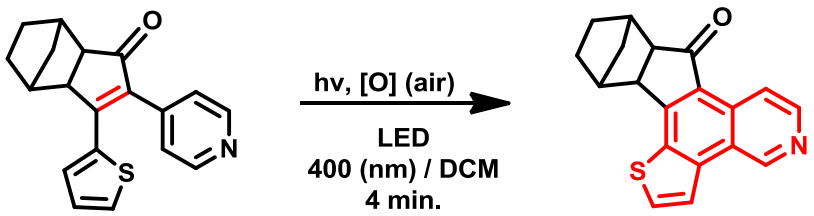

126Aα **126Bα**

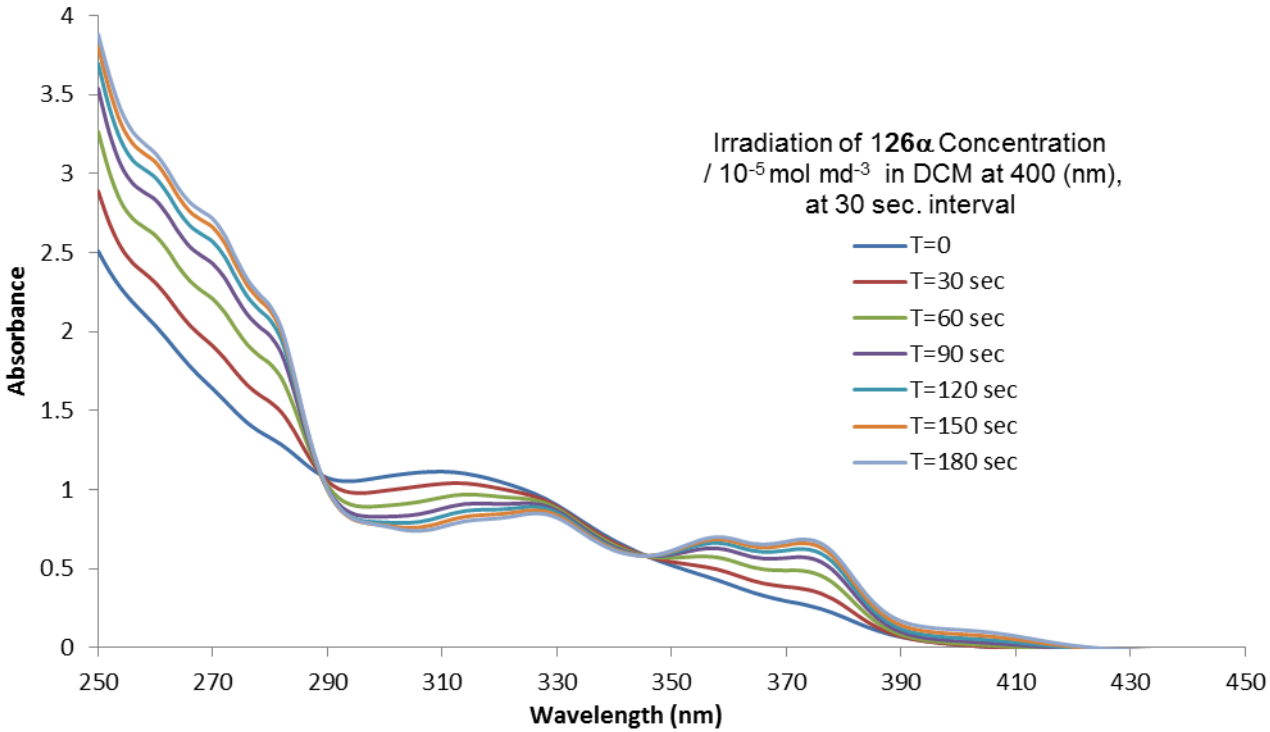

Figure 66 UV–visible irradiation spectroscopic data for compound **126Aα** to form **126B**

9.4 Appendix 4: NMR spectra of prepared compounds

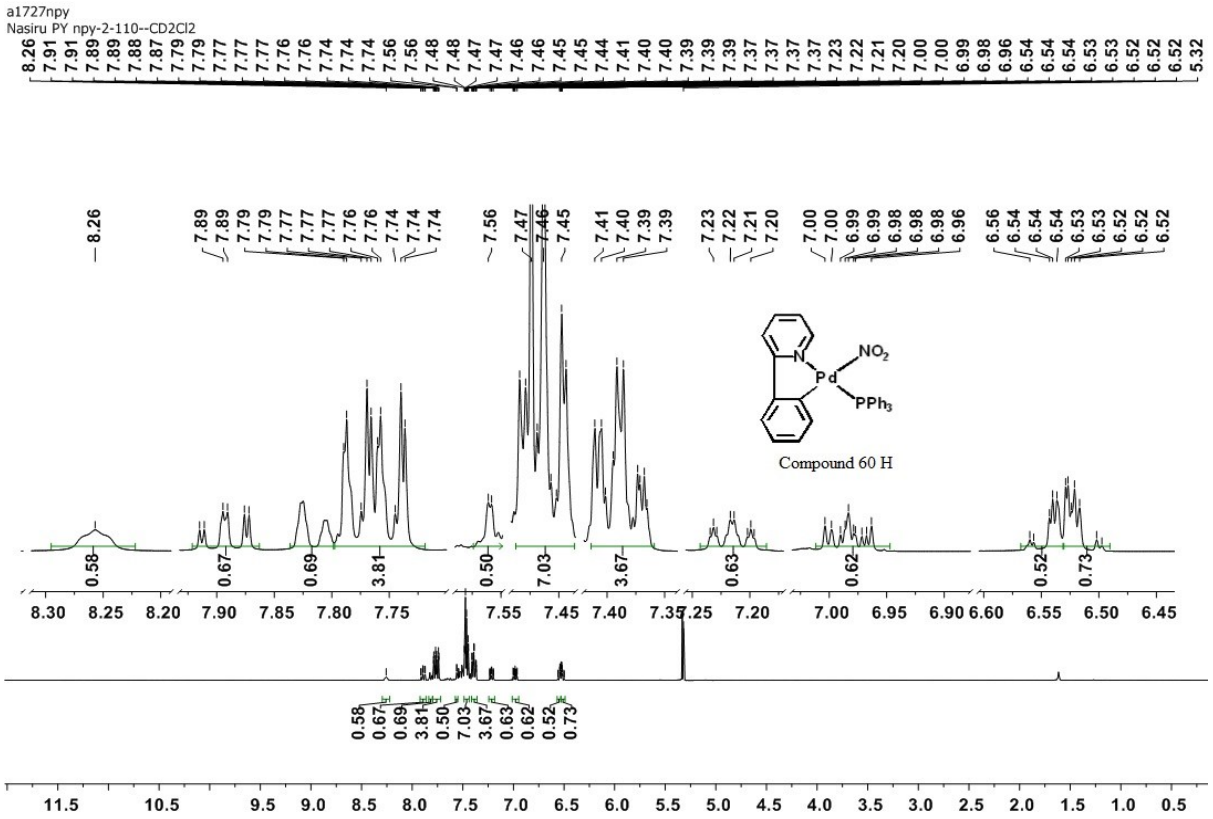

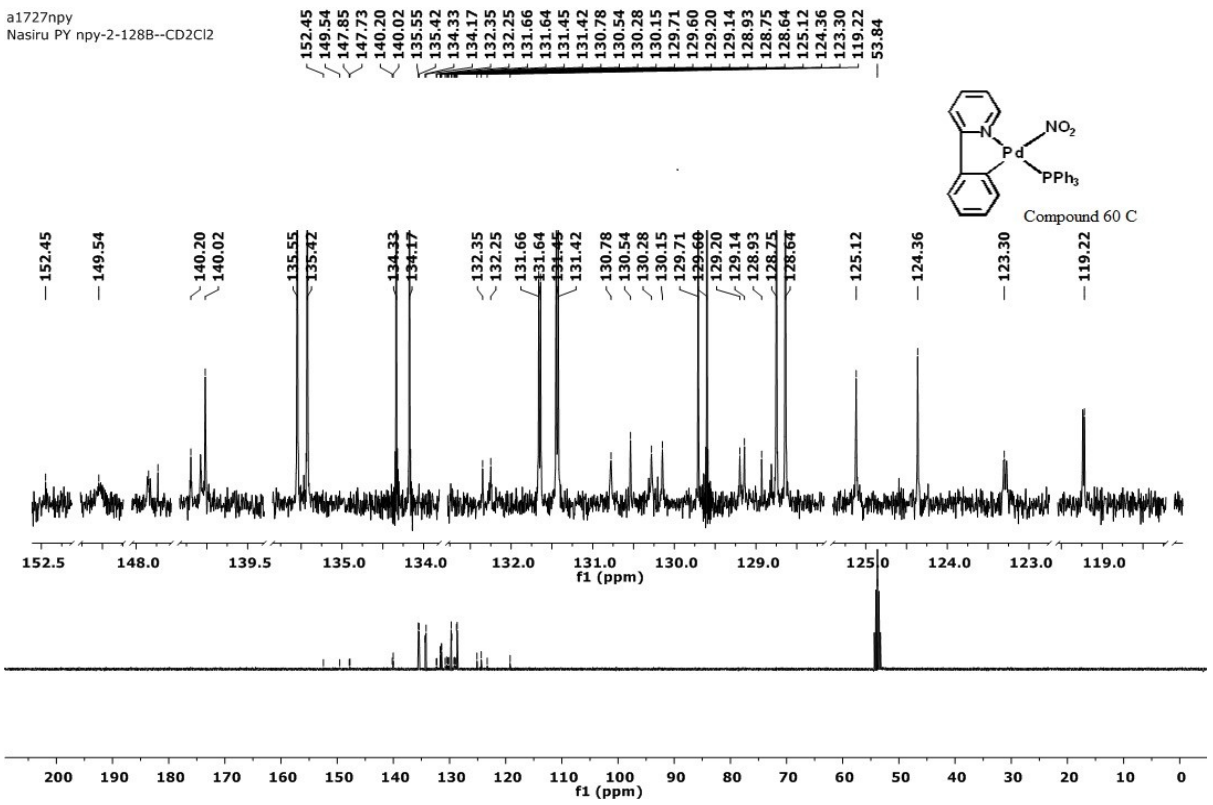

Appendix for (60)

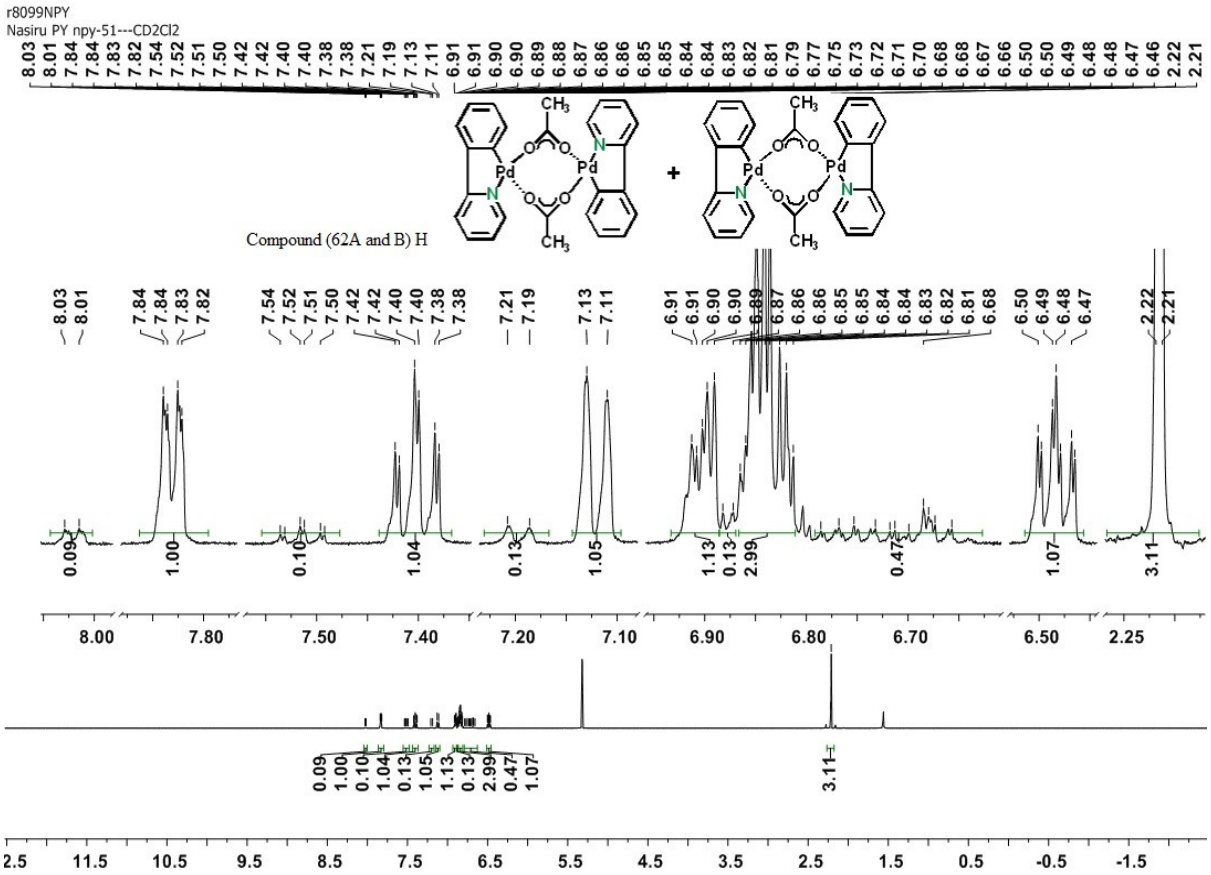

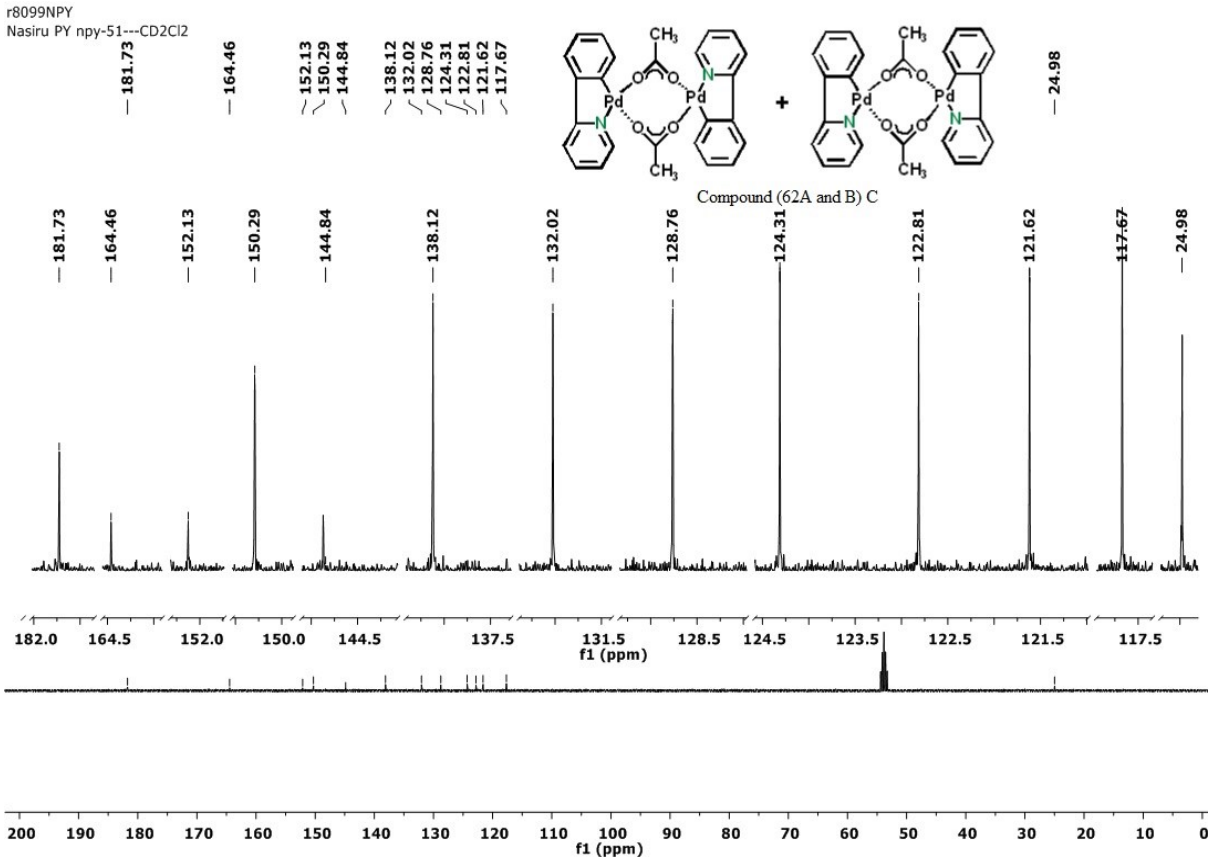

Appendix for (62A and B)

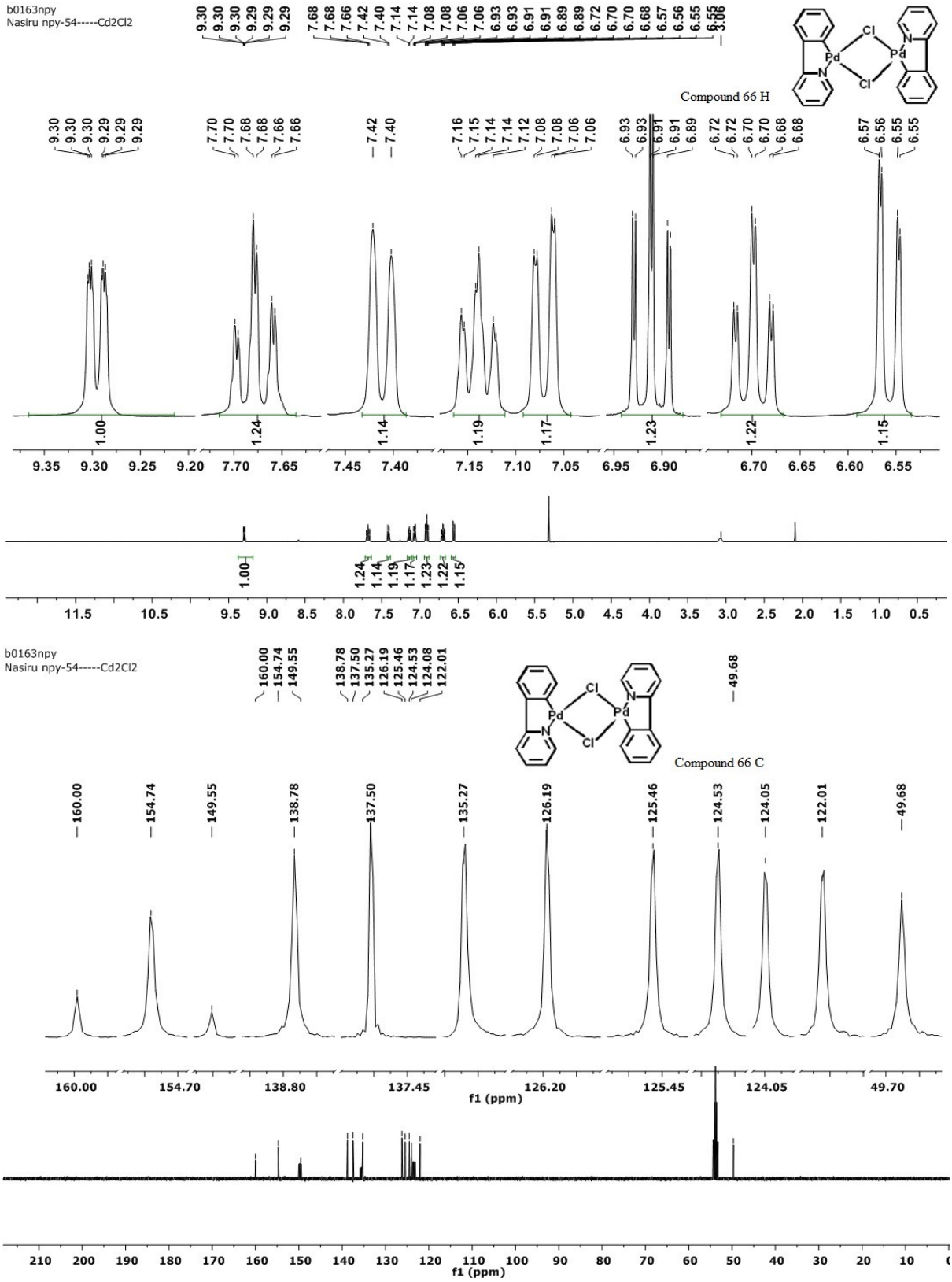

Appendix for 66

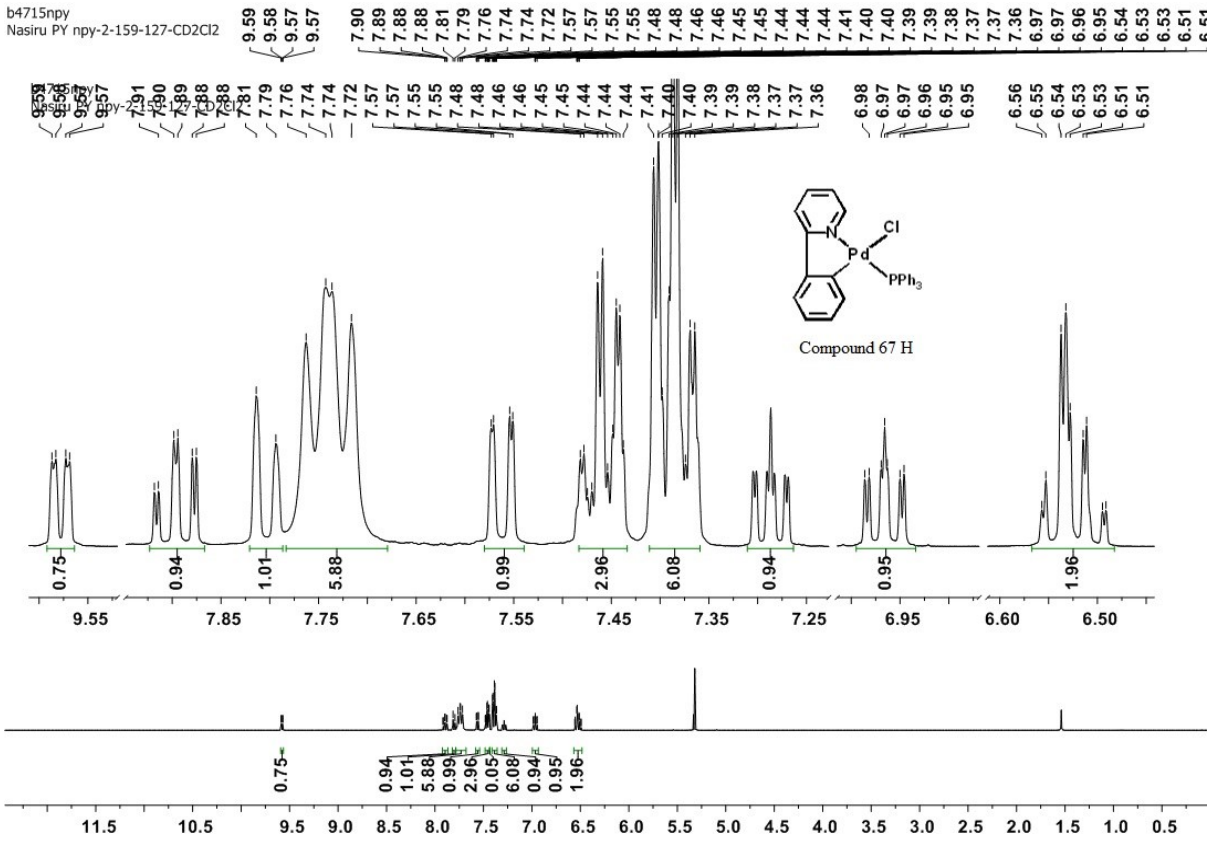

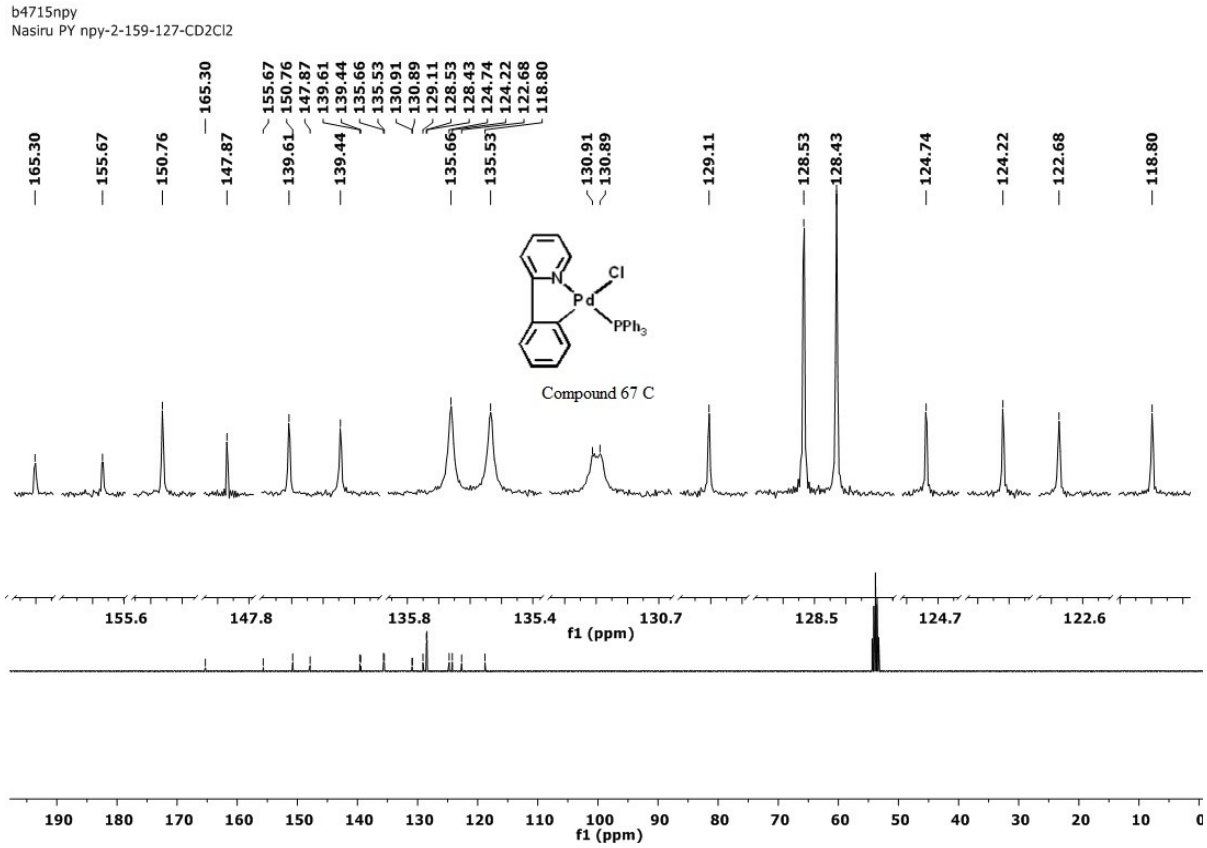

Appendix for (67)

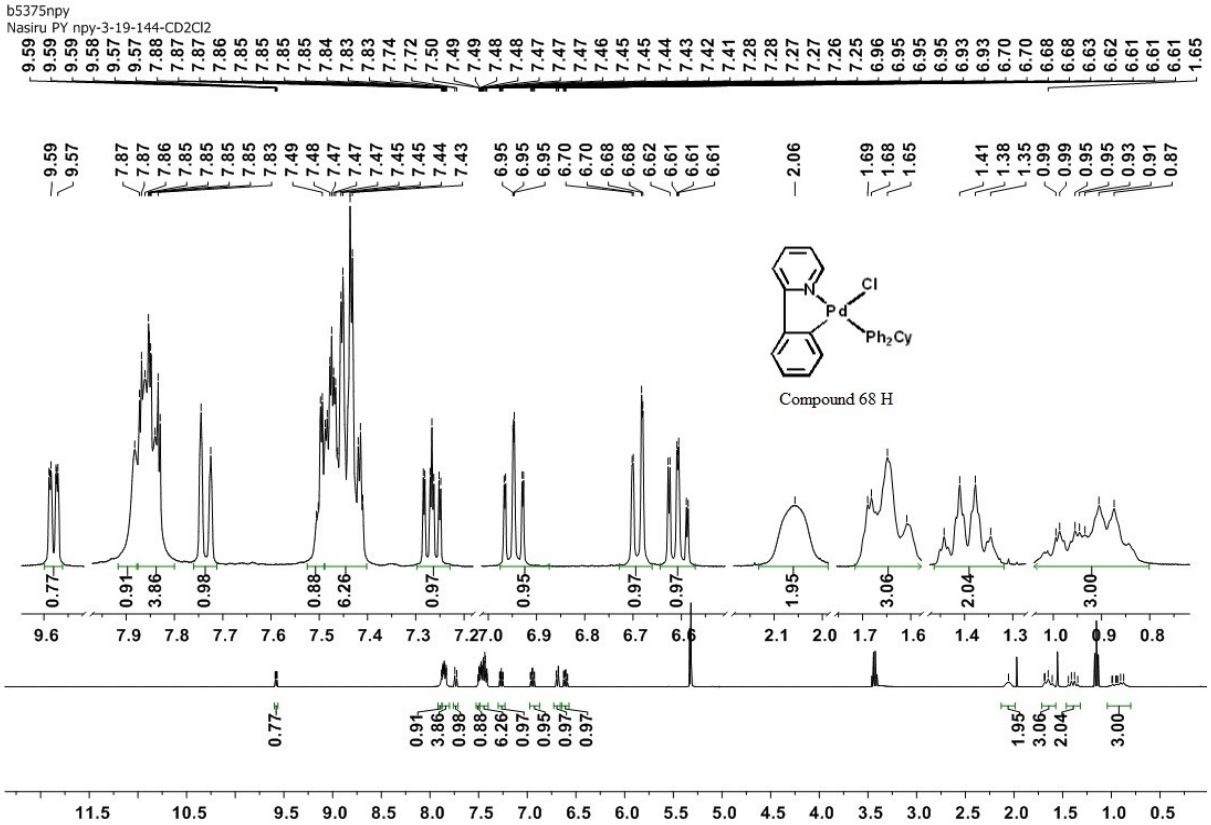

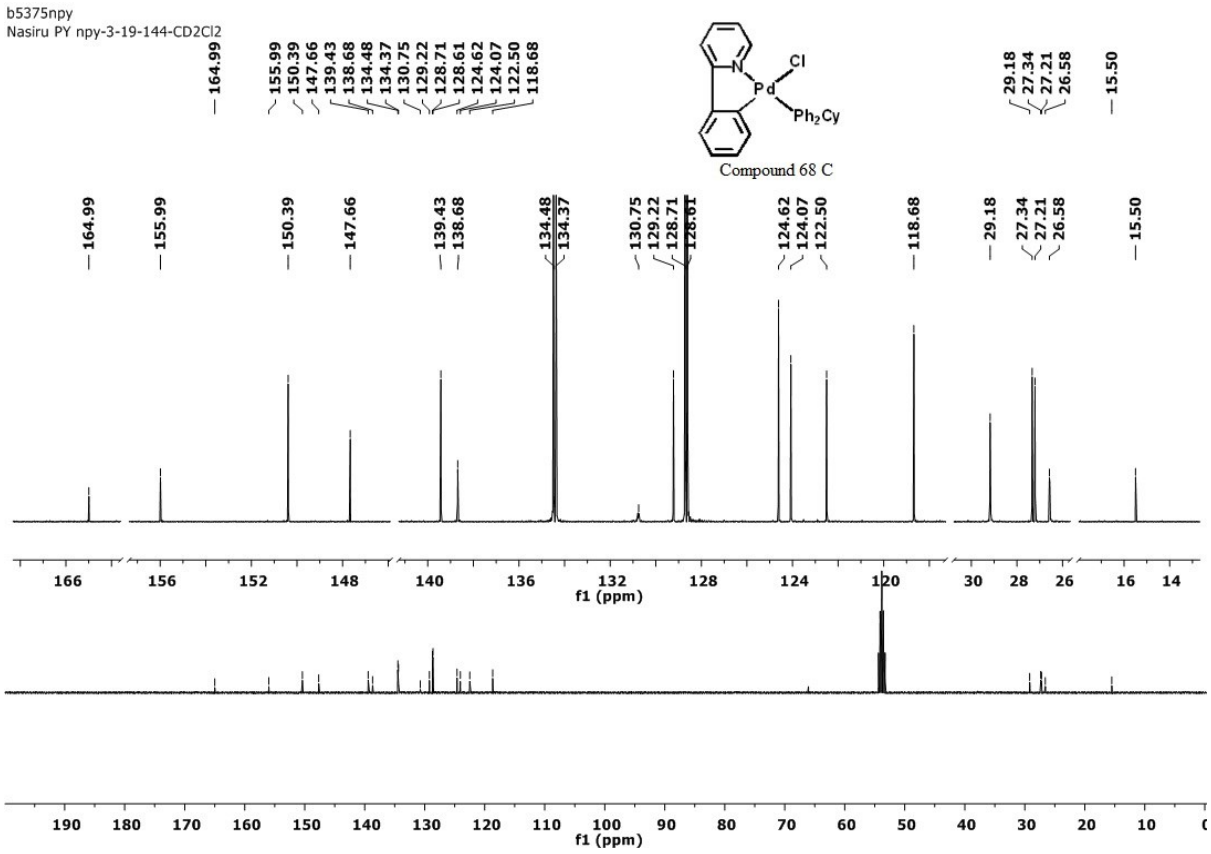

Appendix for (68)

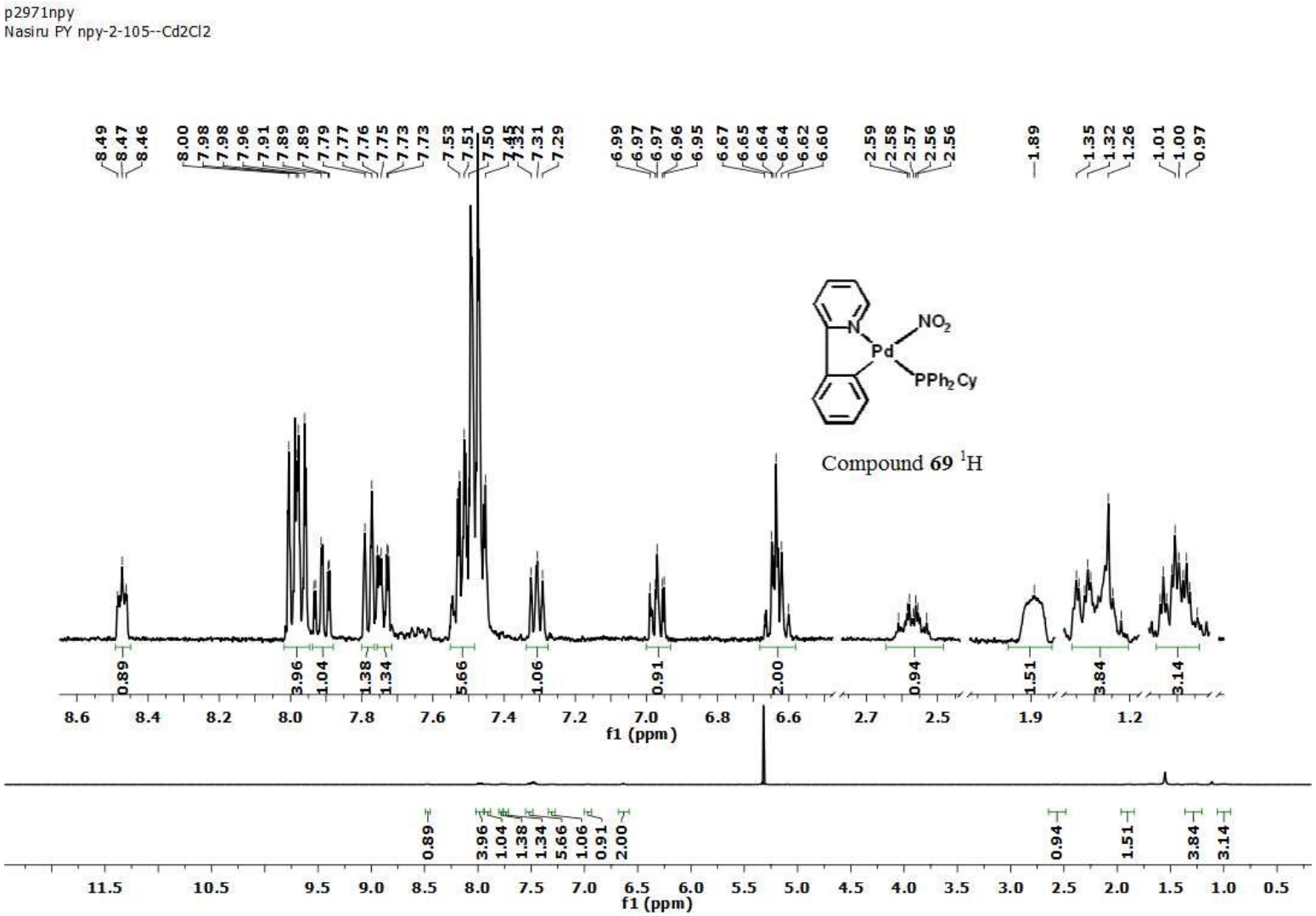

Appendix for (69)

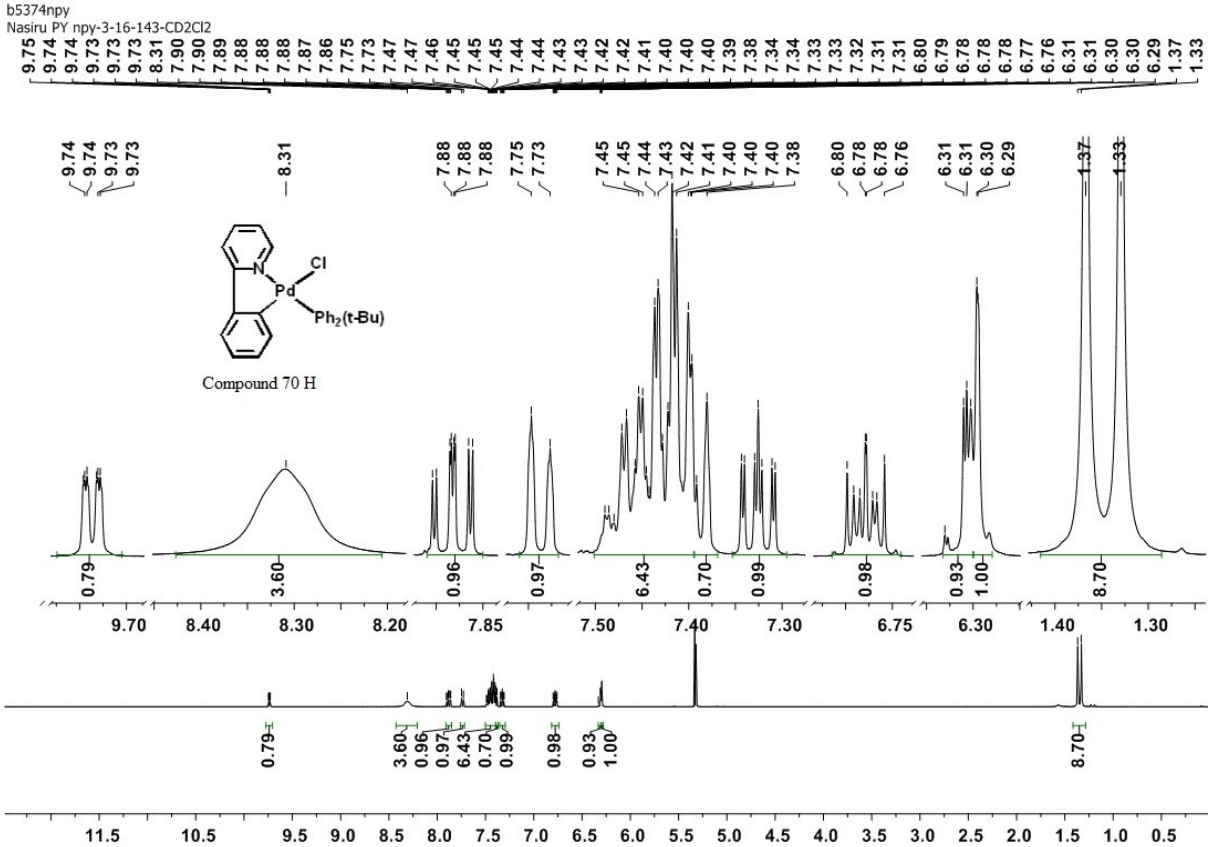

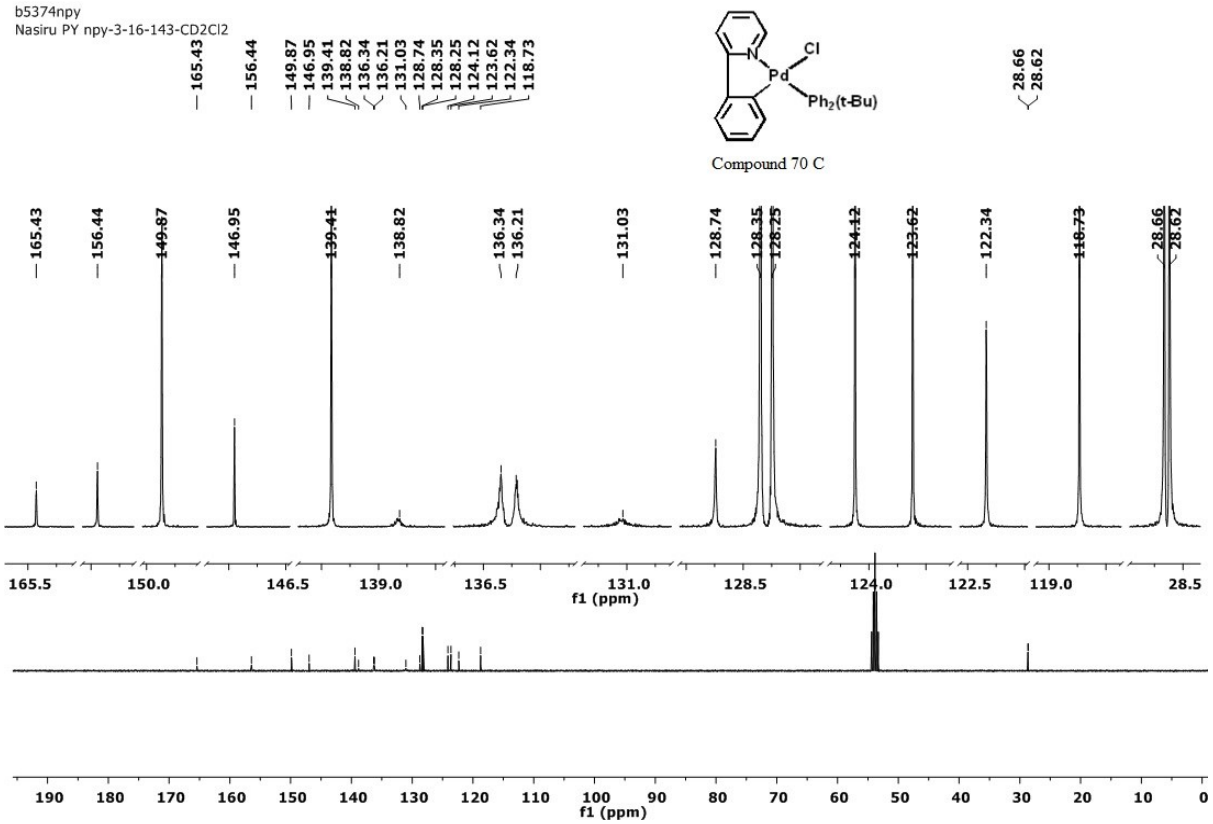

Appendix for (70)

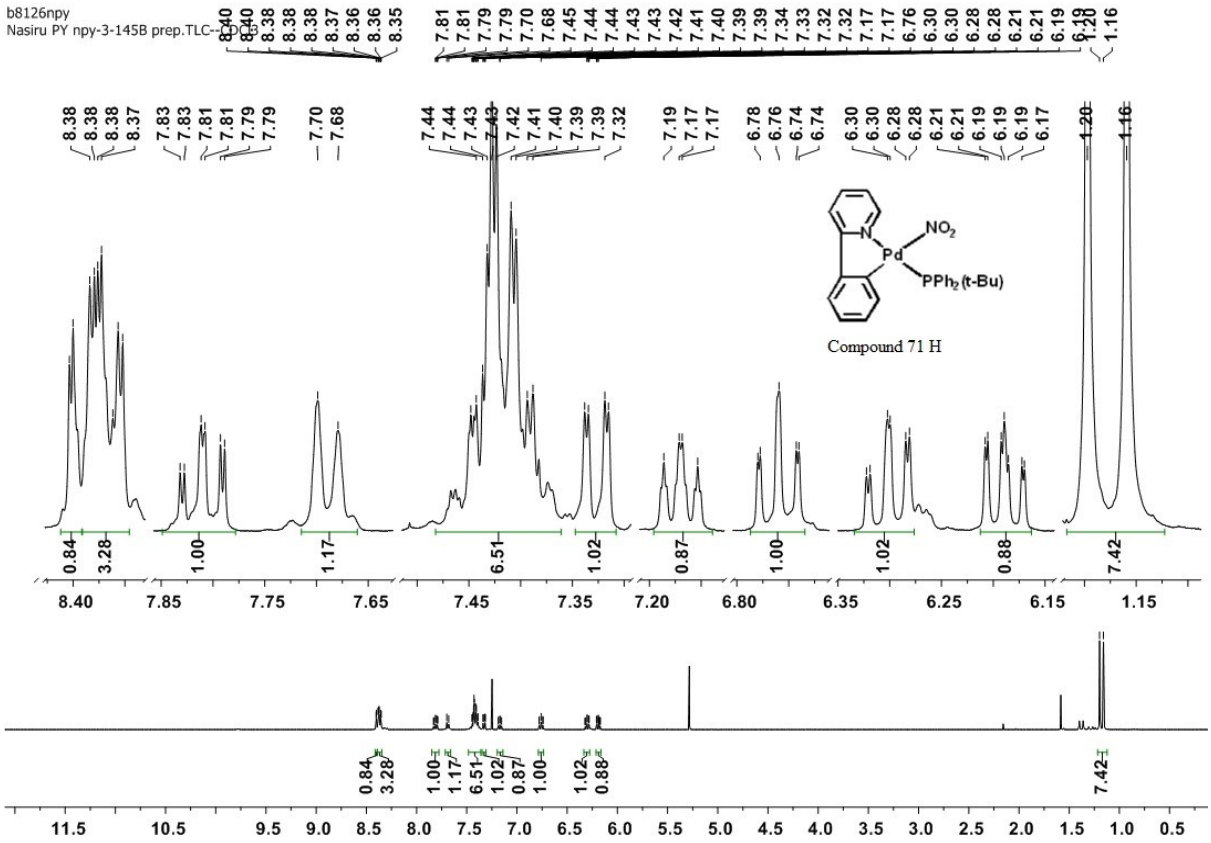

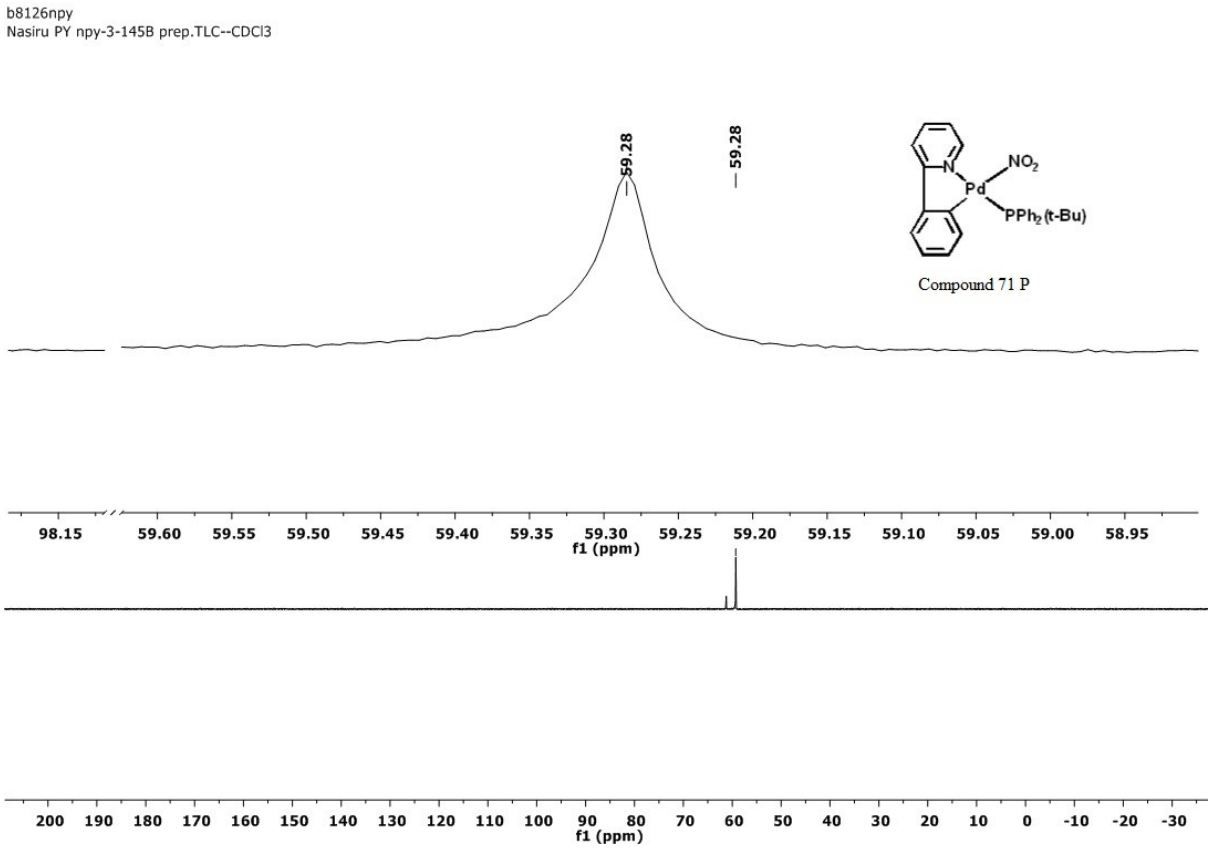

Appendix for (71)

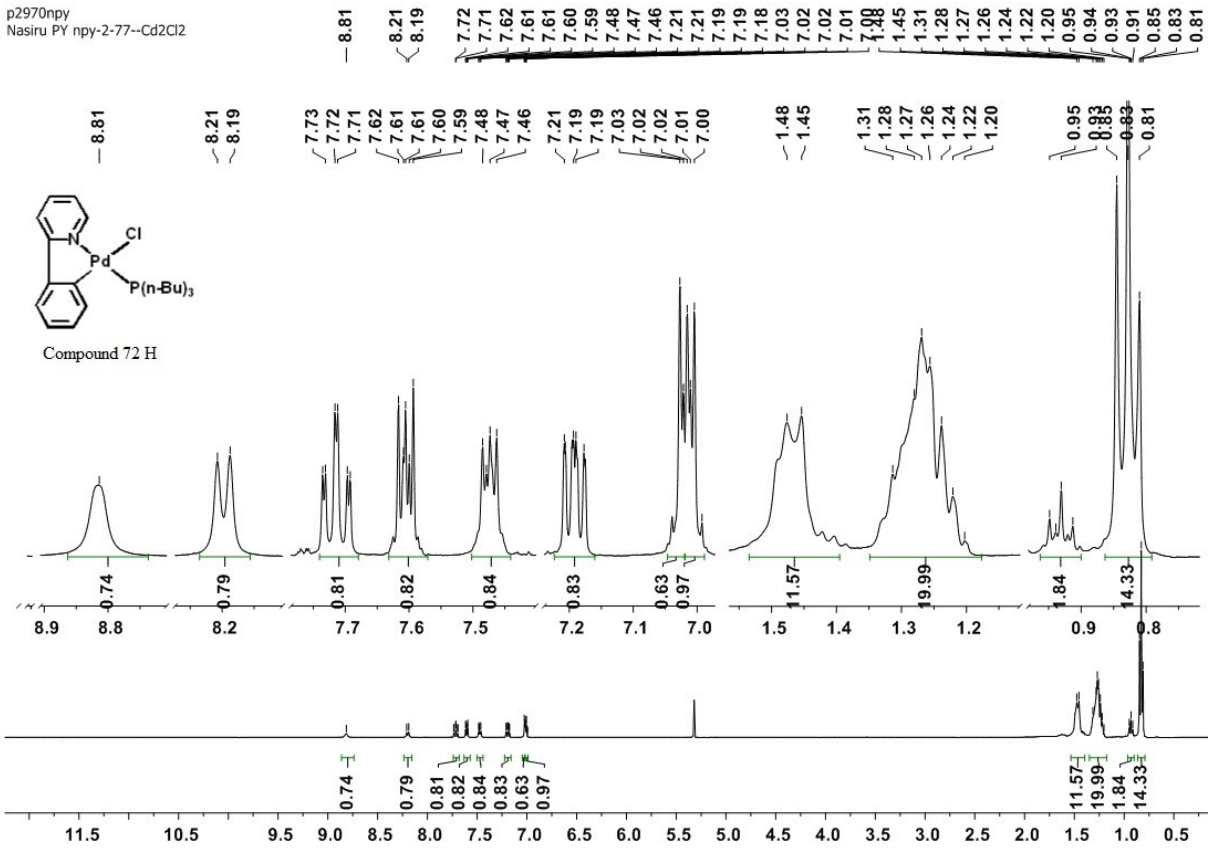

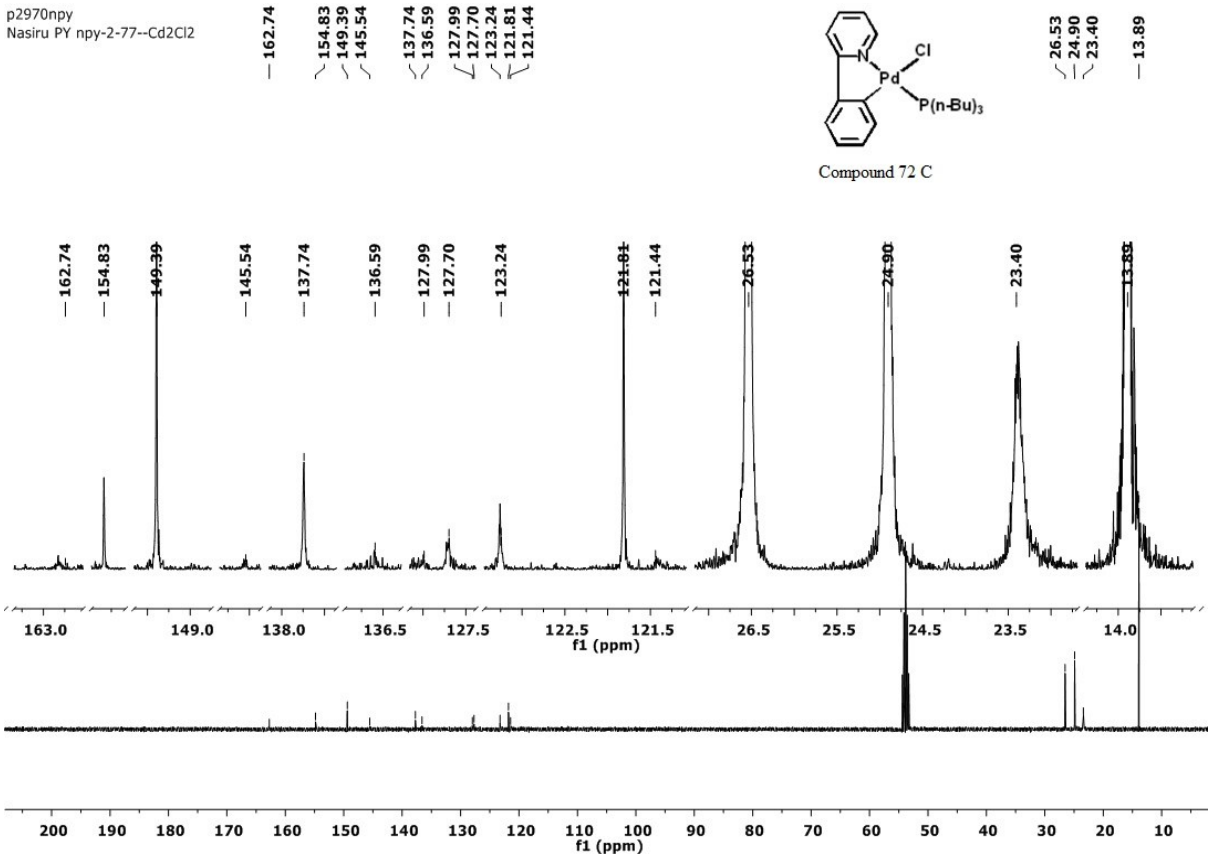

Appendix for (72)

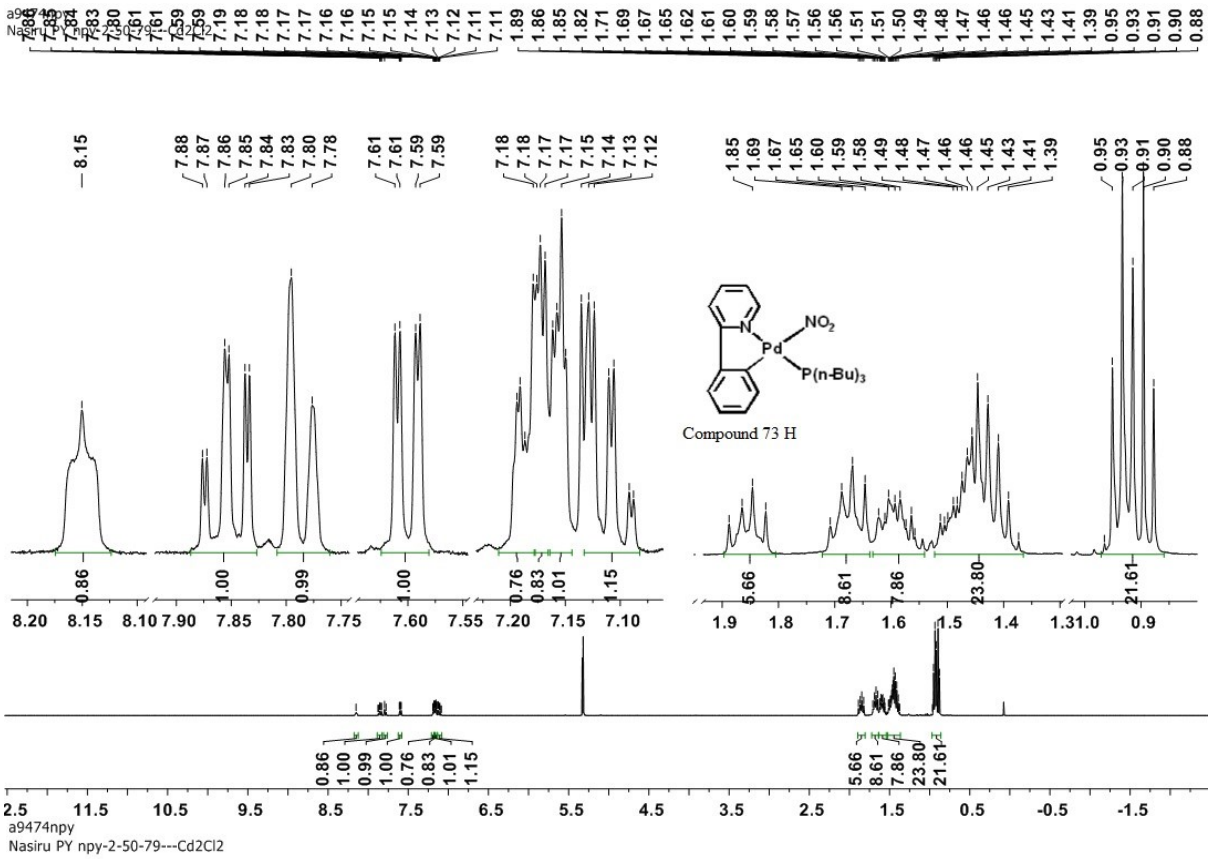

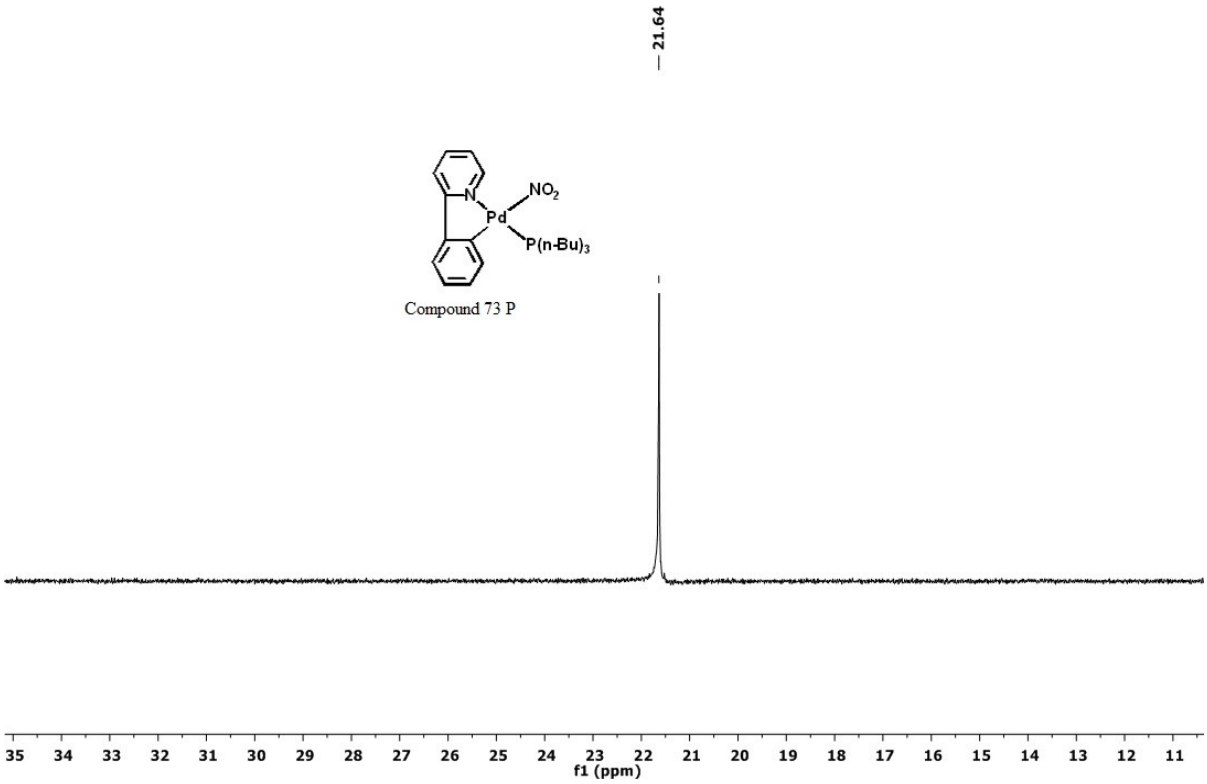

Appendix for (73)

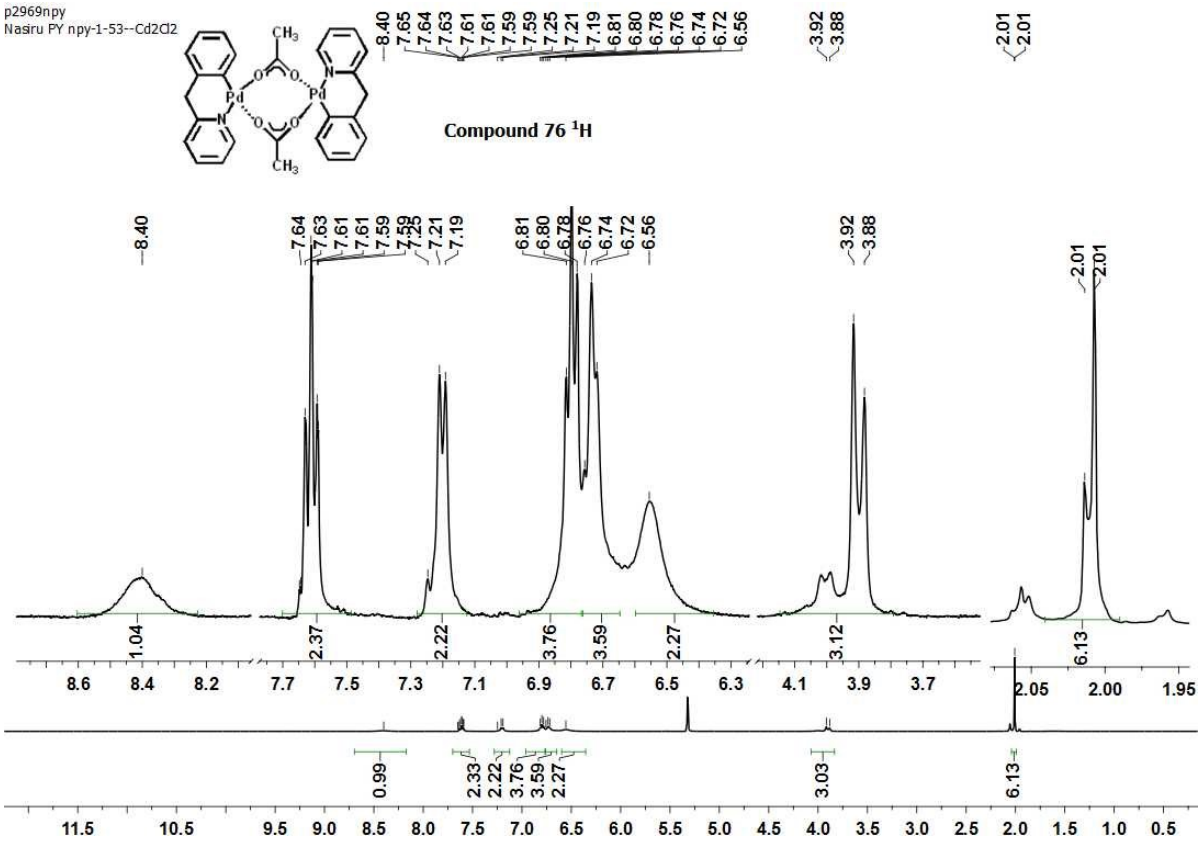

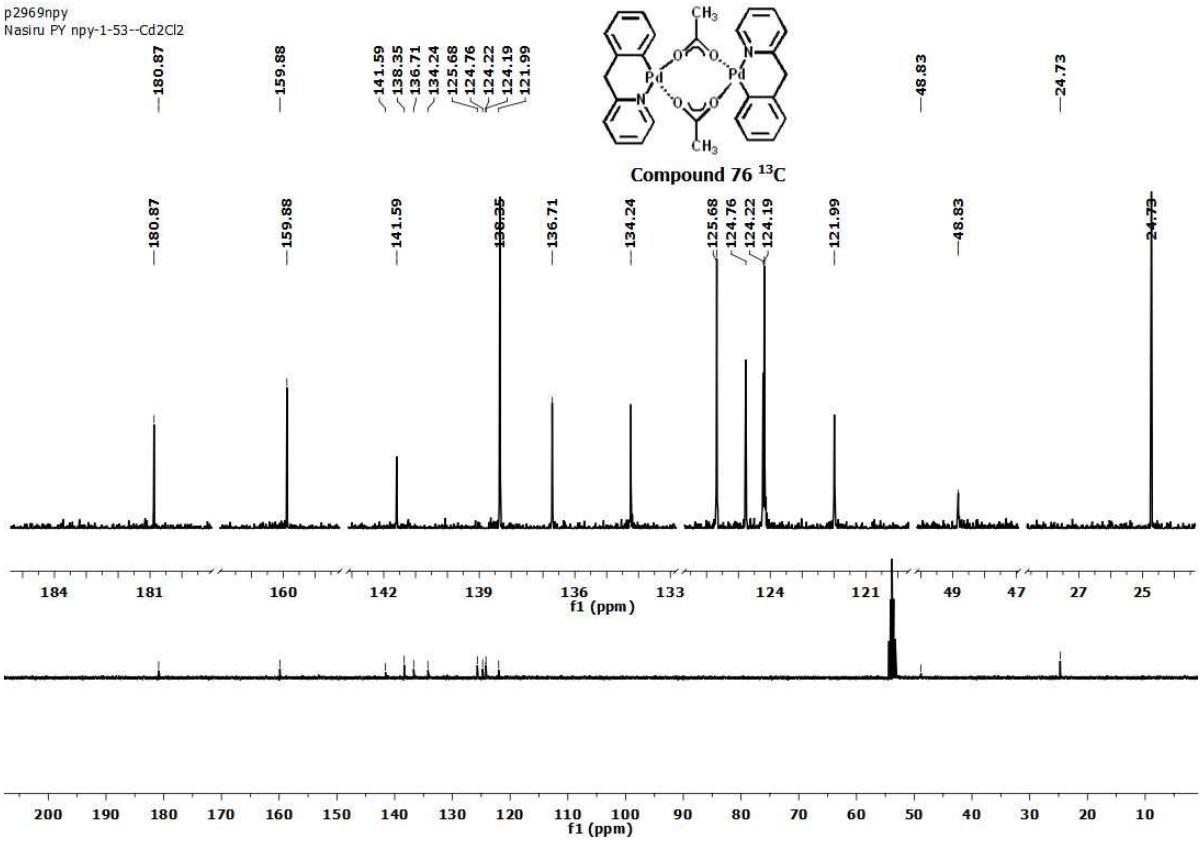

Appendix for (76)

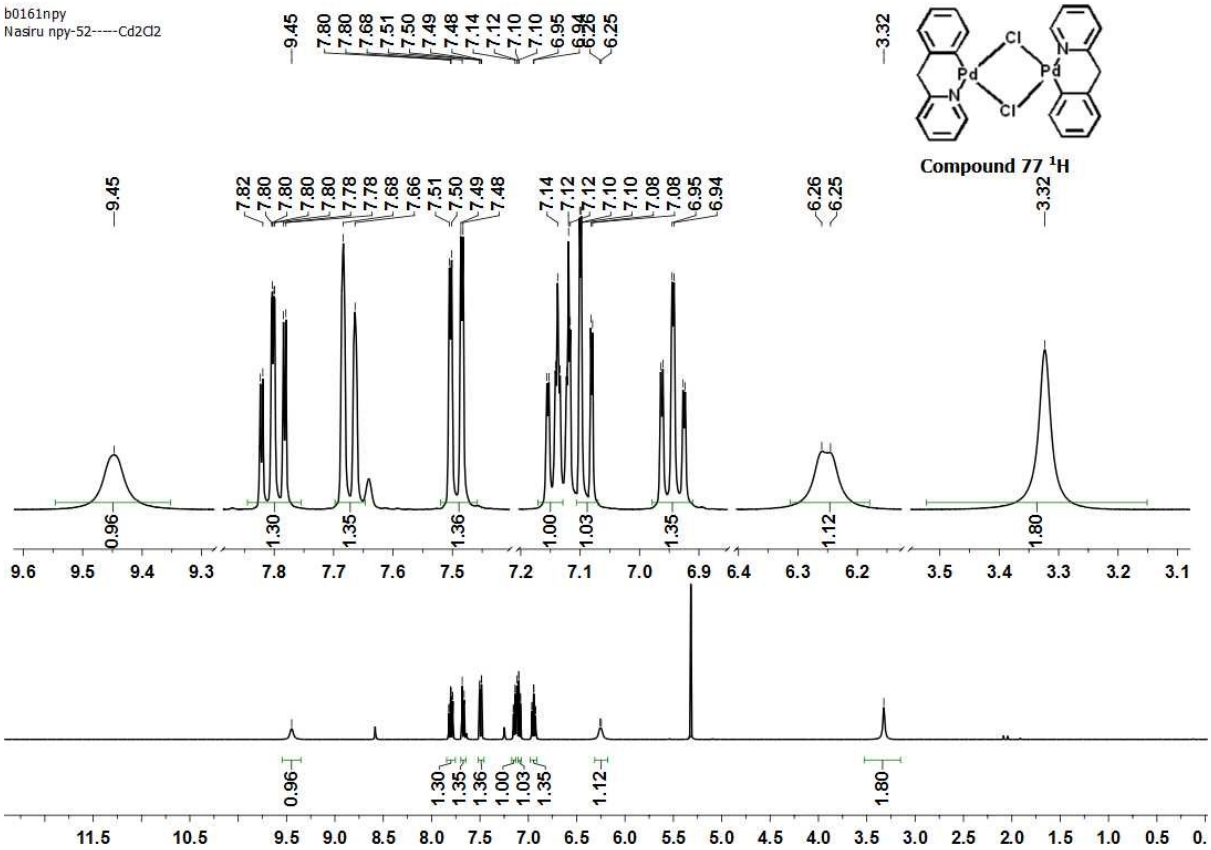

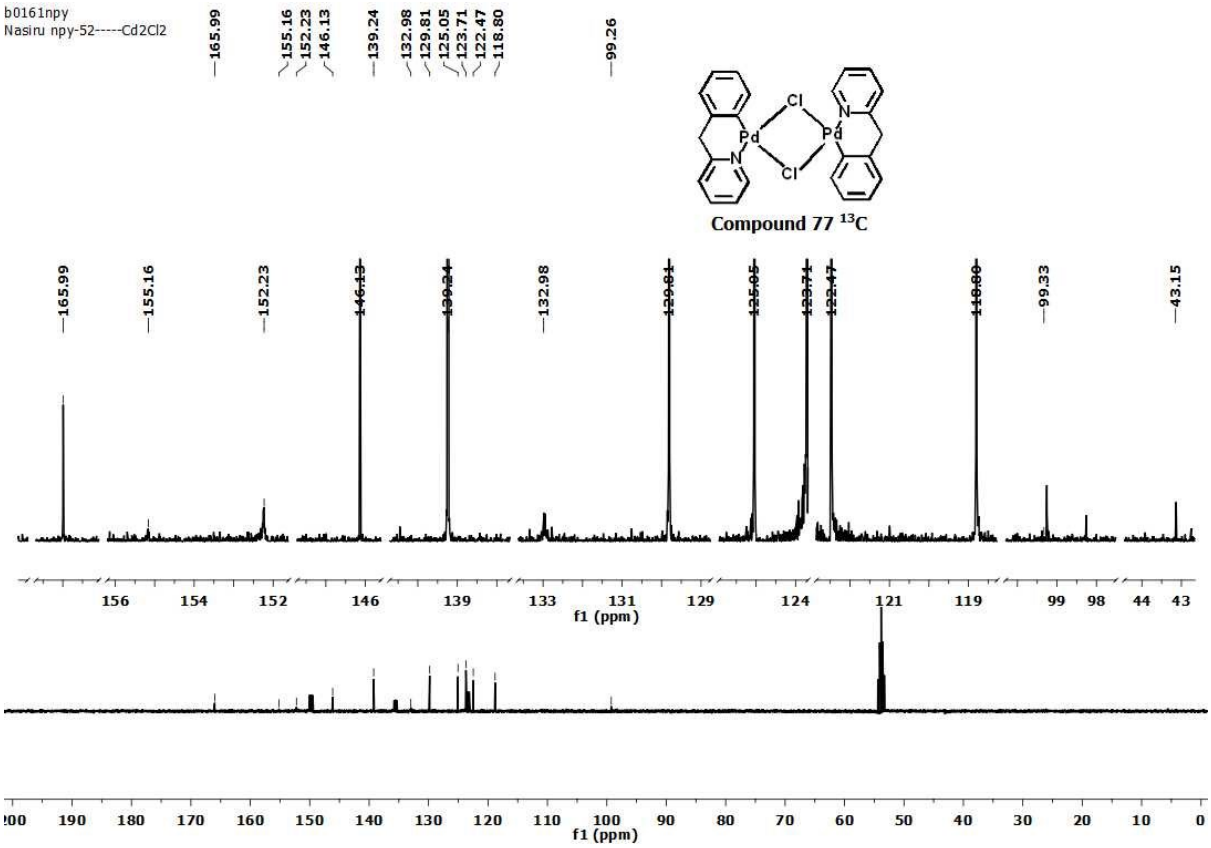

Appendix for (77)

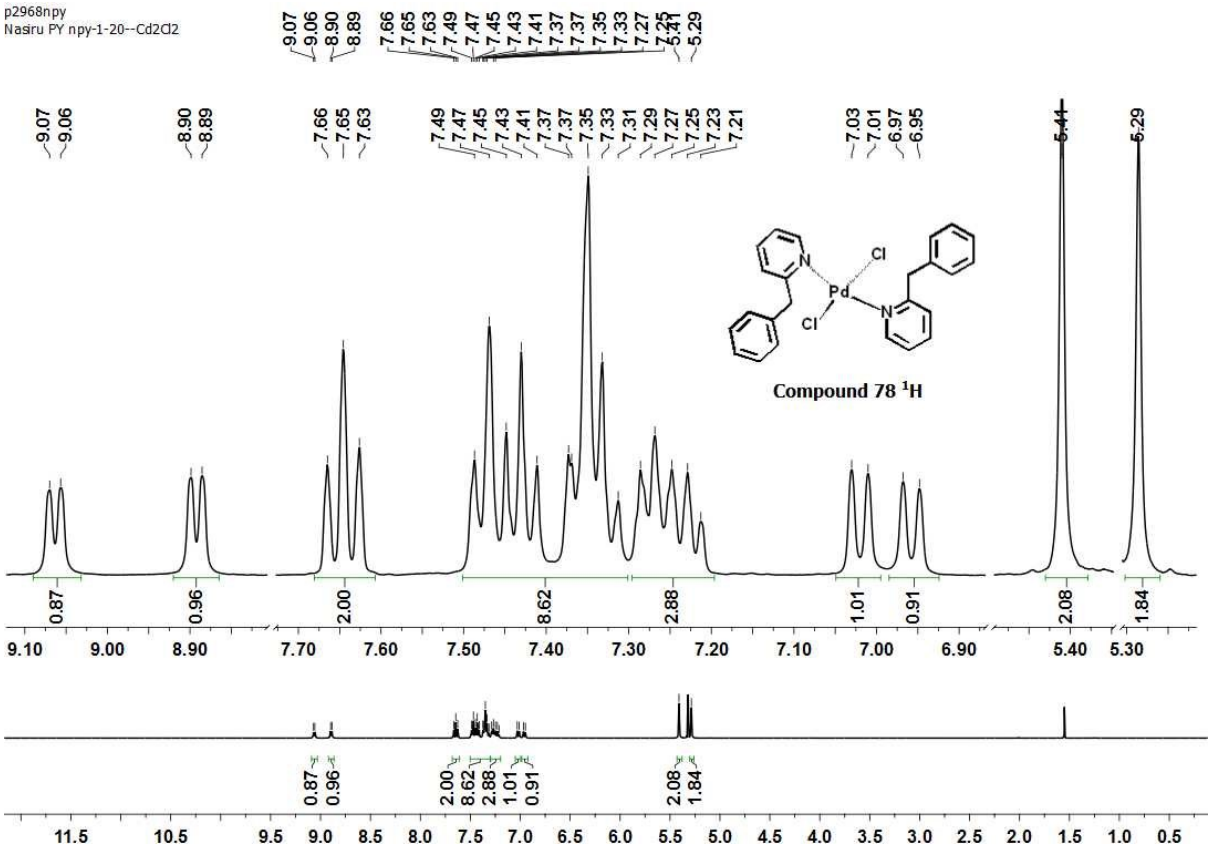

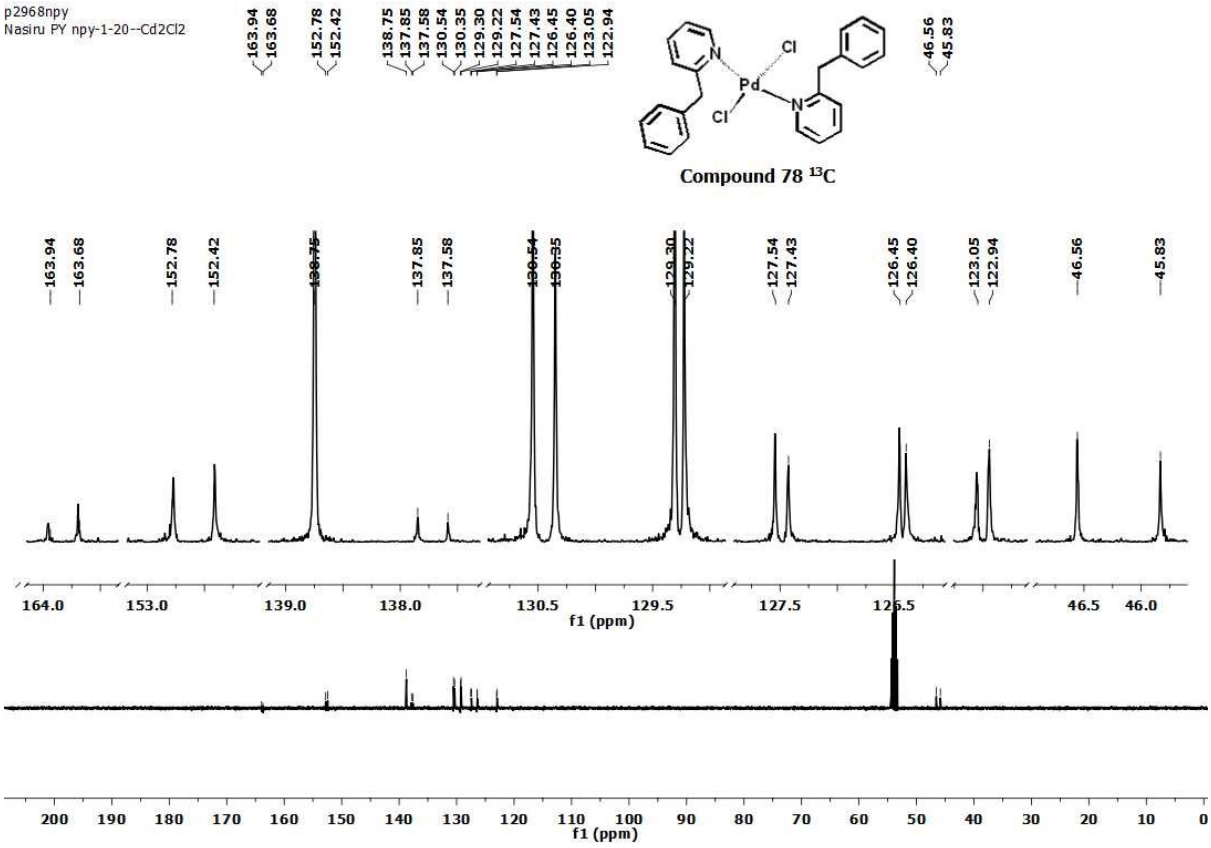

Appendix for (78)

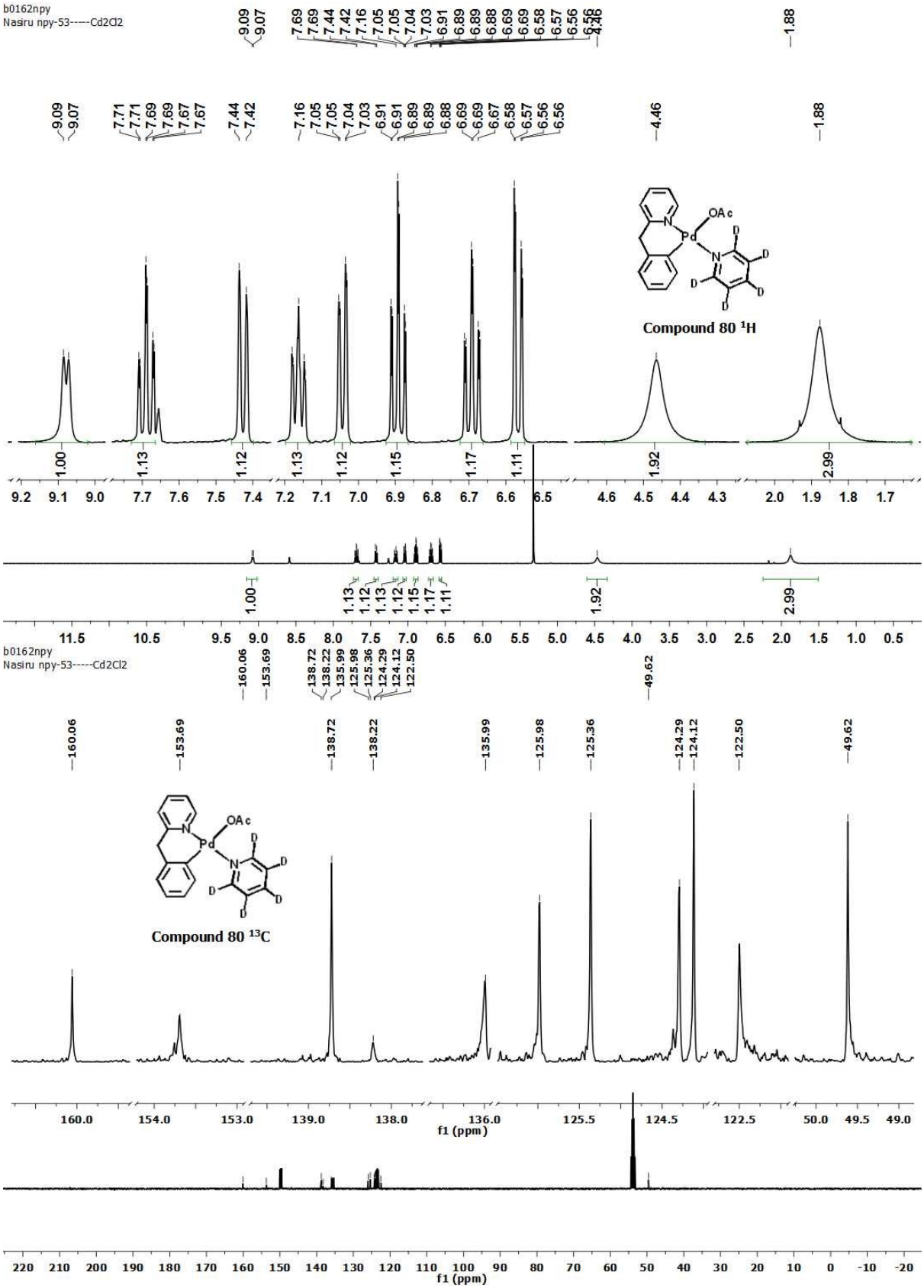

Appendix for (80)

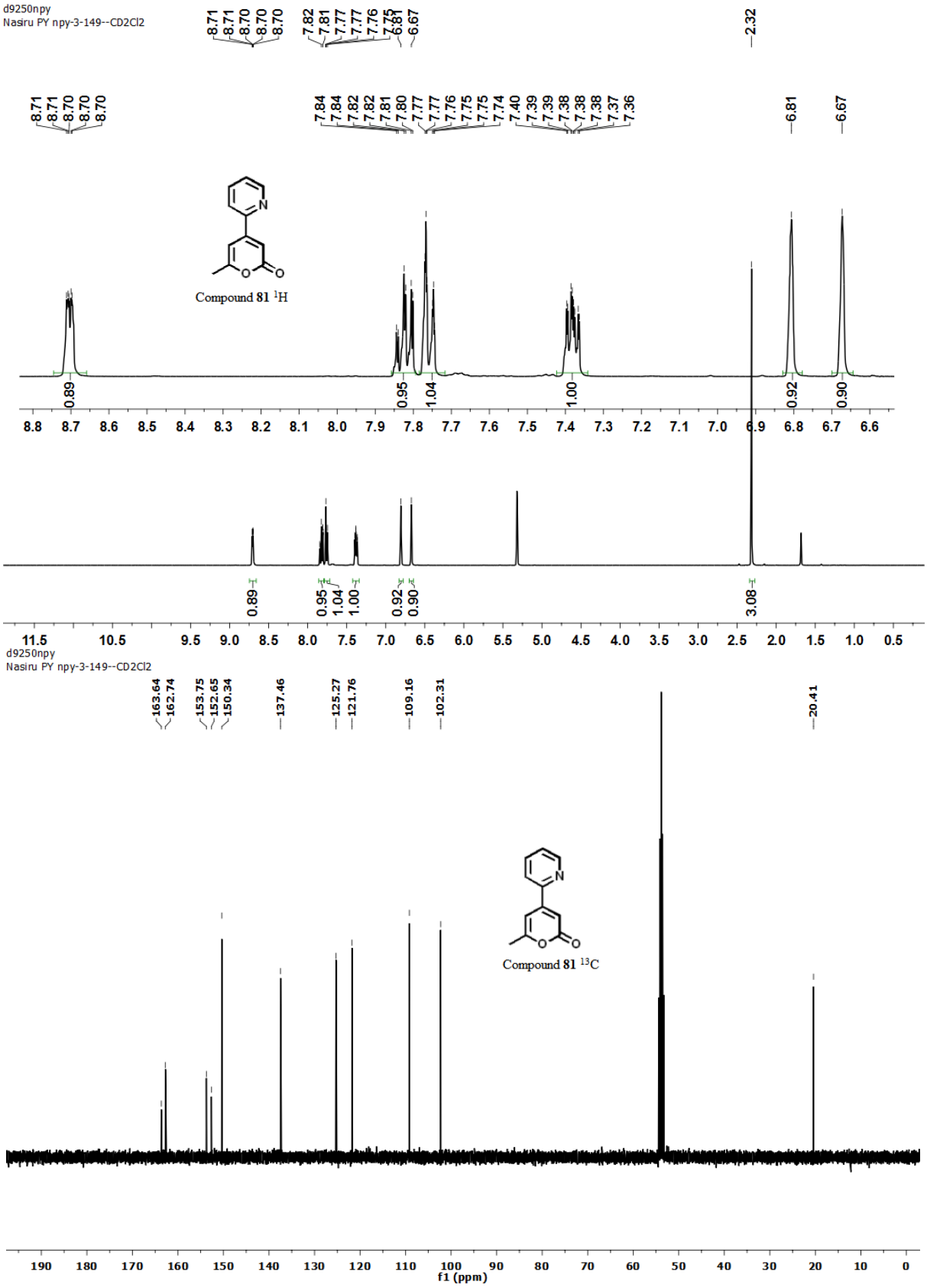

Appendix for (81)

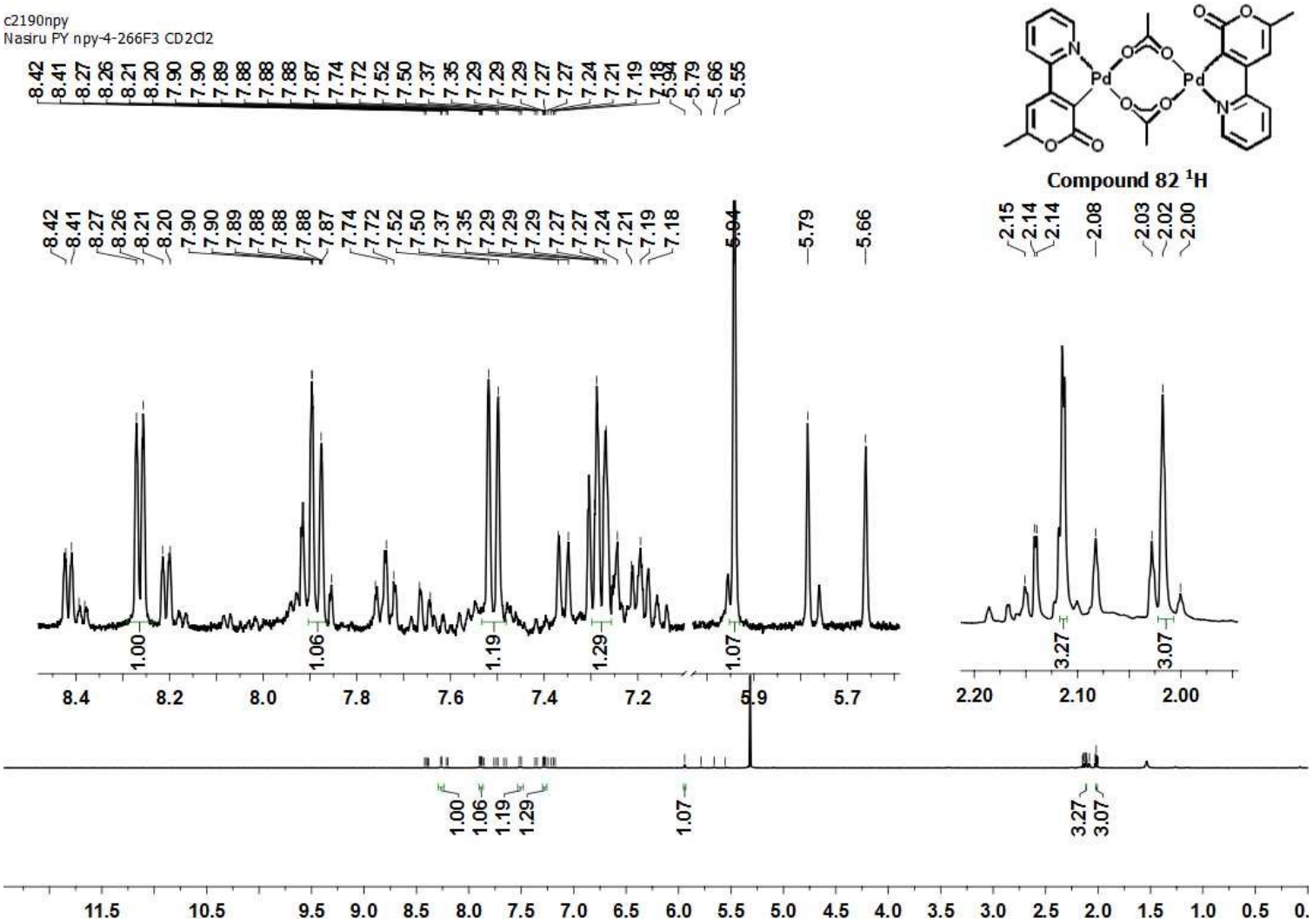

Appendix for (82)

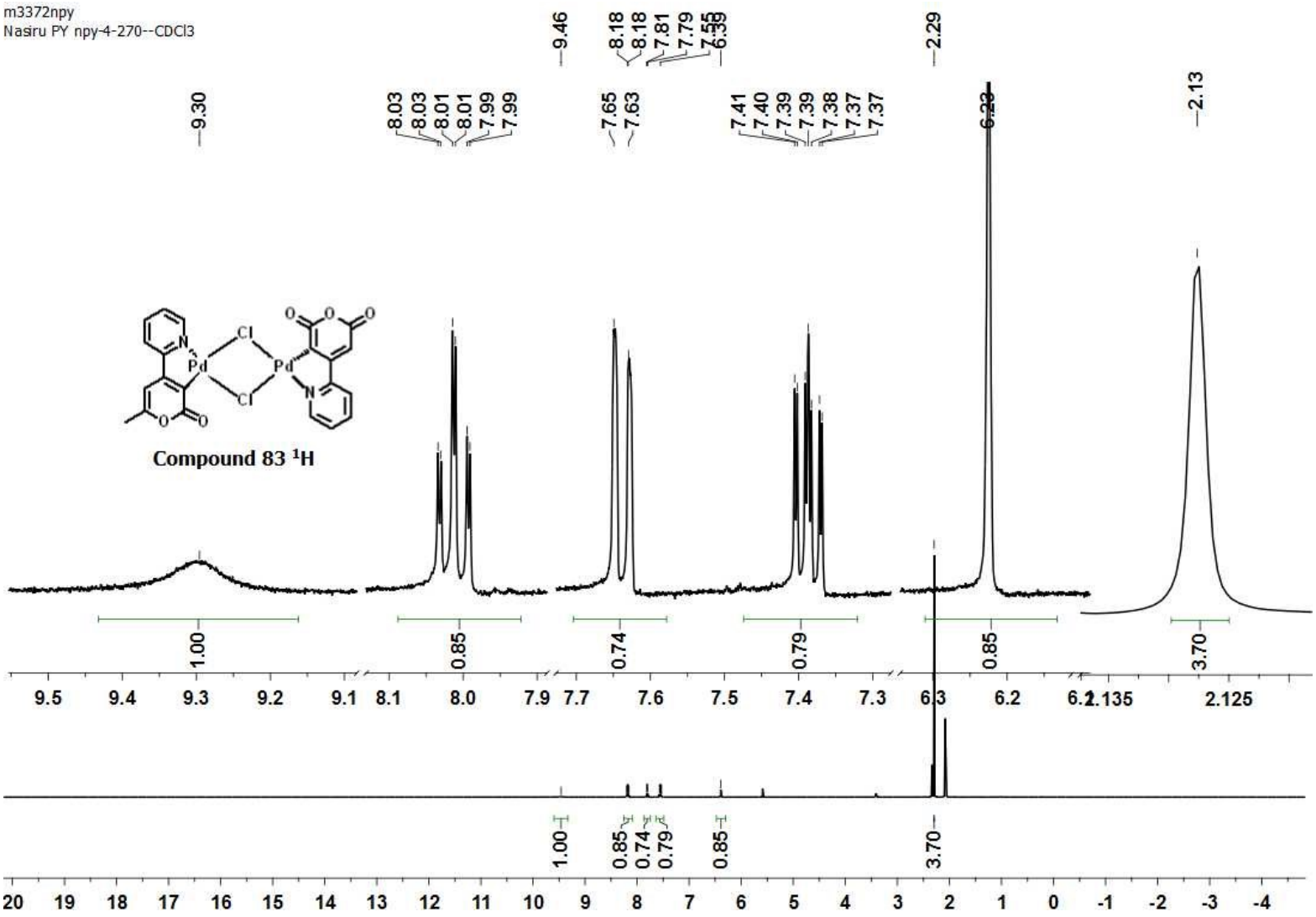

Appendix for (83)

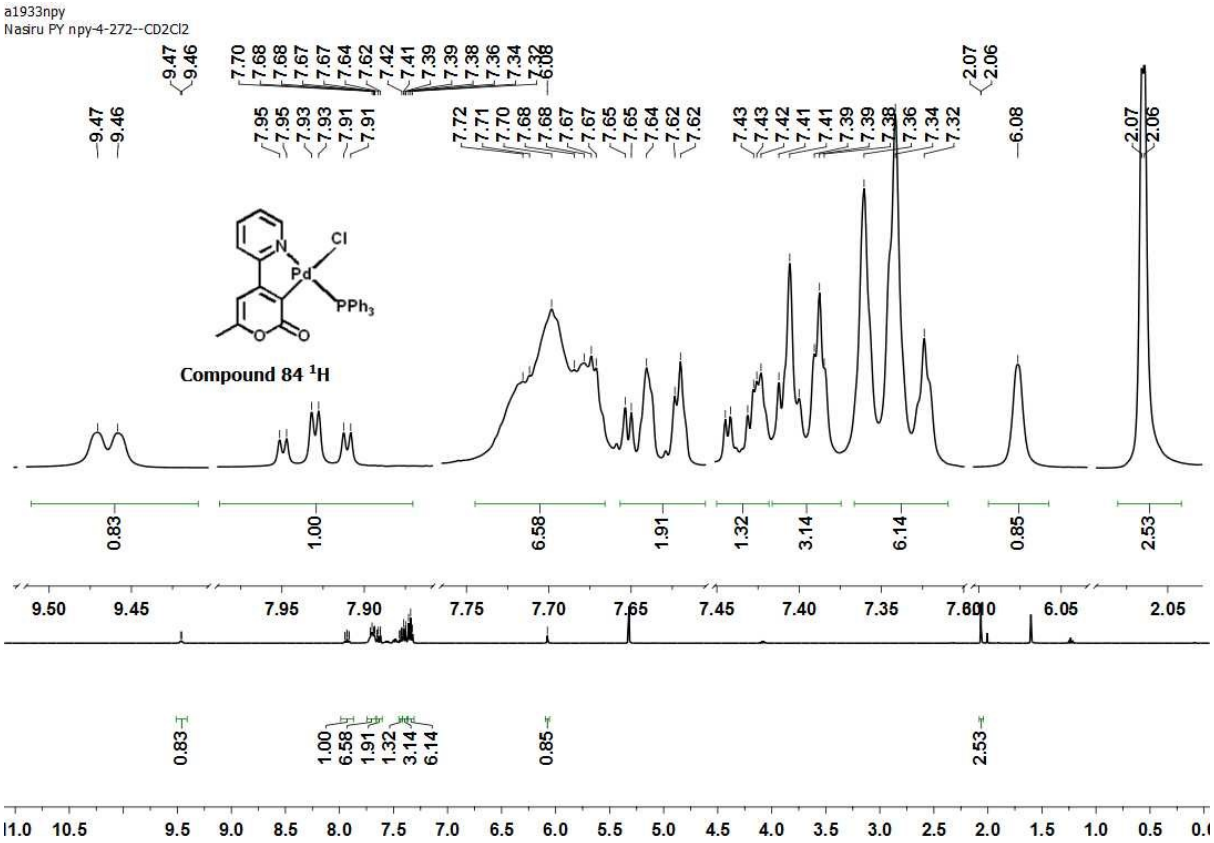

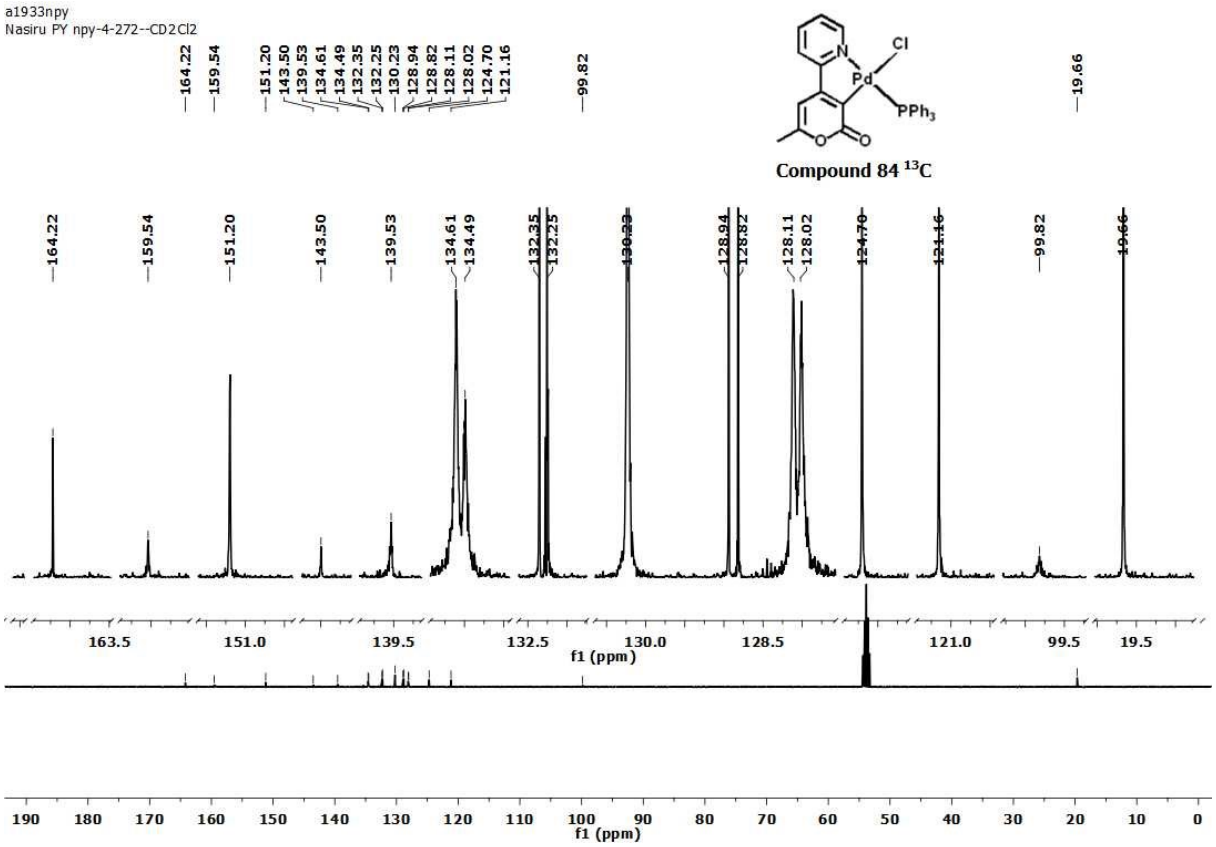

Appendix for (84)

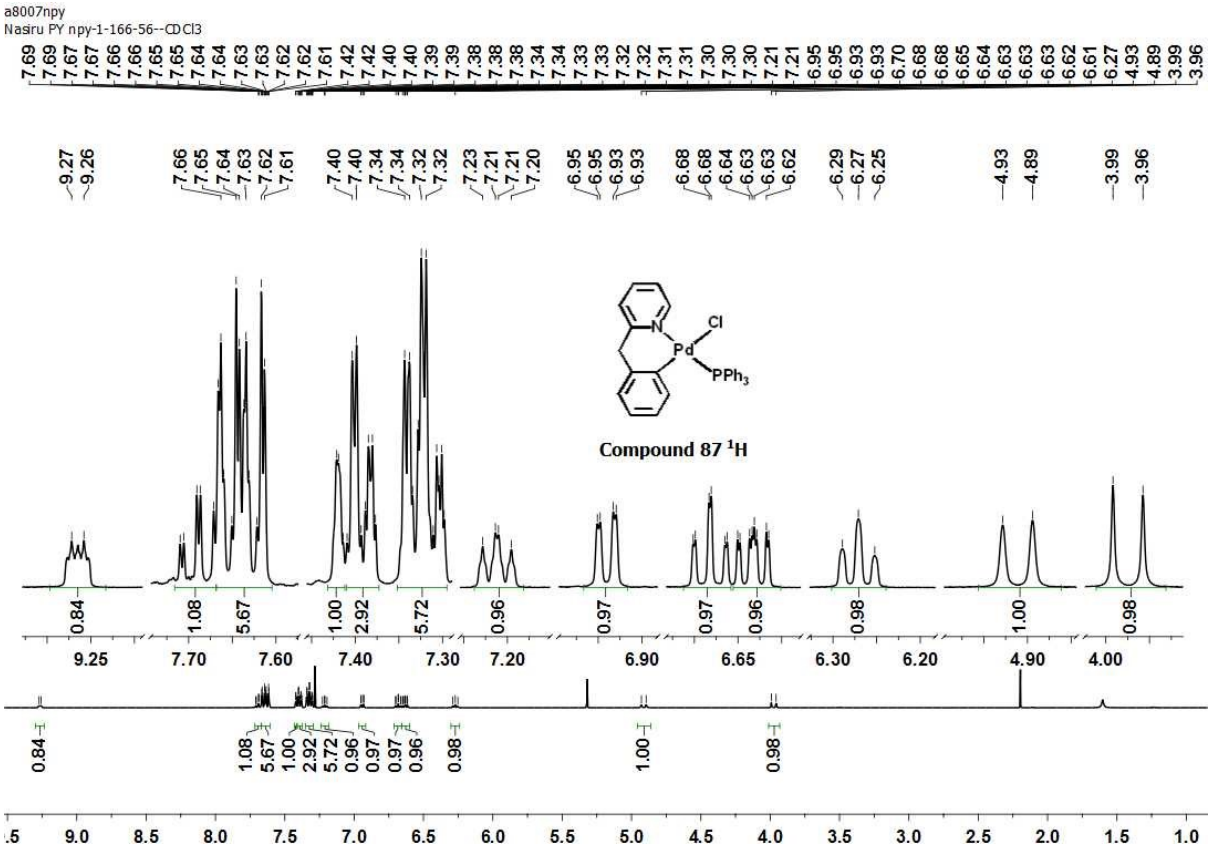

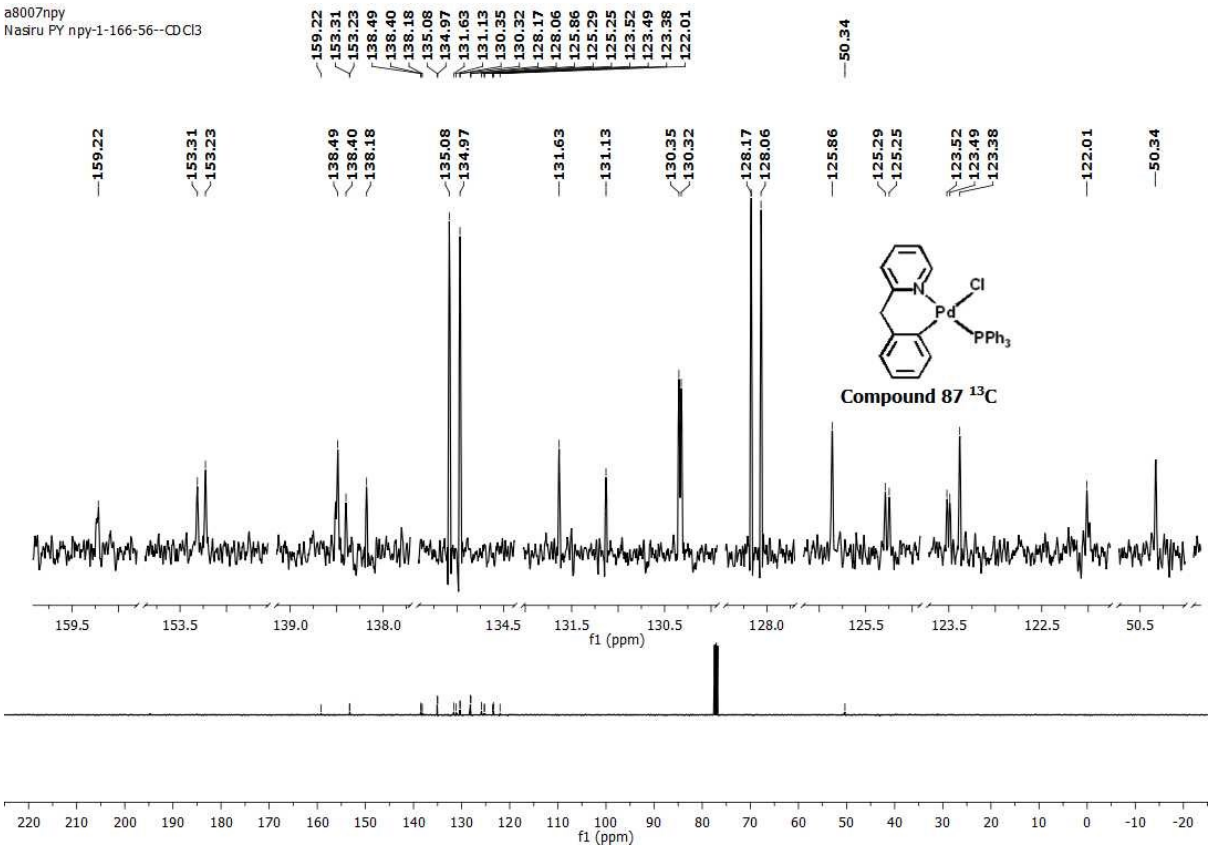

Appendix for (87)

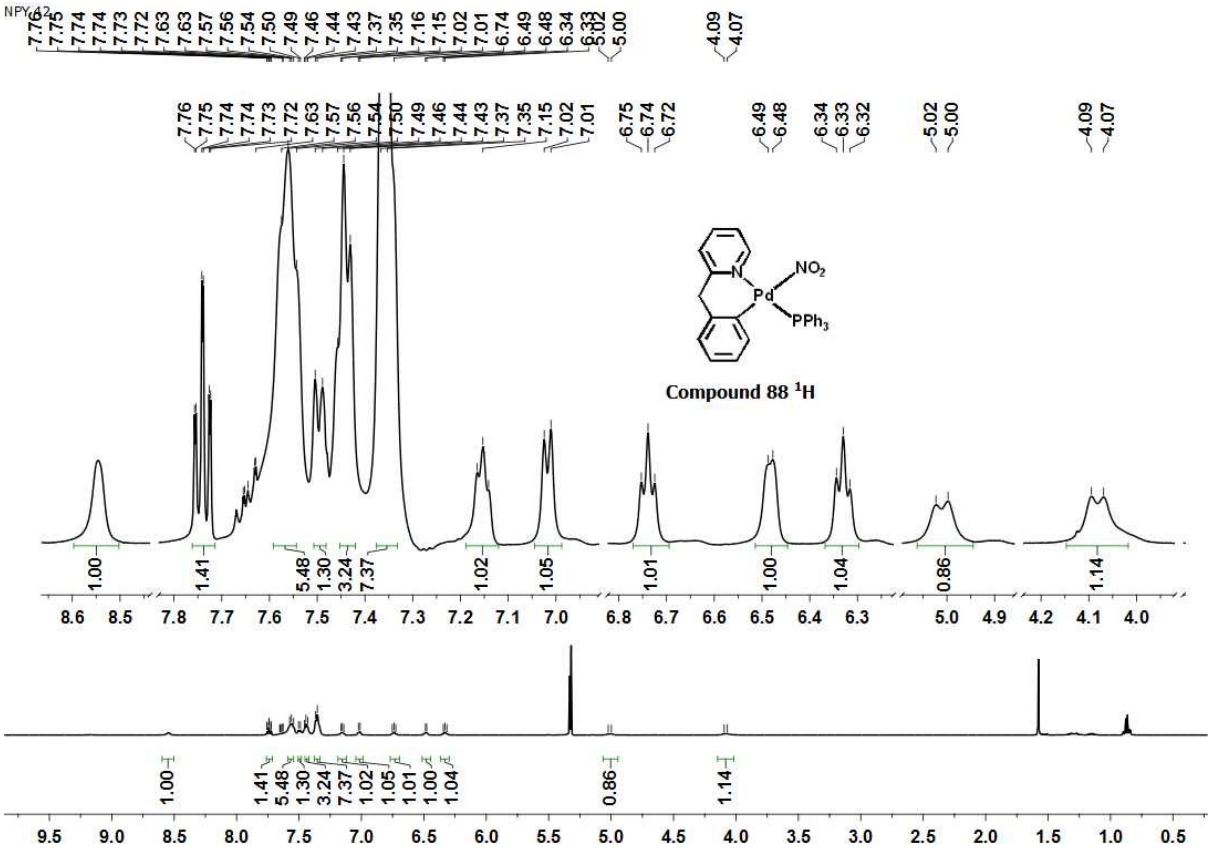

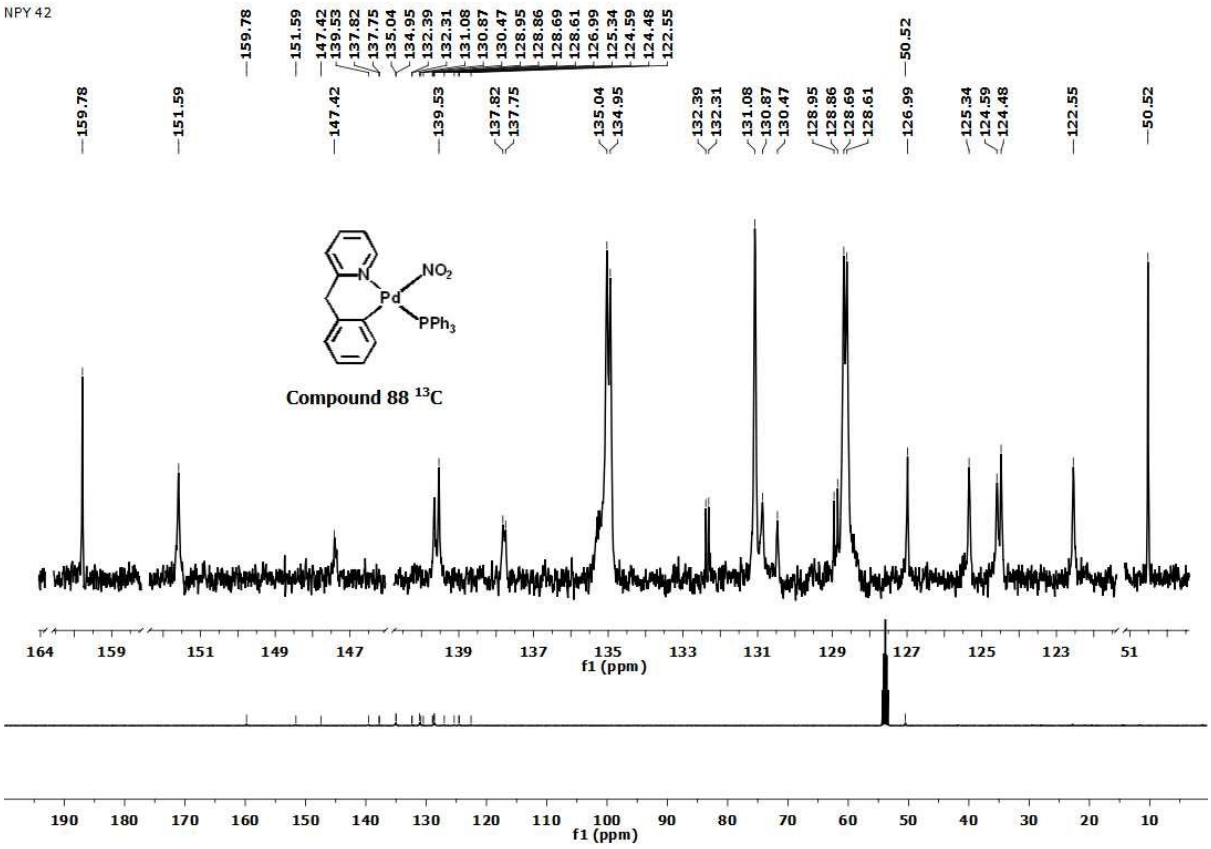

Appendix for (88)

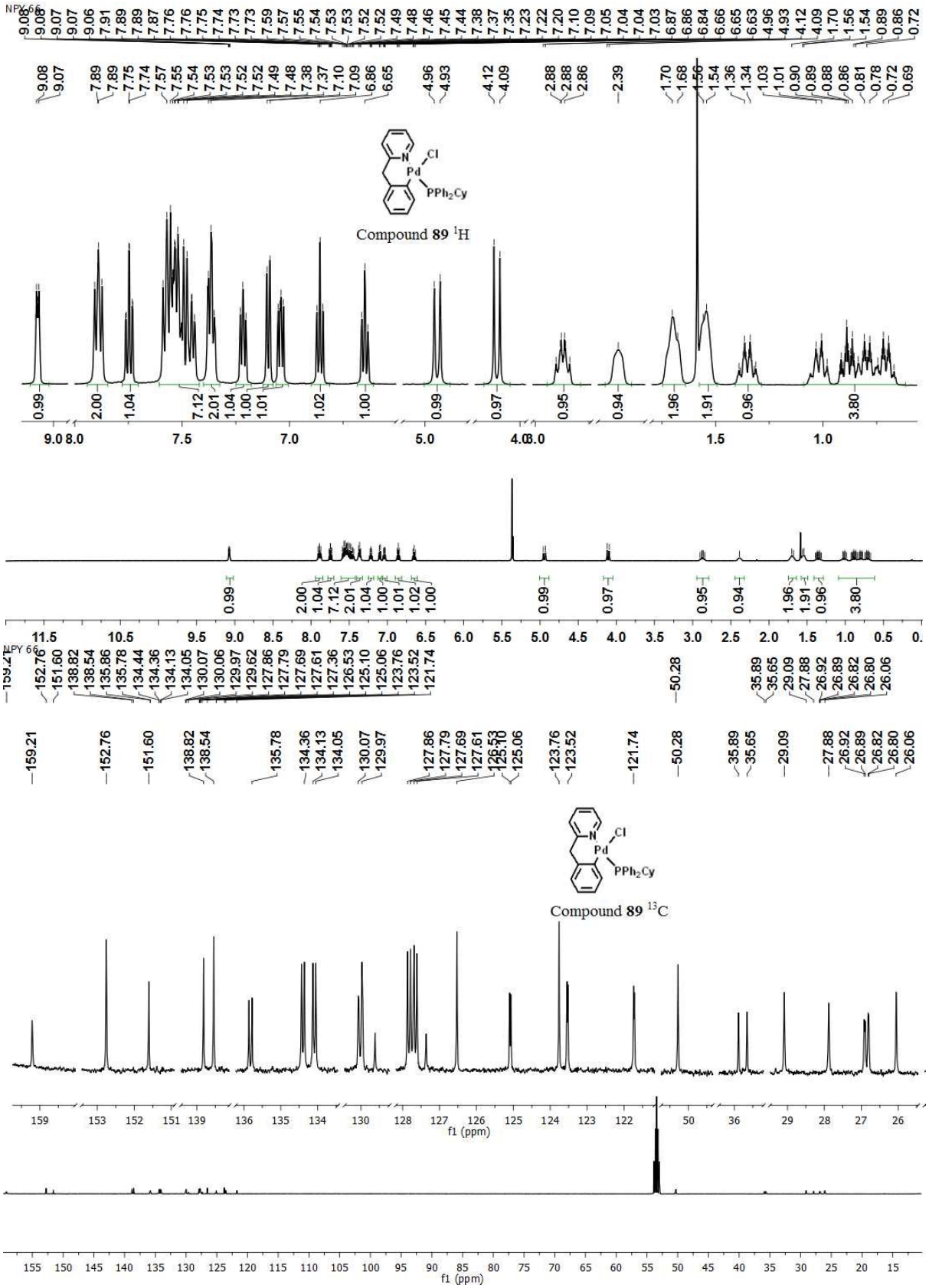

Appendix for (89)

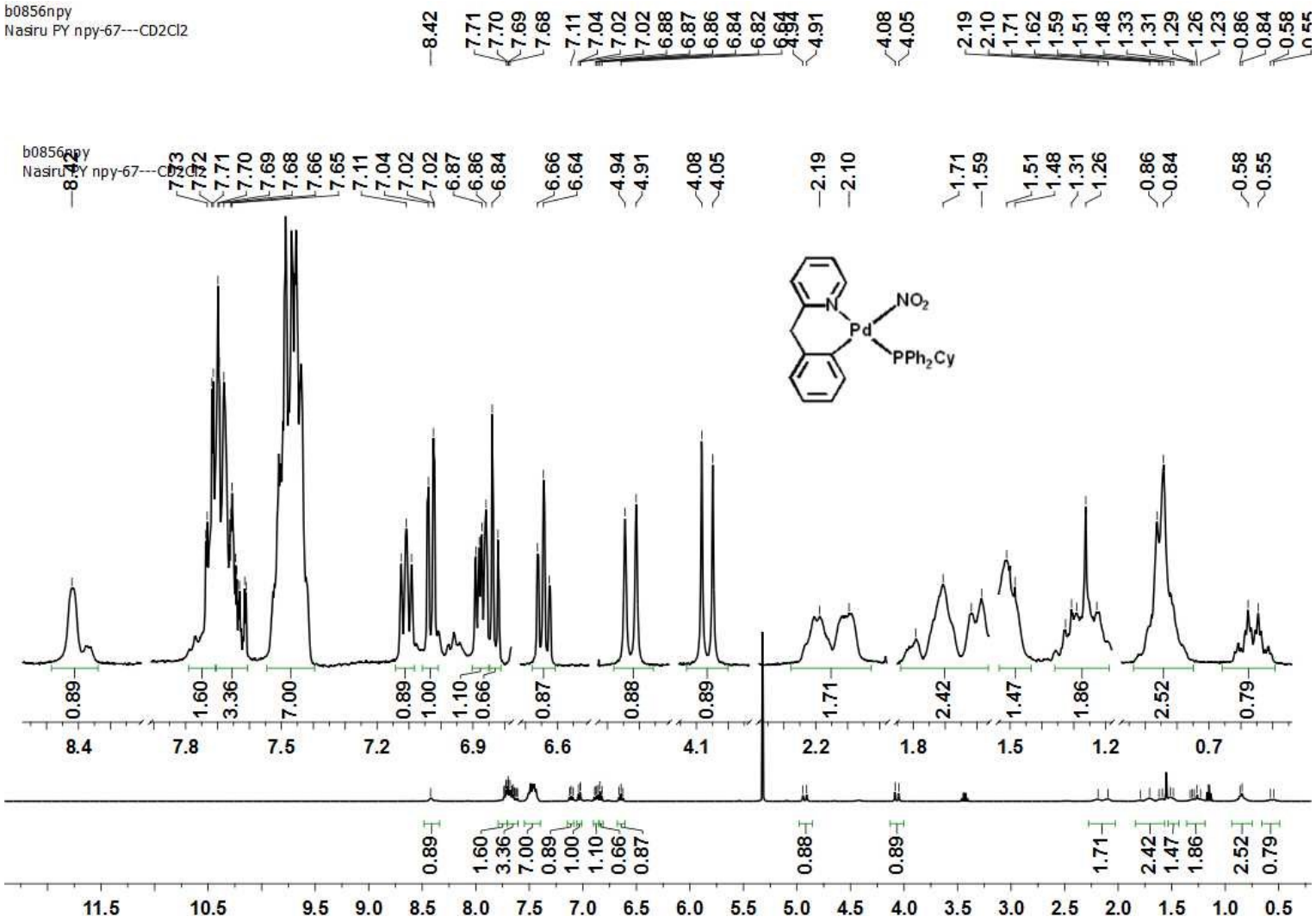

Appendix for (90)

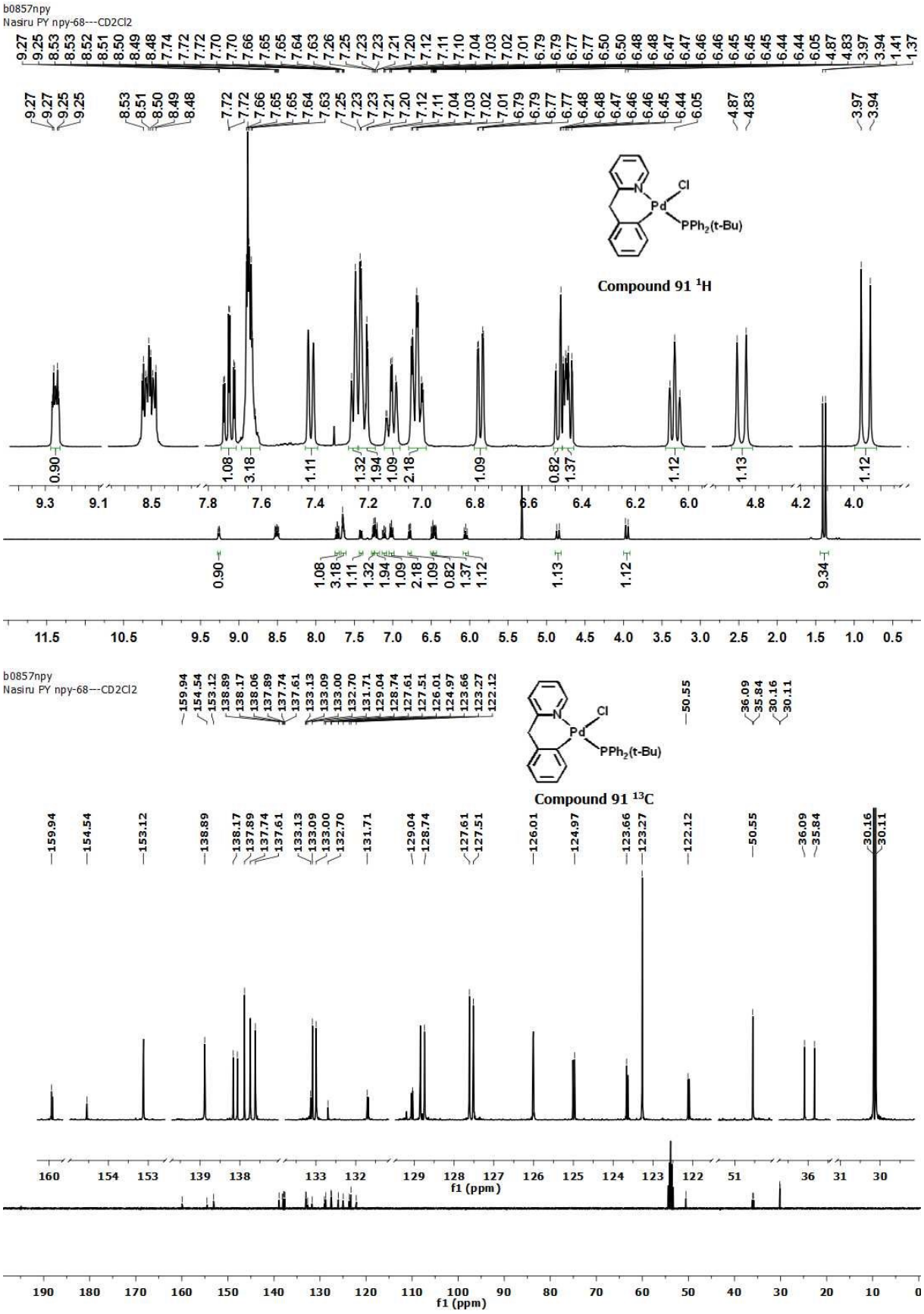

Appendix for (91)

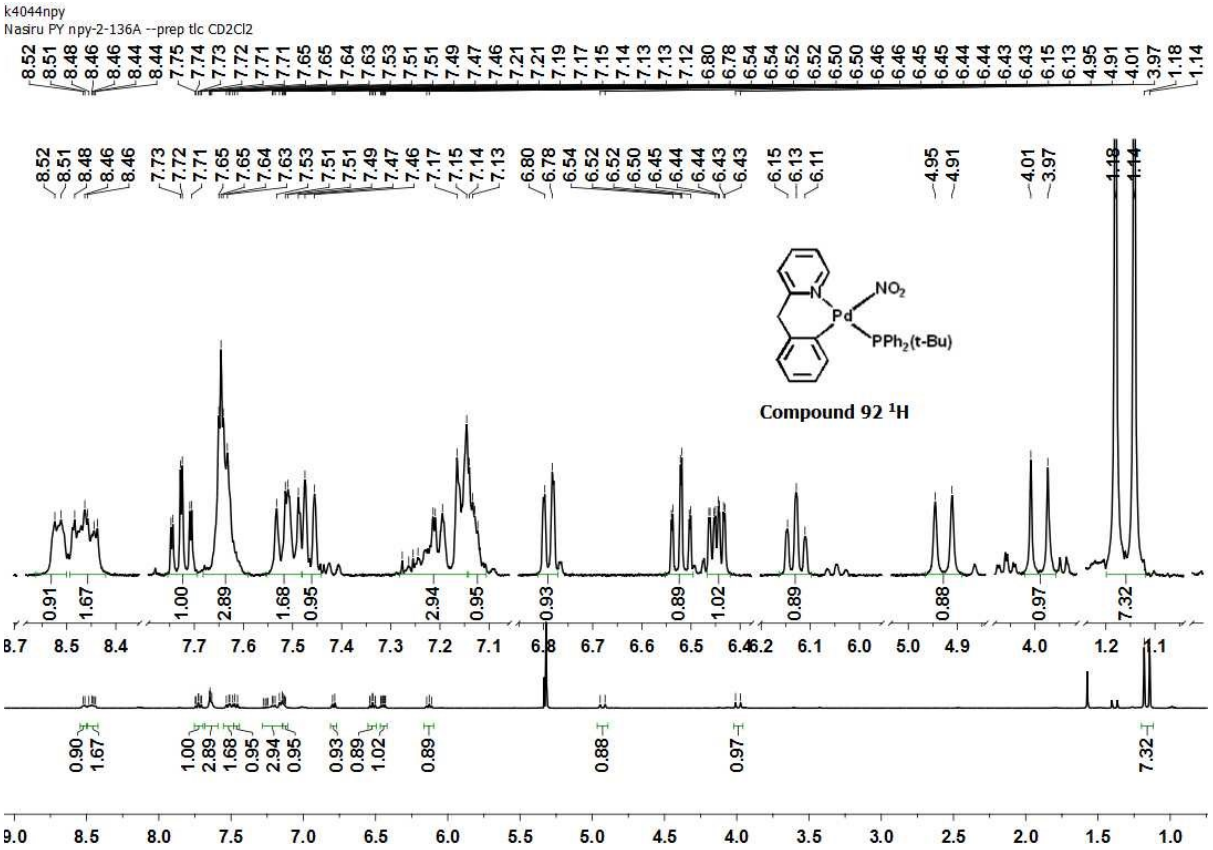

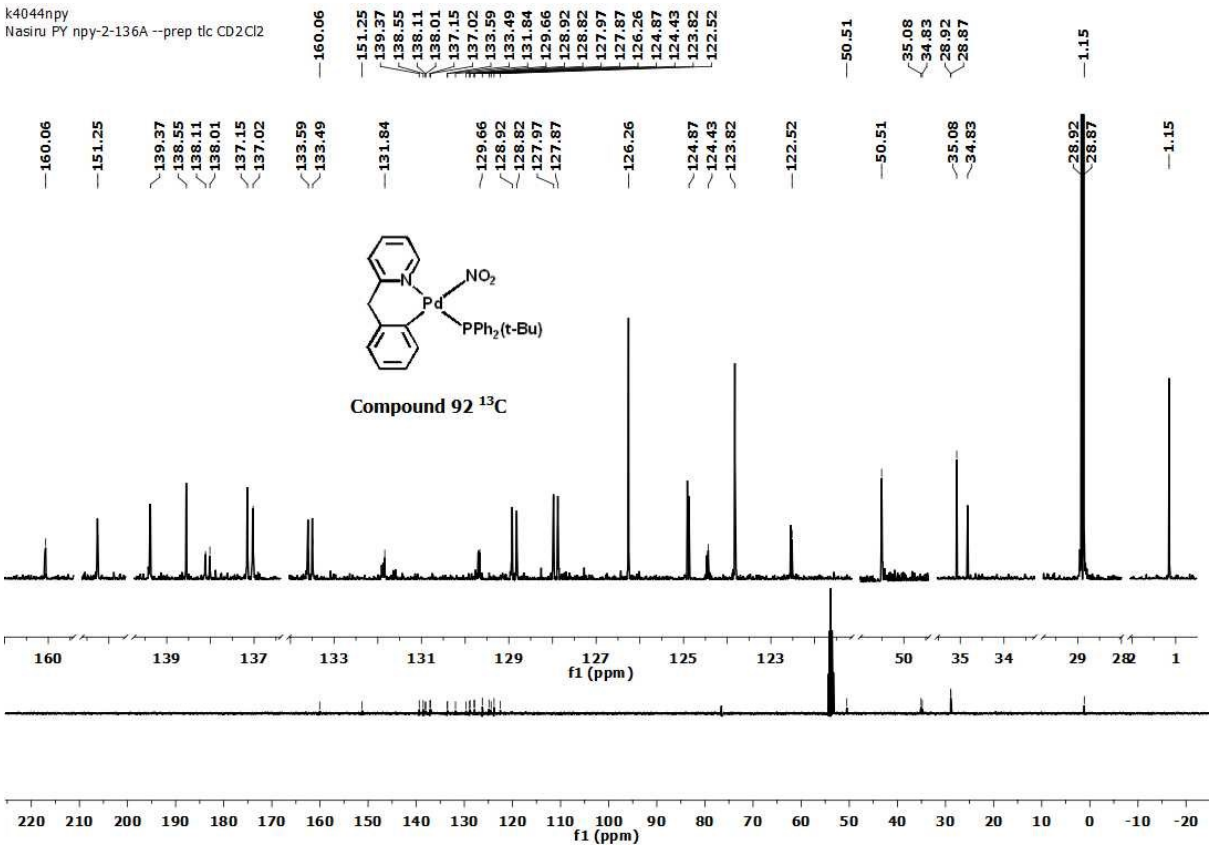

Appendix for (92)

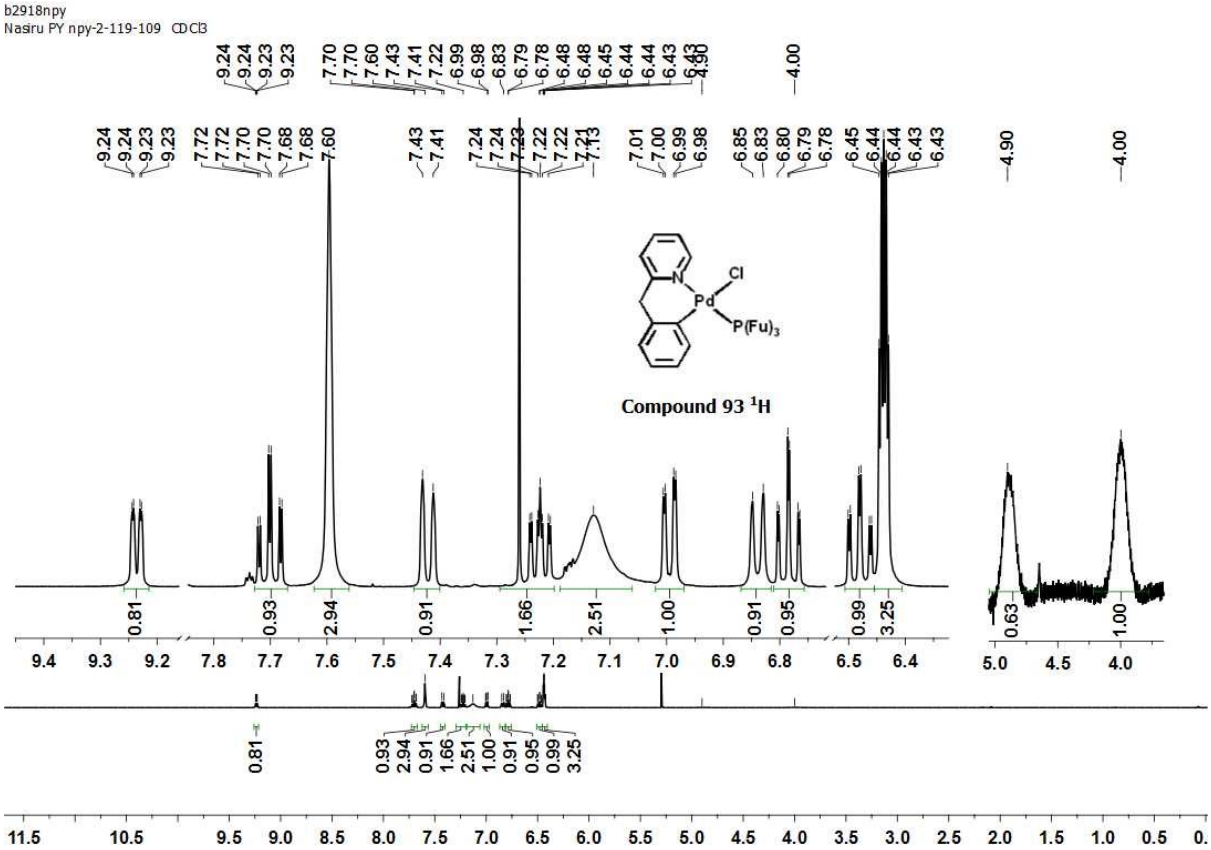

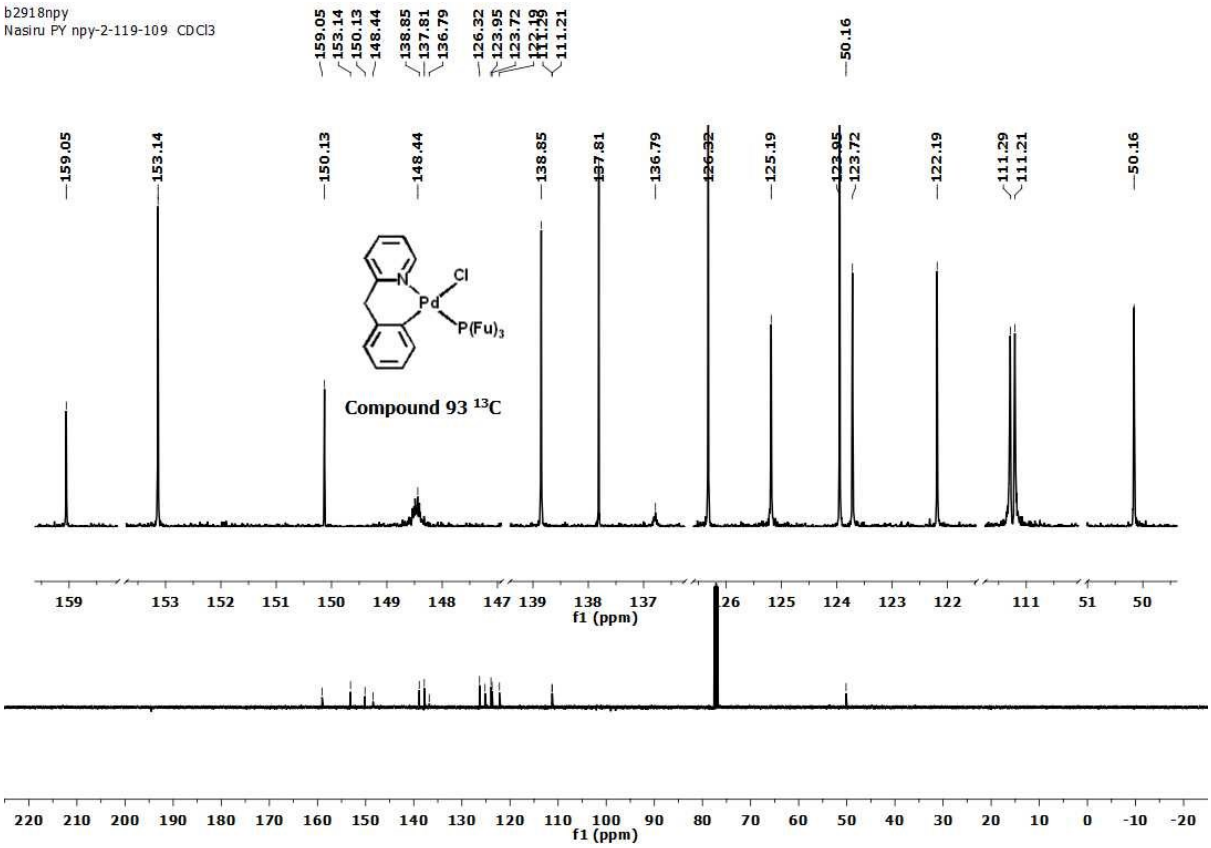

Appendix for (93)

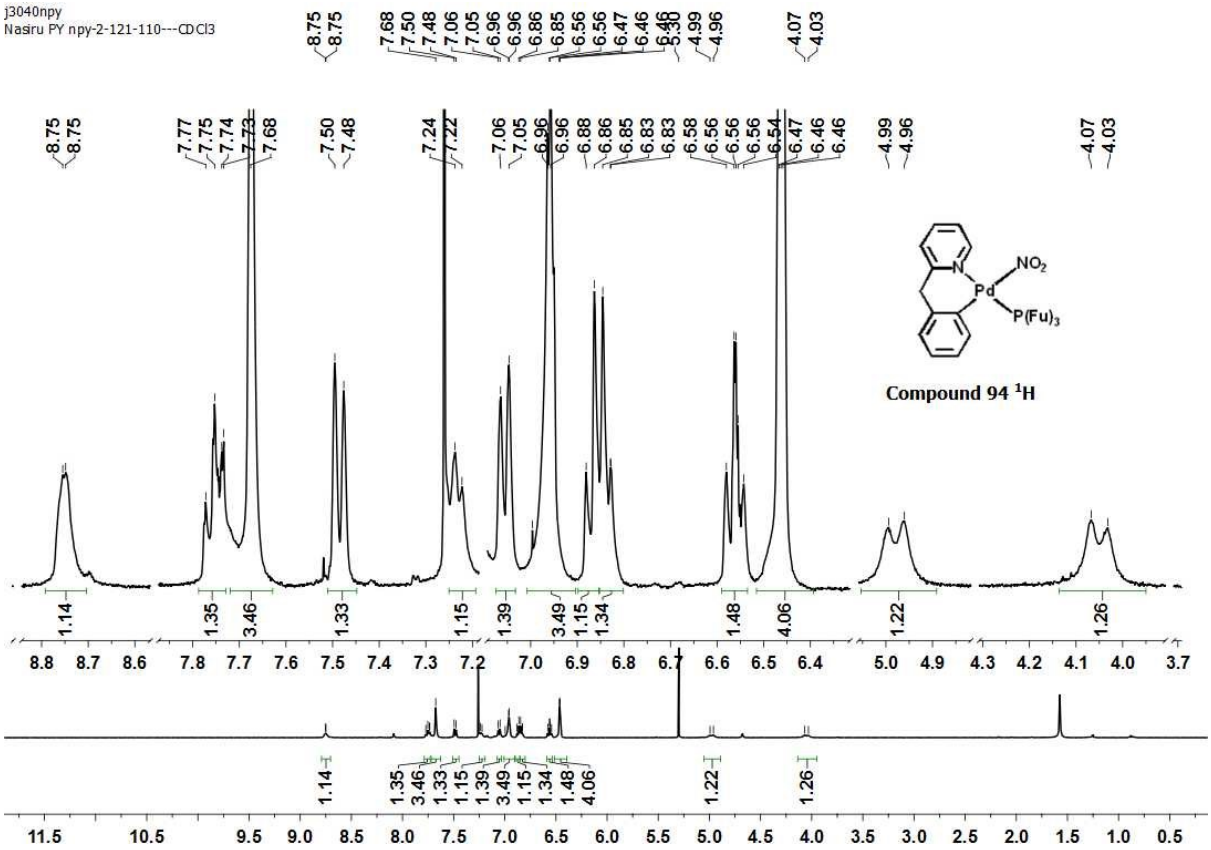

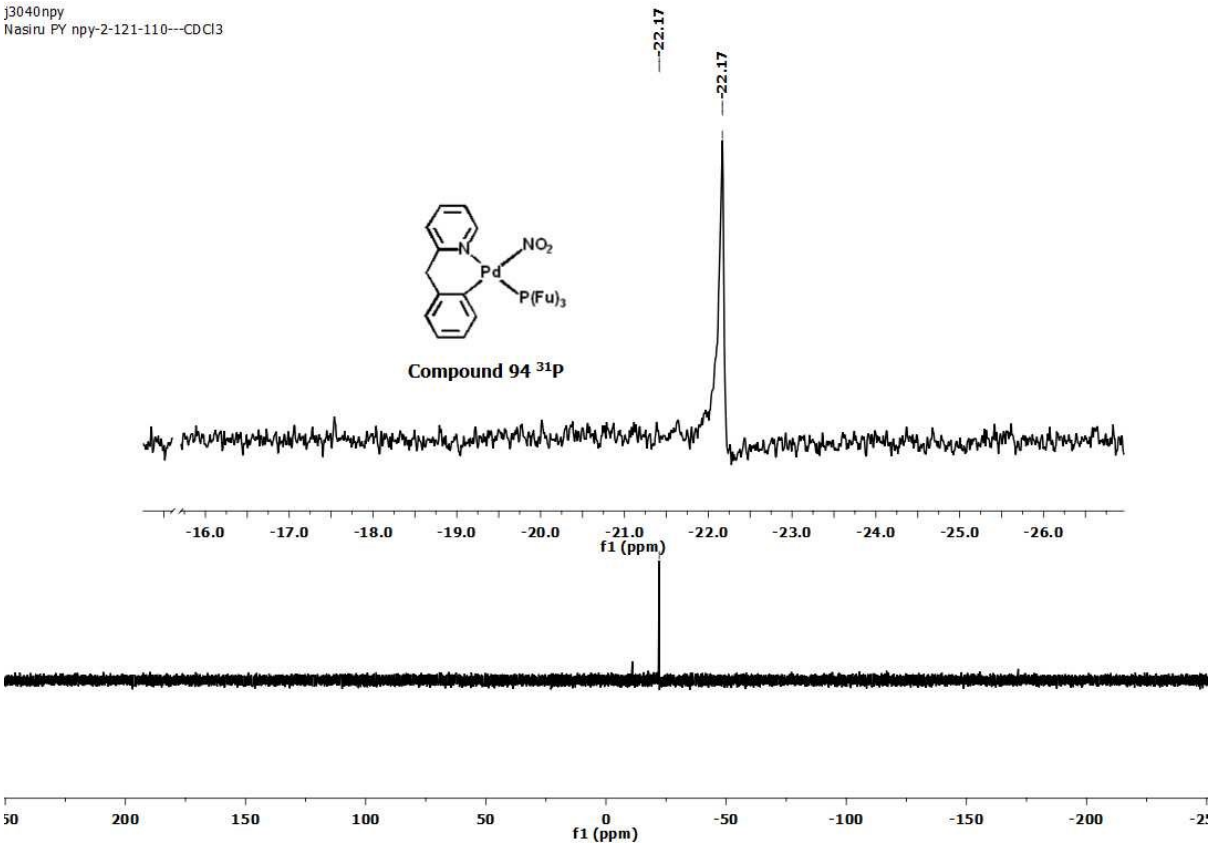

Appendix for (94)

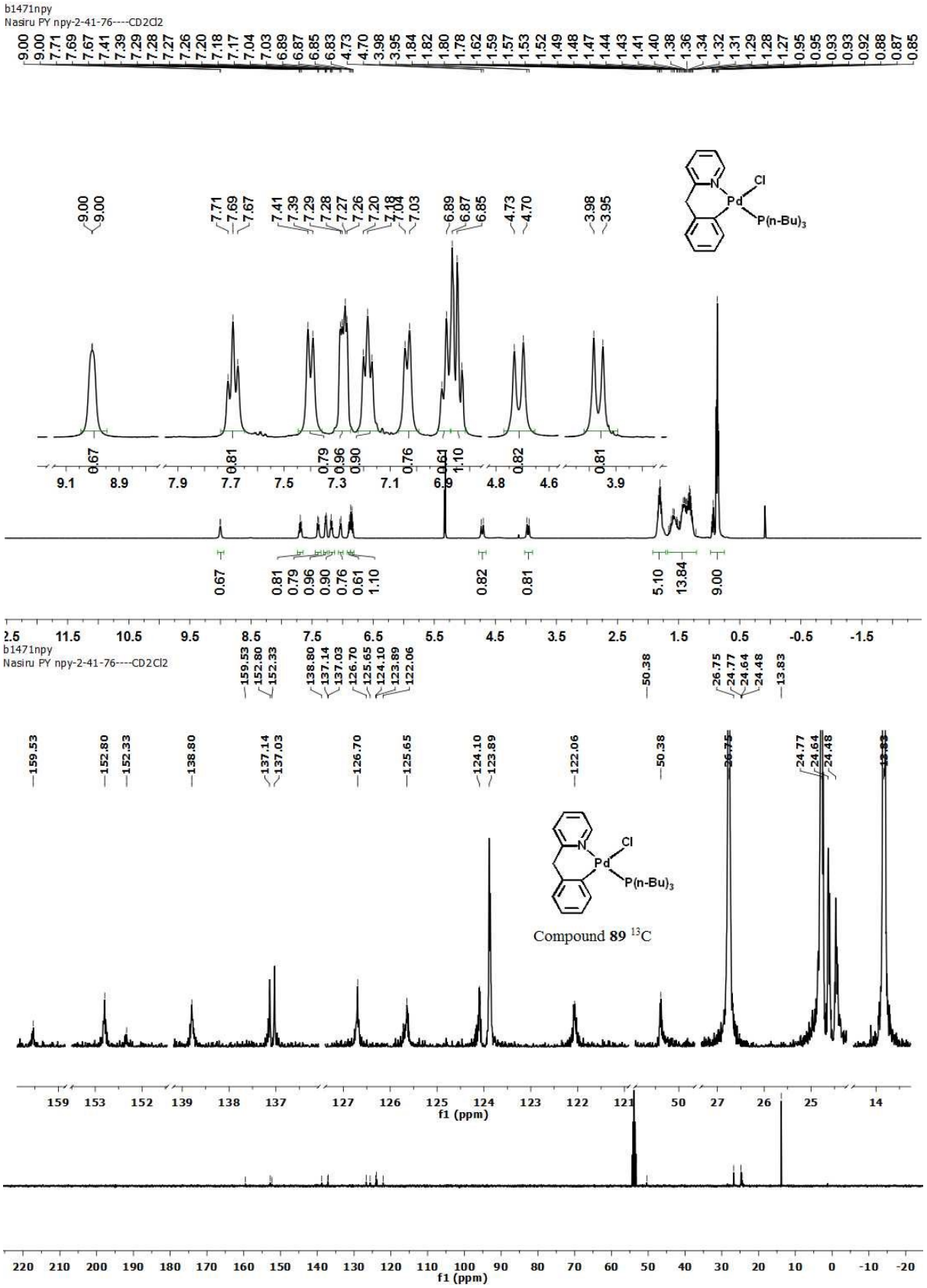

Appendix for (95)

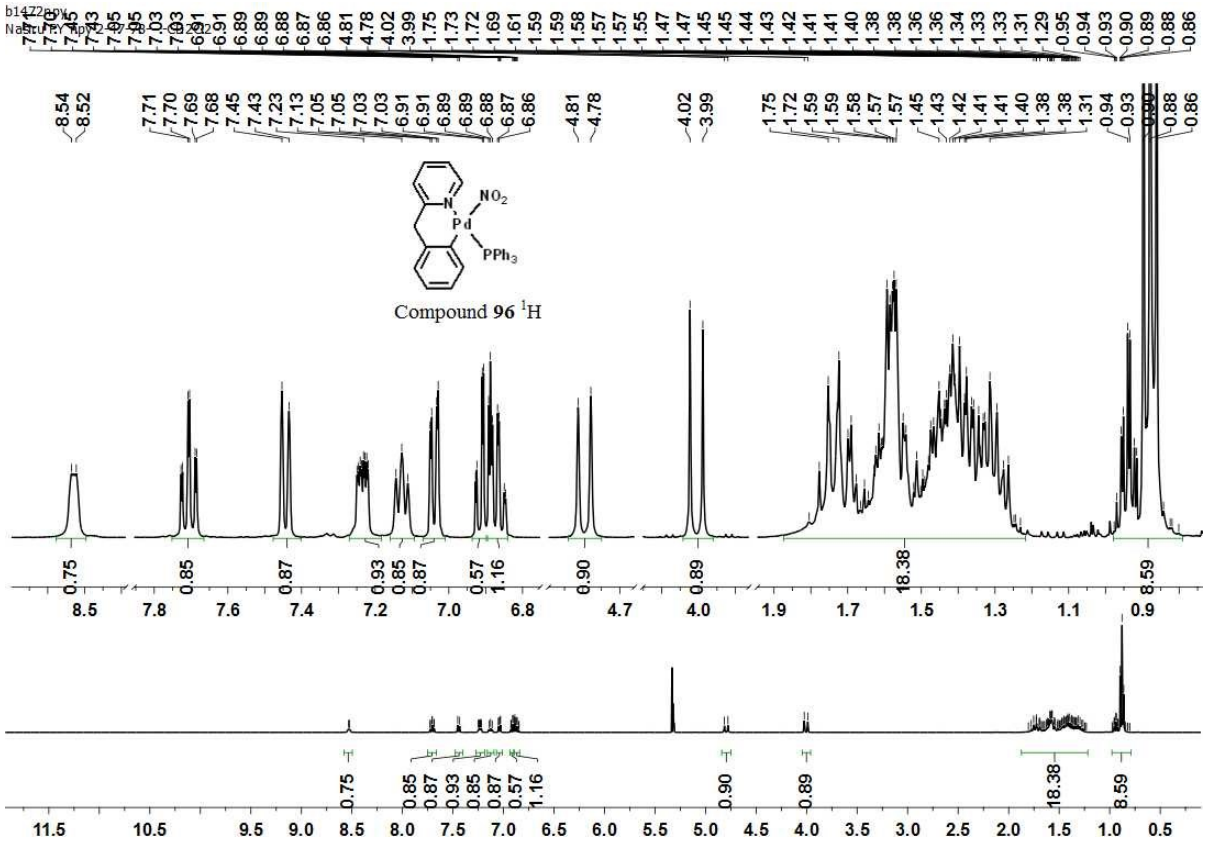

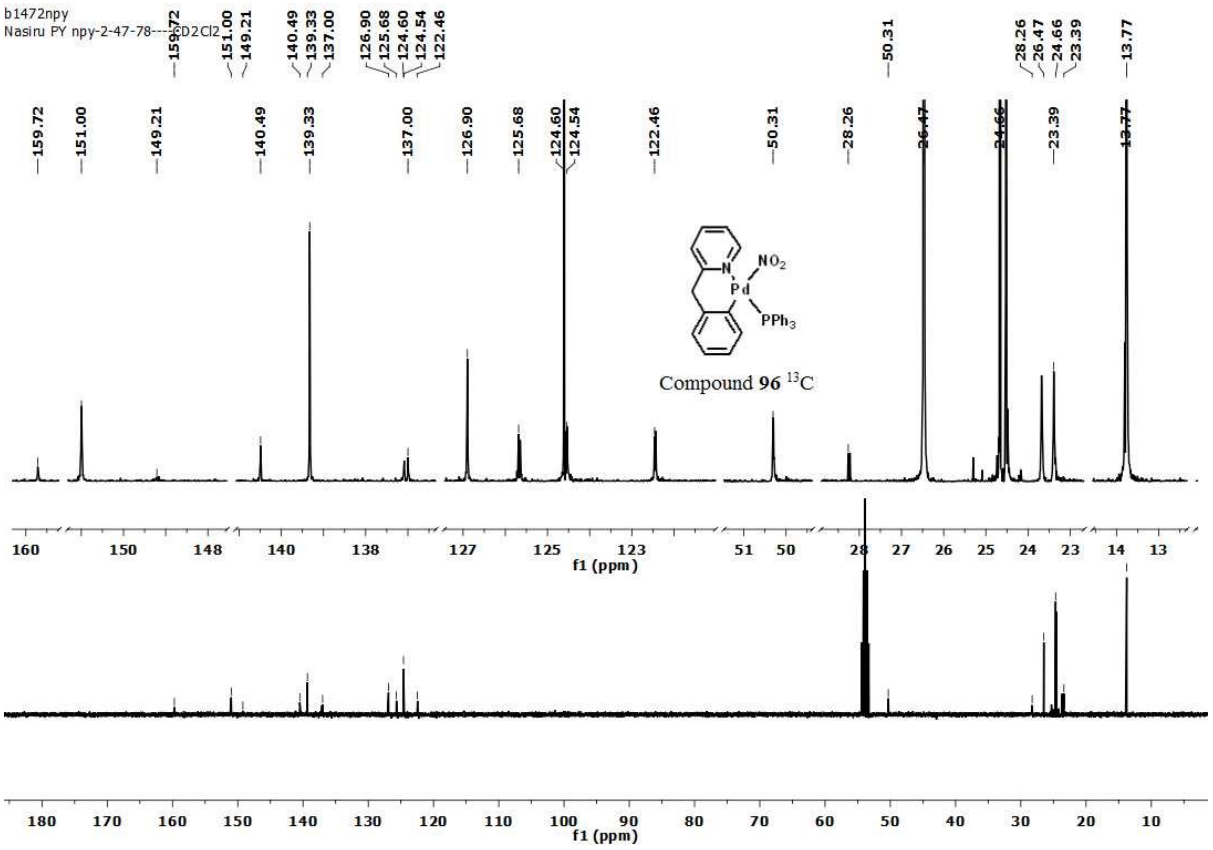

Appendix for (96)

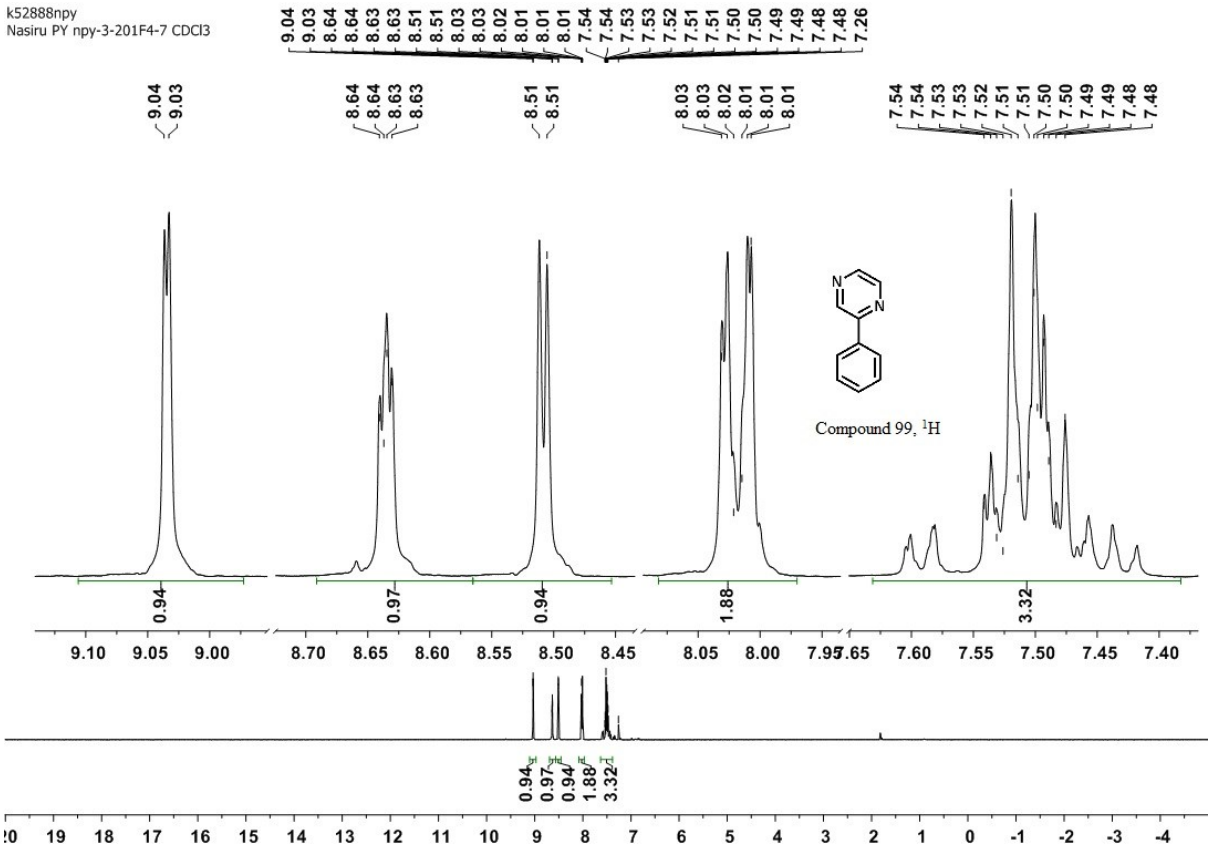

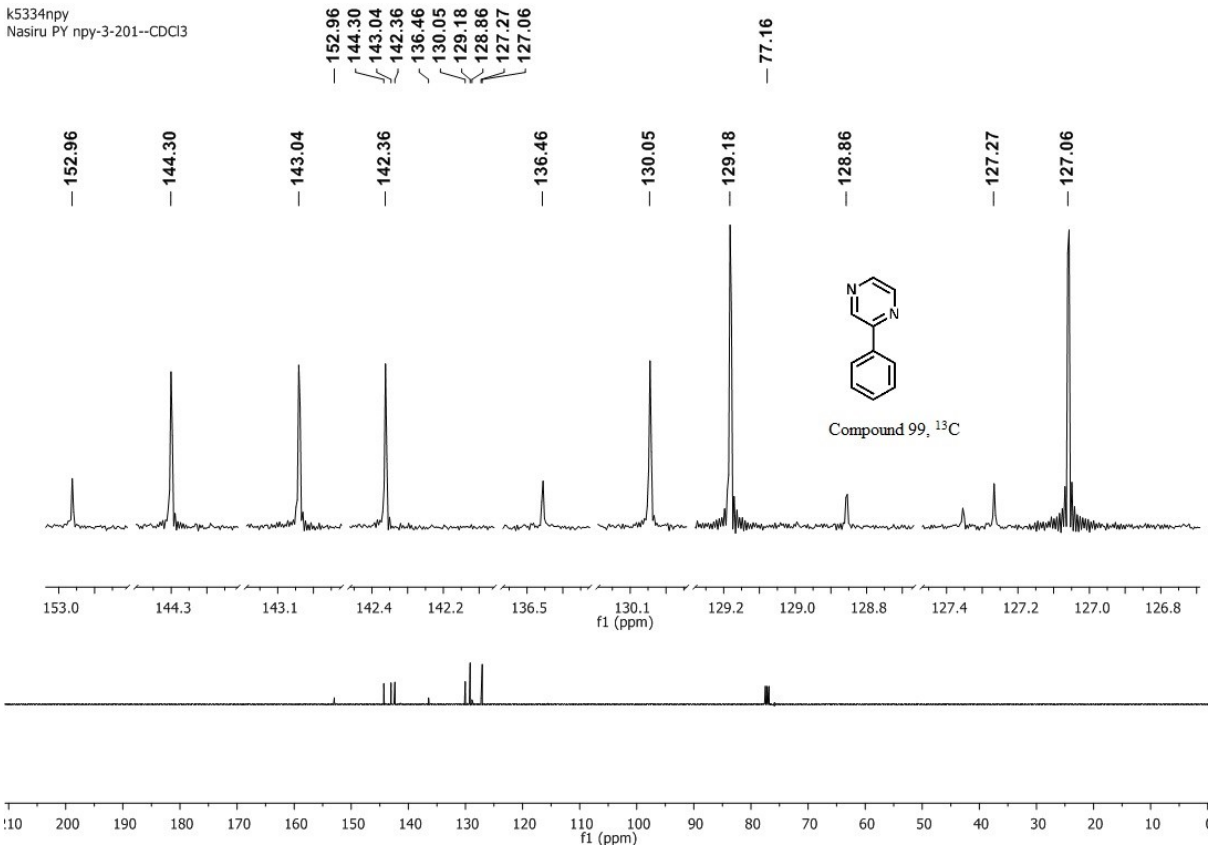

Appendix for (99)

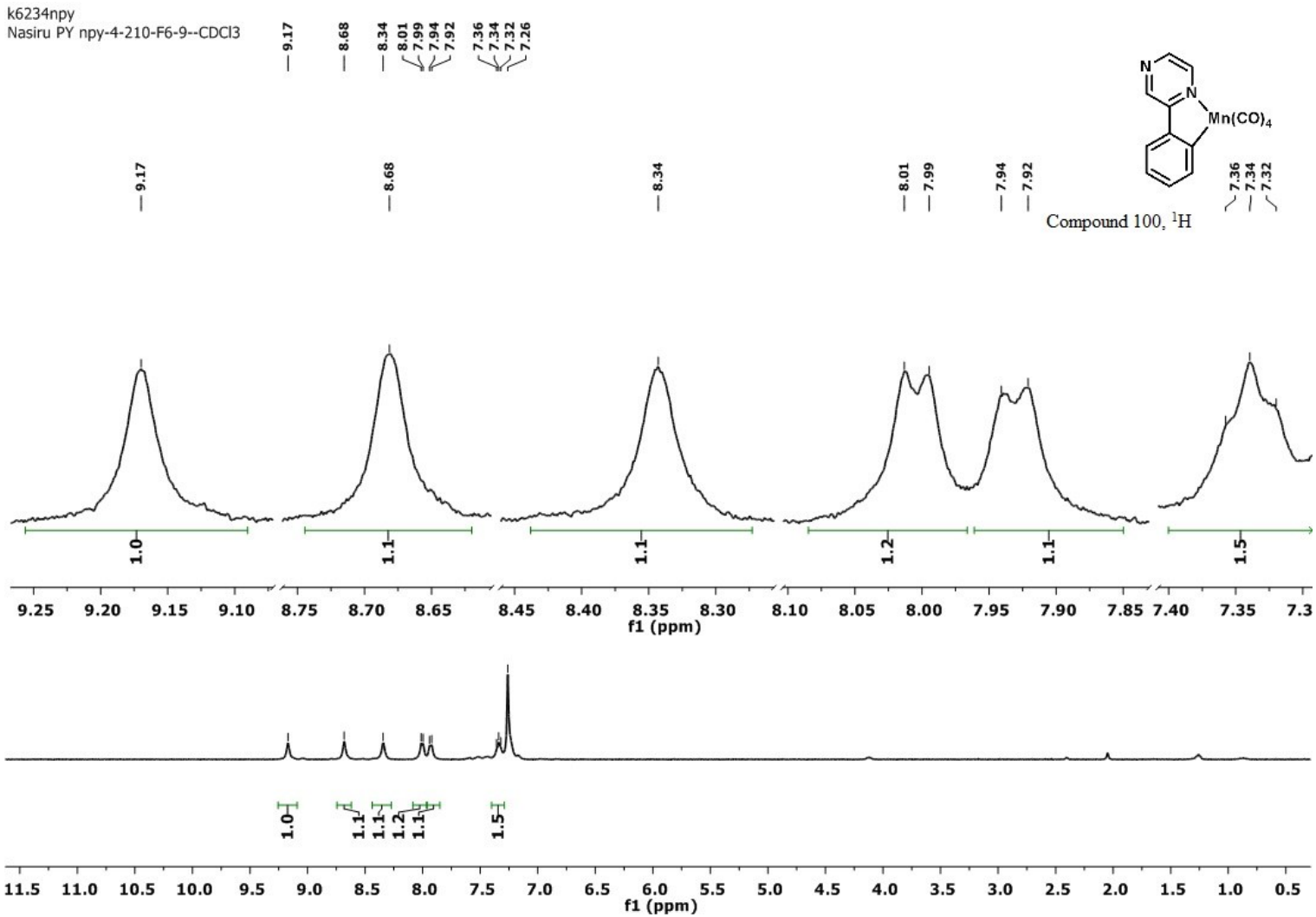

Appendix for (100)

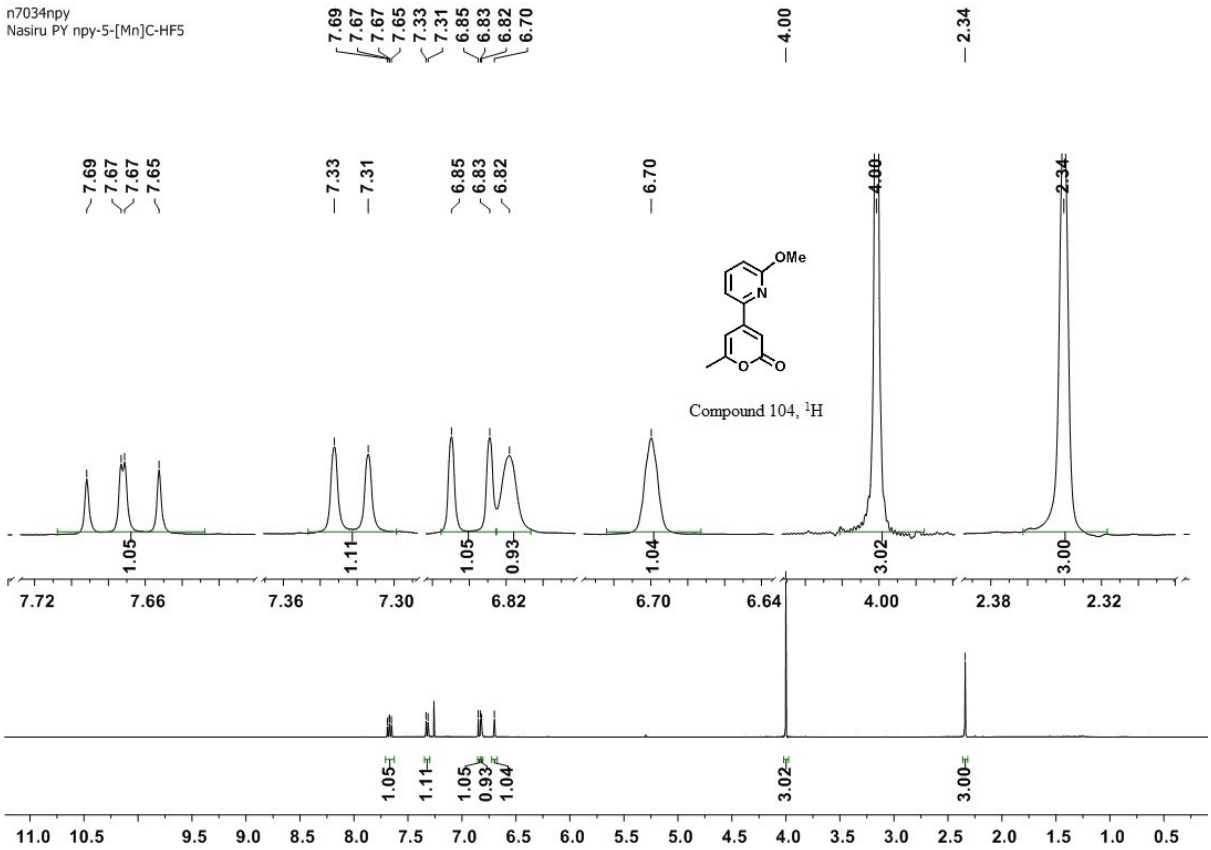

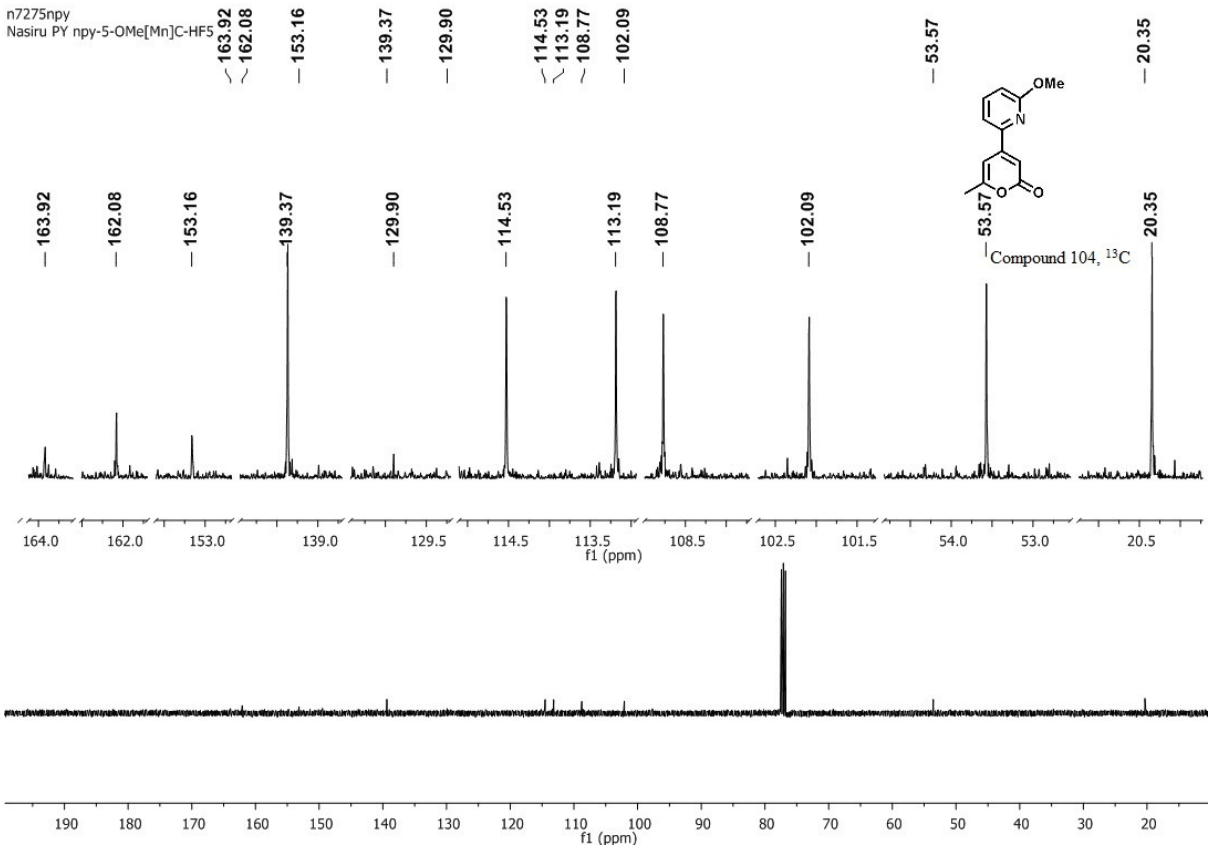

Appendix for (104)

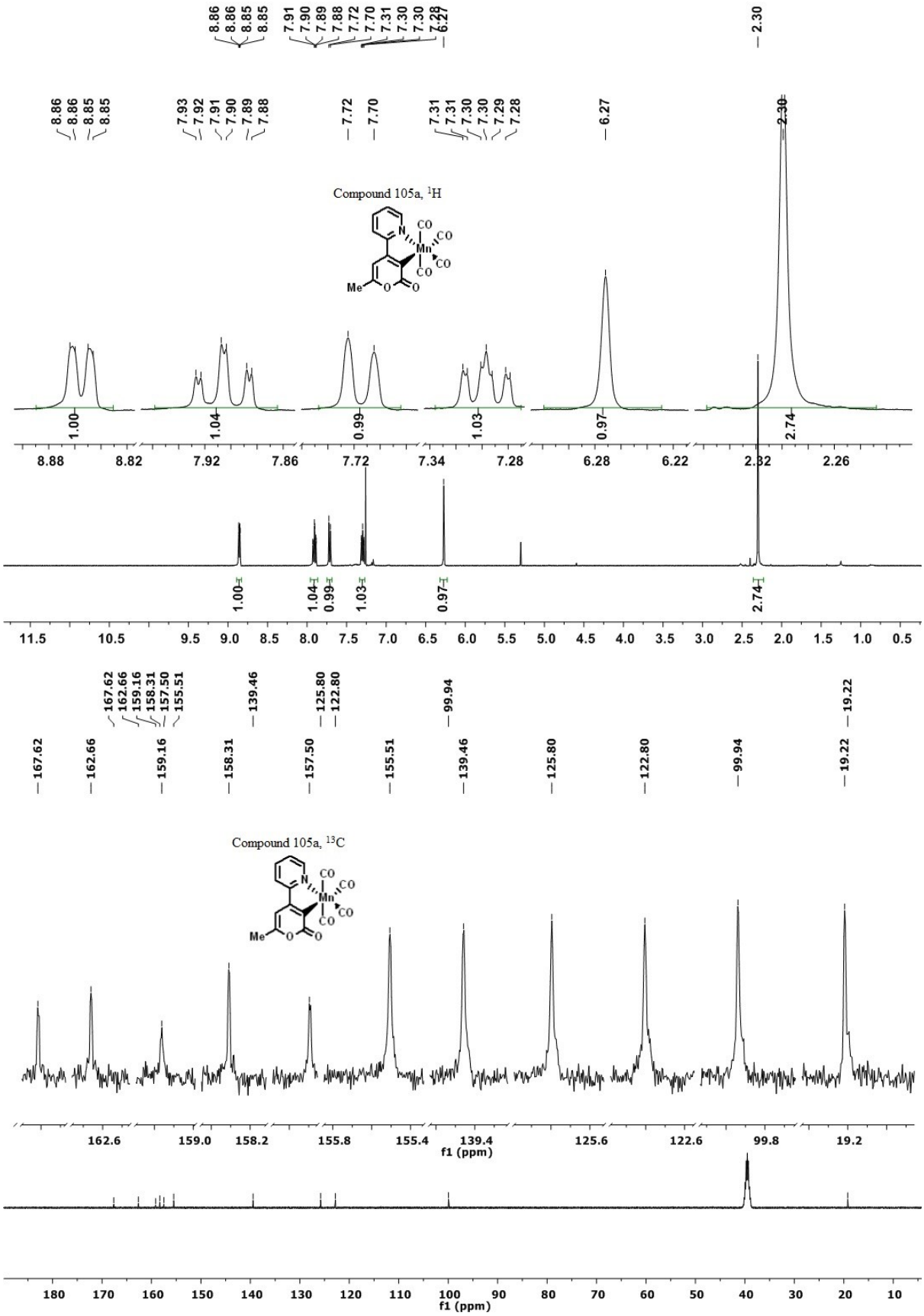

Appendix for (105a)

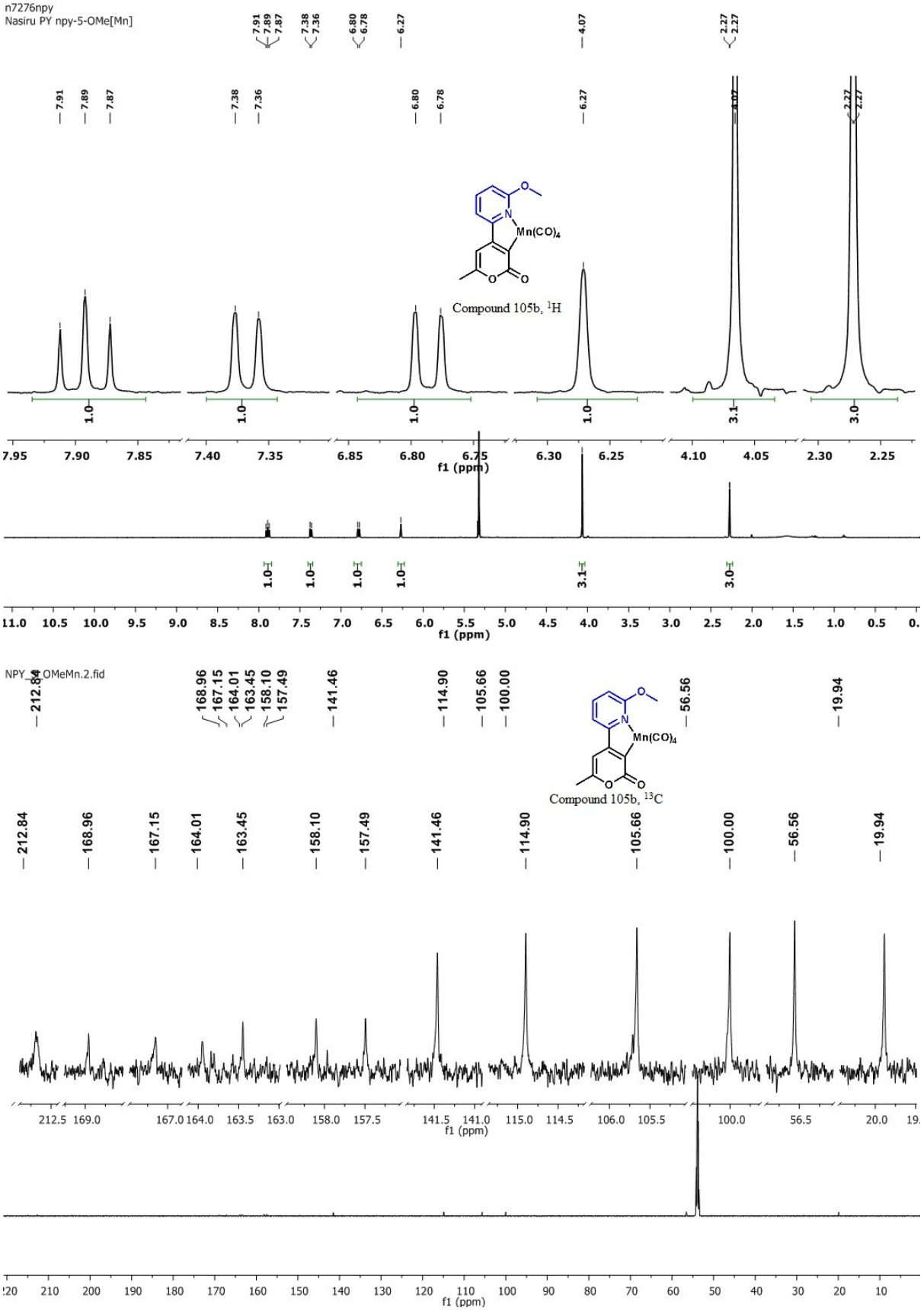

Appendix for (105b)

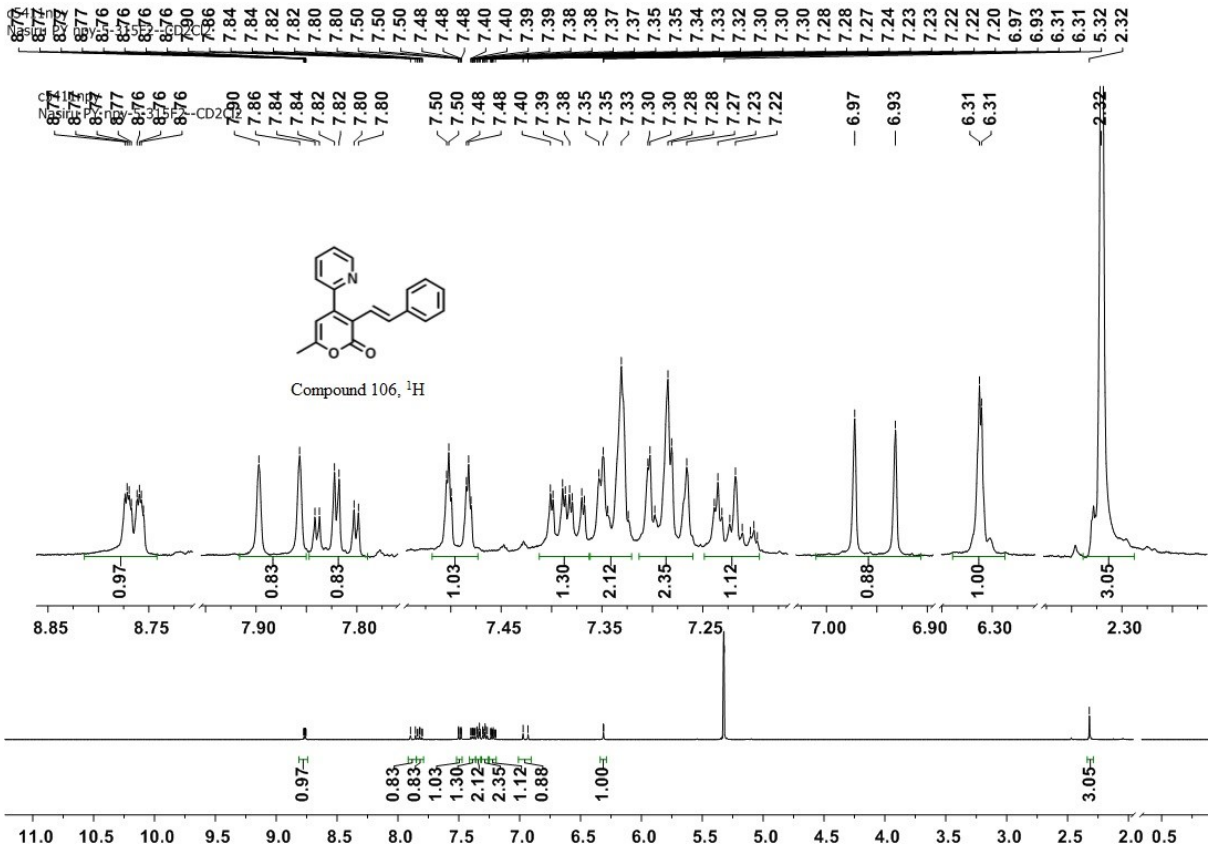

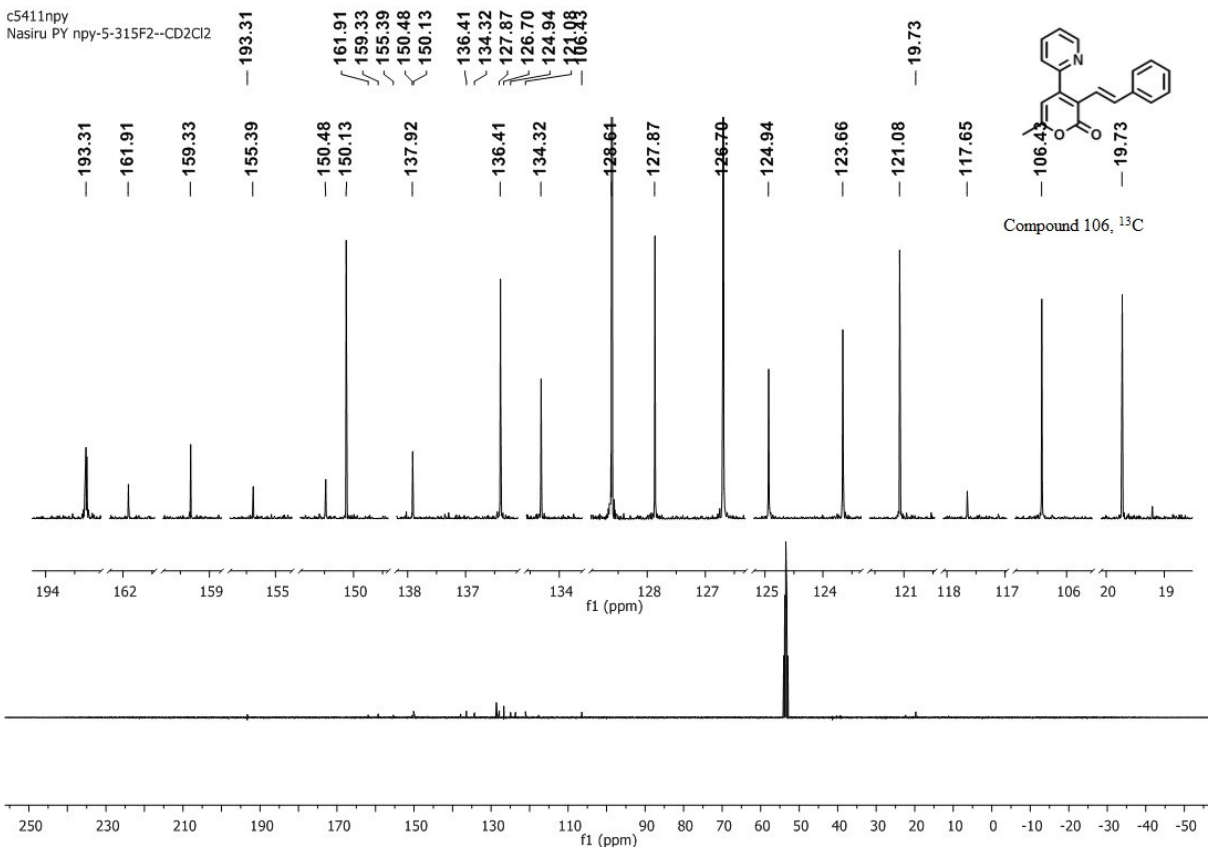

Appendix for (106)

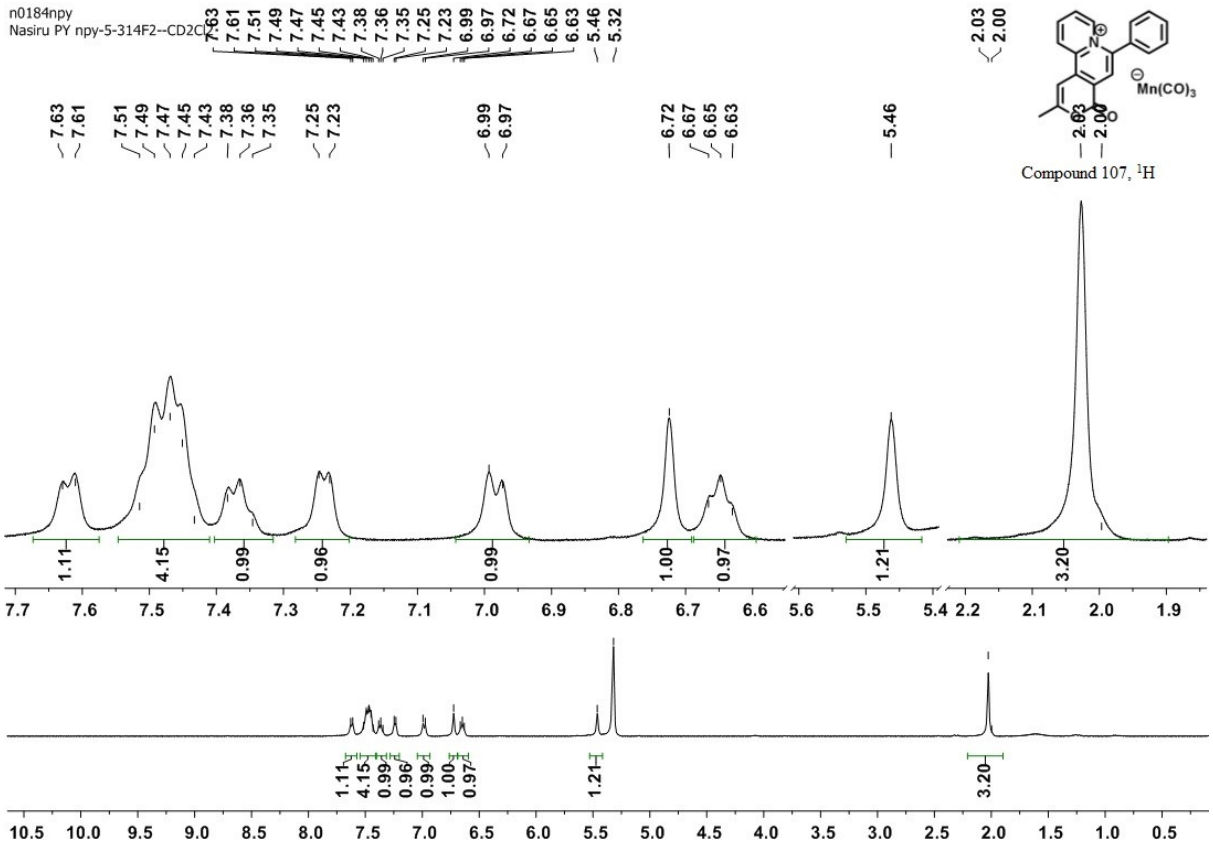

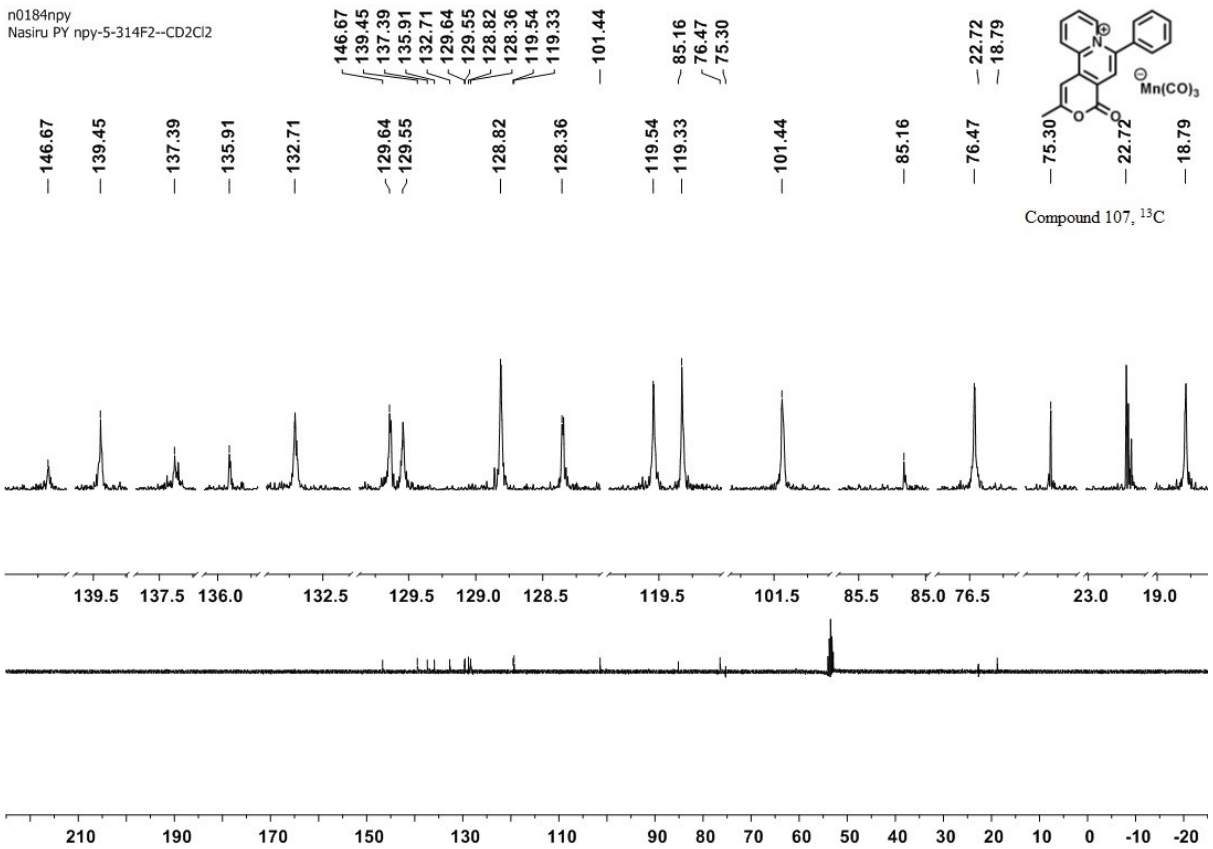

Appendix for (107)

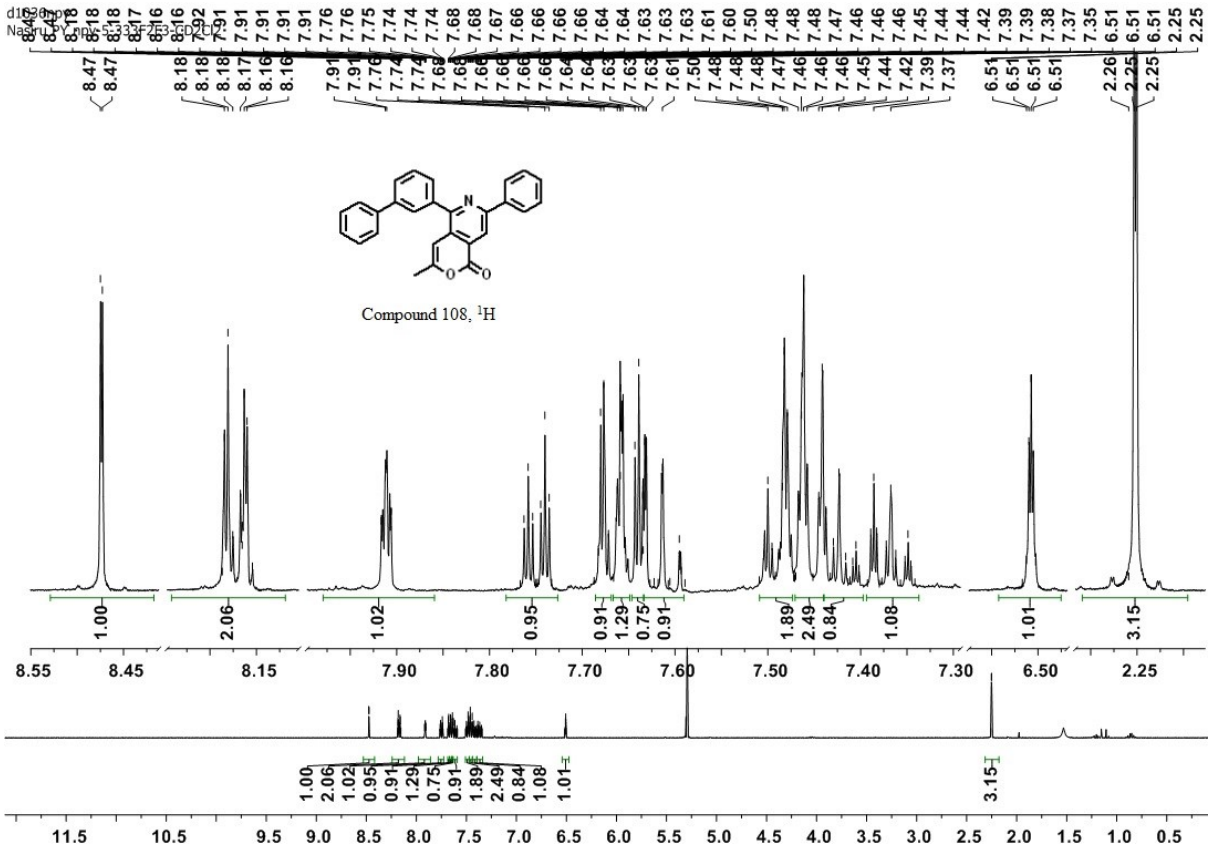

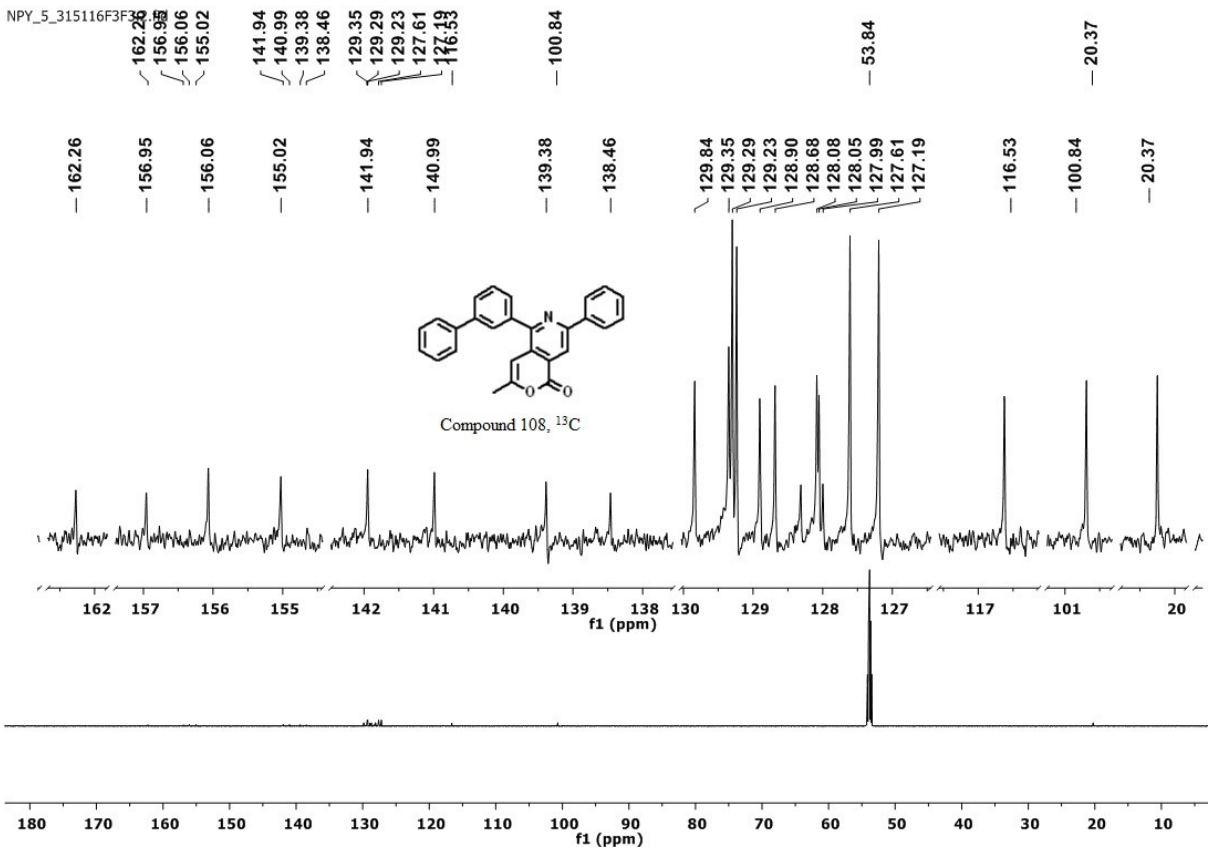

Appendix for (108)

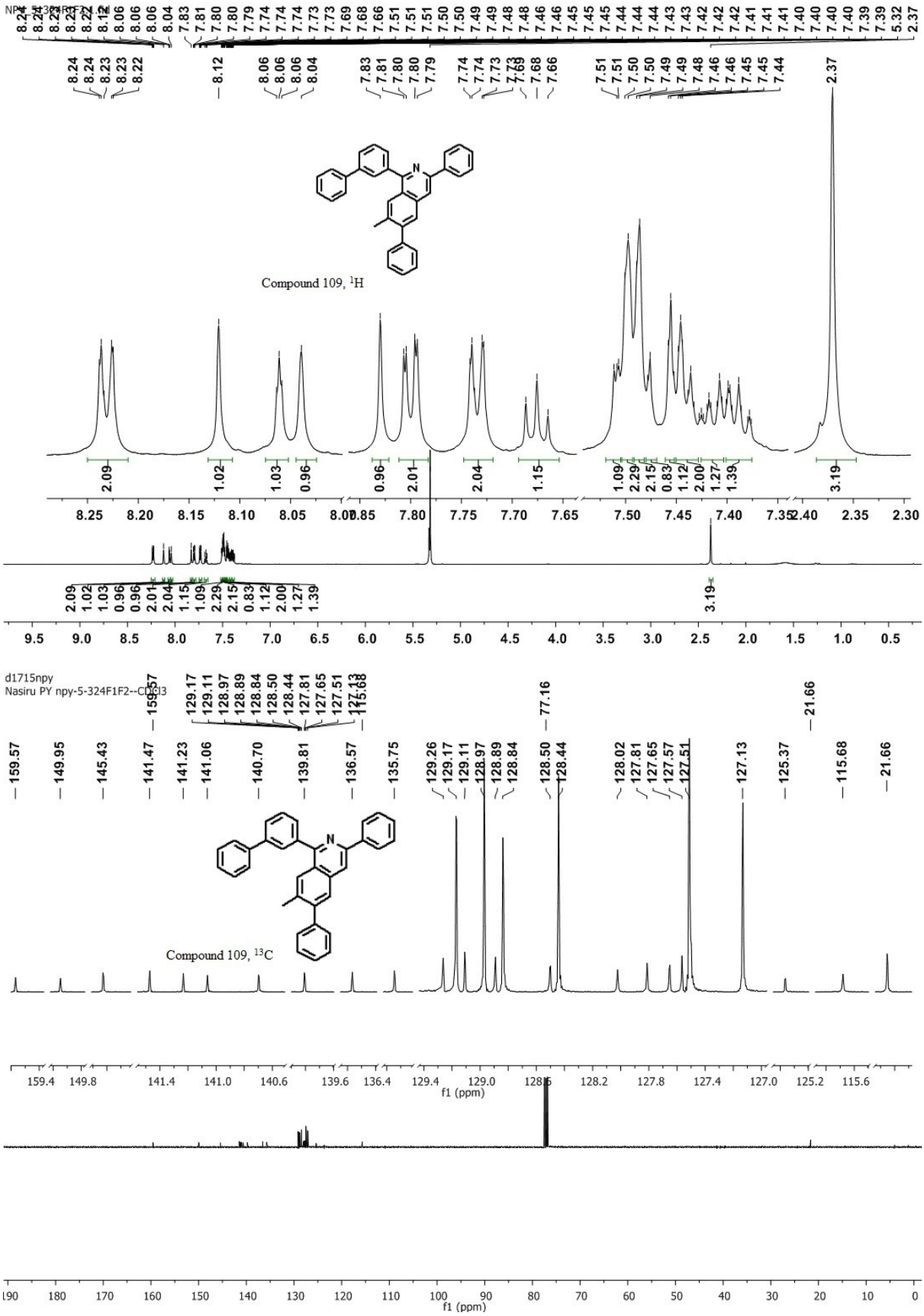

Appendix for (109)

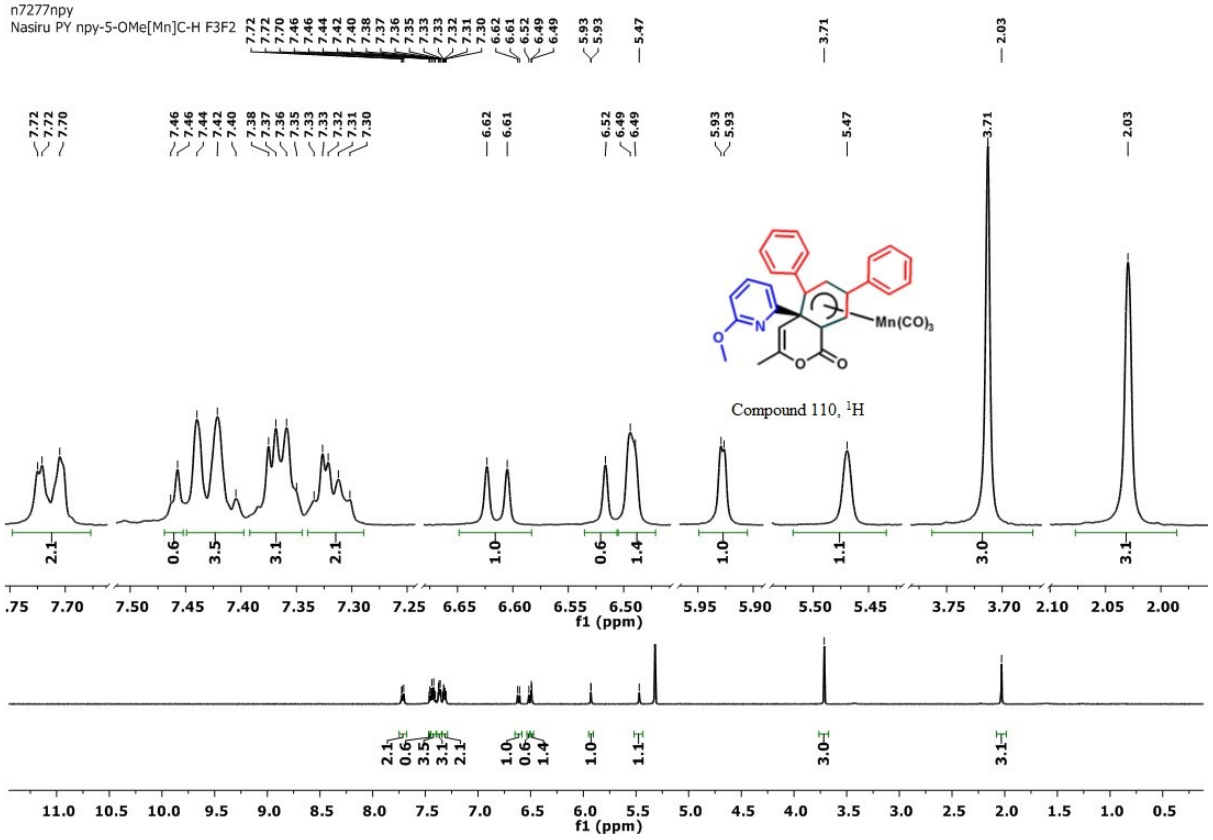

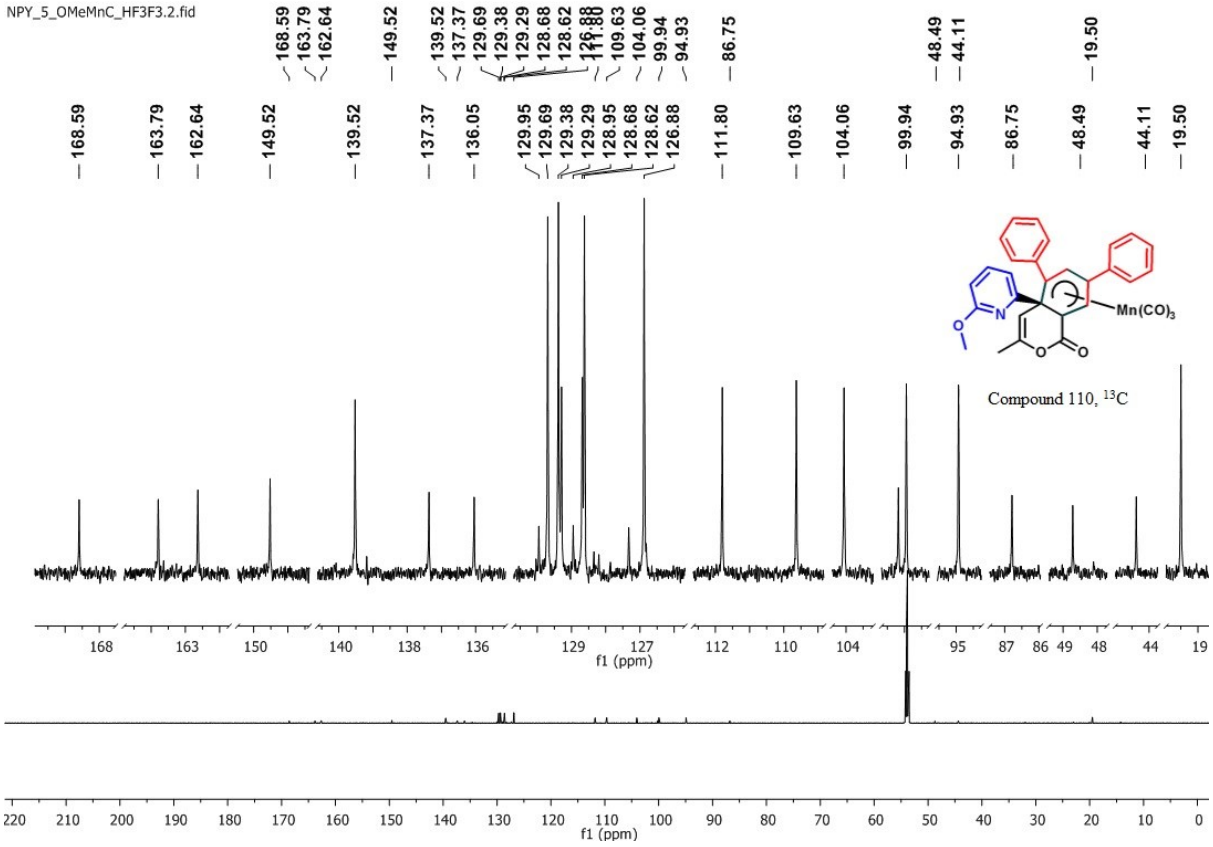

Appendix for (110)

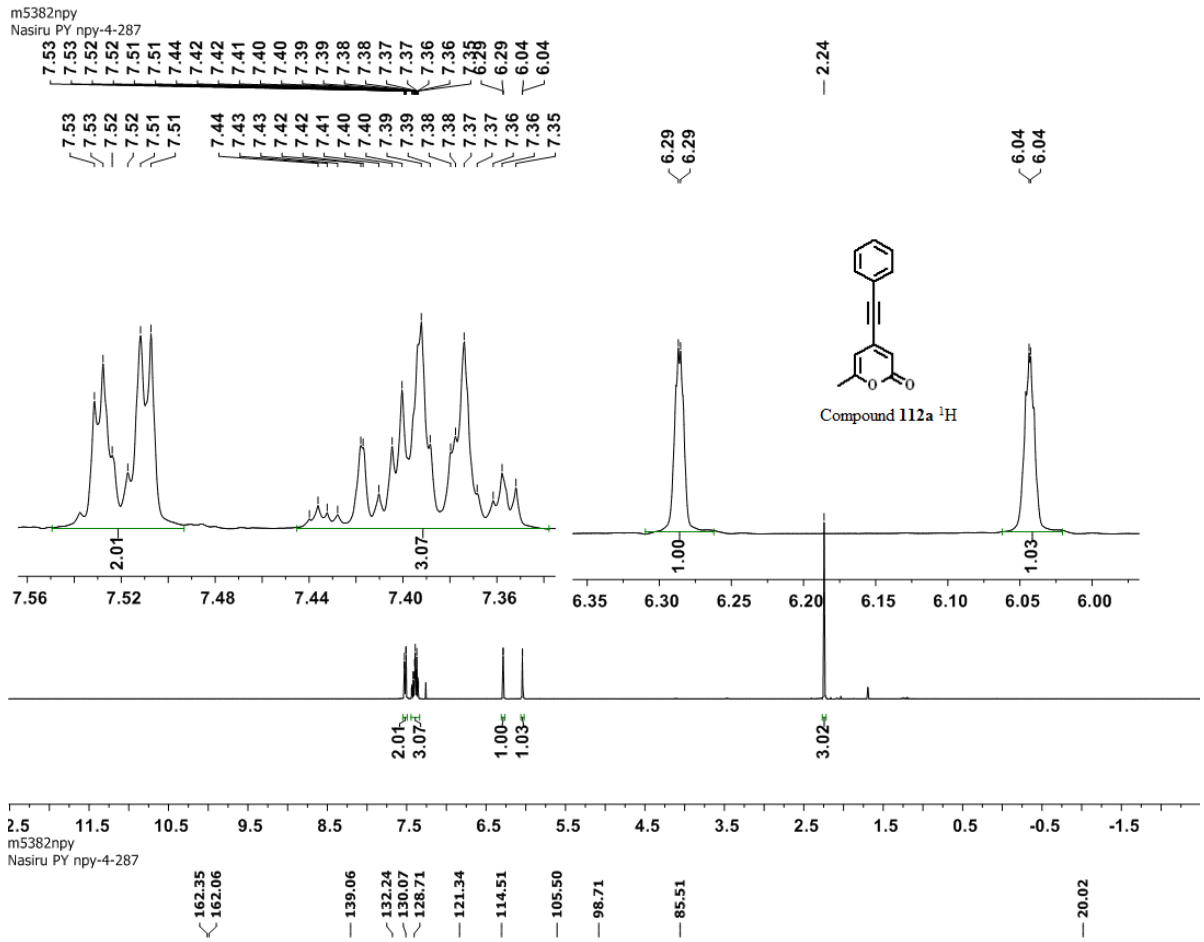

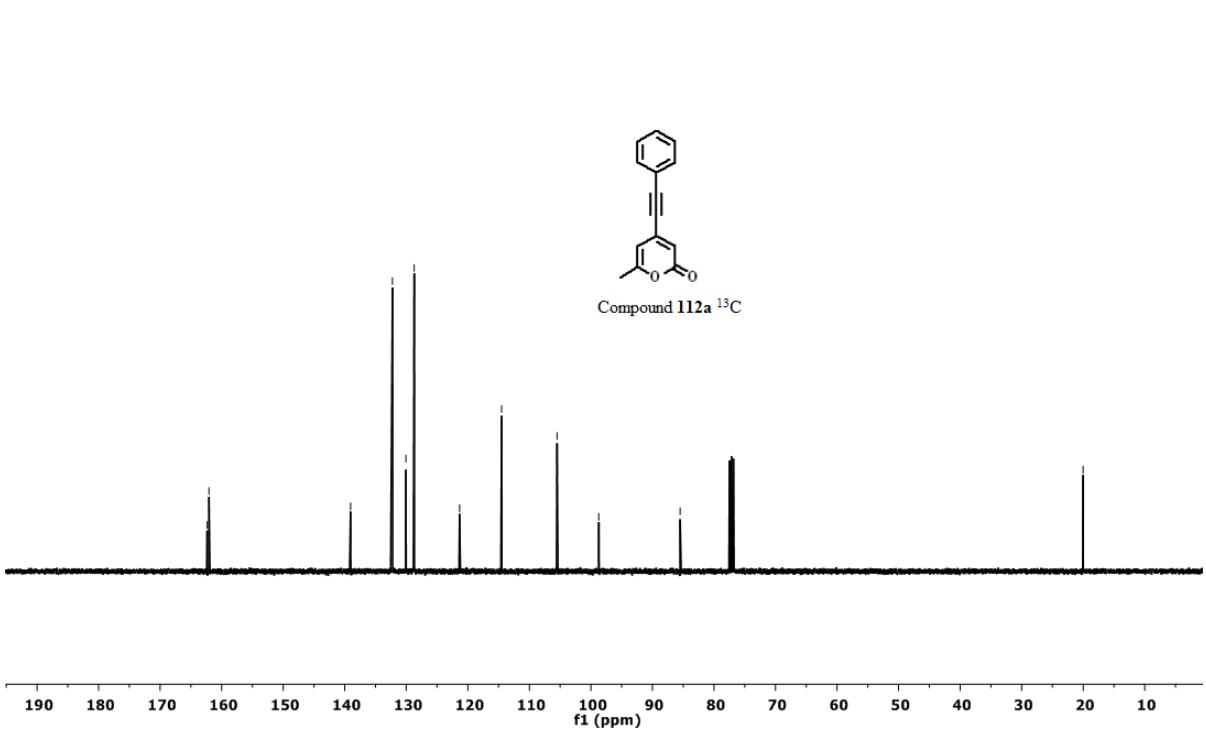

Appendix for (112a)

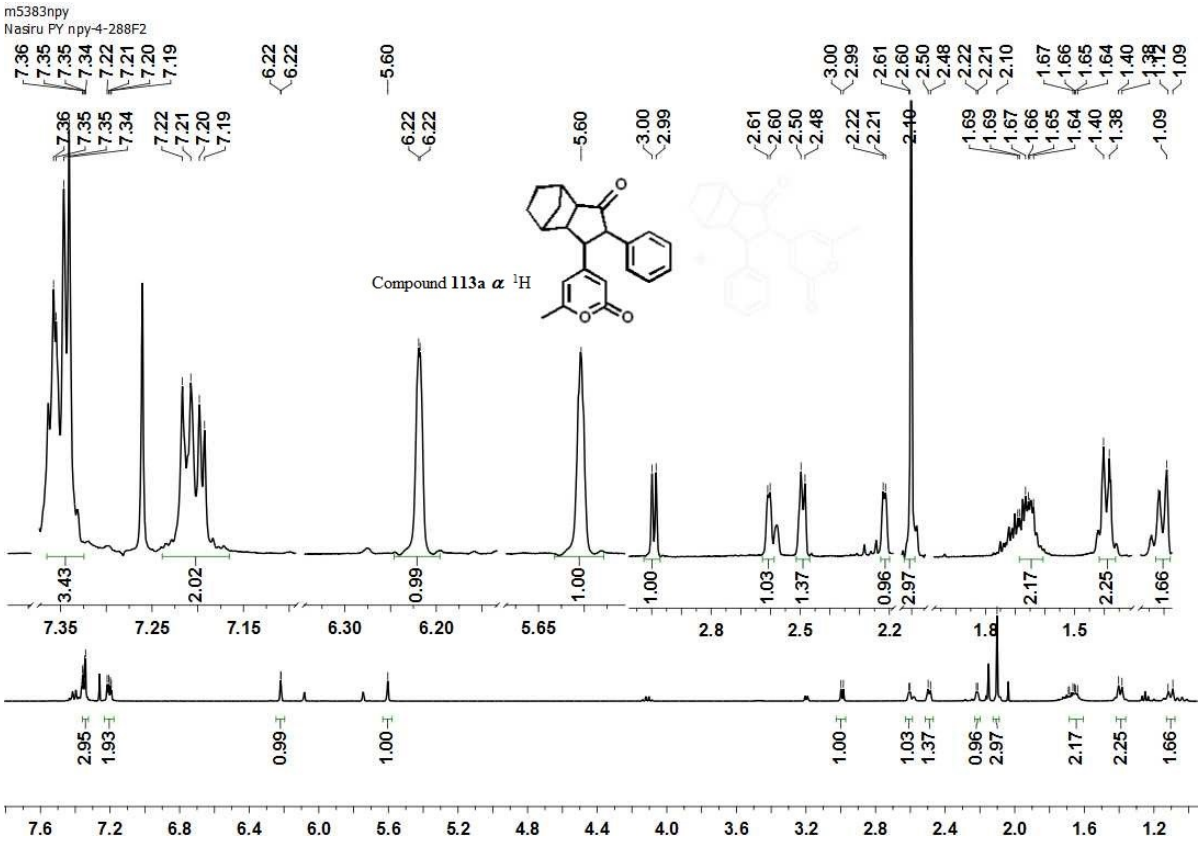

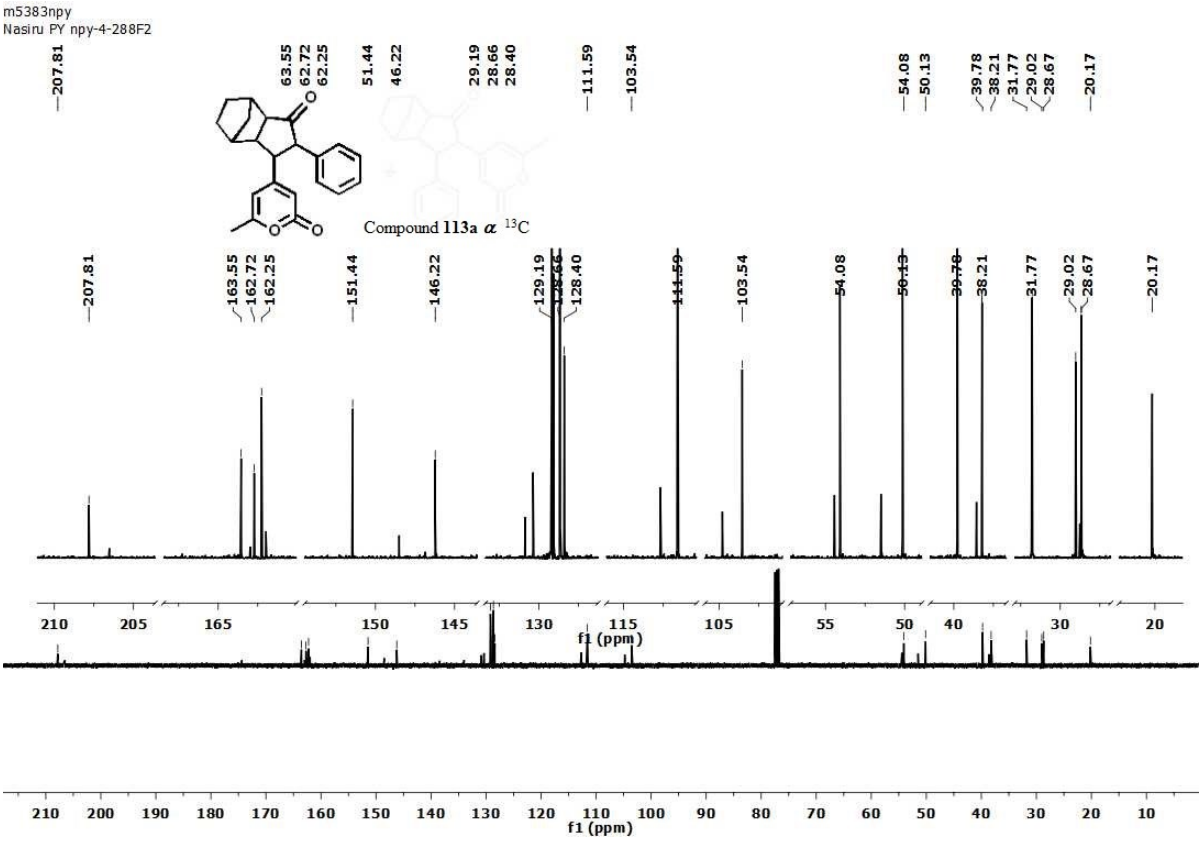

Appendix for (113a α)

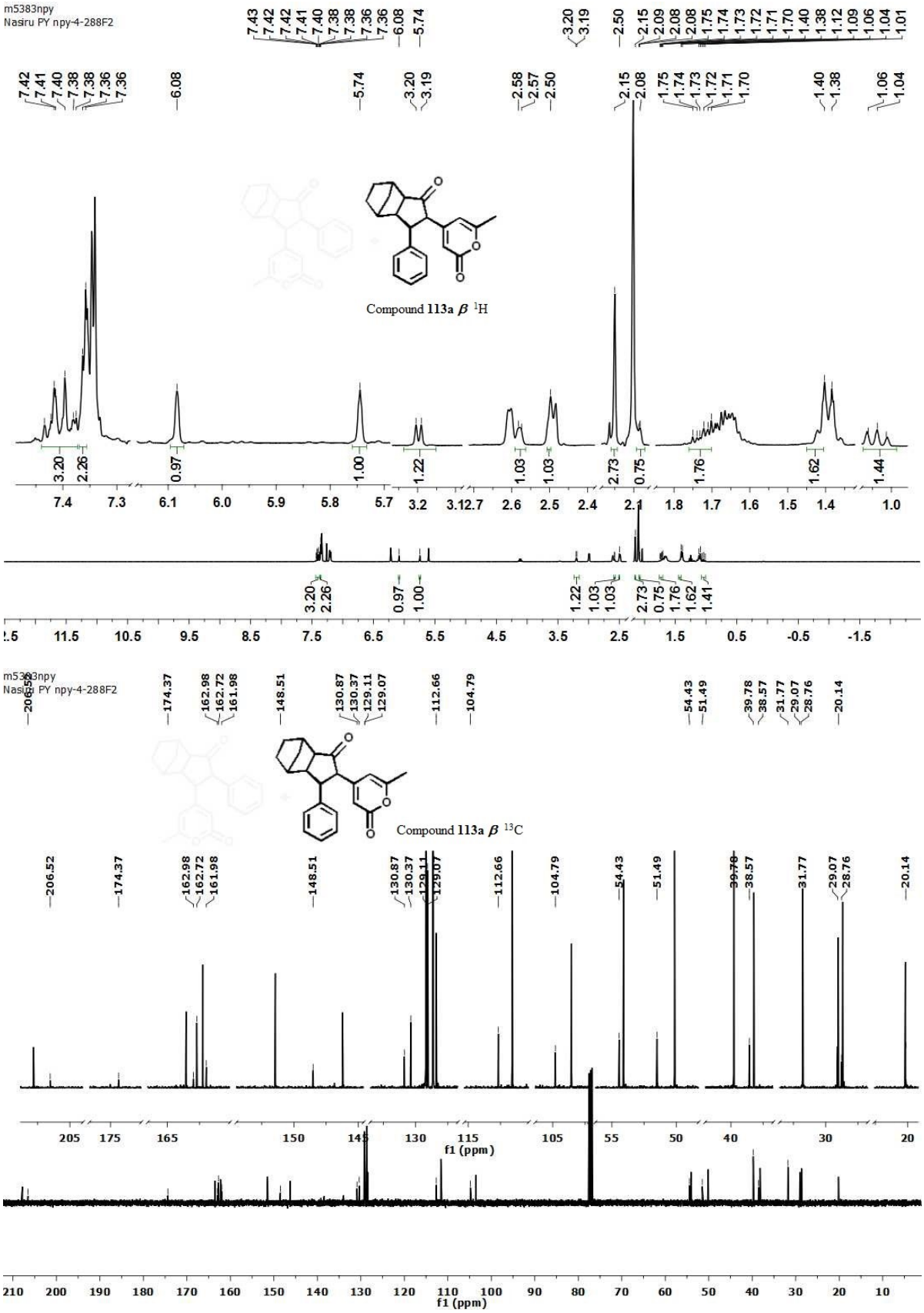

Appendix for (113a *β*)

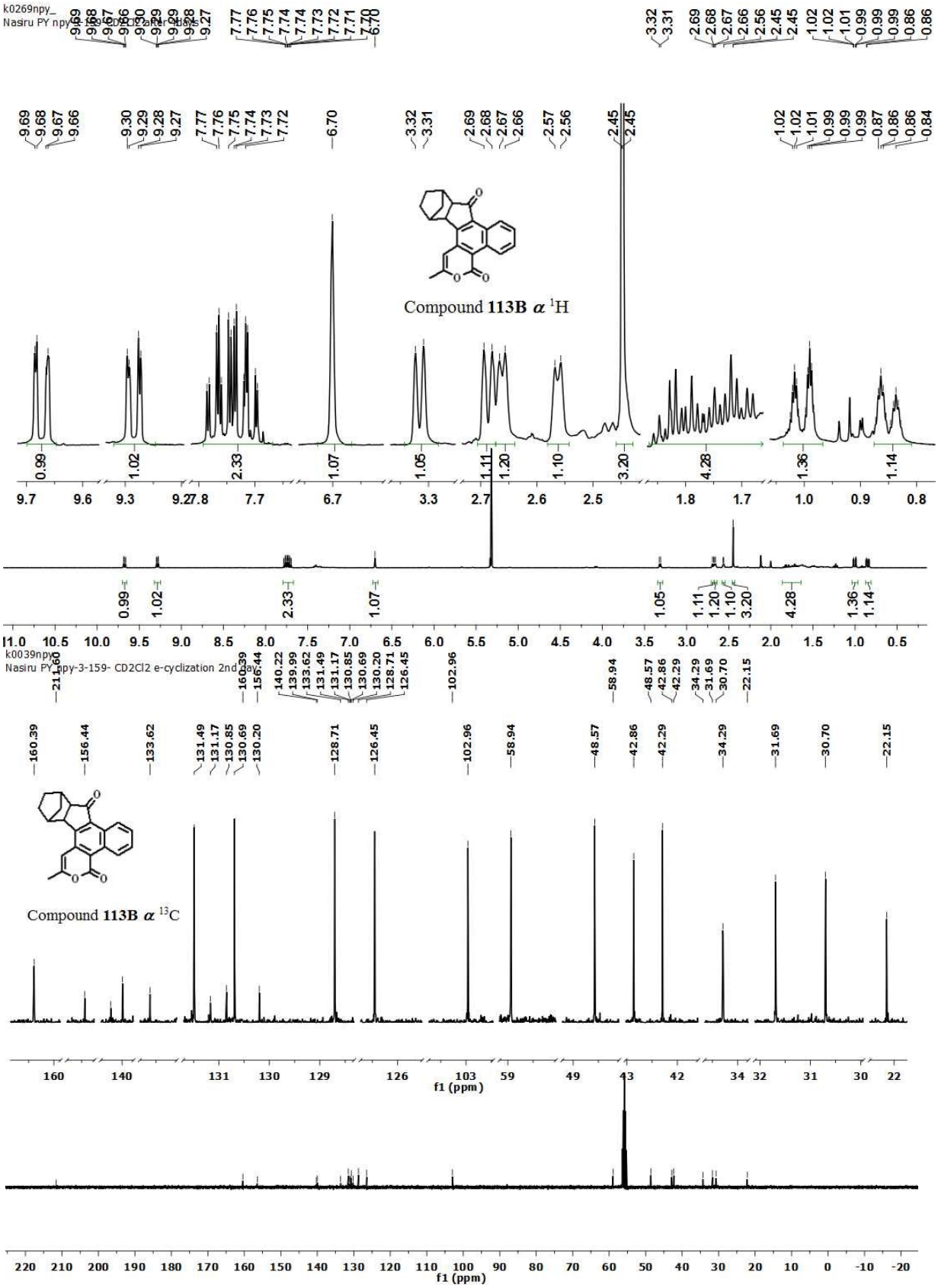

Appendix for (113B α)

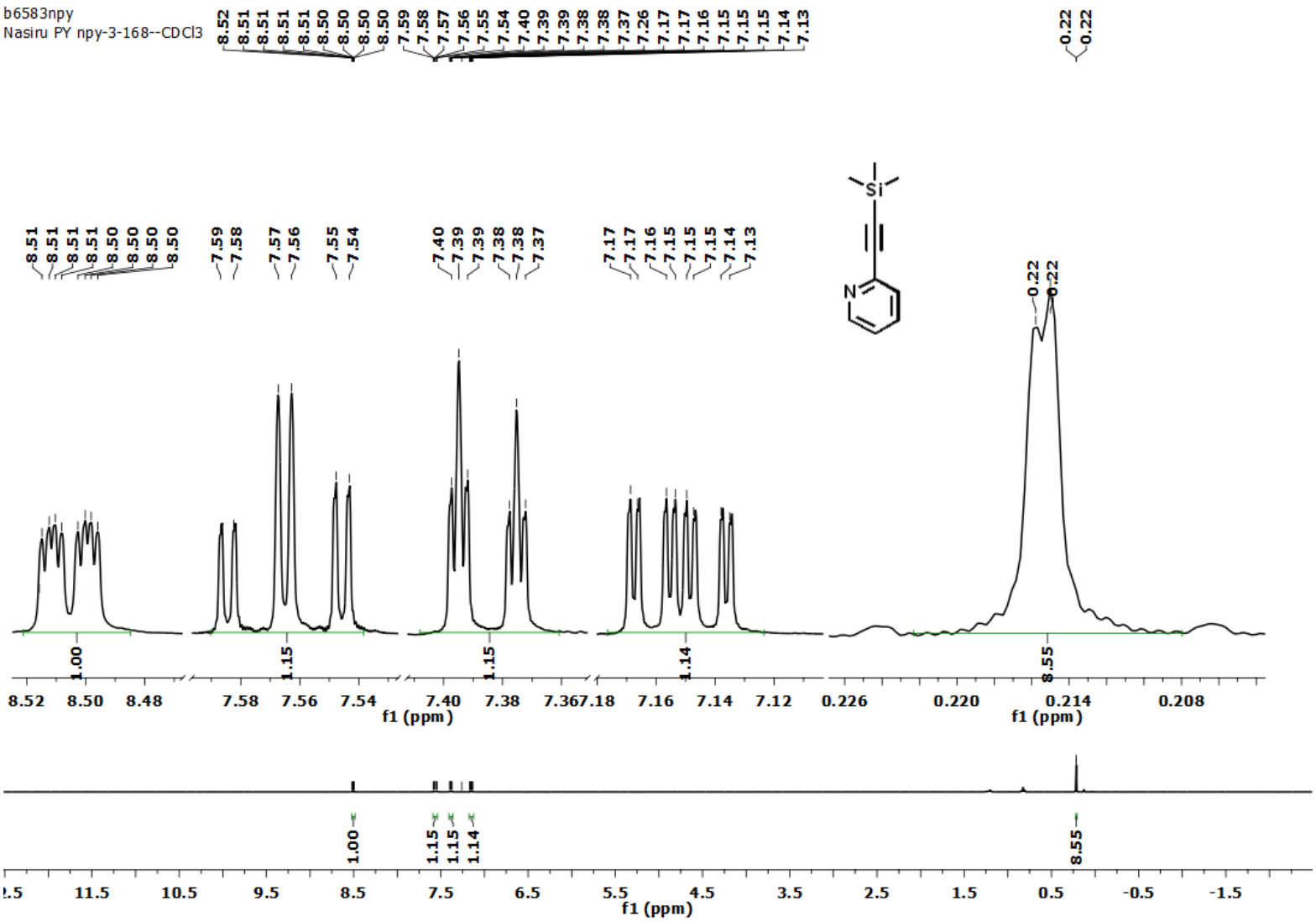

Appendix for (114a)

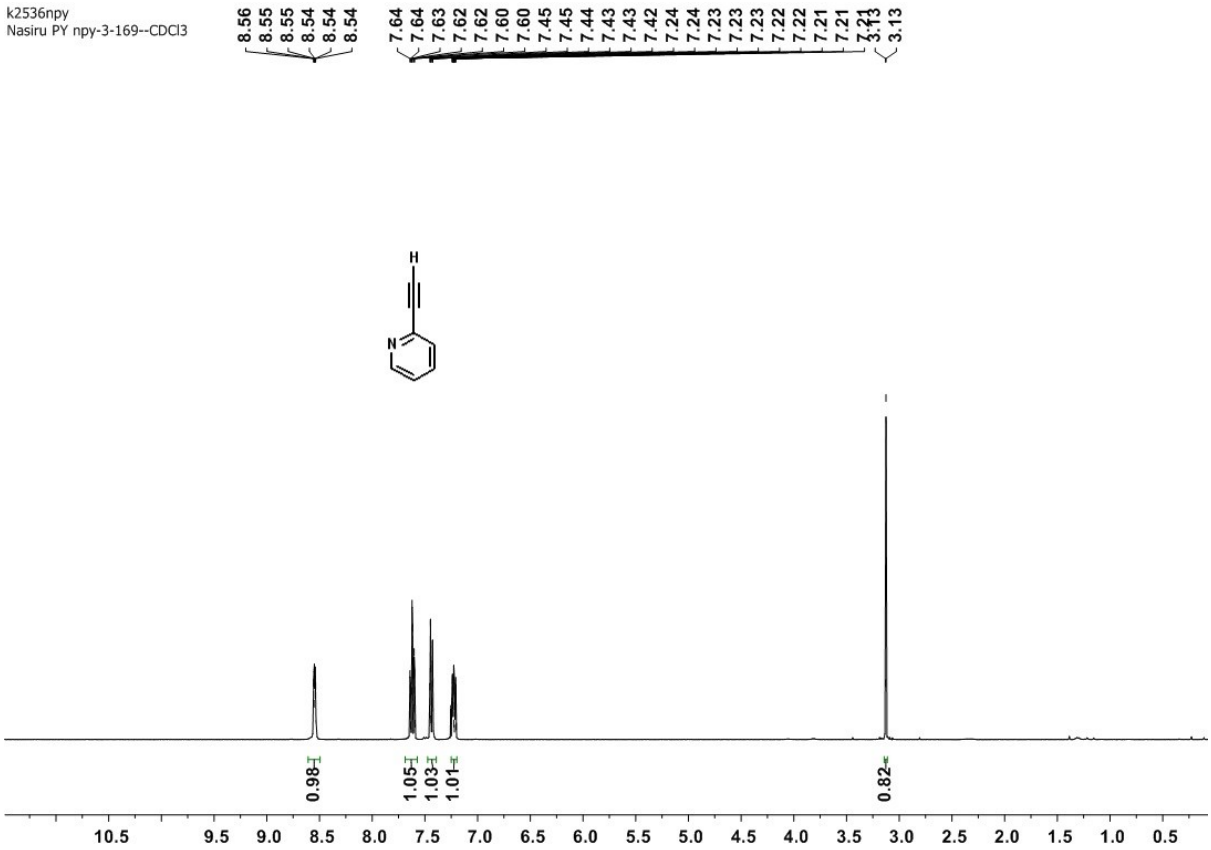

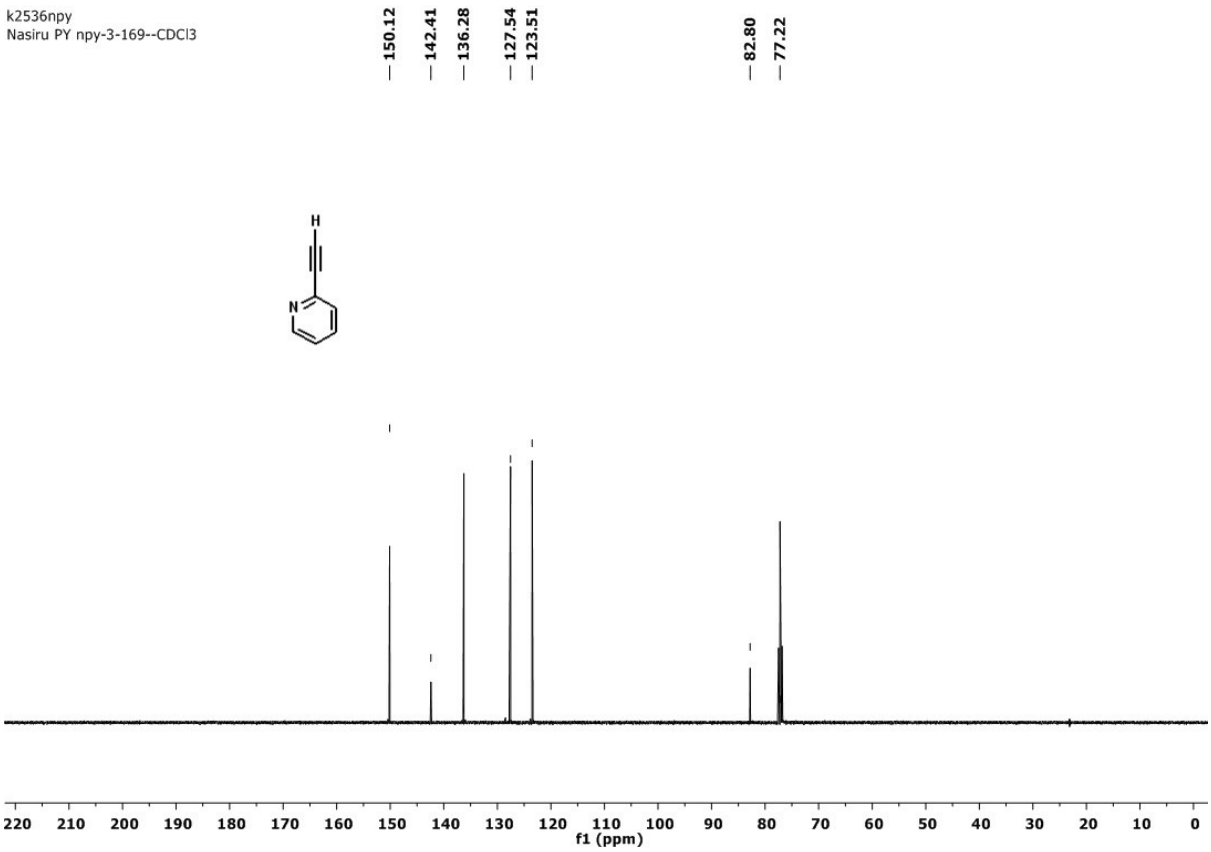

Appendix for (114b)

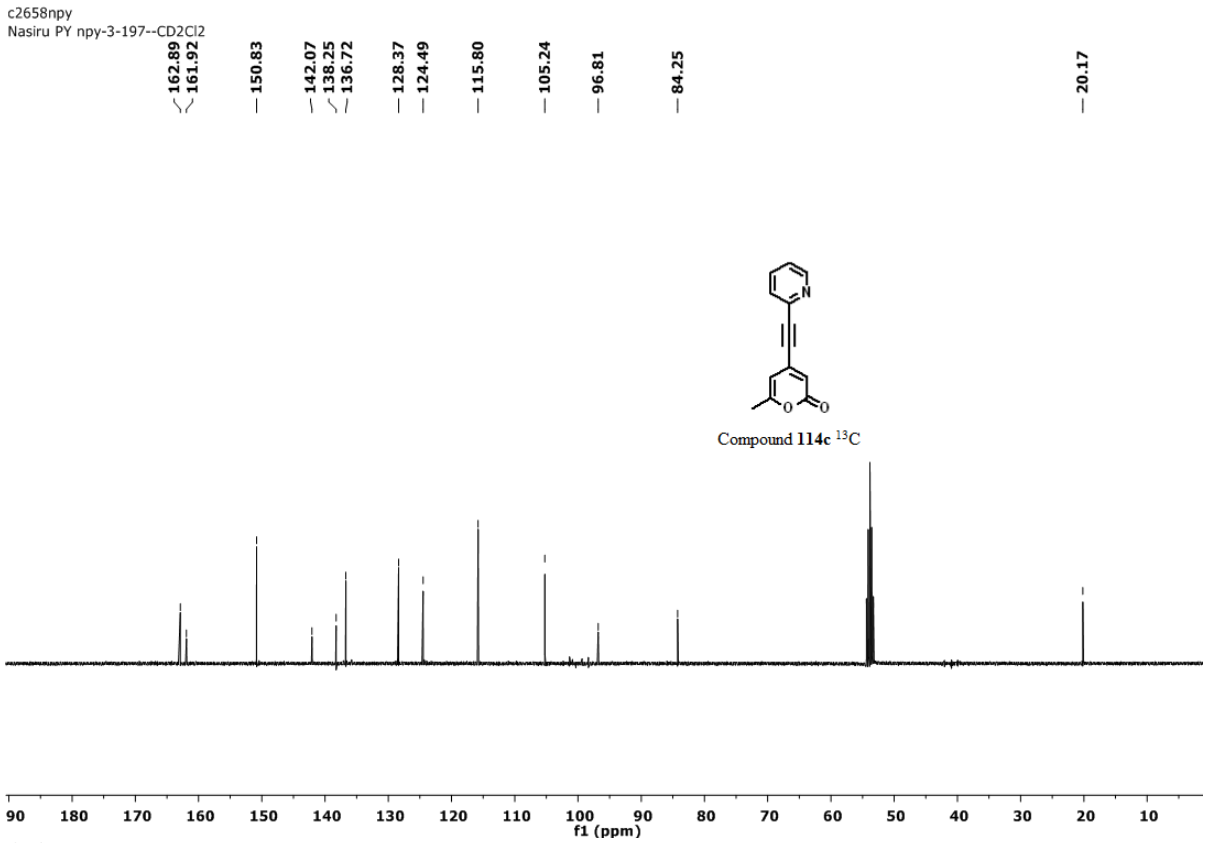

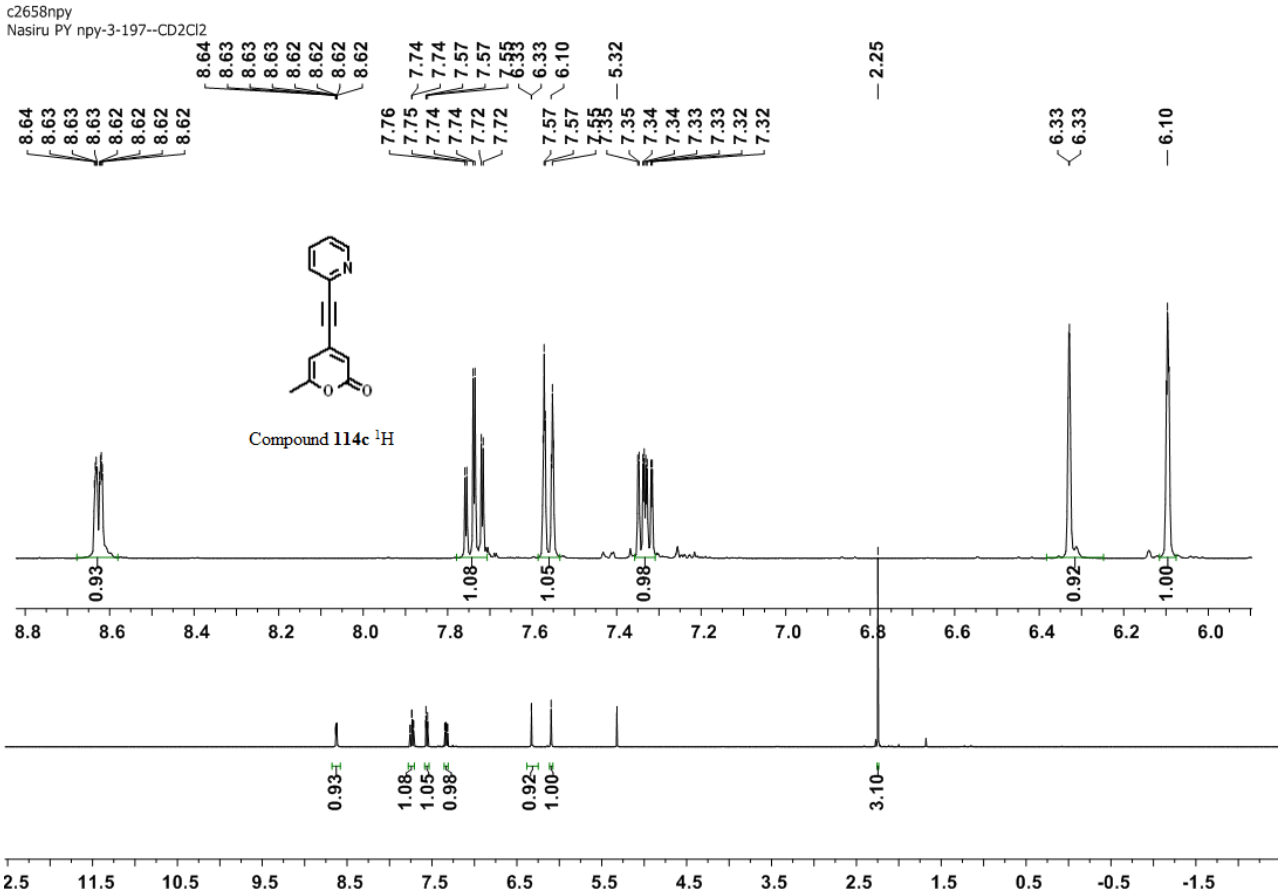

Appendix for (114c)

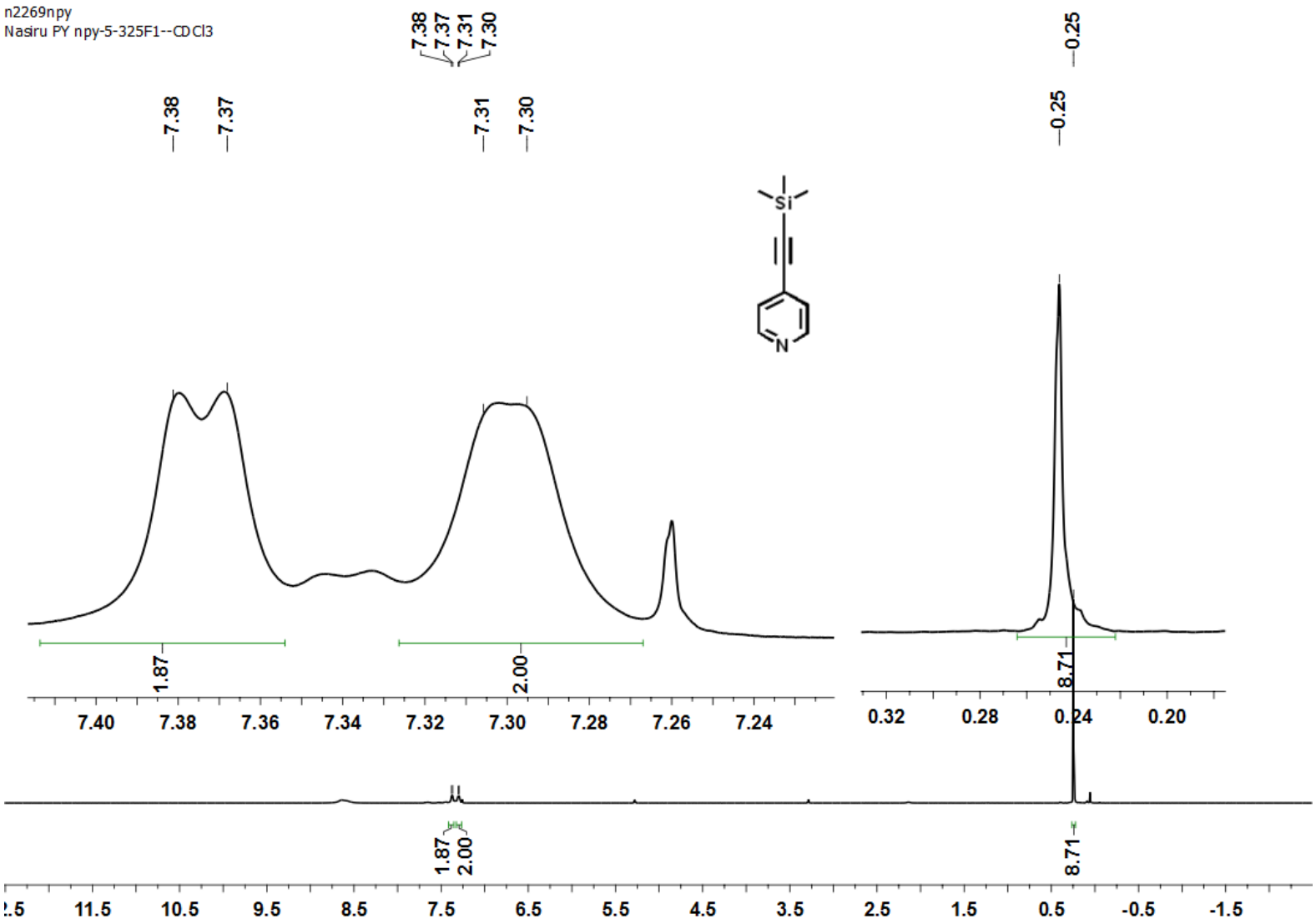

Appendix for (115a)

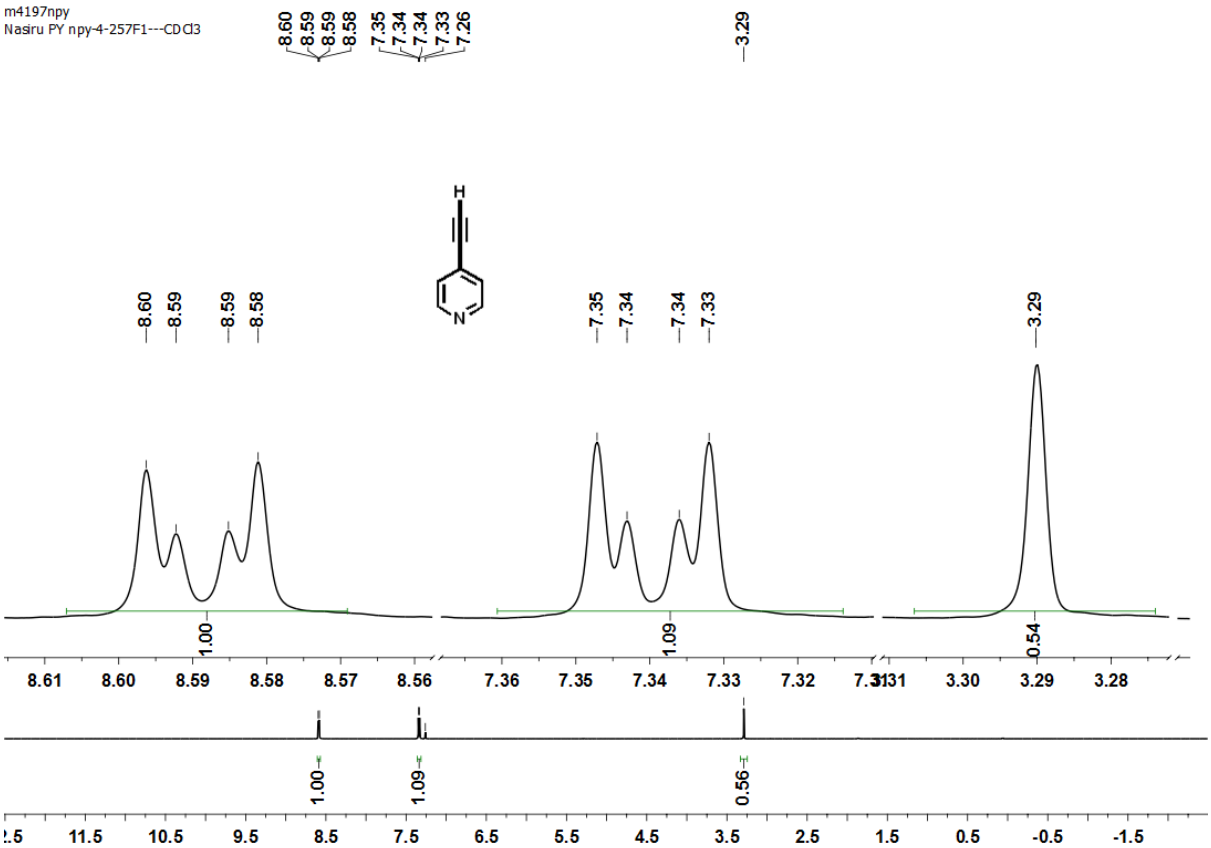

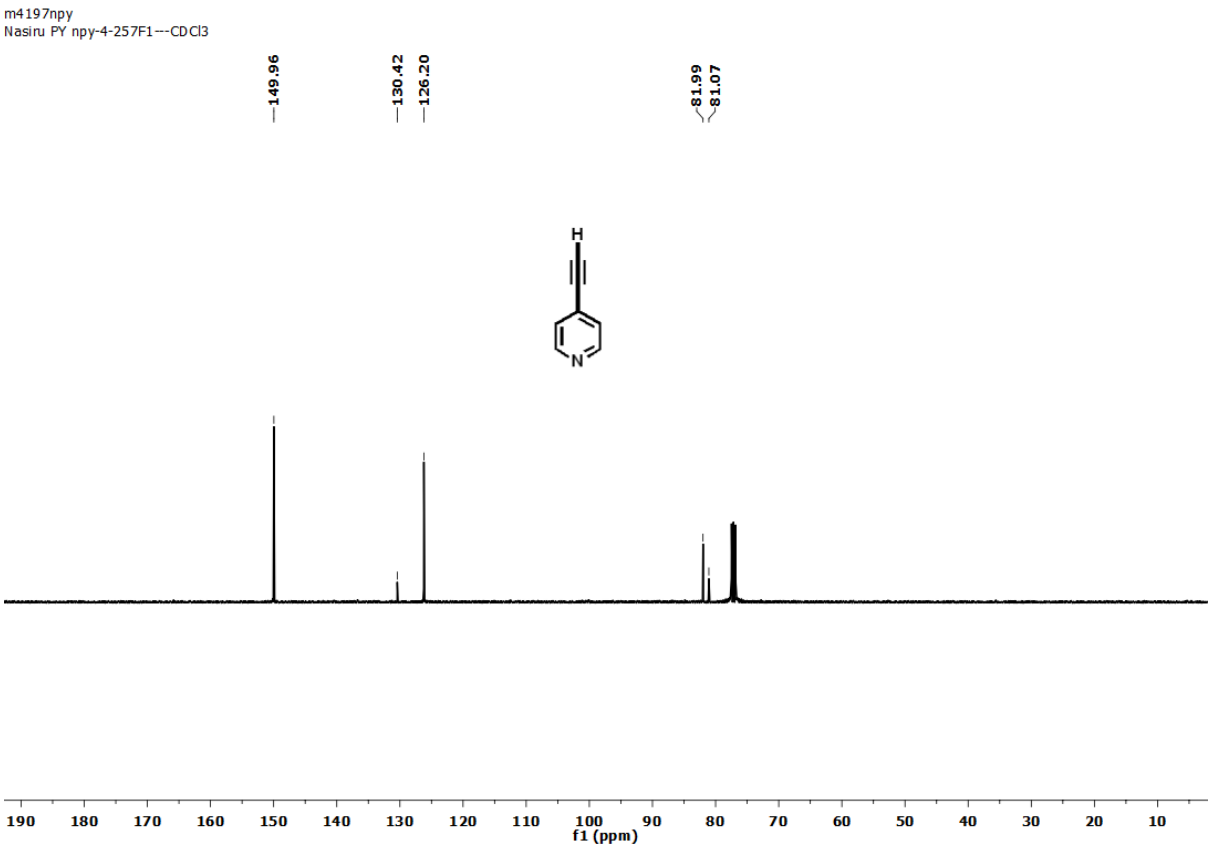

Appendix for (115b)

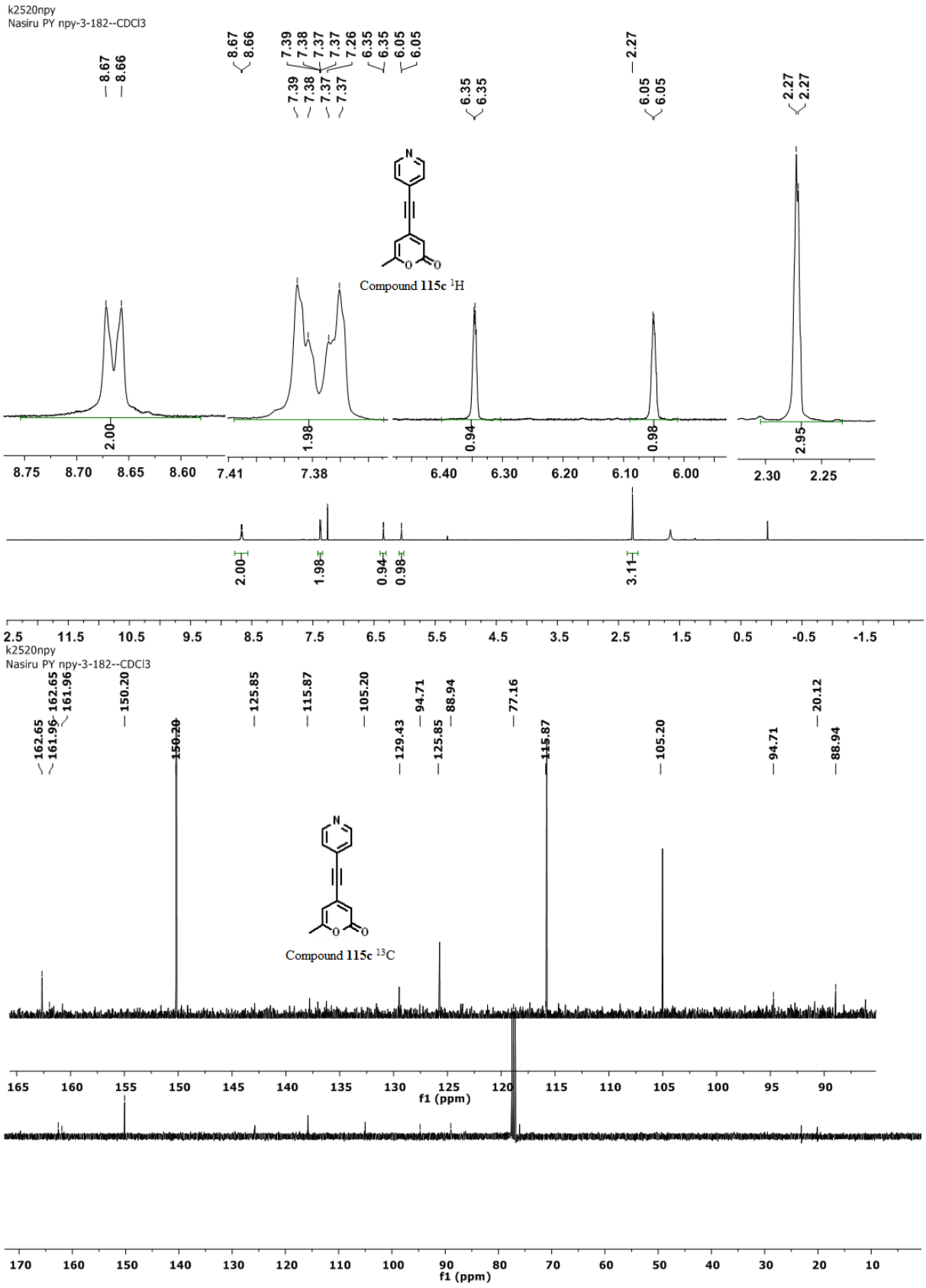

Appendix for (115c)

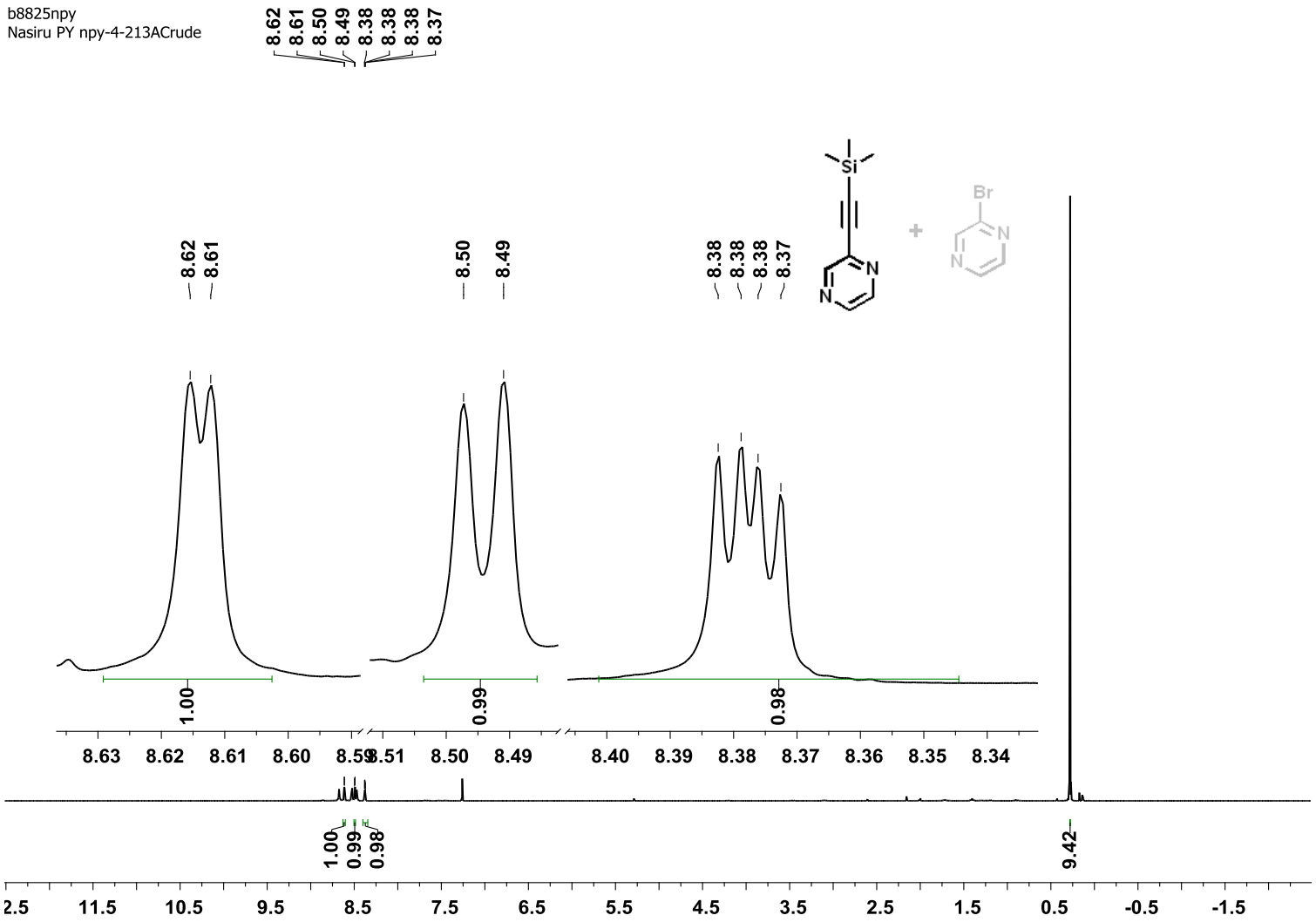

Appendix for (116a)

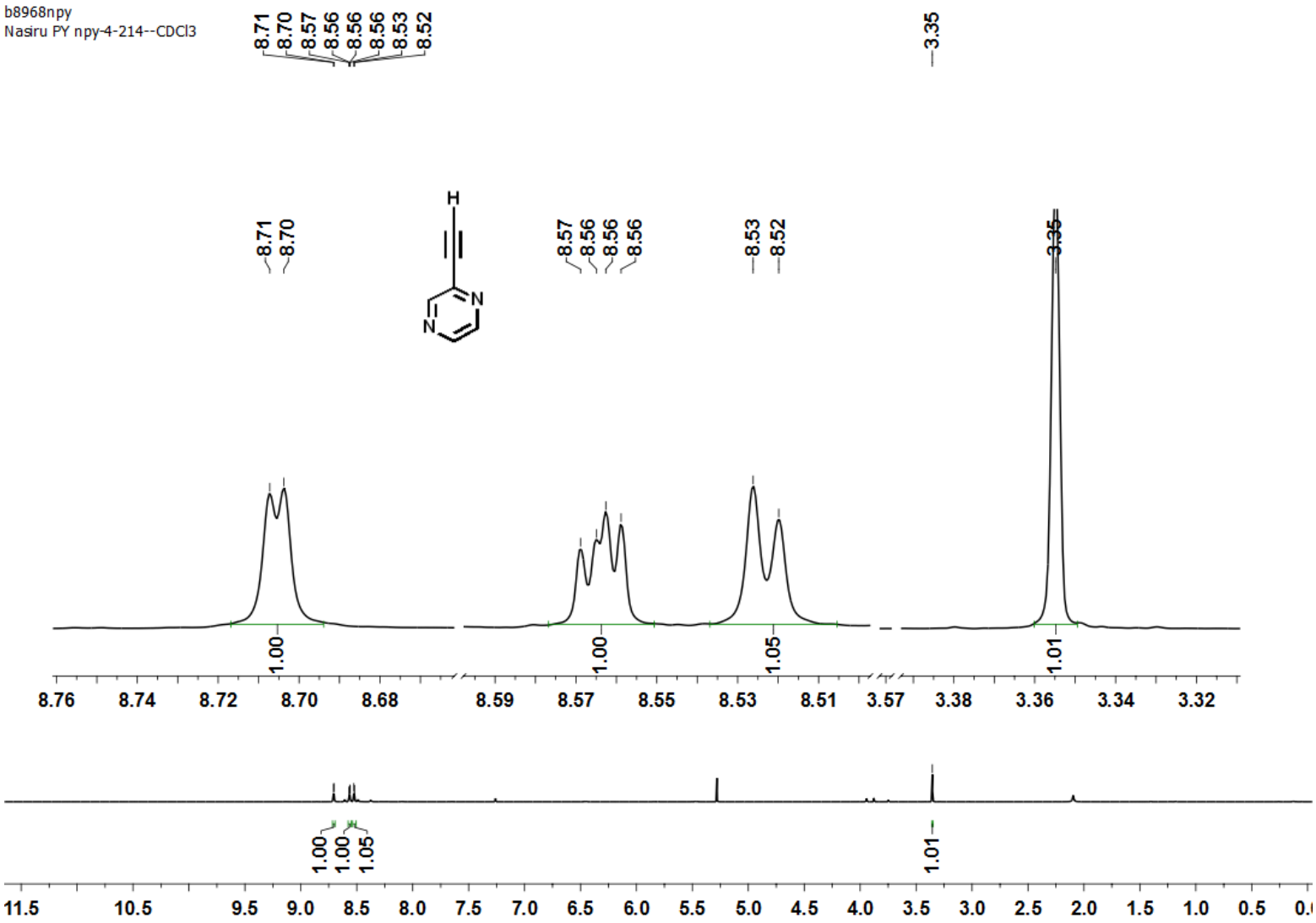

Appendix for (116b)

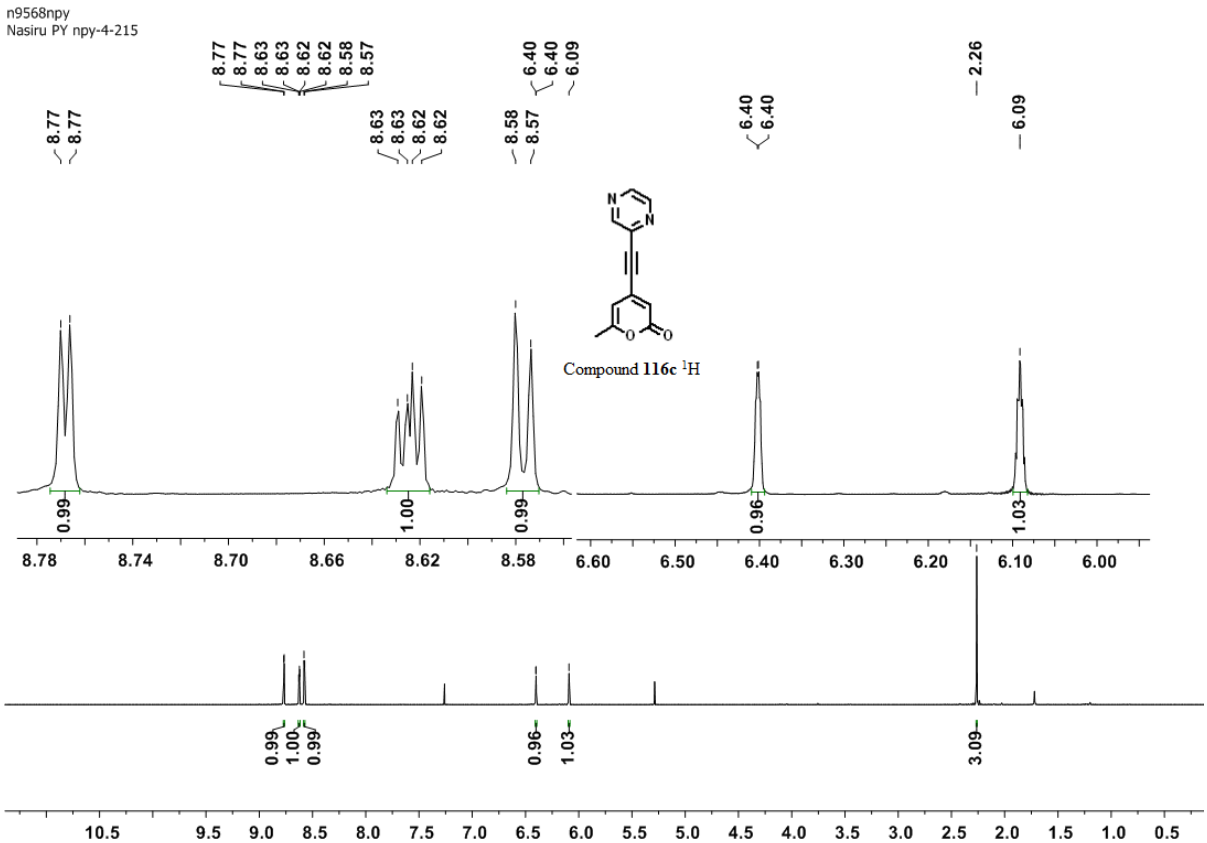

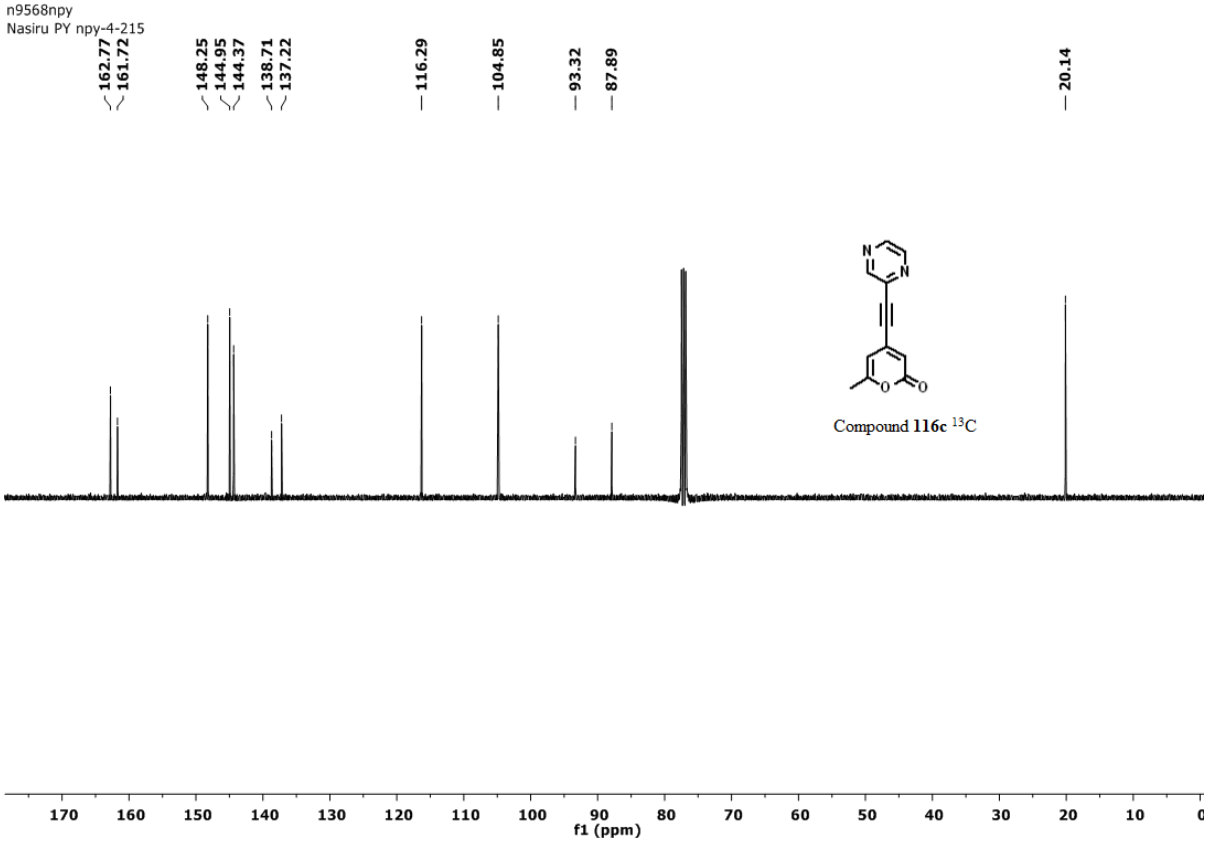

Appendix for (116c)

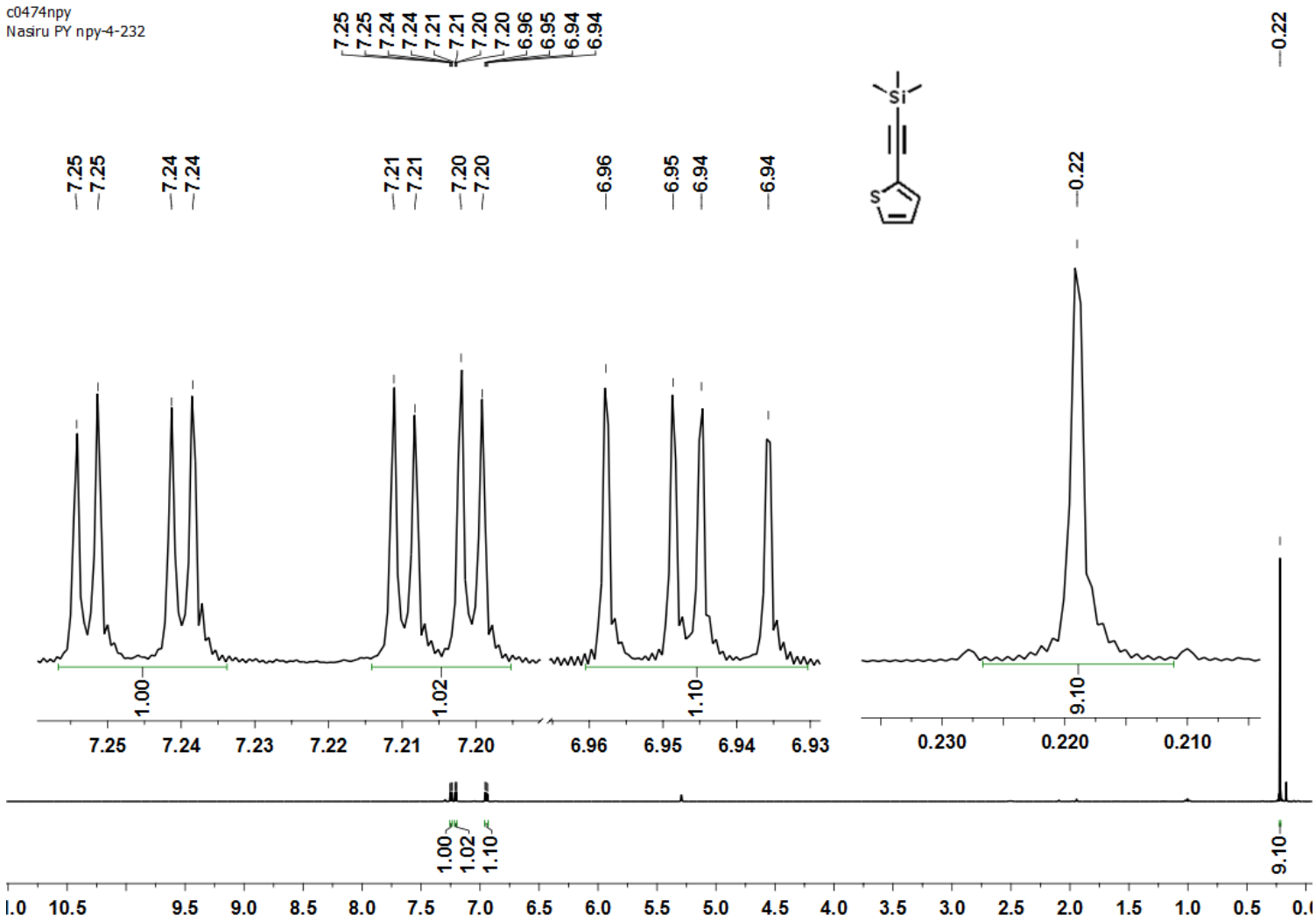

Appendix for (117a)

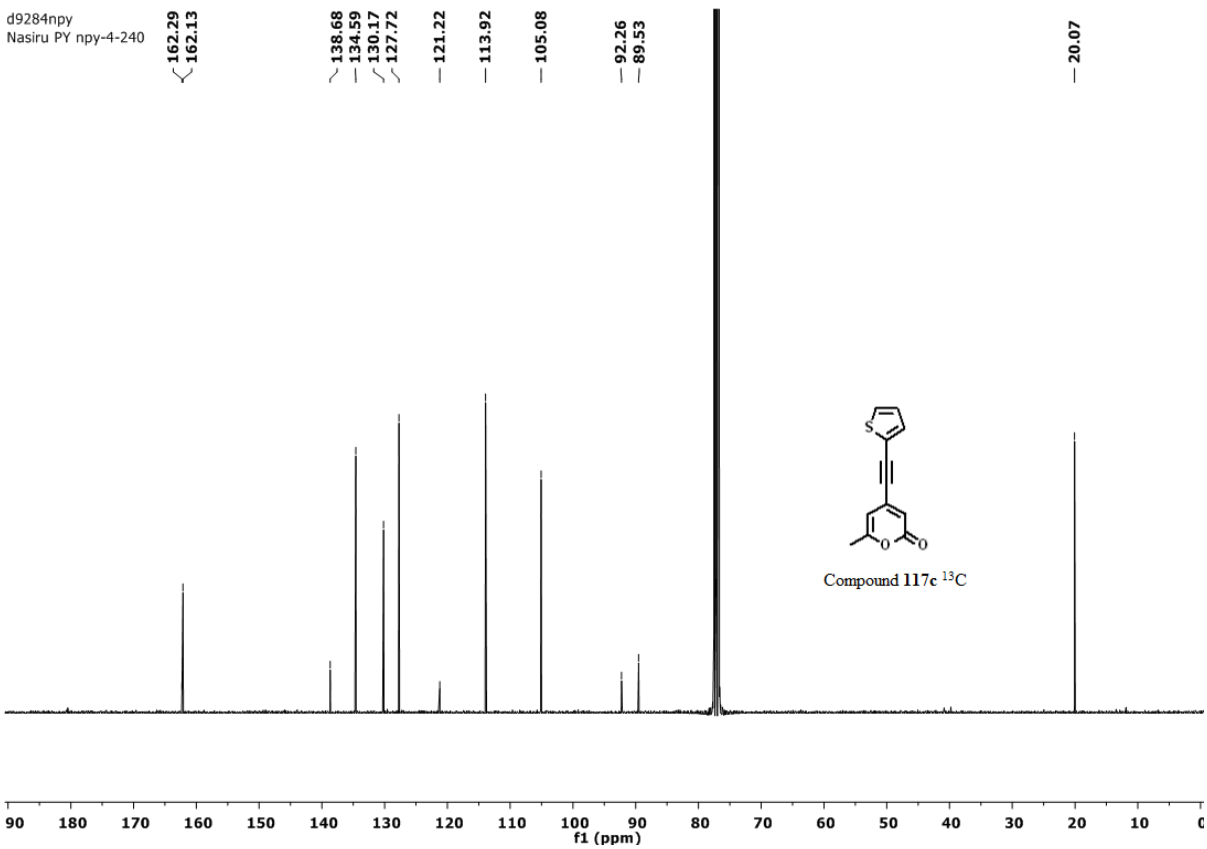

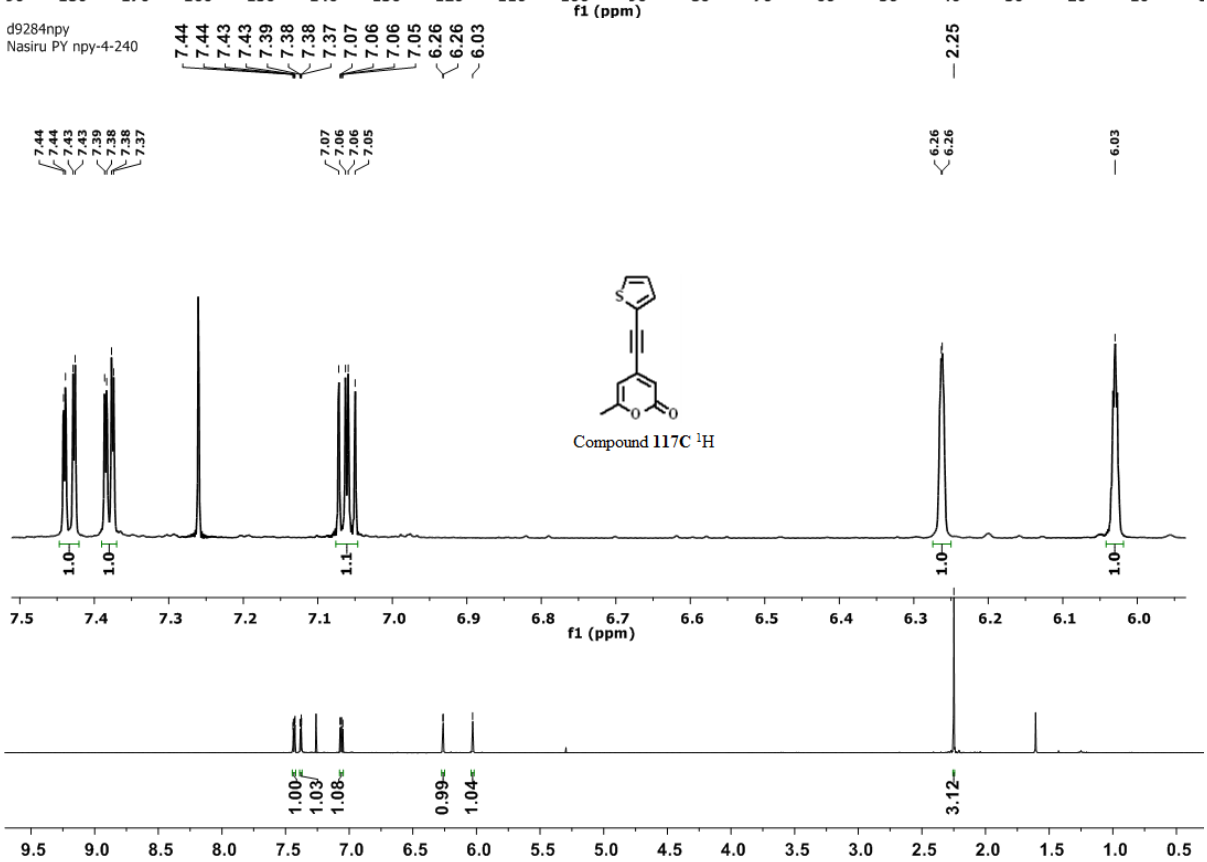

Appendix for (117c)

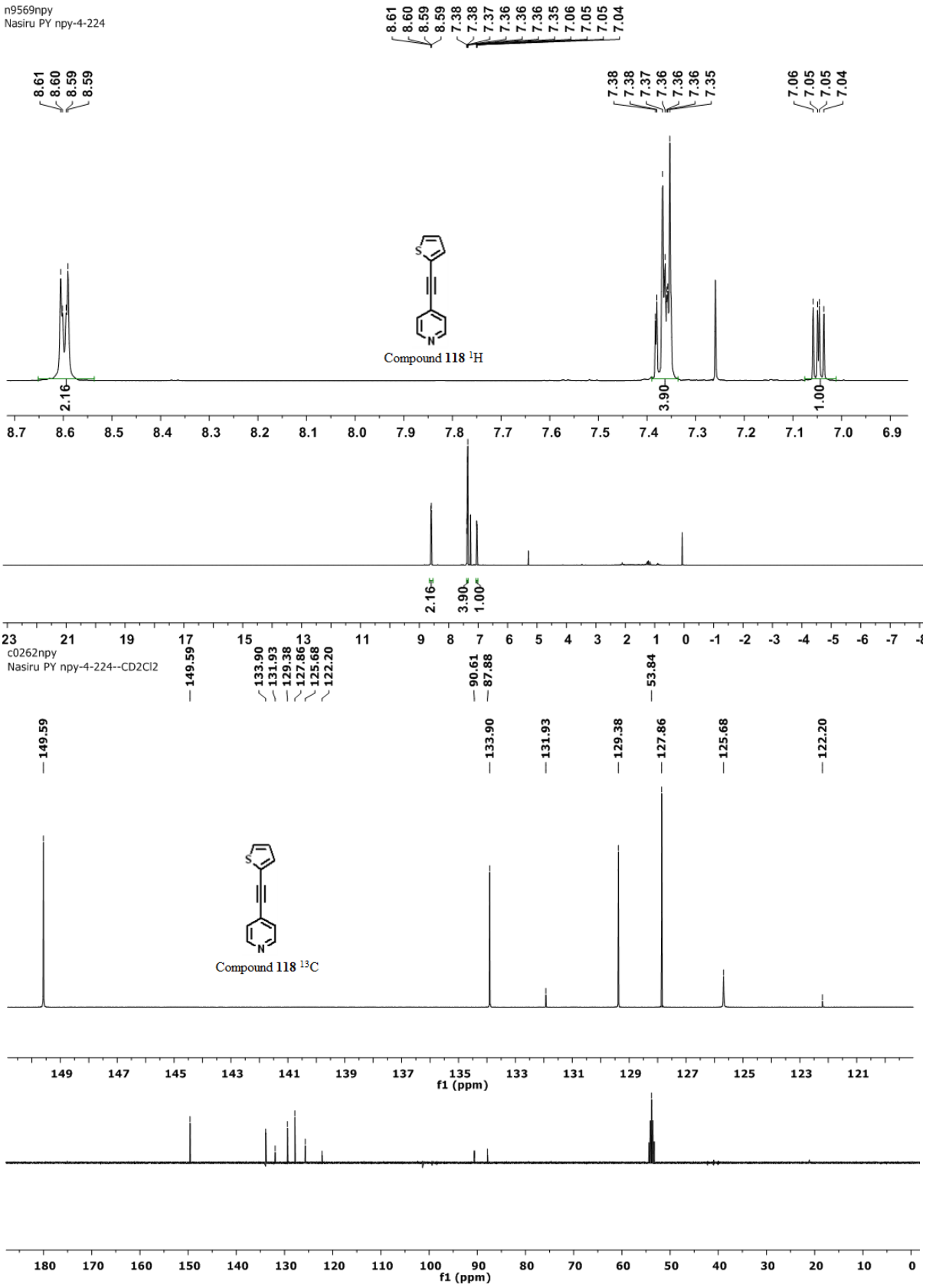

Appendix for (118)

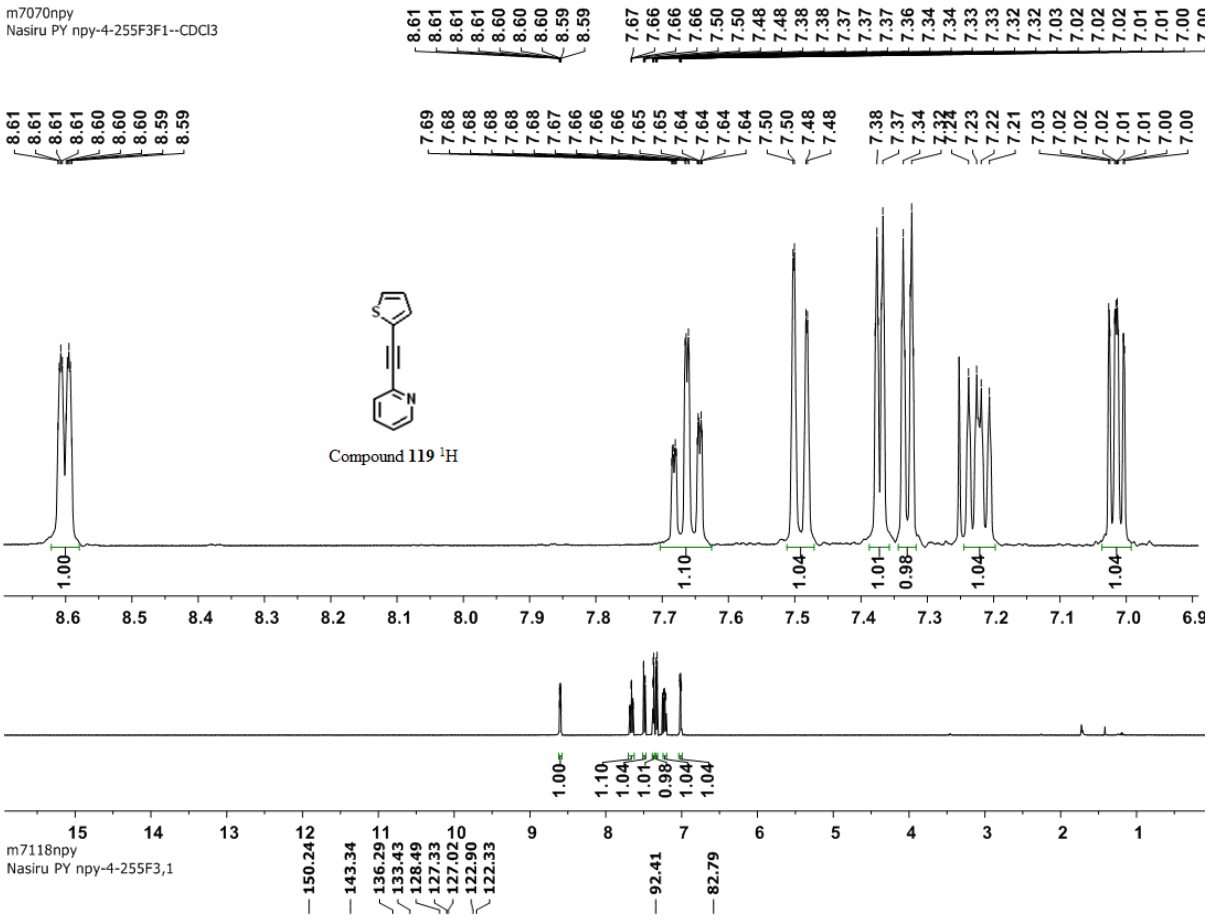

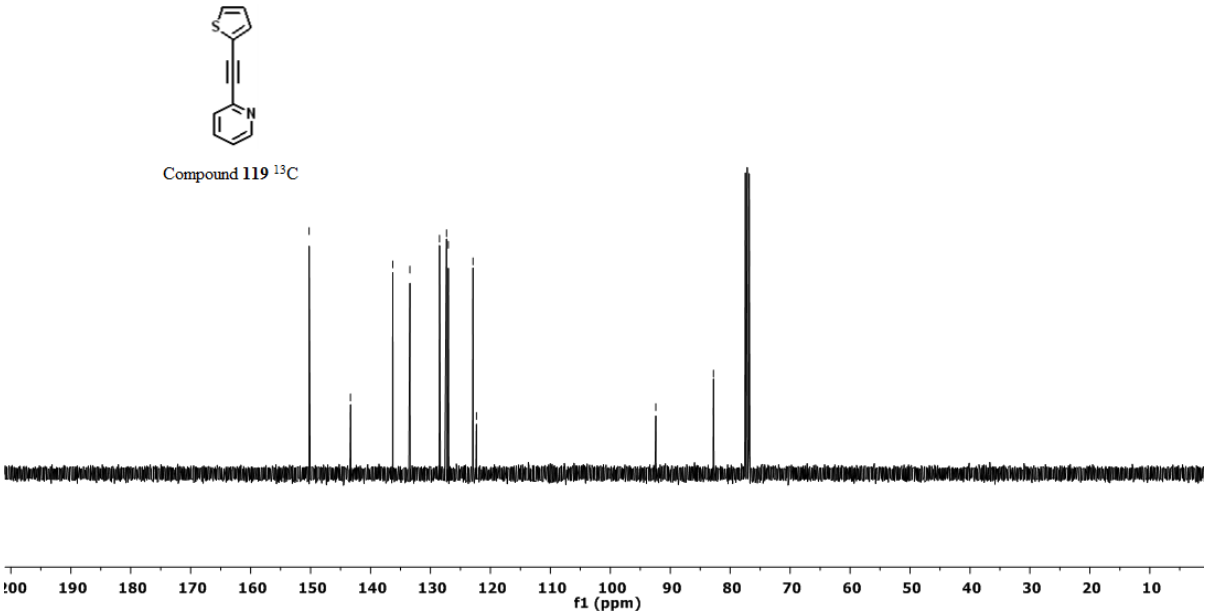

Appendix for (119)

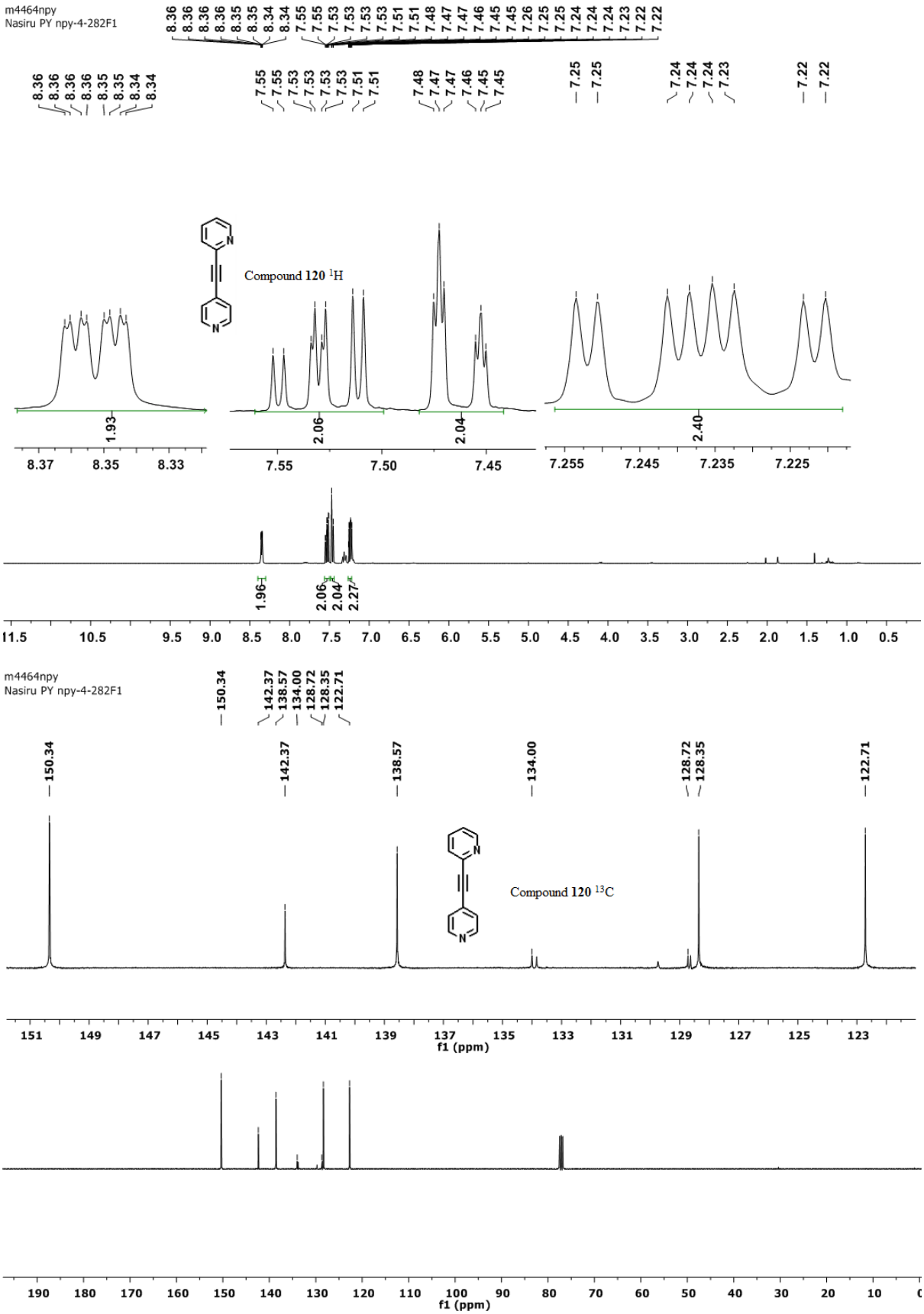

Appendix for (120)

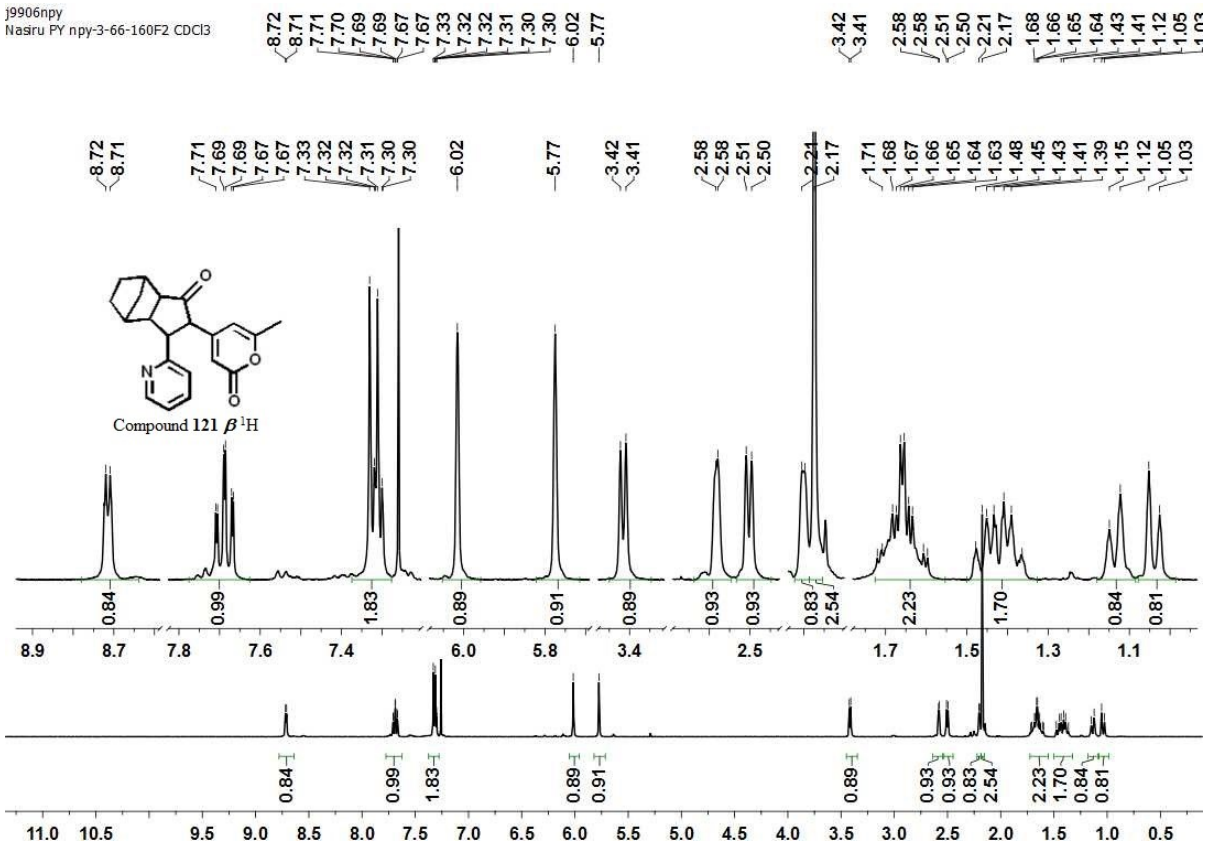

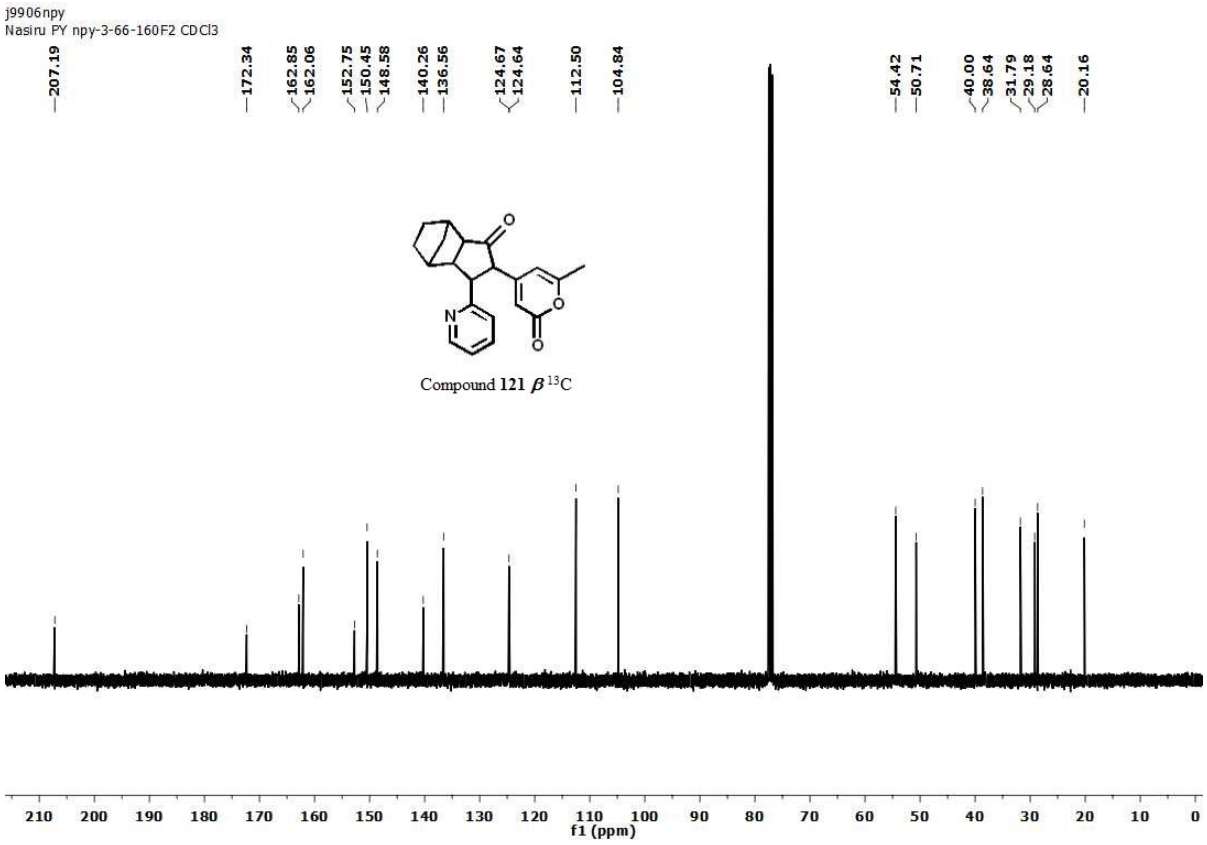

Appendix for (121 β)

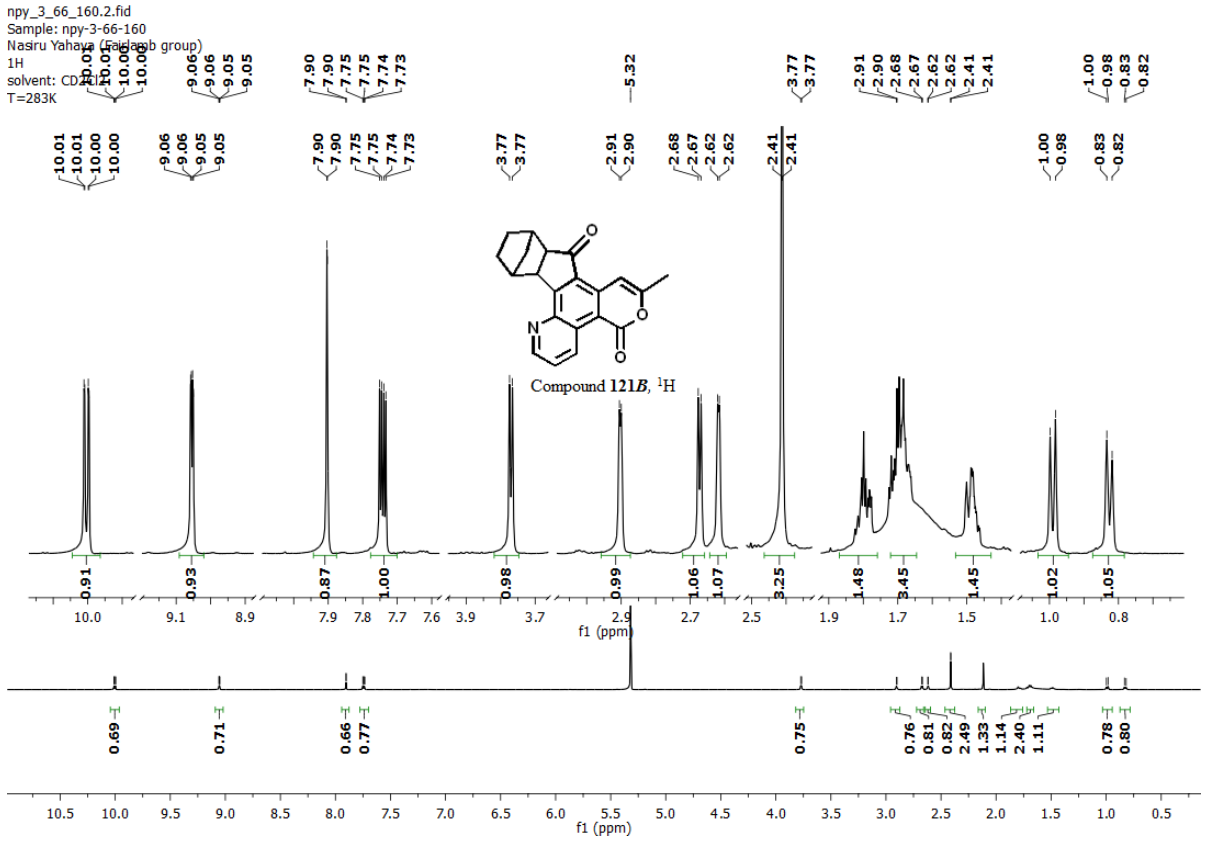

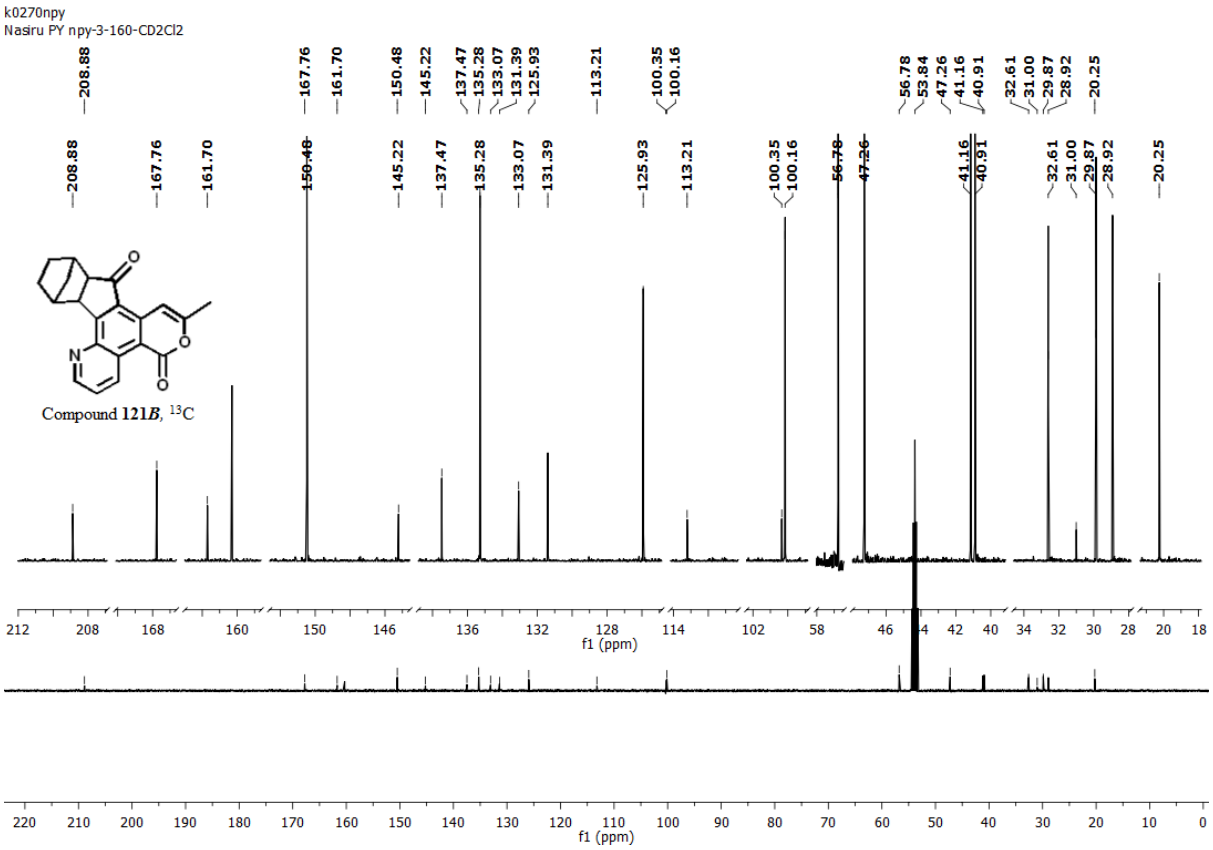

Appendix for (121B *β*)

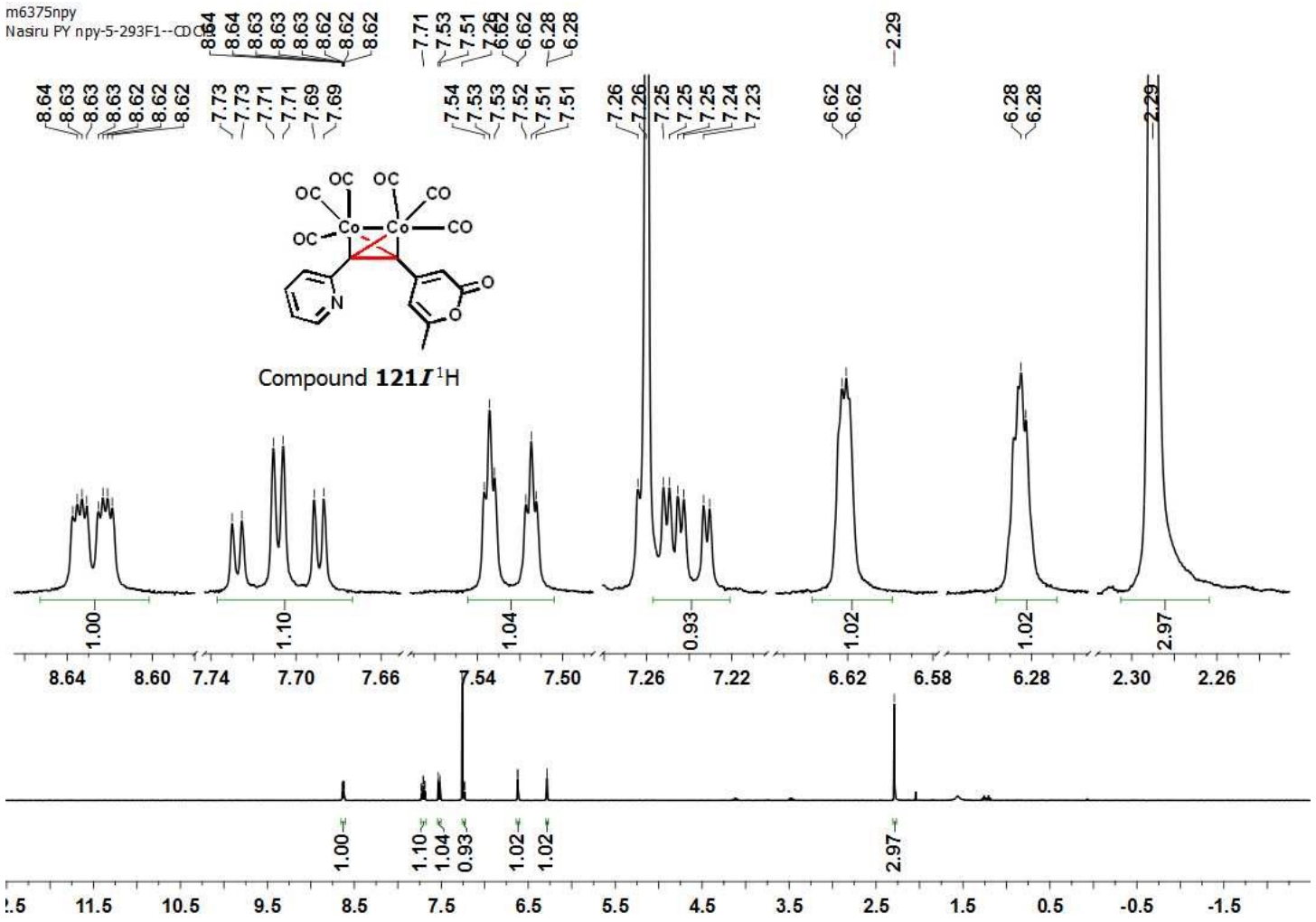

Appendix for (121*I*)

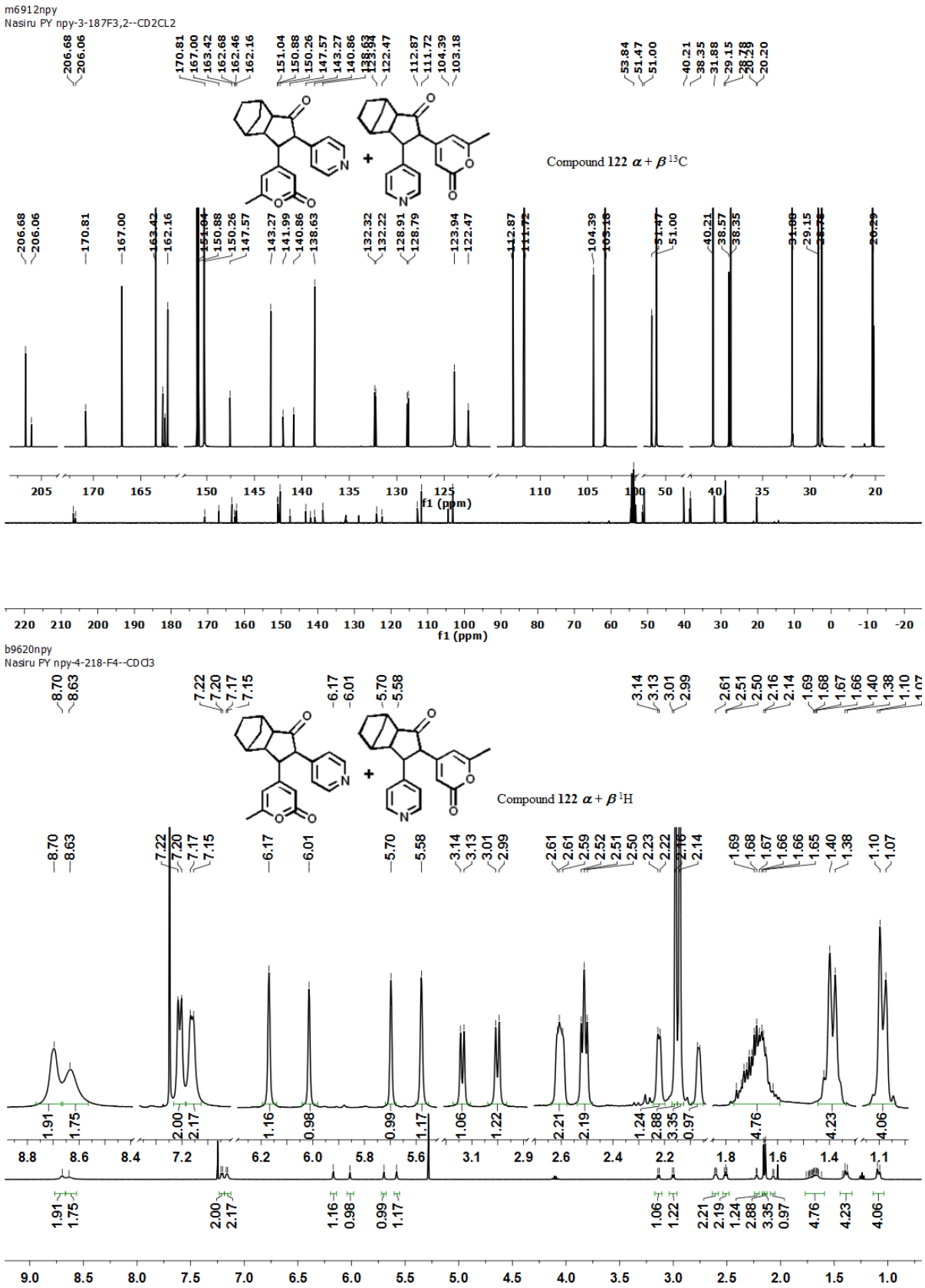

Appendix for (122 $\alpha+\beta$)

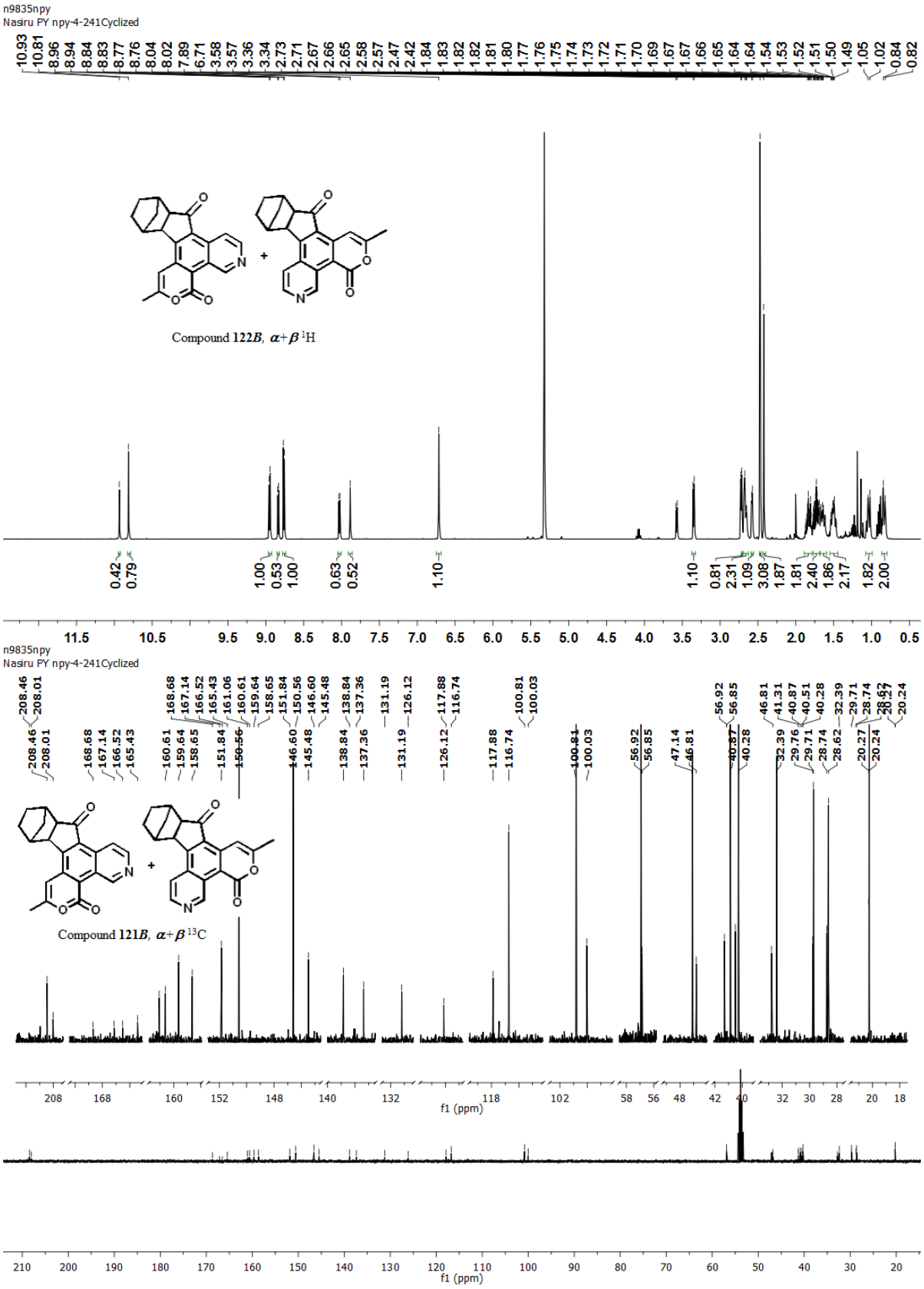

Appendix for (122B $\alpha+\beta$)

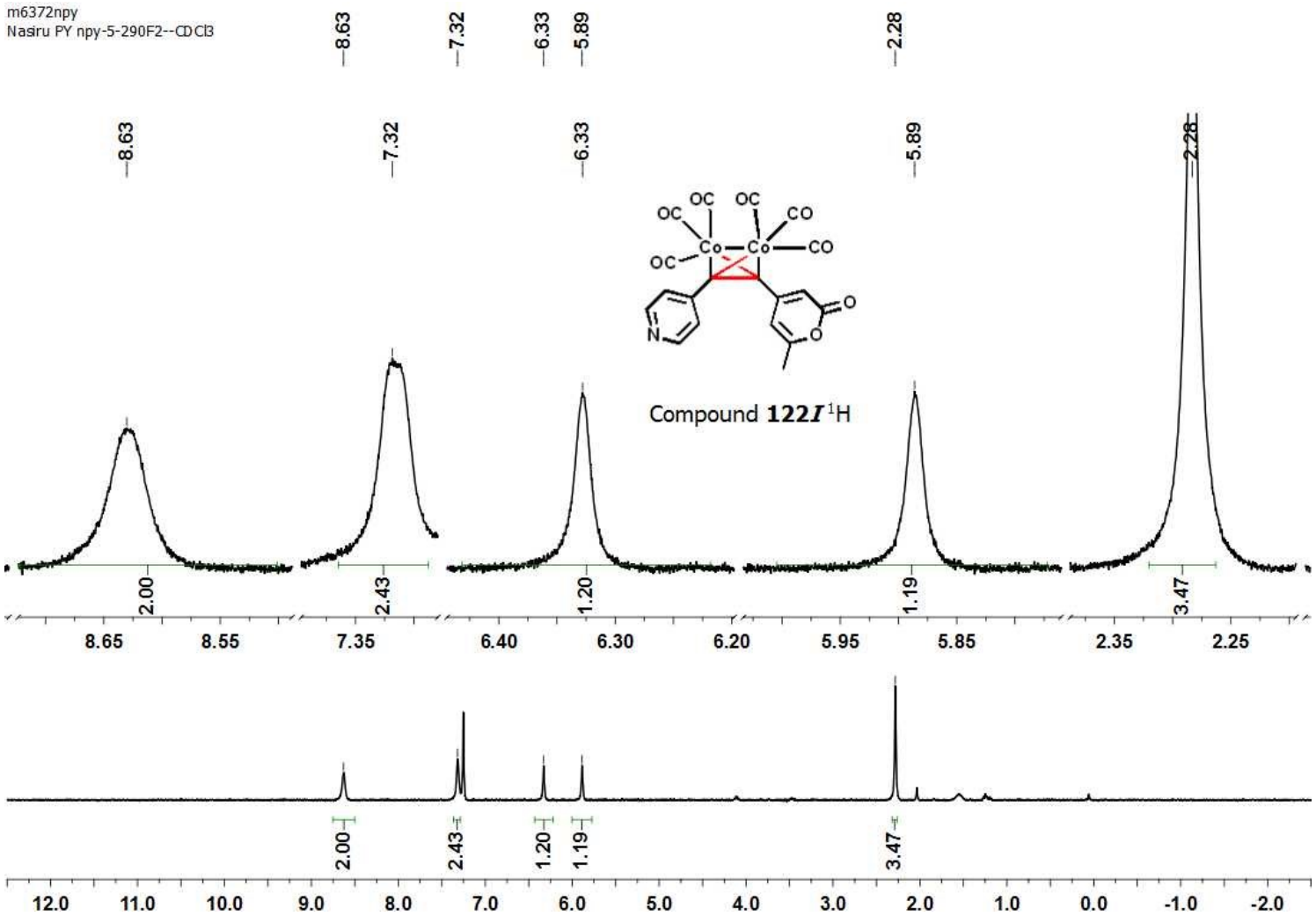

Appendix for (122*I*)

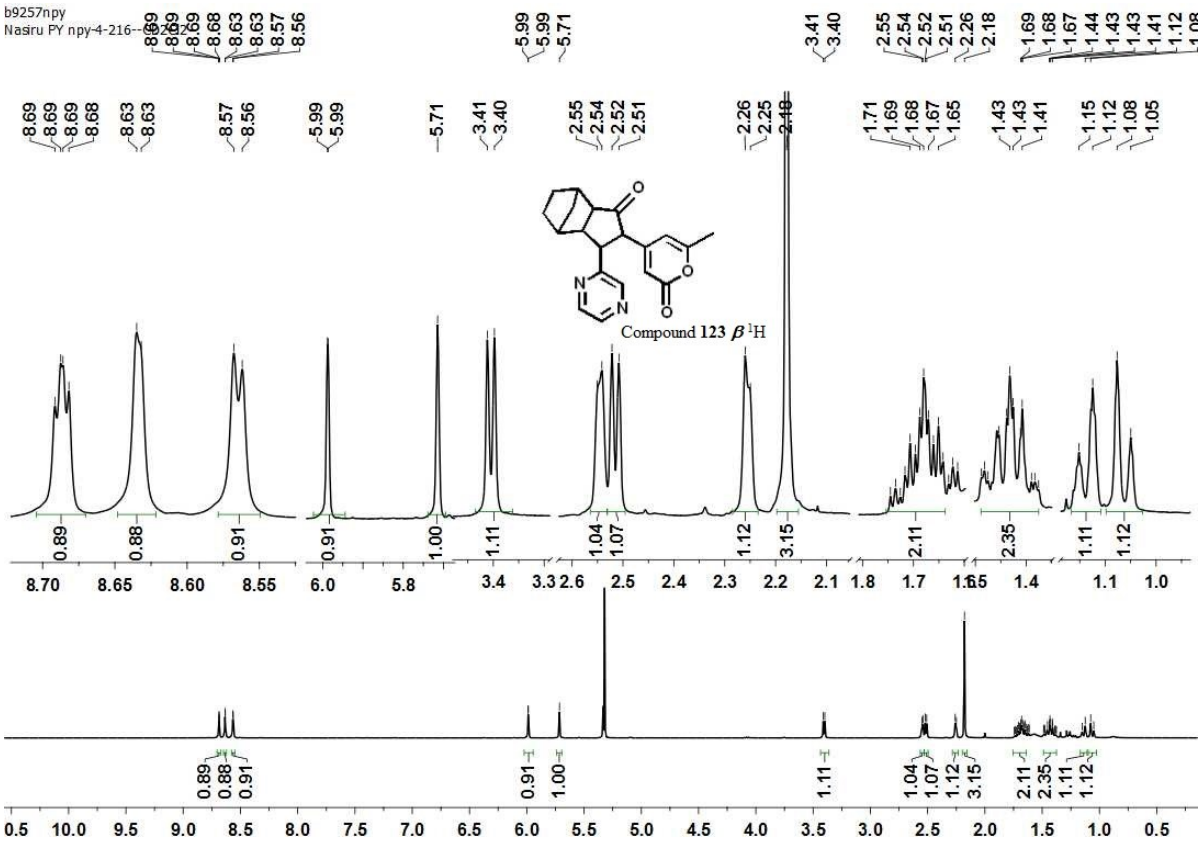

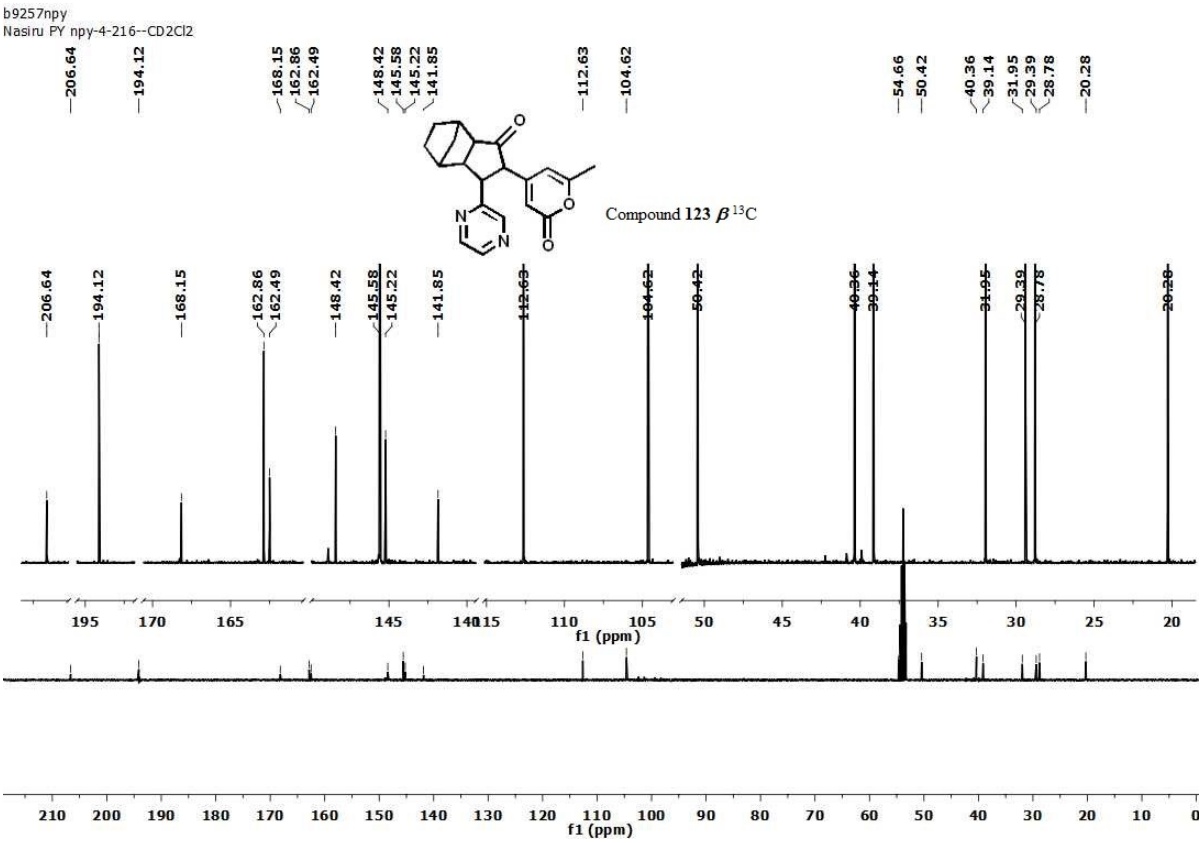

Appendix for (123 β)

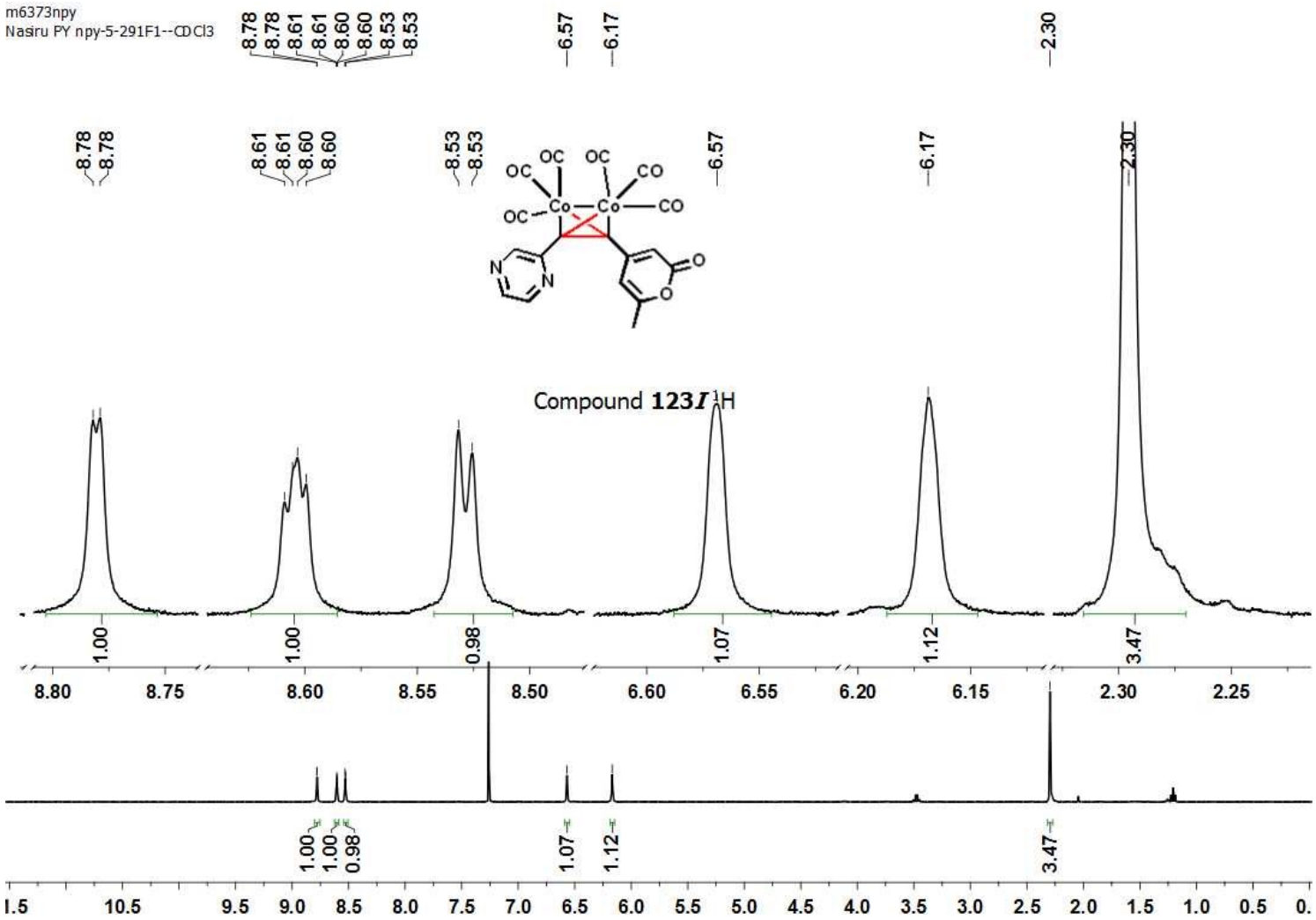

Appendix for (123*I*)

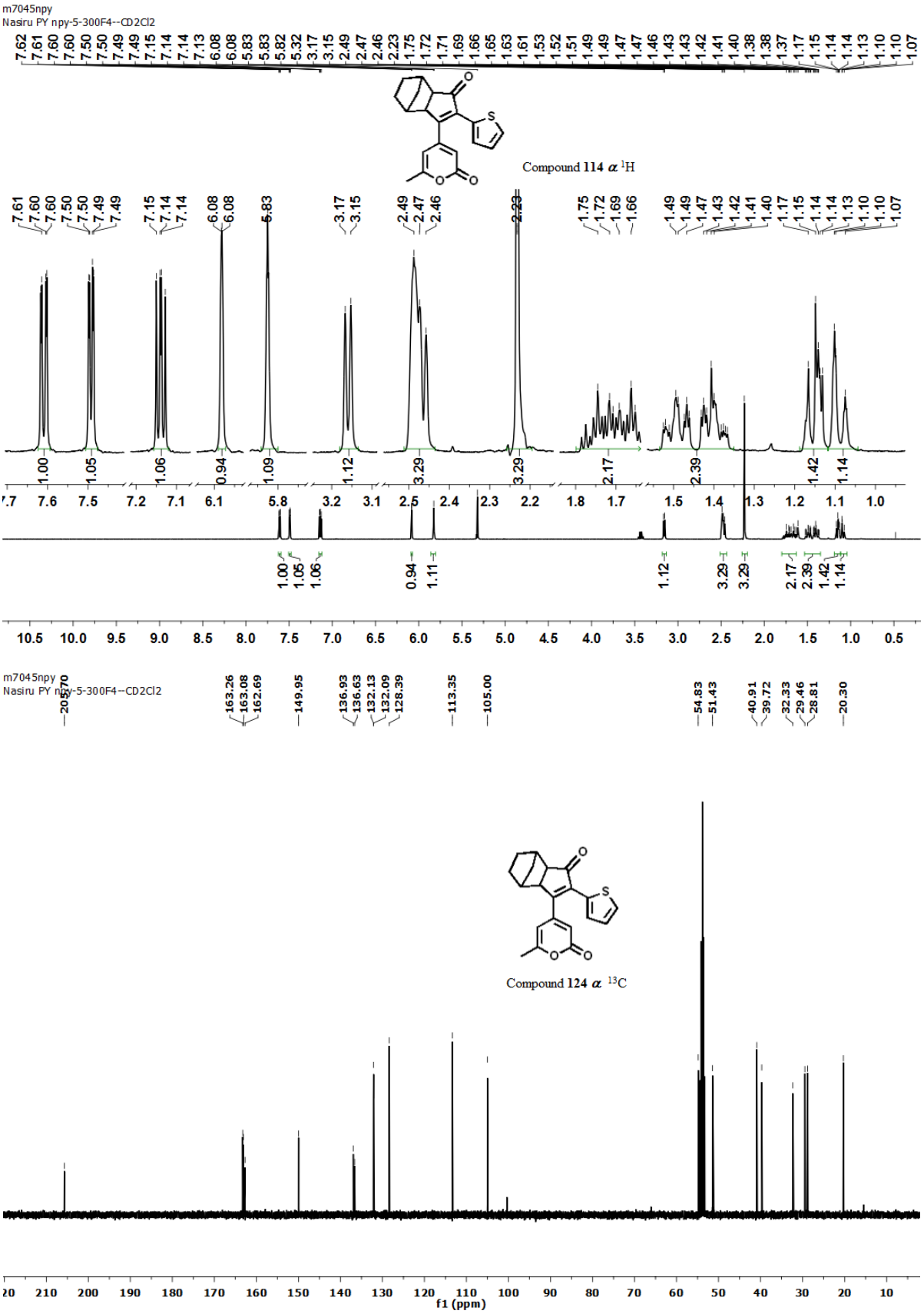

Appendix for (124 α)

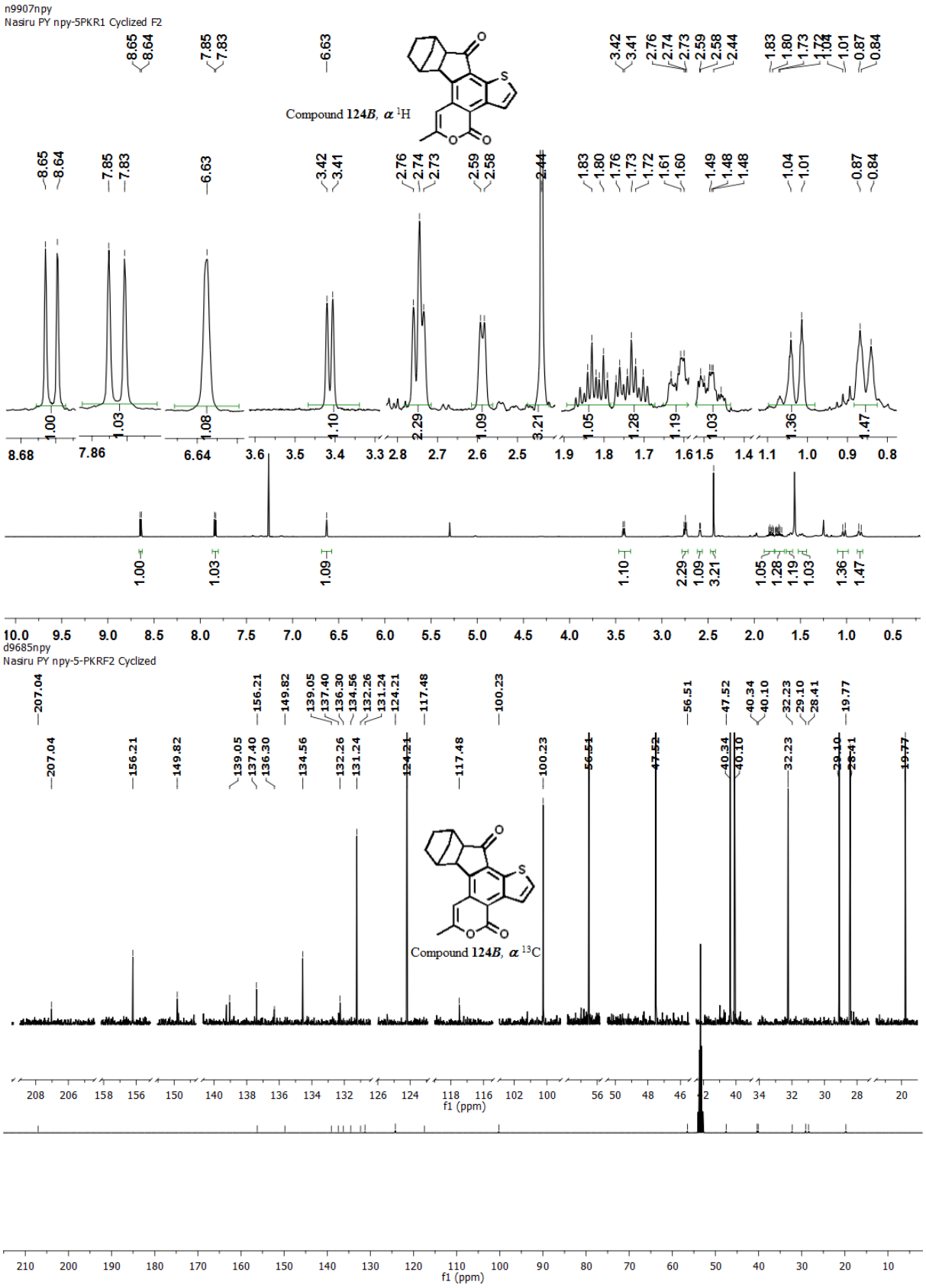

Appendix for (124B α)

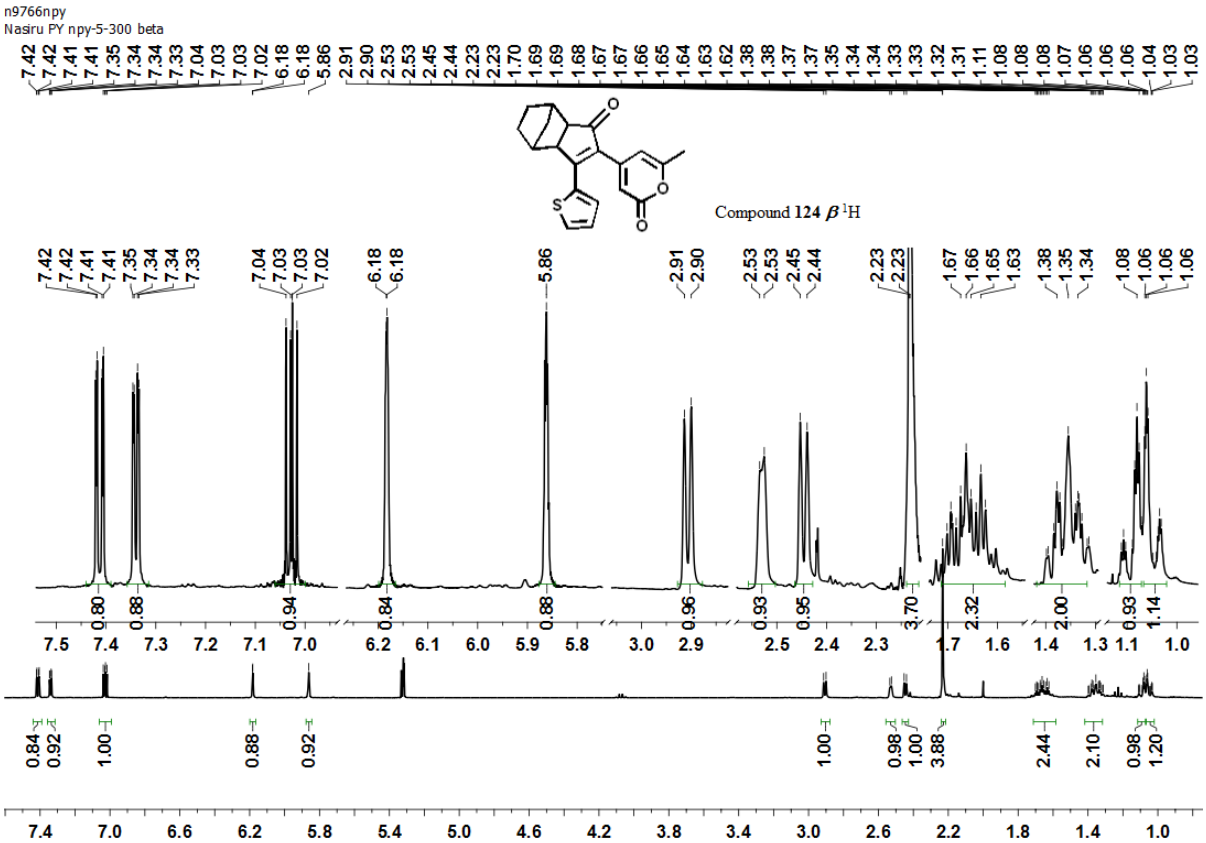

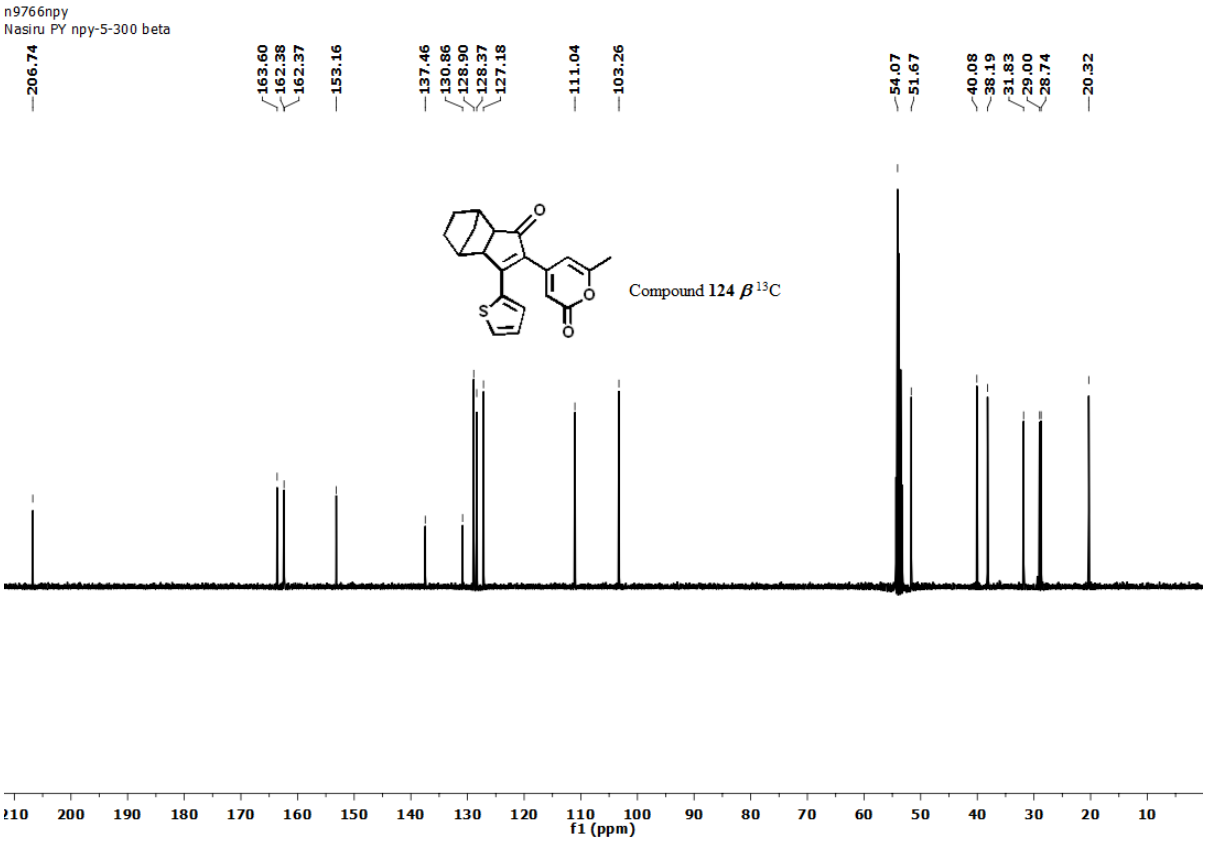

Appendix for (124 *β*)

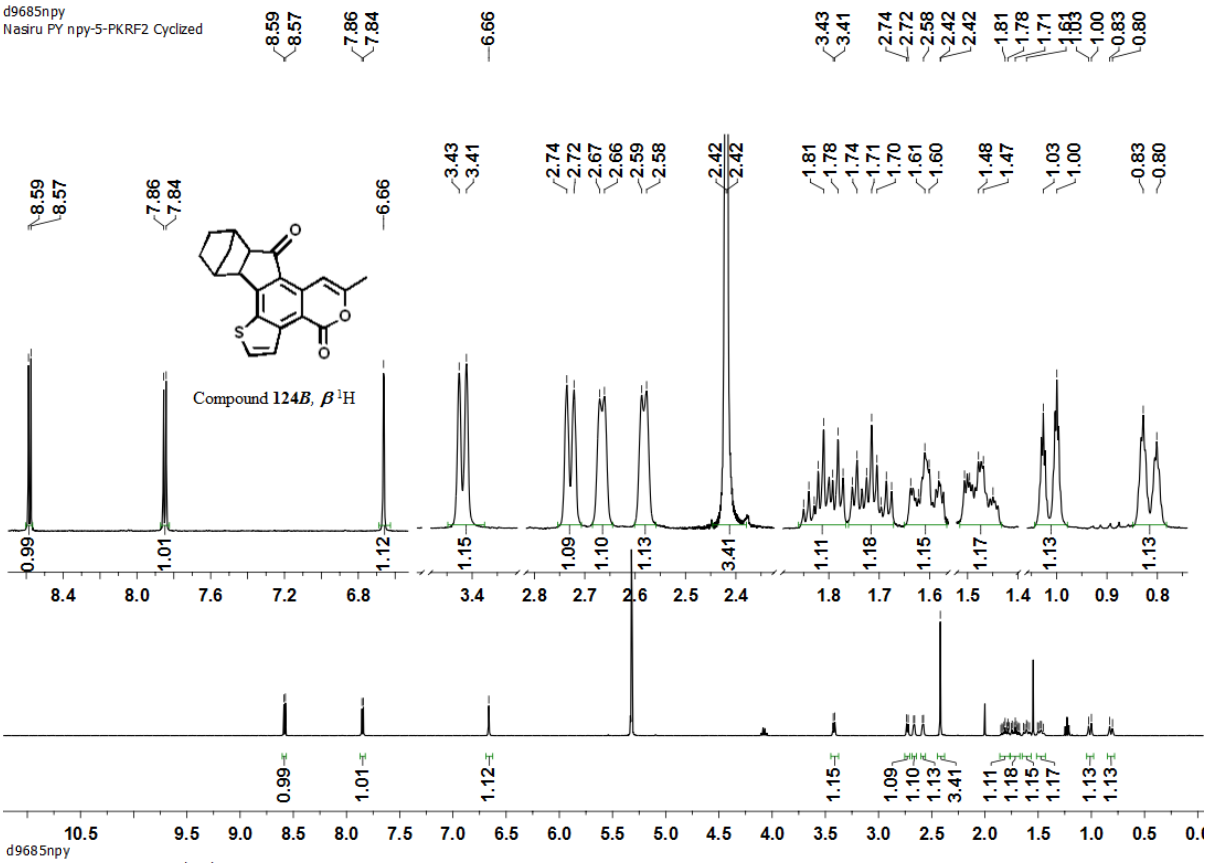

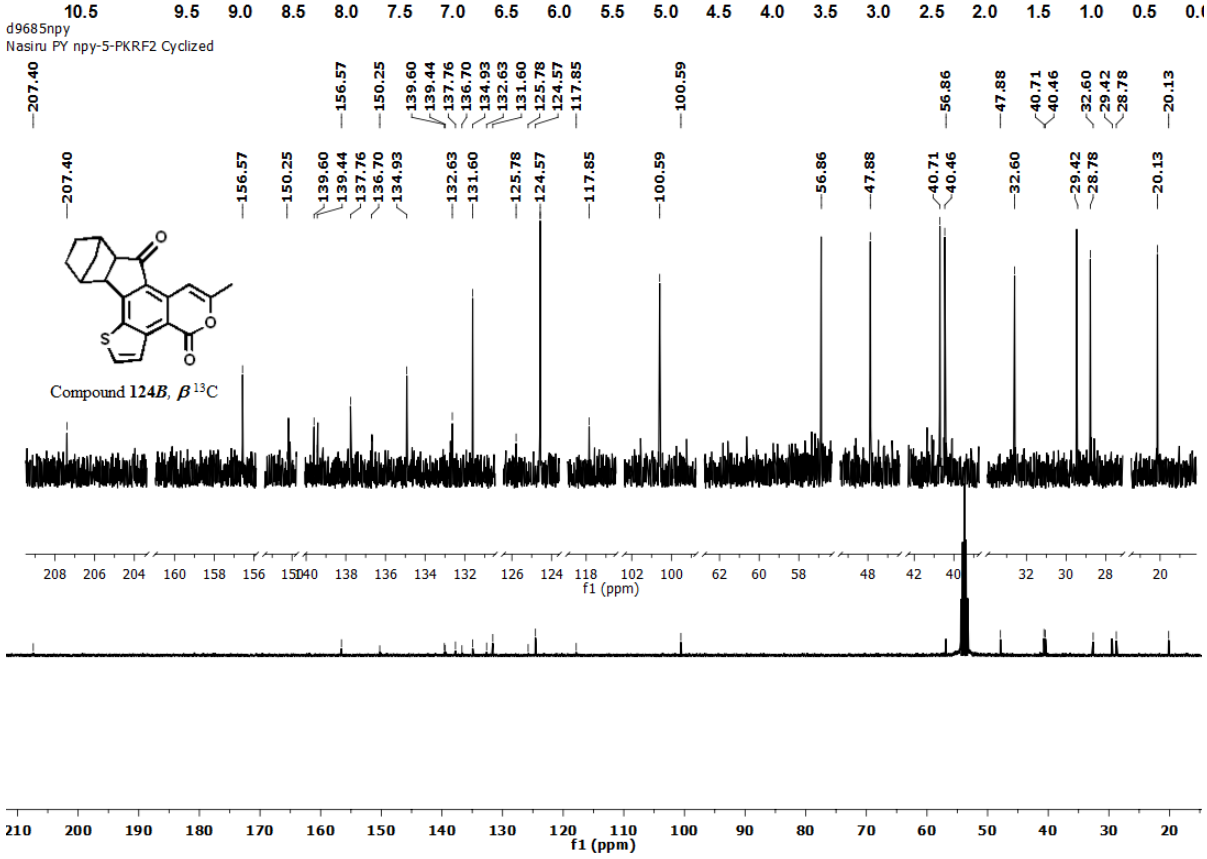

Appendix for (124B *β*)

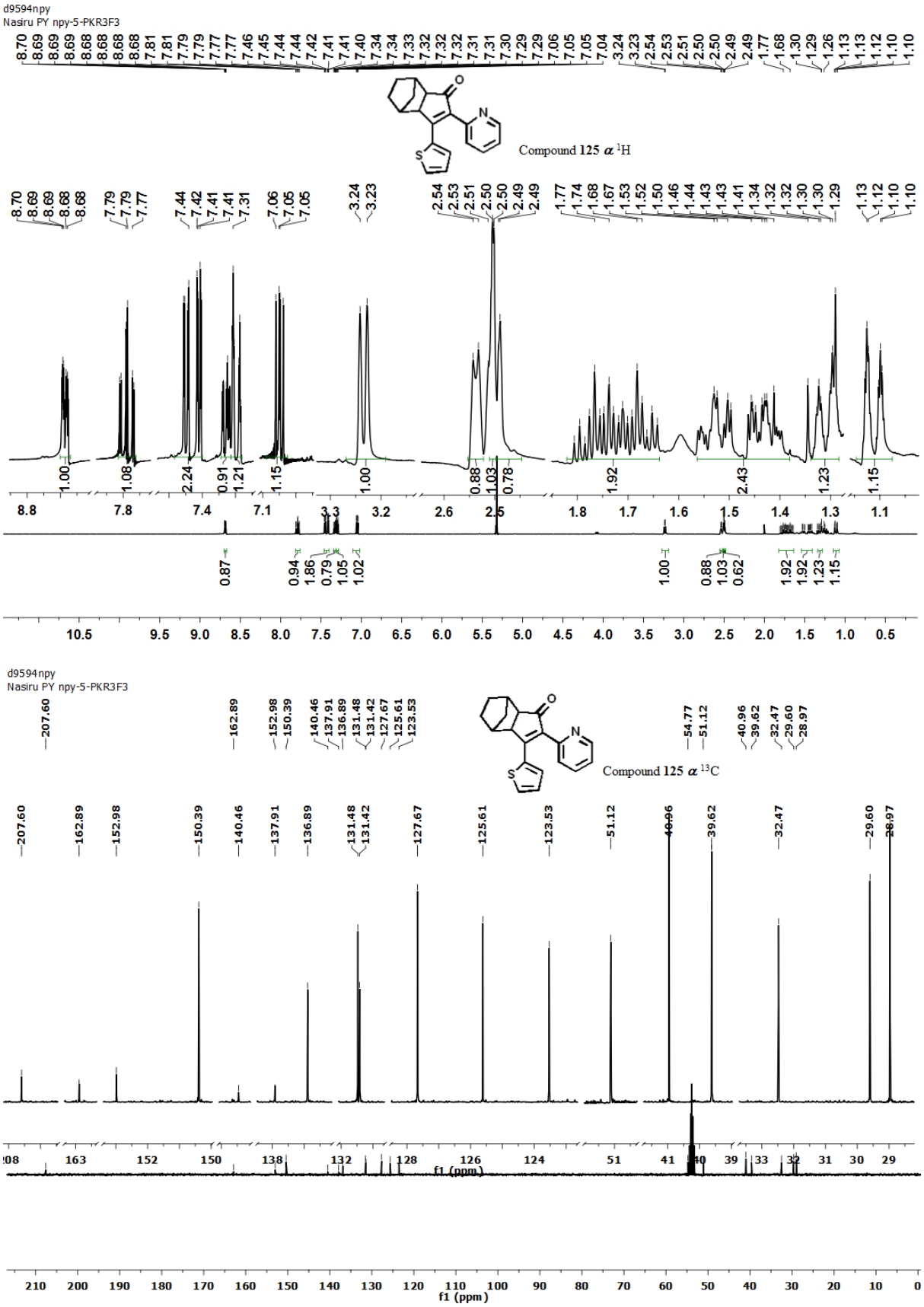

Appendix for (125 α)

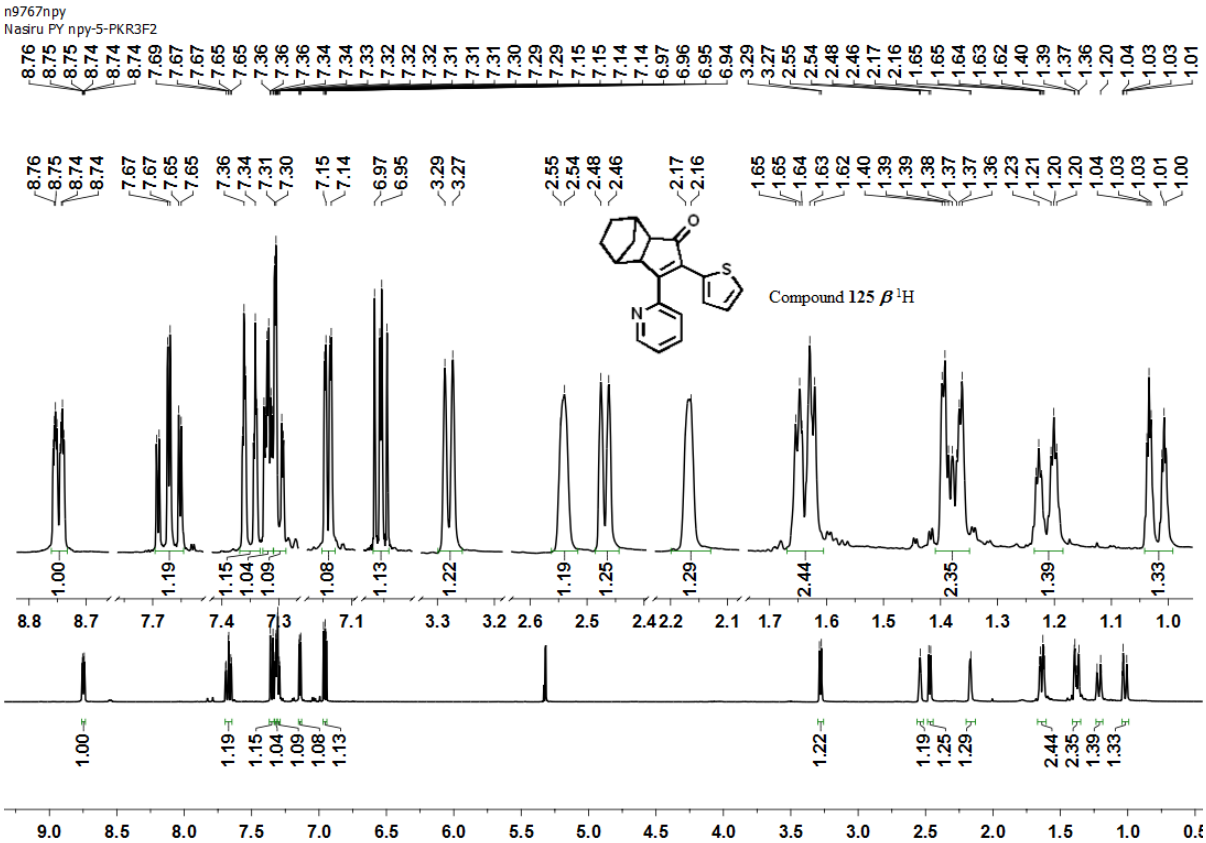

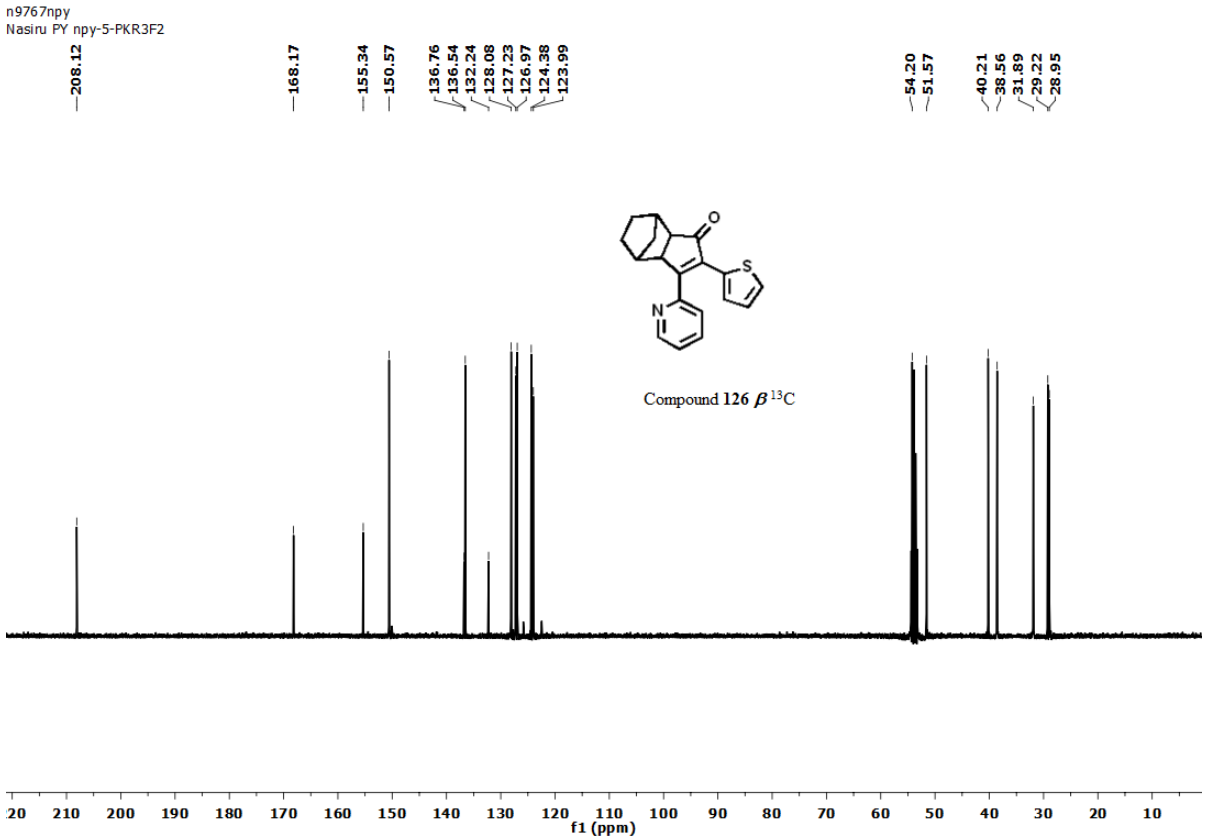

Appendix for (125 β)

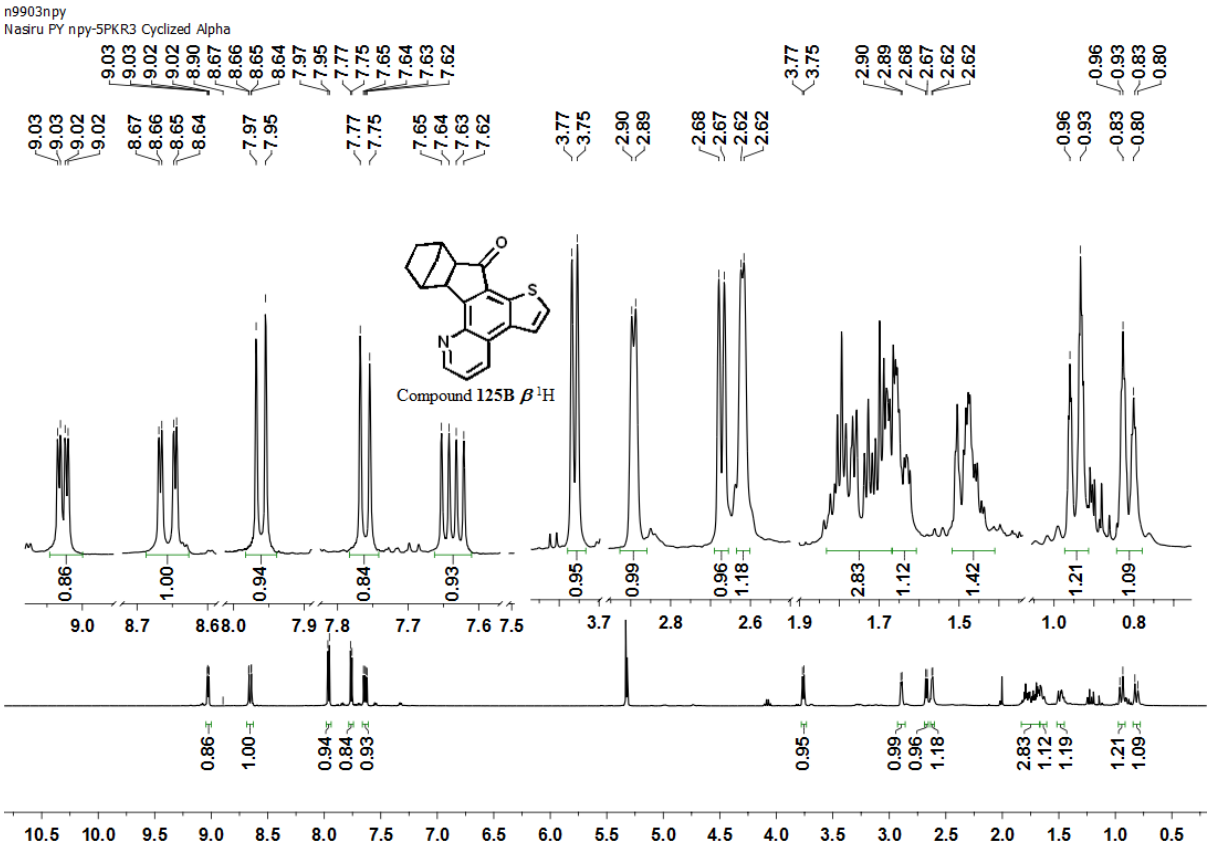

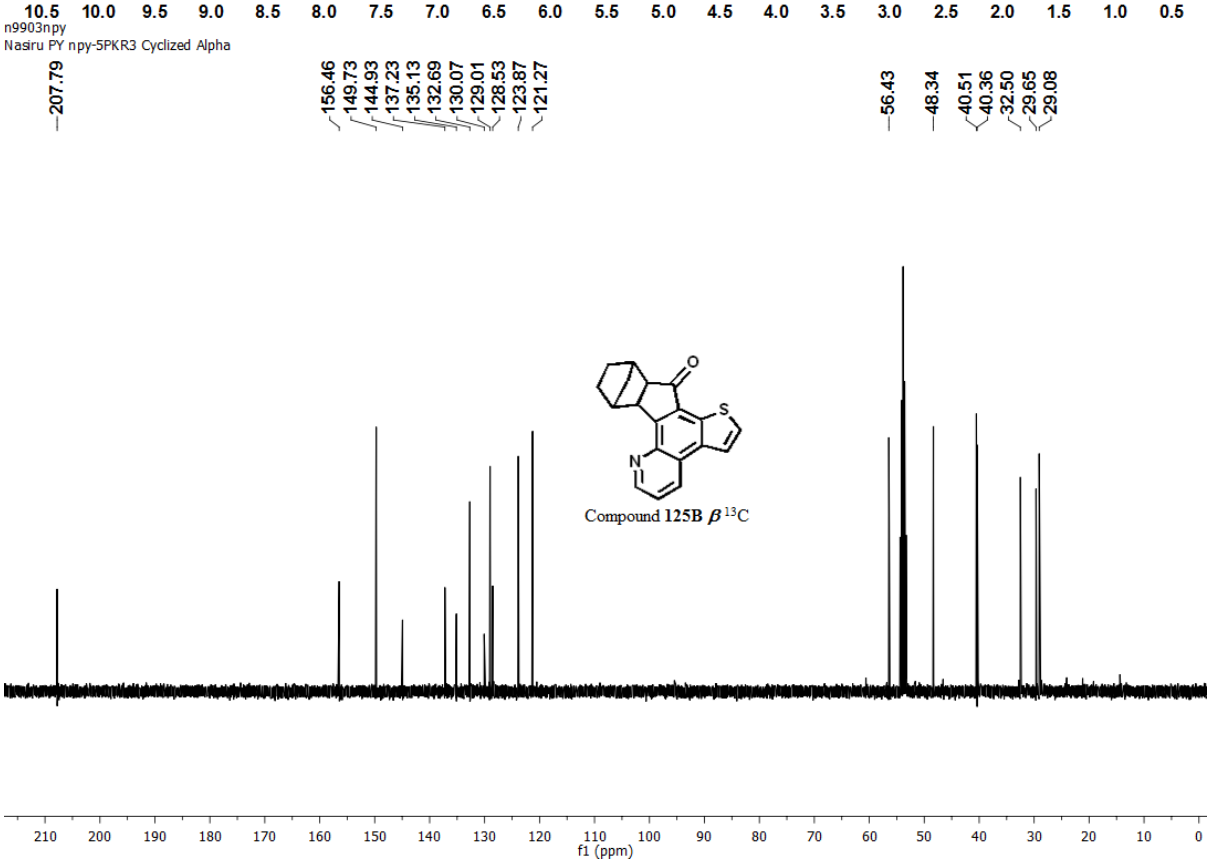

Appendix for (125B β)

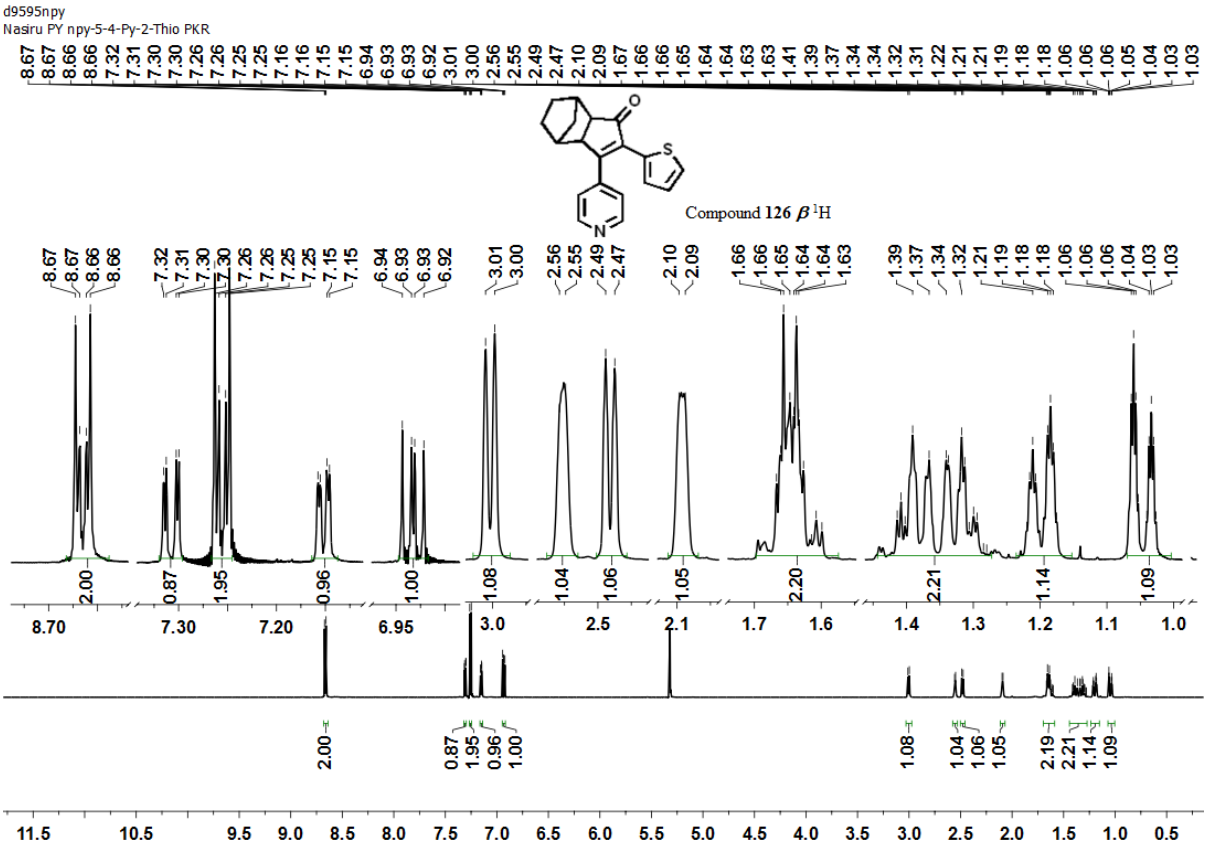

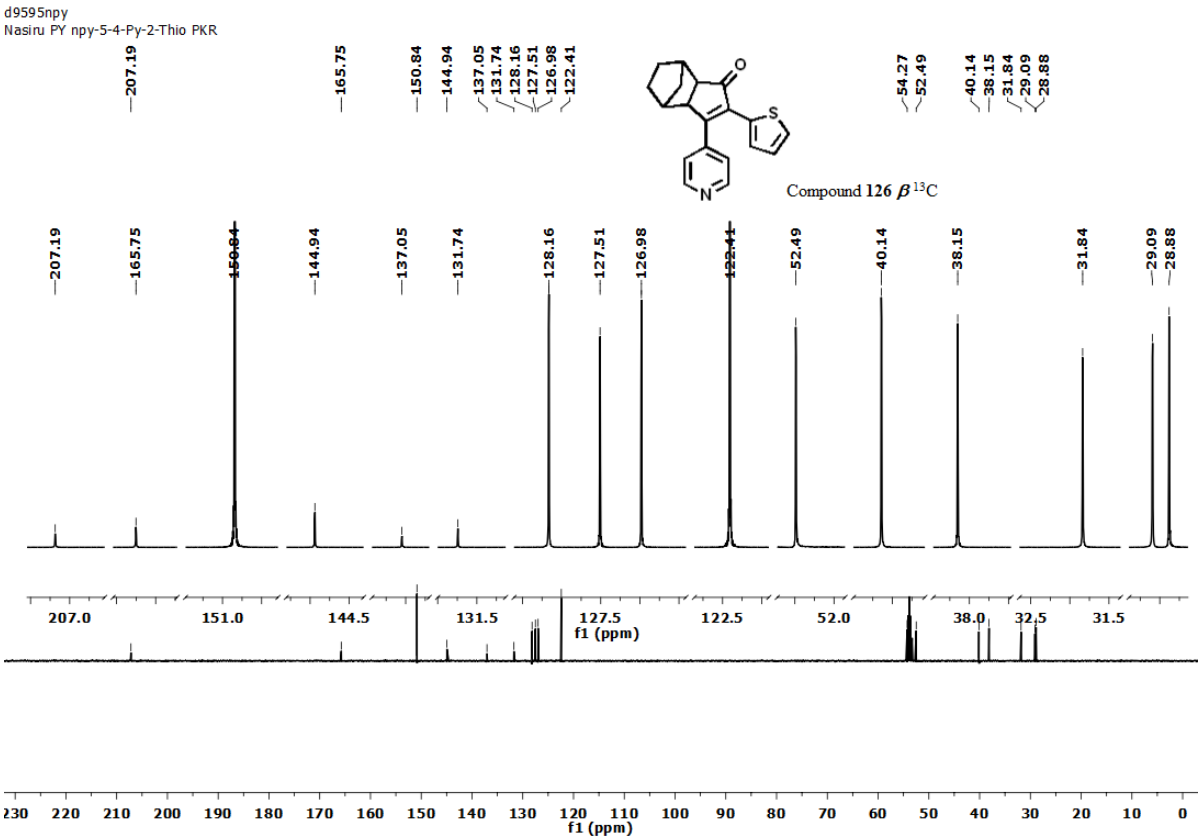

Appendix for (126 *β*)

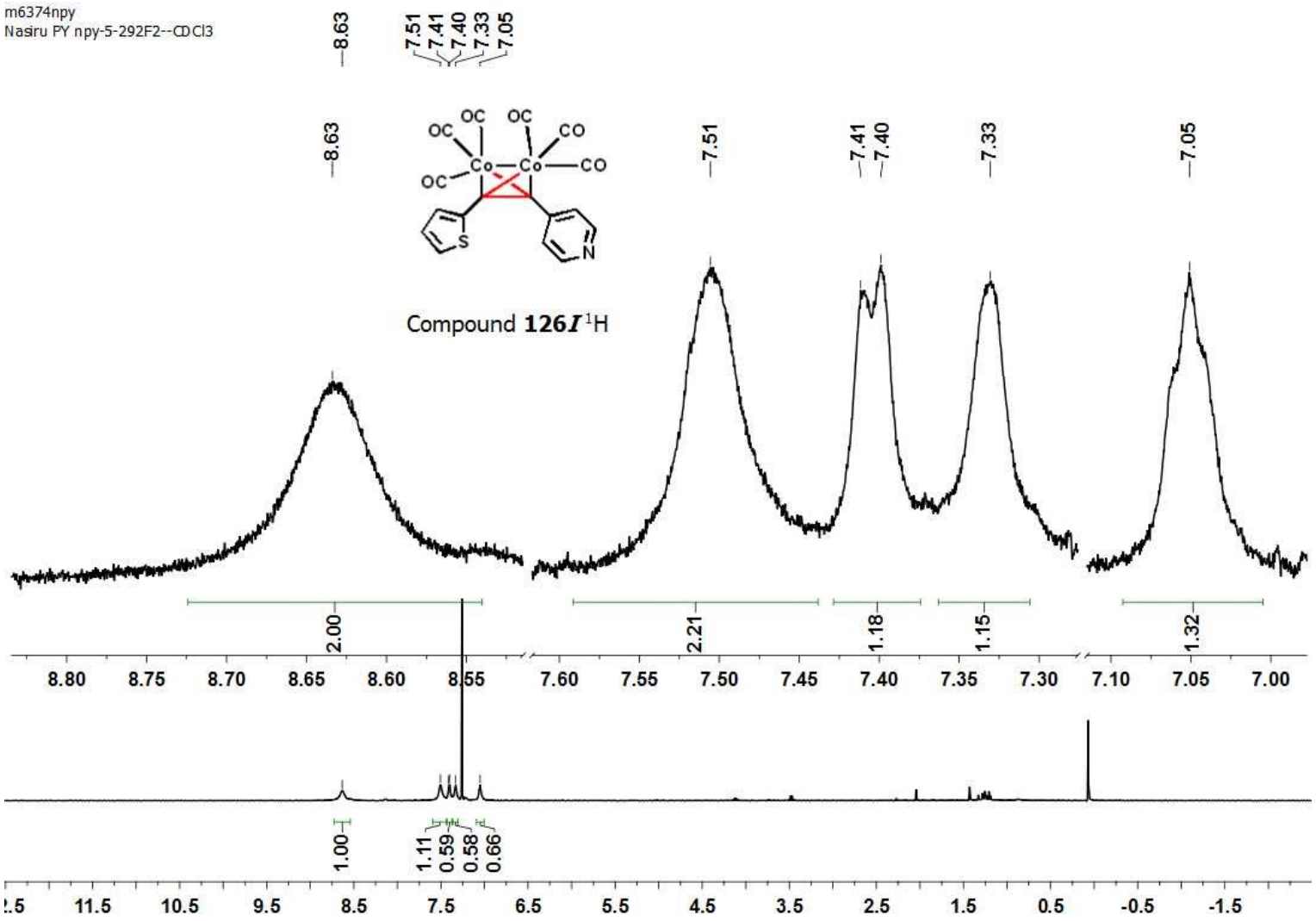

Appendix for (126*I*)

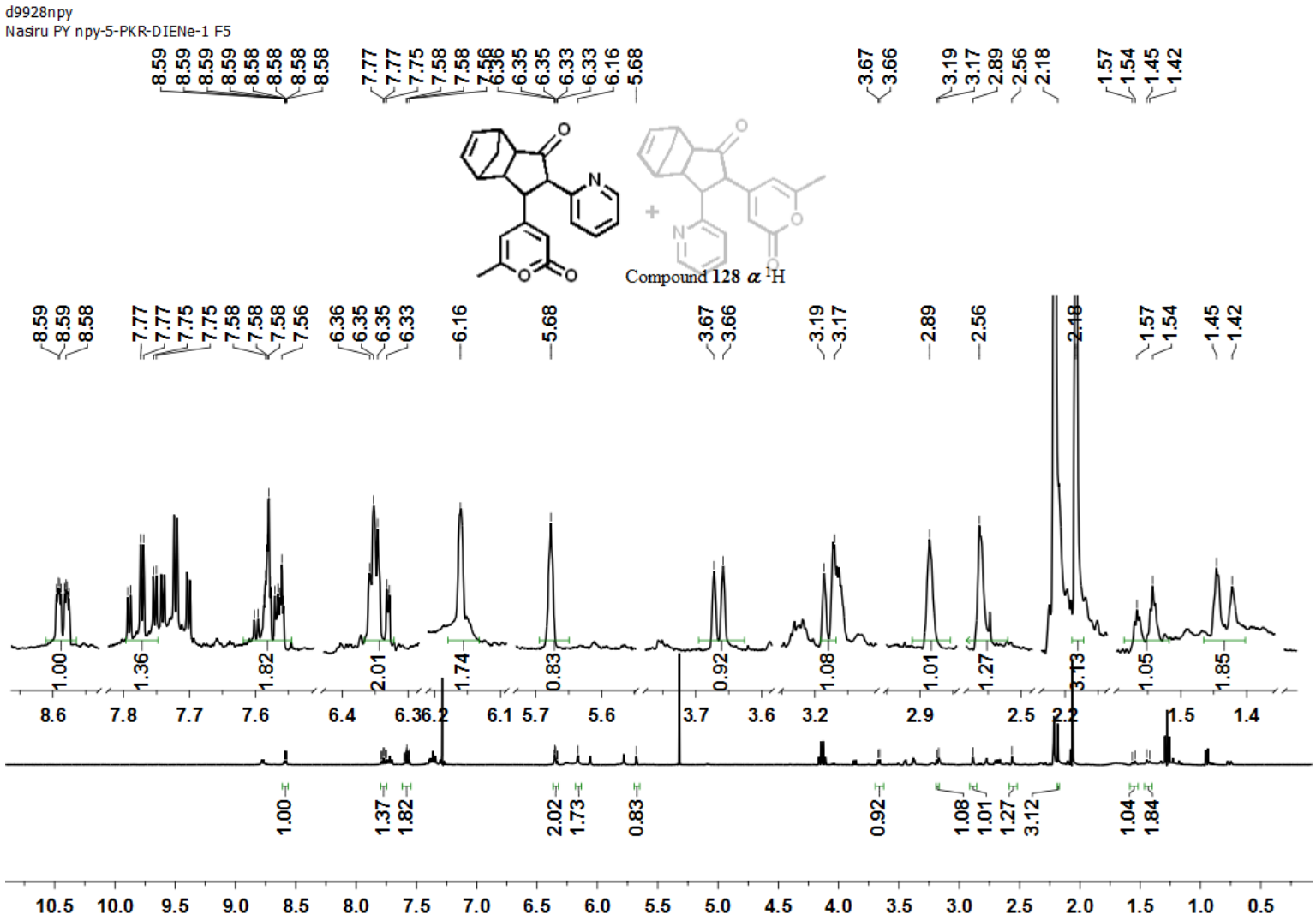

Appendix for (128 *α*)

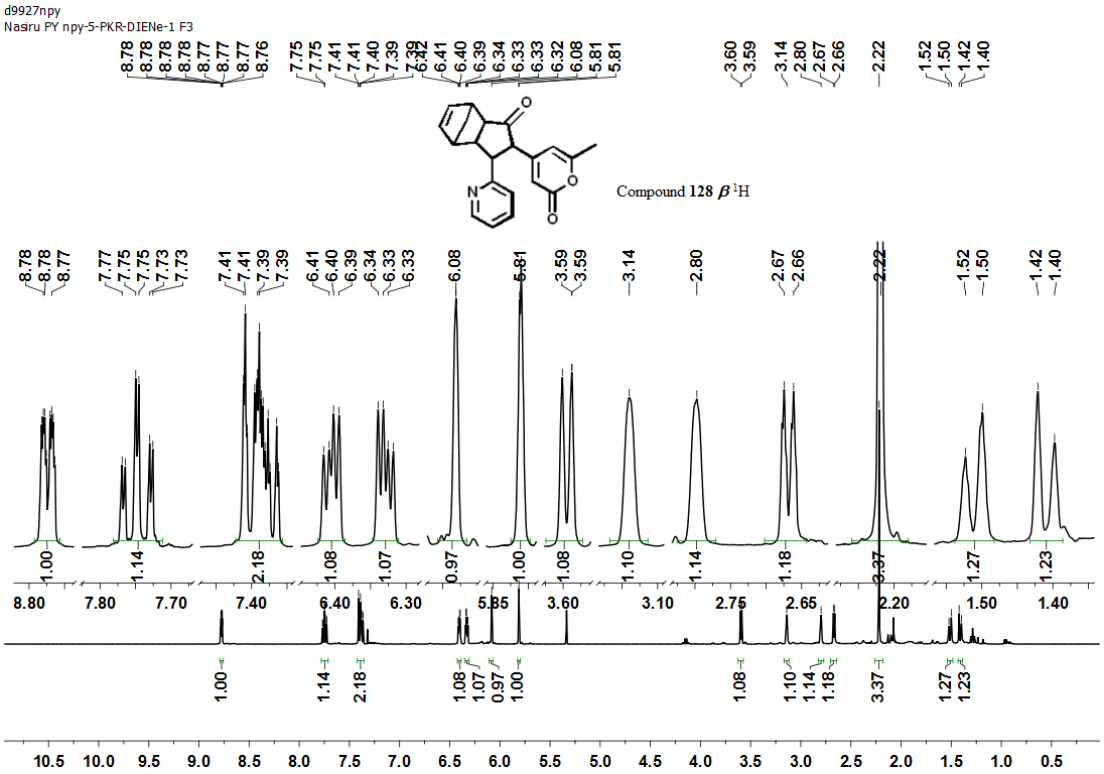

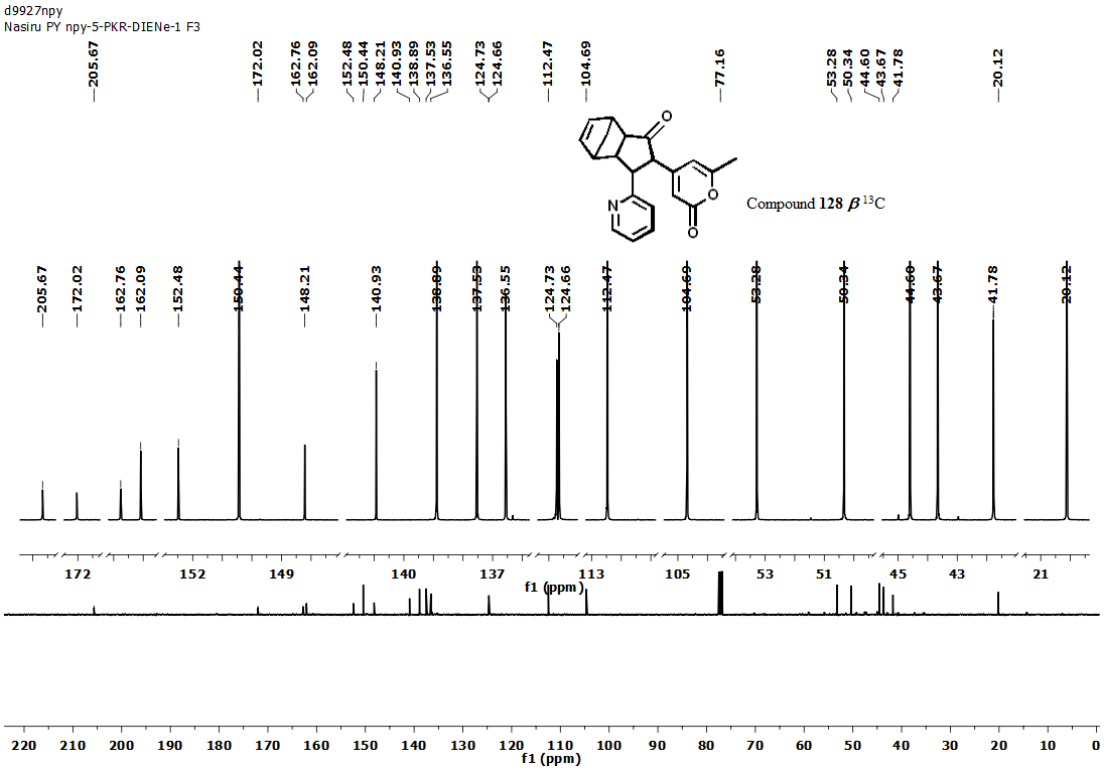

Appendix for (128 *β*)

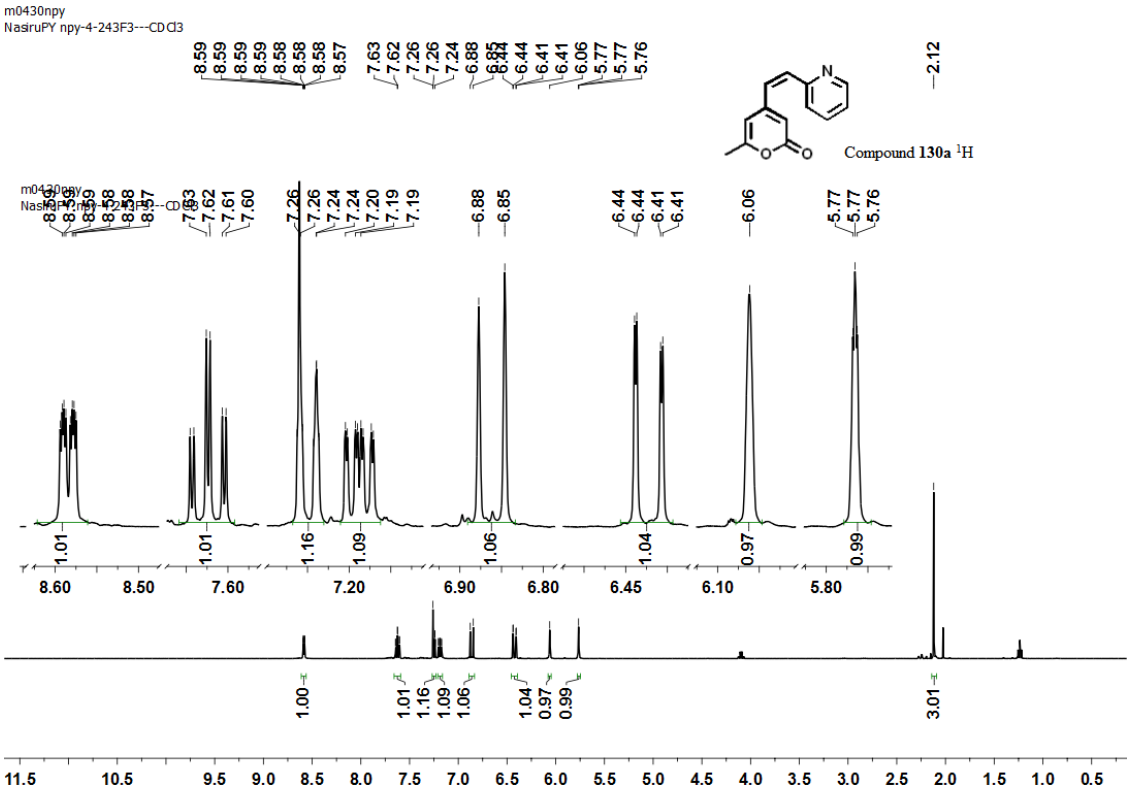

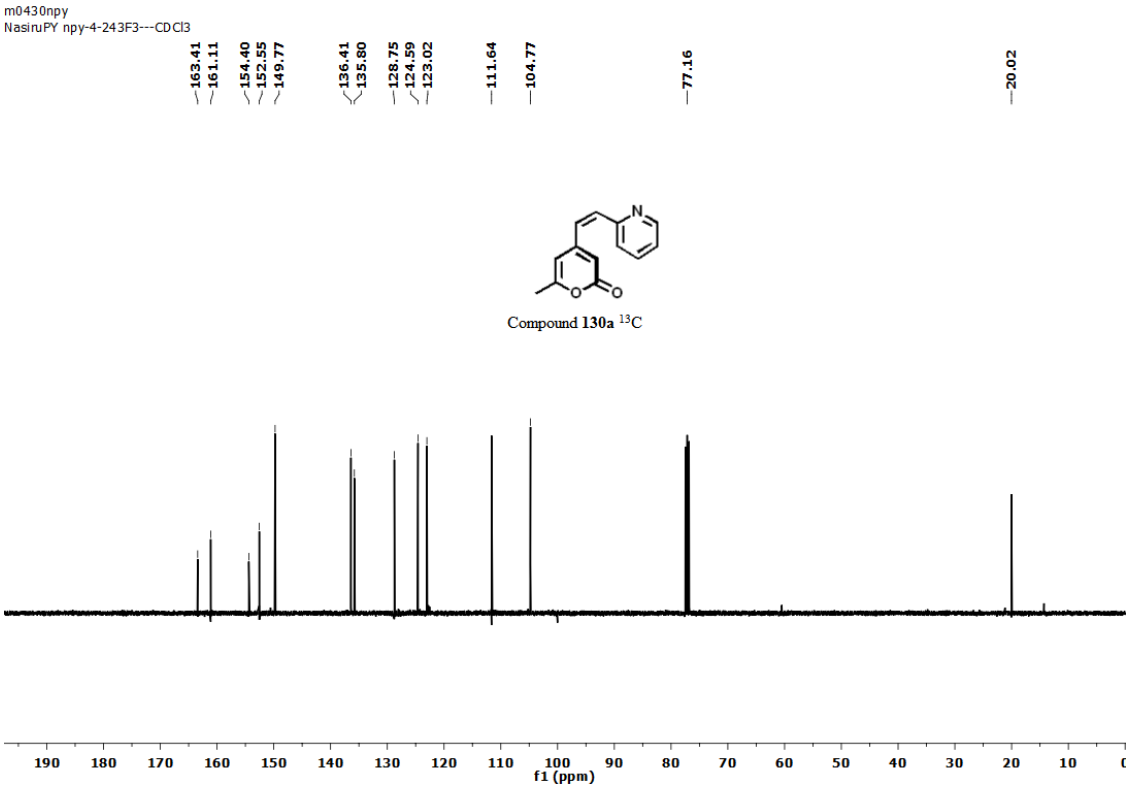

Appendix for (130a)

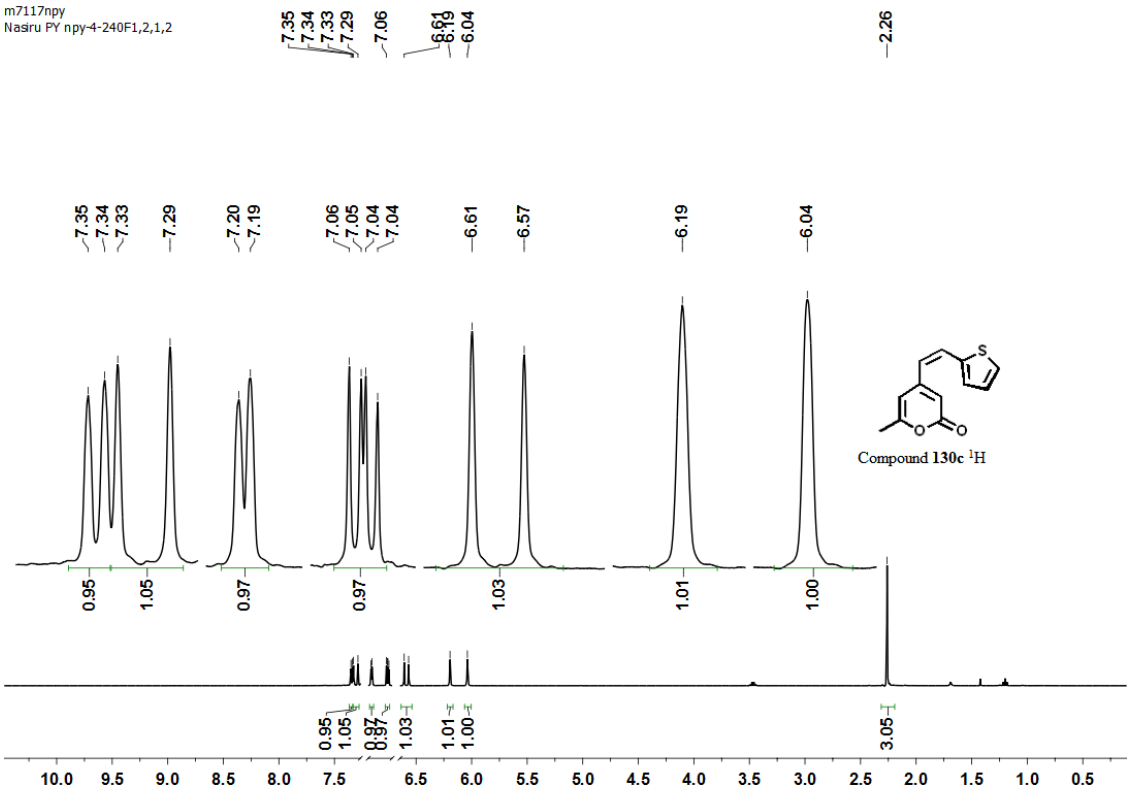

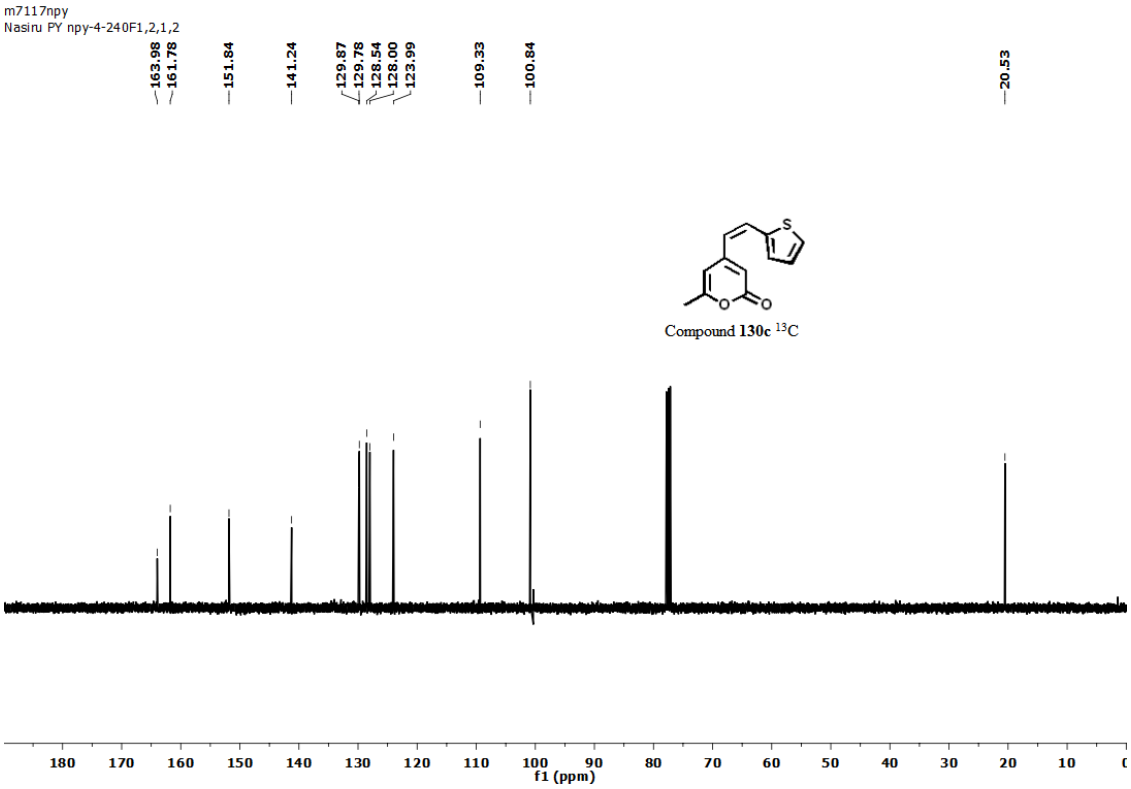

Appendix for (130c)

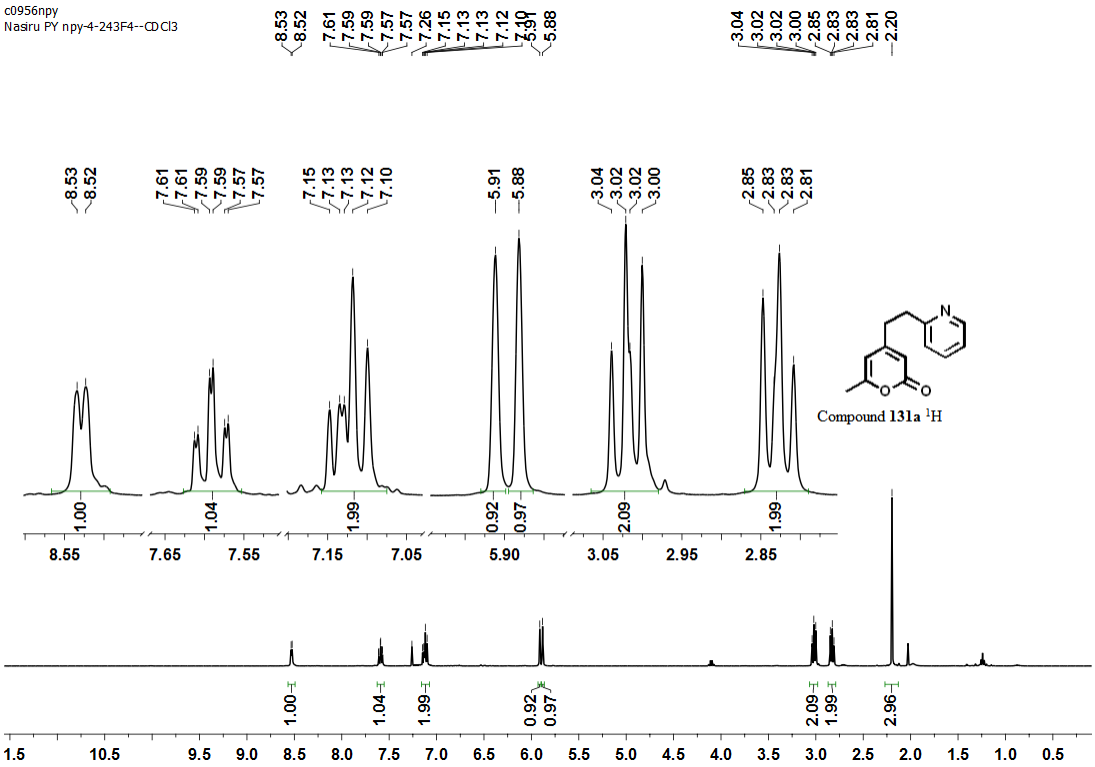

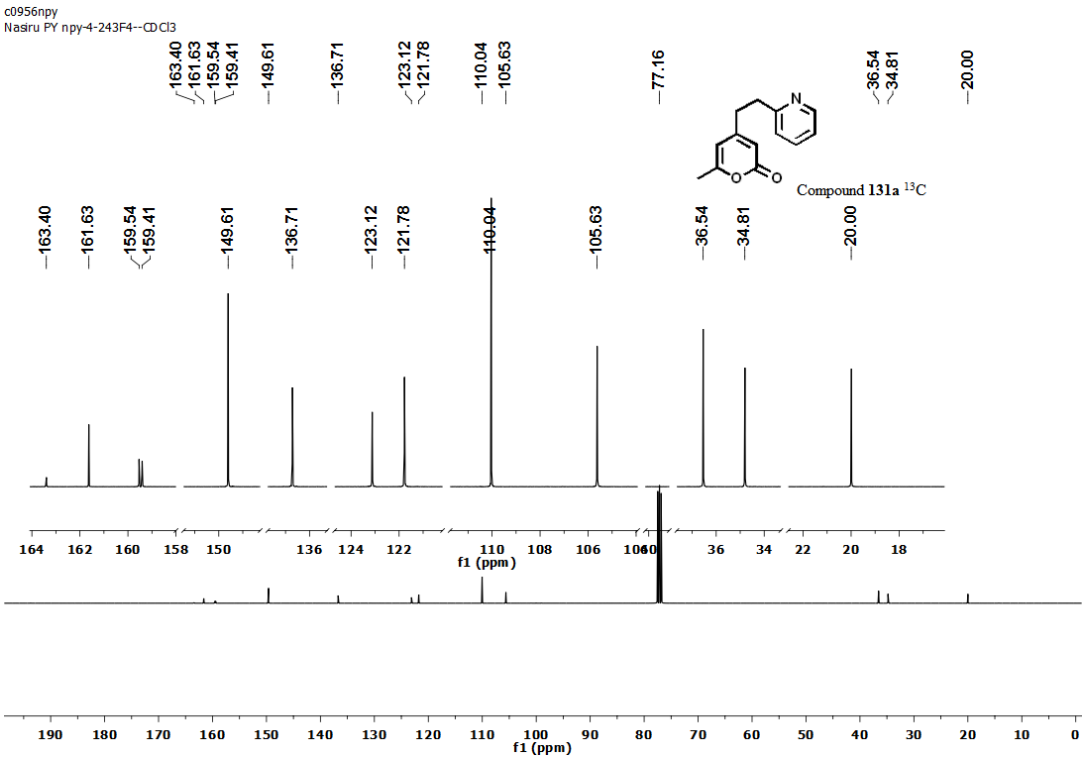

Appendix for (131a)

Abbreviations

2-phpy	2-Phenylpyridine
2-Bnpy	2-Benzylpyridine
Ac	acetyl
APCI	atmospheric pressure chemical ionisation
aq.	aqueous
ATR	attenuated total reflectance
Bn	benzyl
Bu	butyl
C, c.	concentration
c.	concentrated
calcd	calculated
cat.	catalyst, catalytic
cod	1,5-cycloocadiene
conv.	conversion
COSY	correlation spectroscopy
Cp	cyclopentadienyl
Cy	cyclohexyl
d	(NMR) Doublet
dec.	decomposition
DCE	Dichloroethane
DCM	Dichloromethane
DFT	Density functional theory
DMF	dimethylformamide

DMSO	dimethylsulfoxide
dppe	1,2-bis(diphenylphosphino)ethane
dppf	1,1'-bis(diphenylphosphino)ferrocene
EDG	Electron donating group
EI	electron ionisation
eq.	equivalents
ESI	electrospray ionisation
Et	ethyl
EWG	Electron withdrawing group
FG	Functional group
FTIR	Fourier transform infrared spectroscopy
FGI	functional group interconversion
Fu	furyl
G	gram(s)
H	hour(s)
HMBC	heteronuclear multiple-bond correlation spectroscopy
HRMS	high-resolution mass spectrometry
HSQC	heteronuclear single quantum coherence spectroscopy
i-	iso-
IR	infrared
isol.	isolated
J	Spin-spin coupling
L	Ligand
LED	Light emitting diode
LIFDI	liquid introduced field desorption ionisation

lit.	literature
m	Milli
M	(concentration) mol dm-3
m	(nmr) Multiplet
[M]	metal
m-	meta-
m/z	Mass-to-charge ratio
Me	Methyl
min	Minute(s)
mM	millimolar
mm	millimetres
mol	Mole(s)
M.P.	melting point
MS	molecular sieves
MW	Microwave
Mw	molecular weight
n-	normal
NBD	Norbornadiene (Bicyclo[2.2.1]hepta-2,5-diene)
NBN	Norbornene (Bicyclo[2.2.1]hept-2-ene)
nm	nanometres
NMR	nuclear magnetic resonance
Nu	nucleophile
nOe	nuclear Overhauser effect
NOESY	nuclear Overhauser effect spectroscopy

OAc	Acetate
p-	para-
Ph	phenyl
PK	Pauson-Khand
PKR	Pauson-Khand reaction
ppm	parts per million
Pr	propyl
py.	pyridine
quant.	quantitative yield
rel.	relative
q	(NMR) Quartet
R	Substituent
Rf	retention factor
RT	at ambient temperature
SM	starting material
r.t.	Room temperature
s	Second(s)
t	Time
t	(NMR) Triplet
t-	tertiary
temp.	Temperature
t-Bu	tert-Butyl
TFP	tri(2-furyl)phosphine
THF	tetrahydrofuran
TLC	thin layer chromatography

TMS	trimethylsilane
tol	toluene
TS	Transition state
UV	Ultra-violet
Vis	Visible
w.r.t.	with respect to
X	leaving group
δ	Chemical shift downfield from tetramethylsilane
μ	Micro

References

1. J. Tsuji, *Palladium Reagents and Catalysts: New Perspectives for the 21st Century*, Wiley, 2006.

2. J. Tsuji, *Palladium in Organic Synthesis*, Springer, 2005.

3. J. Tsuji, in *Transition Metal Reagents and Catalysts*, John Wiley & Sons, Ltd, 2003, pp. i-xv.

4. J. Tsuji, *Perspectives in Organopalladium Chemistry for the XXI Century*, Elsevier, 1999.

5. K. A. Horn, *Chemical Reviews*, 1995, **95**, 1317-1350.

6. E. Negishi and A. de Meijere, *Handbook of Organopalladium Chemistry for Organic Synthesis, 2 Volume Set*, Wiley, 2003.

7. E. I. Negishi, *Organometallics in organic synthesis*, John Wiley & Sons Australia, Limited, 1980.

8. E.-i. Negishi, in *Handbook of Organopalladium Chemistry for Organic Synthesis*, John Wiley & Sons, Inc., 2003, pp. 229-247.

9. A. Ehrentraut, A. Zapf and M. Beller, *Synlett*, 2000, **2000**, 1589-1592.

10. A. F. Littke and G. C. Fu, *Journal of the American Chemical Society*, 2001, **123**, 6989-7000.

11. K. J. Stowers, A. Kubota and M. S. Sanford, *Chemical Science*, 2012, **3**, 3192-3195.

12. W. Yu and Z. Jin, *Journal of the American Chemical Society*, 2000, **122**, 9840-9841.

13. T. W. Lyons and M. S. Sanford, *Chem Rev*, 2010, **110**, 1147-1169.

14. S. L. Zultanski and S. S. Stahl, *Journal of Organometallic Chemistry*, 2015, **793**, 263-268.

15. C. C. C. Johansson Seechurn, A. DeAngelis and T. J. Colacot, in *New Trends in Cross-Coupling: Theory and Applications*, The Royal Society of Chemistry, 2015, pp. 1-19.

16. E.-i. Negishi, *Angewandte Chemie International Edition*, 2011, **50**, 6738-6764.

17. X. Chen, K. M. Engle, D.-H. Wang and J.-Q. Yu, *Angewandte Chemie International Edition*, 2009, **48**, 5094-5115.

18. K. C. Nicolaou, P. G. Bulger and D. Sarlah, *Angewandte Chemie International Edition*, 2005, **44**, 4442-4489.

19. T. Mizoroki, K. Mori and A. Ozaki, *Bulletin of the Chemical Society of Japan*, 1971, **44**, 581-581.

20. R. F. Heck and J. P. Nolley, *The Journal of Organic Chemistry*, 1972, **37**, 2320-2322.

21. D. Milstein and J. K. Stille, *Journal of the American Chemical Society*, 1978, **100**, 3636-3638.

22. D. Milstein and J. K. Stille, *Journal of the American Chemical Society*, 1979, **101**, 4992-4998.

23. V. Farina, S. Kapadia, B. Krishnan, C. Wang and L. S. Liebeskind, *The Journal of Organic Chemistry*, 1994, **59**, 5905-5911.

24. N. Miyaura, K. Yamada and A. Suzuki, *Tetrahedron Letters*, 1979, **20**, 3437-3440.

25. K. Sonogashira, Y. Tohda and N. Hagihara, *Tetrahedron Letters*, 1975, **16**, 4467-4470.

26. R. Chinchilla and C. Nájera, *Chemical Reviews*, 2007, **107**, 874-922.

27. C. Tsukano and M. Sasaki, *Journal of the American Chemical Society*, 2003, **125**, 14294-14295.

28. C. Tsukano, M. Ebine and M. Sasaki, *Journal of the American Chemical Society*, 2005, **127**, 4326-4335.

29. M. Sasaki, C. Tsukano and K. Tachibana, *Tetrahedron Letters*, 2003, **44**, 4351-4354.

30. M. Sasaki, C. Tsukano and K. Tachibana, *Organic Letters*, 2002, **4**, 1747-1750.

31. M. Satake, M. Shoji, Y. Oshima, H. Naoki, T. Fujita and T. Yasumoto, *Tetrahedron Letters*, 2002, **43**, 5829-5832.

32. F. P. Marmsäter and F. G. West, *Chemistry – A European Journal*, 2002, **8**, 4346-4353.

33. M. Murata and T. Yasumoto, *Natural Product Reports*, 2000, **17**, 293-314.

34. M. Sasaki and H. Fuwa, *Synlett*, 2004, 1851-1874.

35. J. L. Wood, J. A. Porco, J. Taunton, A. Y. Lee, J. Clardy and S. L. Schreiber, *Journal of the American Chemical Society*, 1992, **114**, 5898-5900.

36. J. Taunton, J. L. Wood and S. L. Schreiber, *Journal of the American Chemical Society*, 1993, **115**, 10378-10379.

37. K. C. Nicolaou, A. L. Smith, S. V. Wendeborn and C. K. Hwang, *Journal of the American Chemical Society*, 1991, **113**, 3106-3114.

38. K. C. Nicolaou, C. K. Hwang, A. L. Smith and S. V. Wendeborn, *Journal of the American Chemical Society*, 1990, **112**, 7416-7418.

39. J. Inanaga, K. Hirata, H. Saeki, T. Katsuki and M. Yamaguchi, *Bulletin of the Chemical Society of Japan*, 1979, **52**, 1989-1993.

40. L. Ackermann, *Synlett*, 2007, **2007**, 0507-0526.

41. S. E. Bajwa, T. E. Storr, L. E. Hatcher, T. J. Williams, C. G. Baumann, A. C. Whitwood, D. R. Allan, S. J. Teat, P. R. Raithby and I. J. S. Fairlamb, *Chemical Science*, 2012, **3**, 1656-1661.

42. I. J. S. Fairlamb, *Angewandte Chemie International Edition*, 2015, **54**, 10415-10427.

43. J. Cámpora, P. Palma, D. del Río, E. Carmona, C. Graiff and A. Tiripicchio, *Organometallics*, 2003, **22**, 3345-3347.

44. J. B. Gerken and S. S. Stahl, *ACS Central Science*, 2015.

45. L. Wang, J. Li, H. Yang, Y. Lv and S. Gao, *The Journal of Organic Chemistry*, 2012, **77**, 790-794.

46. V. I. Bakhmutov, J. F. Berry, F. A. Cotton, S. Ibragimov and C. A. Murillo, *Dalton Transactions*, 2005, 1989-1992.

47. T. A. Stephenson, S. M. Morehouse, A. R. Powell, J. P. Heffer and G. Wilkinson, *Journal of the Chemical Society (Resumed)*, 1965, 3632-3640.

48. R. B. Bedford, J. G. Bowen, R. B. Davidson, M. F. Haddow, A. E. Seymour-Julen, H. A. Sparkes and R. L. Webster, *Angewandte Chemie International Edition*, 2015, **54**, 6591-6594.

49. G. Cahiez, D. Bernard and J. F. Normant, *Journal of Organometallic Chemistry*, 1976, **113**, 99-106.

50. G. Cahiez and O. Gager, in *PATAI'S Chemistry of Functional Groups*, John Wiley & Sons, Ltd, 2009.

51. T. Truong, J. Alvarado, L. D. Tran and O. Daugulis, *Organic Letters*, 2010, **12**, 1200-1203.

52. G. Cahiez, A. Moyeux, J. Buendia and C. Duplais, *Journal of the American Chemical Society*, 2007, **129**, 13788-13789.

53. Y. Yuan and Y. Bian, *Applied Organometallic Chemistry*, 2008, **22**, 15-18.

54. G. Cahiez, C. Duplais and J. Buendia, *Angewandte Chemie International Edition*, 2009, **48**, 6731-6734.

55. Z. Zhou and W. Xue, *Journal of Organometallic Chemistry*, 2009, **694**, 599-603.

56. Y.-C. Teo, F.-F. Yong, I. K. Ithnin, S.-H. T. Yio and Z. Lin, *European Journal of Organic Chemistry*, 2013, **2013**, 515-524.

57. Y.-C. Teo, F.-F. Yong and G. S. Lim, *Tetrahedron Letters*, 2011, **52**, 7171-7174.

58. Y.-C. Teo, F.-F. Yong, C.-Y. Poh, Y.-K. Yan and G.-L. Chua, *Chemical Communications*, 2009, 6258-6260.

59. F.-F. Yong and Y.-C. Teo, *Synlett*, 2012, **23**, 2106-2110.

60. F.-F. Yong and Y.-C. Teo, *Tetrahedron Letters*, 2010, **51**, 3910-3912.

61. F. Calderazzo, *Inorganic Chemistry*, 1965, **4**, 293-296.

62. Y. Kuninobu, M. Nishi, A. Kawata, H. Takata, Y. Hanatani, Y. S. Salprima, A. Iwai and K. Takai, *The Journal of Organic Chemistry*, 2010, **75**, 334-341.

63. Y. Kuninobu, A. Kawata and K. Takai, *Journal of the American Chemical Society*, 2006, **128**, 11368-11369.

64. Y. Kuninobu, A. Kawata, M. Nishi, H. Takata and K. Takai, *Chemical Communications*, 2008, 6360-6362.

65. D. A. Valyaev, G. Lavigne and N. Lugan, *Coordination Chemistry Reviews*.

66. H. Chen and J. F. Hartwig, *Angewandte Chemie International Edition*, 1999, **38**, 3391-3393.

67. Y. Kuninobu, Y. Nishina, T. Takeuchi and K. Takai, *Angewandte Chemie International Edition*, 2007, **46**, 6518-6520.

68. Y. Kuninobu, Y. Fujii, T. Matsuki, Y. Nishina and K. Takai, *Organic Letters*, 2009, **11**, 2711-2714.

69. B. Zhou, H. Chen and C. Wang, *Journal of the American Chemical Society*, 2013, **135**, 1264-1267.

70. H. Werner, *Angewandte Chemie International Edition*, 2014, **53**, 3309-3309.

71. I. U. Khand, G. R. Knox, P. L. Pauson and W. E. Watts, *Journal of the Chemical Society, Perkin Transactions 1*, 1973, 975-977.

72. I. U. Khand, G. R. Knox, P. L. Pauson, W. E. Watts and M. I. Foreman, *Journal of the Chemical Society, Perkin Transactions 1*, 1973, 977-981.

73. I. U. Khand, G. R. Knox, P. L. Pauson and W. E. Watts, *Journal of the Chemical Society D: Chemical Communications*, 1971, 36a-36a.

74. S. M. Roberts, M. G. Santoro and E. S. Sickle, *Journal of the Chemical Society, Perkin Transactions 1*, 2002, 1735-1742.

75. A. Rossi, P. Kapahi, G. Natoli, T. Takahashi, Y. Chen, M. Karin and M. G. Santoro, *Nature*, 2000, **403**, 103-118.

76. N. Jeong, S. Lee and B. K. Sung, *Organometallics*, 1998, **17**, 3642-3644.

77. T. Shibata and K. Takagi, *Journal of the American Chemical Society*, 2000, **122**, 9852-9853.

78. A. J. Pearson and R. A. Dubbert, *Organometallics*, 1994, **13**, 1656-1661.

79. A. J. Pearson and R. A. Dubbert, *Journal of the Chemical Society, Chemical Communications*, 1991, 202-203.

80. L. Jordi, A. Segundo, F. Camps, S. Ricart and J. M. Moreto, *Organometallics*, 1993, **12**, 3795-3797.

81. N. Jeong, S. J. Lee, B. Y. Lee and Y. K. Chung, *Tetrahedron Letters*, 1993, **34**, 4027-4030.

82. C. Mukai, M. Uchiyama and M. Hanaoka, *Journal of the Chemical Society, Chemical Communications*, 1992, 1014-1015.

83. T. R. Hoye and J. A. Suriano, *Journal of the American Chemical Society*, 1993, **115**, 1154-1156.

84. T. R. Hoye and J. A. Suriano, *Organometallics*, 1992, **11**, 2044-2050.

85. N. Wu, L. Deng, L. Liu, Q. Liu, C. Li and Z. Yang, *Chemistry – An Asian Journal*, 2013, **8**, 65-68.

86. Y. Lan, L. Deng, J. Liu, C. Wang, O. Wiest, Z. Yang and Y.-D. Wu, *The Journal of Organic Chemistry*, 2009, **74**, 5049-5058.

87. M. E. Krafft, I. L. Scott, R. H. Romero, S. Feibelmann and C. E. Van Pelt, *Journal of the American Chemical Society*, 1993, **115**, 7199-7207.

88. X. Verdaguer, A. Moyano, M. A. Pericas, A. Riera, V. Bernardes, A. E. Greene, A. Alvarez-Larena and J. F. Piniella, *Journal of the American Chemical Society*, 1994, **116**, 2153-2154.

89. C. M. Gordon, M. Kiszka, I. R. Dunkin, W. J. Kerr, J. S. Scott and J. Gebicki, *Journal of Organometallic Chemistry*, 1998, **554**, 147-154.

90. S. M. Draper, C. Long and B. M. Myers, *Journal of Organometallic Chemistry*, 1999, **588**, 195-199.

91. M. K. Pallerla, G. P. A. Yap and J. M. Fox, *The Journal of Organic Chemistry*, 2008, **73**, 6137-6141.

92. E. V. Banide, H. Müller-Bunz, A. R. Manning, P. Evans and M. J. McGlinchey, *Angewandte Chemie International Edition*, 2007, **46**, 2907-2910.

93. Y. Gimbert, D. Lesage, A. Milet, F. Fournier, A. E. Greene and J.-C. Tabet, *Organic Letters*, 2003, **5**, 4073-4075.

94. S. A. Brusey, E. V. Banide, S. Dörrich, P. O'Donohue, Y. Ortin, H. Müller-Bunz, C. Long, P. Evans and M. J. McGlinchey, *Organometallics*, 2009, **28**, 6308-6319.

95. T. Zheng, H. Sun, J. Ding, Y. Zhang and X. Li, *Journal of Organometallic Chemistry*, **695**, 1873-1877.

96. H.-F. Klein, S. Camadanli, R. Beck, D. Leukel and U. Flörke, *Angewandte Chemie International Edition*, 2005, **44**, 975-977.

97. M. Yamanaka and E. Nakamura, *Journal of the American Chemical Society*, 2001, **123**, 1703-1708.

98. S. E. Gibson and N. Mainolfi, *Angewandte Chemie International Edition*, 2005, **44**, 3022-3037.

99. T. J. M. de Bruin, A. Milet, A. E. Greene and Y. Gimbert, *The Journal of Organic Chemistry*, 2004, **69**, 1075-1080.

100. M. E. Krafft, R. H. Romero and I. L. Scott, *The Journal of Organic Chemistry*, 1992, **57**, 5277-5278.

101. T. R. Hoye and J. A. Suriano, *The Journal of Organic Chemistry*, 1993, **58**, 1659-1660.

102. M. E. Krafft, R. H. Romero and I. L. Scott, *Synlett*, 1995, **1995**, 577-578.

103. F. Robert, A. Milet, Y. Gimbert, D. Konya and A. E. Greene, *Journal of the American Chemical Society*, 2001, **123**, 5396-5400.

104. B. E. Moulton, J. M. Lynam, A.-K. Duhme-Klair, W. Zheng, Z. Lin and I. J. S. Fairlamb, *Organic & Biomolecular Chemistry*, 2010, **8**, 5398-5403.

105. B. E. Moulton, A. C. Whitwood, A. K. Duhme-Klair, J. M. Lynam and I. J. S. Fairlamb, *The Journal of Organic Chemistry*, 2011, **76**, 5320-5334.

106. T. Konno, T. Kida, A. Tani and T. Ishihara, *Journal of Fluorine Chemistry*, 2012, **144**, 147-156.

107. N. Aiguabella, C. del Pozo, X. Verdaguer, S. Fustero and A. Riera, *Angewandte Chemie International Edition*, 2013, **52**, 5355-5359.

108. J.-C. Kizirian, N. Aiguabella, A. Pesquer, S. Fustero, P. Bello, X. Verdaguer and A. Riera, *Organic Letters*, 2010, **12**, 5620-5623.

109. B. E. Moulton, H. Dong, C. T. O'Brien, S. B. Duckett, Z. Lin and I. J. S. Fairlamb, *Organic & Biomolecular Chemistry*, 2008, **6**, 4523-4532.

110. R. B. Woodward and R. Hoffmann, *Angewandte Chemie International Edition in English*, 1969, **8**, 781-853.

111. R. B. Woodward and R. Hoffmann, *Journal of the American Chemical Society*, 1965, **87**, 395-397.

112. E. J. Corey and A. G. Hortmann, *Journal of the American Chemical Society*, 1963, **85**, 4033-4034.

113. K. Hiraki, Y. Fuchita and K. Takechi, *Inorganic Chemistry*, 1981, **20**, 4316-4320.

114. S. B. Atla, A. A. Kelkar, V. G. Puranik, W. Bensch and R. V. Chaudhari, *Journal of Organometallic Chemistry*, 2009, **694**, 683-690.

115. B. V. S. Reddy, G. Revathi, A. S. Reddy and J. S. Yadav, *Tetrahedron Letters*, 2011, **52**, 5926-5929.

116. G.-W. Wang, T.-T. Yuan and X.-L. Wu, *The Journal of Organic Chemistry*, 2008, **73**, 4717-4720.

117. M. R. Warren, S. K. Brayshaw, A. L. Johnson, S. Schiffers, P. R. Raithby, T. L. Easun, M. W. George, J. E. Warren and S. J. Teat, *Angewandte Chemie International Edition*, 2009, **48**, 5711-5714.

118. L. E. Hatcher, M. R. Warren, D. R. Allan, S. K. Brayshaw, A. L. Johnson, S. Fuertes, S. Schiffers, A. J. Stevenson, S. J. Teat, C. H. Woodall and P. R. Raithby, *Angewandte Chemie International Edition*, 2011, **50**, 8371-8374.

119. M. R. Warren, S. K. Brayshaw, L. E. Hatcher, A. L. Johnson, S. Schiffers, A. J. Warren, S. J. Teat, J. E. Warren, C. H. Woodall and P. R. Raithby, *Dalton Transactions*, 2012, **41**, 13173-13179.

120. T. W. Lyons and M. S. Sanford, *Chemical reviews*, 2010, **110**, 1147-1169.

121. J. A. Camargo and Á. Alonso, *Environment International*, 2006, **32**, 831-849.

122. F. B. Jensen, *Comparative Biochemistry and Physiology Part A: Molecular & Integrative Physiology*, 2003, **135**, 9-24.

123. X.-Y. Dong, Z.-W. Gao, K.-F. Yang, W.-Q. Zhang and L.-W. Xu, *Catalysis Science & Technology*, 2015, **5**, 2554-2574.

124. W. Zhang, S. Ren, J. Zhang and Y. Liu, *The Journal of Organic Chemistry*, 2015, **80**, 5973-5978.

125. X. Chen, K. M. Engle, D.-H. Wang and J.-Q. Yu, *Angewandte Chemie*, 2009, **121**, 5196-5217.

126. C. Zhou and R. C. Larock, *Journal of the American Chemical Society*, 2004, **126**, 2302-2303.

127. S.-G. Lim, J.-A. Ahn and C.-H. Jun, *Organic Letters*, 2004, **6**, 4687-4690.

128. Y. Kuninobu, Y. Nishina, M. Shouho and K. Takai, *Angewandte Chemie International Edition*, 2006, **45**, 2766-2768.

129. J. S. Ward, J. M. Lynam, J. W. B. Moir, D. E. Sanin, A. P. Mountford and I. J. S. Fairlamb, *Dalton Transactions*, 2012, **41**, 10514-10517.

130. M. Bruce, B. Goodall and I. Matsuda, *Australian Journal of Chemistry*, 1975, **28**, 1259-1264.

131. M. J. Burns, R. J. Thatcher, R. J. K. Taylor and I. J. S. Fairlamb, *Dalton Transactions*, 2010, **39**, 10391-10400.

132. K. Gao, P.-S. Lee, T. Fujita and N. Yoshikai, *Journal of the American Chemical Society*, 2010, **132**, 12249-12251.

133. R. D. Rogers, H. G. Alt and H. E. Maisel, *Journal of Organometallic Chemistry*, 1990, **381**, 233-238.

134. I. J. S. Fairlamb, F. J. Lu and J. P. Schmidt, *Synthesis*, 2003, **2003**, 2564-2570.

135. E. Fager-Jokela, M. Muuronen, M. Patzschke and J. Helaja, *The Journal of Organic Chemistry*, 2012, **77**, 9134-9147.

136. M. P. Coogan, R. L. Jenkins and E. Nutz, *Journal of Organometallic Chemistry*, 2004, **689**, 694-697.

137. Y.-M. Legrand, A. van der Lee and M. Barboiu, *Science*, 2010, **329**, 299-302.

138. W. H. Pirkle and L. H. McKendry, *Journal of the American Chemical Society*, 1969, **91**, 1179-1186.

139. Y. Ji, X. Verdaguer and A. Riera, *Chemistry – A European Journal*, 2011, **17**, 3942-3948.

140. M. Irie, *Chemical Reviews*, 2000, **100**, 1685-1716.

141. X. Rao, C. Liu, J. Qiu and Z. Jin, *Organic & Biomolecular Chemistry*, 2012, **10**, 7875-7883.

142. M. R. R. Prabhath, J. Romanova, R. J. Curry, S. R. P. Silva and P. D. Jarowski, *Angewandte Chemie International Edition*, 2015, **54**, 7949-7953.

143. R. Ul Islam, S. K. Mahato, S. K. Shukla, M. J. Witcomb and K. Mallick, *ChemCatChem*, 2013, **5**, 2453-2461.

144. A. N. Kozhevnikova, M. S. Shvartsberg and I. L. Kotlyarevskii, *Bulletin of the Academy of Sciences of the USSR, Division of chemical science*, 1973, **22**, 1132-1134.